Expanding the Scope of Intramolecular Silver-catalyzed Nitrene Transfer: Enantioselective Aminations and Chemoselective Dearomatizations

By

Emily Z. Schroeder

A dissertation submitted in partial fulfillment of

the requirements for the degree of

Doctor of Philosophy

(Chemistry)

at the

University of Wisconsin-Madison

2024

Date of final oral examination: 01/15/2024

The dissertation is approved by the following members of the Final Oral Committee:

Jennifer M. Schomaker, Professor, Chemistry (Organic)

Daniel J. Weix, Professor, Chemistry (Organic)

John F. Berry, Professor, Chemistry (Inorganic)

Andrew R. Buller, Assistant Professor, Chemistry (Chemical Biology)

Abstract

Nitrene transfer (NT) is a convenient strategy to directly transform C–H bonds into more valuable C–N bonds. Intramolecular NT reactions offer access to various *N*-heterocycles which are common in drugs and natural products. Many of these heterocycles can also be transformed into useful building blocks such as amino alcohols or diamines. However, the high reactivity of nitrenes often results in reactions that are primarily controlled by substrate identity, rendering these reactions less useful. This work will describe our attempts to use silver catalysts to control reactions with challenging selectivity problems such as asymmetric reactions and dearomatization reactions.

Chapter 1 features a broad look at the history of transition metal catalyzed NT, followed by a more in-depth discussion of intramolecular asymmetric NT variants. Chapter 2 describes the use of silver salts ligated to an unusual, quaternary-centered bis(oxazoline) (BOX) ligand, readily accessible through a modular synthetic approach, which enables site- and enantioselective nitrene transfers into benzylic, allylic and unactivated C–H bonds of carbamate esters. The resulting 1,3-aminoalcohol building blocks are delivered in good yields and moderate-to-excellent enantioselectivities. Computational models were employed to rationalize the observed stereochemical outcomes and set the stage for the predictive design of second-generation Ag-BOX catalysts. Chapter 3 presents a combination of silver-catalysts that are able to preferentially undergo either a dearomatization event to form bicyclic azepine structures or an insertion event into the benzylic C(sp^3)–H bond. This chemoselective reaction requires the use of carbamimidate precursors featuring a large sulfamate protecting group, which allows the reaction to be controlled by a combination of ligand sterics and electronics.

Acknowledgements

People who know me know that I often struggle to find the right words to say in the moment. Even when writing it often takes me a long time to find the exact way in which I want to say something, so I end up staring at my computer screen for many minutes before any words hit the page. I am hoping that with these acknowledgements and thanks, I can clearly get across how grateful I am to the many people who have helped me along the way, though I may never say it expressly in person.

I would like to start by recognizing my advisor, Professor Jennifer Schomaker, for all her help on this long Ph.D. process. From the beginning, Jen has been a fantastic example of the scientist that I hope someday I can emulate, excited and curious about chemistry, willing to learn new things, and one of the most hard-working people I know. I have grown so much as a researcher during my time here, and I know that Jen has had a big influence on how I have grown into the scientist I am now. I would also like to thank the other members of my committee, Professor Dan Weix, and Professor John Berry, who have been incredibly helpful not only in giving excellent suggestions for my research, but also challenging me to be an even better scientist. I also can't forget about Prof. Andrew Buller, who graciously agreed to sit on my final oral defense committee.

Scientifically, the other big thank you has to go out to all of my collaborators both in and outside of the Schomaker group. I have been very blessed to work with some excellent computational collaborators, Professor Peng Liu, and Yue Fu, who have strongly impacted how I think about silver-catalyst nitrene transfer. In part, it was their computational insights into the effects of nitrene precursors that led me to be interested in looking into ureas and carbamimidates. Also, without their computations, the asymmetric amination project (Chapter 2) would not have

been half as good as it ended up being. Other people that were instrumental in bringing about success on that project include Minsoo Ju, who was an excellent mentor and scientist; Wentan Liu, a brilliant and hardworking postdoc, who redesigned the synthesis of MinBOX; and Jed Kim, my first ever graduate student mentee who helped fill out the scope of the reaction. Together we spent a long time on this project, and I really think it has turned out well.

In the Schomaker group I have also had the pleasure of working with a different subset of people on the chemoselective project (Chapter 3). In particular, Yun (aka Bob) Hu has been a fantastic colleague to work with, consistently coming to the table with new and interesting ideas and in general being a great person to bounce ideas off of. I do not think the chemoselective project would have come into being without his partnership and early work on optimization of the reaction. I was joined on this work by Chenxi Lin, my second graduate student mentee who has focused on developing the diversification of these products, and Amory Griffin, a superstar undergrad who helped with a few of the substrates in the scope, both of whom have been great to work with and mentor over the past year and a half. Speaking of mentoring, shout out to all my undergrads, Grace, Jack, and Thomas, for teaching me as much as I hopefully taught them.

While I may not have worked directly with other Schomaker group members, such as Logan Vine and Kate Nicastri, these two formed and shaped my first foundational years in the group, and I am very grateful for their guidance, but also their friendship. Kate was and still is a superstar who was a fantastic example for me in the lab and as a person. Logan is an excellent mentor, friend, and dungeon master, and I miss our Sunday D&D sessions.

I would be remiss if I did not mention my friends from the department outside of my research group. We may have started as a random grouping of people that happened to meet on orientation, but my grad school trajectory would have been totally different had that random

meeting not occurred. I enjoyed every crazy get together we had in grad school, and I look forward to having more even though we are now spread across the country. In addition to just being great friends, I have to thank Bethany, Megan, Maggie, and Grace for being my homework partners during first-year classes. Grad school homework was actually fun when we were working together. Also, Megan and Grace were instrumental in keeping me sane during the COVID lockdowns, coming out for walks in the park when I would have otherwise been stuck alone in my apartment.

The last set of thanks is saved for my family. The first thank you goes to my husband, who has been so supportive during this whole process, though sometimes he may wish that I did not have to work quite so much. You are one of the main things that has kept me pushing towards this goal by making sure that I can still have fun when I am not in the lab. The second thank you goes to my dad, who is the best a girl can ask for. Having personal home assistant/chef during my whole life at home allowed me to excel and get where I am today. The final thank you goes to my mom, who showed me and told me that I could do whatever I wanted in life. I thank God everyday that I was raised by such a fantastic family.

Table of Contents

Abbreviations and Acronyms

Å	angstrom(s)
Ar	aryl
aq.	aqueous
bathophen	4,7-diphenyl-1,10-phenanthroline (bathophenanthroline)
BDE	bond dissociation energy
Bn	benzyl
BINAP	2,2′-bis(diphenylphosphino)-1,1′-binaphthalene
BOX	bis(oxazoline)
C	Celsius
CDI	carbonyl-diimidazole
Cp	cyclopentadienyl
d	doublet
DCM	dichloromethane
dd	doublet of doublets
ddd	doublet of doublet of doublets
dddd	doublet of doublet of doublet of doublets
ddt	doublet of doublet of triplets
DFT	density functional theory
dmbox	dimethyl bis(oxazoline)
DMF	dimethyl formamide
dp	doublet of pentets
dpen	1,2-diphenyl-1,2-ethylenediamine

dq	doublet of quartets
dqd	doublet of quartet of doublets
dqt	doublet of quartet of triplets
dr	diastereomeric ratio
dt	doublet of triplets
dtd	doublet of triplet of doublets
ee	enantiomeric excess
equiv	equivalent(s)
er	enantiomeric ratio
ESI	electrospray ionization
esp	α,α,α',α'-tetramethyl-1,3-benzenedipropionic acid
Et	ethyl
Et_2O	diethyl ether
EtOAc	ethyl acetate
g	gram(s)
h	hour(s) or heptet
HAT	hydrogen atom transfer
Hex	hexane
HPLC	high-performance liquid chromatography
HRMS	high resolution mass spectrometry
HTE	high throughput experimentation
iPr	*iso*-propyl
iPrOH	*iso*-propyl alchol

J	spin-spin coupling in hertz
L or L_n	ligand
m	meta
M	molar or metal
m	multiplet
Me	methyl
MeCN	acetonitrile
MeOH	methanol
mg	milligram(s)
MHz	megahertz
min	minute(s)
MinBOX	(4S,4'S)-2,2'-(propane-2,2-diyl)bis(4-(3,5-di-tert-butylphenyl)-4-methyl-4,5-dihydrooxazole)
mL	milliliter(s)
mM	millimolar
mmol	millimole
MS	molecular sieves
NCI	non-covalent interaction
NHC	*N*-heterocyclic carbene
nm	nanometers
NMR	nuclear magnetic resonance
NT	nitrene transfer
NTf_2	bis(trifluoromethanesulfyl)imide

o	ortho
OAc	acetate
OMe	methoxy
OTf	trifluoromethanesulfonate
p	para
Pc	phthalocyanine
PG	protecting group
Ph	phenyl
phen	1,10-phenanthroline
PhIO	iodosobenzene
Por	porphyrin
Py	pyridine
q	quartet
qd	quartet of doublets
qdd	quartet of doublet of doublets
quant.	quantitative
rt	room temperature
s	singlet
t	triplet
td	triplet of doublets
tdd	triplet of doublet of doublets
Tp	trispyrazolylborate
tpa	tris(pyridin-2-ylmethyl)amine

tpy	terpyridine
Tol	toluene
tt	triplet of triplets
tq	triplet of quartets
tBu	*tert*-butyl
Tces	trichloroethylsulfamate
THF	tetrahydrofuran
TLC	thin layer chromatography
TS	transition state
Ts	toluenesulfonyl
TPP	tetraphenyl-porphyrin
δ	chemical shift in ppm
WenBOX	(4S,4'S)-2,2'-(propane-2,2-diyl)bis(4-(3,5-di-phenylphenyl)-4-methyl-4,5-dihydrooxazole)

List of Figures

List of Schemes

List of Tables

Chapter 1. *Introduction to transition metal-catalyzed nitrene transfer*

Portions of the chapter have been published and reprinted with permission from:

Vine, L. E.*; **Zerull, E. E.***; Schomaker, J. M. Taming Nitrene Reactivity with Silver Catalysts. *Synlett* **2021**, *32*, 30–44.

Zerull, E.; Trinh, T. A.; Kim, J.; Schomaker, J. M. C–H Functionalization via Asymmetric Nitrene Transfer. In *Handbook of CH-Functionalization*; Wiley, 2022; pp 1–41.

*Indicates equal authorship.

1.1. Introduction

The presence and importance of nitrogen in natural products, bioactive molecules, pharmaceuticals, polymers, and catalyst ligands has stimulated the development of a diverse array of methods to introduce C–N bonds into readily available starting materials. One attractive strategy is nitrene transfer (NT), which involves the addition of a reactive, electron-deficient nitrogen species, typically supported by a transition metal, to an alkene (aziridination) or into a C–H bond (C–H amination). This class of reactions has been of intense interest in recent years, given that the ability to transform C–H bonds directly into new C–N bonds can streamline the syntheses of many useful compounds and synthetic building blocks.[1] From an academic perspective, the diversity of transition metals that support reactive nitrene species makes the study of NT a rich opportunity to better understand the fundamental details of how electronic structure coupled with ligand design impacts reactivity and selectivity.

Current strategies for NT can be divided into two main approaches: biocatalysis and chemocatalysis. The former takes advantage of specialized enzymes that are capable of selectively oxidizing a specific C–H bond from amongst many candidates. Several research groups, most notably the Arnold group, have developed ways manipulate enzymes to catalyze C–H functionalization reactions beyond the scope of their original purpose, including the direct amination of C–H bonds.[2] Despite the high selectivities and turnover numbers associated with biocatalysis, not all laboratories have the infrastructure or expertise to carry out directed evolution. Substrate scope can also be limited, due to the need to utilize solvent systems compatible with enzymes. Additionally, enzymes are often co-factor dependent and may be inactivated by higher temperatures, extreme pH, high salt concentrations, and polar organic solvents.[3]

While biocatalysis is an excellent choice for optimizing manufacturing routes to commercial drugs and agrochemicals, the early-stage exploration and late-stage functionalization of complex molecules benefit from chemocatalyzed NT. Several broadly accessible and highly modular catalyst systems have been developed to enable expedient reaction screening; in fact, over 10 different transition metals are known to promote NT reactions, with Rh, Ru, Ir, Fe, Mn, Co, Cu, and Ag among the more extensively researched (Figure 1.1).[4] NT transfer reactions are surprisingly robust, despite the intermediacy of a highly reactive nitrene species, and are often insensitive to atmospheric air and water.

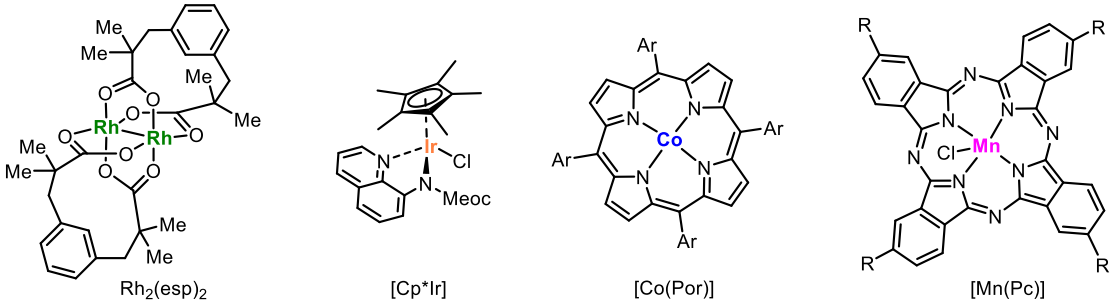

Figure 1.1 – Representative examples of efficient transition metal catalysts for NT.

1.2. Brief summary of chemocatalyzed nitrene transfer

The chemistry of metallonitrenes has a long history, going back to Kwart and Khan's first description of the copper-catalyzed decomposition of benzosulfonyl azides in 1967.[5] In that report, Kwart and Khan proposed the intermediacy of a copper-nitrene species capable of promoting either an alkene aziridination or a C–H insertion process. However, it was not until several years later that Breslow employed catalytic Mn(III)(TPP), Fe(III)(TPP), and $Rh_2(OAc)_4$, in combination with an iminoiodinane nitrogen source, to promote intramolecular C–H amination. Importantly, this work led to a model system for analogous transformations of C–H to C-O bonds performed by the cytochrome P-450 class of enzymes.[6] In the early 1990's, Evans[7]

and Jacobsen[8] expanded on Breslow's initial findings and reported a series of Cu catalysts, supported by bis(oxazoline) (BOX) and salen-type ligands, to promote asymmetric aziridination, albeit with limited scope.

Over the past 20 years, the development of improved NT catalysts has continued unabated. For example, Breslow's initial reports inspired the design of more efficient dinuclear Rh(II) catalysts. Beginning in early 2000's, Du Bois reported a series of Rh_2L_n complexes, commonly referred to as "paddle-wheel" complexes, supported by carboxylate bridging ligands that achieved efficient NT with excellent functional group tolerance.[9] Du Bois' $Rh_2(esp)_2$ (Figure 1.1)[9c] catalyst is particularly powerful for intra- and intermolecular NT with various nitrene precursors and displays excellent utility for the late-stage functionalization of complex molecules.[9h] The Dauban group has described the use of chiral sulfonimidamide nitrene precursors with Rh catalysts to achieve diastereoselective intermolecular C–H amination.[10] Other less expensive precious metals such as Ru and Os have also been well reported as NT catalysts, with Ru in particular showcasing a wide array of available ligand structures ranging from porphyrins and paddle-wheels to PyBOXs and half-sandwiches.[11] NT catalysts based on the first-row transition metals Co, Fe and Mn, are typically supported by ligands that include modified porphyrins, phthalocyanines and other porphyrin mimics,[12] while Cu is utilized with a wide variety of supporting ligand such as bis(oxazolines), diimines, and scorpionates.[13] Of particular note are Co catalysts developed by Zhang, which include several asymmetric versions with chiral extensions off the porphyrin scaffold to enable enantioselective NT.[14]

Recently, the Chang group described a series of Ir catalysts that harness non-covalent interactions to direct both racemic and enantioselective syntheses of γ-lactams from dioxazolones. This innovative strategy circumvents the detrimental Curtius rearrangement that

typically precludes the use of amide derivatives as suitable nitrene precursors.[15] A waterfall of subsequent reports on this relatively new nitrene precursor have resulted in a great expansion of the types of products that NT reactions can easily access.[16] In fact, there are as many nitrene precursors as there are different metals that are able to catalyze reactions, the combinations of which each of which come with specific benefits and challenges (Figure 1.2).

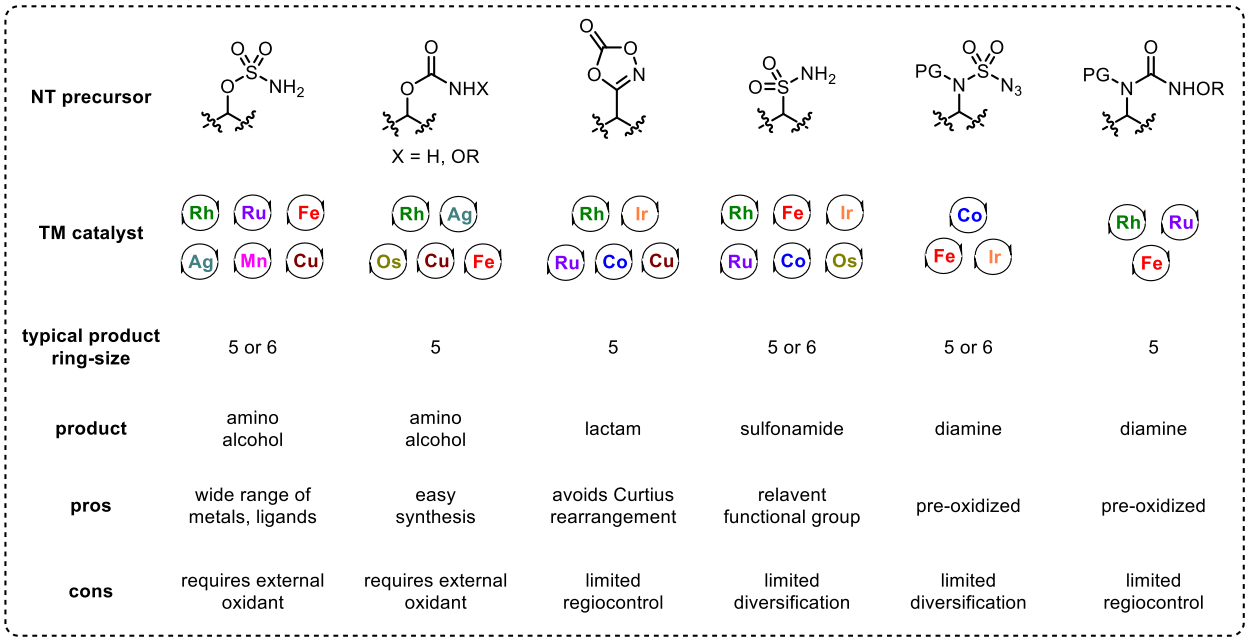

Figure 1.2 – Examples and features of common intramolecular NT precursors.

1.3. Challenges in reactivity and selectivity in nitrene transfer reactions

The relative strength of the C–H bond, compared to other common functional groups, renders it inert to many traditional organic transformations. While extensive research over the past decade has yielded several strategies for C–H bond functionalization, NT remains one of the most efficient methods to directly transform unactivated C–H bonds into new C-N bonds. NT employs a neutral, six-electron nitrogen species (nitrene) that can exist in either a singlet (where the four valence electrons are paired) or triplet (where there are two unpaired electrons) form. Free nitrenes are generated via thermolysis or photolysis of various precursors, typically

azides;[17] however, the extreme reactivity of the free nitrene, coupled with the harsh conditions under which these species are generated, often lead to poorly selective reactions and mixtures of products.

The generation of metal-supported nitrenes offers an attractive alternative method to generate electron deficient nitrenes for C–H functionalization. Along with more controlled reactivity, these species are generated from accessible nitrogen precursors such as carbamates, sulfamates, and sulfonamides. The precursor is treated with a hypervalent iodine oxidant to generate an intermediate imidoiodinane, which is transferred to the metal to form the reactive aminating species (Scheme 1.1). Pre-oxidized nitrenes have also been exploited to generate the metal nitrene species without the need for a hypervalent iodine oxidant.[18] While metal-stabilized nitrenes have been successfully used to limit side reactions and decomposition pathways, the amination of strong secondary and primary aliphatic C–H bonds sites remain challenging.[19]

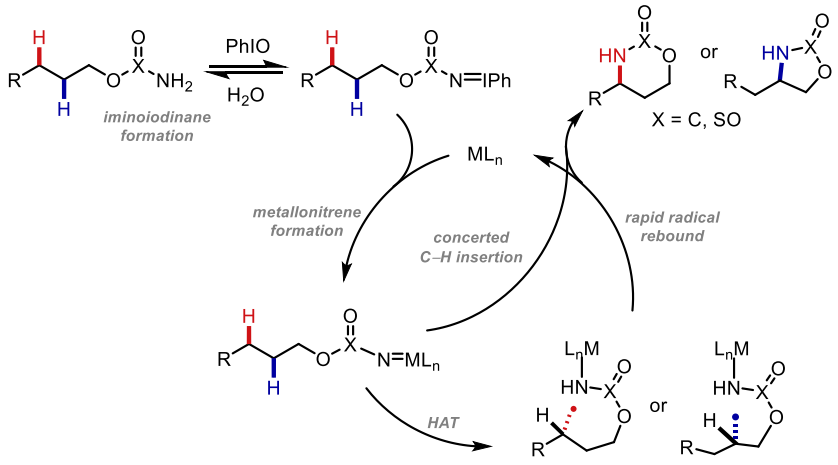

Scheme 1.1 – General catalytic cycle for chemocatalyzed NT.

In addition to meeting the reactivity challenge for C–H bond amination, achieving predictable control over selectivity with broad substrate scope remains the predominant challenge in NT. While certain types of selectivity can be accomplished using particular

catalyst/substrate combinations, the use of one metal to achieve tunable nitrene transfer by altering the ligand is rare, especially when it is desirable to override substrate control.

An exciting opportunity in NT involves identifying strategies to achieve the ultimate goal of tunable catalyst control over chemo-, site-, and stereoselectivity when multiple potential reactive sites are present. Often, site-selectivity is accomplished through substrate control, where potential C–H bonds are differentiated in terms of their reactivity. Substrate parameters that control reactivity include BDE, type of bond (1°, allylic, 2°, benzylic, etc.), and the surrounding steric environment. For example, intramolecular C–H amination of carbamates will typically prefer formation of the 5-membered oxazolidinone ring when the strength of the two competing C–H bonds are the same (Scheme 1.2).[20] However, selectivity is significantly reduced when the C–H bond at the typically unfavored position becomes activated. When the catalyst cannot control the inherent preferences of the substrate, the application of said catalyst is much more limited. On the other hand, catalyst-controlled nitrene transfer, where the metal and its supporting ligands bear primary responsibility for dictating the specific site of amination, is a far more versatile strategy. Ideally, it permits flexible installation of new C–N bonds at diverse C–H bonds in a readily tunable manner. Catalyst features that can control selectivity include the metal, the steric or electronic features of the ligands, the counter anion, and the metal-to-ligand ratio.

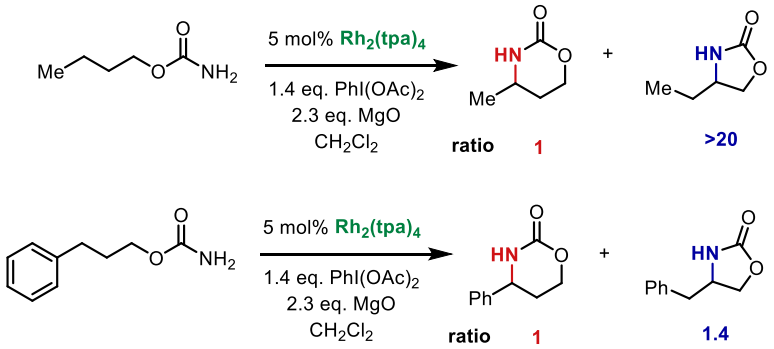

Scheme 1.2 – Example of the influence of substrate-controlled NT on selectivity.

1.4. History of silver-catalyzed nitrene transfer

Two unique features of silver coordination complexes stand out when compared to typical NT catalysts: the diversity of simple *N*-dentate ligands able to support Ag(I) complexes and their dynamic behavior in solution. Both of these features correspond to excellent opportunities to control the NT event using catalyst control. The former characteristic is exemplified by the early reports of silver-catalyzed nitrene transfer published by the He group in 2003.[21] $AgNO_3$ supported by a tBu_3tpy (4,4',4'',-tri-tert-butyl-2,2':6',2''-terpyridine) ligand was proposed to form a dinuclear silver (I) complex that catalyzed intermolecular alkene aziridination (Figure 1.3). A later publication from the same group employed a silver catalyst supported by bathophenanthroline to achieve intramolecular aminations of tertiary and benzylic C–H bonds.[22]

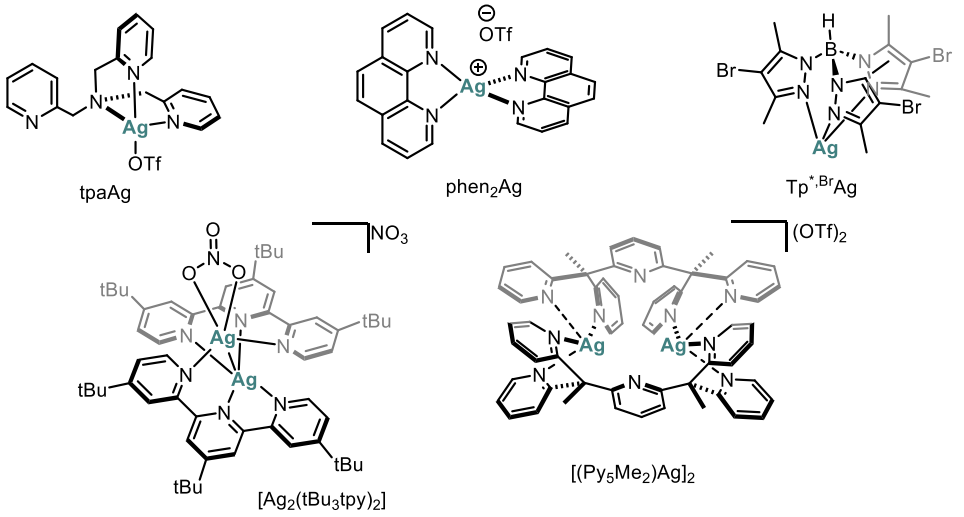

Figure 1.3 – Examples of the varied ligand scaffolds supported by silver salts.

Notably, in both reports, characterization of the silver complex was made through elucidation of the crystal structure. However, efforts made by our group to understand Ag(I) complexes in both the solid- and solution-state have shown that silver complexes in solution often times are under equilibrium, illustrating the second characteristic of Ag(I) complexes. For

example, with (*o*-Me)$_3$tpaAgOTf, the solid-state structure is a dicationic dimer with a five-coordinate geometry at each of the two silver atoms; however, further investigation revealed an equilibrium between monomeric and dimeric structures, as well as rapid exchange of ligands on and off the metal center (Scheme 1.3).[23]

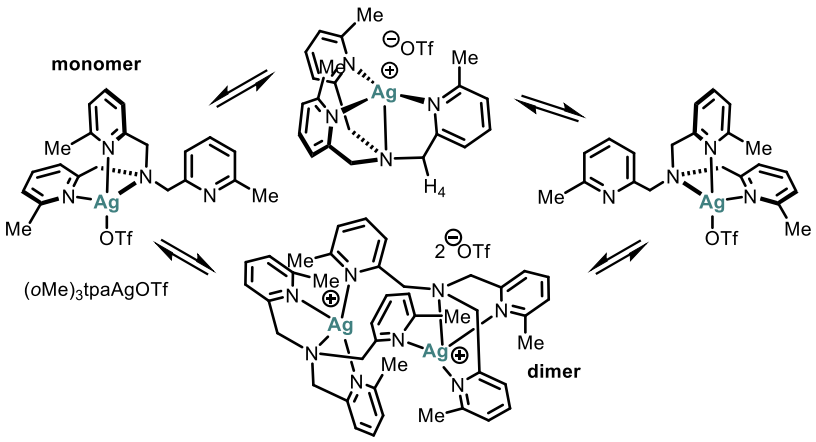

Scheme 1.3 – Solution-state behavior of (*o*-Me)$_3$tpaAgOTf.

Our group has focused on developing and understanding Ag-complexes that achieve catalyst-controlled selectivity for many different types of selectivity challenges. Beginning in 2013, the group has shown that by simply modifying the ligand-to-metal ratio, we can alter the chemoselectivity from aziridine formation at a 1:1 ratio to C–H insertion at a 2:1 ratio (Scheme 1.4a).[24] This difference in ratio leads to an alteration in coordination environment, where the less sterically hindered coordination geometry promotes aziridination and the more sterically demanding coordination environment promotes C–H insertion. The group went on to design a system that could select for either the tertiary aliphatic site or the benzylic site in a molecule. This selectivity is governed by favorable π-π interactions between one of pyridine rings on the ligand and the aryl group on the substrate (Scheme 1.4b).[25] When those π-π interactions are lacking, the selectivity flips to favor tertiary amination. More recently, the group has shown that

by changing the steric environment of the catalyst, we can also change the selectivity for either the β or the γ C-H bond (Scheme 1.4c).[20]

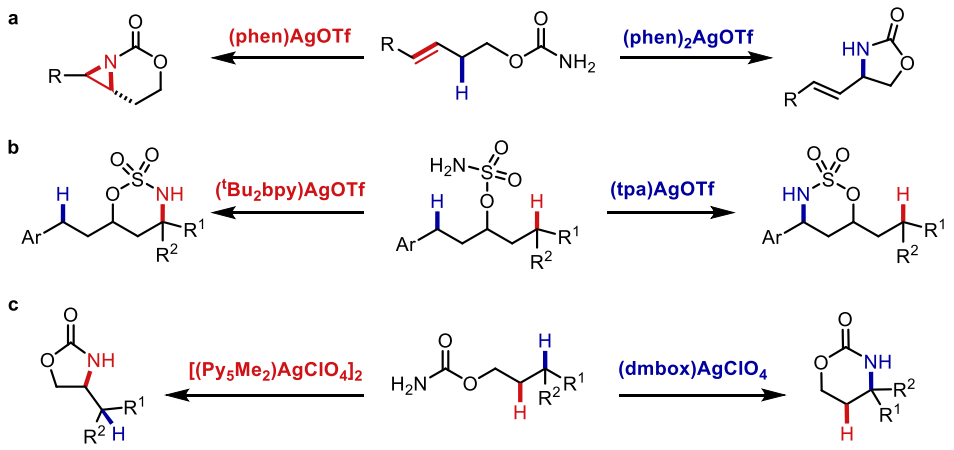

Scheme 1.4 – Tunable, Ag-catalyzed NT. (a) Chemoselective NT controlled by metal-to-ligand ratio. (b) Site-selective NT controlled by NCIs. (c) Site-selective NT controlled by ligand sterics.

Other groups have also published the area of silver-catalyzed NT, with a focus on intermolecular applications. In 2013, Peréz reported sulfonimidamide nitrene precursors and Ag(I) supported by trispyrazolylborate (Tp) scorpionate ligands for intermolecular aminations of benzylic and alkyl C–H bonds.[26] Peréz later published a mechanistic study investigating this catalyst scaffold in aziridination; the concerted mechanism was deemed unlikely, due to a computationally predicted lower energy pathway involving a triplet silver nitrene intermediate.[27] More recently, the Bach group designed an asymmetric nitrene transfer method that relies on hydrogen bonding interactions between a chiral phenanthroline-based silver catalyst and a pyridone directing group built into the substrate.[28]

1.5. Intramolecular asymmetric C–H bond amination via nitrene transfer

The past few decades have seen tremendous interest and growth in the development of catalysts for asymmetric C–H bond amination via NT. Progress has been driven by the desire to

efficiently upgrade hydrocarbons to valuable amine building blocks, as well as apply these methods to tunable, late-stage functionalizations of complex molecules. This section will focus on intramolecular examples of asymmetric C–H amination using transition metal catalysts.

1.5.1. Rhodium-catalyzed intramolecular asymmetric NT

The first account of enantioinduction in C–H amination using a dirhodium(II) catalyst featured an axially chiral binaphthyl phosphate ligand instead of a carboxylate ligand;[29] however, the more modular synthesis of the latter scaffold has yielded the most relevant advances. The chiral tetracarboxylate and tetracarboxamidate ligands used in Rh-catalyzed NT generally follow similar structural patterns, with a bulky chiral center adjacent to the carboxylate or carboxamidate group.

The high reactivity of Rh catalysts has resulted in a significant focus on challenging asymmetric intermolecular NT reactions. However, there are scattered examples of asymmetric intramolecular C–H amination reactions. Du Bois reported a chiral dirhodium tetracarboxamidate Rh_2(*S*-NAP)$_4$ complex was an effective catalyst for intramolecular C–H insertion employing aryl sulfamate precursors (Scheme 1.5a).[30] The donating nature of the carboxamide group was proposed to more effectively stabilize the nitrene-catalyst complex as compared to carboxylate groups, while installation of the proximal sulfonamide group curtailed competing Rh oxidation. This chemistry is compatible with benzylic C–H bonds and furnishes benzylic amines with *ee* values up to 99%, but the catalyst also shows improved chemoselectivity for insertion over aziridination in homoallyl sulfamates. Enantioselectivities for insertions into allylic C–H bonds are generally modest, but it is notable that the *ee* for *cis* alkenes is significantly higher than for *trans*- or mono-substituted substrates (Scheme 1.5b).

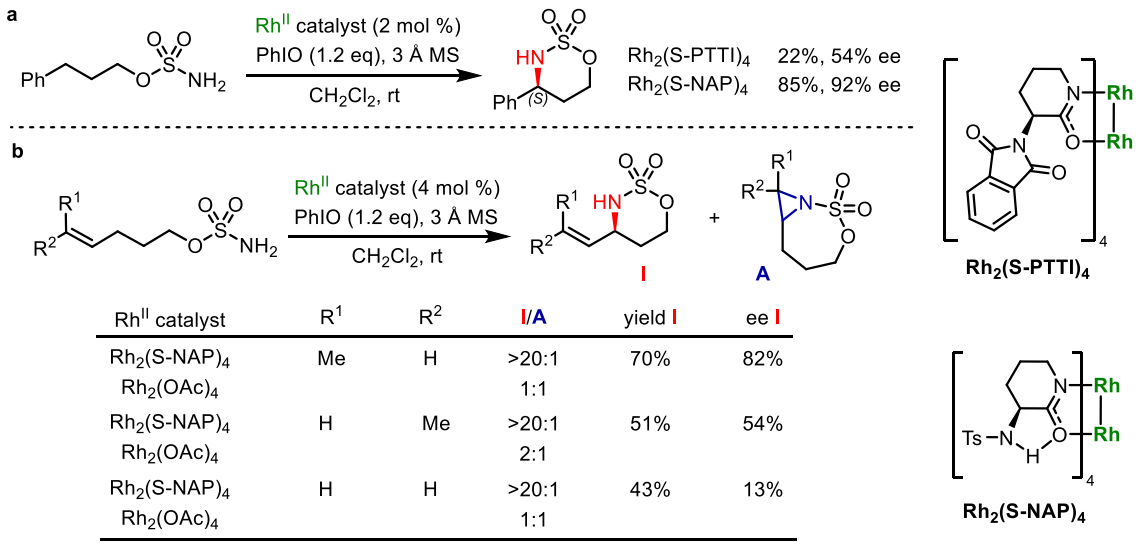

Rh^{II} catalyst	R^1	R^2	I/A	yield I	ee I
Rh_2(S-NAP)$_4$	Me	H	>20:1	70%	82%
$Rh_2(OAc)_4$			1:1		
Rh_2(S-NAP)$_4$	H	Me	>20:1	51%	54%
$Rh_2(OAc)_4$			2:1		
Rh_2(S-NAP)$_4$	H	H	>20:1	43%	13%
$Rh_2(OAc)_4$			1:1		

Scheme 1.5 – (a) Intramolecular NT catalyzed by rhodium tetracarboxamidates. (b) Chemoselectivity of carboamidate catalysts.

Reddy and Davies also reported a dirhodium tetracarboxylate, Rh_2(*S*-TCPTAD)$_4$ complex capable of both intra- and intermolecular asymmetric C–H amination.[31] The catalyst shows moderate *ee* for benzylic, allylic, and unactivated C–H bonds when *N*-tosyloxycarbamates are employed as precursors in intramolecular NT (Table 1.1).

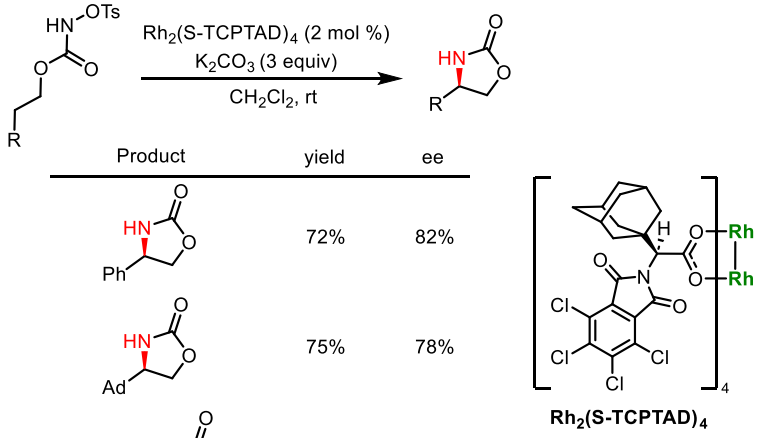

Product	yield	ee
Ph	72%	82%
Ad	75%	78%
Ph	62%	79%

Table 1.1 – Scope of intramolecular C–H amination with *N*-tosyloxycarbamates.

1.5.2. Cobalt-catalyzed intramolecular asymmetric NT

The majority of cobalt NT catalysts have been developed by Zhang and coworkers. In particular, they have specialized in a family of D_2-symmetric chiral porphyrin ligands that are highly effective at controlling the reactivity and enantioselectivity of NT. The radical nature of Co(II) enables the formation of reactive metal-nitrene intermediates from organic azides via homolytic activation, accompanied by the elimination of dinitrogen.[12c] Thus, the use of external oxidants and the generation of toxic byproducts associated with many common nitrene precursors are circumvented. In addition, the steric and electronic properties of the chiral ligands are highly tunable without interfering with the primary coordination sphere, owing to the modularity of porphyrin substituents.

The first example of cobalt-catalyzed enantioselective C–H amination was reported in 2018.[14a] Starting from sulfamoyl azides, an intramolecular, radical-based amination process afforded six-membered cyclic sulfamides via 1,6-C–H activation (Table 1.2). Catalyst screening revealed that both the chiral amide arms and the achiral aryl substituents of the D_2-symmetric porphyrin ligand had remarkable effects on reactivity and enantioselectivity. The optimal catalyst [Co(**P1.1**)] containing bulky substituents on the cyclopropane units, led to high yields and *ee* of various sulfamoyl azides. Intramolecular allylic and propargylic C–H activation furnished the desired sulfamides without chemoselectivity issues potentially arising from radical additions to the C=C and C≡C bonds. In addition, this Co-based catalytic platform proved highly efficient and selective in aminating nonactivated and electron-deficient C–H bonds adjacent to carbonyl functionalities, which are typically less reactive towards NT with other metal catalysts.

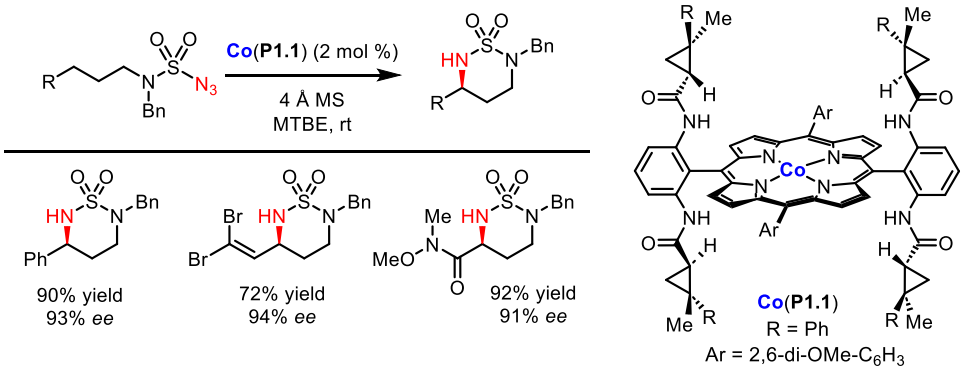

Table 1.2 – Enantioselective intramolecular C–H amination with [Co(Por*)].

In a subsequent publication, Zhang reported asymmetric 1,5-C–H amination reactions that afford five-membered cyclic sulfonamides from aryl- and alkylsulfonyl azides (Scheme 1.6).[14c] The reaction with arylsulfonyl azides in chloroform was catalyzed by [Co(**P1.2**)], whose chiral amide arms were rigidified by intramolecular hydrogen bonding upon replacing the usual cyclopropane rings with tetrahydrofuran units. Benzofused sulfonamides bearing diverse electron-donating and electron-withdrawing substituents could be obtained in up to 99% yield and 93% *ee*. For alkylsulfonyl azides, [Co(**P1.3**)] proved to be an excellent catalyst that efficiently gave the corresponding 5-membered cyclic sulfonamide in high *ee* (92% yield, 94% *ee*). The 1,5-amination products were still obtained as major regioisomers in the presence of competitive 1,6- and 1,7-pathways, albeit in diminished yields and *ee*.

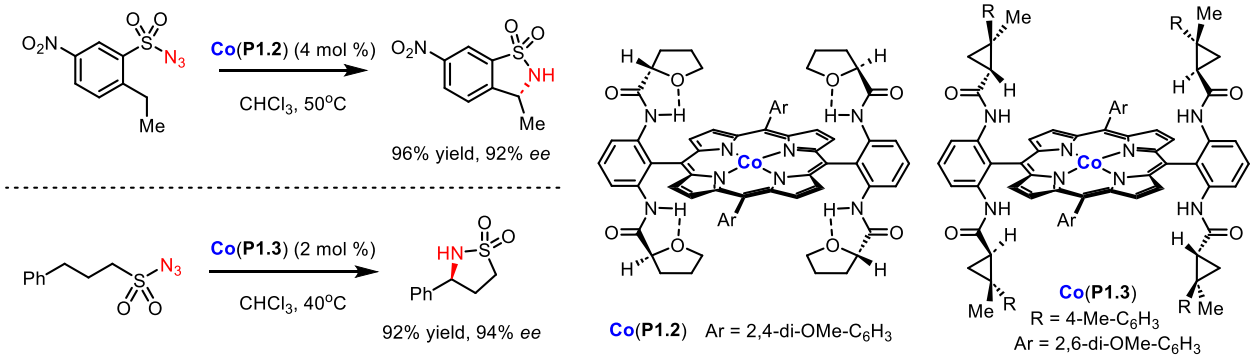

Scheme 1.6 – Enantioselective intramolecular C–H amination of sulfonamides.

Prior to his forays into enantioselective C–H amination, Zhang had introduced another class of cobalt-porphyrin complexes that featured an alkyl chain bridging two opposite cyclopropanecarboxamide arms on each face of porphyrin.[32] This catalyst design resulted in a cavity whose steric environment could be modulated by varying the bridge length and the aryl substituents of porphyrin to dictate both the sense and level of enantioselectivity of C–H amination. As a result, the enantiodivergent formation of several five-membered cyclic sulfamides could be achieved without the need for opposite enantiomers of the chiral catalyst.[14b] Instead, subjecting sulfamoyl azides to 1,5-amination with [Co(**P1.4**)] and [Co(**P1.5**)] yielded (R)-products (up to 98% *ee*) and (S)-products (up to 92% *ee*), respectively (Scheme 1.7).

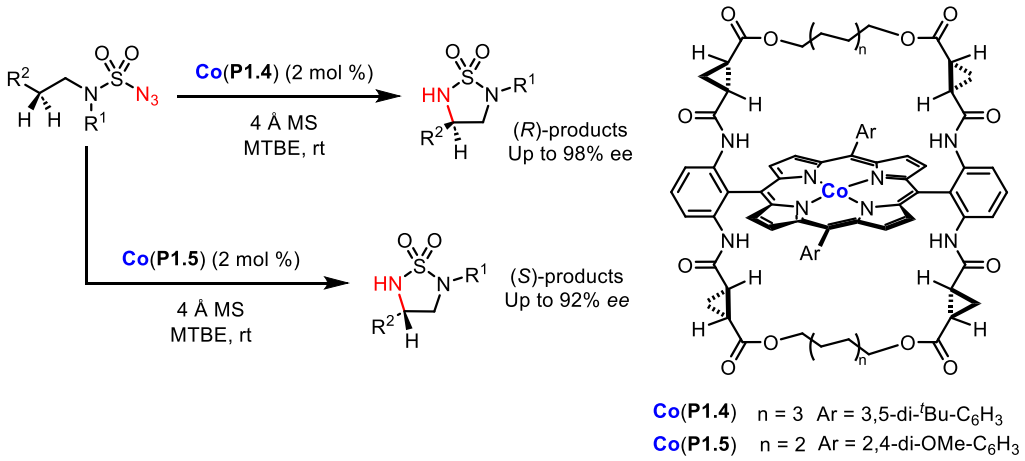

Scheme 1.7 – Enantiodivergent, intramolecular C–H amination with [Co(Por*)].

A major challenge in NT is the stereoselective amination of tertiary C–H bonds, as ablation of the original stereochemical information at such C–H bonds remains elusive. This is largely due to the tendency of NT to proceed through either a concerted mechanism, which retains the stereochemistry, or a stepwise process where the enantiodetermining HAA is followed by barrierless radical recombination to result in either complete or partial stereoretention.[33] The asymmetric installation of a quaternary nitrogen-containing center via catalyst control requires a

pathway for racemization of the starting material to furnish a long-lived, planar carbon radical (Scheme 1.8a). Recently, Zhang explored this new mode of stereoinduction with existing [Co(Por)] designs and discovered a surprising temperature-enantioselectivity relationship dictating the racemization and enantioconvergence of the Co(III)-alkyl radical intermediate.[34] Experiments revealed an optimal temperature of 50 °C, an intermediate point that balanced the requirement for facile interconversion between the two prochiral faces of the radical intermediate and the need for high enantiodifferentiation in the subsequent RS. Starting from racemic mixtures of chiral alkyl sulfamoyl azides, the optimal conditions using catalyst [Co(**P1.1**)] strongly favored the formation of one enantiomer of cyclic sulfamide products in up to 86% ee.

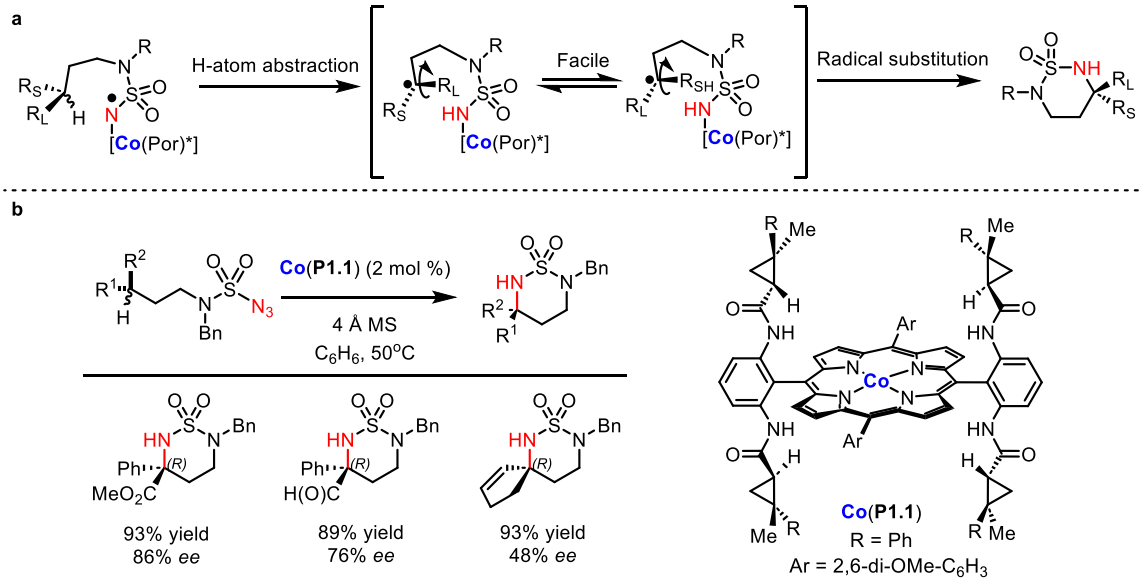

Scheme 1.8 – Enantioconvergent, intramolecular C–H amination of sulfonyl azides. (a) Proposed mechanistic design. (b) Select scope with [Co(Por*)].

1.5.3. Ruthenium, iridium and osmium-catalyzed intramolecular asymmetric NT

Ruthenium, iridium, and osmium complexes are highly valued for their resistance towards oxidative degradation, as well as their ability to support diverse ligands that promote nitrene transfer reactions. In addition, ruthenium and osmium are much less expensive when

compared to noble metals such as Rh and Ir. These attractive features have stimulated extensive efforts to explore the use of Ru, Ir and Os as potential chiral catalysts for nitrene transfer.

The Che group has extensively studied Ru catalysts supported by chiral porphyrin-based ligands to carry out asymmetric C–H bond amination (Table 1.3). Specifically, a series of sulfamate esters underwent intramolecular nitrene transfer using $PhI(OAc)_2$ in the presence of Ru(**L1.1**) to furnish the cyclic sulfamidates in *ee* in up to 82%.[11a]

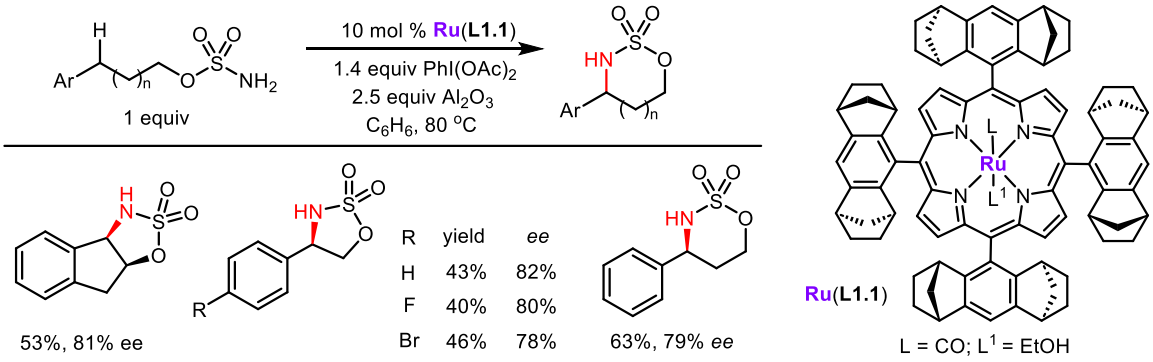

Table 1.3 – Porphyrin-supported ruthenium catalysts for enantioselective C–H amination.

In 2019, the Yu group reported Ru-catalyzed enantioselective cyclizations of 1,4,2-dioxazol-5-ones to deliver γ-lactams in up to 97% yield and 98% *ee* (Table 1.4). Chiral diphenylethylene diamine (dpen) ligands with electron-withdrawing arylsulfonyl groups gave highly chemo- and enantioselective nitrene transfer into a variety of C–H bonds, while suppressing undesirable Curtius-type rearrangement.[35]

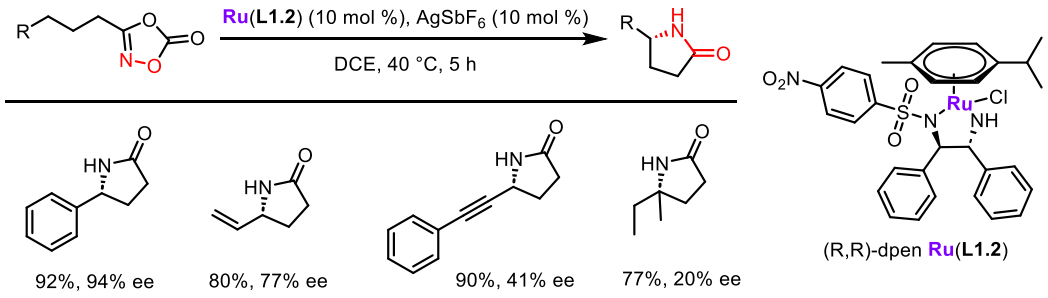

Table 1.4 – Selected scope for enantioselective C-H amination by a ruthenium-dpen catalyst.

Dinuclear metal complexes supported by bridging carboxylate or carboxamidate ligands, have been explored in a variety of transformations. For asymmetric NT, rhodium-based paddlewheel complexes are the most well-studied, due to their stability and high reactivity. In 2011, Du Bois and coworkers showed that achiral tetracarboxylate- and tetraamidate-supported diruthenium(II,III) catalysts are also suitable nitrene transfer catalysts, due to their high oxidation potentials.[9e] However, Du Bois did not investigate the use of chiral ligands to promote asymmetric NT. The Matsunaga group later built on these initial findings and reported a unique diruthenium paddle-wheel complex that successfully promoted asymmetric NT of sulfamates at benzylic C-H bonds in yields ranging from 72-84% and in high *ee* of 91-95% (Table 1.5).[36]

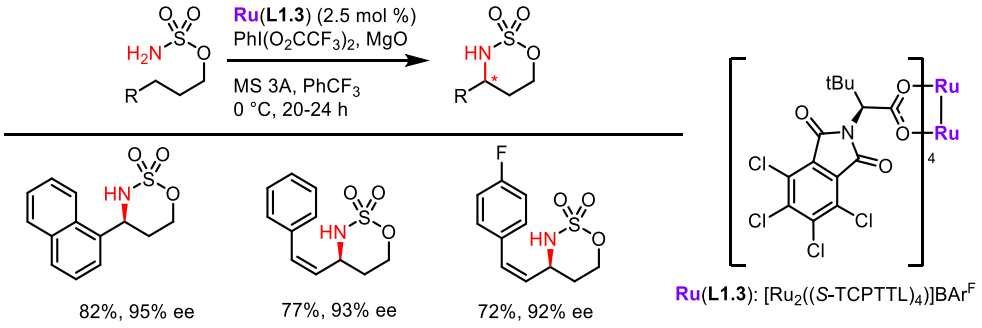

Table 1.5 – Select scope for enantioselective C-H amination with a diruthenium paddle-wheel.

C$_2$-symmetric bis(oxazoline) (BOX) ligands are one of the most widely utilized chiral ligand classes in the field of metal-catalyzed asymmetric synthesis for their ease of synthesis, modularity, and demonstrated ability to induce high levels of enantioselectivity in diverse transformations. In 2008, Blakey reported that a Ru catalyst supported by a pyBOX ligand could transform a variety of sulfamate nitrene precursors to benzylic amines in yields ranging from 42-71% and in good *ee* of 75-92% (Table 1.6).[11d] They proposed that the selectivity of this reaction arose from unfavorable steric interactions between the phenyl group and the pyBOX ligand.

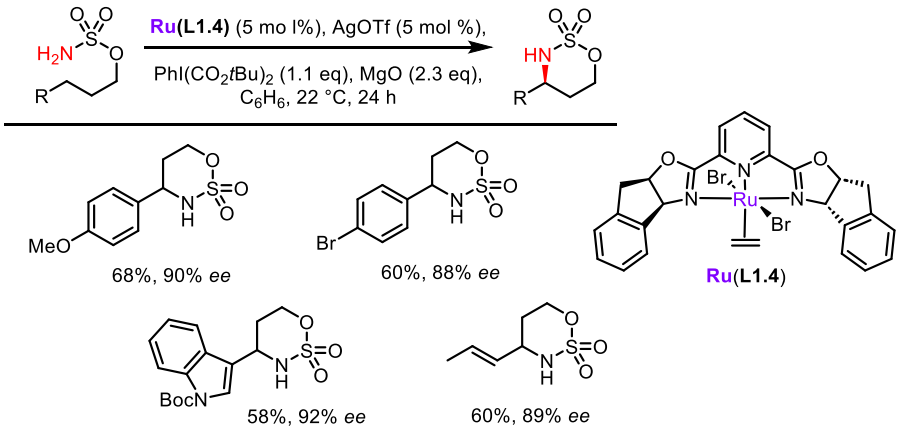

Table 1.6 – Selected scope for enantioselective C-H amination by Ru(**L1.4**).

In 2018, the Meggers group expanded upon Blakey's work with a new catalyst that gave both higher yields and *ee* using sulfonylazides (99% yield, 90% *ee*)[11e] and sulfamoyl azides (55-94% yields, 90-96% *ee*) as nitrene precursors (Table 1.7).[37] In addition to alternating the identity of the 'arms' of the PyBOX ligand, Meggers utilized an additional NHC-type ligand to control the electronics of the Ru metal center. Increasing the sterics of the catalyst arms off of the BOX ligand from H to isopropyl to phenyl groups increased yields and *ee*.

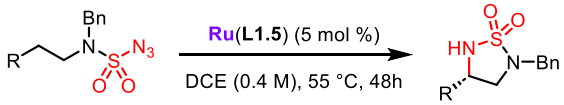

R group	yield	*ee*
	99%	95% *ee*
	93%	96% *ee*
	98%	68% *ee*
	76%	77% *ee*

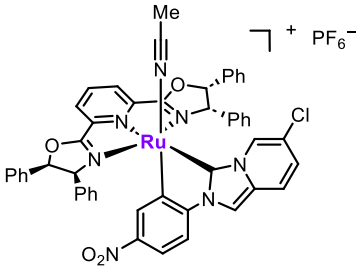

Table 1.7 – Selected scope for enantioselective C-H amination with Ru(**L1.5**).

Typical design strategies for chiral catalysts employ a chiral supporting ligand for the metal to achieve enantioselective transformations. Recently, a new class of "chiral-at-metal" catalysts have been introduced by Meggers and his colleagues. These catalysts contain either Ru and Os as the central metal and utilize achiral *N*-heterocyclic carbene (NHC) and pyridine-derived ligands to furnish either an absolute Λ or Δ stereogenic center (Figure 1.4).[11f] This unusual approach towards the preparation of asymmetric catalysts opens up new strategies for carrying out enantioselective C–H aminations through nitrene transfer.

Meggers demonstrated that this 'chiral-at-metal' strategy can induce enantioselective benzylic C–H aminations to furnish pyrrolidines (76–99% *ee*),[38] 2-imidazolidinones (up to 95% *ee*),[39] and 4-imidazolidinones (up to 99% *ee*). The first of their catalysts to show promise were Ru(**L1.6**) and Ru(**L1.7**), where the R group at the 3-position of the pyridine was varied to optimize the sterics of the catalyst for optimal *ee* and good yields in NT. A similar osmium catalyst (Os(**L1.1**)) showed improved reactivity over a ruthenium variant with sulfonyl azides and azidoformates as nitrene precursors.[11g]

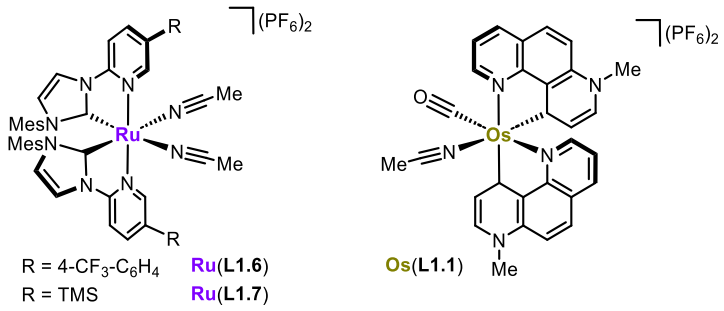

Figure 1.4 – Chiral-at-metal ruthenium and osmium metal complexes.

After developing ruthenium-salen catalysts for intermolecular C–H amination, Katsuki and coworkers went on to employ similar ligands with iridium to explore how the metal identity impacts the reactivity of the metallonitrene. A new Ir^{III}-salen complex Ir(**L1.1**) was developed

for the efficient synthesis of benzosultams via a regio- and enantioselective benzylic C–H bond amination (Table 1.8).[40] Selective activation of 2-ethylbenzenesulfonyl azides at the benzylic position gave 5-membered sultams in high *ee*. However, when the length of the pendant alkyl chain was extended to be longer than an ethyl group, 6-membered sultams could be formed preferentially.

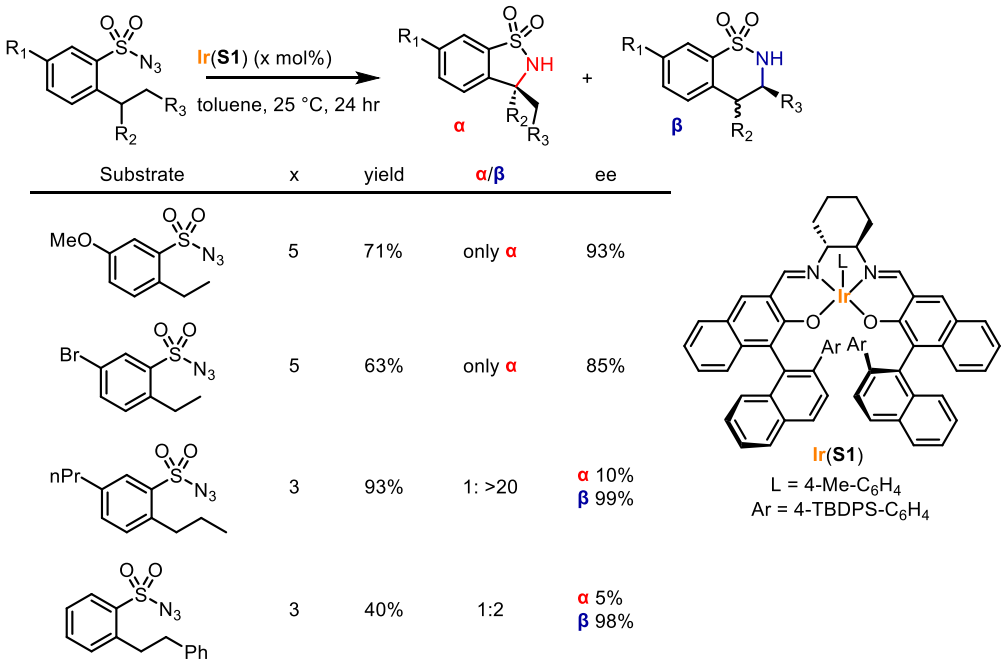

Table 1.8 – Substrate scope for enantioselective allyl amination by Ir(**S1**).

Similar to how azide substrates are typically used in conjunction with porphyrin metal complexes, metal half sandwich catalysts are most well-studied with 3-substituted-1,2,4-dioxazol-5-ones. The Chang group pioneered and developed amination methods utilizing this unique nitrene precursor, introducing 3-substituted-1,2,4-dioxazol-5-ones as an alternative to amides for generating acyl nitrenes.[15] The latter precursor is not used in NT chemistry, due to its proclivity to undergo Curtius rearrangement rather than a productive NT event. Chang and his group met this challenge by utilizing dioxazolones alongside a highly electron-donating

bidentate ligand to generate the iridium complex. However, the initial report only featured racemic C–N bond formation.

The Chang group quickly followed this report with two examples of ligand scaffolds for the asymmetric variant of this reaction. In the first, they designed a catalyst featuring a chiral diamine scaffold (Ir(**L1.2**) that can engage in H-bonding with the ketone oxygen of the substrate,[41] which is the proposed origin for the enantioselectivity. Interestingly, the follow-up to this work also features a catalyst that can engage in attractive non-covalent interactions (Ir(**L1.3**).[42] They propose that this ligand scaffold creates an enzyme-like chiral hydrophobic pocket. This allows the substrate to engage in multiple types of NCIs, including π-π stacking and C–H/π interactions that control the enantioselectivity of the reaction. As a pair, these two NT reactions accommodated diverse substrates, including a variety of benzylic, allylic, propargylic, alkyl and methylene C–H bonds with moderate to high yield and excellent *ee* (Table 1.9).

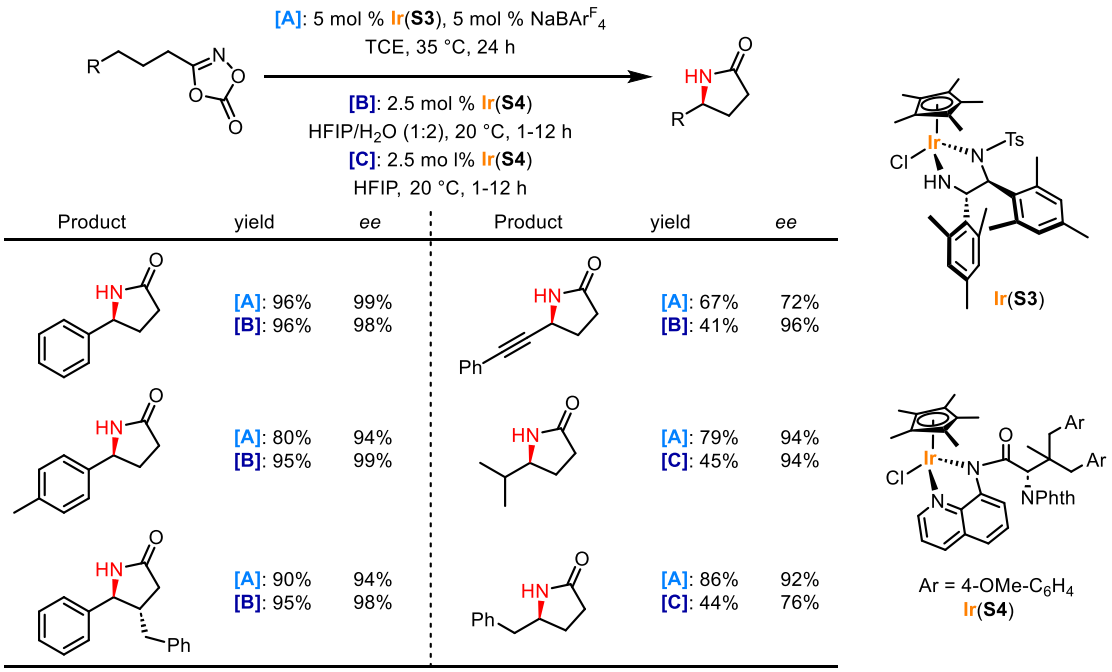

Table 1.9 – Substrate scope for enantioselective amination by iridium half-sandwich catalysts.

1.5.4. Silver-catalyzed intramolecular asymmetric NT

In terms of the noble metals, silver is by far the least expensive; thus, it is somewhat surprising that its utility in asymmetric nitrene transfer has only recently begun to be explored. Following earlier work showing that bis(oxazoline) (BOX) ligands could support asymmetric silver-catalyzed aziridination,[43] the Schomaker group designed a new Min-BOX ligand scaffold (Scheme 1.9) that shows good-to-excellent *ee* in intramolecular aminations of a variety of propargylic and benzylic C–H bonds.[44] Interestingly, installation of a chiral quaternary center on the ligand was key to improved enantioselectivity. DFT and variable temperatureNMR studies revealed that the presence of the methyl group at the chiral center resulted in a greater barrier to rotation of the adjacent phenyl group, rigidifying the transition state and resulting in higher *ee*.

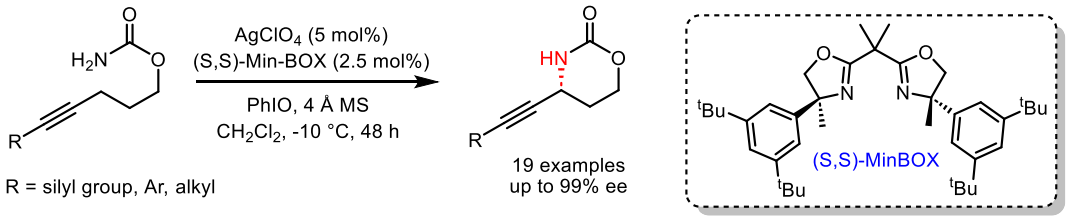

Scheme 1.9 – Asymmetric silver-catalyzed C–H bond aminations.

1.6. Conclusion

Despite the significant progress, many aspects of NT transfer remain challenging. The intramolecular activation of electron-deficient C–H bonds is rare and requires more reactive nitrene species that can display lowered selectivity. Intramolecular asymmetric NT into unactivated and diverse types of allylic C–H bonds that yield non-amide products with broad scope are also lacking. In terms of intermolecular C–H bond amination, the site- and stereoselective activation of tertiary C–H bonds has yet to be achieved. In addition, many intermolecular strategies that do not use pre-oxidized nitrogen sources require a large excess of

substrate, though significant advances have been made towards this end. While remarkable enantioselectivities have been achieved for intramolecular NT involving select nitrene precursors, these products are limited to lactams, pyrrolidines, and a few scattered examples of amino alcohols. Stereoselective intermolecular NT reactions are even more scarce and are mainly reliant on substrate control. Ultimately, a suite of NT catalysts capable of predictable and tunable chemo-, site- and enantioselective transformations of C–H and C=C bond, either in an intra- or intermolecular manner, would revolutionize the way in which chemists approach the synthesis of valuable amines and late-stage functionalization of natural products and pharmaceuticals to prepare useful analogues.

1.7. References

1. (a) Darses, B.; Rodrigues, R.; Neuville, L.; Mazurais, M.; Dauban, P. Transition Metal-Catalyzed Iodine(iii)-Mediated Nitrene Transfer Reactions: Efficient Tools for Challenging Syntheses. *Chem. Commun.* **2017**, *53*, 493–508. (b) Lait, S. M.; Rankic, D. A.; Keay, B. A. 1,3-Aminoalcohols and Their Derivatives in Asymmetric Organic Synthesis. *Chem. Rev.* **2007**, *107*, 767−796. (c) Palchykov, V. A.; Gaponov, A. A., Chapter Four - 1,3-Amino Alcohols and Their Phenol Analogs in Heterocyclization Reactions. In *Advances in Heterocyclic Chemistry*; Scriven, E. F. V.; Ramsden, C. A., Eds.; Academic Press: 2020; Vol. 131, pp 285–350. (d) Ager, D. J.; Prakash, I.; Schaad, D. R. 1,2-Amino Alcohols and Their Heterocyclic Derivatives as Chiral Auxiliaries in Asymmetric Synthesis. *Chem. Rev.* **1996**, *96*, 835−875. (e) Tok, J. B.-H.; Rando, R. R. Simple Aminols as Aminoglycoside Surrogates. *J. Am. Chem. Soc.* **1998**, *120*, 8279−8280. (f) O'Connell, C. E.; Salvato, K. A.; Meng, Z.;

Littlefield B. A.; Schwartz C. E Synthesis and evaluation of hapalosin and analogs as MDR-reversing agents. *Bioorg. Med. Chem. Lett.* **1999**, *9*, 1541–1546.

2. (a) McIntosh, J. A.; Coelho, P. S.; Farwell, C. C.; Wang, Z. J.; Lewis, J. C.; Brown, T. R.; Arnold, F. H. Enantioselective Intramolecular C-H Amination Catalyzed by Engineered Cytochrome P450 Enzymes in Vitro and in Vivo. *Angew. Chem. Int. Ed.* **2013**, *52*, 9309–9312. (b) Hyster, T. K.; Farwell, C. C.; Buller, A. R.; McIntosh, J. A.; Arnold, F. H. Enzyme-Controlled Nitrogen-Atom Transfer Enables Regiodivergent C–H Amination. *J. Am. Chem. Soc.* **2014**, *136*, 15505–15508. (c) Prier, C. K.; Zhang, R. K.; Buller, A. R.; Brinkmann-Chen, S.; Arnold, F. H. Enantioselective, Intermolecular Benzylic C-H Amination Catalysed by an Engineered Iron-Haem Enzyme. *Nat. Chem.* **2017**, *9*, 629–634. (d) Yang, Y.; Cho, I.; Qi, X.; Liu, P.; Arnold, F. H. An Enzymatic Platform for the Asymmetric Amination of Primary, Secondary and Tertiary C(sp^3)–H Bonds. *Nat. Chem.* **2019**, *11*, 987–993. (e) Dydio, P.; Key, H. M.; Hayashi, H.; Clark, D. S.; Hartwig, J. F. Chemoselective, Enzymatic C–H Bond Amination Catalyzed by a Cytochrome P450 Containing an Ir(Me)-PIX Cofactor. *J. Am. Chem. Soc.* **2017**, *139*, 1750–1753. (f) Singh, R.; Bordeaux, M.; Fasan, R. P450-Catalyzed Intramolecular Sp3 C-H Amination with Arylsulfonyl Azide Substrates. *ACS Catal.* **2014**, *4*, 546–552.
3. Bommarius, A. S. Biocatalysis: A Status Report. *Annu. Rev. Chem. Biomol. Eng.* **2015**, *6*, 319–345.
4. For select reviews, see: (a) Muller, P.; Fruit, C. Enantioselective Catalytic Aziridinations and Asymmetric Nitrene Insertions into CH Bonds. *Chem. Rev.* **2003**, *103*, 2905–2920. (b) Driver, T. G. Recent advances in transition metal-catalyzed N-atom transfer reactions of azides. *Org. Biomol. Chem,* **2010**, *8*, 3831–3846. (c) Chang, J. W. W.; Ton, T. M. U.; Chan, P. W. H.

Transition-metal-catalyzed aminations and aziridinations of C–H and C=C bonds with iminoiodinanes. *Chem. Rec.* **2011**, *11*, 331–357. (d) Lu, H.; Zhang, X. P. Catalytic C–H functionalization by metalloporphyrins: recent developments and future directions. *Chem. Soc. Rev.* **2011**, *40*, 1899–1909. (e) Roizen, J. L.; Harvey, M. E.; Du Bois, J. Metal-Catalyzed Nitrogen-Atom Transfer Methods for the Oxidation of Aliphatic C–H Bonds. *Acc. Chem. Res.* **2012**, *45*, 911–922. (f) Gephart III, R. T.; Warren, T. H. Copper-Catalyzed sp^3 C–H Amination. *Organometallics* **2012**, *31*, 7728–7752. (g) Dequirez, G., Pons, V. and Dauban, P. Nitrene Chemistry in Organic Synthesis: Still in Its Infancy? *Angew. Chem. Int. Ed.* **2012**, *51*, 7384–7395. (h) Chu, J. C. K.; Rovis, T. Complementary Strategies for Directed C(sp^3)–H Functionalization: A Comparison of Transition-Metal-Catalyzed Activation, Hydrogen Atom Transfer, and Carbene/Nitrene Transfer. *Angew. Chem. Int. Ed.* **2018**, *57*, 62–101. (i) Alderson, J. M.; Corbin, J. R.; Schomaker, J. M. Tunable, Chemo- and Site-Selective Nitrene Transfer Reactions through the Rational Design of Silver(I) Catalysts. *Acc. Chem. Res.* **2017**, *50*, 2147–2158.

5. Kwart, H.; Kahn, A. A. Copper-Catalyzed Decomposition of Benzenesulfonyl Azide in Cyclohexene Solution. *J. Am. Chem. Soc.* **1967**, *89*, 1951–1953.
6. Breslow, R.; Gellman, S. H. Intramolecular Nitrene C–H Insertions Mediated by Transition-Metal Complexes as Nitrogen Analogues of Cytochrome P-450 Reactions. *J. Am. Chem. Soc.* **1983**, *105*, 6728–6729.
7. Evans, D. A.; Faul, M. M.; Bilodeau, M. T.; Anderson, B. A.; Barnes, D. M. Bis(Oxazoline)-Copper Complexes as Chiral Catalysts for the Enantioselective Aziridination of Olefins. *J. Am. Chem. Soc.* **1993**, *115*, 5328–5329.

8. Li, Z.; Conser, K.R.; Jacobsen, E.N. Asymmetric alkene aziridination with readily available chiral diimine-based catalysts. *J. Am. Chem. Soc.* **1993**, *115*, 5326–5327.

9. (a) Espino, C.G.; Wehn, P.M.; Chow, J.; Du Bois, J. Synthesis of 1,3-Difunctionalized Amine Derivatives through Selective C−H Bond Oxidation. *J. Am. Chem. Soc.* **2001**, *123*, 6935–6936. (b) Espino, C. G.; Du Bois, J. A Rh-Catalyzed C–H Insertion Reaction for the Oxidative Conversion of Carbamates to Oxazolidinones. *Angew. Chem. Int. Ed.* **2001**, *40*, 598–600. (c) Espino, C. G.; Fiori, K. W.; Kim, M.; Du Bois, J. Expanding the Scope of C-H Amination through Catalyst Design. *J. Am. Chem. Soc.* **2004**, *126*, 15378–15379. (d) Fiori, K. W.; Du Bois, J. Catalytic Intermolecular Amination of C–H Bonds: Method Development and Mechanistic Insights. *J. Am. Chem. Soc.* **2007**, *129*, 562–568. (e) Harvey, M. E.; Musaev, D. G.; Du Bois, J. A Diruthenium Catalyst for Selective, Intramolecular Allylic C–H Amination: Reaction Development and Mechanistic Insight Gained through Experiment and Theory. *J. Am. Chem. Soc.* **2011**, *133*, 17207–17216. (f) Roizen, J.L.; Zalatan, D.N.; Du Bois, J. Selective Intermolecular Amination of C–H Bonds at Tertiary Carbon Centers. *Angew. Chem. Int. Ed.* **2013**, *52*, 11343–11346. (g) Bess, E.N.; DeLuca, R.J.; Tindall, D.J.; Oderinde, M.S.; Roizen, J.L.; Du Bois, J.; Sigman, M.S. Analyzing Site Selectivity in $Rh_2(esp)_2$-Catalyzed Intermolecular C–H Amination Reactions. *J. Am. Chem. Soc.* **2014**, *136*, 5783–5789. (h) Chiappini, N. D.; Mack, J. B. C.; Du Bois, J. Intermolecular C(sp^3)−H Amination of Complex Molecules. *Angew. Chem. Int. Ed.* **2018**, *57*, 4956–4959.

10. (a) Fruit, C.; Robert-Peillard, F.; Bernardinelli, G.; Muller, P.; Dodd, R. H.; Dauban, P. Diastereoselective rhodium-catalyzed nitrene transfer starting from chiral sulfonimidamide-derived iminoiodanes. *Tetrahedron Asymmetry* **2005**, *16*, 3484–3487. (b) Liang, C.; Robert-Peillard, F.; Fruit, C.; Müller, P.; Dodd, R. H.; Dauban, P. Efficient Diastereoselective

Intermolecular Rhodium-Catalyzed C–H Amination. *Angew. Chem. Int. Ed.* **2006**, *45*, 4641–4644. (c) Collet, F.; Lescot, C.; Liang, C.; Dauban, P. Studies in catalytic C–H amination involving nitrene C–H insertion. *Dalton Trans.* **2010**, *39*, 10401–10413. (d) Lescot, C.; Darses, B.; Collet, F.; Retailleau, P.; Dauban, P. Intermolecular C-H Amination of Complex Molecules: Insights into the Factors Governing the Selectivity. *J. Org. Chem.* **2012**, *77*, 7232–7240.

11. (a) Liang, J. L.; Yuan, S. X.; Huang, J. S.; Yu, W. Y.; Che, C. M. Highly Diastereo- and Enantioselective Intramolecular Amidation of Saturated C-H Bonds Catalyzed by Ruthenium Porphyrins. *Angew. Chem. Int. Ed.* **2002**, *41*, 3465–3468. (b) Omura, K.; Murakami, M.; Uchida, T.; Irie, R.; Katsuki, T. Enantioselective Aziridination and Amination Using P-Toluenesulfonyl Azide in the Presence of Ru(Salen)(CO) Complex. *Chem. Lett.* **2003**, *32*, 354–355. (c) Omura, K.; Murakami, M.; Uchida, T.; Irie, R.; Katsuki, T. Enantioselective Aziridination and Amination Using P-Toluenesulfonyl Azide in the Presence of Ru(Salen)(CO) Complex. *Chem. Lett.* **2003**, *32*, 354–355. (d) Milczek, E.; Boudet, N.; Blakey, S. Enantioselective C–H Amination Using Cationic Ruthenium(II)-Pybox Catalysts. *Angew. Chem. Int. Ed.* **2008**, *47*, 6825–6828. (e) Li, L.; Han, F.; Nie, X.; Hong, Y.; Ivlev, S.; Meggers, E. Complementing Pyridine-2,6-Bis(Oxazoline) with Cyclometalated N-Heterocyclic Carbene for Asymmetric Ruthenium Catalysis. *Angew. Chem. Int. Ed.* **2020**, *59*, 12392–12395. (f) Zhou, Z.; Chen, S.; Hong, Y.; Winterling, E.; Tan, Y.; Hemming, M.; Harms, K.; Houk, K. N.; Meggers, E. Non-C_2-Symmetric Chiral-at-Ruthenium Catalyst for Highly Efficient Enantioselective Intramolecular C(sp_3)–H Amidation. *J. Am. Chem. Soc.* **2019**, *141*, 19048–19057. (g) Wang, G.; Zhou, Z.; Shen, X.; Ivlev, S.; Meggers, E.

Asymmetric Catalysis with a Chiral-at-Osmium Complex. *Chem. Commun.* **2020**, *56*, 7714–7717.

12. (a) Fantauzzi, S.; Caselli, A.; Gallo, E. Nitrene transfer reactions mediated by metallo-porphyrin complexes. *Dalton Trans.* **2009**, *28*, 5434-5443. (b) Lu, H.; Jiang, H.; Hu, Y.; Wojtas, L.; Zhang, X. P. Chemoselective Intramolecular Allylic C–H Amination versus CC Aziridination through Co(II)-Based Metalloradical Catalysis. *Chem. Sci.* **2011**, *2*, 2361–2366. (c) Lyaskovskyy, V.; Suarez, A. I. O.; Lu, H.; Jiang, H.; Zhang, X. P.; De Bruin, B. Mechanism of Cobalt(II) Porphyrin-Catalyzed C–H Amination with Organic Azides: Radical Nature and H-Atom Abstraction Ability of the Key Cobalt(III)-Nitrene Intermediates. *J. Am. Chem. Soc.* **2011**, *133*, 12264–12273. (d) Lu, H.-J.; Li, C.-Q.; Jiang, H.-L.; Lizardi, C. L.; Zhang, X. P. Chemoselective Amination of Propargylic C(sp^3)–H Bonds by Cobalt(II)-Based Metalloradical Catalysis. *Angew. Chem. Int. Ed.* **2014**, *53*, 7028–7032. (e) Paradine, S.M.; White, M. C. Iron-Catalyzed Intramolecular Allylic C–H Amination. *J. Am. Chem. Soc.* **2012**, *134*, 2036–2039. (f) Paradine, S. M.; Griffin, J. R.; Zhao, J.; Petronico, A. L.; Miller, S. M.; White, M. C. A Manganese Catalyst for Highly Reactive yet Chemoselective Intramolecular C(sp^3)–H Amination. *Nat. Chem.* **2015**, *7*, 987–994. (g) Clark, J. R.; Feng, K.; Sookezian, A.; White, M. C. Manganese-Catalysed Benzylic C(sp^3)–H Amination for Late-Stage Functionalization. *Nat. Chem.* **2018**, *10*, 583–591.

13. (a) Estéoule, A.; Durán, F.; Retailleau, P.; Dodd, R. H.; Dauban, P. Enantioselective Intramolecular Copper-Catalyzed Aziridination of Sulfamates. *Synthesis.* **2007**, *8*, 1251–1260. (b) Barman, D. N.; Nicholas, K. M. Copper-Catalyzed Intramolecular C–H Amination. *Eur. J. Org. Chem.* **2011**, *5*, 908–911. (c) Braga, A. A. C.; Maseras, F.; Urbano, J.; Caballero, A.;

Diaz-Requejo, M. M.; Pérez, P. J. Mechanism of Alkane C−H Bond Activation by Copper and Silver Homoscorpionate Complexes. *Organometallics* **2006**, *25*, 5292–5300.

14. (a) Li, C.; Lang, K.; Lu, H.; Hu, Y.; Cui, X.; Wojtas, L.; Zhang, X. P. Catalytic Radical Process for Enantioselective Amination of C(sp^3)−H Bonds. *Angew. Chem., Int. Ed.* **2018**, *57*, 16837–16841. (b) Lang, K.; Torker, S.; Wojtas, L.; Zhang, X. P. Asymmetric Induction and Enantiodivergence in Catalytic Radical C–H Amination via Enantiodifferentiative H-Atom Abstraction and Stereoretentive Radical Substitution. *J. Am. Chem. Soc.* **2019**, *141*, 12388–12396. (c) Hu, Y.; Lang, K.; Li, C.; Gill, J. B.; Kim, I.; Lu, H.; Fields, K. B.; Marshall, M.; Cheng, Q.; Cui, X.; et al. Enantioselective Radical Construction of 5-Membered Cyclic Sulfonamides by Metalloradical C–H Amination. *J. Am. Chem. Soc.* **2019**, *141*, 18160–18169.
15. Hong, S. Y.; Park, Y.; Hwang, Y.; Kim, Y. B.; Baik, M. H.; Chang, S. Selective Formation of γ-Lactams via C-H Amination Enabled by Tailored Iridium Catalysts. *Science* **2018**, *359*, 1016–1021.
16. Van Vliet, K. M.; De Bruin, B. Dioxazolones: Stable Substrates for the Catalytic Transfer of Acyl Nitrenes. *ACS Catal.* **2020**, *10*, 4751–4769.
17. (a) Smith, P. A. S.; Brown, B. B. The Synthesis of Heterocyclic Compounds from Aryl Azides. I. Bromo and Nitro Carbazoles. *J. Am. Chem. Soc.* **1951**, *73*, 2435–2437. (b) Smith, P. A. S.; Clegg, J. M.; Hall, J. H. Synthesis of Heterocyclic Compounds from Aryl Azides. IV. Benzo-, Methoxy-, and Chloro-carbazoles. *J. Org. Chem.* **1958**, *23*, 524–529. (c) Barton, D. H. R.; Morgan, L. R. Jr. Photochemical transformations. Part XII. The photolysis of azides. *J. Chem. Soc.* **1962**, 622–631.
18. (a) Lebel, H.; Trudel, C.; Spitz, C. Stereoselective Intermolecular C–H Amination Reactions. *Chem. Commun.* **2012**, *48*, 7799–7801. (b) Lebel, H.; Spitz, C.; Leogane, O.; Trudel, C.;

Parmentier, M. Stereoselective Rhodium-Catalyzed Amination of Alkenes. *Org. Lett.* **2011**, *13*, 5460–5463.

19. (a) Fuentes, M. Á.; Gava, R.; Saper, N. I.; Romero, E. A.; Caballero, A.; Hartwig, J. F.; Pérez, P. J. Copper-Catalyzed Dehydrogenative Amidation of Light Alkanes. *Angew. Chem. Int. Ed.* **2021**, *60*, 18467–18471. (b) Lee, J.; Jin, S.; Kim, D.; Hong, S. H.; Chang, S. Cobalt-Catalyzed Intermolecular C-H Amidation of Unactivated Alkanes. *J. Am. Chem. Soc.* **2021**, *143*, 5191–5200. (c) Athavale, S. V.; Gao, S.; Das, A.; Mallojjala, S. C.; Alfonzo, E.; Long, Y.; Hirschi, J. S.; Arnold, F. H. Enzymatic Nitrogen Insertion into Unactivated C-H Bonds. *J. Am. Chem. Soc.* **2022**, *144*, 19097–19105.
20. Ju, M.; Huang, M.; Vine, L. E.; Dehghany, M.; Roberts, J. M.; Schomaker, J. M. Tunable Catalyst-Controlled Syntheses of β- and γ-Amino Alcohols Enabled by Silver-Catalysed Nitrene Transfer. *Nat. Catal.* **2019**, *2*, 899–908.
21. Cui, Y.; He, C. Efficient Aziridination of Olefins Catalyzed by a Unique Disilver(I) Compound. *J. Am. Chem. Soc.* **2003**, *125*, 16202–16203.
22. Li, Z.; Capretto, D. A.; Rahaman, R.; He, C. Silver-Catalyzed Intermolecular Amination of C–H Groups. *Angew. Chem. Int. Ed.* **2007**, *46*, 5184–5186.
23. Huang, M.; Corbin, J. R.; Dolan, N. S.; Fry, C. G.; Vinokur, A. I.; Guzei, I. A.; Schomaker, J. M. Synthesis, Characterization, and Variable-Temperature NMR Studies of Silver(I) Complexes for Selective Nitrene Transfer. *Inorg. Chem.* **2017**, *56*, 6725–6733.
24. (a) Rigoli, J. W.; Weatherly, C. D.; Alderson, J. M.; Vo, B. T.; Schomaker, J. M. Tunable, Chemoselective Amination via Silver Catalysis. *J. Am. Chem. Soc.* **2013**, *135*, 17238–17241. (b) Weatherly, C.; Alderson, J. M.; Berry, J. F.; Hein, J. E.; Schomaker, J. M. Catalyst-

Controlled Nitrene Transfer by Tuning Metal:Ligand Ratios: Insight into the Mechanisms of Chemoselectivity. *Organometallics* **2017**, *36*, 1649–1661.

25. (a) Alderson, J. M.; Phelps, A. M.; Scamp, R. J.; Dolan, N. S.; Schomaker, J. M. Ligand-Controlled, Tunable Silver-Catalyzed C–H Amination. *J. Am. Chem. Soc.* **2014**, *136*, 16720–16723. (b) Huang, M.; Yang, T.; Paretsky, J. D.; Berry, J. F.; Schomaker, J. M. Inverting Steric Effects: Using "Attractive" Noncovalent Interactions to Direct Silver-Catalyzed Nitrene Transfer. *J. Am. Chem. Soc.* **2017**, *139*, 17376–17386.
26. Beltrán, Á.; Lescot, C.; Mar Díaz-Requejo, M.; Pérez, P. J.; Dauban, P. Catalytic C–H Amination of Alkanes with Sulfonimidamides: Silver(I)-Scorpionates vs. Dirhodium(II) Carboxylates. *Tetrahedron* **2013**, *69*, 4488–4492.
27. Llaveria, J.; Beltrán, Á.; Sameera, W. M. C.; Locati, A.; Díaz-Requejo, M. M.; Matheu, M. I.; Castillón, S.; Maseras, F.; Pérez, P. J. Chemo-, Regio-, and Stereoselective Silver-Catalyzed Aziridination of Dienes: Scope, Mechanistic Studies, and Ring-Opening Reactions. *J. Am. Chem. Soc.* **2014**, *136*, 5342–5350.
28. Annapureddy, R. R.; Jandl, C.; Bach, T. A Chiral Phenanthroline Ligand with a Hydrogen-Bonding Site: Application to the Enantioselective Amination of Methylene Groups. *J. Am. Chem. Soc.* **2020**, *142*, 7374–7378.
29. Nägeli, I.; Baud, C.; Bernardinelli, G.; Jacquier, Y.; Moran, M.; Müller, P. Rhodium(II)-Catalyzed CH Insertions with {[(4-Nitrophenyl)Sulfonyl]Imino}phenyl-Λ3-Iodane. *Helv. Chim. Acta* **1997**, *80*, 1087–1105.
30. Zalatan, D. N.; Du Bois, J. A chiral rhodium carboxamidate catalyst for enantioselective C–H amination. *J. Am. Chem. Soc.* **2008,** *130*, 9220-9221.

31. Reddy, R. P. & Davies, H. M. Dirhodium tetracarboxylates derived from adamantylglycine as chiral catalysts for enantioselective C-H aminations. *Org. Lett.* **2006**, *8*, 5013-5016.

32. Hu, Y.; Lang, K.; Tao, J.; Marshall, M. K.; Cheng, Q.; Cui, X.; Wojtas, L.; Zhang, X. P. Next-Generation D_2-Symmetric Chiral Porphyrins for Cobalt(II)-Based Metalloradical Catalysis: Catalyst Engineering by Distal Bridging. *Angew. Chem. Int. Ed.* **2019**, *58*, 2670-2674.

33. Yang, C. J.; Zhang, C.; Gu, Q. S.; Fang, J. H.; Su, X. L.; Ye, L.; Sun, Y.; Tian, Y.; Li, Z. L.; Liu, X. Y. Cu-Catalysed Intramolecular Radical Enantioconvergent Tertiary β-C(sp^3)–H Amination of Racemic Ketones. *Nat. Catal.* **2020**, *3*, 539–546.

34. Lang, K.; Li, C.; Kim, I.; Zhang, X. P. Enantioconvergent Amination of Racemic Tertiary C–H Bonds. *J. Am. Chem. Soc.* **2020**, *142*, 20902–20911.

35. Xing, Q.; Chan, C.-M.; Yeung, Y.-W.; Yu, W.-Y. Ruthenium(II)-Catalyzed Enantioselective γ-Lactams Formation by Intramolecular C–H Amidation of 1,4,2-Dioxazol-5-Ones. *J. Am. Chem. Soc.* **2019**, *141*, 3849–3853.

36. Miyazawa, T.; Suzuki, T.; Kumagai, Y.; Takizawa, K.; Kikuchi, T.; Kato, S.; Onoda, A.; Hayashi, T.; Kamei, Y.; Kamiyama, F.; et al. Chiral Paddle-Wheel Diruthenium Complexes for Asymmetric Catalysis. *Nat. Catal.* **2020**, *3*, 851–858.

37. Nie, X.; Yan, Z.; Ivlev, S.; Meggers, E. Ruthenium Pybox-Catalyzed Enantioselective Intramolecular C-H Amination of Sulfamoyl Azides En Route to Chiral Vicinal Diamines. *J. Org. Chem.* **2021**, *86*, 750–761.

38. Qin, J.; Zhou, Z.; Cui, T.; Hemming, M.; Meggers, E. Enantioselective Intramolecular C-H Amination of Aliphatic Azides by Dual Ruthenium and Phosphine Catalysis. *Chem. Sci.* **2019**, *10*, 3202–3207.

39. Zhou, Z.; Tan, Y.; Yamahira, T.; Ivlev, S.; Xie, X.; Riedel, R.; Hemming, M.; Kimura, M.; Meggers, E. Enantioselective Ring-Closing C–H Amination of Urea Derivatives. *Chem* **2020**, *6*, 2024–2034.
40. Ichinose, M.; Suematsu, H.; Yasutomi, Y.; Nishioka, Y.; Uchida, T.; Katsuki, T. Enantioselective Intramolecular Benzylic C–H Bond Amination: Efficient Synthesis of Optically Active Benzosultams. *Angew. Chem. Int. Ed.* **2011**, *50*, 9884–9887.
41. Park, Y.; Chang, S. Asymmetric Formation of γ-Lactams via C–H Amidation Enabled by Chiral Hydrogen-Bond-Donor Catalysts. *Nat. Catal.* **2019**, *2*, 219–227.
42. Wang, H.; Park, Y.; Bai, Z.; Chang, S.; He, G.; Chen, G. Iridium-Catalyzed Enantioselective C(sp^3)–H Amidation Controlled by Attractive Noncovalent Interactions. *J. Am. Chem. Soc.* **2019**, *141*, 7194–7201.
43. Ju, M.; Weatherly, C. D.; Guzei, I. A.; Schomaker, J. M. Chemo- and Enantioselective Intramolecular Silver-Catalyzed Aziridinations. *Angew. Chem. Int. Ed.* **2017**, *56*, 9944–9948.
44. Ju, M.; Zerull, E. E.; Roberts, J. M.; Huang, M.; Guzei, I. A.; Schomaker, J. M. Silver-Catalyzed Enantioselective Propargylic C–H Bond Amination through Rational Ligand Design. *J. Am. Chem. Soc.* **2020**, *142*, 12930–12936.

Chapter 2. *Scope and computational insights into enantioselective C–H amination through silver-catalyzed nitrene transfer*

This chapter has been adapted from a unpublished preprint manuscript:

Schroeder, E. Z.; Fu, Y.; Kim, J. H.; Liu, W.; Liu, P.; Schomaker, J. M. Scope and computational insights into enantioselective C-H amination through silver-catalyzed nitrene transfer. *ChemRxiv* **2023**. https://doi.org/10.26434/chemrxiv-2023-4xz3w.

2.1. Introduction

Enantioselective transformations of targeted C–H bonds into new C–N bonds is a powerful method for the synthesis of valuable amine building blocks that occur frequently in nitrogen-containing natural products and pharmaceuticals.[1,2] Transition metal-catalyzed nitrene transfer (NT) is a popular strategy to streamline access to these important compounds by facilitating direct C–H to C–N bond amination. However, achieving predictable control over the chemo-, site- and enantioselectivity of an NT event can be challenging. This is particularly true for the preparation of diverse aminoalcohol building blocks that employ inexpensive transition metals supported by modular ligands.[3]

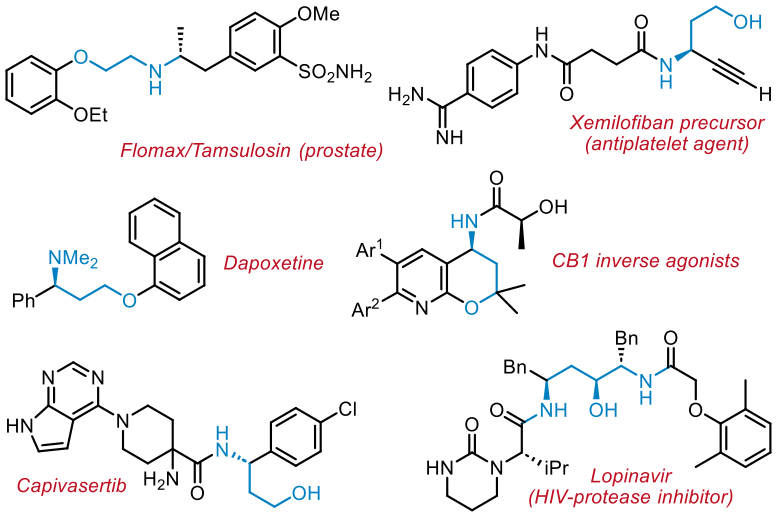

Figure 2.1 – Amino alcohol-containing bioactive molecules.

Enantioselective aminations of benzylic, allylic and unactivated C–H bonds with a variety of nitrene precursors have been reported to form nitrogen-containing heterocycles and acyclic derivatives that include γ-lactams,[4,5] sulfamides,[6-9] sulfamates,[11,12] diamines,[6,13] and amino alcohols.[11,12,14,15] γ-Aminoarylpropanols and β-aminoarylethanols, which are accessible *via* ring-opening of cyclic sulfamates or carbamates following the NT event, are particularly attractive targets, as they are found in diverse bioactive molecules, including dapoxetine,[16] the

anti-cancer candidate capivasertib,[17] and CB1 inverse agonists for the potential treatment of obesity (Figure 2.1), among others.[18] In addition, the alcohol handle can be easily elaborated to furnish other useful enantioenriched amine scaffolds. Despite the utility of enantioenriched 1,2- and 1,3-aminoalcohols, asymmetric NT methods for their formation with broad scope are scarce.

Previous reports of asymmetric C–H bond amination utilize sulfamates and pre-oxidized carbamates as nitrene precursors (Scheme 2.1) and precious metal catalysts. Du Bois found that the electronics of the aryl group impacted the *ee* of asymmetric benzylic C–H aminations catalyzed by dinuclear Rh complexes; the alkene geometry also played a role in the *ee* of the allylic amination. Blakey's Ru(pyBOX) catalyst was less sensitive to arene electronics in terms of *ee*, but in contrast to Rh_2(*S*-NAP)$_4$, the (*Z*)-alkene gave lower *ee* than the *E* isomer. Davies and Meggers employed pre-oxidized carbamate-derived nitrene precursors with asymmetric Rh and Ru catalysts, but these were also limited in scope.[11,12,15] While progress continues to be made in predicting the origins of substrate effects on *ee*, in general, they are still not well understood prior to obtaining experimental results. Thus, it is challenging to rationally design catalysts with high enantioselectivities for different substrate classes without extensive experimental screening.

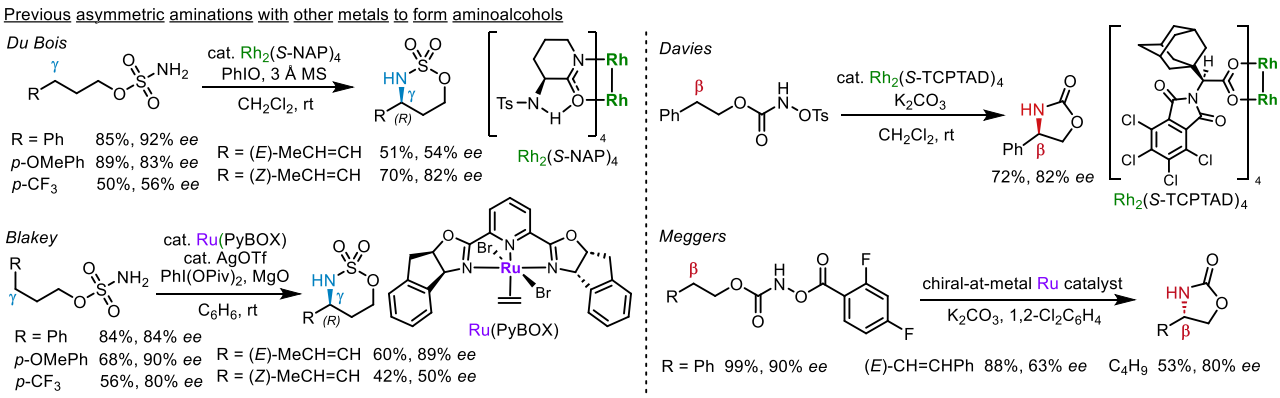

Scheme 2.1 – Prior asymmetric C–H amination via NT to furnish amino alcohols.

We recently developed a new bis(oxazoline) ligand ((*S*,*S*)-Min-BOX, Scheme 2.2, R = Me, R^1 = 3,5-di-*t*-Bu, R^2 = Me) for silver-catalyzed propargylic C–H bond amination in high

ee.[19] Key features of the ligand include a fully substituted stereocenter on the oxazoline ring and significant steric bulk in the form of 3,5-^{t}Bu groups on the aryl ring. Initial attempts to expand the scope to encompass asymmetric aminations of benzylic, allylic and unactivated methylene C–H bonds were not promising, and the limited modularity of our initial ligand synthesis further hampered efforts to identify key interactions between substrate and catalyst that could be tuned to improve scope. In light of these challenges, and to gain a thorough understanding of the factors responsible for high chemo-, site- and enantioselectivity within different substrate classes, we turned to computations to inform choices of substrate and catalyst that would furnish high *ee*. Herein, we report combined experimental and computational explorations of $AgClO_4$/(*S*,*S*)-Min-BOX and related catalysts that provide key insights into the mechanism and stereochemical models to enable future predictive catalyst designs for silver-catalyzed asymmetric intramolecular NT.

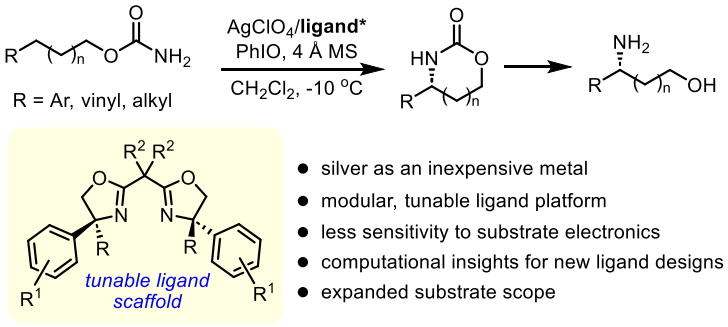

Scheme 2.2 – Silver-catalyzed asymmetric C–H amination with BOX ligands.

2.2. Results and discussion

2.2.1. Benchmarking (S,S)-Min-BOX for asymmetric amination of non-propargylic C–H bonds

Studies to explore site- and enantioselective NT with (*S*,*S*)-Min-BOX were initiated using three simple carbamates **2.1a-c**, bearing a benzylic, allylic and unactivated C–H bond, respectively (Table 2.1).[19] Treatment of **2.1a** with 2 equivalents of PhIO, 5 mol % $AgClO_4$ and

2.5 mol % (S,S)-Min-BOX at -10 °C for 48 h resulted in a moderate 60% yield of **2.2a** in a promising 95:5 *er* (entry 1). The site-selectivity was excellent, and no 5-membered ring product was observed. The role of the excess $AgClO_4$ is to serve as a Lewis acid to break down the polymeric PhIO and increase the overall rate and conversion of the reaction. Control experiments show minimal background reaction promoted by unligated $AgClO_4$. Reducing the temperature in the reaction to -20 °C (entry 2) required increased catalyst loading and time; however, the *er* was similar, suggesting no benefit to temperatures lower than -10 °C. Carrying out the reaction at room temperature reduced the *er* to 91:9 (entry 3), but gave complete conversion to **2.2a** in 99% yield. In cases where the product *er* can be easily increased through a simple recrystallization, this minimal reduction in *er* may be readily compensated for by the higher conversions and yields observed at rt. Ultimately, increasing the catalyst loading to 10 mol % $AgClO_4$ and 5 mol % (S,S)-Min-BOX and running the reaction at -10 °C gave a good balance between conversion and *er* (entry 4); these conditions were adopted for studies of the substrate scope.

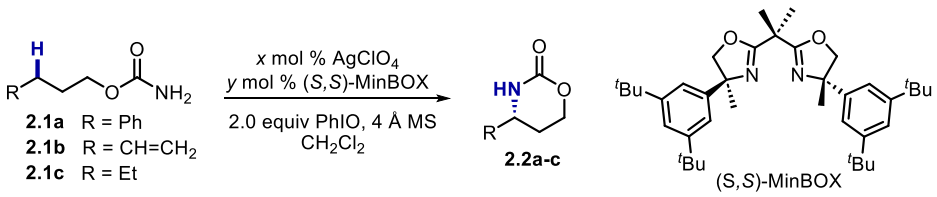

entry	substrate	mol% Ag	mol% MinBOX	T (°C)	t (h)	yield **2.2** (*er*)
1	**2.1a**	5	2.5	-10	48	60% **2.2a** (95:5)
2	**2.1a**	20	10	-20	72	75%[a] **2.2a** (96:4)
3	**2.1a**	20	10	rt	12	99%[a] **2.2a** (91:9)
4	**2.1a**	10	5	-10	48	90%[a] **2.2a** (95:5)
5	**2.1b**	10	5	-10	48	79%[a] **2.2b** (77:23)[b]
6	**2.1c**	10	5	-10	24	26%[a] **2.2c** (69:31)[b,c]

Yields determined by ^{1}H NMR with mesitylene and trimethylphenylsilane internal standards.
[a]Isolated yields. [b]*er* was determined after benzylation. [c]5% of the 5-membered ring.

Table 2.1 – Initial exploration of asymmetric amination of benzylic, allylic, and unactivated C(sp^3)–H bonds.

Substrate **2.1b**, bearing a sterically unhindered allylic C–H bond, showed a significant decrease in *er* to 77:23 when using (S,S)-Min-BOX (entry 5). Both chemo- and site-selectivity were excellent, with no competing formation of the aziridine or the 5-membered ring. Substrate **2.1c**, which displays an unactivated C(sp^3)–H bond (entry 6), showed both poor conversion and low *er* using (S,S)-MinBOX as the ligand. In addition, small amounts of the 5-membered ring were formed. These more challenging substrates (**2.1b** and **2.1c**) merited further investigations into how ligand modifications could impact enantioselectivity (*vida infra*).

2.2.2. Scope of asymmetric benzylic C–H bond amination

With optimized conditions in hand, the scope of the enantioselective C–H amination was explored (Table 2.2). In general, the high *ee* of the reaction was maintained across a variety of carbamates containing benzylic C–H bonds. Changing the electronics of the arene though the addition of electron-withdrawing or electron-donating groups in the *para*-position (**2.2a**, **2.3a-2.7a**) did not significantly impact *er*. Precursor **2.4**, bearing a *p*-OMe group gave **2.4a** in 95:5 *er*, while **2.7**, bearing a *p*-CF_3 group, gave **2.7a** in a similar *er* of 94:6. Interestingly, this is in contrast to results observed with both the Du Bois Rh_2(*S*-NAP)$_4$ and the Blakey Ru(pyBOX) catalysts,[11,12] although steric effects cannot be completely ruled out in these examples. As expected, more electron-poor C–H bonds typically underwent amination at slower rates under the standard conditions, resulting in only ~50% conversion for substrates **2.4a**-**2.6a**. However, increasing the amount of the silver salt to 20 mol % improved the conversion of the nitrene transfer with little impact on the *er*. Substitution at the α-position of the carbamate tether in **2.8** enhanced the reactivity to furnish **2.8a** in excellent yield and *er*, even at reduced catalyst loadings. Interestingly, addition of a Me group at the *meta* position of **2.9** resulted in a

maintained *er* of **2.9a** at 95:5, while moving the Me group to the *ortho* position in **2.10** resulted in an *er* of 90:10 for **2.10a**. Electron-rich heterocycles were also tested in the asymmetric nitrene transfer; furan **2.11a** was obtained in good *er*, with the lower yield attributed to competing oxidative degradation of the sterically accessible furan ring. Finally, the indole derivative **2.12** was poorly reactive at -10 °C but gave moderate yield and *er* of **2.12a** at room temperature.

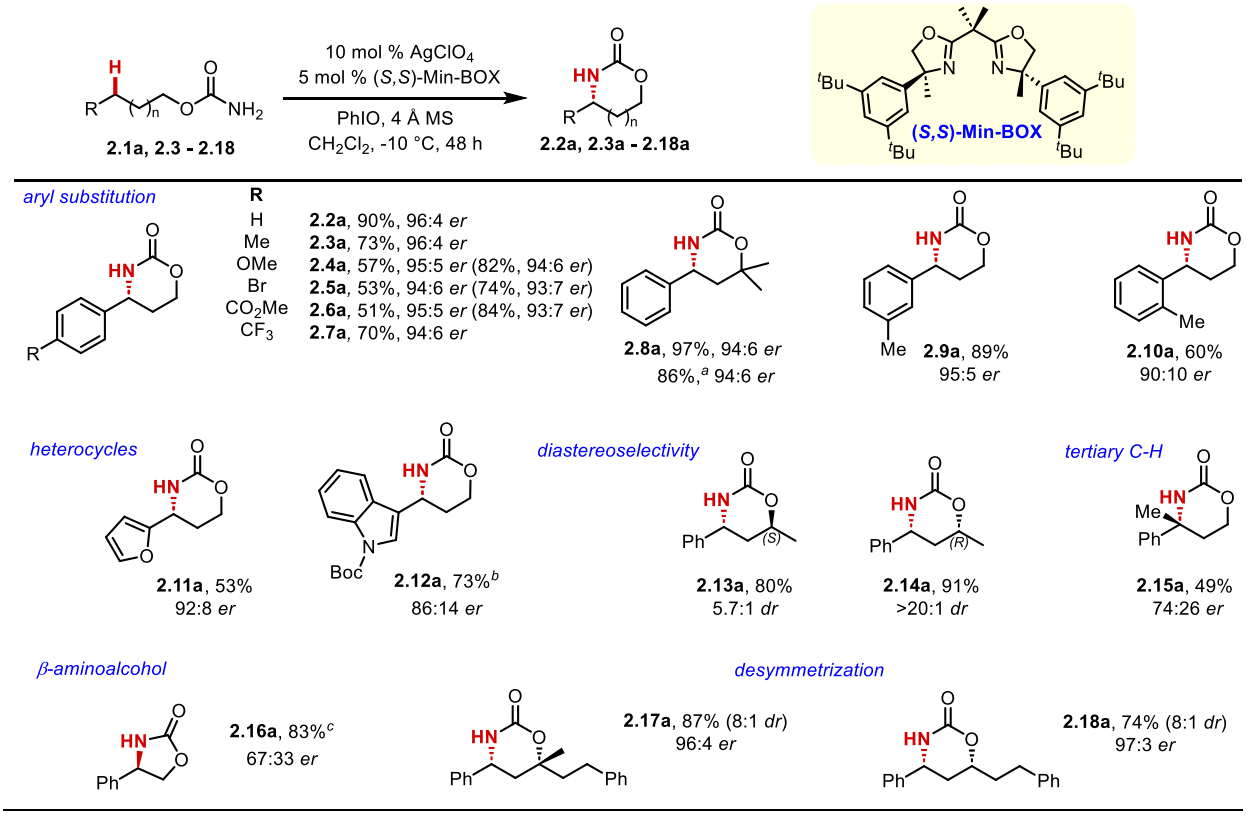

Yields and *er* values in parenthesis were run with 20 mol % $AgClO_4$. [a] 5 mol % $AgClO_4$, 2.5 mol % (*S*,*S*)-Min-BOX. [b] 20 mol % $AgClO_4$, 10 mol % (*S*,*S*)-Min-BOX, room temp. [c] 18-20 h at room temperature.

Table 2.2 – Scope for asymmetric silver-catalyzed amination of benzylic C–H bonds.

Substrates containing a stereogenic carbon were also investigated to probe how the nature of the catalyst impacts the diastereoselectivity of the silver-catalyzed amination. Carbamates **2.13** and **2.14** were prepared in enantioenriched form from the corresponding secondary alcohols and individually subjected to the reaction conditions. Utilizing (*S*,*S*)-Min-BOX with the (*R*) enantiomer **2.14** increased the *dr* for the *syn* diastereomer **2.14a** to >20:1, compared to the 3.4:1

syn:anti ratio observed when the same reaction was run with an achiral bis(oxazoline) ligand (see SI for details). Subjecting the (*S*) enantiomer **2.13** to standard reaction conditions resulted in the catalyst selecting for the typically disfavored *anti*-diastereomer **2.13a** in a 5.7:1 *dr*. This is particularly noteworthy, as enantioenriched *trans*-1,3-aminoalcohols are not accessible using other reported catalyst systems, which overwhelmingly favor the *syn* diastereomer.[3]

To further challenge our asymmetric amination chemistry, a carbamate **2.15** bearing a tertiary benzylic C–H bond was investigated. With a typical racemic catalyst, NT likely occurs via a concerted C–H amination or by H-atom abstraction, followed by rapid radical rebound. However, we were curious whether a mismatch between (*S,S*)-Min-BOX and the stereochemistry at a racemic tertiary C–H bond could lead to a longer-lived radical intermediate, where the initial stereochemistry could be ablated and reset by the catalyst. Running the amination of **2.15** under the standard reaction conditions resulted in 49% yield of the product **2.15a** and 49% recovery of the starting material **2.15**. However, the *er* of both compounds were 74:26. This suggests a scenario involving moderate kinetic resolution by (*S,S*)-Min-BOX, influenced by the small difference between the two activation barriers for C–H amination of (*R*)-**2.15** vs. (*S*)-**2.15**. However, (*S,S*)-Min-BOXAgClO_4 did prove capable of desymmetrizing benzylic C–H bonds in good *er*. Subjecting the achiral carbamates **2.17** and **2.18** to the standard reaction conditions resulted in an effective desymmetrization of both compounds to provide the corresponding benzylic amines **2.17a** and **2.18a** in excellent yield, *dr* and *er*.

We were also curious if the (*S,S*)-Min-BOX ligand would be capable of furnishing good *ee* in the silver-catalyzed amination of homobenzylic carbamates that bear one less carbon in the tether to deliver enantioenriched 1,2-aminoalcohols. Reaction of **2.16** at room temperature gave a good yield of **2.16a**, albeit in a low 67:33 *er*. Additionally, the *er* was not improved by lowering

the temperature. Nonetheless, this result, when combined with results showing the impact of the sterics of arene substitution on the *er* (Table 2.2, **2.9a**-**2.10a**), provided valuable information to inspire our computational investigations on factors affecting catalyst–substrate interactions and the effectiveness of enantioinduction in the selectivity-determining transition states (*vide infra*).

The utility of the asymmetric nitrene transfer was demonstrated in a short synthesis of the drug Dapoxetine (Scheme 2.3). Scale-up of the silver reaction to gram-scale and reaction with the (*R*,*R*)-MinBOX ligand enabled efficient preparation of the desired (*S*)-enantiomer of **2.2a**. After recrystallization of (*S*)-**2.2a** to improve the *ee* to 99%, the carbamate ring was hydrolyzed with NaOH. The free amino alcohol product was carried forward without purification and subjected to Eschweiler-Clarke reaction conditions. Finally, Dapoxetine was synthesized in 48% overall yield and 90% *ee* via a S_NAr reaction of the methylated amino alcohol with 1-fluoronaphthalene.

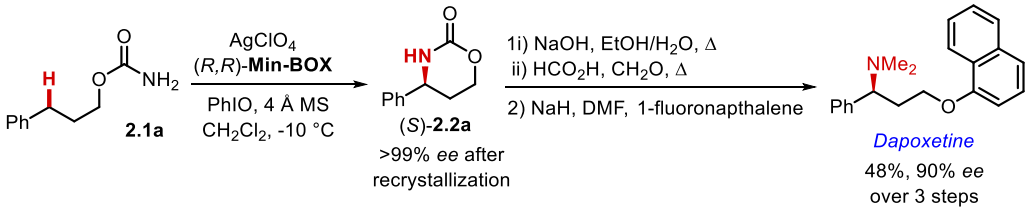

Scheme 2.3 – Short synthesis of Dapoxetine.

2.2.3. Computational explorations of asymmetric silver-catalyzed C–H amination

Density functional theory (DFT) calculations[20] were performed to investigate the origin of enantioselectivity in the Ag-catalyzed benzylic C–H amination and to better understand why the Min-BOX ligand leads to high *ee* with benzylic and heterobenzylic precursors but is less effective with substrates containing sterically unhindered allylic (Table 2.1, **2.1b**) or unactivated methylene C–H bonds (**2.1c**). DFT and local coupled cluster theory [PNO-LCCSD(T)-F12][21] calculations indicated that the singlet Ag nitrene C–H insertion pathway is more favorable than

the competing triplet pathway.[22] This singlet pathway involves concerted C–H bond cleavage and C–N bond formation without the formation of an alkyl radical intermediate; therefore, the enantioselectivity is determined in this concerted C–H insertion transition state (TS). The most stable C–H insertion TS isomers with the benzylic substrate **2.1a** (Figure 2.2) involve a four-coordinate square-planar Ag nitrene complex, where the carbamate carbonyl coordinates to the Lewis acidic Ag center. Several alternative TS isomers were also considered, including a trigonal planar Ag nitrene lacking the carbamate carbonyl–Ag coordination, a TS with a partially dissociated monodentate Min-BOX ligand having only one oxazoline nitrogen bound to the Ag, and finally, a TS having an *N*,*O*-bidentate binding mode for (*S*,*S*)-Min-BOX (Figures S2 and S3). All of these alternative TS isomers are higher in energy than those involving the four-coordinate square-planar Ag nitrene complex where the carbamate carbonyl group is coordinated to Ag. This C–H insertion mechanism involving a singlet square-planar Ag nitrene is consistent with our recent computational study of nitrene transfer using an achiral 2,2ˈ-isopropylidenebis(4,4ˈ-dimethyl-2-oxazoline)-supported (dmBOX) Ag catalyst.

Next, we analyzed the origins of enantioselectivity in the benzylic amination of **2.1a**. Two ring-flipped conformers of the seven-membered cyclic C–H insertion TS were located for the activation of each prochiral benzylic C–H bond (Figure 2). The computed enantioselectivity is consistent with the experimental results, where the most favorable C–H insertion transition state **TS2.1** ($\Delta G^{\ddagger}$ = 6.6 kcal/mol with respect to the Ag nitrene intermediate) leads to the observed major enantiomeric product, (*R*)-**2.2a**. The two transition state conformers (**TS2.2** and **TS2.4**) that lead to the *S* enantiomer of the product (*S*)-**2.2a** are both 3.9 kcal/mol higher in energy than **TS2.1**. The enantioselectivity is attributed to steric repulsions between the Ph substituent on the benzylic substrate and the C2-symmetric (*S*,*S*)-Min-BOX ligand that lead to

greater distortion of the disfavored transition states. In all four C–H insertion transition states (**TS2.1**–**TS2.4**), the nitrene moiety in the four-coordinate Ag complex is slightly distorted from the preferred square planar geometry due to steric repulsions with the Ar group on the (*S*,*S*)-Min-BOX ligand located in quadrant **IV**. This sterically induced distortion is more profound in **TS2.2** and **TS2.4**, where the Ph group of the substrate would be placed in a quadrant (**IV**) occupied by the bulky Ar group if the nitrene was not distorted. In the optimized structures of **TS2.2** and **TS2.4**, the Ph group is placed in the less occupied quadrant **I**, resulting in a more distorted square-planar geometry. Such distortion weakens the Ag–carbamate carbonyl coordination and

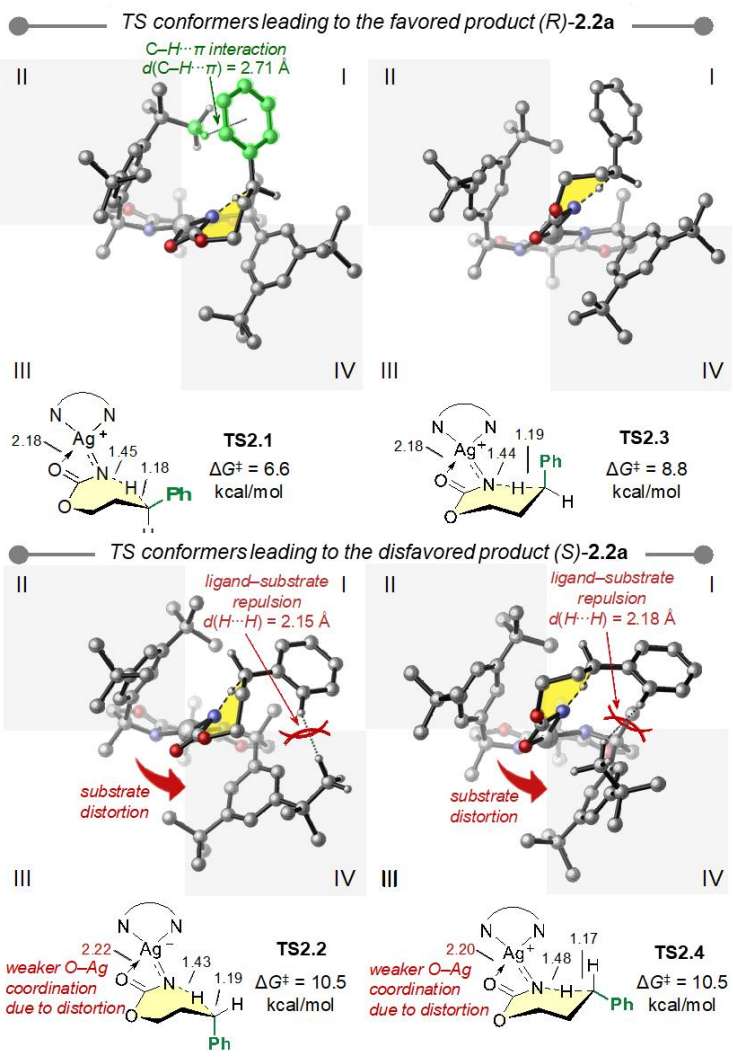

Figure 2.2 – C−H insertion TS structures of the asymmetric NT of benzylic substrate **2.1a**.

leads to longer Ag···O(carbonyl) distances in **TS2.2** and **TS2.4** (2.22 and 2.20 Å, respectively) than those in **TS2.1** and **TS2.3** (both are 2.18 Å). In **TS2.1** and **TS2.3**, the Ph group is placed in the unoccupied quadrant **I**, and thus such ligand–substrate steric repulsions are diminished. In addition, **TS2.1** is stabilized by a C–H/π interaction between the Ph group on the substrate and the *t*-Bu group on the ligand. The ring-flipped TS conformer **TS2.3** is 2.2 kcal/mol less stable than **TS2.1** because the Ph group is in a pseudoaxial position, rather than the pseudoequatorial position as in **TS2.1**.

Next, we investigated substrate effects on enantioselectivity by comparing the C–H insertion TS with the sterically unhindered allylic substrate (**2.1b**) and a benzylic substrate with a shorter tether (**2.16**) (Figure 2.3). The computed enantioselectivities for **2.1b** and **2.16** are both lower than that of **2.1a** ($\Delta\Delta G^{\ddagger}$ = 0.7 and 2.5 kcal/mol for **2.1b** and **2.16**, respectively, compared to $\Delta\Delta G^{\ddagger}$ of 3.9 kcal/mol for **2.1a**), which is consistent with the lower *er* observed experimentally. In the allylic C–H insertion transition state (**TS2.6**) leading to the minor product (*S*)-**2.2b**, the smaller alkenyl group in **2.1b** compared to the Ph group in **2.1a** diminishes the steric repulsion with the (*S,S*)-Min-BOX ligand. This means that the alkenyl group can be placed in the occupied quadrant **IV** without distorting the square planar geometry of the Ag nitrene. Moreover, in **TS2.5** leading to the major product (*R*)-**2.2b**, the stabilizing non-covalent interactions between the ligand and the smaller alkenyl group are weaker than the C–H/π interaction observed in **TS2.1** with the benzylic substrate **2.1a**. Therefore, both factors lead to diminished enantioselectivity with the allylic substrate. Similarly, in the C–H insertion with **2.16**, the ligand–substrate steric repulsion in **TS2.8** leading to the minor product (*S*)-**2.16a** is also diminished, because the six-membered cyclic TS is sterically less encumbered than the seven-membered TS with **2.1a**. The greater ligand–substrate distance allows the Ph group on the substrate to be placed in the

occupied quadrant (**IV**) without distorting the Ag nitrene in order to maintain the preferred square planar geometry. **TS2.7** that leads to the major enantiomeric product contains a ligand–substrate C–H/π interaction similar to **TS2.1**; however, due to the smaller ring size, a greater substrate distortion is required to orient the Ph group towards the Ar group in quadrant **II**. This

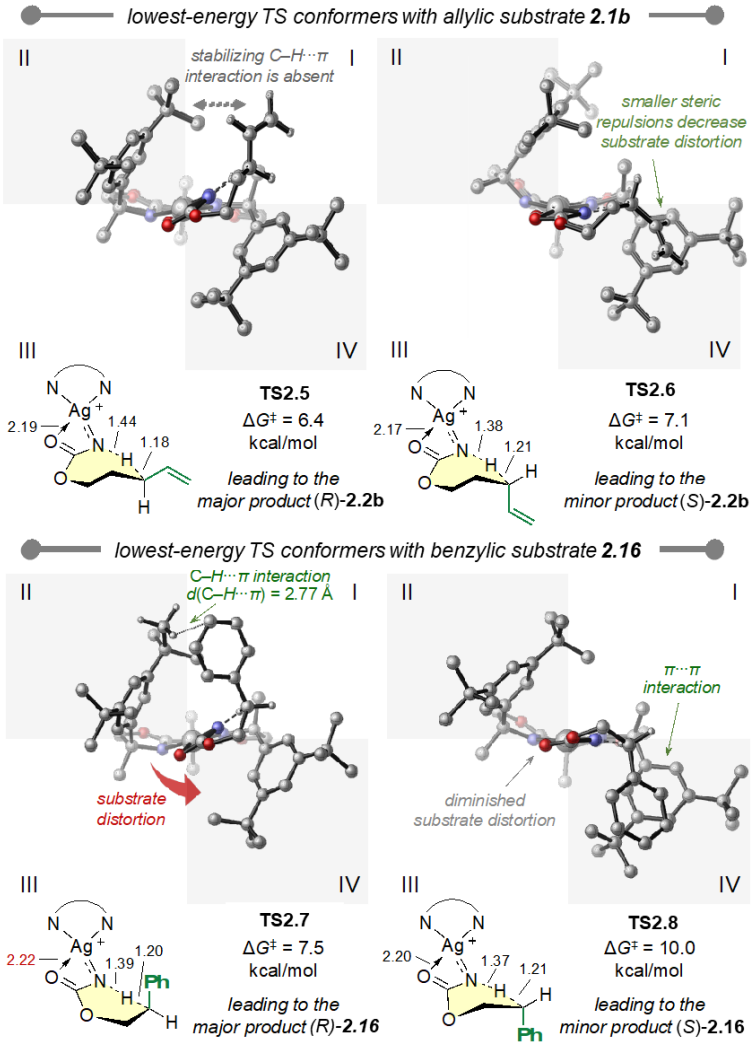

Figure 2.3 – Origins of diminished enantioselectivity in the C–H amination of allylic substrate **2.1b** and benzylic substrate **2.16** with a shorter tether.

distortion leads to a longer Ag···O(carbonyl) distance of 2.22 Å in **TS2.7**, compared to 2.20 Å in **TS2.8**. Taken together, the computed C–H insertion transition states with substrates **2.1a**, **2.1b**, and **2.16** revealed two concurrent factors affecting enantioselectivity: ligand–substrate steric

repulsions that destabilize the TS leading to the minor enantiomeric product, and C–H/π interactions between the *t*-Bu group on the Min-BOX ligand and the Ph group on the benzylic substrate in the TS leading to the major enantiomeric product. The lower *er* observed with less sterically demanding substrates (*e.g.*, **2.1b**) and substrates with a shorter tether (*e.g.*, **2.16**) is because one or both of these interactions are diminished.

We surmised that the enantioselectivities of challenging substrates, such as **2.1b**, might be enhanced by tuning the substituents on the Min-BOX ligand or substrate steric properties to enhance the stabilizing non-covalent interactions in the favored TS, as well as the steric repulsions and substrate distortions in the disfavored TS. To test this hypothesis, transition states with substituted alkenes such as alkene **2.19** were computed (Figure 2.4).

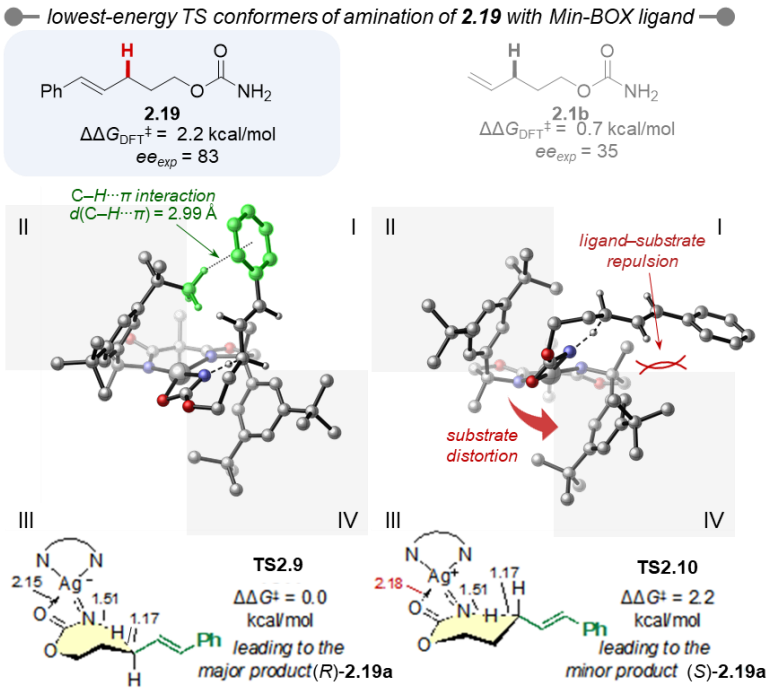

Figure 2.4 – Substrate effects on enantioselectivity.

Gratifyingly, the computed transition states of styrenyl substrate **2.19** with (*S*,*S*)-Min-BOX ligand led to increased *er* (92:8, Table 2.3) compared to the allylic substrate **2.1b** with the

same ligand ($\Delta\Delta G^{\ddagger}$ = 2.2 and 0.7 kcal/mol for **2.19** and **2.1b**, respectively). The newly introduced Ph group on **2.19** enables stabilizing C–H/π interactions with the *tert*-Bu group on the (*S*,*S*)-Min-BOX ligand (quadrant **II**) in **TS2.9** leading to the major enantiomeric product. In addition, replacing the vinyl group with the larger styrenyl moiety increases ligand–substrate steric repulsion in the **TS2.10** that gives the minor enantiomeric product, leading to the same substrate distortion observed in other disfavored TS isomers. Therefore, the higher *er* with **2.19** indicates that the alkenyl substituent on the substrate also affects non-covalent ligand–substrate interactions and substrate distortion, and ultimately, the *er* of the amination product. This prompted us to experimentally explore the scope of diverse allylic substitution patterns to further understand these effects on reactivity and *er*.

2.2.4. Asymmetric amination of allylic and unactivated C–H bonds

The trends in conversion and yield with substituted alkenes **2.19**-**2.26** using (*S*,*S*)-Min-BOX proved puzzling (Table 2.3). Unsubstituted, *cis*- or 2,2'-disubstituted alkenes (**2.1b**, **2.20**, **2.21**) gave poor conversions to the desired **2.2b**, **2.20a** and **2.21a**, with *er* values varying from 66:34 to 90:10. Interestingly, the presence of a *trans*-substituent on the alkene, whether aryl (**2.19**, **2.22**-**2.24**) or alkyl/heteroalkyl (**2.25**, **2.26**), significantly improved the yield of the reaction and resulted in good-to-excellent *er*. For example, an aryl group could be accommodated at the internal alkene carbon of **2.22** to give **2.22a** in 85% yield and 88:12 *er*, while moving the phenyl to the terminal carbon of **2.23** improved the yield and *er* to 90% and >99:1, respectively. We hypothesize that the low conversion and *er* for **2.1b** and **2.20**-**2.21** may result from competing binding of the silver center to the alkene, as alkenes are well-known to serve as ligands for silver. Certain alkene substitution patterns may favor binding to the metal as a hemi-labile ligand that

impedes reactivity and/or promotes background reaction.[23] Decreasing the size of the group *cis* to the group undergoing amination from Ph in **2.23** to a Me in **2.24** resulted in a decreased in *er* of **2.24a** to 89:11. A bulky TBS group in **2.25** gave **2.25a** in excellent *er*, suggesting that steric bulk in the *trans* position is important to achieve high *er*. Replacing the *trans* H group of **2.1b** with a cyclohexyl group in **2.26** improved the *er* of the allylic amine products from 73:27 in **2.2b** to 93:7 in **2.26a**.

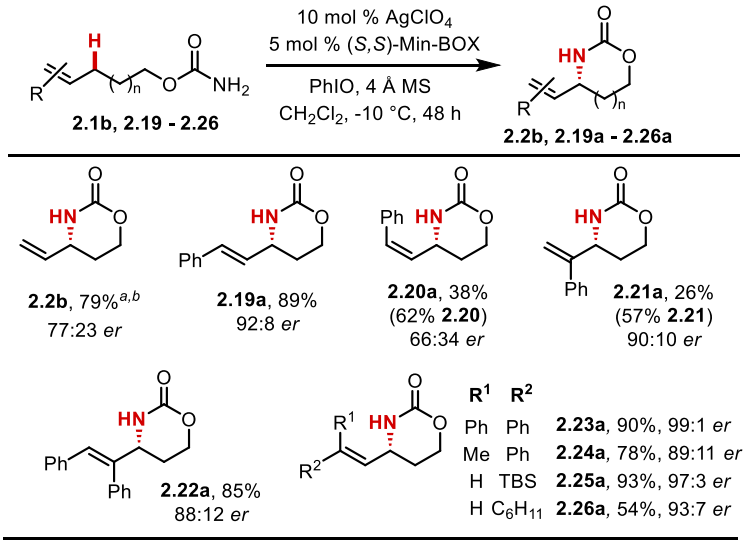

[a] Reaction was run for 24 h. [b] *er* was determined after benzylation.

Table 2.3 – Scope of asymmetric silver-catalyzed amination of allylic C–H bonds.

Chemocatalyzed asymmetric aminations of unactivated prochiral C–H bonds to form enantioenriched 1,3-aminoalcohols remain a challenge in the field of NT. We explored a series of alkyl-substituted carbamates (Table 2.4) using (*S,S*)-Min-BOX. A small alkyl group proximal to the γ site for C–H insertion, such as the ethyl chain in **2.1c**, gave a 69:31 *er*. Increasing the length of the alkyl group in **2.27** improved the *er* of **2.27a** to 79:21. Similar results were obtained with **2.28**, though the slightly increased steric bulk of the alkyl chain increase the amount of competitng 5-membered ring product. Moving the steric bulk closer to the γ C–H bond gave 83:17 *er* for **2.29a** in excellent yield, but too much additional bulk in **2.30a** again decreased the

site- and enantioselectivity. Carbamates **2.31** and **2.32** were tested to assess whether a pendant aryl group might engage in productive non-covalent interactions with the ligand to improve the *ee*; however, **2.31a** and **2.32a** showed a surprising reduction in *er* to 68:32 and 72:28, respectively. These informative results highlight the challenges associated with the asymmetric amination of unactivated C–H bonds when both site- and enantioselectivity must be controlled.

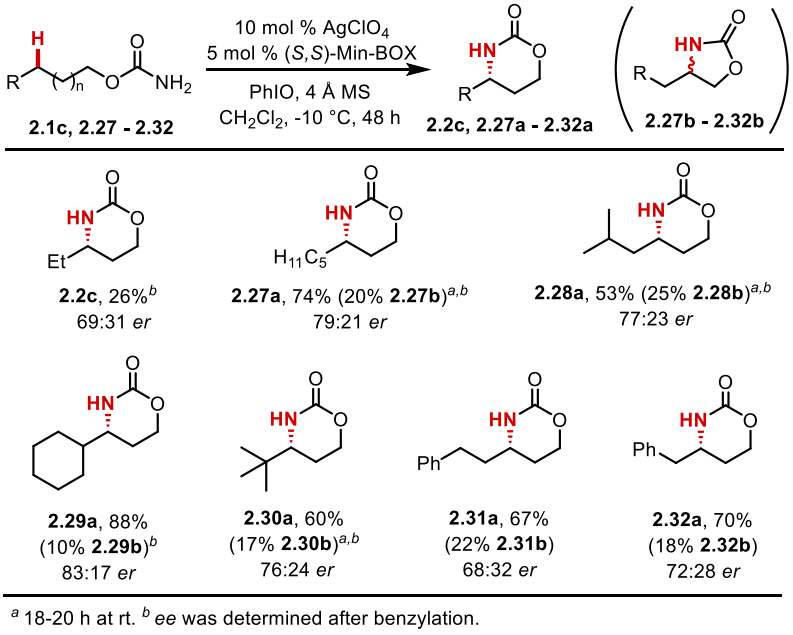

[a] 18-20 h at rt. [b] *ee* was determined after benzylation.

Table 2.4 – Scope of asymmetric silver-catalyzed amination of unactivated C(sp^3)–H bonds.

2.2.5. Modular route to new bis(oxazoline) (BOX) ligands for asymmetric nitrene transfer

With computational and experimental studies in hand to help determine how changing the features of the (*S*,*S*)-Min-BOX ligand and/or the substrate might impact the *er* and expand the scope of silver-catalyzed asymmetric amination, a more modular route to Min-BOX and analogues needed to be developed. Our first-generation synthesis suffered from several drawbacks,[19] including an initial asymmetric Rh-catalyzed hydroformylation that requires the use of bis[(*S*,*S*,*S*)-DiazaPhos-SPE], a complex and commercially unavailable ligand. We had no access to the enantiomer of this ligand; thus only the (*S*,*S*)-Min-BOX enantiomer could be

prepared using our original route. Finally, the use of hydroformylation as a key step limits the modularity of the synthesis to the installation of a Me group at the fully substituted sp^3 carbon of the bis(oxazoline).[24]

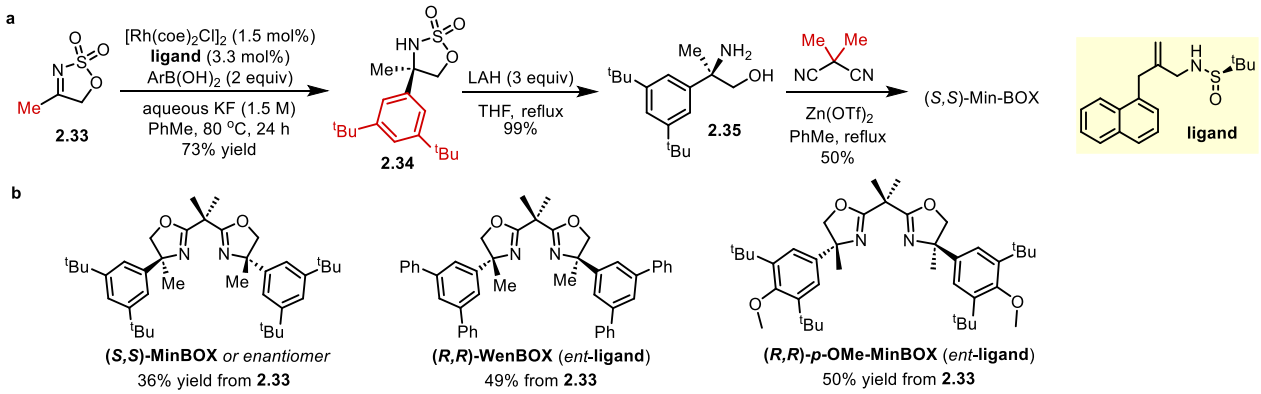

Scheme 2.4 – New modular synthetic route to (*S*,*S*)- and (*R*,*R*)-Min-BOX and analogues informed by computational studies.

To address these issues and provide a reliable and versatile approach to analogues of both (*S*,*S*)-Min-BOX and (*R*,*R*)-Min-BOX, a new route to this class of ligands was developed (Scheme 2.4a). An asymmetric Rh-catalyzed boronic ester addition to imine **2.33** gave **2.34**,[25] which was further elaborated to (*S*,*S*)-Min-BOX using standard procedures. Employing the enantiomer of the *tert*-butylsulfinamide ligand gave facile access to (*R*,*R*)-Min-BOX, which was not available through our previous route.[19] In addition, this new strategy enables easy manipulation of three diverse sites in the ligand, as highlighted in red. Based on guidance from computational studies, additional ligands were synthesized (Scheme 2.4b). The (*R*,*R*)-Wen-BOX ligand was targeted based on computational insight (Figure 2.2) where the *tert*-butyl groups of (*S*,*S*)-Min-BOX are implicated in key interactions in the transition state. Switching these to aryl groups is may to lead to a larger $\Delta\Delta G^{\ddagger}$ between the TS leading to the major and minor enantiomers. The idea behind the design of (*R*,*R*)-*p*-OMe-Min-BOX is to restrict rotation around

the Ar–C(sp^3) bond of the 3,5-di-tert-butyl groups and provide additional rigidity to the catalyst. Computations also suggested that increasing the electron-donor ability of the aryl group could improve selectivity-determining C–H/π interactions (see Figure 2.3, *vide supra*).

2.2.6. Comparing MinBOX with other quaternary-centered BOX ligands

We began by comparing these newly synthesized ligands with the initial set of substrates **2.1a-c**. For the amination of **2.1a**, (*R*,*R*)-Wen-BOX performed slightly worse than (*S*,*S*)-Min-BOX in both conversion and enantioselectivity. In particular, the reaction was much slower, and required the use of more catalyst and higher temperature in order to get to full conversion. This indicated that (*R*,*R*)-Wen-BOX may have a more sterically hindered chiral pocket, which we hoped could improve enantioselectivity in the smaller substrates **2.1b** and **2.1c**. Gratifyingly, though the results for **2.1b** were very similar for both ligands, **2.1c** showed improved enantioselectivity when using (*R*,*R*)-Wen-BOX. However, (*R*,*R*)-Wen-BOX also promoted increased amination at the competing *β*-position up to 24%, again indicating a more sterically hindered transition state. Unfortunately, attempts to utilize (*R*,*R*)-Wen-BOX to improve the *er* of larger substituted substrates such as **2.19** and **2.27** reduced the *er*. This highlights the impact of small changes in the ligand that lead to larger and more varied energetic interactions in the enantiodetermining TS. The greater steric pressure exerted by the (*R*,*R*)-Wen-BOX ligand was also supported by the observation that reaction of **2.27** resulted in reduced reactivity even at rt, and also furnished 28% of the five-membered ring byproduct.

Interestingly, (*R*,*R*)-*p*-OMe-Min-BOX showed small, but noticeable improvements across each of the substrates that were tested. For substrates that performed well with (*S*,*S*)-Min-BOX such as **2.1a** or **2.19**, the increase was very minor and it could be said that the two ligands

performed similarly for those substrates. Happily, for the substrates that still required improvement in *er*, such as **2.1b**, **2.1c**, and **2.27**, the enhanced enantioselectivity was more significant. For example, the *er* of **2.2b** was increased from 77:23 up to 83:17. More impressively, for the unactivated substrates where avoiding 5-membered ring formation also is a key challenge, (*R*,*R*)-*p*-OMe-Min-BOX was able to improve enantioselectivity without negatively impacting the site-selectivity of the reaction. This suggests that while the sterics of the chiral pocket has not changed significantly, another factor such as improving the selectivity-determining C–H/π interactions is contributing to increased *er*. In substrate **2.1c**, (*R*,*R*)-*p*-OMe-Min-BOX catalyzed 5% formation of the 5-membered ring, the same as (*S*,*S*)-Min-BOX, while improving *er* up to 73:27. Similar results were also observed for **2.27**, with improved enantioselectivity (83:17 relative to 79:21) while maintaining good site-selectivity.

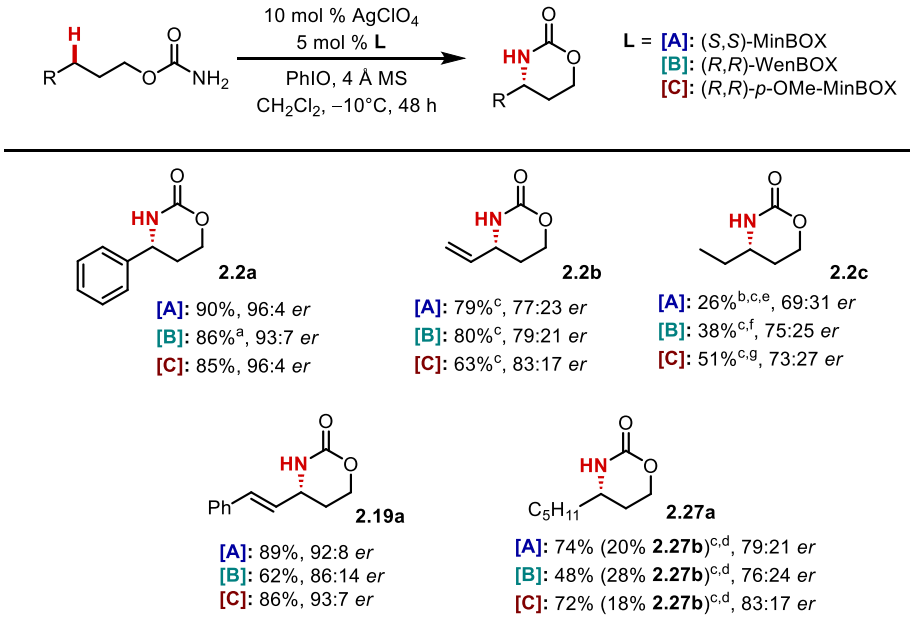

[a]20 mol % [Ag], 10 mol % **L**, room temp, 20 hrs. [b]Reaction run for 24 hours. [c]*ee* was determined after benzylation. [d]Reaction run for 18-21 hours at room temp.[e] 5% of the 5-membered ring. [f]24% of the 5-membered ring in 56:44 *er*. [g]6% of the 5-membered ring.

Table 2.5 – Effects of changing the ligand identity on enantioselectivity for each substrate class.

The response of substituents of varying steric bulk to changing the ligand from (*S*,*S*)-Min-BOX to (*R*,*R*)-Wen-BOX or (*R*,*R*)-*p*-OMe-Min-BOX, combined with computational insights into the major interactions in the transition states that control for site- and enantioselectivity, provides valuable insight for the design of second-generation ligands moving forward.

2.3. Conclusions

In conclusion, we report an enantioselective silver-catalyzed amination of diverse C–H bonds that proceeds via a nitrene transfer pathway. The designer bis(oxazoline) ligands Min-BOX and Wen-BOX are key to furnishing good *ee* for benzylic amination of both electron-rich and electron-poor aromatic rings bearing a variety of functional groups. Other attractive features include high diastereo- and enantioselectivity in the desymmetrization of benzylic C–H bonds, the ability of (*S*,*S*)-Min-BOX to override inherent substrate control to access enantioenriched 1,3-*anti*-aminoalcohols. Computational studies showed that a combination of two key features promote high *er*, including substrate distortion from a square-planar geometry at silver and stabilizing C–H/π interactions between the chiral ligand and the substrate. Computed transition state structures with substrates that furnished lower *er* showed weaker dispersion interactions that diminished stabilizing effects in TS, as well as smaller steric-induced silver nitrene distortion that led to ineffective enantiodiscrimination. These insights were employed to identify other substrates that ultimately gave high *er* for amination of allylic C–H bonds and moderate *er* for amination of unactivated alkyl C(sp^3)–H bonds. Computations also shed insight into an improved ligand design (*p*-OMe-Min-BOX), while highlighting the feasibility of using computed TS structures to rationally design more selective catalysts by fine-tuning catalyst–substrate steric

and non-covalent interactions to improve enantioinduction with challenging substrates that lack sufficient enantioselectivity control with the previous generation catalyst, Min-BOX. Finally, the utility of silver-catalyzed asymmetric benzylic amination was demonstrated in a short synthesis of the drug Dapoxetine. Ultimately, the melding of experimental and detailed computational studies revealed the importance of subtle effects on *er* and sets the stage for the predictive design of second-generation silver catalysts.

2.4. References

1. Heravi, M.; Zadsirjan V. Prescribed Drugs Containing Nitrogen Heterocycles: An Overview *RSC Adv.* **2020**, *10*, 44247–44311.
2. Ricci, A. *Amino Group Chemistry: From Synthesis to the Life Sciences*; Wiley: Weinheim, 2008.
3. For selected reviews see: (a) Collet, F.; Lescot, C.; Dauban, P. Catalytic C–H Amination: The Stereoselectivity Issue. *Chem. Soc. Rev.* **2011**, *40*, 1926–1936. (b) Uchida, T.; Hayashi, H. Recent Development in Asymmetric C-H Amination via Nitrene Transfer Reactions. *Eur. J. Org. Chem*. **2020**, 909-916. (c) Ju, M.; Schomaker, J. M. Nitrene Transfer Catalysts for Enantioselective C–N Bond Formation. *Nat. Rev. Chem.* **2021**, 5, 580-594.
4. Park, Y.; Chang, S. Asymmetric Formation of γ-Lactams via C–H Amination Enabled by Chiral Hydrogen-Bond-Donor Catalysts. *Nat. Catal*. **2019**, *2*, 3, 219–227.
5. Xing, Q.; Chan, C. M.; Yeung, Y. W.; Yu, W. Y. Ruthenium(II)-Catalyzed Enantioselective γ-Lactams Formation by Intramolecular C–H Amination of 1,4,2-Dioxazol-5-Ones. *J. Am. Chem. Soc.* **2019**, *141*, 9, 3849–3853.

6. Li, C.; Lang, K.; Lu, H.; Hu, Y.; Cui, X.; Wojtas, L.; Zhang, X. P. Catalytic Radical Process for Enantioselective Amination of C(sp^3)−H Bonds. *Angew. Chem. Int. Ed.* **2018**, *57*, 16837-16841.
7. Lang, K.; Torker, S.; Wojtas, L.; Zhang, X. P. Asymmetric Induction and Enantiodivergence in Catalytic Radical C–H Amination via Enantiodifferentiative H-Atom Abstraction and Stereoretentive Radical Substitution. *J. Am. Chem. Soc.* **2019**, *141*, 31, 12388–12396.
8. Lang, K.; Li, C.; Kim, I.; Zhang, X. P. Enantioconvergent Amination of Racemic Tertiary C–H Bonds. *J. Am. Chem. Soc.* **2020**, *142*, 20902–20911.
9. Yang, Y.; Cho, I.; Qi, X.; Liu, P.; Arnold, F. H. An Enzymatic Platform for the Asymmetric Amination of Primary, Secondary and Tertiary C(sp^3)–H Bonds. *Nat. Chem.* **2019**, *11*, 987–993.
10. Nasrallah, A.; Lazib, Y.; Boquet, V.; Darses, B.; Dauban, P. Catalytic Intermolecular C(sp^3)–H Amination with Sulfamates for the Asymmetric Synthesis of Amines. *Org. Process Res. Dev.* **2020**, *24*, 724–728.
11. Zalatan, D. N.; Du Bois, J. A chiral rhodium carboxamidate catalyst for enantioselective C–H amination. *J. Am. Chem. Soc.* **2008,** *130*, 9220-9221.
12. Milczek, E.; Boudet, N.; Blakey, S. Enantioselective C–H Amination Using Cationic Ruthenium(II)-Pybox Catalysts. *Angew. Chem., Int. Ed*. **2008**, *47*, 6825-6828.
13. Lang, K.; Torker, S.; Wojtas, L.; Zhang, X. P. Asymmetric Induction and Enantiodivergence in Catalytic Radical C–H Amination via Enantiodifferentiative H-Atom Abstraction and Stereoretentive Radical Substitution. *J. Am. Chem. Soc.* **2019**, *141*, 12388-12396.
14. Reddy, R. P. & Davies, H. M. Dirhodium tetracarboxylates derived from adamantylglycine as chiral catalysts for enantioselective C–H aminations. *Org. Lett.* **2006**, *8*, 5013-5016.

15. Zhou, Z.; Tan, Y.; Shen, X.; Ivlev, S.; Meggers, E. Catalytic Enantioselective Synthesis of β-Amino Alcohols by Nitrene Insertion. *Sci. China Chem.* **2021**, *64*, 452–458.
16. Modi, N. B.; Dresser, M. J.; Simon, M.; Lin, D.; Desai, D.; Gupta, S. Single- and Multiple-Dose Pharmacokinetics of Dapoxetine Hydrochloride, a Novel Agent for the Treatment of Premature Ejaculation *J. Clin. Pharmacol.* **2006**, *46*, 301-309.
17. Lang, L.; Lam, T.; Chen, A.; Jensen, C.; Duncan, L.; Kong, F. C.; Kurago, Z. B.; Shay, C.;Ten, Y. Circumventing AKT-Associated Radioresistance in Oral Cancer by Novel Nanoparticle-Encapsulated Capivasertib. *Cells* **2020**, *9*, 533.
18. Yan, L. et al. Discovery of N-[(4R)-6-(4-Chlorophenyl)-7-(2,4-dichlorophenyl)-2,2-dimethyl-3,4-dihydro-2H-pyrano[2,3-b]pyridin-4-yl]-5-methyl-1H-pyrazole-3-carboxamide (MK-5596) as a Novel Cannabinoid-1 Receptor (CB1R) Inverse Agonist for the Treatment of Obesity. *J. Med. Chem.* **2010**, *53*, 4028–4037.
19. Ju, M.; Zerull, E. E.; Roberts, J. M.; Huang, M.; Guzei, I. A.; Schomaker, J. M. Silver-Catalyzed Enantioselective Propargylic C–H Bond Amination through Rational Ligand Design *J. Am. Chem. Soc.* **2020**, *142*, 12930–12936.
20. DFT calculations were performed at the ωB97X-D/def2-TZVPP/CPCM(DCM)//ωB97X-D/def2-TZVPP(Ag)–def2-SVP level of theory. See the SI for computational details.
21. (a) Ma, Q.; Werner, H.-J. Accurate Intermolecular Interaction Energies Using Explicitly Correlated Local Coupled Cluster Methods [PNO-LCCSD(T)-F12]. *J. Chem. Theory Comput.* **2019**, *15*, 1044–1052. (b) Ma, Q.; Werner, H. J. Scalable Electron Correlation Methods. 8. Explicitly Correlated Open-Shell Coupled-Cluster with Pair Natural Orbitals PNO-RCCSD(T)-F12 and PNO-UCCSD(T)-F12. *J. Chem. Theory Comput.* **2021**, *17*, 902–926.

22. For previous computational studies of the mechanisms of Ag nitrene C–H insertion, see: (a) Fu, Y.; Zerull, E. E.; Schomaker, J. M.; Liu, P. Origins of catalyst-controlled selectivity in the Ag-catalyzed regiodivergent C–H amination. *J. Am. Chem. Soc.* **2022**, *144*, 2735-2746. (b) Dolan, N. S.; Scamp, R. J.; Yang, T.; Berry, J. F.; Schomaker, J. M. Catalyst-controlled and tunable, chemoselective silver-catalyzed intermolecular nitrene transfer: experimental and computational studies. *J. Am. Chem. Soc.* **2016**, *138*, 14658–14667. (c) Huang, M.; Yang, T.; Paretsky, J. D.; Berry, J. F.; Schomaker, J. M. Inverting steric effects: using ″attractive″ noncovalent interactions to direct silver-catalyzed nitrene transfer. *J. Am. Chem. Soc.* **2017**, *139*, 17376–17386. (d) Weatherly, C.; Alderson, J. M.; Berry, J. F.; Hein, J. E.; Schomaker, J. M. Catalyst-controlled nitrene transfer by tuning metal:ligand ratios: insight into the mechanisms of chemoselectivity. *Organometallics* **2017**, *36*, 1649–1661.
23. Motloch, P.; Jašík, J.; Roithová, J. Gold(I) and silver(I) π-complexes with unsaturated hydrocarbons. *Organometallics* **2021**, *40*, 1492-1502.
24. Watkins, A. L.; Hashiguchi, B. G.; Landis, C. R. Highly enantioselective hydroformylation of aryl alkenes with diazaphospholane ligands. *Org. Lett.* **2008**, *10*, 4553-4556.
25. Liu, M.-Q.; Jiang, T. ; Chen, W.-W.; Xu, M.-H. Highly enantioselective Rh/chiral sulfur-olefin-catalyzed arylation of alkyl-substituted non-benzofused cyclic *N*-sulfonyl ketimines. *Org. Chem. Front.* **2017**, *4*, 2159-2162.

2.5. Experimental Details

2.5.1 General information

All glassware was either oven-dried overnight at 130 °C or flame-dried using a Bunsen burner. All glassware was then allowed to cool to room temperature in a desiccator filled with Drierite™

as a desiccant or under a stream of dry nitrogen prior to use. Unless otherwise specified, reagents were used as obtained from Sigma-Aldrich, Oakwood Products, Alfa Aesar, Tokyo Chemical Industry, Combi-Blocks, Acros Organics or Cayman Chemicals and directly used without further purification. Diethyl ether (Et_2O), tetrahydrofuran (THF), dichloromethane (CH_2Cl_2), acetonitrile (CH_3CN), and toluene were passed through an alumina column before use. All other solvents were purified using accepted procedures from the sixth edition of "Purification of Laboratory Chemicals".[1] Air- and moisture-sensitive reactions were performed using standard Schlenk techniques under a nitrogen atmosphere. Analytical thin layer chromatography (TLC) was performed utilizing pre-coated silica gel 60 F_{24} plates containing a fluorescent indicator, while preparative chromatography was performed using SilicaFlash P60 silica gel (230-400 mesh) via Still's method.[2] Column chromatography was typically run using a gradient method employing mixtures of hexanes and ethyl acetate (EtOAc). Various stains were used to visualize reaction products, including *p*-anisaldehyde, $KMnO_4$, ceric ammonium molybdate (CAM stain) and iodine powder. ^1H NMR and ^{13}C NMR spectra were obtained using Bruker Avance-400 (400 and 100 MHz) and Bruker Avance-500 (500 and 125 MHz) spectrometers. Chemical shifts were reported with reference to residual protiated solvent peaks (note: $CDCl_3$ referenced at δ 7.26 and 77.16 ppm, respectively). High-performance liquid chromatography (HPLC) analyses were performed using Shimadzu LC-20AB. A CHIRALPAK® AD-H (0.46 cm diameter x 25 cm), CHIRALCEL® OJ-H column (0.46 cm diameter x 25 cm), CHIRALCEL® OD-H column (0.46 cm diameter x 25 cm), or CHIRALPAK® IC (0.46 cm diameter x 25 cm) was employed, maintained at a temperature of 40 °C, using ^{i}PrOH/hexane or 0.1% HCO_2H/H_2O/MeCN mobile phase. Accurate mass measurements were acquired at the University of Wisconsin-Madison using a Micromass LCT (electrospray ionization, time-of-flight analyzer or electron impact

methods). The following instrumentation in the Paul Bender Chemistry Instrumentation Center was supported by: Thermo Q Exactive™ Plus by NIH 1S10 OD020022-1; Bruker Avance-500 by a generous gift from Paul J. and Margaret M. Bender; Bruker Avance-400 by NSF CHE-1048642 and the University of Wisconsin-Madison.

2.5.2. Synthesis and characterization of carbamate ester substrates

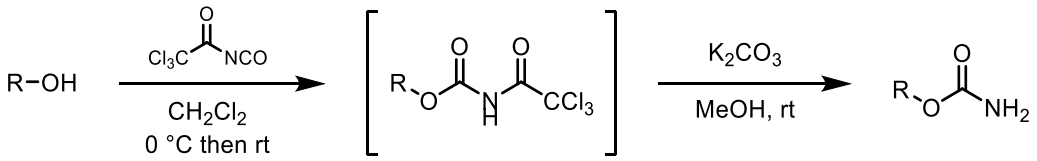

General procedure A. Trichloroacetyl isocyanate (1.43 mL, 12 mmol, 1.2 equiv) was slowly added dropwise to a solution of alcohol (10 mmol, 1.0 equiv) in 20 mL of dry CH_2Cl_2 at 0 °C. The reaction was warmed to ambient temperature and stirred until TLC indicated complete consumption of the starting alcohol (1-6 h). The solvent was then removed under reduced pressure and the crude reaction mixture was dissolved in 17 mL of MeOH. K_2CO_3 (0.14 g, 1 mmol, 0.1 equiv) was added and the mixture was stirred overnight. The mixture was diluted with CH_2Cl_2 (10 mL) and quenched by careful addition of saturated aqueous NH_4Cl (15 mL). The aqueous layer was extracted with CH_2Cl_2 (3 x 15 mL). The combined organic layers were washed with brine, dried over $MgSO_4$, filtered, and concentrated under reduced pressure. IMPORTANT NOTE: The trichloroacetamide contaminant must be removed in order to achieve reproducibility in silver-catalyzed nitrene transfer reactions. This was accomplished by re-dissolving the crude mixture in CH_2Cl_2 (150 mL) and stirring vigorously with a 1 M aqueous NaOH solution (75 mL) for 30 min. The phases were separated, and the aqueous layer was extracted with CH_2Cl_2 (3 x 50 mL). The combined organic layers were washed with brine, dried

over Na_2SO_4, filtered, and concentrated under reduced pressure. The crude product was purified by silica gel column chromatography.

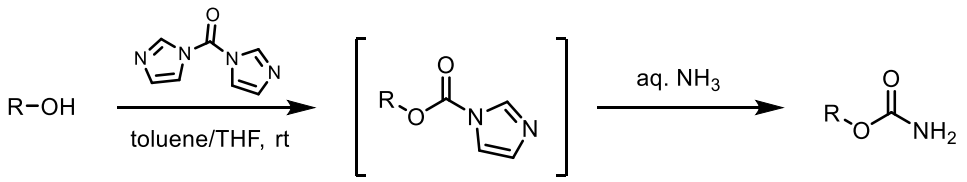

General procedure B for CDI-mediated carbamate synthesis. To a solution of alcohol (10 mmol, 1.0 equiv) in 60 mL of dry toluene was added carbonyl-diimidazole (CDI, 1.96 g, 12.0 mmol, 1.2 equiv) at room temperature. Upon complete consumption of starting alcohol as indicated by TLC (3–5 h), the solvent was evaporated under reduced pressure. The residue was dissolved in 25 mL of dry THF, and the resulting solution was stirred for 1 h before the addition of aqueous NH_4OH (28–30%, 1.2 mL). Stirring was continued overnight, then the mixture was diluted with EtOAc (50 mL). The organic layer was washed with brine, dried over Na_2SO_4, filtered, and concentrated under reduced pressure. The crude product was purified by silica gel column chromatography.

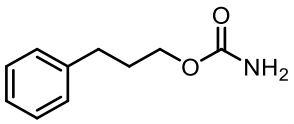

Compound 2.1a. Carbamate ester **2.1a** was prepared from 3-phenyl-1-propanol according to general procedure A on a 3.0 mmol scale. No additional purification of the white solid was necessary (538 mg, 99.9 %). The spectral data were in agreement with literature values.[3]

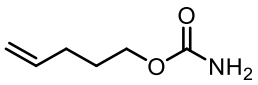

Compound 2.1b. Carbamate ester **2.1b** was prepared from 4-penten-1-ol according to general procedure A on a 3.0 mmol scale. No additional purification was necessary, and a white solid was obtained (0.36 g, 92%). The spectral data were in agreement with literature values.[3]

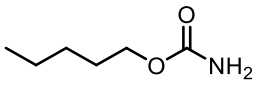

Compound 2.1c. Carbamate ester **2.1c** was prepared from 1-pentanol according to general procedure A on a 5.0 mmol scale. Purification was carried out by silica gel column chromatography (0→30% EtOAc/hexanes) to yield a white solid (0.60 g, 91%); R_f = 0.23 (30% EtOAc/hexanes). The spectral data were in agreement with literature values.[3]

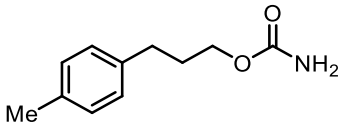

Compound 2.3. Carbamate ester **2.3** was prepared from 4-methylbenzenepropanol according to general procedure A on a 10 mmol scale. No additional purification was necessary, and the product was obtained as a white solid (1.35 g, 70%). The spectral data were in agreement with literature values.[3]

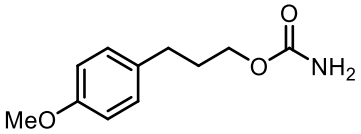

Compound 2.4. Carbamate ester **2.4** was prepared from 4-methoxybenzenepropanol according to general procedure A on a 1.5 mmol scale. No additional purification was necessary, and the product was obtained as a white solid (0.185 g, 59%). The spectral data were in agreement with literature values.[3]

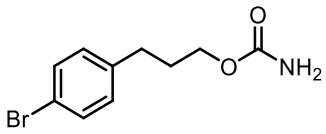

Compound 2.5. Carbamate ester **2.5** was prepared from 3-(4-bromophenyl)-1-propanol according to general procedure A on a 2.6 mmol scale. Purification was carried out by silica gel

column chromatography (0→30% EtOAc/hexanes) to yield a white solid (0.60 g, 89%); R_f = 0.24 (30% EtOAc/hexanes); ^{1}H NMR (500 MHz, $CDCl_3$) δ 7.42 – 7.38 (m, 2H), 7.08 – 7.04 (m, 2H), 4.56 (s, 2H), 4.08 (t, *J* = 6.5 Hz, 2H), 2.65 (dd, *J* = 8.7, 6.8 Hz, 2H), 1.98 – 1.85 (m, 2H); ^{13}C NMR (126 MHz, $CDCl_3$) δ 156.8, 140.3, 131.6, 130.3, 119.9, 64.4, 31.7, 30.5; HRMS (ESI) m/z calcd. for $C_{10}H_{12}BrNO_2$ $[M+H]^+$: 258.1024, found: 258.1022.

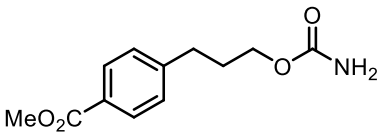

Compound 2.6. Carbamate ester **2.6** was prepared from ethyl 4-(3-hydroxypropyl)benzoate according to general procedure A on a 2.5 mmol scale. No additional purification was necessary and a white solid was obtained (432 mg, 73%); ^{1}H NMR (500 MHz, $CDCl_3$) δ 7.96 (d, *J* = 8.5 Hz, 2H), 7.26 (d, *J* = 8.3 Hz, 2H), 4.58 (s, 2H), 4.09 (t, *J* = 6.5 Hz, 2H), 3.90 (s, 3H), 2.75 (dd, *J* = 8.7, 6.7 Hz, 2H), 2.02 – 1.92 (m, 2H); ^{13}C NMR (126 MHz, $CDCl_3$) δ 167.2, 156.8, 146.9, 129.9, 128.5, 128.2, 64.4, 52.1, 32.3, 30.3.; HRMS (ESI) m/z calcd. for $C_{12}H_{15}NO_4$ $[M+Na]^+$: 260.0893, found: 260.0888.

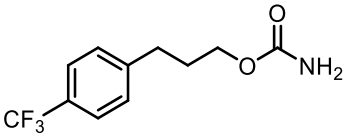

Compound 2.7. Carbamate ester **2.7** was prepared from 4-(trifluoromethyl)benzenepropanol according to general procedure A on a 10 mmol scale. No additional purification was necessary and the product was obtained as a white solid (1.88 g, 76%). The spectral data were in agreement with literature values.[3]

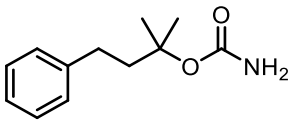

Compound 2.8. Carbamate ester **2.8** was prepared from α,α-dimethylbenzenepropanol according to general procedure A on a 5.0 mmol scale. No additional purification was necessary and a white solid was obtained (1.02 g, 98%). The spectral data were in agreement with literature values.[3]

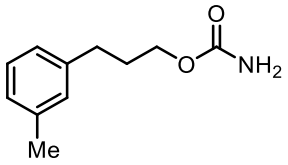

Compound 2.9. Carbamate ester **2.9** was prepared from 3-methylbenzenepropanol according to general procedure A on a 8.7 mmol scale. Purification was carried out by silica gel column chromatography (0→35% EtOAc/hexanes) to yield a white solid (1.30 g, 78%); R_f = 0.20 (30% EtOAc/hexanes). The spectral data were in agreement with literature values.[3]

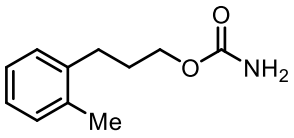

Compound 2.10. Carbamate ester **2.10** was prepared from 2-methylbenzenepropanol according to general procedure A on a 0.34 mmol scale. No additional purification was necessary and a white solid was obtained (58.8 mg, 89%); ^{1}H NMR (500 MHz, $CDCl_3$) δ 7.17 – 7.06 (m, 4H), 4.63 (s, 2H), 4.12 (t, *J* = 6.5 Hz, 2H), 2.71 – 2.64 (m, 2H), 2.31 (s, 3H), 1.96 – 1.87 (m, 2H); ^{13}C NMR (126 MHz, $CDCl_3$) δ 157.0, 139.6, 136.0, 130.4, 128.9, 126.2, 126.1, 64.9, 29.5, 29.5, 19.3; HRMS (ESI) m/z calcd. for $C_{11}H_{15}NO_2$ $[M+Na]^+$: 216.0995, found: 216.0995.

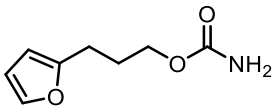

Compound 2.11. Carbamate ester **2.11** was prepared from 3-(2-furyl)-1-propanol according to general procedure A on a 5.3 mmol scale. No additional purification was necessary and a white solid was obtained (0.87 g, 97%); ^{1}H NMR (500 MHz, $CDCl_3$) δ 7.30 (dd, *J* = 1.9, 0.8 Hz, 1H), 6.28 (dd, *J* = 3.2, 1.8 Hz, 1H), 6.01 (dt, *J* = 3.2, 1.0 Hz, 1H), 4.60 (s, 2H), 4.11 (t, *J* = 6.4 Hz, 2H), 2.72 (t, *J* = 7.6 Hz, 2H), 1.98 (tt, *J* = 7.4, 6.5 Hz, 2H); ^{13}C NMR (126 MHz, $CDCl_3$) δ 156.9, 155.1, 141.1, 110.2, 105.3, 64.5, 27.5, 24.6; HRMS (ESI) m/z calcd. for $C_8H_{11}NO_3$ $[M+Na]^+$: 192.0631, found: 192.0633.

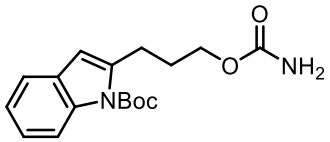

Compound 2.12. Carbamate ester **2.12** was prepared from N-Boc-3-(3-hydroxypropyl)indole according to general procedure A on a 1.9 mmol scale. No additional purification was necessary and a white solid was obtained (0.57 g, 93%); ^{1}H NMR (500 MHz, $CDCl_3$) δ 8.12 (s, 1H), 7.51 (dt, *J* = 7.7, 1.0 Hz, 1H), 7.37 (s, 1H), 7.31 (ddd, *J* = 8.4, 7.2, 1.3 Hz, 1H), 7.23 (td, *J* = 7.5, 1.1 Hz, 1H), 4.63 (s, 2H), 4.16 (t, *J* = 6.5 Hz, 2H), 2.77 (ddd, *J* = 8.8, 6.7, 1.2 Hz, 2H), 2.05 (ddt, *J* = 8.6, 7.6, 6.5 Hz, 2H), 1.67 (s, 9H); ^{13}C NMR (126 MHz, $CDCl_3$) δ 153.8, 149.5, 136.2, 127.4, 125.2, 123.4, 123.0, 120.8, 118.7, 115.9, 84.4, 65.0, 48.3, 28.3, 28.1; HRMS (ESI) m/z calcd. for $C_{17}H_{22}N_2O_4$ $[M+Na]^+$: 341.1472, found: 341.1471.

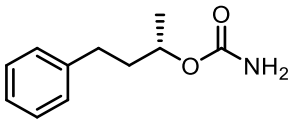

Compound 2.13. Carbamate ester **2.13** was prepared from (S)-4-phenylbutan-2-ol according to general procedure A on a 1.0 mmol scale. No additional purification was necessary and a white

solid was obtained (193 mg, 99.9%); ^{1}H NMR (500 MHz, $CDCl_3$) δ 7.31 – 7.24 (m, 2H), 7.21 – 7.15 (m, 3H), 4.84 (dqd, *J* = 7.7, 6.2, 4.9 Hz, 1H), 4.56 (s, 2H), 2.74 – 2.57 (m, 2H), 1.92 (dddd, *J* = 13.6, 10.0, 7.8, 5.7 Hz, 1H), 1.80 (dddd, *J* = 13.8, 10.1, 6.3, 5.0 Hz, 1H), 1.27 (d, *J* = 6.2 Hz, 3H); ^{13}C NMR (126 MHz, $CDCl_3$) δ 156.8, 141.8, 128.5, 128.5, 126.3, 71.6, 38.0, 31.9, 20.4; HRMS (ESI) m/z calcd. for $C_{11}H_{15}NO_2$ $[M+Na]^+$: 216.0995, found: 216.0994.

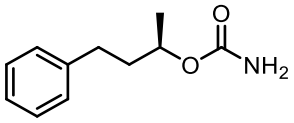

Compound 2.14. Carbamate ester **2.14** was prepared from (R)-4-phenylbutan-2-ol according to general procedure A on a 2.0 mmol scale. No additional purification was necessary and a white solid was obtained (369 mg, 95%); ^{1}H NMR (500 MHz, $CDCl_3$) δ 7.31 – 7.24 (m, 2H), 7.21 – 7.15 (m, 3H), 4.84 (dqd, *J* = 7.7, 6.2, 4.9 Hz, 1H), 4.56 (s, 2H), 2.74 – 2.57 (m, 2H), 1.92 (dddd, *J* = 13.6, 10.0, 7.8, 5.7 Hz, 1H), 1.80 (dddd, *J* = 13.8, 10.1, 6.3, 5.0 Hz, 1H), 1.27 (d, *J* = 6.2 Hz, 3H); ^{13}C NMR (126 MHz, $CDCl_3$) δ 156.8, 141.8, 128.5, 128.5, 126.0, 71.6, 38.0, 31.9, 20.4; HRMS (ESI) m/z calcd. for $C_{11}H_{15}NO_2$ $[M+Na]^+$: 216.0995, found: 216.0994.

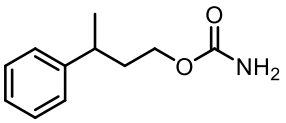

Compound 2.15. Carbamate ester **2.15** was prepared from 3-phenyl-1-butanol according to general procedure A on a 1.7 mmol scale. No additional purification was necessary and a white solid was obtained (0.33 g, 99%); ^{1}H NMR (500 MHz, $CDCl_3$) δ 7.32 – 7.27 (m, 2H), 7.22 – 7.16 (m, 3H), 4.50 (s, 2H), 4.04 – 3.92 (m, 2H), 2.84 (h, *J* = 7.1 Hz, 1H), 1.91 (q, *J* = 6.9 Hz, 2H),

1.29 (d, *J* = 7.0 Hz, 3H); ^{13}C NMR (126 MHz, $CDCl_3$) δ 156.9, 146.5, 128.6, 127.1, 126.3, 63.9, 37.3, 36.7, 22.4; HRMS (ESI) m/z calcd. for $C_{11}H_{15}NO_3$ $[M+H]^+$: 194.1176, found: 194.1174.

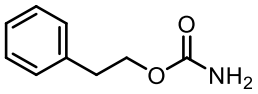

Compound 2.16. Carbamate ester **2.16** was prepared from phenylethanol according to general procedure B on a 25 mmol scale. Purification was carried out by silica gel column chromatography (0→50% EtOAc/hexanes) to yield a white solid (3.70 g, 90%); R_f = 0.30 (30% EtOAc/hexanes); ^{1}H NMR (500 MHz, $CDCl_3$) δ 7.34 – 7.28 (m, 2H), 7.23 (td, *J* = 6.3, 1.7 Hz, 3H), 4.58 (s, 2H), 4.29 (t, *J* = 7.0 Hz, 2H), 2.95 (t, *J* = 7.0 Hz, 2H); ^{13}C NMR (126 MHz, $CDCl_3$) δ 156.8, 138.0, 129.0, 128.6, 126.7, 65.7, 35.5; HRMS (ESI) m/z calcd. for $C_9H_{11}NO_2$ $[M+Na]^+$: 188.0682, found: 188.0681.

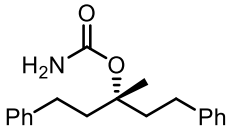

Compound 2.17. Carbamate ester **2.17** was prepared from 3-methyl-1,5-diphenylpentan-3-ol according to general procedure A on a 2.0 mmol scale. No additional purification was necessary and a white solid was obtained (523 mg, 88%); ^{1}H NMR (500 MHz, $CDCl_3$) δ 7.32 – 7.23 (m, 4H), 7.23 – 7.15 (m, 6H), 4.41 (s, 2H), 2.67 (dd, *J* = 9.5, 7.7 Hz, 4H), 2.25 (ddd, *J* = 13.9, 9.5, 7.7 Hz, 2H), 2.10 (ddd, *J* = 13.9, 9.6, 7.7 Hz, 2H), 1.56 (s, 3H); ^{13}C NMR (126 MHz, $CDCl_3$) δ 155.9, 142.3, 128.6, 128.6, 126.0, 83.5, 40.8, 30.4, 24.1; HRMS (ESI) m/z calcd. for $C_{19}H_{23}NO_2$ $[M+Na]^+$: 320.1621, found: 320.1619.

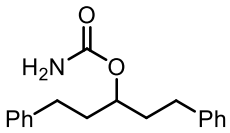

Compound 2.18. Carbamate ester **2.18** was prepared from 1,5-diphenylpentan-3-ol according to general procedure A on a 1.0 mmol scale. No additional purification was necessary and a white solid was obtained (259 mg, 91%); ^{1}H NMR (500 MHz, $CDCl_3$) δ 7.28 (td, *J* = 5.6, 2.8 Hz, 4H), 7.18 (td, *J* = 6.3, 1.6 Hz, 6H), 4.93 – 4.83 (m, 1H), 4.55 (s, 2H), 2.67 (qdd, *J* = 13.8, 9.7, 6.2 Hz, 4H), 2.01 – 1.81 (m, 4H); ^{13}C NMR (126 MHz, $CDCl_3$) δ 156.7, 141.7, 128.3, 125.9, 74.5, 36.2, 31.7; HRMS (ESI) m/z calcd. for $C_{18}H_{21}NO_2$ $[M+H]^+$: 284.1645, found: 284.1644.

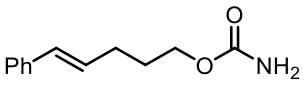

Compound 2.19. Carbamate ester **2.19** was prepared from (E)-5-phenyl-4-penten-1-ol according to general procedure A on a 0.3 mmol scale. No additional purification was necessary and a white solid was obtained (54.1 mg, 86%); ^{1}H NMR (500 MHz, $CDCl_3$) δ 7.42 – 7.38 (m, 2H), 7.08 – 7.04 (m, 2H), 4.56 (s, 2H), 4.08 (t, *J* = 6.5 Hz, 2H), 2.65 (dd, *J* = 8.7, 6.8 Hz, 2H), 1.98 – 1.85 (m, 2H); δ 7.36 – 7.32 (m, 2H), 7.29 (dd, *J* = 8.5, 6.9 Hz, 2H), 7.23 – 7.17 (m, 1H), 6.42 (dt, *J* = 15.6, 1.6 Hz, 1H), 6.21 (dt, *J* = 15.7, 6.9 Hz, 1H), 4.56 (s, 2H), 4.13 (t, *J* = 6.6 Hz, 2H), 2.34 – 2.25 (m, 2H), 1.82 (dq, *J* = 8.4, 6.7 Hz, 2H); ^{13}C NMR (126 MHz, $CDCl_3$) δ 137.6, 130.6, 129.4, 128.5, 127.0, 126.0, 64.7, 29.3, 28.6; HRMS (ESI) m/z calcd. for $C_{12}H_{15}NO_2$ $[M+H]^+$: 206.1176, found: 206.1174.

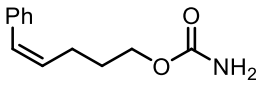

Compound 2.20. Carbamate ester **2.20** was prepared from (Z)-5-phenyl-4-penten-1-ol according to general procedure A on a 1.8 mmol scale. No additional purification was necessary and a

white solid was obtained (330 mg, 91%); ^{1}H NMR (500 MHz, $CDCl_3$) δ 7.33 (t, *J* = 7.6 Hz, 2H), 7.28 – 7.20 (m, 3H), 6.46 (dt, *J* = 11.6, 1.9 Hz, 1H), 5.65 (dt, *J* = 11.6, 7.3 Hz, 1H), 4.59 (s, 2H), 4.08 (t, *J* = 6.6 Hz, 2H), 2.41 (qd, *J* = 7.4, 1.8 Hz, 2H), 1.83 – 1.74 (m, 2H); ^{13}C NMR (126 MHz, $CDCl_3$) δ 157.0, 137.6, 131.5, 129.9, 128.9, 128.3, 126.7, 64.7, 29.3, 25.0; HRMS (ESI) m/z calcd. for $C_{12}H_{15}NO_2$ $[M+H]^+$: 206.1176, found: 206.1174.

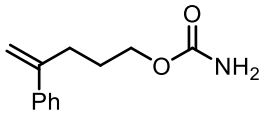

Compound 2.21. Carbamate ester **2.21** was prepared from 4-phenylpent-4-en-1-ol according to general procedure A on a 1.0 mmol scale. No additional purification was necessary and a white solid was obtained (130 mg, 63%); ^{1}H NMR (500 MHz, $CDCl_3$) δ 7.43 – 7.36 (m, 2H), 7.37 – 7.30 (m, 2H), 7.30 – 7.26 (m, 1H), 5.31 (d, *J* = 1.4 Hz, 1H), 5.09 (q, *J* = 1.3 Hz, 1H), 4.57 (s, 2H), 4.09 (t, *J* = 6.6 Hz, 2H), 2.59 (td, *J* = 7.6, 1.3 Hz, 2H), 1.80 (ddt, *J* = 8.8, 7.6, 6.5 Hz, 2H); ^{13}C NMR (126 MHz, $CDCl_3$) δ 157.0, 147.5, 141.1, 128.5, 127.6, 126.2, 113.0, 64.8, 31.7, 27.6; HRMS (ESI) m/z calcd. for $C_{12}H_{15}NO_2$ $[M+Na]^+$: 228.0995, found: 228.0992.

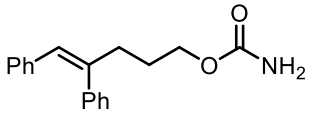

Compound 2.22. Carbamate ester **2.22** was prepared from (Z)-4,5-diphenylpent-4-en-1-ol according to general procedure A on a 2.5 mmol scale. No additional purification was necessary and a white solid was obtained (660 mg, 93%); ^{1}H NMR (500 MHz, $CDCl_3$) δ 7.30 (ddt, *J* = 8.1, 6.5, 1.3 Hz, 2H), 7.18 – 7.12 (m, 2H), 7.12 – 7.01 (m, 3H), 6.94 – 6.88 (m, 2H), 6.46 (s, 1H), 4.54 (s, 2H), 4.10 (t, *J* = 6.6 Hz, 2H), 2.57 (ddd, *J* = 7.6, 6.9, 1.3 Hz, 2H), 1.78 – 1.68 (m, 2H);

^{13}C NMR (126 MHz, $CDCl_3$) δ 141.9, 140.8, 137.2, 129.0, 128.6, 128.6, 127.84, 127.0, 126.9, 126.3, 64.7, 36.8, 27.2; HRMS (ESI) m/z calcd. for $C_{18}H_{19}NO_2$ $[M+H]^+$: 282.1489, found: 282.1487.

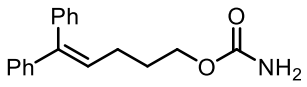

Compound 2.23. Carbamate ester **2.23** was prepared from 5,5-diphenylpent-4-en-1-ol according to general procedure A on a 1.8 mmol scale. No additional purification was necessary and a white solid was obtained (341 mg, 69%); ^{1}H NMR (500 MHz, $CDCl_3$) δ 7.43 – 7.06 (m, 11H), 6.06 (t, *J* = 7.5 Hz, 1H), 4.74 (s, 2H), 4.03 (t, J = 6.6 Hz, 2H), 2.19 (q, *J* = 7.5 Hz, 2H), 1.82 – 1.70 (m, 2H); ^{13}C NMR (126 MHz, $CDCl_3$) δ 142.6, 142.5, 140.0, 129.9, 128.4, 128.2, 128.1, 127.2, 127.0, 64.6, 29.1, 26.1; HRMS (ESI) m/z calcd. for $C_{18}H_{19}NO_2$ $[M+H]^+$: 282.1489, found: 282.1486.

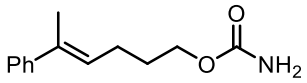

Compound 2.24. Carbamate ester **2.24** was prepared from (E)-5-phenylhex-4-en-1-ol according to general procedure A on a 0.8 mmol scale. No additional purification was necessary and a white solid was obtained (134 mg, 82%); ^{1}H NMR (500 MHz, $CDCl_3$) δ 7.40 – 7.34 (m, 2H), 7.30 (dd, *J* = 8.5, 6.8 Hz, 2H), 7.24 – 7.19 (m, 1H), 5.75 (tq, *J* = 7.5, 1.5 Hz, 1H), 4.60 (s, 2H), 4.12 (t, *J* = 6.6 Hz, 2H), 2.28 (q, *J* = 7.4 Hz, 2H), 2.04 (d, *J* = 1.4 Hz, 3H), 1.84 – 1.74 (m, 2H); ^{13}C NMR (126 MHz, $CDCl_3$) δ 156.9, 143.8, 135.7, 128.2, 127.0, 126.6, 125.6, 64.8, 28.8, 25.1, 15.8; HRMS (ESI) m/z calcd. for $C_{13}H_{17}NO_2$ $[M+NH_4]^+$: 237.1598, found: 237.1592.

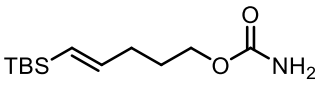

Compound 2.25. Carbamate ester **2.25** was prepared from (E)-5-t-butyldimethylsilyl-4-penten-1-ol according to general procedure A on a 2.1 mmol scale. No additional purification was necessary and a colorless oil was obtained (226 mg, 44%); ^{1}H NMR (500 MHz, $CDCl_3$) δ 6.02 (dt, *J* = 18.6, 6.2 Hz, 1H), 5.66 (dt, *J* = 18.6, 1.5 Hz, 1H), 4.58 (s, 2H), 4.07 (t, *J* = 6.7 Hz, 2H), 2.19 (tdd, *J* = 7.7, 6.2, 1.5 Hz, 2H), 1.74 (dq, *J* = 8.4, 6.8 Hz, 2H), 0.86 (s, 9H), 0.00 (s, 6H); ^{13}C NMR (126 MHz, $CDCl_3$) δ 156.9, 146.8, 127.9, 64.7, 32.9, 28.0, 26.4, 16.4, -6.1; HRMS (ESI) m/z calcd. for $C_{12}H_{25}NO_2Si$ $[M+H]^+$: 244.1727, found: 244.1725.

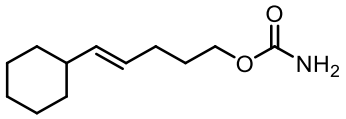

Compound 2.26. Carbamate ester **2.26** was prepared from (*E*)-5-cyclohexylpent-4-en-1-ol according to general procedure A on a 1.8 mmol scale. No additional purification was necessary and a white solid was obtained (327 mg, 86%); ^{1}H NMR (500 MHz, $CDCl_3$) δ 5.43 – 5.28 (m, 2H), 4.55 (s, 2H), 4.06 (t, *J* = 6.7 Hz, 2H), 2.08 – 2.00 (m, 2H), 1.89 (tdd, *J* = 11.0, 6.6, 3.2 Hz, 1H), 1.75 – 1.59 (m, 7H), 1.25 (dddd, *J* = 16.7, 13.5, 9.9, 3.5 Hz, 2H), 1.14 (qt, *J* = 12.6, 3.1 Hz, 1H), 1.09 – 0.98 (m, 2H); ^{13}C NMR (126 MHz, $CDCl_3$) δ 156.9, 137.5, 126.1, 64.7, 40.6, 33.2, 28.8, 28.8, 26.2, 26.1; HRMS (ESI) m/z calcd. for $C_{12}H_{21}NO_2$ $[M+H]^+$: 212.1645, found: 212.1644.

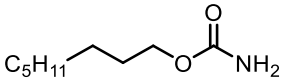

Compound 2.27. Carbamate ester **2.27** was prepared from 1-ocatanol according to general procedure A on a 3.0 mmol scale. No additional purification was necessary and a white solid was

obtained (441 mg, 85%); ^{1}H NMR (500 MHz, $CDCl_3$) δ 4.53 (s, 2H), 4.06 (t, *J* = 6.8 Hz, 2H), 1.67 – 1.55 (m, 2H), 1.40 – 1.20 (m, 10H), 0.88 (t, *J* = 6.9 Hz, 3H); ^{13}C NMR (126 MHz, $CDCl_3$) δ 156.9, 65.4, 31.8, 29.2, 29.2, 28.9, 25.8, 22.6, 14.1; HRMS (ESI) m/z calcd. for $C_9H_9NO_2$ $[M+H]^+$: 174.1489, found: 174.1486.

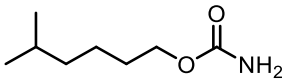

Compound 2.28. Carbamate ester **2.28** was prepared from 5-methyl-1-hexanol according to general procedure A on a 2.0 mmol scale. No additional purification was necessary and a white solid was obtained (259 mg, 81%); ^{1}H NMR (500 MHz, $CDCl_3$) δ 4.57 (s, 2H), 4.06 (t, *J* = 6.8 Hz, 2H), 1.63 – 1.57 (m, 2H), 1.54 (dt, *J* = 13.3, 6.6 Hz, 1H), 1.38 – 1.30 (m, 2H), 1.22 – 1.15 (m, 2H), 0.87 (d, *J* = 6.6 Hz, 6H); ^{13}C NMR (126 MHz, $CDCl_3$δ 157.0, 65.4, 38.5, 29.1, 27.9, 23.6, 22.5; HRMS (ESI) m/z calcd. for $C_8H_{17}NO_2$ $[M+H]^+$: 160.1332, found: 160.1331.

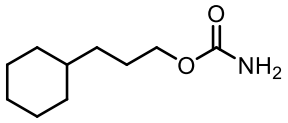

Compound 2.29. Carbamate ester **2.29** was prepared from 3-cyclohexylpropan-1-olaccording to general procedure A on a 2.1 mmol scale. No additional purification was necessary and a white solid was obtained (337.6mg, 97%); ^{1}H NMR (500 MHz, $CDCl_3$) δ 4.54 (s, 2H), 4.04 (t, *J* = 6.8 Hz, 2H), 1.74 – 1.58 (m, 4H), 1.55 (dd, *J* = 2.7, 1.1 Hz, 1H), 1.28 – 1.07 (m, 5H), 0.90 (dd, *J* = 11.3, 3.1 Hz, 1H), 0.87 (s, 1H); ^{13}C NMR (126 MHz, $CDCl_3$) δ 157.0, 65.7, 37.4, 33.4, 33.3, 26.7, 26.4, 26.3.; HRMS (ESI) m/z calcd. for $C_{10}H_{19}NO_2$ $[M+H]^+$: 186.1489, found: 186.1488.

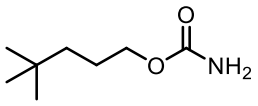

Compound 2.30. Carbamate ester **2.30** was prepared from 4,4-dimethyl-1-pentanol according to general procedure A on a 0.6 mmol scale. No additional purification was necessary and a white solid was obtained (78 mg, 78%); ^{1}H NMR (500 MHz, $CDCl_3$) δ 4.59 (s, 2H), 4.04 (t, *J* = 6.8 Hz, 2H), 1.65 – 1.52 (m, 2H), 1.26 – 1.14 (m, 2H), 0.89 (s, 9H); ^{13}C NMR (126 MHz, $CDCl_3$) δ 157.0, 66.1, 39.9, 30.0, 29.3, 24.3; HRMS (ESI) m/z calcd. for $C_8H_{17}NO_2$ $[M+Na]^+$: 182.1152, found: 182.1149.

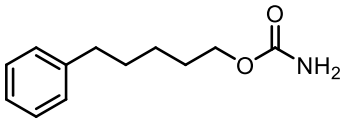

Compound 2.31. Carbamate ester **2.31** was prepared from 5-phenylpentan-1-ol according to general procedure A on a 10.0 mmol scale. No additional purification was necessary and a white solid was obtained (1.72 g, 84%); ^{1}H NMR (500 MHz, $CDCl_3$) δ 7.31 – 7.24 (m, 2H), 7.18 (ddd, *J* = 7.6, 5.9, 1.6 Hz, 3H), 4.56 (s, 2H), 4.05 (t, *J* = 6.7 Hz, 2H), 2.65 – 2.58 (m, 2H), 1.70 – 1.60 (m, 4H), 1.45 – 1.35 (m, 2H); ^{13}C NMR (126 MHz, $CDCl_3$) δ 157.0, 142.4, 128.4, 128.3, 125.7, 65.2, 35.8, 31.1, 28.8, 25.5; HRMS (ESI) m/z calcd. for $C_{12}H_{17}NO_2$ $[M+H]^+$: 208.1332, found: 208.1331.

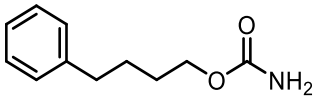

Compound 2.32. Carbamate ester **2.32** was prepared from 4-phenylbutan-1-ol according to general procedure A on a 5.1 mmol scale. No additional purification was necessary and a white

solid was obtained (819 mg, 84%); ^{1}H NMR (500 MHz, $CDCl_3$) ^{1}H NMR (500 MHz, $CDCl_3$) δ 7.28 (dd, *J* = 8.6, 6.8 Hz, 2H), 7.22 – 7.15 (m, 3H), 4.55 (s, 2H), 4.08 (t, *J* = 6.1 Hz, 2H), 2.64 (t, *J* = 7.1 Hz, 2H), 1.68 (tdq, *J* = 9.1, 4.7, 2.8 Hz, 4H); ^{13}C NMR (126 MHz, CDCl3) δ 156.9, 142.1, 128.4, 128.3, 125.8, 65.1, 35.5, 28.5, 27.6.HRMS (ESI) m/z calcd. for $C_{11}H_{15}NO_2$ $[M+H]^+$: 194.1176, found: 194.1175.

2.5.3. Asymmetric amination of activated C–H bonds

General procedure C for Ag-catalyzed asymmetric C–H amination. A pre-dried 16 x 100 mm glass test tube equipped with a magnetic stir bar was charged with $AgClO_4$ (4.2 mg, 20 μmol, 10 mol %), (*S*,*S*)-Min-BOX ligand (5.9 mg, 10 μmol, 5 mol %), and dry CH_2Cl_2 (4 mL). The test tube was capped with a rubber septum and the reaction mixture was stirred vigorously for 15 min at room temperature. Powdered 4 Å molecular sieves (200 mg, 1 g of sieves/mmol of substrate) were added, followed by carbamate ester substrate (0.2 mmol, 1.0 equiv). After adjusting the reaction temperature to –10 °C using a chiller, iodosobenzene (88 mg, 0.4 mmol, 2.0 equiv) was added in one portion and the reaction mixture was stirred at –10 °C for 48 h. The mixture was filtered through a pad of Celite® rinsing with EtOAc, and the filtrate concentrated under reduced pressure. The crude C–H amination product was purified by silica gel column chromatography.

General procedure D for benzylation of C–H amination product. To a solution of oxazinanone (1.0 equiv) in anhydrous THF (0.05 M) were added KO^{t}Bu (2.0 equiv) and BnBr (1.5 equiv). The reaction mixture was stirred at room temperature overnight and diluted with EtOAc and washed with saturated aqueous NH_4Cl. The aqueous layer was extracted with EtOAc three times. The combined organic layer was washed with brine, dried over Na_2SO_4, filtered, and

concentrated under reduced pressure. The crude material was purified by silica gel column chromatography.

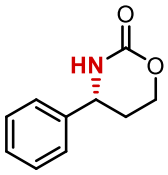

Compound 2.2a. The title compound was obtained from carbamate ester **2.1a** following the general procedure C. Silica gel column chromatography (0→100% EtOAc/hexanes) afforded oxazinanone **2.2a** as a white solid (31.9 mg, 90% yield); R_f = 0.24 (80% EtOAc/hexanes); ^{1}H NMR (500 MHz, $CDCl_3$) δ 7.45 – 7.37 (m, 2H), 7.37 – 7.29 (m, 3H), 5.27 (s, 1H), 4.71 – 4.62 (m, 1H), 4.37 – 4.27 (m, 2H), 2.32 – 2.21 (m, 1H), 2.05 – 1.95 (m, 1H); ^{13}C NMR (126 MHz, $CDCl_3$) δ 153.8, 141.2, 129.2, 128.6, 126.1, 65.2, 55.3, 30.7; HRMS (ESI) m/z calcd. for $C_{10}H_{11}NO_2$ $[M+Na]^+$: 200.0682, found: 200.0681.

The *ee* value (91%) was determined by chiral HPLC analysis of oxazinanone **2a** in comparison with an authentic sample of racemic material (CHIRALCEL® OJ-H, 5→35% iPrOH/hexane gradient over 22 min, 0.7 mL/min, 210 nm): t_R = 19.3 min (major), 20.1 min (minor).

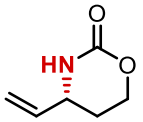

Compound 2.2b. The title compound was obtained from carbamate ester **2.1b** following the general procedure C and run for 48 h. Silica gel column chromatography (0→100% EtOAc/hexanes) afforded oxazinanone **2.2b** as a white solid (79% yield); R_f = 0.25 (80% EtOAc/hexanes); ^{1}H NMR (500 MHz, $CDCl_3$) δ 5.79 (ddd, *J* = 16.7, 10.2, 6.1 Hz, 1H), 5.47 (s, 1H), 5.32 (dt, *J* = 17.1, 1.1 Hz, 1H), 5.25 (dt, *J* = 10.3, 1.0 Hz, 1H), 4.30 (ddd, *J* = 11.1, 6.5, 3.6

Hz, 1H), 4.23 (ddd, *J* = 11.2, 8.2, 3.2 Hz, 1H), 4.06 (dtd, *J* = 7.2, 5.8, 1.5 Hz, 1H), 2.10 (dtd, *J* = 14.6, 6.0, 3.2 Hz, 1H), 1.80 (dddd, *J* = 14.1, 8.3, 7.2, 3.7 Hz, 1H); ^{13}C NMR (126 MHz, $CDCl_3$) δ 153.9, 137.6, 117.5, 64.7, 53.1, 27.4; HRMS (ESI) m/z calcd. for $C_6H_9NO_2$ $[M+H]^+$: 128.0706, found: 128.0705.

The *ee* value (54%) was determined by chiral HPLC analysis of **2.2d** obtained by benzylation of oxazinanone **2.2b** in comparison with an authentic sample of racemic material (CHIRALPAK® OJ-H, 5→35% iPrOH/hexane gradient over 22 min, 0.7 mL/min, 220 nm): t_R = 16.6 min (major), 17.4 min (minor). Use of (*R*,*R*)-Wen-BOX gave 80% yield and 58% *ee* of *ent*-**2b**.

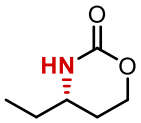

Compound 2.2c. The title compound was obtained from carbamate ester **2.1c** following the general procedure C. Silica gel column chromatography (0→100% EtOAc/hexanes) afforded oxazinanone **2.2c** as a white solid (6.7 mg, 26% yield); R_f = 0.25 (80% EtOAc/hexanes); ^{1}H NMR (500 MHz, $CDCl_3$) δ 5.53 (s, 1H), 4.33 (dt, *J* = 11.1, 4.1 Hz, 1H), 4.21 (td, *J* = 10.8, 2.9 Hz, 1H), 3.39 (dq, *J* = 11.8, 6.3 Hz, 1H), 2.05 – 1.96 (m, 1H), 1.69 (tdd, *J* = 13.8, 9.2, 4.0 Hz, 1H), 1.64 – 1.47 (m, 2H), 0.96 (t, *J* = 7.5 Hz, 3H); ^{13}C NMR (126 MHz, $CDCl_3$) δ 154.4, 65.7, 52.5, 29.4, 27.0, 9.6; HRMS (ESI) m/z calcd. for $C_6H_{11}NO_2$ $[M+H]^+$: 130.0863, found: 130.0682.

The *ee* value (40%) was determined by chiral HPLC analysis of compound **2.2e** obtained by benzylation of oxazinanone **2.2c** in comparison with an authentic sample of racemic material (CHIRALPAK® OJ-H, 5→35% iPrOH/hexane gradient over 22 min, 0.7 mL/min, 220 nm): t_R = 16.3 min (major), 16.7 min (minor).

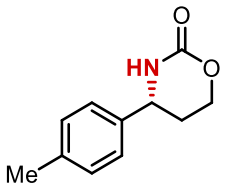

Compound 2.3a. The title compound was obtained from carbamate ester **2.3** following the general procedure C. Silica gel column chromatography (0→100% EtOAc/hexanes) afforded oxazinanone **2.3a** as a white solid (29.2 mg, 76% yield); R_f = 0.22 (80% EtOAc/hexanes); ^{1}H NMR (500 MHz, $CDCl_3$) δ 7.23 – 7.16 (m, 4H), 5.54 (s, 1H), 4.62 (ddd, *J* = 8.3, 5.1, 1.6 Hz, 1H), 4.33 – 4.22 (m, 2H), 2.23 (dq, *J* = 14.0, 4.7 Hz, 1H), 2.02 – 1.91 (m, 1H); ^{13}C NMR (126 MHz, $CDCl_3$) δ 154.1, 138.2, 138.1, 129.7, 125.9, 65.0, 54.8, 30.5, 21.1; HRMS (ESI) m/z calcd. for $C_{11}H_{13}NO_2$ $[M+Na]^+$: 214.0839, found: 214.0836.

The *ee* value (91%) was determined by chiral HPLC analysis of oxazinanone **2.3a** in comparison with an authentic sample of racemic material (CHIRALCEL® OJ-H, 5→35% iPrOH/hexane gradient over 22 min, 0.7 mL/min, 210 nm): t_R = 17.6 min (major), 18.3 min (minor).

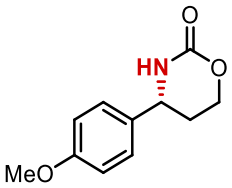

Compound 2.4a. The title compound was obtained from carbamate ester **2.4** following the general procedure C. Silica gel column chromatography (0→100% EtOAc/hexanes) afforded oxazinanone **2.4a** as a white solid (23.7 mg, 57% yield); R_f = 0.22 (80% EtOAc/hexanes); ^{1}H NMR (500 MHz, $CDCl_3$) δ 7.25 – 7.19 (m, 2H), 6.94 – 6.87 (m, 2H), 5.49 (s, 1H), 4.63 – 4.56 (m, 1H), 4.30 (dt, *J* = 8.7, 3.8 Hz, 2H), 3.81 (s, 3H), 2.25 – 2.15 (m, 1H), 2.02 – 1.91 (m, 1H);

^{13}C NMR (126 MHz, $CDCl_3$) δ 159.7, 154.0, 133.1, 127.4, 114.5, 65.2, 55.5, 54.7, 30.7; HRMS (ESI) m/z calcd. for $C_{11}H_{13}NO_3$ $[M+H]^+$: 208.0968, found: 208.0966.

The *ee* value (90%) was determined by chiral HPLC analysis of oxazinanone **2.4a** in comparison with an authentic sample of racemic material (CHIRALCEL® OJ-H, 5→28% iPrOH/hexane gradient over 22 min, 0.7 mL/min, 210 nm): t_R = 27.6 min (major), 28.7 min (minor).

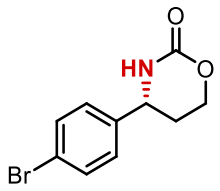

Compound 2.5a. The title compound was obtained from carbamate ester **2.5** following the general procedure C. Silica gel column chromatography (0→100% EtOAc/hexanes) afforded oxazinanone **2.5a** as a white solid (27.1 mg, 53% yield); R_f = 0.18 (80% EtOAc/hexanes); ^{1}H NMR (500 MHz, $CDCl_3$) δ 7.53 (d, *J* = 8.5 Hz, 2H), 7.21 (d, *J* = 8.6 Hz, 2H), 5.29 (s, 1H), 4.64 (t, *J* = 6.6 Hz, 1H), 4.31 (dd, *J* = 6.4, 4.4 Hz, 2H), 2.26 (dq, *J* = 13.4, 4.0 Hz, 1H), 1.96 (dq, *J* = 14.0, 6.9 Hz, 1H); ^{13}C NMR (126 MHz, $CDCl_3$) δ 153.5, 140.1, 132.3, 127.7, 122.4, 64.9, 54.7, 30.4; HRMS (ESI) m/z calcd. for $C_{10}H_{10}BrNO_2$ $[M+H]^+$: 255.9968, found: 255.9963.

The *ee* value (88%) was determined by chiral HPLC analysis of oxazinanone **2.5a** in comparison with an authentic sample of racemic material (CHIRALCEL® IC, 5→80% H_2O/acetonitrile (0.1% formic acid) gradient over 20 min, 0.7 mL/min, 210 nm): t_R = 24.4 min (major), 24.7 min (minor).

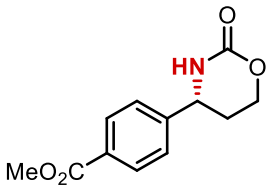

Compound 2.6a. The title compound was obtained from carbamate ester **2.6** following the general procedure C. Silica gel column chromatography (0→100% EtOAc/hexanes) afforded oxazinanone **2.6a** as a white solid (24.1 mg, 51% yield); R_f = 0.17 (80% EtOAc/hexanes); ^{1}H NMR (400 MHz, $CDCl_3$) δ 8.05 (d, *J* = 8.4 Hz, 2H), 7.41 (d, *J* = 8.4 Hz, 2H), 6.26 (s, 1H), 4.74 (t, *J* = 6.3 Hz, 1H), 4.33 – 4.19 (m, 2H), 3.92 (s, 3H), 2.29 (dtd, *J* = 13.8, 7.1, 4.2 Hz, 1H), 1.96 (dtd, *J* = 13.4, 7.8, 3.7 Hz, 1H); ^{13}C NMR (101 MHz, $CDCl_3$) δ 166.5, 154.2, 146.1, 130.3, 130.2, 126.1, 64.7, 54.5, 52.3, 30.1; HRMS (ESI) m/z calcd. for $C_{12}H_{13}NO_4$ $[M+H]^+$: 236.0917, found: 236.0913.

The *ee* value (91%) was determined by chiral HPLC analysis of oxazinanone **2.6a** in comparison with an authentic sample of racemic material (CHIRALCEL® OJ-H, 5→38% iPrOH/hexane gradient over 22 min, 0.7 mL/min, 210 nm): t_R = 27.6 min (major), 28.7 min (minor).

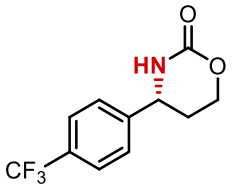

Compound 2.7a. The title compound was obtained from carbamate ester **2.7** following the general procedure C. Silica gel column chromatography (0→100% EtOAc/hexanes) afforded oxazinanone **2.7a** as a colorless oil (34.2 mg, 70% yield); R_f = 0.15 (80% EtOAc/hexanes); ^{1}H NMR (500 MHz, $CDCl_3$) δ 7.67 (d, *J* = 8.1 Hz, 2H), 7.47 (d, *J* = 8.1 Hz, 2H), 5.43 (s, 1H), 4.76 (td, *J* = 6.6, 6.1, 3.0 Hz, 1H), 4.37 – 4.26 (m, 2H), 2.32 (dtdd, *J* = 14.2, 5.2, 3.7, 0.9 Hz, 1H),

1.99 (dtd, *J* = 14.2, 7.9, 4.8 Hz, 1H); ^{13}C NMR (126 MHz, $CDCl_3$) δ 153.6, 145.2, δ 131.0 (q, *J* = 32.6 Hz), 126.6, 126.3 (q, *J* = 3.7 Hz), 124.0 (q, *J* = 271.8 Hz), 64.9, 54.9, 30.5; ^{19}F NMR (377 MHz, $CDCl_3$) δ -62.66; HRMS (ESI) m/z calcd. for $C_{11}H_{10}F_3NO_2$ $[M+H]^+$: 246.0736, found: 246.0734.

The *ee* value (86%) was determined by chiral HPLC analysis of oxazinanone **2.7a** in comparison with an authentic sample of racemic material (CHIRALCEL® OJ-H, 5→35% iPrOH/hexane gradient over 22 min, 0.7 mL/min, 220 nm): t_R = 19.2 min (minor), 20.3 min (major).

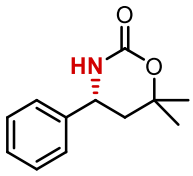

Compound 2.8a. The title compound was obtained from carbamate ester **2.8** following the general procedure C. Silica gel column chromatography (0→100% EtOAc/hexanes) afforded oxazinanone **2.8a** as a white solid (39.9 mg, 97% yield); R_f = 0.42 (80% EtOAc/hexanes); ^{1}H NMR (500 MHz, $CDCl_3$) δ 7.41 – 7.29 (m, 5H), 5.85 (s, 1H), 4.61 (dd, *J* = 11.8, 4.8 Hz, 1H), 2.01 (ddd, *J* = 14.0, 4.8, 1.6 Hz, 1H), 1.82 (dd, *J* = 13.9, 11.8 Hz, 1H), 1.51 (s, 3H), 1.42 (s, 3H); ^{13}C NMR (126 MHz, $CDCl_3$) 154.0, 141.0, 129.2, 128.6, 126.3, 78.7, 53.2, 42.2, 29.6, 25.4; HRMS (ESI) m/z calcd. for $C_{12}H_{15}NO_2$ $[M+Na]^+$: 228.0995, found: 228.0993.

The *ee* value (86%) was determined by chiral HPLC analysis of oxazinanone **2.8a** in comparison with an authentic sample of racemic material (CHIRALCEL® OJ-H, 5→35% iPrOH/hexane gradient over 22 min, 0.7 mL/min, 210 nm): t_R = 13.6 min (major), 14.9 min (minor).

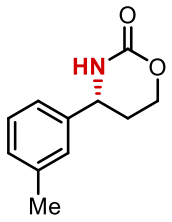

Compound 2.9a. The title compound was obtained from carbamate ester **2.9** following the general procedure C. Silica gel column chromatography (0→100% EtOAc/hexanes) afforded oxazinanone **2.9a** as a white solid (34.0 mg, 89% yield); R_f = 0.21 (80% EtOAc/hexanes); ^{1}H NMR (500 MHz, $CDCl_3$) δ 7.27 (m, *J* = 7.7 Hz, 1H), 7.13 (m, *J* = 7.2 Hz, 3H), 5.60 (s, 1H), 4.62 (ddd, *J* = 7.2, 5.2, 1.5 Hz, 1H), 4.37 – 4.24 (m, 2H), 2.37 (s, 3H), 2.25 (dq, *J* = 14.0, 4.9 Hz, 1H), 1.98 (dp, *J* = 13.6, 4.5, 3.8 Hz, 1H); ^{13}C NMR (126 MHz, $CDCl_3$) δ 154.1, 141.2, 139.0, 129.2, 129.0, 126.7, 123.2, 65.1, 55.1, 55.1, 30.5, 21.5; HRMS (ESI) m/z calcd. for $C_{11}H_{13}NO_2$ $[M+H]^+$: 192.1019, found: 192.1017.

The *ee* value (90%) was determined by chiral HPLC analysis of oxazinanone **2.9a** in comparison with an authentic sample of racemic material (CHIRALCEL® OJ-H, 5→35% iPrOH/hexane gradient over 22 min, 0.7 mL/min, 210 nm): t_R = 17.9 min (major), 18.6 min (minor).

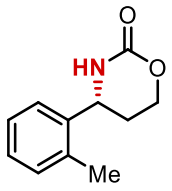

Compound 2.10a. The title compound was obtained from carbamate ester **2.10** following the general procedure C. Silica gel column chromatography (0→100% EtOAc/hexanes) afforded oxazinanone **2.10a** as a white solid (23.0 mg, 60% yield); R_f = 0.22 (80% EtOAc/hexanes); ^{1}H NMR (500 MHz, $CDCl_3$) δ 7.41 (d, *J* = 7.6 Hz, 1H), 7.27 (t, *J* = 7.5 Hz, 1H), 7.23 (t, *J* = 7.3 Hz, 2H), 7.18 (d, *J* = 7.6 Hz, 1H), 5.46 (s, 1H), 4.90 (ddd, *J* = 7.3, 5.3, 1.8 Hz, 1H), 4.37 – 4.24 (m,

2H), 2.34 (s, 3H), 2.28 (dtd, *J* = 14.7, 5.7, 3.5 Hz, 1H), 1.89 (dtd, *J* = 14.6, 7.3, 4.0 Hz, 1H); ^{13}C NMR (126 MHz, $CDCl_3$) δ 154.3, 139.1, 134.5, 131.2, 128.2, 126.9, 125.6, 64.8, 51.6, 28.5, 19.0; HRMS (ESI) m/z calcd. for $C_{11}H_{13}NO_2$ $[M+Na]^+$: 214.0839, found: 214.0836.

The *ee* value (72%) was determined by chiral HPLC analysis of oxazinanone **2.10a** in comparison with an authentic sample of racemic material (CHIRALCEL® OJ-H, 5→35% iPrOH/hexane gradient over 22 min, 0.7 mL/min, 220 nm): t_R = 18.0 min (major), 19.4 min (minor).

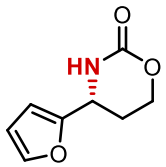

Compound 2.11a. The title compound was obtained from carbamate ester **2.11** following the general procedure C. Silica gel column chromatography (0→100% EtOAc/hexanes) afforded oxazinanone **2.11a** as a yellowish solid (17.7 mg, 53% yield); R_f = 0.21 (80% EtOAc/hexanes); ^{1}H NMR (500 MHz, $CDCl_3$) δ 7.39 (dd, *J* = 1.8, 0.8 Hz, 1H), 6.36 (dd, *J* = 3.3, 1.8 Hz, 1H), 6.30 (dt, *J* = 3.3, 0.9 Hz, 1H), 5.46 (s, 1H), 4.76 – 4.69 (m, 1H), 4.41 – 4.26 (m, 2H), 2.35 – 2.24 (m, 1H), 2.24 – 2.14 (m, 1H); ^{13}C NMR (126 MHz, $CDCl_3$) δ 153.3, 153.3, 142.9, 110.6, 107.1, 64.8, 48.8, 26.4; HRMS (ESI) m/z calcd. for $C_8H_9NO_3$ $[M+H]^+$: 168.0655, found: 168.0654.

The *ee* value (84%) was determined by chiral HPLC analysis of oxazinanone **2.11a** in comparison with an authentic sample of racemic material (CHIRALCEL® OJ-H, 5→35% iPrOH/hexane gradient over 22 min, 0.7 mL/min, 210 nm): t_R = 18.0 min (major), 19.1 min (minor).

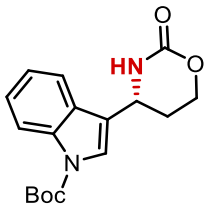

Compound 2.12a. The title compound was obtained from carbamate ester **2.12** following the general procedure C (2x higher catalyst loading) on a 0.1 mmol scale. Silica gel column chromatography (0→100% EtOAc/hexanes) afforded oxazinanone **2.12a** as a yellow oil (21.0 mg, 66% yield); R_f = 0.22 (80% EtOAc/hexanes); ^{1}H NMR (500 MHz, $CDCl_3$) δ 8.19 (d, *J* = 8.4 Hz, 1H), 7.59 (s, 1H), 7.51 (d, *J* = 7.8 Hz, 1H), 7.36 (ddd, *J* = 8.4, 7.2, 1.2 Hz, 1H), 7.29 – 7.23 (m, 1H), 5.69 (s, 1H), 5.00 – 4.93 (m, 1H), 4.42 – 4.28 (m, 2H), 2.35 (dtd, *J* = 14.8, 6.0, 3.4 Hz, 1H), 2.21 (dtd, *J* = 14.2, 7.5, 3.6 Hz, 1H), 1.68 (s, 9H); ^{13}C NMR (126 MHz, $CDCl_3$) δ 153.9, 149.5, 136.3, 127.5, 125.3, 123.4, 123.1, 120.8, 118.7, 115.9, 84.5, 65.0, 48.3, 28.3, 28.1; HRMS (ESI) m/z calcd. for $C_{17}H_{20}N_2O_2$ $[M+H]^+$: 317.1496, found: 317.1493.

The *ee* value (72%) was determined by chiral HPLC analysis of oxazinanone **2.12a** in comparison with an authentic sample of racemic material (CHIRALCEL® OJ-H, 5→35% iPrOH/hexane gradient over 22 min, 1 mL/min, 210 nm): t_R = 19.8 min (major), 21.0 min (minor).

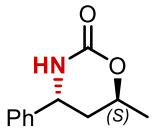

Compound 2.13a. The title compound was obtained from carbamate ester **2.13** following the general procedure C. Silica gel column chromatography (0→100% EtOAc/hexanes) afforded oxazinanone **2.13a** as a white solid mixture of diastereomers (30.5 mg, 80% yield, 5.7:1 *anti:syn*); oxazinanone **2.13a-*anti*:** R_f = 0.29 (80% EtOAc/hexanes); ^{1}H NMR (500 MHz, $CDCl_3$)

δ 7.41 – 7.27 (m, 5H), 6.31 (s, 1H), 4.73 (dt, *J* = 6.4, 3.5 Hz, 1H), 4.34 (dqt, *J* = 8.8, 6.1, 2.6 Hz, 1H), 2.10 (ddd, *J* = 14.0, 9.8, 5.9 Hz, 1H), 1.96 (dt, *J* = 14.0, 3.3 Hz, 1H), 1.31 (d, *J* = 6.4 Hz, 3H); ^{13}C NMR (126 MHz, $CDCl_3$) δ 154.8, 142.2, 128.9, 127.9, 126.0, 70.0, 52.6, 36.0, 20.6; HRMS (ESI) m/z calcd. for $C_{11}H_{13}NO_2$ $[M+H]^+$: 192.1019, found: 192.1017.

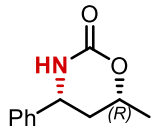

Compound 2.14a. The title compound was obtained from carbamate ester **2.14** following the general procedure C. Silica gel column chromatography (0→100% EtOAc/hexanes) afforded oxazinanone **2.14a** as a white solid mixture of diastereomers (34.9 mg, 91% yield, >20:1 *syn:anti*); oxazinanone **2.14a-*syn*:** R_f = 0.33 (80% EtOAc/hexanes); ^{1}H NMR (500 MHz, $CDCl_3$) δ 7.42 – 7.27 (m, 5H), 5.64 (s, 1H), 4.57 (dd, *J* = 11.6, 4.7 Hz, 1H), 4.51 (dtd, *J* = 12.6, 6.3, 1.9 Hz, 1H), 2.14 (ddt, *J* = 13.9, 4.1, 1.9 Hz, 1H), 1.71 (dt, *J* = 14.0, 11.6 Hz, 1H), 1.38 (d, *J* = 6.3 Hz, 3H); ^{13}C NMR (126 MHz, $CDCl_3$) δ 154.5, 140.9, 129.2, 128.6, 126.1, 73.7, 55.6, 38.6, 21.0; HRMS (ESI) m/z calcd. for $C_{11}H_{13}NO_2$ $[M+H]^+$: 192.1019, found: 192.1018.

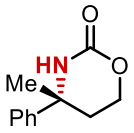

Compound 2.15a. The title compound was obtained from carbamate ester **2.15** following the general procedure C. Silica gel column chromatography (0→100% EtOAc/hexanes) afforded oxazinanone **2.15a** as a white solid (18.6 mg, 49% yield); R_f = 0.29 (80% EtOAc/hexanes); ^{1}H NMR (500 MHz, $CDCl_3$) δ 7.38 (dd, *J* = 4.1, 1.3 Hz, 4H), 7.29 (hept, *J* = 3.8 Hz, 1H), 6.10 (s, 1H), 4.19 (dt, *J* = 11.3, 3.9 Hz, 1H), 3.90 (td, *J* = 11.0, 3.5 Hz, 1H), 2.25 – 2.11 (m, 2H), 1.66 (s,

3H); ^{13}C NMR (126 MHz, $CDCl_3$) δ 154.2, 145.3, 128.9, 127.6, 127.6, 125.2, 64.04 57.4, 36.2, 30.9; HRMS (ESI) m/z calcd. for $C_{13}H_{17}NO_2$ $[M+H]^+$: 192.1019, found: 192.1016.

The *ee* value (48%) was determined by chiral HPLC analysis of oxazinanone **2.15a** in comparison with an authentic sample of racemic material (CHIRALCEL® AD-H, 5→60% iPrOH/hexane gradient over 22 min, 0.7 mL/min, 210 nm): t_R = 12.9 min (major), 13.8 min (minor).

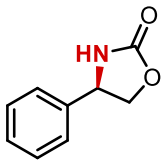

Compound 2.16a. The title compound was obtained from carbamate ester **2.16** following the general procedure C on a 0.10 mmol scale for 18 hours at room temperature. Silica gel column chromatography (0→100% EtOAc/hexanes) afforded oxazinanone **2.16a** as a white solid (13.6 mg, 83% yield); R_f = 0.54 (80% EtOAc/hexanes); ^{1}H NMR (500 MHz, $CDCl_3$) δ 7.46 – 7.31 (m, 5H), 5.65 (s, 1H), 4.99 – 4.91 (t, *J* = 8.0 Hz, 1H), 4.74 (t, *J* = 8.7 Hz, 1H), 4.20 (dd, *J* = 8.6, 6.9 Hz, 1H); ^{13}C NMR (126 MHz, $CDCl_3$) δ 159.4, 139.4, 129.3, 128.9, 126.1, 72.5, 56.4; HRMS (ESI) m/z calcd. for $C_9H_9NO_2$ $[M+Na]^+$: 186.0526, found: 186.0524.

The *ee* value (34%) was determined by chiral HPLC analysis of oxazinanone **2.16a** in comparison with an authentic sample of racemic material (CHIRALCEL® OJ-H, 5→35% iPrOH/hexane gradient over 22 min, 0.7 mL/min, 210 nm): t_R = 17.4 min (minor), 18.2 min (major).

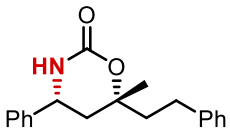

Compound 2.17a. The title compound was obtained from carbamate ester **2.17** following the general procedure C. Silica gel column chromatography (0→100% EtOAc/hexanes) afforded oxazinanone **2.17a** as a white solid mixture of diastereomers (51.1 mg, 87% yield, 8:1 *syn:anti*).

Oxazinanone **2.17a-*syn***: R_f = 0.50 (80% EtOAc/hexanes); ^{1}H NMR (500 MHz, $CDCl_3$) δ 7.43 – 7.33 (m, 5H), 7.30 – 7.24 (m, 2H), 7.21 – 7.14 (m, 3H), 5.26 (s, 1H), 4.67 (dd, *J* = 11.6, 4.8 Hz, 1H), 2.83 – 2.70 (m, 2H), 2.05 – 1.88 (m, 4H), 1.57 (s, 3H); ^{13}C NMR (126 MHz, $CDCl_3$) δ 153.7, 141.4, 140.9, 129.2, 128.7, 128.5, 128.3, 126.2, 126.1, 80.3, 53.0, 44.1, 40.2, 29.5, 23.7.

Oxazinanone **2.17a-*anti***: R_f = 0.55 (80% EtOAc/hexanes); ^{1}H NMR (500 MHz, $CDCl_3$) δ 7.40 – 7.31 (m, 5H), 7.28 – 7.21 (m, 5H), 5.24 (s, 1H), 4.55 (dd, *J* = 11.8, 4.7 Hz, 1H), 2.87 (ddd, *J* = 13.7, 11.7, 4.9 Hz, 1H), 2.79 – 2.65 (m, 1H), 2.22 (ddd, *J* = 13.9, 11.6, 4.9 Hz, 1H), 2.12 (ddd, *J* = 14.2, 4.7, 1.6 Hz, 1H), 2.08 – 1.96 (m, 1H), 1.84 (dd, *J* = 14.2, 11.8 Hz, 1H), 1.49 (s, 3H); ^{13}C NMR (126 MHz, $CDCl_3$) δ 153.5, 141.3, 140.8, 129.2, 128.7, 128.6, 128.4, 126.3, 126.1, 80.6, 52.8, 41.1, 39.8, 30.2, 26.3.

HRMS (ESI) m/z calcd. for $C_{19}H_{21}NO_2$ $[M+Na]^+$: 318.1465, found: 318.1460.

The *ee* value (91%) was determined by chiral HPLC analysis of oxazinanone **2.17a** in comparison with an authentic sample of racemic material (CHIRALCEL® OJ-H, 5→35% iPrOH/hexane gradient over 22 min, 0.7 mL/min, 210 nm): t_R = 20.1 min (major), 28.1 min (minor).

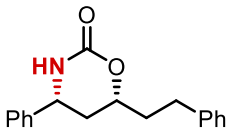

Compound 2.18a. The title compound was obtained from carbamate ester **2.18** following the general procedure C. Silica gel column chromatography (0→100% EtOAc/hexanes) afforded oxazinanone **2.18a** as a white solid as a mixture of diastereomers (42.2 mg, 74% yield, 8:1 *syn:anti*).

Oxazinanone **2.18a-*syn***: R_f = 0.35 (80% EtOAc/hexanes); ^{1}H NMR (500 MHz, $CDCl_3$) δ 7.43 – 7.32 (m, 3H), 7.30 (ddd, *J* = 9.7, 8.3, 6.7 Hz, 4H), 7.25 – 7.17 (m, 3H), 5.51 (s, 1H), 4.55 (dd, *J* = 11.5, 4.6 Hz, 1H), 4.36 (dddd, *J* = 11.8, 8.2, 4.3, 2.0 Hz, 1H), 2.92 – 2.75 (m, 2H), 2.18 – 2.00 (m, 2H), 1.95 – 1.84 (m, 1H), 1.77 (dt, *J* = 13.9, 11.6 Hz, 1H); ^{13}C NMR (126 MHz, $CDCl_3$) δ 154.3, 140.9, 140.8, 129.2, 128.6, 128.6, 128.5, 126.2, 126.0, 76.1, 55.6, 36.9, 36.8, 30.8.

HRMS (ESI) m/z calcd. for $C_{18}H_{19}NO_2$ $[M+H]^+$: 282.1489, found: 282.1487.

Oxazinanone **2.18a-*anti***: R_f = 0.55 (80% EtOAc/hexanes); ^{1}H NMR (500 MHz, $CDCl_3$) δ 7.43 – 7.36 (m, 2H), 7.39 – 7.29 (m, 1H), 7.33 – 7.26 (m, 2H), 7.26 – 7.20 (m, 2H), 7.20 – 7.14 (m, 1H), 7.17 – 7.09 (m, 2H), 5.30 (s, 1H), 4.74 (dt, *J* = 6.4, 3.6 Hz, 1H), 4.30 – 4.22 (m, 1H), 2.86 (ddd, *J* = 13.6, 10.1, 5.5 Hz, 1H), 2.68 (ddd, *J* = 13.8, 9.8, 6.3 Hz, 1H), 2.23 – 2.13 (m, 1H), 2.06 (dddd, *J* = 13.8, 9.8, 8.2, 5.6 Hz, 1H), 1.98 (dddd, *J* = 13.9, 3.9, 2.7, 1.1 Hz, 1H), 1.87 – 1.77 (m, 1H); ^{13}C NMR (126 MHz, $CDCl_3$) δ 129.0, 128.5, 128.4, 128.1, 126.1, 125.9, 73.0, 52.8, 36.4, 34.5, 31.2.

HRMS (ESI) m/z calcd. for $C_{18}H_{19}NO_2$ $[M+H]^+$: 282.1489, found: 282.1487.

The *ee* value (94%) was determined by chiral HPLC analysis of oxazinanone **2.18a-syn** in comparison with an authentic sample of racemic material (CHIRALCEL® OJ-H, 5→30%

iPrOH/hexane gradient over 22 min, 0.7 mL/min, 210 nm): t_R = 15.9 min (major), 18.7 min (minor).

The *ee* value (72%) was determined by chiral HPLC analysis of oxazinanone **2.18a-anti** in comparison with an authentic sample of racemic material (CHIRALCEL® OJ-H, 5→35% iPrOH/hexane gradient over 22 min, 0.7 mL/min, 220 nm): t_R = 24.7 min (major), 22.6 min (minor).

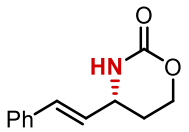

Compound 2.19a. The title compound was obtained from carbamate ester **2.19a** following the general procedure C. Silica gel column chromatography (0→100% EtOAc/hexanes) afforded oxazinanone **2.19a** as a white solid (36.2 mg, 89% yield); R_f = 0.15 (80% EtOAc/hexanes); ^{1}H NMR (500 MHz, $CDCl_3$) δ 7.40 – 7.33 (m, 2H), 7.33 – 7.27 (m, 1H), 7.22 – 7.15 (m, 2H), 6.67 (d, *J* = 11.4 Hz, 1H), 5.59 (dd, *J* = 11.4, 9.5 Hz, 1H), 5.54 (s, 1H), 4.47 (td, *J* = 9.3, 5.0 Hz, 1H), 4.36 (dt, *J* = 11.2, 4.1 Hz, 1H), 4.23 (td, *J* = 10.9, 2.8 Hz, 1H), 2.10 – 2.02 (m, 1H), 1.96 – 1.85 (m, 1H); ^{13}C NMR (126 MHz, $CDCl_3$) δ 153.7, 135.6, 133.2, 130.6, 128.6, 128.4, 127.8, 65.5, 48.6, 28.1; HRMS (ESI) m/z calcd. for $C_{12}H_{13}NO_2$ $[M+H]^+$: 204.1019, found: 204.1018.

The *ee* value (83%) was determined by chiral HPLC analysis of oxazinanone **2.19a** in comparison with an authentic sample of racemic material (CHIRALCEL® OJ-H, 5→35% iPrOH/hexane gradient over 27 min, 0.7 mL/min, 210 nm): t_R = 30.9 min (major), 33.8 min (minor).

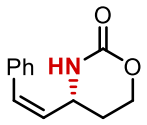

Compound 2.20a. The title compound was obtained from carbamate ester **2.20** following the general procedure C. Silica gel column chromatography (0→100% EtOAc/hexanes) afforded oxazinanone **2.20a** as a white solid (15.3 mg, 38% yield); R_f = 0.27 (80% EtOAc/hexanes); ^{1}H NMR (500 MHz, $CDCl_3$) δ 7.37 (dd, *J* = 8.1, 6.7 Hz, 2H), 7.34 – 7.28 (m, 1H), 7.19 (dd, *J* = 7.2, 1.8 Hz, 2H), 6.68 (d, *J* = 11.4 Hz, 1H), 5.60 (dd, *J* = 11.4, 9.4 Hz, 1H), 5.22 (s, 1H), 4.49 (td, *J* = 9.3, 5.0 Hz, 1H), 4.37 (dt, *J* = 11.2, 4.1 Hz, 1H), 4.24 (td, *J* = 11.0, 2.7 Hz, 1H), 2.13 – 2.03 (m, 1H), 1.92 (dtd, *J* = 14.0, 10.2, 4.0 Hz, 1H); ^{13}C NMR (126 MHz, $CDCl_3$) δ 153.4, 135.6, 133.3, 130.6, 128.6, 128.4, 127.9, 65.5, 48.7, 28.1; HRMS (ESI) m/z calcd. for $C_{12}H_{13}NO_2$ $[M+H]^+$: 204.1019, found: 204.1020.

The *ee* value (31%) was determined by chiral HPLC analysis of oxazinanone **2.20a** in comparison with an authentic sample of racemic material (CHIRALCEL® OJ-H, 5→35% iPrOH/hexane gradient over 27 min, 0.7 mL/min, 210 nm): t_R = 27.2 min (major), 29.3 min (minor).

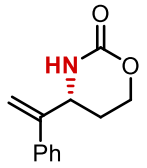

Compound 2.21a. The title compound was obtained from carbamate ester **2.21** following the general procedure C. Silica gel column chromatography (0→100% EtOAc/hexanes) afforded oxazinanone **2.21a** as a white solid (10.5 mg, 26% yield); R_f = 0.26 (80% EtOAc/hexanes); ^{1}H NMR (500 MHz, $CDCl_3$) δ 7.40 – 7.30 (m, 5H), 5.48 (s, 1H), 5.40 (d, *J* = 1.4 Hz, 2H), 4.65 – 4.57 (m, 1H), 4.29 (ddd, *J* = 11.3, 8.0, 3.2 Hz, 1H), 4.21 (ddd, *J* = 10.9, 6.9, 3.5 Hz, 1H), 2.13

(dddd, *J* = 13.8, 8.8, 5.6, 3.4 Hz, 1H), 1.76 (dtd, *J* = 13.6, 6.3, 3.2 Hz, 1H); ^{13}C NMR (126 MHz, $CDCl_3$) δ 153.8, 148.5, 138.5, 128.8, 128.4, 126.6, 114.5, 64.2, 53.4, 26.1; HRMS (ESI) m/z calcd. for $C_{12}H_{13}NO_2$ $[M+H]^+$: 204.1019, found: 204.1019.

The *ee* value (80%) was determined by chiral HPLC analysis of oxazinanone **2.21a** in comparison with an authentic sample of racemic material (CHIRALCEL® OJ-H, 5→35% iPrOH/hexane gradient over 22 min, 0.7 mL/min, 210 nm): t_R = 18.3 min (minor), 19.5 min (major).

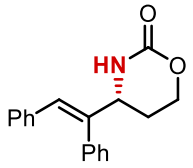

Compound 2.22a. The title compound was obtained from carbamate ester **2.22** following the general procedure C. Silica gel column chromatography (0→100% EtOAc/hexanes) afforded oxazinanone **2.22a** as a white solid (46.7 mg, 85% yield); R_f = 0.24 (80% EtOAc/hexanes); ^{1}H NMR (500 MHz, $CDCl_3$) δ 7.43 – 7.32 (m, 3H), 7.21 – 7.07 (m, 5H), 6.96 – 6.88 (m, 2H), 6.69 (d, *J* = 1.3 Hz, 1H), 5.25 (s, 1H), 4.48 – 4.41 (m, 1H), 4.33 (ddd, *J* = 10.9, 7.3, 3.4 Hz, 1H), 4.23 (ddd, *J* = 11.0, 7.7, 3.2 Hz, 1H), 2.12 – 2.02 (m, 1H), 1.84 (dtd, *J* = 14.1, 7.2, 3.4 Hz, 1H); ^{13}C NMR (126 MHz, $CDCl_3$) δ 154.0, 141.2, 137.7, 135.6, 129.3, 129.2, 129.0, 128.2, 128.1, 128.0, 127.3, 64.5, 57.0, 25.8.; HRMS (ESI) m/z calcd. for $C_{18}H_{17}NO_2$ $[M+H]^+$: 280.1332, found: 280.1330.

The *ee* value (76%) was determined by chiral HPLC analysis of oxazinanone **2.22a** in comparison with an authentic sample of racemic material (CHIRALCEL® OJ-H, 5→35% iPrOH/hexane gradient over 22 min, 0.7 mL/min, 220 nm): t_R = 21.3 min (major), 33.7 min (minor).

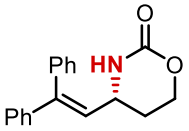

Compound 2.23a. The title compound was obtained from carbamate ester **2.23** following the general procedure C. Silica gel column chromatography (0→100% EtOAc/hexanes) afforded oxazinanone **2.23a** as a white solid (35.2 mg, 63% yield); R_f = 0.24 (80% EtOAc/hexanes); ^{1}H NMR (500 MHz, $CDCl_3$) δ 7.45 – 7.36 (m, 4H), 7.30 (dd, *J* = 4.9, 2.1 Hz, 3H), 7.23 – 7.20 (m, 2H), 7.17 – 7.11 (m, 2H), 5.96 (d, *J* = 9.4 Hz, 1H), 4.98 (s, 1H), 4.35 (dt, *J* = 11.2, 4.1 Hz, 1H), 4.21 – 4.03 (m, 3H), 2.04 – 1.86 (m, 2H); ^{13}C NMR (126 MHz, $CDCl_3$) δ 153.7, 145.8, 140.7, 138.5, 129.3, 128.7, 128.4, 128.2, 128.0, 127.4, 127.0, 65.4, 50.2, 28.2.; HRMS (ESI) m/z calcd. for $C_{18}H_{17}NO_2$ $[M+H]^+$: 280.1332, found: 280.1331.

The *ee* value (99%) was determined by chiral HPLC analysis of oxazinanone **2.23a** in comparison with an authentic sample of racemic material (CHIRALCEL® OJ-H, 5→35% iPrOH/hexane gradient over 45 min, 0.7 mL/min, 220 nm): t_R = 30.1 min (major), 36.4 min (minor).

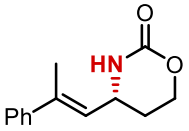

Compound 2.24a. The title compound was obtained from carbamate ester **2.24** following the general procedure C. Silica gel column chromatography (0→100% EtOAc/hexanes) afforded oxazinanone **2.24a** as a white solid (34.0 mg, 78% yield); R_f = 0.15 (80% EtOAc/hexanes); ^{1}H NMR (500 MHz, $CDCl_3$) δ 7.42 – 7.27 (m, 5H), 5.67 (dq, *J* = 8.9, 1.5 Hz, 1H), 5.22 (s, 1H), 4.50 – 4.42 (m, 1H), 4.39 (dt, *J* = 11.2, 4.1 Hz, 1H), 4.31 (td, *J* = 10.8, 2.8 Hz, 1H), 2.11 (d, *J* = 1.4 Hz, 4H), 1.89 (dtd, *J* = 13.9, 9.7, 4.0 Hz, 1H); ^{13}C NMR (126 MHz, $CDCl_3$) δ 153.6, 142.0,

139.4, 128.4, 127.8, 126.80, 125.8, 65.6, 49.6, 27.9, 16.3; HRMS (ESI) m/z calcd. for $C_{13}H_{15}NO_2$ $[M+H]^+$: 218.1176, found: 218.1172.

The *ee* value (77%) was determined by chiral HPLC analysis of oxazinanone **2.24a** in comparison with an authentic sample of racemic material (CHIRALCEL® OJ-H, 5→35% iPrOH/hexane gradient over 27 min, 0.7 mL/min, 220 nm): t_R = 31.9 min (major), 34.0 min (minor).

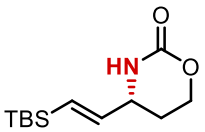

Compound 2.25a. The title compound was obtained from carbamate ester **2.25** following the general procedure C. Silica gel column chromatography (0→100% EtOAc/hexanes) afforded oxazinanone **2.25a** as a white solid (44.8 mg, 93% yield); R_f = 0.32 (80% EtOAc/hexanes); ^{1}H NMR (500 MHz, $CDCl_3$) δ 5.94 (apparent d, *J* = 3.2 Hz, 2H), 5.29 (s, 1H), 4.29 – 4.18 (m, 2H), 4.10 – 4.02 (m, 1H), 2.16 – 2.07 (m, 1H), 1.78 (dtd, *J* = 14.3, 7.3, 3.9 Hz, 1H), 0.86 (s, 9H), 0.03 (s, 6H); ^{13}C NMR (126 MHz, $CDCl_3$) δ 153.7, 145.6, 130.1, 64.5, 54.6, 27.1, 26.3, 16.4, -6.2; HRMS (ESI) m/z calcd. for $C_{12}H_{23}NO_2Si$ $[M+H]^+$: 242.1571, found: 242.1569.

The *ee* value (94%) was determined by chiral HPLC analysis of oxazinanone **2.25a** in comparison with an authentic sample of racemic material (CHIRALCEL® OJ-H, 5→20% iPrOH/hexane gradient over 12 min, 0.7 mL/min, 210 nm): t_R = 9.2 min (major), 10.4 min (minor).

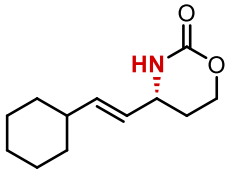

Compound 2.26a. The title compound was obtained from carbamate ester **2.26** following the general procedure C. Silica gel column chromatography (0→100% EtOAc/hexanes) afforded oxazinanone **2.26a** as a white solid (22.5 mg, 54% yield); R_f = 0.29 (80% EtOAc/hexanes); ^{1}H NMR (500 MHz, $CDCl_3$) δ 5.66 (dd, *J* = 15.4, 6.7 Hz, 1H), 5.32 (ddd, *J* = 15.4, 6.9, 1.4 Hz, 1H), 5.06 (s, 1H), 4.30 (ddd, *J* = 11.2, 5.7, 3.8 Hz, 1H), 4.21 (ddd, *J* = 11.5, 9.1, 3.0 Hz, 1H), 4.02 – 3.90 (m, 1H), 2.09 – 2.00 (m, 1H), 1.96 (tdd, *J* = 10.6, 6.8, 3.2 Hz, 1H), 1.82 – 1.60 (m, 6H), 1.32 – 1.19 (m, 2H), 1.15 (dtd, *J* = 12.5, 9.2, 3.2 Hz, 1H), 1.05 (qd, *J* = 12.6, 11.9, 3.7 Hz, 2H); ^{13}C NMR (126 MHz, $CDCl_3$) δ 153.6, 140.1, 126.9, 64.9, 53.0, 40.1, 32.7, 32.7, 28.0, 26.0, 25.9; HRMS (ESI) m/z calcd. for $C_{12}H_{19}NO_2$ $[M+H]^+$: 210.1489, found: 210.1487.

The *ee* value (85%) was determined by chiral HPLC analysis of compound **2.26b** obtained by benzylation of oxazinanone **2.26a** in comparison with an authentic sample of racemic material (CHIRALCEL® OJ-H, 5→20% iPrOH/hexane gradient over 22 min, 0.7 mL/min, 220 nm): t_R = 13.7 min (major), 14.3 min (minor).

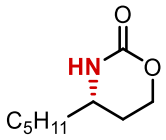

Compound 2.27a. The title compound was obtained from carbamate ester **2.27** following the general procedure C on a 0.10 mmol scale for 20 hours at room temperature. Silica gel column chromatography (0→100% EtOAc/hexanes) afforded oxazinanone **2.27a** as a colorless oil (12.6 mg, 74% yield); R_f = 0.24 (80% EtOAc/hexanes); ^{1}H NMR (500 MHz, $CDCl_3$) δ 5.51 (s, 1H),

4.33 (dt, *J* = 11.1, 4.2 Hz, 1H), 4.21 (td, *J* = 10.8, 2.8 Hz, 1H), 3.56 – 3.38 (m, 1H), 2.00 (dtdd, *J* = 13.6, 4.4, 3.6, 2.8, 1.2 Hz, 1H), 1.76 – 1.56 (m, 1H), 1.56 – 1.44 (m, 2H), 1.39 – 1.16 (m, 7H), 0.91 – 0.84 (m, 3H); ^{13}C NMR (126 MHz, $CDCl_3$) δ 154.2, 65.6, 51.0, 36.4, 31.5, 27.3, 24.7, 22.5, 13.9; HRMS (ESI) m/z calcd. for $C_9H_{17}NO_2$ $[M+H]^+$: 172.1332, found: 172.1332.

The *ee* value (58%) was determined by chiral HPLC analysis of compound **2.27b** obtained by benzylation of oxazinanone **2.27a** in comparison with an authentic sample of racemic material (CHIRALCEL® OD-H, 5→12% iPrOH/hexane gradient over 22 min, 0.7 mL/min, 210 nm): t_R = 19.6 min (major), 20.3 min (minor).

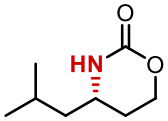

Compound 2.28a. The title compound was obtained from carbamate ester **2.28** following the general procedure C on a 0.10 mmol scale for 20 hours at room temperature. Silica gel column chromatography (0→100% EtOAc/hexanes) afforded 95xazinanones **2.28a** as a white solid (8.4 mg, 53% yield); R_f = 0.21 (80% EtOAc/hexanes); ^{1}H NMR (500 MHz, $CDCl_3$) δ 5.35 (s, 1H), 4.34 (dt, *J* = 11.1, 4.2 Hz, 1H), 4.22 (td, *J* = 10.8, 2.8 Hz, 1H), 3.54 (dddd, *J* = 12.2, 8.9, 5.5, 1.1 Hz, 1H), 2.00 (dtdd, *J* = 13.6, 4.5, 2.8, 1.3 Hz, 1H), 1.72 – 1.62 (m, 2H), 1.46 – 1.31 (m, 2H), 0.94 (d, *J* = 6.6 Hz, 6H); ^{13}C NMR (126 MHz, $CDCl_3$) δ 154.1, 65.6, 49.0, 45.6, 27.8, 24.2, 22.7, 22.3; HRMS (ESI) m/z calcd. For $C_8H_{15}NO_2$ $[M+H]^+$: 158.1176, found: 158.1175.

The *ee* value (54%) was determined by chiral HPLC analysis of compound **2.28b** obtained by benzylation of oxazinanone **2.28a** in comparison with an authentic sample of racemic material (CHIRALCEL® OJ-H, 5→20% iPrOH/hexane gradient over 22 min, 0.7 mL/min, 210 nm): t_R = 16.5 min (major), 17.7 min (minor).

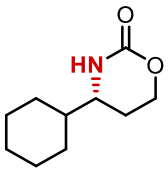

Compound 2.29a. The title compound was obtained from carbamate ester **2.29** following the general procedure C. Silica gel column chromatography (0→100% EtOAc/hexanes) afforded oxazinanone **2.29a** as a white solid (32.3 mg, 88% yield); R_f = 0.24 (80% EtOAc/hexanes); ^{1}H NMR (500 MHz, $CDCl_3$) δ 5.15 (s, 1H), 4.42 – 4.27 (m, 1H), 4.18 (t, *J* = 10.7 Hz, 1H), 3.24 (dt, *J* = 11.2, 6.0 Hz, 1H), 1.92 (d, *J* = 13.1 Hz, 1H), 1.85 – 1.65 (m, 7H), 1.49 – 0.90 (m, 5H); ^{13}C NMR (126 MHz, $CDCl_3$) δ 154.3, 79.4, 65.7, 56.0, 42.5, 28.6, 28.3, 26.2, 25.8, 25.8, 24.6; HRMS (ESI) m/z calcd. for $C_{10}H_{17}NO_2$ $[M+H]^+$: 184.1332, found: 184.1332.

The *ee* value (65%) was determined by chiral HPLC analysis compound **2.29b** obtained by benzylation of oxazinanone **2.29a** in comparison with an authentic sample of racemic material (CHIRALCEL® IC, 35→70% H_2O/acetonitrile (0.1% formic acid) gradient over 15 min, 0.7 mL/min, 210 nm): t_R = 10.9 min (major), 10.4 min (minor).

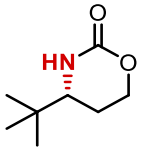

Compound 2.30a. The title compound was obtained from carbamate ester **2.30** following the general procedure C on a 0.10 mmol scale for 20 hours at room temperature. Silica gel column chromatography (0→100% EtOAc/hexanes) afforded oxazinanone **2.30a** as a white solid (9.5 mg, 60% yield); R_f = 0.21 (80% EtOAc/hexanes); ^{1}H NMR (500 MHz, $CDCl_3$) δ 5.12 (s, 1H), 4.35 (ddd, *J* = 11.0, 4.3, 2.6 Hz, 1H), 4.17 (ddd, *J* = 12.0, 11.0, 2.5 Hz, 1H), 3.21 (dd, *J* = 10.9, 5.0 Hz, 1H), 1.92 – 1.84 (m, 1H), 1.78 (dddd, *J* = 13.8, 12.0, 10.9, 4.3 Hz, 1H), 0.94 (s, 9H); ^{13}C

NMR (126 MHz, $CDCl_3$) δ 154.7, 65.9, 60.4, 33.6, 25.3, 22.9; HRMS (ESI) m/z calcd. for $C_8H_{15}NO_2$ $[M+H]^+$: 158.1176, found: 158.1173.

The *ee* value (52%) was determined by chiral HPLC analysis of compound **2.30b** obtained by benzylation of oxazinanone **2.30a** in comparison with an authentic sample of racemic material (CHIRALCEL® OJ-H, 5→20% iPrOH/hexane gradient over 22 min, 0.7 mL/min, 210 nm): t_R = 16.4 min (minor), 18.6 min (major).

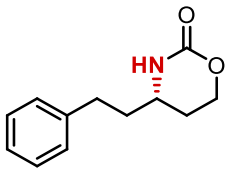

Compound 2.31a. The title compound was obtained from carbamate ester **2.31** following the general procedure D. Silica gel column chromatography (0→100% EtOAc/hexanes) afforded oxazinanone **2.31a** as a white solid (27.5 mg, 67% yield); R_f = 0.24 (80% EtOAc/hexanes); ^{1}H NMR (500 MHz, $CDCl_3$) δ 7.32 – 7.25 (m, 2H), 7.24 – 7.15 (m, 3H), 6.32 (s, 0H), 4.32 (ddd, *J* = 10.9, 5.4, 3.6 Hz, 1H), 4.24 – 4.15 (m, 1H), 3.47 (dt, *J* = 12.1, 6.0 Hz, 1H), 2.77 – 2.63 (m, 2H), 2.08 – 1.97 (m, 1H), 2.00 – 1.67 (m, 3H).; ^{13}C NMR (126 MHz, CDCl3) δ 154.6, 140.6, 128.6, 128.3, 126.3, 65.5, 50.2, 37.9, 31.4, 27.2; HRMS (ESI) m/z calcd. for $C_{12}H_{15}NO_2$ $[M+H]^+$: 206.1176 found: 206.1177.

The *ee* value (35%) was determined by chiral HPLC analysis of oxazinanone **2.31a** in comparison with an authentic sample of racemic material (CHIRALCEL® OJ-H, 5→15% iPrOH/hexane gradient over 33 min, 0.7 mL/min, 220 nm): t_R = 28.4 min (major), 31.1 min (minor).

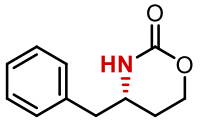

Compound 2.32a. The title compound was obtained from carbamate ester **2.32** following the general procedure D. Silica gel column chromatography (0→100% EtOAc/hexanes) afforded oxazinanone **2.32a** as a white solid (26.8 mg, 70% yield); R_f = 0.23 (80% EtOAc/hexanes); ^{1}H NMR (500 MHz, $CDCl_3$) δ 7.33 (dd, *J* = 8.1, 6.6 Hz, 2H), 7.30 – 7.23 (m, 1H), 7.21 – 7.15 (m, 2H), 5.61 (d, *J* = 17.1 Hz, 1H), 4.34 (dt, *J* = 11.3, 4.2 Hz, 1H), 4.20 (td, *J* = 10.9, 2.8 Hz, 1H), 3.76 – 3.67 (m, 1H), 2.85 (dd, *J* = 13.5, 6.4 Hz, 1H), 2.76 (ddd, *J* = 13.5, 7.8, 1.8 Hz, 1H), 2.08 – 1.95 (m, 1H), 1.78 (tdd, *J* = 13.8, 9.2, 4.0 Hz, 1H).^{13}C NMR (126 MHz, CDCl3) δ 154.1, 136.1, 129.2, 129.0, 127.2, 65.5, 52.1, 42.7, 27.3.; HRMS (ESI) m/z calcd. for $C_{11}H_{13}NO_2$ $[M+H]^+$: 192.1019, found: 192.1020.

The *ee* value (43%) was determined by chiral HPLC analysis of oxazinanone **2.32a** in comparison with an authentic sample of racemic material (CHIRALCEL® IC, 35→70% H_2O/acetonitrile (0.1% formic acid) gradient over 15 min, 0.7 mL/min, 210 nm): t_R = 10.4 min (major), 10.9 min (minor).

2.5.4. Racemic amination of chiral carbamate **13**

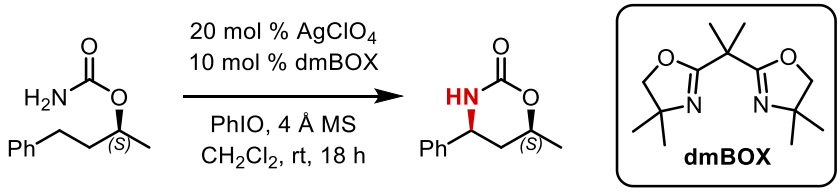

A pre-dried 1.5 dram vial equipped with a magnetic stir bar was charged with $AgClO_4$ (4.2 mg, 20 μmol, 20 mol %), dmBOX (2.4 mg, 10 μmol, 10 mol %), and dry CH_2Cl_2 (2 mL). The reaction mixture was stirred vigorously for 15 min at room temperature. Powdered 4 Å

molecular sieves (100 mg, 1 g of sieves/mmol of substrate) were added, followed by carbamate ester substrate **13** (19.3 mg, 0.1 mmol, 1.0 equiv). Iodosobenzene (44 mg, 0.2 mmol, 2.0 equiv) was added in one portion and the reaction mixture was stirred at room temperature for 18 hours. The mixture was filtered through a pad of Celite® rinsing with EtOAc, and the filtrate concentrated under reduced pressure. The yield and diastereoselectivity was determined by ^{1}H NMR, using trimethylphenyl silane as the internal standard (74%, 3.4:1 *syn*:*anti*).

2.5.5. Large scale reaction set-up

A flame-dried 250 mL round bottom flask equipped with a magnetic stir bar was charged with $AgClO_4$ (82.9 mg, 0.4 mmol, 10 mol %), (*R*,*R*)-Min-BOX ligand (117 mg, 0.2 mmol, 5 mol %), and dry CH_2Cl_2 (25 mL). The flask was capped with a rubber septum and the reaction mixture was stirred vigorously for 15 min at room temperature. Powdered 4 Å molecular sieves (2.0 g, 0.5 g of sieves/mmol of substrate) were added, followed by carbamate ester **1a** (717 mg, 4.0 mmol, 1.0 equiv), rinsing with dry CH_2Cl_2 (15 mL). After adjusting the reaction temperature to –10 °C using a chiller, iodosobenzene (1.32 g, 6.0 mmol, 1.5 equiv) was added in one portion and the reaction mixture was stirred at –10 °C for 4 days. (NOTE: The rate of the reaction and overall conversion can be increased by increasing the catalyst loading). The mixture was filtered through a pad of Celite® rinsing with EtOAc, and the filtrate concentrated under reduced pressure. Silica gel column chromatography (0→100% EtOAc/hexanes) afforded the (*S*)-enantiomer of oxazinanone **2a** as a yellowish solid (497 mg, 70% yield, 88% *ee*); R_f = 0.24 (80% EtOAc/hexanes). The product was further purified by recrystallization from MeOH to afford the (*S*)-enantiomer of oxazinanone **2a** as a white solid with improved enantioselectivity (209 mg, 30% yield, >99% *ee*).

2.5.6. Synthesis of Dapoxetine

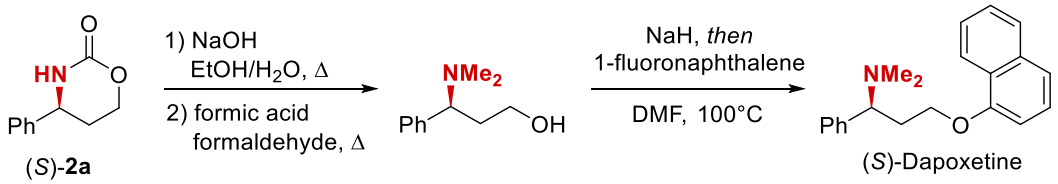

Ring opening: To a round-bottom flask containing the (*S*)-enantiomer of oxazinanone **2.2a** (177 mg, 1.00 mmol, 1 equiv) were added EtOH (7 mL), H_2O (3.5 mL), and NaOH (160 mg, 4.00 mmol, 4 equiv). The resulting mixture was refluxed at 80 °C until TLC indicated the reaction was complete (~18 h). After cooling to room temperature, EtOH was evaporated under reduced pressure and the residue was extracted with EtOAc three times. The total combined organic phase was dried over Na_2SO_4 and concentrated under reduced pressure and used directly in the next step without further purification.

Eschweiler-Clarke methylation: A mixture of (S)-3-amino-3-phenyl-1-propanol (151 mg, 1.00 mmol, 1 equiv), 37 wt.% formaldehyde in H_2O (0.30 mL, 4.00 mmol, 4 equiv), and formic acid (75.4 µL, 2.00 mmol, 2 equiv) in H_2O (2 mL) was stirred at 100 °C overnight. After cooling to room temperature, the reaction was basified with 1M NaOH. The mixture was extracted with CH_2Cl_2 three times and washed with brine. The organic layer was dried with $MgSO_4$ and concentrated in vacuo. Silica gel chromatography (0-10% MeOH/EtOAc) afforded the amino alcohol (129 mg, 72%); ^{1}H NMR (500 MHz, $CDCl_3$) δ 7.38 – 7.32 (m, 2H), 7.32 – 7.27 (m, 1H), 7.20 – 7.16 (m, 2H), 5.26 (s, 1H), 3.90 – 3.82 (m, 2H), 3.76 (dd, *J* = 10.5, 3.7 Hz, 1H), 2.41 (dddd, *J* = 14.5, 10.5, 9.1, 5.4 Hz, 1H), 2.18 (s, 6H), 1.67 (dq, *J* = 14.5, 3.6 Hz, 1H); ^{13}C NMR (126 MHz, $CDCl_3$) δ 136.3, 129.0, 128.1, 127.7, 70.3, 63.6, 41.2, 32.3; HRMS (ESI) m/z calcd. for $C_{11}H_{17}NO$ $[M+H]^+$: 180.1383, found: 180.1381.

S_NAr: A mixture of 3-(dimethylamino)-3-phenylpropan-1-ol (129 mg, 0.72 mmol, 1 equiv) dissolved in 5 ml of DMF was cooled to 0 °C and 60 wt.% NaH in mineral oil (58 mg, 1.44 mmol, 2 equiv) was added. The mixture was heated for an hour at 60 °C and 1-fluoronaphthalene (92.9 µL, 0.72 mmol, 1 equiv) was added to the reaction mixture. The mixture was then stirred overnight at about 100 °C under a nitrogen atmosphere. The reaction mixture was cooled to room temperature and poured into approximately 10 mL of cold water and extracted with EtOAc three times. The combined organics were washed with water twice and then brine. The organic layer was dried with Na_2SO_4 and concentrated in vacuo. Silica gel chromatography (0-10% MeOH/EtOAc) afforded (*S*)-Dapoxetine (173 mg, 79%). ^{1}H NMR (500 MHz, $CDCl_3$ δ 8.27 – 8.21 (m, 1H), 7.82 – 7.76 (m, 1H), 7.51 – 7.42 (m, 2H), 7.38 (d, *J* = 8.2 Hz, 1H), 7.35 – 7.27 (m, 6H), 6.65 (dd, *J* = 7.6, 0.9 Hz, 1H), 4.08 (ddd, *J* = 9.2, 6.7, 5.2 Hz, 1H), 3.91 (ddd, *J* = 9.3, 7.6, 6.2 Hz, 1H), 3.60 (dd, *J* = 9.2, 5.5 Hz, 1H), 2.68 – 2.58 (m, 1H), 2.33 – 2.26 (m, 1H), 2.25 (s, 6H); ^{13}C NMR (126 MHz, $CDCl_3$) δ 154.8, 139.8, 134.6, 128.7, 128.4, 127.6, 127.5, 126.4, 126.0, 125.8, 125.2, 122.2, 120.2, 104.7, 67.8, 65.8, 43.0, 33.2; HRMS (ESI) m/z calcd. for $C_{21}H_{23}NO$ $[M+H]^+$: 306.1852, found: 306.1850.

The *ee* value (90%) was determined by chiral HPLC analysis of (*S*)-Dapoxetine in comparison with an authentic sample of racemic material (CHIRALCEL® OD-H, 0.2→1.6% iPrOH/hexane gradient over 12 min, 1.0 mL/min, 210 nm): t_R = 14.2 min (minor), 14.5 min (major).

2.5.7. Synthesis of (*R*,*R*)-MinBOX, (*R*,*R*)-WenBOX, and (*R*,*R*)-pOMe-MinBOX

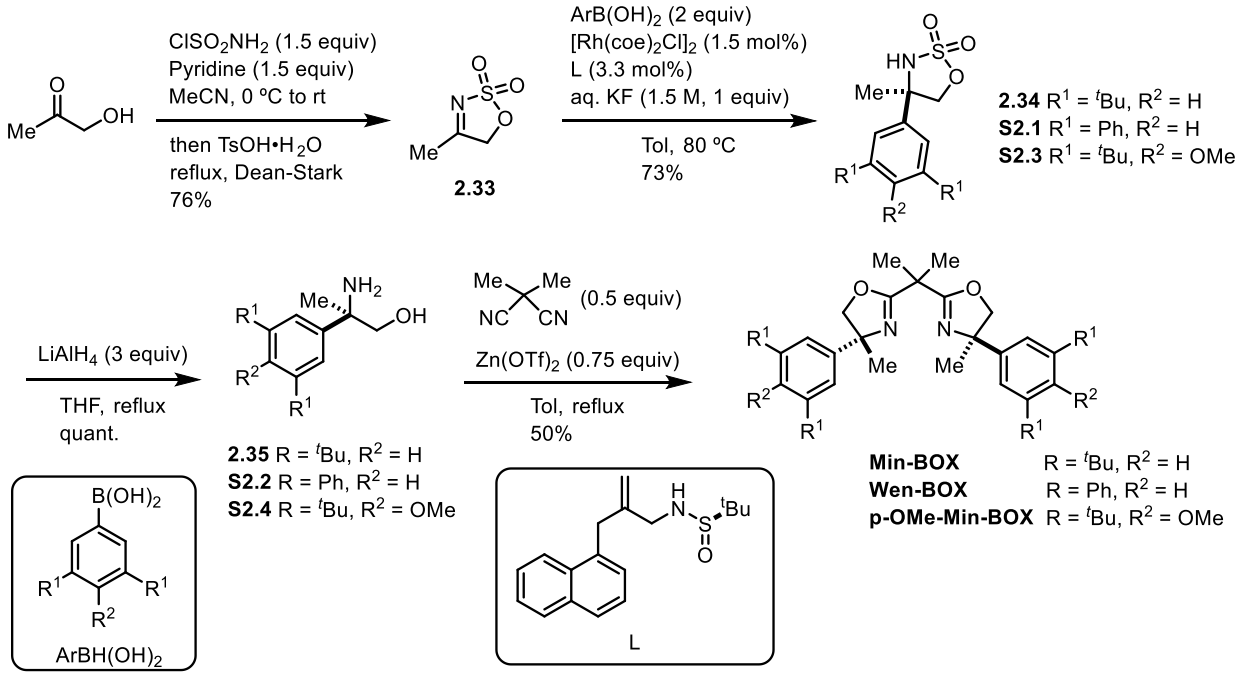

Compound 2.33. *a*-Hydroxyacetone (90%, 2.47 g, 30 mmol) in a 100 mL flame-dried round bottom flask was dissolved in MeCN (30 mL) under N_2, followed by pyridine (3.7 mL, 45 mmol, 1.5 equiv), cooled to 0 °C. Sulfamoyl chloride (5.2 g, 45 mmol, 1.5 equiv) in MeCN (20 mL) was added dropwise, then the mixture gradually warmed to rt overnight. The solution was filtered through a short pad of silica and washed with EtOAc. The solvent was removed under vacuo, then *p*-toluenesulfonic acid (571 mg, 3 mmol, 10 mol%) and toluene (50 mL) were added, and the reaction mixture was heated at reflux for 2 h with azeotropic removal of H_2O. The solvent was evaporated, and the residue was purified by silica gel chromatography (hexanes/EtOAc = 1/1 to 1/2) to afford the desired product as a light brown solid (3.1 g, 76%); ^{1}H NMR (500 MHz, $CDCl_3$) δ 5.08 (s, 2H), 2.42 (s, 3H); ^{13}C NMR (126 MHz, $CDCl_3$) δ 181.5, 77.1, 17.9.

Compound 2.34. A 100 mL 2-neck round bottom flask equipped with a stir bar and a condenser was charged with **2.33** (811 mg, 6 mmol), 3,5-di*t*Bu-phenylboronic acid (2.81 g, 12 mmol, 2 equiv) and **L** (60 mg, 0.2 mmol, 3.3 mol%). $[Rh(coe)_2Cl]_2$ (65 mg, 0.09 mmol, 1.5 mol%) was added to the mixture in a glovebox, then toluene (60 mL) was added under N_2. The mixture was stirred at rt for 30 min, followed by addition of aqueous KF (1.5 M, 4 mL, 6 mmol, 1 equiv), then stirred at 80 °C for 24 h. The reaction was cooled to rt, extracted with EtOAc, washed with brine, dried over Na_2SO_4, filtered and concentrated. The crude product was purified by silica gel chromatography (hexanes/EtOAc = 3/1 to 2/1) to afford the desired product as a white solid (1.43 g, 73%); ^{1}H NMR (500 MHz, $CDCl_3$) δ 7.42 (t, *J* = 1.7 Hz, 1H), 7.21 (d, *J* = 1.7 Hz, 2H), 4.65 (s, 1H), 4.65 (dd, *J* = 22.5, 8.5 Hz, 2H), 1.85 (s, 3H), 1.33 (s, 18H); ^{13}C NMR (126 MHz, $CDCl_3$) δ 152.0, 140.4, 122.87, 119.0, 80.8, 65.9, 35.2, 31.6, 27.8; HRMS (ESI, *m*/*z*) $[M+Na]^+$ calcd for $[C_{17}H_{27}NO_3S]^+$: 348.1604; found: 348.1597.

The *ee* value (99%) was determined by chiral HPLC analysis of compound **2.34** in comparison with an authentic sample of racemic material (CHIRALCEL® AD-H, 5% iPrOH/hexane, 0.7 mL/min, 210 nm): t_R = 10.1 min (major), 11.4 min (minor).

Compound 2.35. A flame-dried 15 mL 2-neck round bottom flask equipped with a stir bar and a condenser under N_2 was charged with $LiAlH_4$ (40.6 mg, 1.07 mmol, 3 equiv) followed by dry THF (2.5 mL). A solution of **2.34** (116.1 mg, 0.357 mmol, 1 equiv) in THF (1.5 mL, then 1 mL to rinse vial containing sulfamate) was added dropwise to the stirred grey suspension at rt, then the mixture was refluxed for 5 hours. The reaction mixture was first cooled to rt, then 0 °C in an ice-water bath and quenched by the dropwise addition of 0.5 mL water. The mixture was filtered through a short pad of Celite, washed with EtOAc, dried over Na_2SO_4, and filtered. The resulting

solution was concentrated carefully to result in **2.35** as a flakey white solid (93 mg, 99%). NMR analysis determined the product was of high purity. ^{1}H NMR (500 MHz, $CDCl_3$) δ 7.34 (t, *J* = 1.8 Hz, 1H), 7.29 (d, *J* = 1.8 Hz, 2H), 3.64 (d, *J* = 10.6 Hz, 1H), 3.59 (d, *J* = 10.6 Hz, 1H), 1.64 (br, 3H, NH_2 + OH) 1.48 (s, 3H), 1.34 (s, 18H); ^{13}C NMR (126 MHz, $CDCl_3$) δ 150.7, 145.5, 121.0, 119.3, 71.9, 56.6, 35.0, 31.5, 27.2; HRMS (ESI, *m*/*z*) $[M+H]^+$ calcd for $[C_{17}H_{30}NO]^+$: 264.2322; found: 264.2317.

(*R*,*R*)-MinBOX. A flame-dried 15 mL 2-neck round bottom flask equipped with a stir bar and a condenser was charged with $Zn(OTf)_2$ (96.3 mg, 0.265 mmol, 0.75 equiv). The apparatus was placed in a pre-heated 120°C oil bath and heated under vacuum for 2 h. The reaction vessel was allowed to cool to room temperature under vacuum, then carefully placed under N_2. A portion of 2,2-dicyanopropane (16.4 mg, 0.174 mmol, 0.5 equiv) was added, followed by toluene (2 mL). The resulting reaction mixture was allowed to stir for 5 min, after which the amino alcohol **S3** (93.0 mg, 0.353 mmol, 1 equiv) was added. The vial containing the amino alcohol was rinsed with toluene (1.5 mL) and the solution was added to the reaction flask. The reaction was stirred at reflux for 72 h. After cooling to rt, the yellow reaction mixture was transferred to a separatory funnel. Brine was added and the mixture extracted with EtOAc, dried over Na_2SO_4, and filtered. Silica gel chromatography (Hexanes/EtOAC = 9/1 to 2/1) gave **(*R*,*R*)-Min-BOX** as a white solid (51.3 mg, 50%). ^{1}H NMR (500 MHz, $CDCl_3$) δ 7.29 (t, *J* = 1.8 Hz, 2H), 7.22 (d, *J* = 1.8 Hz, 4H), 4.29 (d, *J* = 7.9 Hz, 2H), 4.26 (d, *J* = 8.2 Hz, 2H), 1.67 (d, *J* = 5.9 Hz, 12H), 1.31 (s, 36H); ^{13}C NMR (126 MHz, $CDCl_3$) δ 168.4, 150.6, 146.0, 121.0, 119.8, 81.6, 72.7, 38.8, 35.1, 31.6, 28.5, 24.8; HRMS (ESI, *m*/*z*) $[M+H]^+$ calcd for $[C_{39}H_{59}N_2O_2]^+$: 587.4571; found: 587.4571.

Compound S2.1: The title compound was synthesized on a 3.7 mmol scale using an analogous to procedure as in compound **2.34** with 3,5-diphenylphenylboronic acid. Silica gel chromatography (hexanes/EtOAc = 3/1 to 2/1) afforded the desired product as a white solid (0.81g, 61%). ^{1}H NMR (500 MHz, $CDCl_3$) δ 7.78 (t, *J* = 1.6 Hz, 1H), 7.66 – 7.59 (m, 6H), 7.52 – 7.45 (m, 4H), 7.44 – 7.37 (m, 2H), 4.78 (d, *J* = 8.7 Hz, 1H), 4.68 (d, *J* = 8.7 Hz, 1H), 4.61 (s, 1H), 1.94 (s, 3H); ^{13}C NMR (126 MHz, $CDCl_3$) δ 143.0, 142.3, 140.4, 129.0, 128.0, 127.3, 126.5, 122.7, 80.3, 65.4, 27.8; HRMS (ESI, *m*/*z*) $[M+NH_4]^+$ calcd for $[C_{21}H_{19}NO_3S]^+$: 383.1424; found: 383.1422.

Compound S2.2: The title compound was synthesized on a 3.6 mmol scale using an analogous to procedure as in compound **2.35**. The product was obtained as a white solid (1.13 g, 99.9%). ^{1}H NMR (500 MHz, $CDCl_3$) δ 7.69 (t, *J* = 1.7 Hz, 1H), 7.68 – 7.61 (m, 5H), 7.47 (dd, *J* = 8.4, 6.9 Hz, 4H), 7.41 – 7.34 (m, 2H), 3.76 (d, *J* = 10.6 Hz, 1H), 3.69 (d, *J* = 10.6 Hz, 1H), 1.69 (broad s, 3H), 1.57 (s, 3H); ^{13}C NMR (126 MHz, $CDCl_3$) δ 147.6, 142.1, 141.3, 128.8, 127.5, 127.4, 124.9, 123.4, 71.9, 56.6, 27.4; HRMS (ESI, *m*/*z*) $[M+H]^+$ calcd for $[C_{21}H_{21}NO]^+$: 304.1696; found: 304.1695.

(*R*,*R*)-WenBOX: The title compound was synthesized on a 3.5 mmol scale using an analogous to procedure as in **(*R*,*R*)-Min-BOX**. Silica gel chromatography (Hexanes/EtOAC = 4/1 to 2/1) gave **(*R*,*R*)-Wen-BOX** as a white solid (1.17 g, 71%). ^{1}H NMR (500 MHz, $CDCl_3$) δ 7.67 (t, *J* = 1.7 Hz, 2H), 7.65 – 7.60 (m, 8H), 7.58 (d, *J* = 1.7 Hz, 4H), 7.46 – 7.40 (m, 8H), 7.37 – 7.32 (m, 4H), 4.31 (s, 4H), 1.74 (s, 6H), 1.73 (s, 6H); ^{13}C NMR (126 MHz, $CDCl_3$) δ 168.7, 147.7, 141.9,

141.3, 128.7, 127.4, 127.3, 124.8, 123.4, 81.1, 72.5, 38.8, 28.4, 24.5; HRMS (ESI, *m*/*z*) $[M+H]^+$ calcd for $[C_{47}H_{42}N_2O_2]^+$: 667.3319; found: 667.3314.

Compound S2.3: The title compound was synthesized on a 2.5 mmol scale using an analogous to procedure as in compound **2.34** with 3,5-di^{t}Bu-4-OMe-phenylboronic acid. Silica gel chromatography (hexanes/EtOAc = 3/1 to 2/1) afforded the desired product as a white solid (553 mg, 62%). ^{1}H NMR (500 MHz, $CDCl_3$) δ 7.25 (s, 2H), 4.64 (d, *J* = 8.6 Hz, 1H), 4.58 (d, *J* = 8.6 Hz, 1H), 4.47 (s, 1H), 3.69 (s, 3H), 1.83 (s, 3H), 1.43 (s, 18H); ^{13}C NMR (126 MHz, $CDCl_3$) δ 159.6, 144.6, 134.7, 123.0, 80.6, 65.4, 64.3, 36.0, 32.0, 27.4; HRMS (ESI, *m*/*z*) $[M+NH_4]^+$ calcd for $[C_{18}H_{29}NO_4S]^+$: 373.2156; found: 373.2153.

Compound S2.4: The title compound was synthesized on a 1.6 mmol scale using an analogous to procedure as in compound **2.35**. The product was obtained as a white solid (424 mg, 93%). ^{1}H NMR (500 MHz, $CDCl_3$) δ 7.30 (s, 2H), 3.69 (s, 3H), 3.64 – 3.51 (m, 2H), 1.63 (broad s, 3H), 1.43 (s, 18H); ^{13}C NMR (126 MHz, $CDCl_3$) δ 158.1, 143.2, 139.8, 123.4, 71.9, 64.0, 56.2, 35.9, 32.1, 27.1; HRMS (ESI, *m*/*z*) $[M+H]^+$ calcd for $[C_{18}H_{31}NO_2]^+$: 294.2428; found: 294.2424.

(*R*,*R*)-*p*-OMe-Min-BOX: The title compound was synthesized on a 0.5 mmol scale using an analogous to procedure as in **(*R*,*R*)-Min-BOX**. Silica gel chromatography (Hexanes/EtOAC = 4/1 to 2/1) gave **(*R*,*R*)-*p*-OMe-Min-BOX** as a white solid (281 mg, 87%). ^{1}H NMR (500 MHz, $CDCl_3$) δ 7.22 (s, 4H), 4.29 – 4.19 (m, 4H), 3.66 (s, 6H), 1.67 (s, 6H), 1.64 (s, 6H), 1.41 (s, 36H); ^{13}C NMR (126 MHz, $CDCl_3$) δ 168.3, 158.2, 143.1, 140.2, 123.8, 81.7, 72.1, 64.1, 38.6, 35.9, 32.1, 27.8, 24.6; HRMS (ESI, *m*/*z*) $[M+H]^+$ calcd for $[C_{41}H_{62}N_2O_4]^+$: 647.4782; found: 647.4782.

2.5.8. DFT calculations

Density functional theory (DFT) calculations, including geometry optimization and single-point energy calculations, were performed with the Gaussian 16 software package.[4] Geometries were optimized in the gas phase using the ωB97X-D[5] functional and a mixed basis set of def2-TZVPP for Ag and def2-SVP for other atoms. Single-point energies were calculated using ωB97X-D and the def2-TZVPP basis set for all atoms in dichloromethane (DCM) using the CPCM solvation model.[6] Conformers of each ground state and transition state structure were studied by manual conformational search and automated conformational sampling using CREST[7] and GFN2-xTB.[8] Low-energy conformers from the CREST/xTB conformational sampling were then re-optimized using DFT at the aforementioned level of theory. Gibbs free energies were calculated at the standard conditions (298 K, 1 M solution). Quasiharmonic approximation from Grimme[9] was applied for vibrational entropy calculations using 100 cm^{-1} as the frequency cut-off. Quasiharmonic approximations and "free-volume" theory translational entropy calculations were computed using GoodVibes.[10] The 3D images of optimized structures were prepared using CYLView.[11] PNO-LCCSD(T)-F12 benchmark calculations were performed using Molpro 2020.2.[12-14]

Benchmark of DFT methods for spin state energies of silver nitrene complexes [(dmbox)Ag^{+}=NCO_2R] and C–H insertion transition states

Using a similar approach described in our previous benchmark study,[15] we computed both singlet and triplet states of the Ag nitrene intermediate and the C–H insertion transition state using different levels of theory,[16] including several DFT methods [(U)B3LYP[17]-D3,[18] (U)BP86,[19] and (U)ωB97X-D], and explicitly correlated local coupled cluster [PNO-LCCSD(T)-F12]. The open-

shell PNO-RCCSD(T)-F12 method was used for triplet complexes. In the local coupled-cluster theory calculations, the ECP28MDF effective core potential and the AWCVTZ basis set were used for Ag, VDZ was used for H, and VDZ-F12 was used for other atoms. The aug-cc-pVTZ-PP/JKFIT (Ag), VTZ/JKFIT (H), and AVTZ/JKFIT (other atoms) fitting auxiliary basis sets were used to compute the Fock matrix and as the RI basis set. For the density fitting of all other two-electron integrals, the aug-cc-pVTZ-PP/MP2FIT (Ag), VDZ/MP2FIT (H), and AVDZ/MP2FIT (other atoms) basis sets were used. These basis sets are similar to those used by Werner et al. in recent computational studies. T1/D1 diagnostic values were calculated for all structures in the PNO-LCCSD(T)-F12 benchmark study and compared with the criteria recommended by Wilson et al. for 4d transition metals (T1 < 0.045 and D1 < 0.12).[20] The computed T1 values were all smaller than 0.045 and the D1 values were in the range of 0.09−0.26, suggesting small or moderate multireference character. All PNO-LCCSD(T)-F12 were performed in the gas phase using the DFT-optimized geometries.

The singlet Ag nitrene favors a four-coordinate square planar geometry (**^{1}2.34**) with strong coordination of the carbonyl oxygen to the Ag center. In contrast, the triplet Ag nitrene favors a three-coordinate trigonal planar geometry (**^{3}2.35**), in which the carbonyl of the carbamate does not bind to the Ag (Figure S2.1). The PNO-LCCSD(T)-F12 calculations predicted that the singlet Ag nitrene (**^{1}2.34**) and the C–H insertion transition states (**^{1}TS2.1-^{1}TS2.4**) are significantly more stable than the triplet structures (**^{3}35** and **^{3}TS2.11-^{3}TS2.14**). DFT calculations with three different functionals (ωB97X-D, B3LYP-D3, and BP86-D3) also predicted that the singlet pathway is more favorable, albeit to a lesser extent. For example, PNO-LCCSD(T)-F12 predicted the singlet Ag nitrene **^{1}2.34** is 20.0 kcal/mol more stable than the triplet **^{3}2.35**, but ωB97X-D, B3LYP-D3, and BP86-D3 predicted the singlet nitrene is 1.6, 2.2, and 8.6 kcal/mol more stable, respectively.

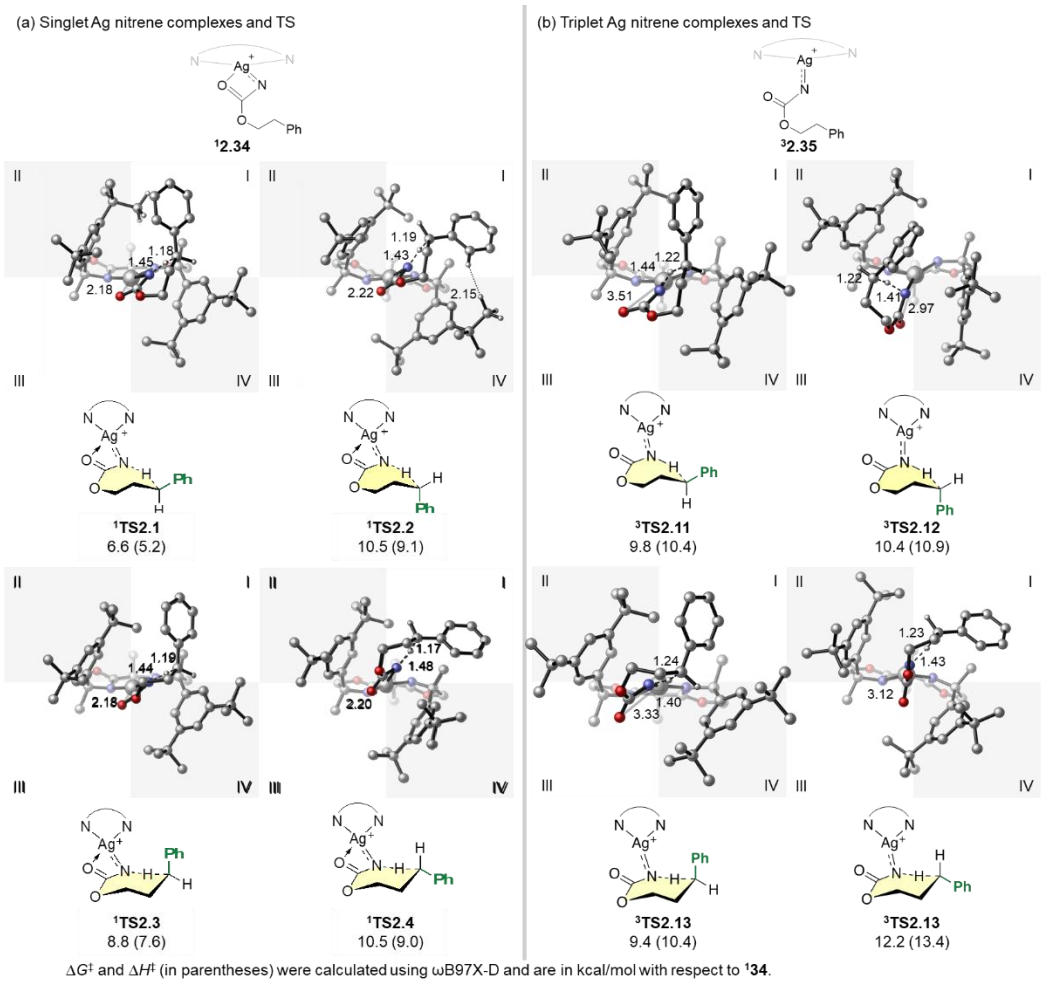

$\Delta G^{\ddagger}$ and $\Delta H^{\ddagger}$ (in parentheses) were calculated using ωB97X-D and are in kcal/mol with respect to **^{1}34**.

	^{1}2.34	^{3}2.35	^{1}TS2.1	^{1}TS2.2	^{1}TS2.3	^{1}TS2.4	^{3}TS2.11	^{3}TS2.12	^{3}TS2.13	^{3}TS2.14	Predicted enantioselectivity $\Delta\Delta E_{(TS2\text{-}TS1)}^{\ddagger}$ or $\Delta\Delta E_{(TS4\text{-}TS1)}^{\ddagger}$
PNO-LCCSD(T)-F12 (Δ*E*)	0.0	20.0	**8.6**	11.8	10.8	**11.4**	31.9	35.9	29.7	32.9	2.8
ωB97X-D (Δ*E*)	0.0	1.6	**6.6**	9.6	8.3	**9.2**	13.9	14.6	12.9	16.1	2.6
B3LYP-D3 (Δ*E*)	0.0	2.2	**1.9**	5.0	3.9	**4.6**	12.1	12.3	11.7	12.6	2.7
BP86-D3 (Δ*E*)	0.0	8.6	**-1.8**	**0.9**	0.1	0.9	15.1	12.9	14.3	15.4	2.7
ωB97X-D (Δ*G*)	0.0	0.7	**6.6**	**10.5**	8.8	10.5	9.8	10.4	9.4	12.2	3.9 ($\Delta\Delta G^{\ddagger}$)
ωB97X-D (Δ*H*)	0.0	1.9	**5.2**	9.1	7.6	**9.0**	10.4	10.9	10.4	13.4	2.8 ($\Delta\Delta H^{\ddagger}$)

Energy values in the most favorable pathways leading to the (*R*)- (**TS2.1**) and (*S*)- (**TS2.2** or **TS2.4**) amination products are in bold.

Figure S2.1 – Benchmark of DFT methods for spin state energies of silver nitrene complexes [(dmbox)Ag^{+}=NCO_2R] and C–H insertion transition states. All energies are with respect to **^{1}2.34**.

A possible source of error of the DFT calculations is the underestimation of the binding energy of the carbonyl oxygen to the Ag center, which has also been observed in other systems.[21,22]

Among the tested DFT methods, ωB97X-D provided the best agreement for activation energy ($\Delta E_{(\mathbf{TS1})}^{\ddagger}$ = 6.6 kcal/mol) compared with the PNO-LCCSD(T)-F12 results ($\Delta E_{(\mathbf{TS1})}^{\ddagger}$ = 8.6 kcal/mol) while all three DFT methods predicted essentially the same enantioselectivity ($\Delta\Delta E^{\ddagger}$ = 2.6, 2.7, and 2.7 kcal/mol, respectively) compared with PNO-LCCSD(T)-F12 ($\Delta\Delta E^{\ddagger}$ = 2.8 kcal/mol). Therefore, we used ωB97X-D for geometry optimizations and single point energy calculations in the present study.

A higher-energy C–H insertion TS isomer lacking carbamate carbonyl–Ag coordination

While the majority of the C–H insertion transition states with *singlet* Ag nitrene have relatively strong coordination of the carbamate carbonyl oxygen and the Ag center, we have located a higher energy singlet C–H insertion TS isomer where such coordination is absent (**^{1}TS2.3'**, Figure S2.2). **^{1}TS2.3'** is 3.3 kcal/mol less stable than **^{1}TS2.3**, although these two TS isomers have the same seven-membered ring conformation. Here, **^{1}TS2.3'**, which has a trigonal planar geometry with a long distance between the carbamate carbonyl oxygen and the Ag center (3.23 Å, compared with 2.18 Å in **^{1}TS2.3**), is destabilized due to the lack of carbonyl–Ag coordination.

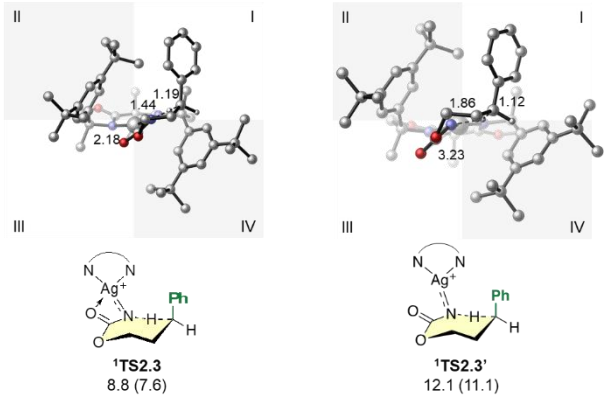

Figure S2.2 – An alternative TS isomer (**^{1}TS2.3'**) that lacks the carbamate carbonyl–Ag coordination. Gibbs free energies and enthalpies (in parentheses) are in kcal/mol with respect to the singlet Ag nitrene **^{1}2.34**.

Effects of ligand binding mode on C–H insertion transition state energy

We have compared three possible ligand binding modes (*i.e.*, *N*,*N*-bidentate, *N*-monodentate, and *N*,*O*-bidentate) by computing the corresponding isomers of an example C–H insertion transition state (Figure S3). In **^{1}TS2.15**, both N atoms of the oxazoline rings of the Min-BOX ligand bind to the Ag. **^{1}TS2.16** has an *N*,*O*-bidentate binding mode, in which one of the oxazoline rings coordinates to the Ag via its oxygen atom, rather than nitrogen. In **^{1}TS2.17**, one of the oxazoline rings is dissociated, leaving only one oxazoline nitrogen bound to the Ag in a monodentate binding mode. Both **^{1}TS2.16** and **^{1}TS2.17** are significantly less stable than **^{1}TS2.15** by more than 10 kcal/mol [$(\Delta\Delta G(\mathbf{TS16\text{-}TS15})^{\ddagger}$ = 10.1 kcal/mol, $(\Delta\Delta G(\mathbf{TS17\text{-}TS15})^{\ddagger}$ = 13.8 kcal/mol], indicating that these alternatively binding modes to the singlet Ag nitrene are not likely involved. Therefore, all computed transition states in the present study involve the *N*,*N*-bidentate binding mode.

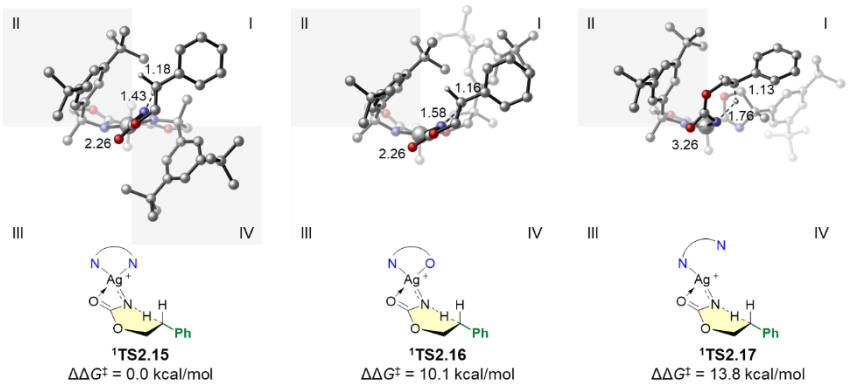

Figure S2.3 – Alternative TS isomers with different ligand binding modes. Gibbs free energies are in kcal/mol with respect to **^{1}TS2.15**.

2.5.9. Cartesian Coordinates (Å) and Energies of Optimized Structures

2.34
ωB97X-D SCF energy: -2518.42593683 a.u.
ωB97X-D enthalpy: -2517.261989 a.u.
ωB97X-D free energy: -2517.417459 a.u.
ωB97X-D SCF energy in solution: -2521.01743212 a.u.
ωB97X-D enthalpy in solution: -2519.853484 a.u.
ωB97X-D free energy in solution: -2520.008954 a.u.

Cartesian coordinates

ATOM	X	Y	Z
C	0.751245	-5.240433	0.289446
C	0.472109	-3.908409	1.043388
N	1.498925	-3.016095	0.442470
C	2.128545	-3.652172	-0.470689
O	1.806134	-4.921215	-0.638412
C	3.252231	-3.123603	-1.332445
C	3.034150	-1.688049	-1.771110
N	2.185750	-0.811670	-1.368751
C	2.408973	0.457288	-2.124603
C	3.741973	0.137423	-2.845349
O	3.903983	-1.280831	-2.678123
C	3.428648	-4.003790	-2.583377
C	4.537693	-3.146007	-0.466269
H	-0.107393	-5.605144	-0.287771
H	1.115465	-6.037208	0.951340
H	3.720077	0.358058	-3.919248
H	4.607367	0.631821	-2.382935
H	4.270923	-3.635118	-3.179958
H	2.524269	-3.997966	-3.208045
H	3.630851	-5.038558	-2.282919
H	5.394927	-2.808758	-1.063720
H	4.432354	-2.496414	0.414641
H	4.732655	-4.172159	-0.125009
Ag	0.994581	-0.925513	0.407228
N	0.133942	0.866122	0.458225
C	-0.232565	0.708769	1.696709
O	-0.861239	1.567042	2.447748
C	-1.085253	2.896010	1.934389
C	-2.456180	3.033509	1.300438
C	-2.661445	2.168762	0.053968
O	0.099798	-0.432571	2.206184
H	-0.277391	3.139263	1.225830
H	-0.992523	3.549319	2.811088
H	-3.226317	2.803322	2.054544
H	-2.591013	4.096381	1.038994
H	-2.557395	1.103994	0.319912
H	-1.855576	2.374797	-0.668402
C	-0.890445	-3.298009	0.698148
C	-3.205646	-1.943244	-0.013980
C	-1.140706	-2.970045	-0.643607
C	-1.831019	-2.964645	1.663431
C	-3.014210	-2.289705	1.323093
C	-2.285485	-2.273640	-1.020959
H	-0.410049	-3.248786	-1.404489
H	-1.637694	-3.198183	2.708212
H	-4.101238	-1.387930	-0.293822
C	2.546103	1.620082	-1.148273
C	2.589051	3.581929	0.807808
C	1.940122	2.845829	-1.375675
C	3.230992	1.405373	0.053959
C	3.230129	2.358980	1.065723
C	1.961225	3.859364	-0.405107
H	1.409662	3.023464	-2.310094
H	3.723221	0.446287	0.218861
H	2.584872	4.337995	1.592554
C	-2.548851	-1.844236	-2.468909
C	-4.009969	-1.869441	2.413575
C	1.312841	5.217132	-0.714336
C	3.841983	2.095432	2.447214
C	0.738297	-4.031087	2.539203
H	0.643405	-3.054336	3.033147
H	1.756793	-4.408723	2.707848
H	0.030781	-4.731932	3.004768
C	1.256961	0.614195	-3.113420
H	0.306236	0.740805	-2.577845
H	1.186931	-0.276312	-3.754844
H	1.415147	1.483430	-3.766187
C	-4.002412	2.373764	-0.603310
C	-5.168964	1.892448	0.003813
C	-4.113282	3.034490	-1.829944
C	-6.411668	2.054118	-0.604551
H	-5.101948	1.382338	0.969010
C	-5.355392	3.200408	-2.442754
H	-3.211733	3.416622	-2.317208
C	-6.507738	2.707575	-1.833571
H	-7.310000	1.668690	-0.117264
H	-5.422829	3.716379	-3.402982
H	-7.480234	2.834469	-2.313393
C	2.720308	2.167263	3.501334
H	1.949949	1.403693	3.312272
H	3.129136	1.991117	4.508201
H	2.228737	3.151247	3.511410
C	4.488740	0.706990	2.536332
H	4.914530	0.559168	3.539511
H	3.751994	-0.096866	2.373897
H	5.307546	0.586128	1.810111
C	4.915234	3.155725	2.750531
H	5.720777	3.126593	2.001150

H	4.497271	4.172925	2.755952	H	-2.510245	-0.637288	3.440139
H	5.362075	2.976753	3.740478	H	-3.463176	0.241712	2.232142
C	-0.113693	5.023169	-1.261016	H	-4.199142	-0.187106	3.797901
H	-0.573443	6.000301	-1.472564	C	-5.424202	-1.681426	1.843433
H	-0.131685	4.447044	-2.197574	H	-5.784012	-2.597979	1.351245
H	-0.753883	4.502304	-0.534061	H	-6.123441	-1.437709	2.656941
C	2.172648	5.927548	-1.776988	H	-5.480343	-0.859814	1.115419
H	3.199578	6.081030	-1.412646	C	-3.843160	-2.506840	-2.972872
H	2.228822	5.342075	-2.707260	H	-3.761391	-3.604145	-2.947469
H	1.745698	6.912023	-2.023620	H	-4.711648	-2.218118	-2.363149
C	1.227792	6.111821	0.528865	H	-4.049850	-2.202372	-4.010430
H	0.647059	5.636861	1.335357	C	-1.398203	-2.245398	-3.400377
H	2.222101	6.366284	0.924533	H	-0.444703	-1.797623	-3.079619
H	0.728330	7.057772	0.273314	H	-1.270433	-3.337793	-3.451795
C	-4.087525	-2.924916	3.529492	H	-1.604626	-1.891607	-4.421223
H	-4.863784	-2.642711	4.256054	C	-2.700546	-0.313176	-2.508908
H	-4.345378	-3.916158	3.126141	H	-3.582168	0.029470	-1.949128
H	-3.146663	-3.014547	4.091479	H	-1.819023	0.180681	-2.070293
C	-3.516710	-0.537043	3.007419	H	-2.818510	0.037455	-3.545821

2.35

ωB97X-D SCF energy: -2518.42699329 a.u.
ωB97X-D enthalpy: -2517.263699 a.u.
ωB97X-D free energy: -2517.419648 a.u.
ωB97X-D SCF energy in solution: -2521.013757 a.u.
ωB97X-D enthalpy in solution: -2519.889257 a.u.
ωB97X-D free energy in solution: -2520.045206 a.u.

Cartesian coordinates

ATOM	X	Y	Z				
C	2.289308	3.431436	1.879261	H	-4.250729	3.181416	0.615998
C	1.673097	2.001713	1.785327	H	-0.187016	4.347060	-2.747127
N	0.573207	2.215944	0.816617	H	0.524395	2.820203	-2.153137
C	0.559703	3.446191	0.468811	H	1.387819	4.367407	-1.912618
O	1.479467	4.232291	1.004398	H	-0.958352	5.772952	0.684842
C	-0.318437	4.102197	-0.581482	H	0.498162	6.088314	-0.290294
C	-1.668499	3.413647	-0.641847	H	-1.110258	6.062162	-1.061865
N	-1.866346	2.187943	-0.951965	Ag	-0.619055	0.542986	-0.075080
C	-3.334252	1.958935	-1.022474	N	-0.329150	-1.361224	0.543597
C	-3.883079	3.275328	-0.414143	C	0.377085	-2.099096	1.484471
O	-2.741048	4.152262	-0.399860	O	1.035691	-3.161570	1.075425
C	0.398262	3.890024	-1.936919	C	1.027966	-3.505522	-0.319184
C	-0.483059	5.599736	-0.289254	C	2.081392	-2.744964	-1.103488
H	3.327559	3.484824	1.528387	C	1.860136	-2.906317	-2.607771
H	2.221653	3.858319	2.888650	O	0.334658	-1.751846	2.643362
H	-4.662392	3.739362	-1.030105	H	0.023091	-3.327271	-0.730406

H	1.215492	-4.586633	-0.340239
H	2.052299	-1.677310	-0.826735
H	3.082517	-3.098891	-0.824605
H	1.768872	-3.975326	-2.858051
H	2.756023	-2.551974	-3.137705
C	2.668548	1.005604	1.191768
C	4.628132	-0.634310	0.116833
C	3.170081	1.249085	-0.091853
C	3.146527	-0.083468	1.916212
C	4.142243	-0.920710	1.395437
C	4.164664	0.444878	-0.649207
H	2.796689	2.109208	-0.649679
H	2.753178	-0.279063	2.910431
H	5.418811	-1.265977	-0.294722
C	-3.628091	0.694776	-0.215087
C	-3.807887	-1.652275	1.263232
C	-3.498311	0.717162	1.175433
C	-3.865525	-0.526605	-0.853014
C	-3.948910	-1.717224	-0.129525
C	-3.601507	-0.450254	1.942903
H	-3.303624	1.663976	1.684603
H	-3.960053	-0.556029	-1.935433
H	-3.867139	-2.575867	1.835970
C	4.799840	0.751255	-2.013775
C	4.751871	-2.067134	2.218390
C	-3.516347	-0.363110	3.472505
C	-4.110701	-3.073808	-0.829042
C	1.087491	1.570160	3.124686
H	0.621241	0.579680	3.054681
H	0.327371	2.295149	3.448976
H	1.870086	1.530425	3.895727
C	-3.727135	1.865765	-2.495894
H	-3.165087	1.075063	-3.003973
H	-3.504433	2.816886	-3.001679
H	-4.802479	1.659964	-2.599325
C	0.649948	-2.163289	-3.126239
C	0.526899	-0.776257	-2.945840
C	-0.361072	-2.832988	-3.820311
C	-0.569127	-0.084124	-3.459236
H	1.315240	-0.226047	-2.419949
C	-1.458049	-2.144154	-4.337994
H	-0.283351	-3.912714	-3.971874
C	-1.563612	-0.767754	-4.161394
H	-0.644028	0.997237	-3.322450
H	-2.227419	-2.687214	-4.890726
H	-2.409602	-0.226851	-4.590959
C	-5.076386	-3.982727	-0.050010
H	-6.060053	-3.504512	0.071735
H	-5.223133	-4.928045	-0.593551
H	-4.698049	-4.243041	0.948768
C	-4.648400	-2.919677	-2.258869
H	-5.612764	-2.389058	-2.273201
H	-3.943554	-2.381922	-2.909546
H	-4.805349	-3.912584	-2.705560
C	-2.718425	-3.729396	-0.895591
H	-2.027854	-3.098315	-1.477064
H	-2.297327	-3.871605	0.112370
H	-2.774818	-4.715862	-1.382606
C	-2.212188	0.342861	3.878268
H	-2.143519	1.361710	3.467245
H	-2.149681	0.428030	4.973959
H	-1.343245	-0.232892	3.530645
C	-3.529309	-1.748227	4.130823
H	-2.680414	-2.364113	3.796636
H	-3.447040	-1.639108	5.222105
H	-4.462671	-2.294231	3.927212
C	-4.728213	0.438906	3.982421
H	-5.672899	-0.044138	3.690156
H	-4.705715	0.508937	5.080838
H	-4.736125	1.464535	3.582725
C	4.048065	-2.241896	3.571013
H	4.492435	-3.091595	4.109806
H	4.164361	-1.355186	4.212653
H	2.973284	-2.448025	3.452113
C	4.642140	-3.397427	1.454142
H	3.588210	-3.684900	1.329063
H	5.116620	-3.349416	0.461991
H	5.144295	-4.198271	2.017754
C	6.235853	-1.740692	2.473332
H	6.807961	-1.673130	1.535838
H	6.342565	-0.781958	3.003277
H	6.698792	-2.525529	3.091122
C	6.297898	1.042144	-1.803617
H	6.828566	0.174512	-1.385203
H	6.777326	1.295488	-2.761657
H	6.441390	1.888111	-1.114454
C	4.159485	1.971359	-2.689180
H	4.291211	2.888542	-2.094814
H	4.632232	2.144697	-3.666958
H	3.082594	1.822728	-2.868803
C	4.634414	-0.452091	-2.955832
H	3.572021	-0.617135	-3.188962

H	5.159409	-0.270868	-3.906064	H	5.040690	-1.378351	-2.522925

2.1b_Ag_complex

ωB97X-D SCF energy: -2364.92163067 a.u.
ωB97X-D enthalpy: -2363.808779 a.u.
ωB97X-D free energy: -2363.960492 a.u.
ωB97X-D SCF energy in solution: -2367.35561484 a.u.
ωB97X-D enthalpy in solution: -2366.242763 a.u.
ωB97X-D free energy in solution: -2366.394476 a.u.

Cartesian coordinates

ATOM	X	Y	Z				
C	4.321747	-2.198337	-1.777994	H	-2.281222	4.996494	-0.462613
C	3.295299	-1.031211	-1.824155	H	-3.772473	2.298964	-0.568839
N	2.067514	-1.704939	-1.321273	H	-2.534627	2.820800	-1.718196
C	2.328169	-2.934657	-1.085697	C	3.616057	0.096070	-0.840590
O	3.555433	-3.341185	-1.350421	C	3.820847	2.109337	1.049953
C	1.360297	-3.995017	-0.612798	C	3.582652	-0.206593	0.526773
C	0.362940	-3.476109	0.404808	C	3.792306	1.415234	-1.243240
N	0.065553	-2.272543	0.740991	C	3.901786	2.446768	-0.302669
C	-1.084040	-2.295170	1.687193	C	3.653657	0.793304	1.495783
C	-1.320217	-3.825106	1.838820	H	3.457475	-1.244544	0.838252
O	-0.351315	-4.430297	0.968089	H	3.799275	1.657709	-2.302878
C	2.122346	-5.187661	-0.007759	H	3.870769	2.909400	1.791346
C	0.544756	-4.444716	-1.853367	C	-2.280401	-1.604525	1.032227
H	5.126447	-2.041421	-1.048257	C	-4.371985	-0.274575	-0.228172
H	4.754972	-2.429296	-2.759455	C	-3.209578	-0.887462	1.779288
H	-1.131315	-4.188316	2.857861	C	-2.435627	-1.671331	-0.351852
H	-2.317080	-4.143925	1.510586	C	-3.449277	-0.975586	-1.011340
H	2.814590	-5.601014	-0.750513	C	-4.282878	-0.229823	1.167401
H	1.412800	-5.967798	0.290763	H	-3.096707	-0.819736	2.861335
H	2.704949	-4.884852	0.873681	H	-1.723713	-2.245092	-0.947951
H	1.228785	-4.836661	-2.618755	H	-5.180106	0.259363	-0.722372
H	-0.156213	-5.241018	-1.570403	C	3.475160	0.503603	2.990777
H	-0.018245	-3.603741	-2.283620	C	4.033829	3.920776	-0.708330
Ag	0.627776	-0.493732	-0.273351	C	-5.290549	0.535784	2.038302
N	-0.457580	0.851452	0.717205	C	-3.472311	-0.971389	-2.545567
C	-0.147651	1.784625	-0.136601	C	3.033203	-0.558836	-3.250530
O	-0.546696	3.024876	-0.122340	H	3.936584	-0.108534	-3.685766
C	-1.597773	3.398383	0.792550	H	2.223845	0.183934	-3.271840
C	-2.694425	4.090229	0.009883	H	2.740493	-1.412369	-3.878930
C	-3.333265	3.188343	-1.049283	C	-0.654558	-1.657873	3.005672
O	0.631994	1.397469	-1.090597	H	0.263041	-2.139125	3.373108
H	-1.148635	4.061760	1.544243	H	-1.429731	-1.790617	3.772914
H	-1.974032	2.495931	1.298553	H	-0.469494	-0.584278	2.869565
H	-3.458189	4.432636	0.727341	C	-2.137657	-0.388792	-3.053224

H	-1.277094	-1.014841	-2.765644	C	4.096062	4.097731	-2.230520
H	-2.139451	-0.320770	-4.151877	H	4.957346	3.571786	-2.670530
H	-1.966845	0.620911	-2.649478	H	3.177982	3.740963	-2.722026
C	-3.639176	-2.411003	-3.063325	H	4.204605	5.164672	-2.474418
H	-3.646349	-2.424808	-4.164111	C	2.805327	4.688321	-0.182643
H	-2.820728	-3.067101	-2.728380	H	2.858315	5.745000	-0.487252
H	-4.585300	-2.848510	-2.710847	H	1.872685	4.260453	-0.580421
C	-4.612879	-0.112815	-3.104617	H	2.746625	4.664367	0.915961
H	-4.523864	0.940353	-2.798688	C	4.716796	0.973713	3.767403
H	-4.592551	-0.137238	-4.204124	H	4.590922	0.782562	4.844242
H	-5.598708	-0.484790	-2.786896	H	5.618694	0.441751	3.428609
C	-5.889089	-0.421986	3.084912	H	4.894676	2.051526	3.640636
H	-6.630190	0.105581	3.704556	C	3.265142	-0.991802	3.261188
H	-6.394225	-1.269729	2.597693	H	4.135032	-1.592079	2.952812
H	-5.123546	-0.827898	3.762533	H	3.116083	-1.158548	4.338257
C	-6.440418	1.126691	1.214005	H	2.374130	-1.375869	2.739437
H	-7.152298	1.634355	1.881202	C	2.226813	1.262898	3.481257
H	-6.082963	1.876632	0.493029	H	2.024027	1.029018	4.537998
H	-6.995546	0.350570	0.665792	H	2.356220	2.352365	3.402735
C	-4.566199	1.694313	2.748307	H	1.341816	0.990564	2.884499
H	-4.172324	2.412201	2.012710	C	-4.362405	3.899293	-1.877669
H	-5.262159	2.236972	3.406296	H	-4.017774	4.808994	-2.385666
H	-3.726415	1.342576	3.366353	C	-5.628217	3.515753	-2.041107
C	5.319120	4.505139	-0.095235	H	-6.320046	4.083296	-2.667625
H	6.208684	3.966733	-0.456180	H	-6.023637	2.616005	-1.559371
H	5.426169	5.565031	-0.372517				
H	5.314170	4.449409	1.003415				

2.16_Ag_complex

ωB97X-D SCF energy: -2479.14873306 a.u.
ωB97X-D enthalpy: -2478.014470 a.u.
ωB97X-D free energy: -2478.166656 a.u.
ωB97X-D SCF energy in solution: -2481.69767289 a.u.
ωB97X-D enthalpy in solution: -2480.563410 a.u.
ωB97X-D free energy in solution: -2480.715596 a.u.

Cartesian coordinates

ATOM	X	Y	Z				
C	5.383716	-0.919581	-0.032662	C	-0.644547	-2.340783	1.770962
C	4.132339	-0.451942	-0.827664	C	-0.489789	-3.785656	2.311089
N	3.109747	-1.431170	-0.364622	O	0.925402	-4.034673	2.264442
C	3.627019	-2.184555	0.530909	C	3.661888	-3.523022	2.646025
O	4.909195	-2.001569	0.790072	C	3.083728	-4.578132	0.408046
C	2.960731	-3.309791	1.289052	H	5.795999	-0.147617	0.628928
C	1.488227	-3.070668	1.558482	H	6.178567	-1.312102	-0.680603
N	0.717321	-2.105902	1.207575	H	-0.826108	-3.901055	3.348528

H	-0.983651	-4.532784	1.674993
H	3.193646	-4.361197	3.175344
H	3.593210	-2.624243	3.275816
H	4.722061	-3.751097	2.485672
H	2.667561	-5.443656	0.939375
H	2.550707	-4.449924	-0.545141
H	4.143490	-4.774590	0.195074
Ag	1.088240	-0.679143	-0.330677
N	-0.575760	0.397932	-0.254111
C	-0.364427	0.896363	-1.439009
O	-1.152381	1.717937	-2.077341
C	-2.383367	2.040542	-1.406777
C	-2.184136	3.143986	-0.370569
O	0.723992	0.495565	-2.003749
H	-2.773115	1.125402	-0.934704
H	-3.074356	2.345187	-2.202227
H	-1.268693	2.927249	0.199553
H	-2.036578	4.109260	-0.878224
C	3.623757	0.929016	-0.398213
C	2.331877	3.248601	0.415248
C	3.192348	1.079125	0.931914
C	3.436133	1.974331	-1.289229
C	2.790378	3.160065	-0.896358
C	2.517548	2.219242	1.353315
H	3.359243	0.265990	1.639562
H	3.750433	1.865953	-2.326712
H	1.799831	4.145247	0.731056
C	-1.700809	-2.255023	0.672246
C	-3.504973	-1.931823	-1.402220
C	-2.974544	-1.752611	0.925054
C	-1.366774	-2.655819	-0.623394
C	-2.239066	-2.452802	-1.692605
C	-3.914274	-1.614800	-0.103578
H	-3.246036	-1.449961	1.933734
H	-0.386787	-3.095747	-0.809436
H	-4.208866	-1.780987	-2.223425
C	1.925873	2.351256	2.761535
C	2.578245	4.276737	-1.926891
C	-5.352595	-1.135462	0.148711
C	-1.846870	-2.754026	-3.144958
C	4.318112	-0.604477	-2.332479
H	3.385629	-0.373512	-2.865592
H	4.607937	-1.637664	-2.570774
H	5.108421	0.066487	-2.698185
C	-0.852160	-1.331193	2.898675
H	-0.882188	-0.310974	2.493192
H	-0.029862	-1.403069	3.625691
H	-1.790100	-1.526651	3.435438
C	-1.985405	-1.465056	-3.977084
H	-1.329490	-0.670547	-3.590142
H	-1.704035	-1.655501	-5.024158
H	-3.016955	-1.083950	-3.977730
C	-0.395380	-3.238153	-3.262151
H	-0.151768	-3.426827	-4.317915
H	0.316085	-2.481106	-2.893192
H	-0.226975	-4.179061	-2.715387
C	-2.776482	-3.843246	-3.709195
H	-2.694312	-4.772781	-3.125473
H	-3.830173	-3.528215	-3.692111
H	-2.513412	-4.070194	-4.753842
C	-5.649361	-0.968933	1.643969
H	-6.692825	-0.648571	1.779993
H	-5.517288	-1.913157	2.194751
H	-5.014172	-0.197395	2.102570
C	-6.332299	-2.178265	-0.422158
H	-6.232564	-2.289193	-1.511735
H	-6.168071	-3.166228	0.034507
H	-7.370219	-1.875310	-0.216109
C	-5.579619	0.220602	-0.542875
H	-4.952406	1.003362	-0.091565
H	-5.358505	0.174279	-1.620312
H	-6.628967	0.533947	-0.431113
C	3.950641	4.753742	-2.436549
H	3.823544	5.560816	-3.174165
H	4.566527	5.140379	-1.610315
H	4.511712	3.944265	-2.926996
C	1.745071	3.730676	-3.101378
H	2.241112	2.889866	-3.607804
H	0.760870	3.376831	-2.760897
H	1.586054	4.521440	-3.850585
C	1.836355	5.478935	-1.330014
H	2.389811	5.932714	-0.493842
H	1.710569	6.254325	-2.099753
H	0.831255	5.204042	-0.974263
C	2.561484	3.551747	3.483009
H	3.648527	3.417227	3.589766
H	2.390500	4.491684	2.938195
H	2.130206	3.667218	4.489293
C	2.163396	1.089022	3.600706
H	1.713498	0.200809	3.129084
H	3.235385	0.895615	3.760543
H	1.701318	1.208106	4.591783

C	0.405064	2.559931	2.628649	H	-2.432435	1.912198	2.033223
H	0.162381	3.515162	2.140009	C	-5.636867	3.871812	1.075333
H	-0.043493	1.754535	2.025772	H	-4.559180	4.474300	-0.692549
H	-0.073557	2.570171	3.620172	C	-5.598393	3.148167	2.266143
C	-3.361215	3.196441	0.570857	H	-4.401030	1.893049	3.550877
C	-3.334277	2.469632	1.766930	H	-6.537367	4.424639	0.800041
C	-4.523647	3.898060	0.236185	H	-6.467337	3.132751	2.926994
C	-4.440878	2.452121	2.613293				

TS2.1

ωB97X-D SCF energy: -2518.41748372 a.u.
ωB97X-D enthalpy: -2517.258291 a.u.
ωB97X-D free energy: -2517.410701 a.u.
ωB97X-D SCF energy in solution: -2521.00438091 a.u.
ωB97X-D enthalpy in solution: -2519.845188 a.u.
ωB97X-D free energy in solution: -2519.997598 a.u.
Imaginary frequency: -282.8408 cm-1

Cartesian coordinates

ATOM	X	Y	Z				
C	1.874006	-2.600767	-2.968679	O	1.014983	1.748394	2.677202
C	1.488810	-1.372613	-2.101425	C	1.853124	3.558579	1.244888
N	0.275144	-1.878804	-1.410552	C	1.670380	2.980050	-0.143536
C	-0.071624	-2.989350	-1.944616	O	-0.240523	-0.061531	2.425500
O	0.722893	-3.453976	-2.901485	H	0.962959	4.103432	1.591811
C	-1.267419	-3.885458	-1.683972	H	2.677824	4.290065	1.237523
C	-2.201167	-3.373580	-0.609422	H	1.175450	1.917493	-0.008794
N	-1.918628	-2.663002	0.413395	H	2.637733	2.691320	-0.578590
C	-3.172923	-2.367642	1.155167	C	2.585155	-1.033754	-1.094300
C	-4.194118	-3.261393	0.399840	C	4.526428	-0.426360	0.796223
O	-3.463533	-3.765448	-0.731126	C	2.703890	-1.789611	0.068008
C	-0.747400	-5.263938	-1.209208	C	3.485183	0.011548	-1.319201
C	-2.035255	-4.028904	-3.015520	C	4.482807	0.318188	-0.392319
H	2.732199	-3.154835	-2.563587	C	3.652911	-1.484268	1.050714
H	2.059580	-2.350360	-4.020487	H	2.023572	-2.628843	0.230373
H	-4.526701	-4.121517	0.997246	H	3.409555	0.595664	-2.233695
H	-5.068258	-2.714197	0.026717	H	5.289741	-0.182008	1.534550
H	-0.112679	-5.712607	-1.984044	C	-3.420840	-0.866743	0.955224
H	-1.598646	-5.932767	-1.022251	C	-3.560147	1.856903	0.439519
H	-0.165990	-5.166716	-0.280996	C	-3.556688	-0.394121	-0.353037
H	-2.882076	-4.712898	-2.886438	C	-3.372142	0.049661	2.006288
H	-2.424013	-3.057784	-3.355700	C	-3.431650	1.425523	1.764959
H	-1.366362	-4.429820	-3.786291	C	-3.622845	0.970973	-0.639070
Ag	-0.453821	-1.028839	0.485296	H	-3.579550	-1.107098	-1.180552
N	0.604115	0.732736	0.592118	H	-3.247233	-0.308798	3.024550
C	0.475890	0.839081	1.900652	H	-3.601218	2.927681	0.242518

C	3.693870	-2.313218	2.341684
C	5.548154	1.396582	-0.647986
C	-3.640791	1.449557	-2.096365
C	-3.357606	2.459271	2.897799
C	1.063521	-0.182736	-2.961097
H	0.724519	0.650503	-2.330325
H	0.237068	-0.475591	-3.624694
H	1.890409	0.165199	-3.595301
C	-3.009267	-2.785466	2.610953
H	-3.928782	-2.587146	3.180145
H	-2.180041	-2.241816	3.084075
H	-2.789503	-3.860752	2.669144
C	0.814426	3.679577	-1.141785
C	1.109229	3.552746	-2.508265
C	-0.319711	4.417602	-0.772942
C	0.305598	4.149894	-3.475241
H	1.991089	2.982851	-2.813549
C	-1.115778	5.028122	-1.738370
H	-0.588835	4.521153	0.279544
C	-0.809988	4.893866	-3.092481
H	0.557538	4.044667	-4.532428
H	-1.982240	5.617315	-1.430438
H	-1.437244	5.372579	-3.846967
C	4.771369	-1.816262	3.313106
H	4.599025	-0.771904	3.615745
H	4.759108	-2.428775	4.226525
H	5.780825	-1.890999	2.881386
C	2.328358	-2.218914	3.047113
H	2.081054	-1.178897	3.306326
H	1.509897	-2.609047	2.421985
H	2.337491	-2.805927	3.978243
C	3.994670	-3.781319	1.988262
H	4.962221	-3.872260	1.471814
H	4.036497	-4.394014	2.901883
H	3.221417	-4.213510	1.335051
C	5.546665	2.433406	0.489536
H	5.712843	1.972677	1.474305
H	6.347647	3.171588	0.332743
H	4.593917	2.982667	0.525219
C	2.179387	2.485319	2.271064
H	2.928623	1.772470	1.887408
H	2.552209	2.927169	3.201927
C	6.926356	0.709282	-0.708421
H	7.714993	1.448702	-0.916430
H	7.176476	0.211650	0.239970
H	6.951039	-0.050419	-1.504178
C	5.323273	2.136994	-1.972692
H	6.105107	2.898052	-2.110194
H	5.372266	1.457913	-2.837098
H	4.354141	2.659907	-1.997708
C	-3.010699	1.811292	4.244344
H	-2.050060	1.275689	4.197266
H	-2.926630	2.587862	5.018807
H	-3.789552	1.108121	4.576057
C	-2.270192	3.503170	2.581510
H	-2.487847	4.060427	1.658507
H	-2.203368	4.237579	3.398729
H	-1.284372	3.025029	2.476769
C	-4.723610	3.160021	3.014069
H	-4.995339	3.676123	2.080766
H	-5.519086	2.434126	3.240763
H	-4.704787	3.909157	3.820821
C	-4.114353	2.903489	-2.215899
H	-4.158731	3.195482	-3.275722
H	-5.118369	3.037109	-1.784891
H	-3.425388	3.601078	-1.721408
C	-4.569633	0.573973	-2.954401
H	-5.594466	0.568002	-2.553187
H	-4.610038	0.964338	-3.982371
H	-4.224599	-0.468529	-3.023082
C	-2.197293	1.341178	-2.623699
H	-1.512085	1.967278	-2.030640
H	-1.838808	0.301275	-2.564420
H	-2.134640	1.668128	-3.673791

TS2.2

ωB97X-D SCF energy: -2518.41443861 a.u.
ωB97X-D enthalpy: -2517.254361 a.u.
ωB97X-D free energy: -2517.406382 a.u.
ωB97X-D SCF energy in solution: -2520.99915312 a.u.
ωB97X-D enthalpy in solution: -2519.839076 a.u.
ωB97X-D free energy in solution: -2519.991097 a.u.
Imaginary frequency: -221.5875 cm-1

Cartesian coordinates

ATOM	X	Y	Z
C	4.129534	2.725693	-0.771093
C	3.155085	2.024777	0.216295
N	1.844105	2.237283	-0.448989
C	2.051778	2.762392	-1.595772
O	3.309571	3.065499	-1.897898
C	1.064176	3.107830	-2.688286
C	-0.312783	2.527615	-2.448530
N	-0.624035	1.422759	-1.884972
C	-2.107299	1.313837	-1.843493
C	-2.532049	2.530776	-2.710869
O	-1.310845	3.248346	-2.944191
C	1.567878	2.521076	-4.027441
C	0.991292	4.647163	-2.766286
H	4.942874	2.077474	-1.119770
H	4.549879	3.655381	-0.362606
H	-2.941242	2.231251	-3.685923
H	-3.235562	3.205662	-2.208317
H	2.538922	2.958908	-4.290315
H	0.848110	2.755979	-4.823531
H	1.674781	1.428450	-3.963598
H	0.335220	4.953672	-3.589625
H	0.598019	5.072998	-1.831904
H	1.996149	5.051171	-2.943501
Ag	0.379057	0.582995	-0.078913
N	-0.388000	-1.337179	0.053266
C	-0.030934	-1.509536	1.311190
O	-0.135136	-2.608560	2.022048
C	-0.067608	-3.919985	1.440979
C	-1.317285	-4.313644	0.669331
C	-1.366147	-3.653751	-0.692761
O	0.447023	-0.472009	1.847441
H	0.087310	-4.578398	2.303171
H	0.830887	-3.966860	0.803121
H	-1.309396	-5.409507	0.551565
H	-2.196478	-4.072262	1.283689
H	-0.565131	-4.045116	-1.339024
H	-1.022517	-2.544258	-0.533772
C	3.370565	0.506346	0.275522
C	3.500249	-2.268716	0.317014
C	3.173912	-0.236463	-0.892287
C	3.674027	-0.165363	1.460344
C	3.756599	-1.558948	1.499190
C	3.209286	-1.634835	-0.892448
H	2.970952	0.282792	-1.832233
H	3.824725	0.402914	2.374537
H	3.546605	-3.357224	0.347621
C	-2.502848	1.479064	-0.372809
C	-2.930527	1.769018	2.356232
C	-1.980569	2.582538	0.321572
C	-3.250550	0.538167	0.320513
C	-3.488341	0.675834	1.699222
C	-2.153885	2.731913	1.692287
H	-1.394452	3.323481	-0.221660
H	-3.629540	-0.340869	-0.201121
H	-3.079866	1.873241	3.430443
C	2.940814	-2.394549	-2.199332
C	4.122585	-2.322790	2.779890
C	-1.478662	3.856064	2.486687
C	-4.251406	-0.424882	2.447315
C	3.140123	2.700372	1.581698
H	2.891633	3.764933	1.467715
H	4.122370	2.627034	2.069983
H	2.387872	2.239997	2.236803
C	-2.537865	-0.008549	-2.460804
H	-3.633429	-0.097498	-2.493507
H	-2.141236	-0.852109	-1.883925
H	-2.154787	-0.085474	-3.488037
C	-2.649219	-3.547234	-1.447231
C	-3.889962	-3.393961	-0.812126
C	-2.610030	-3.505096	-2.849692
C	-5.050859	-3.193920	-1.556041
H	-3.961252	-3.429010	0.276041
C	-3.768888	-3.308082	-3.594359
H	-1.651328	-3.624422	-3.361783
C	-4.994846	-3.145541	-2.948708
H	-6.008333	-3.081941	-1.042714
H	-3.716734	-3.285335	-4.684809
H	-5.906530	-2.993302	-3.529820
C	-4.646402	-0.001226	3.867598
H	-3.769168	0.181202	4.505668
H	-5.266959	0.907840	3.861779
H	-5.230434	-0.802126	4.344721
C	-5.533274	-0.801643	1.684378
H	-6.198164	0.068737	1.576946
H	-5.322632	-1.191730	0.678360
H	-6.083210	-1.582957	2.231252

C	-3.316373	-1.644254	2.535176	C	4.265262	-1.388118	3.987630
H	-3.829488	-2.503409	2.997174	H	5.072620	-0.653393	3.847348
H	-2.972696	-1.939975	1.533566	H	3.329654	-0.846828	4.196068
H	-2.423009	-1.415270	3.135285	H	4.514138	-1.976352	4.882989
C	-0.610108	4.749845	1.590593	C	3.027060	-3.354027	3.103453
H	0.185474	4.172257	1.092193	H	3.279384	-3.896522	4.027334
H	-1.205202	5.263412	0.819439	H	2.054803	-2.860228	3.247874
H	-0.126274	5.527114	2.200415	H	2.920118	-4.105104	2.306038
C	-0.565938	3.217633	3.551157	C	4.088778	-2.106291	-3.183869
H	-1.135750	2.625317	4.281382	H	4.165418	-1.032431	-3.413183
H	0.169442	2.545537	3.082030	H	5.054680	-2.431052	-2.768752
H	-0.021669	3.996274	4.107726	H	3.926883	-2.640659	-4.132863
C	-2.549218	4.726667	3.166592	C	1.605786	-1.926392	-2.809813
H	-3.210000	5.192824	2.420025	H	1.396103	-2.482214	-3.736749
H	-3.177609	4.139620	3.852383	H	0.774926	-2.084296	-2.107781
H	-2.076263	5.529113	3.753494	H	1.615855	-0.856442	-3.066667
C	5.464531	-3.044165	2.554057	C	2.853815	-3.908986	-1.974361
H	5.405938	-3.767209	1.726649	H	2.053784	-4.166961	-1.262204
H	6.263473	-2.325235	2.317127	H	2.629061	-4.416111	-2.924242
H	5.759477	-3.595962	3.459914	H	3.798175	-4.327584	-1.596400

TS2.3

ωB97X-D SCF energy: -2518.41476454 a.u.
ωB97X-D enthalpy: -2517.255413 a.u.
ωB97X-D free energy: -2517.408242 a.u.
ωB97X-D SCF energy in solution: -2521.00076036 a.u.
ωB97X-D enthalpy in solution: -2519.841409 a.u.
ωB97X-D free energy in solution: -2519.994238 a.u.
Imaginary frequency: -379.0289 cm-1

Cartesian coordinates

ATOM	X	Y	Z				
C	-4.409488	-2.924394	-0.360476	H	-4.980826	-3.715203	0.144065
C	-3.435354	-2.179428	0.596457	H	2.719946	-2.975650	-3.430575
N	-2.113853	-2.544718	0.027088	H	2.884698	-3.659103	-1.778382
C	-2.297127	-3.252481	-1.019881	H	-1.033192	-4.287954	-4.057593
O	-3.554012	-3.544043	-1.333215	H	-1.945611	-2.789432	-3.723744
C	-1.264759	-3.867527	-1.936385	H	-2.719070	-4.375996	-3.477477
C	0.072875	-3.157715	-1.923255	H	-0.376061	-5.847661	-2.150155
N	0.412915	-2.036140	-1.409672	H	-0.664716	-5.369663	-0.452819
C	1.800465	-1.723531	-1.834557	H	-2.034471	-5.852820	-1.492071
C	2.238397	-3.076745	-2.450239	Ag	-0.562676	-0.973461	0.272587
O	1.008414	-3.796025	-2.618054	N	0.497500	0.814627	0.456114
C	-1.774684	-3.825142	-3.394538	C	0.076794	1.033746	1.686215
C	-1.068668	-5.330216	-1.474715	O	0.328409	2.083883	2.434203
H	-5.099688	-2.254903	-0.889312	C	1.930756	3.525577	1.251630

C	2.112821	2.785023	-0.057587
O	-0.637460	0.106621	2.162355
H	2.132741	4.600383	1.116207
H	2.655775	3.161929	1.995318
H	1.460997	1.795743	0.013776
H	3.110941	2.336834	-0.146282
C	-3.552065	-0.653975	0.495400
C	-3.485771	2.112297	0.260104
C	-3.845383	0.151567	1.596574
C	-3.258901	-0.048128	-0.729506
C	-3.202965	1.343368	-0.869551
C	-3.821008	1.543813	1.497113
H	-4.066137	-0.310764	2.555152
H	-3.046580	-0.673736	-1.600982
H	-3.450723	3.198623	0.181972
C	2.663686	-1.342441	-0.635166
C	4.142051	-0.632708	1.600311
C	3.720598	-0.441381	-0.749530
C	2.390356	-1.917596	0.608730
C	3.090762	-1.543552	1.755041
C	4.497864	-0.091035	0.362524
H	3.951942	-0.006701	-1.720068
H	1.597382	-2.661204	0.685137
H	4.721473	-0.351694	2.481734
C	-4.125153	2.459325	2.691169
C	-2.801578	1.951358	-2.220274
C	5.739708	0.808508	0.252692
C	2.742775	-2.085309	3.147644
C	-3.517096	-2.712545	2.022620
H	-3.348662	-3.798793	2.023018
H	-4.506983	-2.519361	2.460132
H	-2.753115	-2.243883	2.658368
C	1.697409	-0.624258	-2.891336
H	2.677208	-0.398306	-3.334241
H	1.285513	0.292780	-2.449383
H	1.030944	-0.948031	-3.704566
C	1.701123	3.432483	-1.336802
C	2.201135	2.915610	-2.542564
C	0.803305	4.507124	-1.402305
C	1.806482	3.436914	-3.769871
H	2.917970	2.092247	-2.508548
C	0.410560	5.035863	-2.630155
H	0.407136	4.956454	-0.489586
C	0.902330	4.498386	-3.818179
H	2.213120	3.020922	-4.693989
H	-0.285408	5.876697	-2.657937
H	0.593363	4.914934	-4.778873
C	-5.339448	3.342790	2.351016
H	-5.580387	4.003444	3.198020
H	-5.151924	3.980956	1.474679
H	-6.226069	2.727260	2.135853
C	-4.441492	1.663675	3.963540
H	-5.328936	1.024716	3.838134
H	-3.594374	1.031799	4.271289
H	-4.652889	2.357105	4.790724
C	-2.897900	3.345241	2.974050
H	-2.648464	3.985494	2.113836
H	-3.096295	4.008652	3.829964
H	-2.019372	2.727626	3.213998
C	-1.367067	1.501953	-2.555849
H	-1.292782	0.406316	-2.645847
H	-1.034518	1.941035	-3.509283
H	-0.663223	1.820583	-1.772446
C	0.540101	3.375735	1.852350
H	0.394766	4.072918	2.685908
H	-0.252773	3.549179	1.107145
C	-3.769546	1.465046	-3.313342
H	-3.496688	1.902123	-4.286169
H	-3.748984	0.370619	-3.427173
H	-4.804611	1.760815	-3.084713
C	-2.833682	3.483435	-2.191630
H	-3.839852	3.868001	-1.965766
H	-2.127355	3.891361	-1.453329
H	-2.536095	3.879016	-3.173951
C	3.941484	-2.881297	3.694816
H	3.712718	-3.280184	4.695055
H	4.185953	-3.728648	3.036172
H	4.841139	-2.254664	3.784651
C	2.429248	-0.902875	4.083604
H	3.282960	-0.216747	4.182924
H	1.566724	-0.327119	3.716091
H	2.183625	-1.271495	5.091371
C	1.514196	-3.004186	3.118743
H	0.620626	-2.474248	2.751416
H	1.678431	-3.896950	2.495641
H	1.290899	-3.354536	4.137119
C	5.873616	1.452129	-1.133818
H	5.007936	2.086038	-1.383080
H	6.765128	2.095489	-1.159709
H	5.993584	0.701096	-1.928995
C	6.981594	-0.069204	0.504234
H	7.900825	0.531563	0.424251

H	6.959311	-0.520834	1.507146	H	6.595342	2.561030	1.221285
H	7.040876	-0.885837	-0.231137	H	4.820953	2.585994	1.156922
C	5.695087	1.933487	1.302354	H	5.660242	1.546459	2.330572

TS2.3'

ωB97X-D SCF energy: -2518.40809960 a.u.
ωB97X-D enthalpy: -2517.246583 a.u.
ωB97X-D free energy: -2517.398874 a.u.
ωB97X-D SCF energy in solution: -2520.99726150 a.u.
ωB97X-D enthalpy in solution: -2519.835745 a.u.
ωB97X-D free energy in solution: -2519.988036 a.u.
Imaginary frequency: -190.3396 cm-1

Cartesian coordinates

ATOM	X	Y	Z				
C	3.834998	3.414631	-0.166022	H	-1.160457	-3.788140	2.455754
C	3.104780	2.302899	0.629698	H	-0.984061	-1.846327	0.693296
N	1.687113	2.581708	0.274718	H	-2.460640	-2.754113	0.785352
C	1.630749	3.712959	-0.319152	C	3.471231	0.902242	0.150818
O	2.786975	4.326978	-0.534507	C	3.916164	-1.691169	-0.733002
C	0.415724	4.521149	-0.719749	C	4.165801	-0.002422	0.953971
C	-0.820810	3.690581	-0.977225	C	3.046407	0.499194	-1.114532
N	-0.991801	2.423787	-0.915534	C	3.231209	-0.810275	-1.570373
C	-2.371756	2.110062	-1.362358	C	4.415178	-1.305242	0.520809
C	-3.004472	3.524136	-1.403211	H	4.494256	0.304498	1.943071
O	-1.877317	4.409781	-1.334313	H	2.531656	1.217435	-1.758273
C	0.716013	5.322569	-2.004157	H	4.083077	-2.716085	-1.064402
C	0.118604	5.481000	0.459007	C	-3.063523	1.197411	-0.352372
H	4.303965	3.047747	-1.089966	C	-4.229554	-0.512975	1.495915
H	4.575026	3.960369	0.431368	C	-4.074386	0.320356	-0.744273
H	-3.554448	3.732356	-2.329032	C	-2.682609	1.237450	0.993378
H	-3.649429	3.725783	-0.536219	C	-3.235563	0.366498	1.935895
H	-0.155485	5.931760	-2.272530	C	-4.678294	-0.548284	0.172119
H	0.950903	4.652856	-2.844319	H	-4.386156	0.294535	-1.786333
H	1.574859	5.983356	-1.839156	H	-1.948247	1.975218	1.316927
H	-0.722518	6.138064	0.203284	H	-4.678771	-1.197726	2.218153
H	-0.129597	4.918881	1.371080	C	5.204852	-2.312658	1.369546
H	1.002151	6.102244	0.658231	C	2.665301	-1.212252	-2.937874
Ag	0.198394	0.937497	0.152675	C	-5.780160	-1.538049	-0.233155
N	0.528700	-0.796824	0.983954	C	-2.787136	0.349156	3.403190
C	1.074023	-1.212748	2.117031	C	3.252692	2.509228	2.135999
O	1.024709	-2.461741	2.529947	H	2.914700	3.520716	2.406471
C	-0.700543	-3.835306	1.457245	H	4.304718	2.415456	2.440433
C	-1.399859	-2.871045	0.511877	H	2.655439	1.770151	2.684694
O	1.651781	-0.330071	2.744746	C	-2.261402	1.491547	-2.758405
H	-0.826491	-4.874295	1.115230	H	-3.251491	1.329184	-3.205585

H	-1.733413	0.527823	-2.714157	C	3.389031	-0.416277	-4.038571
H	-1.702039	2.166659	-3.422702	H	2.995145	-0.686319	-5.030736
C	-1.296870	-3.138112	-0.968782	H	3.256975	0.669102	-3.911230
C	-2.040139	-2.326868	-1.839088	H	4.469129	-0.626623	-4.030937
C	-0.500891	-4.143517	-1.526820	C	2.841987	-2.709237	-3.215936
C	-2.005851	-2.521934	-3.215563	H	3.903203	-2.997219	-3.256694
H	-2.662405	-1.537294	-1.415164	H	2.339773	-3.323523	-2.453325
C	-0.458990	-4.338543	-2.908853	H	2.393298	-2.962794	-4.187939
H	0.091276	-4.803306	-0.889628	C	-3.978957	0.741802	4.295474
C	-1.212052	-3.533082	-3.758346	H	-3.683120	0.732596	5.355662
H	-2.604075	-1.883713	-3.870503	H	-4.338385	1.752561	4.049571
H	0.165406	-5.133682	-3.321430	H	-4.823569	0.046862	4.178613
H	-1.183780	-3.694198	-4.837767	C	-2.310185	-1.068544	3.768096
C	6.434824	-2.782906	0.571386	H	-3.107091	-1.817854	3.651763
H	7.031371	-3.488303	1.170116	H	-1.464128	-1.372616	3.135065
H	6.151445	-3.295509	-0.359817	H	-1.974320	-1.101756	4.815386
H	7.079513	-1.931657	0.304900	C	-1.631467	1.322623	3.671354
C	5.685142	-1.700608	2.691604	H	-0.732045	1.071879	3.086076
H	6.358955	-0.846045	2.526627	H	-1.912782	2.366159	3.461403
H	4.842199	-1.367242	3.316004	H	-1.345478	1.271735	4.731889
H	6.244553	-2.453361	3.266333	C	-6.102617	-1.463308	-1.731009
C	4.308686	-3.518040	1.703678	H	-5.227692	-1.713657	-2.351309
H	3.920063	-4.008169	0.797889	H	-6.892703	-2.188084	-1.975418
H	4.877921	-4.271616	2.269449	H	-6.470158	-0.468242	-2.024888
H	3.457290	-3.201301	2.323967	C	-7.058207	-1.210681	0.561074
C	1.159076	-0.893153	-2.970665	H	-7.868969	-1.900573	0.281243
H	0.962307	0.184941	-2.853968	H	-6.902465	-1.303548	1.646067
H	0.719479	-1.203423	-3.930472	H	-7.397390	-0.183972	0.355817
H	0.625874	-1.429841	-2.170754	C	-5.323251	-2.974251	0.085594
C	0.784316	-3.551829	1.620909	H	-6.114988	-3.691359	-0.179226
H	1.301395	-4.401239	2.083189	H	-4.424028	-3.240563	-0.491425
H	1.271516	-3.322394	0.658714	H	-5.101299	-3.110923	1.154511

TS2.4

ωB97X-D SCF energy: -2518.41364918 a.u.
ωB97X-D enthalpy: -2517.254527 a.u.
ωB97X-D free energy: -2517.406566 a.u.
ωB97X-D SCF energy in solution: -2520.99810990 a.u.
ωB97X-D enthalpy in solution: -2519.838988 a.u.
ωB97X-D free energy in solution: -2519.991027 a.u.
Imaginary frequency: -413.4387 cm-1

Cartesian coordinates

ATOM	X	Y	Z				
C	4.155953	-3.102975	0.109531	N	1.886453	-2.482898	0.017144
C	3.143289	-2.305787	-0.756749	C	2.169960	-3.034284	1.134013

O	3.430932	-3.414099	1.310304
C	1.243912	-3.363453	2.282990
C	0.018005	-2.475001	2.348721
N	-0.209248	-1.347181	1.790670
C	-1.586941	-0.916647	2.129935
C	-1.991676	-1.981740	3.188913
O	-0.937078	-2.951642	3.139467
C	1.990451	-3.199669	3.624681
C	0.800673	-4.831668	2.085891
H	5.048546	-2.528904	0.386386
H	4.458416	-4.049982	-0.359064
H	-2.026487	-1.568657	4.207350
H	-2.937497	-2.488800	2.963406
H	2.350340	-2.168466	3.754865
H	2.852624	-3.876414	3.662440
H	1.311841	-3.443004	4.452419
H	1.688181	-5.476252	2.028859
H	0.182204	-5.157033	2.931241
H	0.221289	-4.947606	1.158376
Ag	0.555484	-0.720910	-0.212339
N	-0.156377	1.203444	-0.456078
C	-0.272498	1.110365	-1.771256
O	-0.772177	2.033184	-2.562889
C	-1.684494	3.008631	-2.045439
C	-0.971872	4.145950	-1.325431
C	-0.382096	3.742517	0.015221
O	0.130102	0.025356	-2.262561
H	-2.398166	2.492876	-1.382493
H	-2.219727	3.378496	-2.927970
H	-0.182440	4.524853	-1.990627
H	-1.692877	4.968693	-1.194211
H	0.640542	4.119859	0.155738
H	-0.181185	2.568780	-0.038406
C	3.410538	-0.792803	-0.751711
C	3.553464	1.977804	-0.595684
C	3.460178	-0.024920	-1.917801
C	3.465241	-0.146452	0.486168
C	3.509359	1.245926	0.591045
C	3.539989	1.369444	-1.858502
H	3.404758	-0.517852	-2.885134
H	3.431543	-0.739476	1.403614
H	3.596620	3.065301	-0.545578
C	-2.444140	-1.026951	0.863042
C	-3.934809	-1.293754	-1.469084
C	-2.203649	-2.073423	-0.025510
C	-3.471531	-0.120514	0.577753
C	-4.251900	-0.260196	-0.572865
C	-2.916207	-2.210965	-1.222542
H	-1.430352	-2.808847	0.202069
H	-3.665652	0.699439	1.267406
H	-4.520802	-1.386789	-2.382850
C	3.613281	2.243268	-3.118841
C	3.428416	1.889891	1.980641
C	-2.548620	-3.348131	-2.184802
C	-5.462005	0.637919	-0.872650
C	2.971154	-2.901665	-2.147425
H	2.157909	-2.398752	-2.688757
H	2.717640	-3.967999	-2.067459
H	3.896556	-2.807819	-2.733672
C	-1.551300	0.487160	2.722366
H	-2.530364	0.772221	3.132659
H	-1.270310	1.223947	1.959583
H	-0.816886	0.529046	3.538909
C	-1.193972	3.898065	1.255242
C	-2.595131	3.853003	1.242365
C	-0.544932	4.009933	2.494389
C	-3.323652	3.896644	2.427937
H	-3.133569	3.790251	0.294899
C	-1.270015	4.055203	3.681216
H	0.545649	4.062412	2.525402
C	-2.663244	3.990281	3.653033
H	-4.414798	3.862574	2.393769
H	-0.745359	4.148832	4.634218
H	-3.234157	4.028339	4.582899
C	-5.646457	1.732534	0.184066
H	-4.769458	2.393002	0.240766
H	-6.516713	2.355043	-0.070829
H	-5.823320	1.312597	1.185854
C	-5.295584	1.312162	-2.245984
H	-4.400695	1.951566	-2.267709
H	-5.202554	0.580064	-3.060846
H	-6.168554	1.944520	-2.468917
C	-6.728996	-0.239278	-0.883752
H	-7.620071	0.377907	-1.076677
H	-6.684125	-1.013375	-1.663638
H	-6.865508	-0.743904	0.084695
C	-1.055141	-3.239843	-2.550963
H	-0.402756	-3.365563	-1.672127
H	-0.783804	-4.024704	-3.273946
H	-0.828406	-2.260439	-2.998625
C	-3.367966	-3.291179	-3.479498
H	-3.209080	-2.345642	-4.019961

H	-3.064673	-4.110081	-4.148291	H	3.401827	3.845108	2.921752
H	-4.445691	-3.406794	-3.289273	H	4.415444	3.782400	1.467097
C	-2.815443	-4.697367	-1.492590	C	2.516078	3.322987	-3.075559
H	-2.557151	-5.530539	-2.164363	H	2.581265	3.961400	-3.969913
H	-2.217967	-4.812272	-0.574927	H	1.515277	2.867377	-3.061612
H	-3.876260	-4.797319	-1.217236	H	2.612054	3.981208	-2.198867
C	2.092142	1.470188	2.624133	C	3.416661	1.422308	-4.399445
H	1.966734	1.948881	3.608227	H	3.444085	2.087873	-5.274629
H	1.241379	1.758458	1.988680	H	4.212747	0.674826	-4.536032
H	2.029022	0.381393	2.772071	H	2.444642	0.905365	-4.402752
C	4.601438	1.406274	2.850722	C	4.997791	2.916294	-3.164976
H	5.566379	1.685149	2.401445	H	5.089120	3.544793	-4.064291
H	4.547995	1.859271	3.852670	H	5.167416	3.558639	-2.287651
H	4.594448	0.313738	2.981939	H	5.800333	2.163726	-3.191479
C	3.475277	3.420396	1.909421				
H	2.641444	3.828057	1.317630				

TS2.5

ωB97X-D SCF energy: -2364.91358170 a.u.
ωB97X-D enthalpy: -2363.805851 a.u.
ωB97X-D free energy: -2363.955729 a.u.
ωB97X-D SCF energy in solution: -2367.34187539 a.u.
ωB97X-D enthalpy in solution: -2366.234145 a.u.
ωB97X-D free energy in solution: -2366.384023 a.u.
Imaginary frequency: -273.8516 cm-1

Cartesian coordinates

ATOM	X	Y	Z				
C	-4.445072	2.499588	-0.936943	H	-2.336972	3.695813	2.454357
C	-3.393036	1.469780	-1.436053	H	-3.057115	5.055331	1.555554
N	-2.126209	2.074276	-0.946738	H	-0.688462	4.897878	-1.397673
C	-2.404342	3.106692	-0.247989	H	-2.150366	5.700126	-0.758387
O	-3.684890	3.448583	-0.171526	H	-0.569096	5.982450	0.017921
C	-1.460205	4.043908	0.471417	Ag	-0.575206	0.583059	-0.441340
C	-0.136261	3.416679	0.859601	N	0.566762	-1.037948	0.141138
N	0.250538	2.197506	0.819390	C	0.406123	-1.686258	-0.997529
C	1.583531	2.098641	1.466806	O	0.946833	-2.829318	-1.345227
C	1.955315	3.597434	1.614126	C	1.984207	-3.792209	0.669477
O	0.721769	4.289663	1.375005	C	1.900070	-2.652202	1.661950
C	-2.117469	4.537027	1.780191	O	-0.355282	-1.101811	-1.819439
C	-1.195696	5.232948	-0.481488	H	1.084575	-4.427198	0.714562
H	-5.208631	2.064032	-0.280462	H	2.838275	-4.443228	0.919613
H	-4.933750	3.040007	-1.759021	H	1.264397	-1.801073	1.137726
H	2.313984	3.861811	2.616463	H	2.865893	-2.139692	1.786285
H	2.683578	3.930002	0.861075	C	-3.503780	0.108829	-0.737770
H	-1.441192	5.232235	2.292760	C	-3.357284	-2.305700	0.625746

C	-3.566967	-1.097275	-1.437534	H	-0.905592	-0.911562	2.631562
C	-3.398506	0.080294	0.655108	H	-1.726218	0.659072	2.763037
C	-3.302373	-1.122051	1.362356	C	2.167503	-3.305193	-0.759180
C	-3.496001	-2.321733	-0.768942	H	2.916966	-2.498699	-0.816551
H	-3.633815	-1.083931	-2.522293	H	2.475506	-4.123112	-1.419940
H	-3.354583	1.021994	1.209369	C	-4.209695	-0.306909	3.561388
H	-3.283117	-3.258286	1.149211	H	-4.050440	-0.272228	4.650120
C	2.573278	1.356379	0.572393	H	-4.274744	0.732167	3.204773
C	4.287230	-0.049704	-1.091763	H	-5.181313	-0.788352	3.374293
C	3.598988	0.582899	1.112509	C	-3.002290	-2.487155	3.489271
C	2.447181	1.449079	-0.815644	H	-2.837790	-2.413581	4.574500
C	3.269430	0.716362	-1.672253	H	-3.936348	-3.047479	3.333225
C	4.492149	-0.113447	0.289554	H	-2.172221	-3.075211	3.069086
H	3.707748	0.517029	2.192869	C	1.856092	1.530464	-3.625536
H	1.669259	2.087218	-1.234647	H	0.932033	1.116498	-3.190905
H	4.961068	-0.604753	-1.748058	H	1.935717	2.592151	-3.345406
C	-3.540499	-3.667002	-1.506825	H	1.750622	1.490078	-4.719537
C	-3.070249	-1.082726	2.878170	C	4.338877	1.347752	-3.846109
C	5.689113	-0.900341	0.847469	H	4.490147	2.381215	-3.498933
C	3.089793	0.725330	-3.196223	H	5.249132	0.776989	-3.609462
C	-3.349019	1.386105	-2.956909	H	4.232616	1.366827	-4.941667
H	-3.205988	2.389680	-3.381726	C	2.907780	-0.720790	-3.694352
H	-4.287122	0.973267	-3.354816	H	3.775563	-1.353526	-3.456031
H	-2.516410	0.750838	-3.289158	H	2.011401	-1.181575	-3.252744
C	1.379354	1.427504	2.826193	H	2.785636	-0.732727	-4.788160
H	2.299922	1.455464	3.425256	C	6.982516	-0.224614	0.352340
H	1.071953	0.380643	2.698628	H	7.027399	0.824559	0.681243
H	0.597584	1.955119	3.391985	H	7.865956	-0.746611	0.751158
C	-2.278989	-4.482222	-1.164880	H	7.053483	-0.236132	-0.745275
H	-2.302011	-5.449965	-1.689211	C	5.653946	-2.357180	0.352110
H	-1.368077	-3.949798	-1.475937	H	4.767631	-2.885771	0.734613
H	-2.203082	-4.696211	-0.088129	H	5.646466	-2.425526	-0.745607
C	-4.795441	-4.438345	-1.058151	H	6.541738	-2.901246	0.708248
H	-5.709878	-3.870908	-1.288717	C	5.709888	-0.918160	2.381400
H	-4.855067	-5.407267	-1.577480	H	4.808116	-1.390856	2.802320
H	-4.787692	-4.639593	0.023565	H	6.575529	-1.497293	2.734528
C	-3.590864	-3.487553	-3.029131	H	5.799554	0.093759	2.804012
H	-2.708028	-2.946463	-3.402715	C	1.224398	-2.905744	2.953972
H	-3.607660	-4.472884	-3.517607	H	0.347034	-3.562983	2.926319
H	-4.495796	-2.949687	-3.350689	C	1.592823	-2.357927	4.116763
C	-1.725326	-0.377373	3.135789	H	2.464359	-1.699122	4.185639
H	-1.500496	-0.345321	4.213527	H	1.046533	-2.559879	5.040713

TS2.6

ωB97X-D SCF energy: -2364.91231213 a.u.

ωB97X-D enthalpy: -2363.804695 a.u.

ωB97X-D free energy: -2363.950758 a.u.
ωB97X-D SCF energy in solution: -2367.34291781 a.u.
ωB97X-D enthalpy in solution: -2366.235301 a.u.
ωB97X-D free energy in solution: -2366.381364 a.u.
Imaginary frequency: -459.6175 cm-1

Cartesian coordinates

ATOM	X	Y	Z
C	4.632647	-1.734811	-2.089420
C	3.808929	-0.436585	-1.939884
N	2.428279	-0.974279	-2.078674
C	2.478882	-2.237259	-1.893514
O	3.685013	-2.783675	-1.814126
C	1.278257	-3.141112	-1.685174
C	0.552322	-2.655655	-0.435412
N	0.164389	-1.458383	-0.198797
C	-0.635110	-1.450352	1.041562
C	-0.386454	-2.894149	1.565364
O	0.235086	-3.571541	0.460805
C	1.710392	-4.603660	-1.534572
C	0.307270	-2.987518	-2.877740
H	5.472193	-1.829575	-1.392357
H	4.995032	-1.874328	-3.118230
H	0.314581	-2.926243	2.411602
H	-1.305074	-3.432505	1.823841
H	0.828380	-5.240983	-1.396611
H	2.377792	-4.745631	-0.675775
H	2.240770	-4.926663	-2.439417
H	-0.602354	-3.576162	-2.693495
H	0.019243	-1.939511	-3.038366
H	0.783467	-3.359930	-3.794981
Ag	0.752116	0.304132	-1.377745
N	-0.637977	1.743257	-0.726917
C	-0.237648	2.643350	-1.612594
O	-0.683337	3.862373	-1.776089
C	-1.968806	4.291382	-1.307887
C	-2.047880	4.355680	0.211563
C	-2.218068	2.994725	0.845642
O	0.702902	2.243623	-2.356559
H	-2.735117	3.617149	-1.722575
H	-2.092672	5.284152	-1.754414
H	-1.135567	4.844808	0.584084
H	-2.889322	5.012567	0.485120
H	-1.707414	2.898083	1.815676
H	-1.540887	2.228287	0.195085
C	3.836693	0.150513	-0.520317
C	3.519656	1.107310	2.072801
C	4.061463	-0.678427	0.576716
C	3.455373	1.480903	-0.296613
C	3.282207	1.976043	0.997321
C	3.919115	-0.216347	1.891799
H	4.341854	-1.721765	0.420853
H	3.280139	2.136909	-1.147089
H	3.389105	1.487454	3.085348
C	-2.116523	-1.228819	0.727106
C	-4.826695	-0.893493	0.215519
C	-3.047402	-1.286054	1.774863
C	-2.567275	-0.998324	-0.563582
C	-3.928748	-0.811587	-0.844269
C	-4.411898	-1.129321	1.538385
H	-2.693003	-1.468436	2.790613
H	-1.847805	-0.959066	-1.379367
H	-5.891260	-0.765142	0.021781
C	4.217797	-1.167583	3.060108
C	2.816339	3.412827	1.272657
C	-5.461824	-1.198567	2.656313
C	-4.353002	-0.519829	-2.289645
C	4.114596	0.570096	-3.041196
H	5.111368	1.010795	-2.897139
H	3.374100	1.380404	-3.057749
H	4.082501	0.077786	-4.023009
C	-0.094839	-0.381873	1.993884
H	-0.571649	-0.459171	2.981430
H	-0.295311	0.619008	1.589612
H	0.993209	-0.489821	2.115780
C	-3.550161	2.351521	0.861720
C	-4.681489	2.836613	0.338235
H	-4.741740	3.812079	-0.152866
C	-3.924768	-1.691896	-3.191656
H	-4.391888	-2.632555	-2.862581
H	-4.228539	-1.505430	-4.233219
H	-2.833533	-1.835590	-3.186281
C	-5.868903	-0.332817	-2.420879
H	-6.229049	0.512348	-1.814525

H	-6.129602	-0.121134	-3.468345	C	2.739394	4.252327	-0.008705
H	-6.421282	-1.235660	-2.119669	H	2.407809	5.272350	0.235486
C	-3.661581	0.774061	-2.759854	H	3.720926	4.334115	-0.499772
H	-2.564560	0.695121	-2.714266	H	2.027912	3.841509	-0.739186
H	-3.942303	1.004835	-3.799025	C	1.411816	3.350044	1.901744
H	-3.961384	1.619528	-2.121713	H	1.411502	2.786709	2.847324
C	-6.415685	-2.374296	2.374979	H	1.040501	4.364843	2.116928
H	-6.941461	-2.255651	1.416136	H	0.708581	2.857641	1.213036
H	-5.866134	-3.327371	2.342124	C	3.299518	-2.400477	2.973215
H	-7.177954	-2.446643	3.165963	H	3.538386	-3.114077	3.776426
C	-6.259605	0.118487	2.688979	H	2.245930	-2.104812	3.091035
H	-7.008887	0.091270	3.494812	H	3.400675	-2.934249	2.016007
H	-5.597991	0.979905	2.870288	C	3.992465	-0.499439	4.421905
H	-6.799160	0.296042	1.746750	H	4.653293	0.368161	4.566809
C	-4.825295	-1.408423	4.035740	H	2.950673	-0.166075	4.548823
H	-4.270238	-2.357347	4.092662	H	4.209587	-1.215699	5.227917
H	-4.141387	-0.587335	4.301525	C	5.689127	-1.614354	2.972400
H	-5.610210	-1.443711	4.805328	H	5.896829	-2.163686	2.042021
C	3.792015	4.103631	2.242175	H	6.364906	-0.746864	3.010123
H	4.809748	4.127795	1.824509	H	5.938909	-2.279183	3.813439
H	3.474395	5.141730	2.423820	H	-5.609187	2.264364	0.407864
H	3.838736	3.599927	3.218468	H	-3.578391	1.366834	1.339346

TS2.7

ωB97X-D SCF energy: -2479.13519112 a.u.
ωB97X-D enthalpy: -2478.006292 a.u.
ωB97X-D free energy: -2478.158765 a.u.
ωB97X-D SCF energy in solution: -2481.68052406 a.u.
ωB97X-D enthalpy in solution: -2480.551625 a.u.
ωB97X-D free energy in solution: -2480.704098 a.u.
Imaginary frequency: -569.5116 cm-1

Cartesian coordinates

ATOM	X	Y	Z				
C	4.618656	-3.046415	0.571327	C	1.150910	-5.183417	1.919300
C	3.650752	-2.396542	-0.457936	H	5.329647	-2.336018	1.011940
N	2.328754	-2.648715	0.169492	H	5.166678	-3.904223	0.159077
C	2.507894	-3.234369	1.290058	H	-2.321013	-2.344548	3.910928
O	3.760689	-3.527629	1.618226	H	-2.663910	-3.273356	2.413495
C	1.468667	-3.712575	2.280279	H	2.284390	-2.581799	3.975971
C	0.176817	-2.919570	2.261043	H	2.945923	-4.225037	3.795527
N	-0.154538	-1.876647	1.597359	H	1.293035	-3.995799	4.429475
C	-1.490624	-1.422003	2.060388	H	2.076603	-5.774425	1.939969
C	-1.933646	-2.630988	2.925443	H	0.448433	-5.605622	2.649044
O	-0.729736	-3.387371	3.112179	H	0.709629	-5.255368	0.914788
C	2.034929	-3.620718	3.714260	C	3.802225	-0.874220	-0.547042

C	3.762325	1.901324	-0.637516
C	4.024317	-0.208081	-1.752590
C	3.592326	-0.124758	0.613807
C	3.556834	1.273606	0.591870
C	4.004862	1.186558	-1.818248
H	4.177187	-0.782546	-2.662554
H	3.425408	-0.641852	1.562917
H	3.724895	2.989178	-0.687324
C	-2.433360	-1.201299	0.880375
C	-4.077625	-0.801583	-1.321760
C	-2.321209	-2.012952	-0.244047
C	-3.412674	-0.204286	0.903936
C	-4.266114	-0.003245	-0.183007
C	-3.114484	-1.810136	-1.379138
H	-1.574508	-2.810391	-0.252888
H	-3.516845	0.422664	1.786733
H	-4.727692	-0.643368	-2.181822
C	4.204577	1.949109	-3.134986
C	3.227981	2.041245	1.879041
C	-2.895125	-2.690475	-2.616892
C	-5.434405	0.995522	-0.138616
C	3.694528	-3.104663	-1.807349
H	2.921036	-2.709846	-2.480557
H	3.514809	-4.180351	-1.669297
H	4.676078	-2.978833	-2.286343
C	-1.276389	-0.167548	2.908718
H	-2.207745	0.142959	3.401630
H	-0.908586	0.658564	2.285336
H	-0.534087	-0.368437	3.695078
C	-5.400206	1.875525	1.117791
H	-4.467430	2.457924	1.189979
H	-6.233311	2.592978	1.092285
H	-5.508261	1.285149	2.039784
C	-5.423339	1.919587	-1.369021
H	-4.537009	2.572022	-1.375083
H	-5.443091	1.361380	-2.315951
H	-6.308541	2.573113	-1.357967
C	-6.745334	0.184238	-0.129437
H	-7.614596	0.857090	-0.067511
H	-6.851977	-0.421051	-1.041790
H	-6.777984	-0.498333	0.733122
C	-1.436758	-2.542896	-3.089983
H	-0.716696	-2.866147	-2.321729
H	-1.260653	-3.161220	-3.983507
H	-1.201141	-1.500012	-3.348883
C	-3.818238	-2.296561	-3.776261
H	-3.653416	-1.255729	-4.094787
H	-3.619384	-2.941082	-4.644995
H	-4.880633	-2.416505	-3.515603
C	-3.174033	-4.158610	-2.246343
H	-3.028036	-4.808942	-3.122490
H	-2.501241	-4.516491	-1.452210
H	-4.209067	-4.286704	-1.894989
C	1.767592	1.730236	2.256150
H	1.477690	2.270026	3.171532
H	1.085805	2.031172	1.445228
H	1.618134	0.653841	2.437994
C	4.166688	1.597595	3.014482
H	5.219003	1.781699	2.750369
H	3.943454	2.160485	3.933703
H	4.060329	0.528640	3.252969
C	3.370163	3.555999	1.697600
H	2.666829	3.944687	0.948004
H	3.148332	4.067006	2.646427
H	4.391848	3.835868	1.398518
C	2.962959	2.819291	-3.404422
H	3.073950	3.356660	-4.358893
H	2.055003	2.199522	-3.461236
H	2.816965	3.572056	-2.615738
C	4.393335	1.003982	-4.327803
H	4.528343	1.591663	-5.247717
H	5.285256	0.369223	-4.212722
H	3.516378	0.355349	-4.475503
C	5.451344	2.844237	-3.014479
H	5.613013	3.403096	-3.949189
H	5.352726	3.577629	-2.200216
H	6.351123	2.241781	-2.817494
Ag	0.819992	-1.064072	-0.212350
N	-0.366145	0.624920	-0.510882
O	0.815644	-0.084134	-2.202760
O	-0.574215	1.621017	-2.611081
C	-1.758947	2.265428	-2.144746
H	-1.930644	3.115308	-2.818624
C	-1.626413	2.692042	-0.696046
H	-1.179465	1.703521	-0.181589
C	-0.041714	0.736886	-1.789669
H	-2.593104	1.553481	-2.243282
H	-2.612023	2.754243	-0.212750
C	-0.743101	3.831502	-0.337294
C	-0.906158	4.456859	0.909000
C	0.264909	4.294507	-1.196675
C	-0.099295	5.527320	1.279775

H	-1.686181	4.104721	1.589823	H	-0.244918	6.008627	2.248736
C	1.065035	5.373195	-0.828455	H	1.834505	5.733571	-1.514671
H	0.425751	3.814698	-2.163524	H	1.512797	6.839926	0.692355
C	0.884780	5.993684	0.407295				

TS2.8

ωB97X-D SCF energy: -2479.12903518 a.u.
ωB97X-D enthalpy: -2477.999965 a.u.
ωB97X-D free energy: -2478.150622 a.u.
ωB97X-D SCF energy in solution: -2481.67757453 a.u.
ωB97X-D enthalpy in solution: -2480.548504 a.u.
ωB97X-D free energy in solution: -2480.699161 a.u.
Imaginary frequency: -617.1651 cm-1

Cartesian coordinates

ATOM	X	Y	Z				
C	4.142274	-3.144427	-1.309390	C	4.583107	1.387747	1.128491
C	3.498648	-1.759260	-1.588507	C	4.543376	0.530594	-1.110485
N	2.072658	-2.034068	-1.279742	C	3.759824	-0.817365	0.722355
C	1.927143	-3.289899	-1.098680	C	4.041008	0.206732	1.634431
O	3.020363	-4.035545	-1.169986	C	4.846939	1.573614	-0.234819
C	0.612265	-4.019709	-0.911324	H	4.710246	0.664369	-2.176235
C	-0.252758	-3.389096	0.168428	H	3.330113	-1.754438	1.088698
N	-0.331446	-2.163306	0.538490	H	4.804234	2.205694	1.813317
C	-1.494330	-2.023109	1.447733	C	-2.651493	-1.311855	0.738156
C	-1.848588	-3.510936	1.714904	C	-4.831966	-0.124725	-0.515359
O	-1.117716	-4.228774	0.714385	C	-3.851018	-1.111140	1.437155
C	0.858896	-5.502458	-0.595204	C	-2.575464	-0.914466	-0.587827
C	-0.184159	-3.877819	-2.234339	C	-3.652714	-0.292632	-1.234930
H	4.717590	-3.175551	-0.373919	C	-4.962524	-0.538689	0.821943
H	4.767474	-3.506840	-2.134541	H	-3.921535	-1.439938	2.474694
H	-1.499414	-3.857989	2.699074	H	-1.658847	-1.090321	-1.148951
H	-2.913510	-3.740289	1.597199	H	-5.689938	0.334969	-1.004913
H	-0.097021	-6.033596	-0.526862	C	5.398226	2.921715	-0.716810
H	1.398133	-5.629709	0.353155	C	3.717739	0.004752	3.120315
H	1.460904	-5.954834	-1.392261	C	-6.319076	-0.407739	1.531554
H	-1.160224	-4.373033	-2.139204	C	-3.473608	0.166528	-2.687348
H	-0.341606	-2.820293	-2.487029	C	3.587250	-1.393455	-3.068490
H	0.371613	-4.356214	-3.052891	H	3.184872	-2.214397	-3.680012
Ag	0.830361	-0.471630	-0.313866	H	4.630440	-1.223310	-3.370598
N	-0.123901	1.184271	0.609188	H	3.004304	-0.486844	-3.281309
C	0.708949	2.050676	0.044527	C	-1.087924	-1.303932	2.732095
O	0.744969	3.336082	0.340036	H	-1.929492	-1.266031	3.437449
C	-1.389276	3.079003	1.445156	H	-0.771338	-0.277942	2.508508
O	1.506834	1.566801	-0.794596	H	-0.256809	-1.831765	3.220063
C	3.986669	-0.661182	-0.645494	C	6.741620	3.205283	-0.020819

H	7.147546	4.172410	-0.355188	H	-1.356767	0.725503	-2.428735
H	6.638376	3.251031	1.073409	H	-2.175472	1.545191	-3.774936
H	7.480998	2.424998	-0.257534	C	-3.150043	-1.051829	-3.571042
C	5.623442	2.945319	-2.233661	H	-2.220548	-1.550632	-3.257332
H	6.346678	2.179375	-2.553532	H	-3.961266	-1.794698	-3.532428
H	4.685088	2.795206	-2.789164	H	-3.020165	-0.741056	-4.619135
H	6.028405	3.923358	-2.532452	C	-6.231358	-0.766483	3.020529
C	4.380062	4.022350	-0.361982	H	-5.515093	-0.123051	3.555139
H	4.232187	4.107376	0.725126	H	-7.214869	-0.631491	3.493940
H	4.733239	4.999767	-0.725760	H	-5.939607	-1.816066	3.176464
H	3.401134	3.812377	-0.817902	C	-7.311099	-1.371218	0.852034
C	2.220923	-0.325133	3.255678	H	-8.297669	-1.313926	1.337593
H	1.961372	-1.259811	2.735701	H	-7.445348	-1.129405	-0.212850
H	1.941120	-0.446708	4.313949	H	-6.956870	-2.411139	0.918697
H	1.599176	0.475077	2.823317	C	-6.851329	1.031239	1.417836
C	-0.021533	3.728370	1.476296	H	-7.820044	1.119107	1.932457
H	-0.075017	4.824683	1.448164	H	-6.160376	1.752557	1.881167
H	0.524659	3.426601	2.383450	H	-7.013683	1.330253	0.372067
C	4.558255	-1.160648	3.672006	H	-1.120615	1.921774	1.202445
H	4.336788	-1.325292	4.737958	C	-2.373407	3.520670	0.424424
H	4.352773	-2.101684	3.139701	C	-3.696433	3.060750	0.514103
H	5.633522	-0.948077	3.575903	C	-2.025533	4.374517	-0.634688
C	4.012608	1.257459	3.953741	C	-4.652322	3.468438	-0.408134
H	5.077540	1.531346	3.920368	H	-3.974124	2.370026	1.314534
H	3.423993	2.123405	3.612989	C	-2.986608	4.784544	-1.555140
H	3.753960	1.073467	5.007086	H	-0.998633	4.725768	-0.748723
C	-4.733708	0.843172	-3.238707	C	-4.301910	4.337265	-1.442513
H	-4.560488	1.163078	-4.276868	H	-5.677978	3.107856	-0.317190
H	-5.596772	0.160217	-3.244109	H	-2.704253	5.457463	-2.366874
H	-4.998475	1.737978	-2.656820	H	-5.054588	4.662619	-2.163329
C	-2.310703	1.174863	-2.746996	H	-1.827240	2.995437	2.450395
H	-2.506620	2.037477	-2.094386				

TS2.9

ωB97X-D SCF energy: -2595.73722716 a.u.
ωB97X-D enthalpy: -2594.541497 a.u.
ωB97X-D free energy: -2594.702019 a.u.
ωB97X-D SCF energy in solution: -2598.40770823 a.u.
ωB97X-D enthalpy in solution: -2597.211978 a.u.
ωB97X-D free energy in solution: -2597.372500 a.u.
Imaginary frequency: -237.7762 cm-1

Cartesian coordinates

ATOM	X	Y	Z				
C	2.229001	-0.559165	-3.666598	N	0.521893	-0.874404	-2.090170
C	1.741504	-0.047077	-2.286152	C	0.251831	-1.477339	-3.186918

O	1.112113	-1.298373	-4.181392
C	-0.929014	-2.343737	-3.575484
C	-1.887057	-2.634856	-2.442544
N	-1.661225	-2.642884	-1.185229
C	-2.926450	-2.954632	-0.470576
C	-3.885703	-3.259728	-1.655054
O	-3.111101	-2.968564	-2.829842
C	-0.401681	-3.706782	-4.082669
C	-1.677993	-1.600641	-4.704642
H	3.083729	-1.245498	-3.588266
H	2.465988	0.247235	-4.371356
H	-4.184637	-4.315974	-1.699131
H	-4.779609	-2.624025	-1.669256
H	0.248639	-3.556778	-4.953612
H	-1.248420	-4.339789	-4.380273
H	0.167447	-4.225749	-3.297854
H	-2.513798	-2.212040	-5.064368
H	-2.078236	-0.639737	-4.348553
H	-0.991640	-1.409094	-5.538416
Ag	-0.315537	-1.280507	-0.109596
N	0.626004	0.137883	1.030908
C	0.348585	-0.467752	2.165645
O	0.709812	-0.103883	3.371635
C	1.500033	2.228345	3.248693
C	1.586180	2.484106	1.755228
O	-0.344607	-1.522301	2.030978
H	0.497911	2.470006	3.638463
H	2.208256	2.876856	3.789674
H	1.244633	1.496669	1.238174
H	2.627320	2.565616	1.411221
C	2.762993	-0.327283	-1.187426
C	4.523182	-0.880098	0.886281
C	2.857821	-1.612225	-0.661588
C	3.602957	0.673507	-0.692637
C	4.514171	0.408710	0.331428
C	3.709585	-1.908106	0.408325
H	2.227452	-2.404002	-1.073157
H	3.544996	1.676547	-1.110101
H	5.212922	-1.088832	1.703817
C	-3.308695	-1.682639	0.294764
C	-3.705442	0.729028	1.620437
C	-3.328903	-0.472818	-0.410610
C	-3.523649	-1.663407	1.668466
C	-3.730191	-0.459238	2.354881
C	-3.506872	0.750601	0.234171
H	-3.173122	-0.478824	-1.492810
H	-3.497092	-2.594455	2.233668
H	-3.843563	1.671920	2.143617
C	3.715239	-3.325675	0.996371
C	5.526426	1.452707	0.830469
C	-3.424022	2.049388	-0.579001
C	-3.941379	-0.486836	3.875087
C	1.296362	1.413799	-2.348610
H	0.893022	1.739013	-1.380249
H	0.513475	1.538169	-3.110957
H	2.134838	2.069463	-2.621917
C	-2.707824	-4.171482	0.420211
H	-1.947770	-3.962459	1.185846
H	-2.364155	-5.021277	-0.186399
H	-3.641457	-4.462937	0.922193
C	4.648490	-3.443629	2.207445
H	5.695828	-3.235147	1.942024
H	4.352889	-2.760721	3.018793
H	4.610170	-4.467165	2.608209
C	2.290214	-3.695791	1.449303
H	1.575513	-3.698774	0.611053
H	2.279621	-4.705073	1.888557
H	1.912059	-2.993389	2.206825
C	4.187809	-4.314851	-0.084773
H	4.204471	-5.340620	0.314668
H	3.523358	-4.310719	-0.962281
H	5.202911	-4.066193	-0.429441
C	6.944748	0.933713	0.521912
H	7.699880	1.668854	0.840247
H	7.156710	-0.010716	1.044183
H	7.071813	0.757887	-0.556955
C	1.817221	0.782376	3.602979
H	2.685897	0.411520	3.033037
H	2.021898	0.670817	4.673662
C	5.354274	2.810772	0.137558
H	6.096506	3.522999	0.526435
H	5.508095	2.738800	-0.949618
H	4.359705	3.248633	0.316809
C	5.382684	1.660843	2.348865
H	4.398914	2.083320	2.602738
H	5.506778	0.723589	2.910865
H	6.147694	2.364521	2.710442
C	-4.160206	0.916436	4.454320
H	-3.289029	1.568937	4.288561
H	-5.047934	1.406098	4.025766
H	-4.314915	0.847288	5.541117
C	-5.181771	-1.341365	4.195105

H	-6.080866	-0.928482	3.712710	H	-3.599682	4.193647	-0.334594
H	-5.063923	-2.381565	3.856932	C	0.714700	3.517961	1.159963
H	-5.358010	-1.365986	5.281459	H	-0.266727	3.660656	1.627410
C	-2.699064	-1.099059	4.548188	C	1.005410	4.161974	0.016964
H	-1.797906	-0.505371	4.335397	H	1.976396	3.963032	-0.453275
H	-2.838970	-1.133987	5.639786	C	0.109446	5.052672	-0.732077
H	-2.503696	-2.124762	4.203412	C	-0.990155	5.693383	-0.140816
C	-4.478686	2.031716	-1.699375	C	0.328221	5.235665	-2.106161
H	-4.423520	2.960339	-2.288087	C	-1.857245	6.466230	-0.906207
H	-4.330187	1.191156	-2.394190	H	-1.163452	5.597977	0.933163
H	-5.494546	1.949700	-1.284207	C	-0.544295	6.001506	-2.875111
C	-2.015050	2.149497	-1.192471	H	1.191451	4.759345	-2.578910
H	-1.809287	1.313507	-1.879893	C	-1.644244	6.615581	-2.277663
H	-1.898393	3.088508	-1.756404	H	-2.703855	6.963522	-0.428057
H	-1.245020	2.129249	-0.405569	H	-0.361120	6.126648	-3.944289
C	-3.662750	3.290173	0.288377	H	-2.325853	7.223715	-2.875665
H	-4.656222	3.274588	0.761535				
H	-2.903270	3.387513	1.079456				

TS2.10

ωB97X-D SCF energy: -2595.73491820 a.u.
ωB97X-D enthalpy: -2594.539670 a.u.
ωB97X-D free energy: -2594.699631 a.u.
ωB97X-D SCF energy in solution: -2598.40375638 a.u.
ωB97X-D enthalpy in solution: -2597.208508 a.u.
ωB97X-D free energy in solution: -2597.368469 a.u.
Imaginary frequency: -228.6781 cm-1

Cartesian coordinates

ATOM	X	Y	Z				
C	4.725210	2.126486	-1.233110	H	-2.684290	3.588726	-1.807170
C	3.806991	1.518276	-0.136525	H	0.981123	2.937232	-4.762150
N	2.463730	1.959873	-0.589527	H	1.746917	1.448538	-4.140624
C	2.581464	2.499955	-1.741413	H	2.738429	2.900368	-4.453451
O	3.813652	2.627381	-2.221349	H	0.900311	5.042819	-3.296590
C	1.510568	3.049296	-2.655963	H	1.386144	4.959415	-1.583225
C	0.113400	2.606062	-2.281920	H	2.626680	4.900056	-2.866618
N	-0.261632	1.553563	-1.659304	Ag	0.815110	0.573378	0.008360
C	-1.741410	1.586934	-1.514605	N	-0.242268	-1.191689	0.310147
C	-2.110315	2.836270	-2.361648	C	0.379007	-1.464412	1.438806
O	-0.845455	3.411647	-2.720987	O	0.285141	-2.574620	2.135632
C	1.763037	2.547470	-4.096604	C	0.080879	-3.844928	1.495040
C	1.609797	4.589071	-2.594345	C	-1.367059	-4.097283	1.113625
H	5.382952	1.391189	-1.712374	C	-1.809703	-3.287270	-0.090617
H	5.323932	2.970773	-0.862965	O	1.132611	-0.536588	1.851198
H	-2.641450	2.577640	-3.288189	H	0.424451	-4.574210	2.237653

H	0.747602	-3.900581	0.618096
H	-1.476993	-5.173813	0.903844
H	-2.001703	-3.882054	1.987505
H	-1.375687	-3.673536	-1.026951
H	-1.277909	-2.244887	-0.000562
C	3.798031	-0.016362	-0.165431
C	3.530623	-2.781807	-0.228259
C	3.271540	-0.658714	-1.288538
C	4.229229	-0.789272	0.913658
C	4.115019	-2.180436	0.896604
C	3.103491	-2.046900	-1.335197
H	2.962166	-0.065814	-2.152427
H	4.637421	-0.298860	1.793569
H	3.421734	-3.866293	-0.237176
C	-2.020777	1.789161	-0.023167
C	-2.246430	2.125639	2.726476
C	-1.366042	2.840757	0.625603
C	-2.804662	0.917031	0.725928
C	-2.938059	1.078167	2.111260
C	-1.441496	3.015153	2.007025
H	-0.745727	3.527563	0.044287
H	-3.291181	0.074215	0.234792
H	-2.322895	2.241603	3.804788
C	2.466060	-2.683179	-2.578698
C	4.602220	-3.057710	2.058601
C	-0.589140	4.102591	2.674174
C	-3.733741	0.049814	2.926533
C	4.090323	2.106043	1.240456
H	3.975299	3.198601	1.208669
H	5.115877	1.878174	1.564176
H	3.389227	1.706534	1.986055
C	-2.331202	0.309359	-2.094256
H	-3.429810	0.318701	-2.041183
H	-1.963012	-0.564126	-1.543582
H	-2.034003	0.206477	-3.147833
C	-3.253537	-2.993598	-0.222064
C	-3.851567	-2.708649	-1.392279
H	-3.240757	-2.746359	-2.302630
C	-5.049470	-0.304433	2.213691
H	-5.681325	0.586944	2.081743
H	-4.888189	-0.747324	1.220917
H	-5.616979	-1.036285	2.809247
C	-2.853720	-1.207423	3.051254
H	-1.925168	-0.989075	3.600423
H	-3.387194	-2.011112	3.584301
H	-2.568501	-1.576758	2.056938
C	-4.075547	0.558498	4.333553
H	-4.699499	-0.182918	4.854349
H	-3.178856	0.712648	4.951484
H	-4.637690	1.504045	4.296385
C	0.893979	3.737790	2.460430
H	1.116309	2.748721	2.891574
H	1.158022	3.701397	1.391621
H	1.549133	4.478912	2.944708
C	-0.853901	4.202350	4.181308
H	-1.906869	4.440643	4.394972
H	-0.595644	3.270809	4.706927
H	-0.238066	5.004051	4.614970
C	-0.886014	5.471507	2.037222
H	-0.655215	5.489388	0.961311
H	-1.945936	5.741133	2.159092
H	-0.278565	6.254907	2.515773
C	5.727940	-3.975808	1.547165
H	6.572864	-3.385544	1.161119
H	6.101724	-4.613456	2.363076
H	5.382124	-4.637316	0.738785
C	5.144615	-2.222186	3.224870
H	6.014209	-1.616317	2.927969
H	4.375342	-1.552912	3.639620
H	5.474347	-2.888783	4.035175
C	3.434381	-3.910455	2.585354
H	3.044028	-4.591632	1.814011
H	3.769036	-4.532393	3.429662
H	2.609284	-3.270678	2.932440
C	3.378722	-2.432795	-3.793003
H	3.511627	-1.357865	-3.988947
H	4.375477	-2.870902	-3.633777
H	2.946957	-2.885676	-4.698945
C	1.084011	-2.049137	-2.828739
H	0.609807	-2.504836	-3.711828
H	0.424530	-2.191656	-1.960567
H	1.147369	-0.965091	-3.010510
C	2.273932	-4.195728	-2.415821
H	1.621289	-4.433786	-1.560945
H	1.800904	-4.611687	-3.317556
H	3.230119	-4.721080	-2.274813
H	-3.827358	-2.935713	0.709098
C	-5.245364	-2.292635	-1.592311
C	-6.227096	-2.408603	-0.593746
C	-5.613915	-1.734149	-2.826641
C	-7.523405	-1.958618	-0.817161
H	-5.981536	-2.870497	0.364641

C	-6.911688	-1.281178	-3.050107	H	-8.274338	-2.060636	-0.031148
H	-4.867483	-1.653890	-3.621762	H	-7.178383	-0.848763	-4.016606
C	-7.869810	-1.388596	-2.043779	H	-8.889562	-1.039191	-2.216905

TS2.11

ωB97X-D SCF energy: -2518.40809706 a.u.
ωB97X-D enthalpy: -2517.251215 a.u.
ωB97X-D free energy: -2517.406273 a.u.
ωB97X-D SCF energy in solution: -2520.99386854 a.u.
ωB97X-D enthalpy in solution: -2519.836986 a.u.
ωB97X-D free energy in solution: -2519.992044 a.u.
Imaginary frequency: -1088.8897 cm-1

Cartesian coordinates

ATOM	X	Y	Z				
C	-4.005446	3.165588	-0.987918	H	0.949136	-4.053082	-2.138981
C	-3.003719	2.084487	-1.488602	H	2.547807	-4.075225	-1.384015
N	-1.727126	2.581594	-0.923646	H	0.513892	-1.800844	-0.901547
C	-1.966878	3.586451	-0.176993	H	1.963373	-2.058544	0.004983
O	-3.229654	4.000846	-0.112562	C	-3.257321	0.710420	-0.858340
C	-0.959640	4.429080	0.581326	C	-3.584597	-1.741744	0.417289
C	0.142902	3.609797	1.224795	C	-3.378610	0.637621	0.533029
N	0.390635	2.357422	1.143407	C	-3.307907	-0.467909	-1.600666
C	1.531945	2.049154	2.041986	C	-3.480016	-1.711879	-0.975989
C	2.058366	3.471793	2.358405	C	-3.543257	-0.578175	1.195244
O	0.972782	4.328572	1.978219	H	-3.336267	1.558837	1.120736
C	-1.661808	5.235574	1.691110	H	-3.201586	-0.427131	-2.684504
C	-0.305039	5.383979	-0.445981	H	-3.707122	-2.700332	0.914948
H	-4.848766	2.758231	-0.416921	C	2.553580	1.190498	1.299103
H	-4.387367	3.794859	-1.803843	C	4.385047	-0.327765	-0.140875
H	2.272883	3.632344	3.421745	C	2.957828	1.582559	0.023828
H	2.939308	3.748323	1.761035	C	3.091371	0.022701	1.849682
H	-0.930408	5.865910	2.210709	C	4.023869	-0.747069	1.149062
H	-2.140501	4.571697	2.425162	C	3.872015	0.832035	-0.725781
H	-2.437097	5.875405	1.253634	H	2.551762	2.504572	-0.401128
H	0.223122	4.817028	-1.226050	H	2.792456	-0.284734	2.849217
H	-1.080909	5.997115	-0.925263	H	5.115926	-0.919494	-0.692287
H	0.404761	6.051794	0.059876	C	-3.655084	-0.593796	2.725893
Ag	-0.124764	1.028391	-0.577212	C	-3.547960	-2.986665	-1.830476
N	0.396008	-0.604422	-1.692133	C	4.295762	1.330764	-2.115244
C	0.329269	-0.945839	-3.039142	C	4.705097	-1.978818	1.768069
O	1.178418	-1.849308	-3.505944	C	-2.905699	2.058602	-3.009048
C	1.712180	-3.413871	-1.669002	H	-2.109397	1.378516	-3.341228
C	1.190117	-2.706735	-0.438678	H	-2.677603	3.066591	-3.383698
O	-0.504678	-0.430617	-3.743304	H	-3.856872	1.732015	-3.454407

C	0.970291	1.385815	3.298321	H	2.861606	-2.927442	-3.444366
H	0.214515	2.038113	3.759245	C	-2.205523	-3.171179	-2.560621
H	1.761385	1.208950	4.040453	H	-1.378024	-3.208125	-1.833907
H	0.488781	0.429890	3.054383	H	-2.201334	-4.113281	-3.130856
C	0.412874	-3.407671	0.601052	H	-2.010908	-2.354318	-3.269333
C	-0.221837	-4.640922	0.386705	C	-3.818005	-4.236576	-0.983943
C	0.299993	-2.804886	1.868385	H	-3.869580	-5.120684	-1.636810
C	-0.935269	-5.256709	1.412036	H	-3.020279	-4.413360	-0.247826
H	-0.154621	-5.133542	-0.584926	H	-4.776062	-4.167450	-0.446801
C	-0.410124	-3.420973	2.890644	C	4.146507	-2.313963	3.157021
H	0.794995	-1.844791	2.041476	H	4.318451	-1.501123	3.878618
C	-1.032261	-4.651103	2.664402	H	3.067622	-2.532434	3.123098
H	-1.416098	-6.220305	1.232874	H	4.648739	-3.209612	3.550834
H	-0.480066	-2.945666	3.871196	C	4.514784	-3.215923	0.871878
H	-1.588240	-5.139536	3.467078	H	4.844782	-3.038973	-0.162973
C	-3.928839	-1.999944	3.272723	H	5.103892	-4.058784	1.263639
H	-3.123079	-2.702976	3.016711	H	3.461078	-3.532385	0.854305
H	-4.003483	-1.964340	4.369960	C	6.209501	-1.673319	1.905827
H	-4.876699	-2.407041	2.889425	H	6.373476	-0.777390	2.523446
C	-2.324669	-0.088930	3.311405	H	6.729159	-2.517877	2.383755
H	-1.498578	-0.743396	2.994507	H	6.683122	-1.499897	0.928164
H	-2.091675	0.932080	2.972411	C	5.305587	0.390968	-2.785412
H	-2.357762	-0.081004	4.412478	H	4.895892	-0.620684	-2.930469
C	-4.802866	0.329482	3.172762	H	5.572155	0.779569	-3.779026
H	-4.635704	1.375344	2.874962	H	6.236146	0.306207	-2.204581
H	-5.760116	0.003687	2.738668	C	4.951369	2.716765	-1.963738
H	-4.902575	0.311651	4.269007	H	5.294510	3.086370	-2.942037
C	-4.680181	-2.850860	-2.864801	H	4.250592	3.460979	-1.556634
H	-5.650702	-2.704610	-2.367018	H	5.821814	2.668625	-1.292280
H	-4.517638	-2.003968	-3.547257	C	3.061648	1.445017	-3.028716
H	-4.746001	-3.761632	-3.479713	H	2.279811	2.090646	-2.600286
C	2.223099	-2.425123	-2.709156	H	3.344195	1.869308	-4.003833
H	2.810473	-1.622510	-2.231386	H	2.619196	0.456583	-3.219383

TS2.12

ωB97X-D SCF energy: -2518.40712604 a.u.
ωB97X-D enthalpy: -2517.249952 a.u.
ωB97X-D free energy: -2517.405213 a.u.
ωB97X-D SCF energy in solution: -2520.99333826 a.u.
ωB97X-D enthalpy in solution: -2519.836164 a.u.
ωB97X-D free energy in solution: -2519.991425 a.u.
Imaginary frequency: -1065.3944 cm-1

Cartesian coordinates

ATOM	X	Y	Z				
C	1.689317	-4.139748	-1.595992	C	1.469835	-2.596773	-1.624261

N	0.154294	-2.481892	-0.969939
C	-0.319581	-3.647851	-0.758427
O	0.442707	-4.672215	-1.118925
C	-1.708790	-3.991976	-0.259410
C	-2.172064	-3.085736	0.863850
N	-1.636646	-2.011295	1.309282
C	-2.575371	-1.380963	2.276052
C	-3.700315	-2.447787	2.368421
O	-3.343283	-3.430286	1.384733
C	-1.773305	-5.454665	0.211292
C	-2.671430	-3.755841	-1.452765
H	2.479302	-4.447455	-0.897874
H	1.888026	-4.567268	-2.587111
H	-3.727953	-2.944817	3.347547
H	-4.700267	-2.065698	2.129691
H	-1.084557	-5.637306	1.048121
H	-1.497504	-6.125228	-0.611271
H	-2.793053	-5.692374	0.536718
H	-3.693113	-4.041950	-1.170127
H	-2.663658	-2.700505	-1.763160
H	-2.359023	-4.374891	-2.305330
Ag	-0.661791	-0.597807	-0.107109
N	-0.413515	1.072964	-1.231505
C	-0.983886	1.036096	-2.495276
O	-0.765218	2.039170	-3.333259
C	0.063205	3.162037	-3.005444
C	1.545805	2.791564	-2.964302
C	1.931638	2.105511	-1.669719
O	-1.676642	0.093064	-2.816349
H	-0.267131	3.599240	-2.049838
H	-0.139983	3.881170	-3.806911
H	1.758396	2.138148	-3.823838
H	2.142421	3.704216	-3.122523
H	2.691207	1.317166	-1.773006
H	0.938486	1.454507	-1.398881
C	2.516981	-1.853963	-0.795286
C	4.399942	-0.560369	0.788251
C	2.430425	-1.901791	0.594650
C	3.568695	-1.145758	-1.385360
C	4.525750	-0.489740	-0.606841
C	3.360961	-1.249719	1.412699
H	1.611602	-2.458582	1.054956
H	3.641703	-1.103182	-2.470262
H	5.137788	-0.044425	1.401286
C	-3.014385	-0.074851	1.604446
C	-3.583810	2.213459	0.144156
C	-2.523869	1.165434	2.021248
C	-3.800538	-0.144616	0.448864
C	-4.110126	0.995669	-0.298859
C	-2.792032	2.327200	1.292350
H	-1.910638	1.226475	2.916764
H	-4.172404	-1.114234	0.112408
H	-3.803491	3.116317	-0.425872
C	3.196731	-1.314912	2.936503
C	5.700131	0.286797	-1.220638
C	-2.229920	3.696828	1.695531
C	-5.051785	0.922428	-1.509189
C	1.336087	-2.069108	-3.052456
H	1.144125	-0.987181	-3.050719
H	0.494176	-2.562496	-3.557915
H	2.246794	-2.263668	-3.636013
C	-1.886938	-1.189616	3.621780
H	-0.997696	-0.554569	3.529990
H	-1.562946	-2.161988	4.018868
H	-2.574032	-0.726426	4.344868
C	2.114410	2.911846	-0.430919
C	2.130595	4.312107	-0.415236
C	2.230933	2.227320	0.791380
C	2.269697	5.008624	0.784826
H	2.042395	4.877839	-1.344525
C	2.358825	2.921551	1.987767
H	2.221210	1.133836	0.791205
C	2.378508	4.318346	1.989070
H	2.289935	6.100193	0.776076
H	2.444649	2.374201	2.929300
H	2.480868	4.865156	2.928349
C	-4.715715	1.999901	-2.553074
H	-4.878368	3.018806	-2.172850
H	-3.676003	1.915098	-2.901641
H	-5.370569	1.881727	-3.428909
C	-4.974217	-0.447521	-2.202197
H	-5.335245	-1.264908	-1.559697
H	-5.615139	-0.445819	-3.096123
H	-3.945096	-0.666926	-2.522492
C	-6.485383	1.150859	-0.991445
H	-6.768359	0.382340	-0.255703
H	-6.580070	2.133709	-0.505103
H	-7.206020	1.109589	-1.823020
C	-1.348209	4.224528	0.550005
H	-1.921662	4.355268	-0.380639
H	-0.915712	5.201314	0.815851
H	-0.518253	3.529010	0.352665

C	-1.365122	3.619080	2.959709	C	5.721540	1.726130	-0.672778
H	-0.493809	2.961315	2.816440	H	4.795349	2.266083	-0.920219
H	-0.979147	4.619562	3.205014	H	5.838438	1.755198	0.420032
H	-1.937976	3.265039	3.830461	H	6.565585	2.282503	-1.108017
C	-3.393346	4.670436	1.955087	C	4.194121	-0.405867	3.664321
H	-3.006405	5.658901	2.246885	H	4.096006	0.644195	3.348567
H	-4.020195	4.809785	1.062059	H	4.015175	-0.448275	4.748841
H	-4.039952	4.303881	2.766718	H	5.235009	-0.718451	3.493936
C	7.010743	-0.428088	-0.841129	C	3.420667	-2.766351	3.399237
H	7.874616	0.100397	-1.272839	H	2.697849	-3.455879	2.937034
H	7.152413	-0.465040	0.249151	H	4.431682	-3.110651	3.134674
H	7.019109	-1.462213	-1.217759	H	3.308348	-2.844624	4.491743
C	5.609623	0.358086	-2.750376	C	1.769333	-0.874814	3.311399
H	4.686564	0.858053	-3.085395	H	1.561084	0.148937	2.960631
H	6.456557	0.937990	-3.145037	H	1.008202	-1.538653	2.875725
H	5.652915	-0.638306	-3.215555	H	1.635985	-0.893037	4.404180

TS2.13

ωB97X-D SCF energy: -2518.41066846 a.u.
ωB97X-D enthalpy: -2517.254321 a.u.
ωB97X-D free energy: -2517.410171 a.u.
ωB97X-D SCF energy in solution: -2520.99322825 a.u.
ωB97X-D enthalpy in solution: -2519.836881 a.u.
ωB97X-D free energy in solution: -2519.992731 a.u.
Imaginary frequency: -1220.2468 cm-1

Cartesian coordinates

ATOM	X	Y	Z				
C	3.716422	3.525829	0.028541	H	0.732481	4.194625	-2.848709
C	2.961251	2.379437	0.757990	H	1.469066	5.676932	-2.183146
N	1.558576	2.646069	0.365523	H	-0.677332	6.391354	-0.108306
C	1.514676	3.767418	-0.236658	H	-0.084431	5.405764	1.256133
O	2.674086	4.401655	-0.422107	H	1.068420	6.333081	0.257759
C	0.312911	4.546405	-0.722512	Ag	0.112912	0.845442	0.017668
C	-0.974393	3.750495	-0.775899	N	0.431338	-1.078322	0.749959
N	-1.163907	2.485469	-0.802473	C	1.183565	-1.448561	1.860739
C	-2.594602	2.237826	-1.106144	O	1.534799	-2.715211	2.001193
C	-3.198575	3.646594	-0.892702	C	-0.270519	-4.095618	1.071173
O	-2.057664	4.512834	-0.919826	C	-1.159579	-3.100497	0.352669
C	0.575215	5.041462	-2.164305	O	1.448470	-0.611933	2.691876
C	0.140814	5.746868	0.235181	H	-0.386919	-5.103451	0.641005
H	4.277164	3.179297	-0.851199	H	-0.563234	-4.177732	2.128296
H	4.385710	4.092047	0.688476	H	-0.581022	-2.025709	0.564826
H	-3.891347	3.954044	-1.685530	H	-2.130091	-2.907782	0.833664
H	-3.687412	3.753356	0.086664	C	3.371387	0.997411	0.250306
H	-0.283349	5.626992	-2.518241	C	3.949708	-1.552881	-0.694500

C	4.110304	0.106071	1.031102
C	2.969066	0.602387	-1.025195
C	3.215790	-0.687829	-1.509698
C	4.437826	-1.169115	0.563977
H	4.430827	0.408289	2.024616
H	2.434718	1.315159	-1.658265
H	4.183095	-2.553375	-1.058194
C	-3.179575	1.204863	-0.146490
C	-4.141243	-0.714125	1.613907
C	-4.177041	0.316544	-0.547617
C	-2.700679	1.141355	1.167153
C	-3.156702	0.172246	2.064273
C	-4.675415	-0.659892	0.323848
H	-4.559403	0.364665	-1.564803
H	-1.960038	1.870437	1.496137
H	-4.515182	-1.474386	2.302755
C	5.362018	-2.112865	1.349372
C	2.704725	-1.079854	-2.902715
C	-5.756539	-1.667175	-0.094368
C	-2.618828	0.055198	3.496552
C	3.047785	2.518727	2.277393
H	2.662166	3.503071	2.580705
H	4.088316	2.445365	2.624290
H	2.452457	1.736084	2.767288
C	-2.663749	1.810041	-2.574324
H	-3.702038	1.701561	-2.916684
H	-2.138261	0.855072	-2.719176
H	-2.182642	2.570777	-3.206594
C	-1.245797	-3.128755	-1.127116
C	-2.072130	-2.185801	-1.764809
C	-0.513601	-4.019674	-1.927949
C	-2.183825	-2.151627	-3.149129
H	-2.634312	-1.477034	-1.154326
C	-0.625512	-3.984275	-3.316166
H	0.136329	-4.769864	-1.473541
C	-1.461082	-3.054002	-3.931953
H	-2.841971	-1.419925	-3.623356
H	-0.058302	-4.694297	-3.921123
H	-1.550369	-3.033272	-5.019825
C	6.688617	-2.222407	0.572696
H	7.398658	-2.865893	1.115013
H	6.537798	-2.655445	-0.427755
H	7.152920	-1.232757	0.444887
C	5.656659	-1.586567	2.760170
H	6.205675	-0.633167	2.739703
H	4.732203	-1.446388	3.341431
H	6.285099	-2.309396	3.300923
C	4.734905	-3.509963	1.491476
H	4.484653	-3.959244	0.518514
H	5.442779	-4.189677	1.989552
H	3.822904	-3.460931	2.102529
C	1.203068	-0.760234	-3.018609
H	0.993459	0.314516	-2.900448
H	0.824020	-1.057446	-4.007916
H	0.620855	-1.308683	-2.261998
C	1.208378	-3.710895	1.023076
H	1.845003	-4.561887	1.290144
H	1.514099	-3.353304	0.025101
C	3.484997	-0.275460	-3.958545
H	3.143135	-0.535822	-4.972398
H	3.345802	0.808187	-3.825226
H	4.563203	-0.486077	-3.896058
C	2.892510	-2.575629	-3.183733
H	3.953719	-2.864836	-3.197756
H	2.371516	-3.195348	-2.437187
H	2.471591	-2.825090	-4.169078
C	-3.769179	0.312500	4.487269
H	-3.407001	0.231181	5.523568
H	-4.186778	1.321322	4.349734
H	-4.588538	-0.410740	4.361918
C	-2.062479	-1.364587	3.711360
H	-2.838967	-2.135880	3.599275
H	-1.260950	-1.581780	2.990138
H	-1.637910	-1.463503	4.721496
C	-1.495207	1.061381	3.776924
H	-0.630293	0.913624	3.112100
H	-1.843747	2.100989	3.680321
H	-1.133306	0.933456	4.807458
C	-6.146964	-1.517188	-1.570154
H	-5.288301	-1.685428	-2.239046
H	-6.913262	-2.262645	-1.828012
H	-6.571795	-0.525164	-1.786249
C	-7.008770	-1.437676	0.771936
H	-7.804679	-2.143960	0.489896
H	-6.797680	-1.582449	1.841864
H	-7.396129	-0.415984	0.640507
C	-5.234746	-3.101170	0.117633
H	-6.004547	-3.831982	-0.173267
H	-4.341654	-3.292524	-0.497497
H	-4.978259	-3.298448	1.169107

TS2.14

ωB97X-D SCF energy: -2518.40439098 a.u.
ωB97X-D enthalpy: -2517.247637 a.u.
ωB97X-D free energy: -2517.404075 a.u.
ωB97X-D SCF energy in solution: -2520.98890621 a.u.
ωB97X-D enthalpy in solution: -2519.832152 a.u.
ωB97X-D free energy in solution: -2519.988590 a.u.
Imaginary frequency: -1131.7234 cm-1

Cartesian coordinates

ATOM	X	Y	Z
C	2.720967	2.894103	2.395048
C	2.217007	1.512795	1.880631
N	0.770792	1.770160	1.693469
C	0.522931	2.983120	2.003228
O	1.545422	3.716849	2.430619
C	-0.827663	3.669159	2.045849
C	-1.732744	3.276596	0.896359
N	-1.526777	2.457015	-0.061768
C	-2.754433	2.381538	-0.895050
C	-3.690898	3.398094	-0.181454
O	-2.921773	3.872407	0.931335
C	-0.658283	5.200411	2.019167
C	-1.509778	3.224316	3.362253
H	3.450693	3.368190	1.726268
H	3.134305	2.845997	3.411547
H	-3.940657	4.259348	-0.815557
H	-4.616908	2.951857	0.203075
H	-0.158076	5.529572	1.097300
H	-0.051499	5.526253	2.872234
H	-1.642423	5.680846	2.077231
H	-2.473747	3.736251	3.479238
H	-1.676127	2.137399	3.367142
H	-0.868487	3.484768	4.215806
Ag	-0.299428	0.573901	0.080554
N	-0.112956	-1.395175	-0.467913
C	0.468238	-1.756816	-1.676731
O	0.507779	-3.033625	-2.032074
C	-0.142639	-4.068922	-1.285800
C	0.606759	-4.427687	-0.009751
C	0.308265	-3.449877	1.110171
O	0.925714	-0.891651	-2.388395
H	-0.167924	-4.917343	-1.979038
H	-1.182805	-3.767890	-1.071129
H	0.303193	-5.441018	0.301121
H	1.679247	-4.483924	-0.245908
H	-0.729090	-3.558106	1.457715
H	0.189979	-2.374265	0.524316
C	2.807512	1.153532	0.516676
C	3.762617	0.573118	-2.025330
C	2.525354	1.995169	-0.561195
C	3.586247	0.014873	0.302577
C	4.089608	-0.283332	-0.968961
C	2.975517	1.712234	-1.851938
H	1.920065	2.890284	-0.394996
H	3.800428	-0.652719	1.135616
H	4.118363	0.328446	-3.023057
C	-3.253762	0.939163	-0.795501
C	-3.947066	-1.728886	-0.459849
C	-3.552775	0.435480	0.480470
C	-3.333116	0.092080	-1.891875
C	-3.688408	-1.260443	-1.746050
C	-3.898293	-0.896588	0.672926
H	-3.498086	1.107407	1.338563
H	-3.115360	0.475744	-2.888250
H	-4.219635	-2.775100	-0.321565
C	2.559009	2.624823	-3.011329
C	4.897781	-1.563327	-1.228314
C	-4.204307	-1.474061	2.060975
C	-3.821682	-2.139815	-2.997839
C	2.386710	0.422832	2.931823
H	1.950630	-0.525442	2.589461
H	1.879222	0.716633	3.861821
H	3.448540	0.252783	3.160034
C	-2.432727	2.826863	-2.316268
H	-1.684407	2.170671	-2.778031
H	-2.024418	3.847297	-2.305382
H	-3.339581	2.823315	-2.938505
C	1.244247	-3.255204	2.240874
C	0.733288	-2.899454	3.502259
C	2.636517	-3.376950	2.098634
C	1.580903	-2.680397	4.583229
H	-0.347295	-2.807978	3.635717

C	3.484649	-3.154977	3.179512	H	-3.307129	-2.956066	3.396047
H	3.068236	-3.652654	1.135087	H	-3.130846	-3.353229	1.672432
C	2.961409	-2.805427	4.425033	H	-2.135060	-2.059079	2.390224
H	1.162456	-2.417296	5.556690	C	5.921332	-1.365770	-2.358683
H	4.563782	-3.264289	3.051624	H	6.540164	-2.269410	-2.463695
H	3.628791	-2.639321	5.272951	H	5.443993	-1.192718	-3.333430
C	-4.965754	-1.578761	-3.864385	H	6.590824	-0.518032	-2.148069
H	-5.913343	-1.566041	-3.304974	C	5.665605	-2.008580	0.025709
H	-4.757831	-0.551984	-4.200254	H	6.341183	-1.216335	0.382937
H	-5.106267	-2.200377	-4.761986	H	4.995859	-2.281034	0.852917
C	-2.510576	-2.118630	-3.803139	H	6.274958	-2.895722	-0.202791
H	-2.208227	-1.101594	-4.091314	C	3.901195	-2.663075	-1.637424
H	-1.682600	-2.564014	-3.233405	H	3.356850	-2.389714	-2.553238
H	-2.624703	-2.701615	-4.729639	H	4.418383	-3.620264	-1.811501
C	-4.149125	-3.597315	-2.650824	H	3.150952	-2.814433	-0.846387
H	-4.214967	-4.192646	-3.573231	C	3.095631	4.046090	-2.765543
H	-3.370707	-4.054666	-2.019884	H	2.707450	4.476217	-1.829634
H	-5.113787	-3.692153	-2.130221	H	4.194588	4.046875	-2.706305
C	-5.597925	-2.127011	2.057336	H	2.798350	4.716002	-3.587248
H	-5.666335	-2.952819	1.334506	C	1.020830	2.649841	-3.075010
H	-5.830331	-2.538094	3.051649	H	0.628871	1.629278	-3.206913
H	-6.375128	-1.391055	1.802254	H	0.580104	3.064425	-2.155312
C	-4.176629	-0.398666	3.154589	H	0.677698	3.270481	-3.917798
H	-4.917167	0.394004	2.969024	C	3.089616	2.124830	-4.359940
H	-4.416392	-0.851673	4.127741	H	4.189593	2.099995	-4.384003
H	-3.183129	0.067736	3.246906	H	2.712546	1.118181	-4.595431
C	-3.132888	-2.525059	2.397731	H	2.759100	2.800482	-5.162789

TS2.15

ωB97X-D SCF energy: -2479.13005601 a.u.
ωB97X-D enthalpy: -2478.000653 a.u.
ωB97X-D free energy: -2478.153515 a.u.
ωB97X-D SCF energy in solution: -2481.67474965 a.u.
ωB97X-D enthalpy in solution: -2480.545347 a.u.
ωB97X-D free energy in solution: -2480.698209 a.u.
Imaginary frequency: -374.9467 cm-1

Cartesian coordinates

ATOM	X	Y	Z				
C	4.417807	-2.972867	0.309384	N	-0.157749	-1.750531	1.756961
C	3.384367	-2.295871	-0.634167	C	-1.515892	-1.341488	2.187706
N	2.102024	-2.643733	0.029272	C	-1.906615	-2.505208	3.146776
C	2.357680	-3.214859	1.143085	O	-0.786727	-3.398785	3.102546
O	3.635894	-3.445322	1.418423	C	2.025461	-3.816112	3.556233
C	1.369006	-3.735903	2.163146	C	0.941514	-5.144472	1.684885
C	0.126890	-2.875832	2.293371	H	5.179794	-2.284706	0.695428

H	4.908440	-3.840540	-0.152969
H	-2.038489	-2.173442	4.185816
H	-2.798102	-3.056064	2.821254
H	2.357337	-2.824826	3.897354
H	2.898441	-4.478798	3.523903
H	1.303093	-4.214387	4.279286
H	1.830993	-5.780456	1.576596
H	0.269077	-5.603676	2.420425
H	0.428177	-5.091480	0.713920
Ag	0.600079	-1.028954	-0.226406
N	-0.151523	0.888056	-0.343472
C	-0.144699	0.945620	-1.668592
O	-0.516550	2.005757	-2.357855
C	-0.424156	3.324559	-0.332728
O	0.248698	-0.094391	-2.248354
H	0.585332	3.718004	-0.523415
H	-0.220052	2.246424	0.102221
C	3.476666	-0.762258	-0.614780
C	3.413443	2.012125	-0.476398
C	3.551393	0.003046	-1.780868
C	3.384836	-0.109121	0.618759
C	3.334901	1.285061	0.712343
C	3.526155	1.399897	-1.731726
H	3.609517	-0.496149	-2.744696
H	3.326299	-0.701393	1.536261
H	3.393284	3.099942	-0.431237
C	-2.427500	-1.287448	0.959675
C	-3.988406	-1.196088	-1.337805
C	-2.236277	-2.206960	-0.069501
C	-3.455423	-0.346721	0.843833
C	-4.267689	-0.303069	-0.290892
C	-2.989302	-2.164141	-1.249728
H	-1.476645	-2.983921	0.037724
H	-3.629290	0.357033	1.655493
H	-4.592409	-1.140616	-2.242689
C	3.660789	2.261186	-2.996047
C	3.152843	1.943539	2.086471
C	-2.704487	-3.184999	-2.359707
C	-5.444099	0.676126	-0.429166
C	3.400706	-2.899390	-2.033103
H	2.578686	-2.497334	-2.641384
H	3.275117	-3.989308	-1.969229
H	4.352233	-2.689898	-2.542533
C	-1.422239	-0.007884	2.924784
H	-2.380462	0.250329	3.397214
H	-1.143350	0.797398	2.232776
H	-0.662618	-0.070528	3.716666
C	-1.157732	4.063889	0.729302
C	-2.381400	3.572370	1.210085
C	-0.624131	5.227681	1.296940
C	-3.064250	4.240998	2.220090
H	-2.787262	2.643348	0.799137
C	-1.310840	5.899684	2.305974
H	0.332116	5.616079	0.937457
C	-2.531283	5.409297	2.768105
H	-4.015997	3.850041	2.586631
H	-0.890434	6.811944	2.733499
H	-3.067409	5.935843	3.560054
C	-5.725623	1.433008	0.875290
H	-4.881251	2.069856	1.176691
H	-6.594526	2.093701	0.740926
H	-5.954266	0.745936	1.704153
C	-5.126964	1.700282	-1.533035
H	-4.257078	2.315802	-1.256355
H	-4.906583	1.212558	-2.494150
H	-5.979273	2.379735	-1.686650
C	-6.717673	-0.105701	-0.803955
H	-7.577944	0.578081	-0.864875
H	-6.628015	-0.606207	-1.778519
H	-6.944654	-0.873323	-0.048742
C	-1.209893	-3.145827	-2.732010
H	-0.563685	-3.438421	-1.888551
H	-1.005915	-3.850522	-3.552720
H	-0.907129	-2.138925	-3.055068
C	-3.521130	-2.898020	-3.625584
H	-3.302870	-1.898657	-4.032015
H	-3.271939	-3.634374	-4.403685
H	-4.603747	-2.971221	-3.442926
C	-3.072136	-4.588408	-1.842821
H	-2.881187	-5.345307	-2.619253
H	-2.481260	-4.863785	-0.955456
H	-4.136479	-4.641904	-1.568078
C	1.800067	1.495350	2.668930
H	1.645636	1.929606	3.668872
H	0.972420	1.823250	2.023241
H	1.729980	0.400473	2.759133
C	4.294547	1.508896	3.022358
H	5.272895	1.801547	2.612374
H	4.182358	1.983383	4.009269
H	4.307120	0.420031	3.180381
C	3.151157	3.474496	1.999367
H	2.321601	3.846177	1.378156

H	3.022316	3.903930	3.003755	H	2.446909	0.948453	-4.262863
H	4.094919	3.864822	1.589777	C	5.084512	2.848846	-3.021255
C	2.634441	3.408332	-2.985346	H	5.228827	3.469677	-3.919119
H	2.732945	4.005939	-3.904021	H	5.274798	3.479000	-2.139029
H	1.607638	3.016510	-2.946517	H	5.840720	2.049337	-3.033384
H	2.781973	4.097390	-2.140316	C	-1.165013	3.043780	-1.626339
C	3.432477	1.439182	-4.271973	H	-1.184185	3.920078	-2.287077
H	3.473577	2.098862	-5.151014	H	-2.201209	2.730125	-1.429806
H	4.206085	0.669707	-4.413568				

TS2.16

ωB97X-D SCF energy: -2479.10806505 a.u.
ωB97X-D enthalpy: -2477.978316 a.u.
ωB97X-D free energy: -2478.129260 a.u.
ωB97X-D SCF energy in solution: -2481.65969063 a.u.
ωB97X-D enthalpy in solution: -2480.529942 a.u.
ωB97X-D free energy in solution: -2480.680886 a.u.
Imaginary frequency: -221.3889 cm-1

Cartesian coordinates

ATOM	X	Y	Z				
C	2.831688	-3.772801	1.407832	C	2.723338	1.888428	-1.552429
C	3.397420	-2.549695	0.631458	O	2.971163	3.169962	-1.486464
N	2.602049	-2.601487	-0.622307	C	0.676624	3.569286	-0.788005
C	1.801718	-3.601579	-0.570655	O	3.651824	1.046170	-1.652774
O	1.860460	-4.349309	0.517211	H	0.942715	3.456378	0.273600
C	0.815733	-4.004288	-1.654057	H	0.519679	2.479138	-1.146135
C	-0.251869	-2.935299	-1.809994	C	3.074340	-1.203120	1.289945
N	-1.492931	-3.111891	-1.716235	C	2.325861	1.303973	2.227061
C	-2.185829	-1.874867	-2.092868	C	4.026907	-0.194578	1.443251
C	-1.016858	-0.893871	-2.412168	C	1.742660	-0.935587	1.628676
O	0.168835	-1.683610	-2.191513	C	1.344467	0.316890	2.103900
C	0.145255	-5.336726	-1.305111	C	3.669482	1.077433	1.904978
C	1.582195	-4.118782	-2.990474	H	5.062933	-0.388764	1.175678
H	2.321737	-3.507364	2.342790	H	0.989208	-1.719691	1.505817
H	3.593995	-4.534704	1.615460	H	2.037898	2.286405	2.595123
H	-1.005761	-0.557106	-3.457876	C	-3.065441	-1.373218	-0.953344
H	-0.976399	-0.024797	-1.743803	C	-4.665362	-0.416493	1.096114
H	-0.422070	-5.268656	-0.369278	C	-3.392876	-2.194115	0.116344
H	0.903986	-6.123345	-1.200775	C	-3.564976	-0.066151	-1.002188
H	-0.551742	-5.613930	-2.104992	C	-4.362504	0.437300	0.021873
H	2.346446	-4.904788	-2.916305	C	-4.204039	-1.730112	1.163991
H	0.881567	-4.392852	-3.791418	H	-3.006525	-3.213797	0.125095
H	2.077698	-3.177817	-3.262787	H	-3.310738	0.568279	-1.853268
Ag	2.146705	-0.623615	-1.415837	H	-5.287122	-0.030896	1.903585
N	1.527895	1.324838	-1.513371	C	4.727582	2.173180	2.098705

C	-0.132839	0.561328	2.429017
C	-4.574710	-2.684189	2.308101
C	-4.882010	1.881415	0.032253
C	4.871152	-2.735504	0.285231
H	5.217776	-1.951582	-0.401996
H	5.017668	-3.706437	-0.208663
H	5.493193	-2.710643	1.191629
C	-3.038434	-2.161228	-3.334055
H	-3.549608	-1.246510	-3.668152
H	-3.799766	-2.915967	-3.096419
H	-2.412300	-2.537881	-4.157327
C	-0.592095	4.335787	-0.971955
C	-1.118365	4.566817	-2.252725
C	-1.269363	4.854290	0.139902
C	-2.273381	5.324613	-2.416807
H	-0.624294	4.147221	-3.133054
C	-2.424960	5.613855	-0.025124
H	-0.877957	4.675771	1.144289
C	-2.924719	5.856162	-1.303079
H	-2.670114	5.500407	-3.418421
H	-2.934559	6.021427	0.849922
H	-3.828738	6.454322	-1.432997
C	-4.496598	2.642101	-1.241469
H	-4.896486	2.157778	-2.145559
H	-4.908911	3.660935	-1.203353
H	-3.404669	2.741208	-1.348315
C	-6.416825	1.876079	0.148563
H	-6.872190	1.336694	-0.695742
H	-6.759626	1.397684	1.077409
H	-6.804441	2.906646	0.145065
C	-4.270954	2.622834	1.236085
H	-4.642526	3.658845	1.276640
H	-4.526488	2.137777	2.190165
H	-3.173425	2.662414	1.153940
C	-5.449563	-3.815059	1.735101
H	-4.917182	-4.386712	0.960250
H	-5.740608	-4.517480	2.531675
H	-6.367922	-3.410111	1.283676
C	-5.356213	-1.976916	3.422125
H	-6.317084	-1.579104	3.062826
H	-5.580017	-2.689717	4.229548
H	-4.780534	-1.147386	3.861771
C	-3.298230	-3.284261	2.924088
H	-3.557966	-3.971749	3.743712
H	-2.711804	-3.855642	2.189386
H	-2.652867	-2.494038	3.334872
C	-0.957825	0.365943	1.147996
H	-2.030895	0.479971	1.353948
H	-0.674884	1.105680	0.382337
H	-0.822175	-0.638089	0.719117
C	-0.596141	-0.444335	3.497276
H	-0.011915	-0.335699	4.423430
H	-1.657583	-0.278379	3.738092
H	-0.496983	-1.484211	3.152962
C	-0.389843	1.976781	2.957733
H	-0.106085	2.744249	2.221755
H	-1.462615	2.104820	3.164523
H	0.157089	2.175884	3.891569
C	4.120945	3.574597	1.917681
H	4.913221	4.333852	1.991181
H	3.650208	3.675661	0.927919
H	3.377202	3.817578	2.690502
C	5.875625	2.022708	1.086728
H	6.568576	2.871569	1.181368
H	6.468760	1.112665	1.258727
H	5.499039	1.999306	0.052889
C	5.284219	2.043995	3.529299
H	6.053347	2.809997	3.713957
H	4.487758	2.170710	4.278427
H	5.742400	1.055912	3.687665
C	1.866954	4.073785	-1.583583
H	2.229761	5.035610	-1.199564
H	1.621177	4.196204	-2.649348

TS2.17

ωB97X-D SCF energy: -2479.09238974 a.u.
ωB97X-D enthalpy: -2477.961841 a.u.
ωB97X-D free energy: -2478.118340 a.u.
ωB97X-D SCF energy in solution: -2481.65085668 a.u.
ωB97X-D enthalpy in solution: -2480.520308 a.u.
ωB97X-D free energy in solution: -2480.676807 a.u.
Imaginary frequency: -298.5943 cm-1

Cartesian coordinates

ATOM	X	Y	Z
C	2.632008	-3.767073	1.715945
C	2.930816	-2.934282	0.435011
N	1.560234	-2.695365	-0.076900
C	0.716834	-3.320186	0.660380
O	1.213221	-4.002780	1.671843
C	-0.776321	-3.346320	0.429985
C	-1.194331	-1.929578	0.121352
N	-1.716342	-1.510410	-0.957449
C	-2.137969	-0.120232	-0.703922
C	-1.296448	0.230366	0.546114
O	-1.008891	-1.045506	1.121973
C	-1.529288	-3.816583	1.685632
C	-1.063659	-4.269089	-0.764332
H	2.856284	-3.231933	2.647825
H	3.139239	-4.739958	1.723651
H	-0.336256	0.700682	0.267514
H	-1.806295	0.854662	1.288014
H	-1.305853	-3.180749	2.551464
H	-1.254925	-4.851394	1.928136
H	-2.610541	-3.775218	1.493529
H	-0.717137	-5.288018	-0.540962
H	-2.144431	-4.298660	-0.955313
H	-0.568379	-3.910296	-1.675960
Ag	1.372948	-1.114369	-1.483232
N	2.041629	0.591352	-2.538073
C	3.234036	1.129572	-2.407380
O	3.607189	2.261655	-1.915903
C	1.354858	2.540791	-0.980944
O	3.934404	0.267249	-2.951956
H	1.601111	1.956551	-0.080897
H	1.019453	1.796356	-1.764113
C	3.567962	-1.575775	0.742303
C	4.647461	0.908869	1.341466
C	4.778582	-1.179605	0.177699
C	2.891077	-0.697139	1.599322
C	3.424711	0.552001	1.926462
C	5.342951	0.070905	0.466712
H	5.304457	-1.852980	-0.494936
H	1.931900	-1.004020	2.021843
H	5.091078	1.869430	1.602204
C	-3.635206	-0.081403	-0.380133
C	-6.336095	0.047786	0.232840
C	-4.437685	-1.204849	-0.514621
C	-4.203139	1.125339	0.051930
C	-5.557445	1.211091	0.363144
C	-5.806191	-1.163400	-0.203011
H	-3.985956	-2.129303	-0.874470
H	-3.565477	2.007565	0.143263
H	-7.395193	0.104323	0.482808
C	6.724978	0.473156	-0.070015
C	2.769929	1.465534	2.973506
C	-6.648064	-2.437398	-0.359087
C	-6.220468	2.510738	0.840608
C	3.696599	-3.764238	-0.593063
H	3.803937	-3.222807	-1.544083
H	3.154686	-4.699863	-0.792039
H	4.699519	-4.021240	-0.223707
C	-1.837730	0.762133	-1.911318
H	-2.062313	1.816857	-1.698747
H	-2.448398	0.440725	-2.765303
H	-0.779098	0.680454	-2.204154
C	0.188302	3.458369	-0.749868
C	-0.382975	4.158401	-1.821349
C	-0.378609	3.587223	0.523425
C	-1.494081	4.972464	-1.622505
H	0.026386	4.048274	-2.829457
C	-1.491089	4.402154	0.722946
H	0.054115	3.047460	1.367792
C	-2.050931	5.095565	-0.348869
H	-1.932443	5.508582	-2.466206
H	-1.921245	4.498308	1.721686
H	-2.923470	5.732320	-0.191699
C	-5.225479	3.676053	0.897437
H	-4.787333	3.884159	-0.090821
H	-5.739526	4.588923	1.234073
H	-4.404452	3.478629	1.604374
C	-7.351327	2.891650	-0.132665
H	-6.960539	3.038701	-1.151174
H	-8.130435	2.117180	-0.180648
H	-7.834260	3.827737	0.188307
C	-6.799167	2.296665	2.251244
H	-7.275687	3.220262	2.615249
H	-7.560191	1.502916	2.265610
H	-6.007413	2.015817	2.962776
C	-6.643260	-2.862722	-1.839057
H	-5.625591	-3.070800	-2.202210

H	-7.241833	-3.776546	-1.977966
H	-7.072257	-2.073597	-2.475031
C	-8.101832	-2.229856	0.082829
H	-8.609469	-1.465470	-0.524643
H	-8.663916	-3.168192	-0.034922
H	-8.170038	-1.933538	1.140743
C	-6.036506	-3.558657	0.501899
H	-6.637353	-4.477440	0.418188
H	-5.011822	-3.805517	0.184430
H	-6.003582	-3.267270	1.563092
C	1.287775	1.121994	3.177463
H	0.821667	1.849755	3.858088
H	0.732350	1.138838	2.227783
H	1.145019	0.127895	3.624659
C	3.514803	1.257987	4.306833
H	4.579198	1.520153	4.212642
H	3.076879	1.887407	5.097126
H	3.454054	0.208387	4.631473
C	2.876350	2.946989	2.571806
H	2.414542	3.138622	1.591737
H	2.358641	3.576527	3.310844
H	3.916912	3.297557	2.528120
C	6.765624	1.964875	-0.443018
H	7.754674	2.217777	-0.852847
H	6.009989	2.207126	-1.203892
H	6.605572	2.621412	0.424650
C	7.109864	-0.337605	-1.316487
H	8.065226	0.030983	-1.717470
H	7.252193	-1.405464	-1.093384
H	6.351321	-0.244903	-2.108861
C	7.753136	0.200719	1.045439
H	8.766913	0.464439	0.706351
H	7.531098	0.792382	1.946689
H	7.754284	-0.862152	1.331398
C	2.603223	3.218031	-1.518470
H	3.082199	3.841788	-0.754146
H	2.384107	3.842184	-2.396591

2.5.9. References

1. Armarego, W. L. F.; Chai, C. L. L. *Purification of Laboratory Chemicals*; 2013.
2. Still, W. C., Kahn, M., Mitra, A. J. Rapid chromatographic technique for preparative separations with moderate resolution. *J. Org. Chem.* **1978**, *43*, 2923–2925.
3. Ju, M.; Huang, M.; Vine, L. E.; Dehghany, M.; Roberts, J. M.; Schomaker, J. M. Tunable Catalyst-Controlled Syntheses of β- and γ-Amino Alcohols Enabled by Silver-Catalysed Nitrene Transfer. *Nat. Catal.* **2019**, *2*, 899–908.
4. Frisch, M. J.; Trucks, G. W.; Schlegel, H. B.; Scuseria, G. E.; Robb, M. A.; Cheeseman, J. R.; Scalmani, G.; Barone, V.; Petersson, G. A.; Nakatsuji, H.; Li, X.; Caricato, M.; Marenich, A. V.; Bloino, J.; Janesko, B. G.; Gomperts, R.; Mennucci, B.; Hratchian, H. P.; Ortiz, J. V.; Izmaylov, A. F.; Sonnenberg, J. L.; Williams; Ding, F.; Lipparini, F.; Egidi, F.; Goings, J.; Peng, B.; Petrone, A.; Henderson, T.; Ranasinghe, D.; Zakrzewski, V. G.; Gao, J.; Rega, N.; Zheng, G.; Liang, W.; Hada, M.; Ehara, M.; Toyota, K.; Fukuda, R.; Hasegawa, J.; Ishida, M.;

Nakajima, T.; Honda, Y.; Kitao, O.; Nakai, H.; Vreven, T.; Throssell, K.; Montgomery Jr. J. A.; Peralta, J. E.; Ogliaro, F.; Bearpark, M. J.; Heyd, J. J.; Brothers, E. N.; Kudin, K. N.; Staroverov, V. N.; Keith, T. A.; Kobayashi, R.; Normand, J.; Raghavachari, K.; Rendell, A. P.; Burant, J. C.; Iyengar, S. S.; Tomasi, J.; Cossi, M.; Millam, J. M.; Klene, M.; Adamo, C.; Cammi, R.; Ochterski, J. W.; Martin, R. L.; Morokuma, K.; Farkas, O.; Foresman, J. B.; Fox, D. J. *Gaussian 16 Rev. B.01*, Gaussian, Inc.: Wallingford, CT, **2016**.

5. Chai, J.-D.; Head-Gordon, M. Long-Range Corrected Hybrid Density Functionals with Damped Atom–Atom Dispersion Corrections. *Phys. Chem. Chem. Phys.* **2008**, *10*, 6615–6620.
6. Barone, V.; Cossi, M.; Tomasi, J. Geometry Optimization of Molecular Structures in Solution by the Polarizable Continuum Model. *J. Comput. Chem.* **1998**, *19*, 404–417.
7. Pracht, P.; Bohle, F.; Grimme, S. Automated Exploration of the Low-Energy Chemical Space with Fast Quantum Chemical Methods. *Phys. Chem. Chem. Phys.* **2020**, *22*, 7169–7192.
8. Bannwarth, C.; Ehlert, S.; Grimme, S. GFN2-XTB—An Accurate and Broadly Parametrized Self-Consistent Tight-Binding Quantum Chemical Method with Multipole Electrostatics and Density-Dependent Dispersion Contributions. *J. Chem. Theory Comput.* **2019**, *15*, 1652–1671.
9. Grimme, S. Supramolecular Binding Thermodynamics by Dispersion-Corrected Density Functional Theory. *Chem. – A Eur. J.* **2012**, *18*, 9955–9964.
10. Luchini, G.; Alegre-Requena, J. V.; Funes-Ardoiz, I.; Paton, R. S. GoodVibes: Automated Thermochemistry for Heterogeneous Computational Chemistry Data. *F1000Research* **2020,** *9*, 291.
11. CYLview, 1.0b; Legault, C. Y., Université de Sherbrooke, **2009** (http://www.cylview.org)

12. (a) Werner, H.-J.; Knowles, P. J.; Knizia, G.; Manby, F. R.; Schütz, M. Molpro: A General-Purpose Quantum Chemistry Program Package. *WIREs Comput. Mol. Sci.* **2012**, *2*, 242–253. (b) Werner, H.-J.; Knowles, P. J.; Manby, F. R.; Black, J. A.; Doll, K.; Heßelmann, A.; Kats, D.; Köhn, A.; Korona, T.; Kreplin, D. A.; Ma, Q.; Miller, T. F.; Mitrushchenkov, A.; Peterson, K. A.; Polyak, I.; Rauhut, G.; Sibaev, M. The Molpro Quantum Chemistry Package. *J. Chem. Phys.* **2020**, *152*, 144107.
13. Ma, Q.; Werner, H. J. Scalable Electron Correlation Methods. 8. Explicitly Correlated Open-Shell Coupled-Cluster with Pair Natural Orbitals PNO-RCCSD(T)-F12 and PNO-UCCSD(T)-F12. *J. Chem. Theory Comput.* **2021**, *17*, 902–926.
14. Ma, Q.; Werner, H.-J. Accurate Intermolecular Interaction Energies Using Explicitly Correlated Local Coupled Cluster Methods [PNO-LCCSD(T)-F12]. *J. Chem. Theory Comput.* **2019**, *15*, 1044–1052.
15. Fu, Y.; Zerull, E. E.; Schomaker, J. M.; Liu, P. Origins of Catalyst-Controlled Selectivity in Ag-Catalyzed Regiodivergent C–H Amination. *J. Am. Chem. Soc.* **2022**, *144*, 2735–2746.
16. (a) Maestre, L.; Sameera, W. M. C.; Díaz-Requejo, M. M.; Maseras, F.; Pérez, P. J. A General Mechanism for the Copper- and Silver-Catalyzed Olefin Aziridination Reactions: Concomitant Involvement of the Singlet and Triplet Pathways. *J. Am. Chem. Soc.* **2013**, *135*, 1338–1348. (b) Dolan, N. S.; Scamp, R. J.; Yang, T.; Berry, J. F.; Schomaker, J. M. Catalyst-Controlled and Tunable, Chemoselective Silver-Catalyzed Intermolecular Nitrene Transfer: Experimental and Computational Studies. *J. Am. Chem. Soc.* **2016**, *138*, 14658–14667.
17. (a) Lee, C.; Yang, W.; Parr, R. G. Development of the Colle-Salvetti Correlation-Energy Formula into a Functional of the Electron Density. *Phys. Rev. B* **1988**, *37*, 785–789. (b)

Becke, A. D. Density-Functional Thermochemistry. III. The Role of Exact Exchange. *J. Chem. Phys.* **1993**, *98*, 5648–5652.

18. Grimme, S.; Antony, J.; Ehrlich, S.; Krieg, H. A Consistent and Accurate Ab Initio Parametrization of Density Functional Dispersion Correction (DFT-D) for the 94 Elements H-Pu. *J. Chem. Phys.* **2010**, *132*, 154104.
19. (a) Perdew, J. P. Density-Functional Approximation for the Correlation Energy of the Inhomogeneous Electron Gas. *Phys. Rev. B* **1986**, *33*, 8822–8824. (b) Becke, A. D. Density-Functional Exchange-Energy Approximation with Correct Asymptotic Behavior. *Phys. Rev. A* **1988**, *38*, 3098–3100.
20. Jiang, W.; DeYonker, N. J.; Wilson, A. K. Multireference Character for 3d Transition-Metal-Containing Molecules *J. Chem. Theory Comput.* **2012**, *8*, 460–468.
21. For κ^2-coordinated Cu nitrene complexes, see: (a) Moegling, J.; Hoffmann, A.; Thomas, F.; Orth, N.; Liebhäuser, P.; Herber, U.; Rampmaier, R.; Stanek, J.; Fink, G.; Ivanović-Burmazović, I.; Herres-Pawlis, S. Designed to React: Terminal Copper Nitrenes and Their Application in Catalytic C−H Aminations. *Angew. Chemie Int. Ed.* **2018**, *57*, 9154–9159. (b) Thomas, F.; Oster, M.; Schön, F.; Göbgen, K. C.; Amarouch, B.; Steden, D.; Hoffmann, A.; Herres-Pawlis, S. A New Generation of Terminal Copper Nitrenes and Their Application in Aromatic C–H Amination Reactions. *Dalt. Trans.* **2021**, *50*, 6444–6462.
22. Oláh, J.; Harvey, J. N. No Bonding to Heme Groups: DFT and Correlated Ab Initio Calculations. *J. Phys. Chem. A* **2009**, *113*, 7338–7345.

2.5.10. HPLC chromatograms

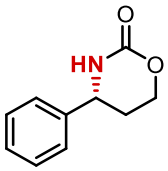

HPLC analysis for compound **2.2a** (CHIRALPAK® OJ-H, 5→35% iPrOH/hexane gradient over 22 min, 0.7 mL/min, 210 nm): t_R = 19.3 min (major), 20.1 min (minor); 92% ee

Racemic **2.2a**:

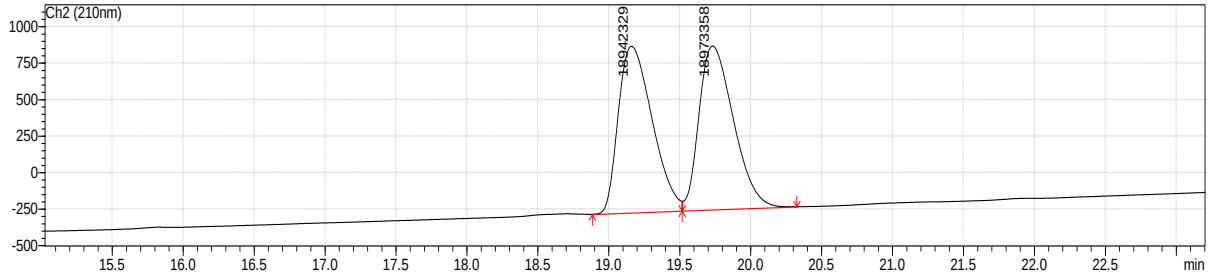

Peak #	Retention Time	Area	Area %
1	19.157	18942329	50.0
2	19.729	18973358	50.0

Enantioenriched **2.2a**:

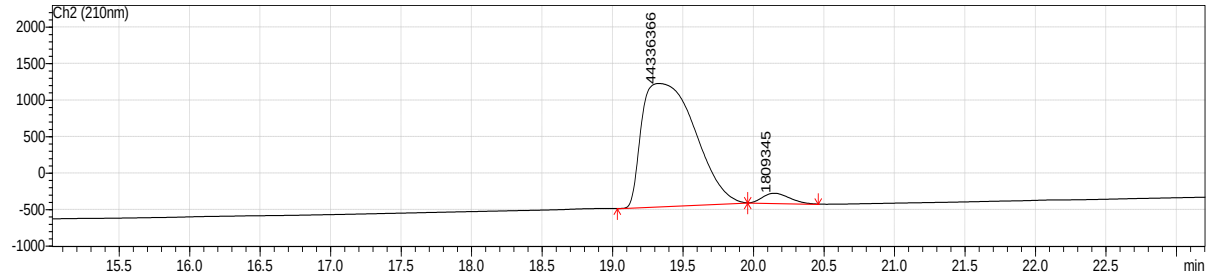

Peak #	Retention Time	Area	Area %
1	19.327	44336366	96.1
2	20.144	1809345	3.9

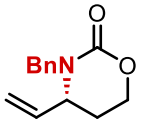

HPLC analysis for compound **2.2d** (CHIRALPAK® OJ-H, 5→35% iPrOH/hexane gradient over 22 min, 0.7 mL/min, 220 nm): t_R = 16.6 min (major), 17.4 min (minor); 46% ee

Racemic **2.2d**:

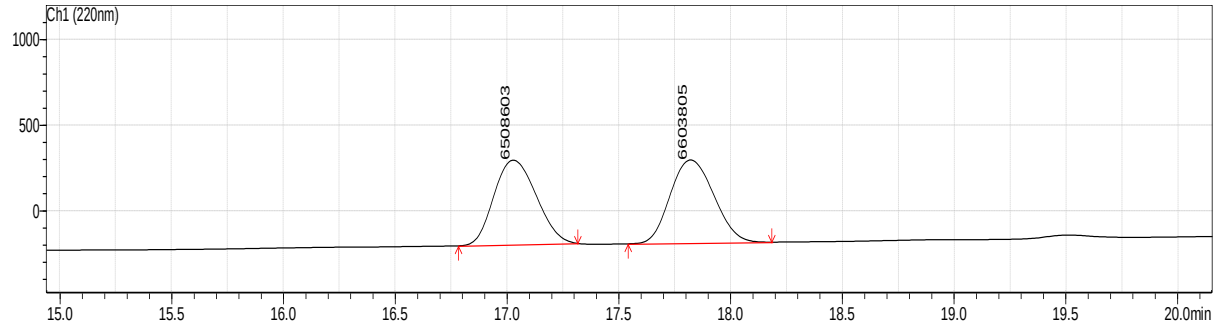

Peak #	Retention Time	Area	Area %
1	17.025	6508603	49.6
2	17.817	6603805	50.4

Enantioenriched **2.2d**:

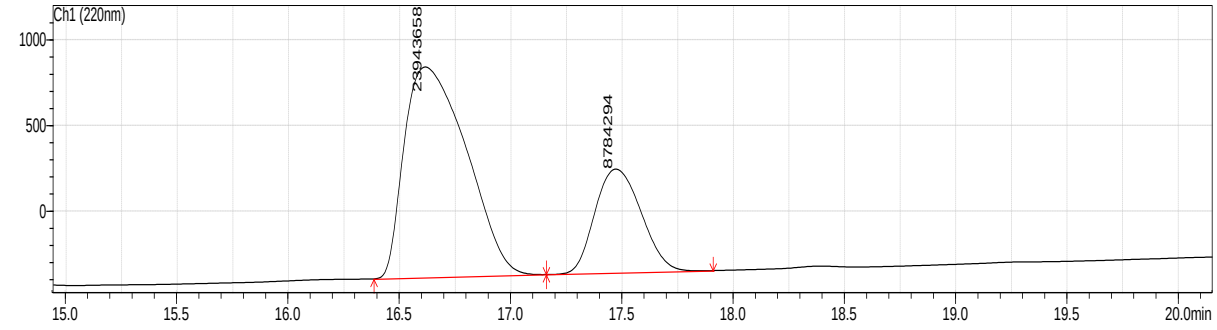

Peak #	Retention Time	Area	Area %
1	16.611	23943658	73.2
2	17.438	8784294	26.8

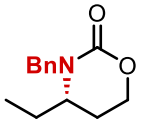

HPLC analysis for compound **2.2e** (CHIRALPAK® OJ-H, 5→35% iPrOH/hexane gradient over 22 min, 0.7 mL/min, 220 nm): t_R = 16.3 min (major), 16.7 min (minor); 39% ee

Racemic **2.2e**:

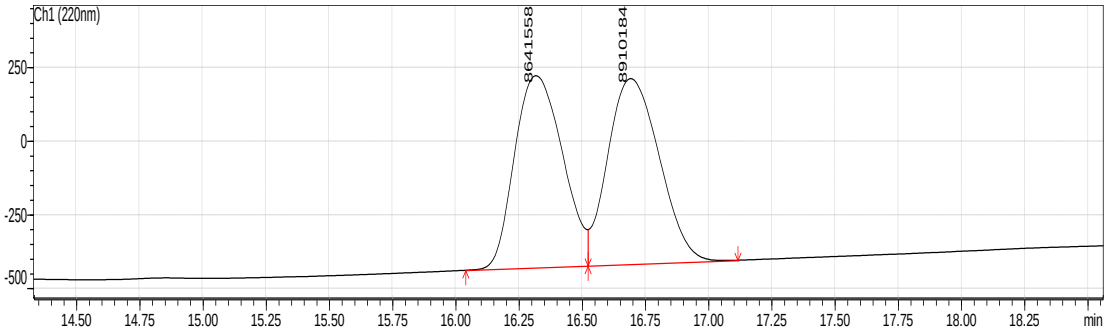

Peak #	Retention Time	Area	Area %
1	16.315	8641558	49.2
2	16.690	8910184	50.8

Enantioenriched **2.2e**:

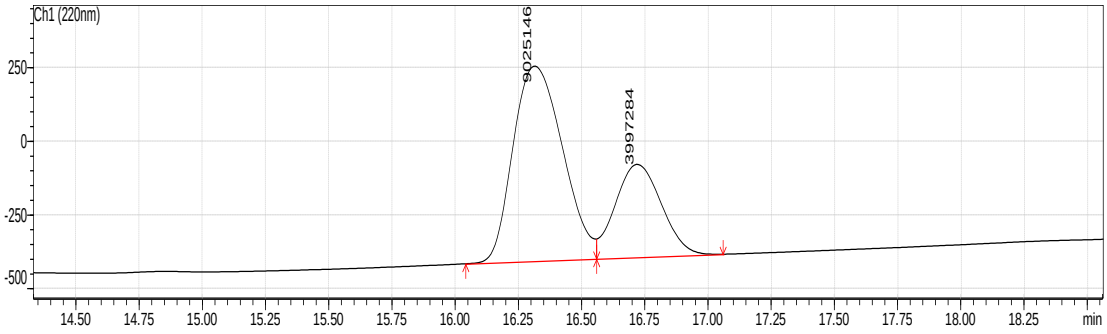

Peak #	Retention Time	Area	Area %
1	16.311	9025146	69.3
2	16.716	3997284	30.7

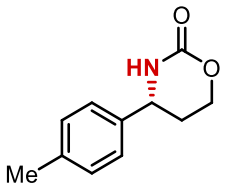

HPLC analysis for compound **2.3a** (CHIRALPAK® OJ-H, 5→35% iPrOH/hexane gradient over 22 min, 0.7 mL/min, 210 nm): t_R = 17.6 min (major), 18.3 min (minor); 91% ee

Racemic **2.3a**:

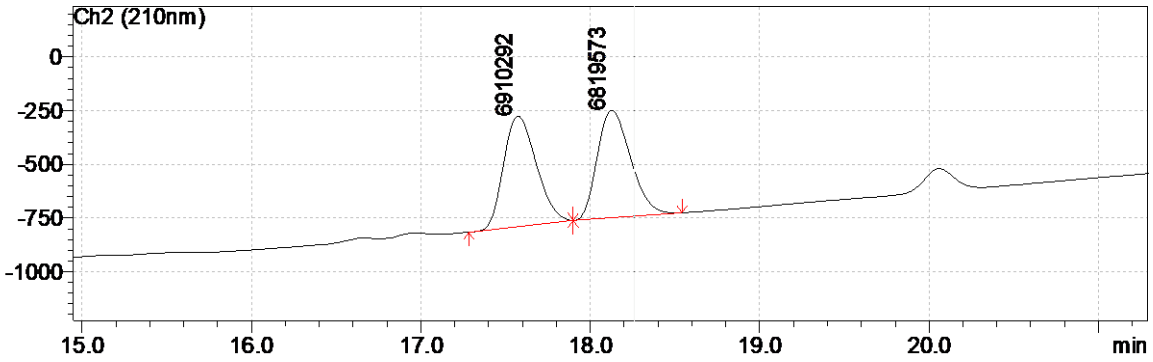

Peak #	Retention Time	Area	Area %
1	17.569	6910292	50.3
2	18.122	6819573	49.7

Enantioenriched **2.3a**:

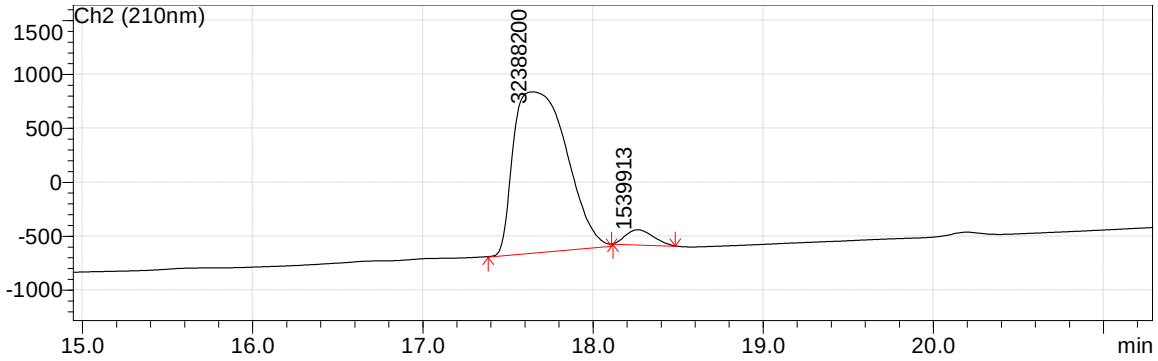

Peak #	Retention Time	Area	Area %
1	17.641	32388200	95.5
2	18.261	138169	4.5

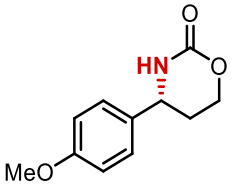

HPLC analysis for compound **2.4a** (CHIRALPAK® OJ-H, 5→28% iPrOH/hexane gradient over 22 min, 0.7 mL/min, 210 nm): t_R = 27.6 min (major), 28.7 min (minor); 90% ee

Racemic **2.4a**:

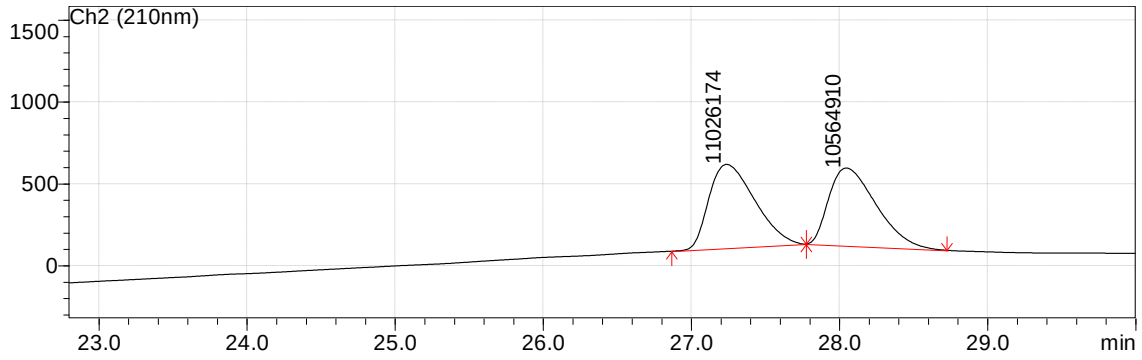

Peak #	Retention Time	Area	Area %
1	27.236	11026174	51.1
2	28.044	10564910	48.9

Enantioenriched **2.4a**:

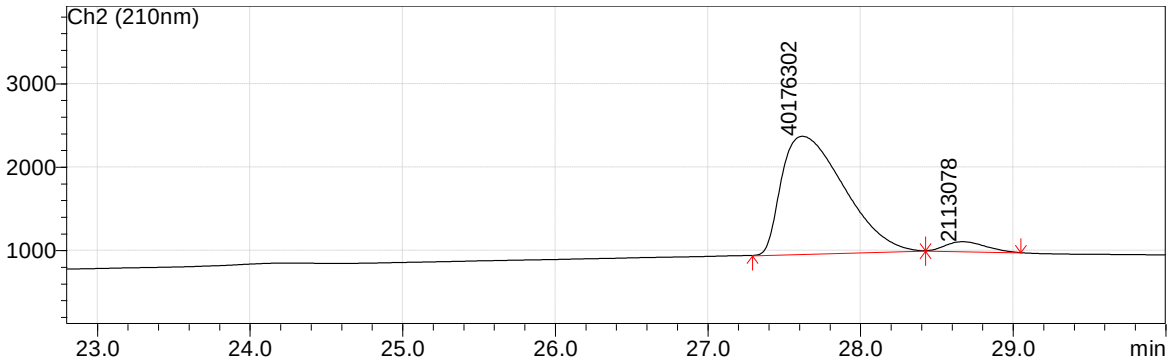

Peak #	Retention Time	Area	Area %
1	27.617	40176302	95.0
2	28.665	2113078	5.0

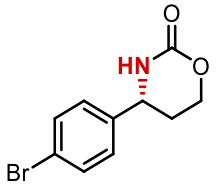

HPLC analysis for compound **2.5a** (CHIRALPAK® IC, 5→80% H_2O/acetonitrile (0.1% formic acid) over 22 min, 0.7 mL/min, 235 nm): t_R = 24.4 min (major), 24.7 min (minor); 88% ee

Racemic **2.5a**:

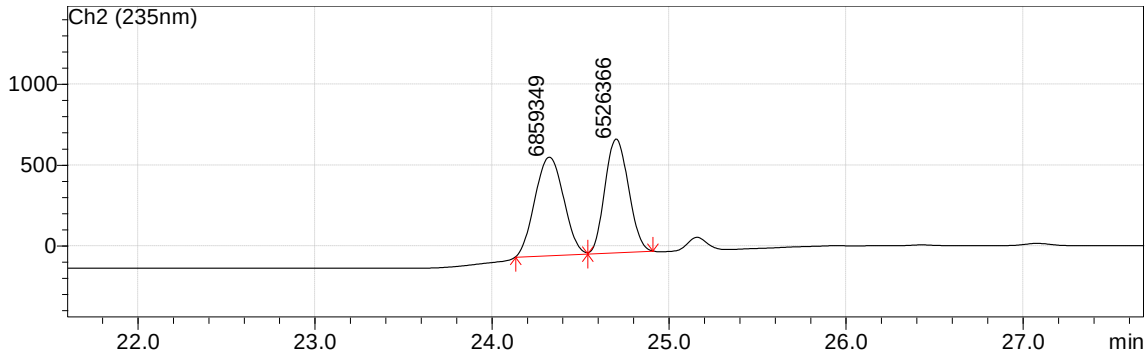

Peak #	Retention Time	Area	Area %
1	24.325	6859349	51.2
2	24.703	6526366	48.8

Enantioenriched **5a**:

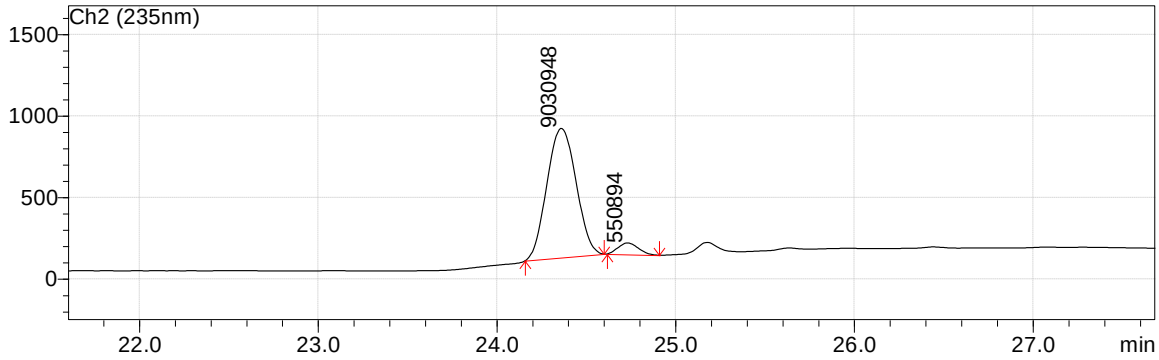

Peak #	Retention Time	Area	Area %
1	24.362	9030948	94.3
2	24.732	550894	5.7

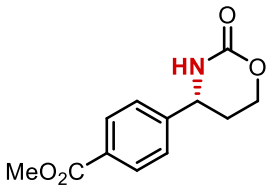

HPLC analysis for compound **2.6a** (CHIRALPAK® OJ-H, 5→38% iPrOH/hexane gradient over 22 min, 0.7 mL/min, 210 nm): t_R = 28.1 min (minor), 29.1 min (major); 91% ee

Racemic **2.6a**:

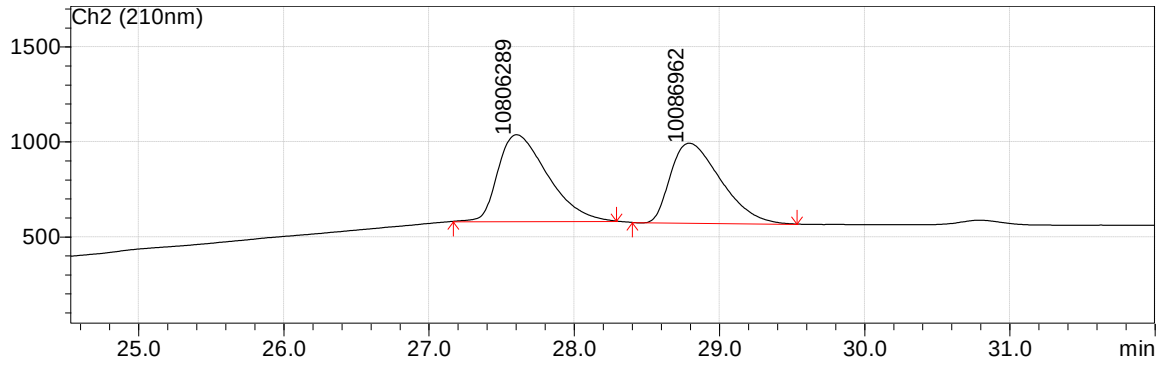

Peak #	Retention Time	Area	Area %
1	27.601	10806289	50.6
2	28.790	10086962	49.4

Enantioenriched **2.6a**:

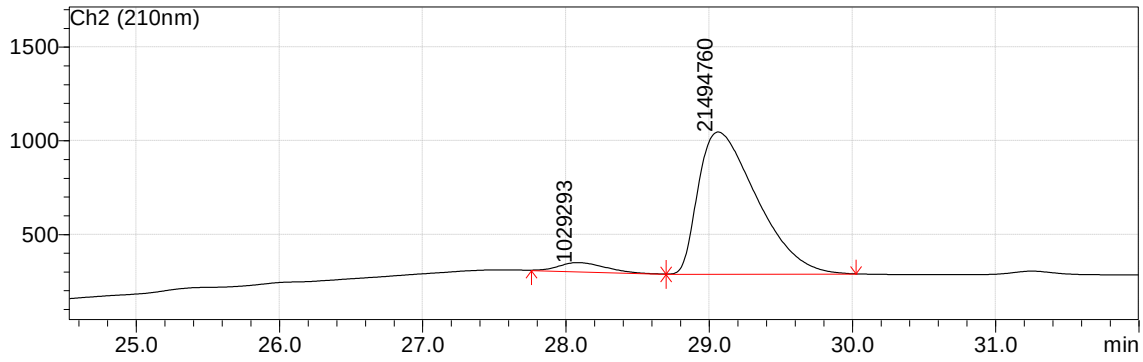

Peak #	Retention Time	Area	Area %
1	28.080	1029293	4.6
2	29.061	21494760	95.4

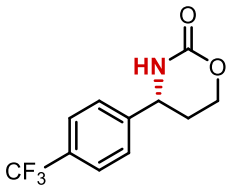

HPLC analysis for compound **2.7a** (CHIRALPAK® OJ-H, 5→35% iPrOH/hexane gradient over 22 min, 0.7 mL/min, 220 nm): t_R = 19.2 min (minor), 20.3 min (major); 88% ee

Racemic **2.7a**:

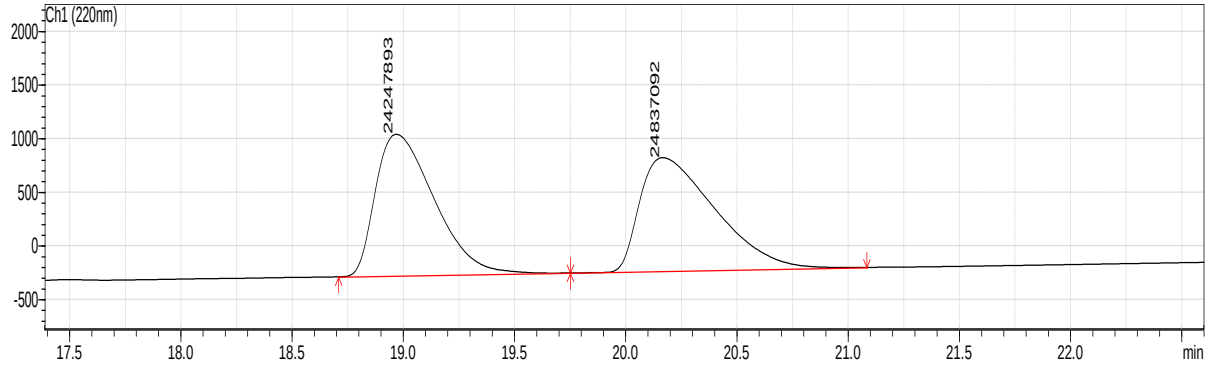

Peak #	Retention Time	Area	Area %
1	18.965	24247893	49.4
2	20.163	24837092	50.6

Enantioenriched **2.7a**:

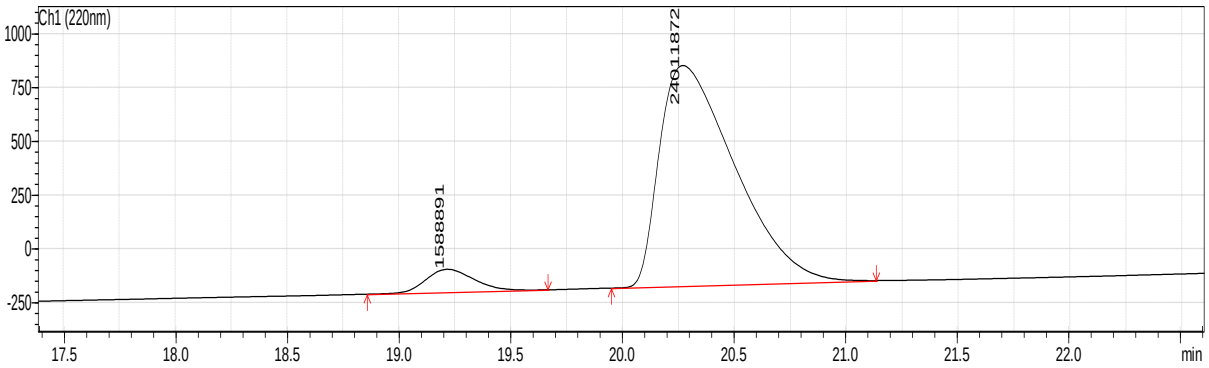

Peak #	Retention Time	Area	Area %
1	19.214	1588891	6.2
2	20.266	24011872	93.8

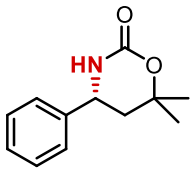

HPLC analysis for compound **2.8a** (CHIRALPAK® OJ-H, 5→35% iPrOH/hexane gradient over 22 min, 0.7 mL/min, 220 nm): t_R = 13.9 min (major), 15.4 min (minor); 88% ee

Racemic **2.8a**:

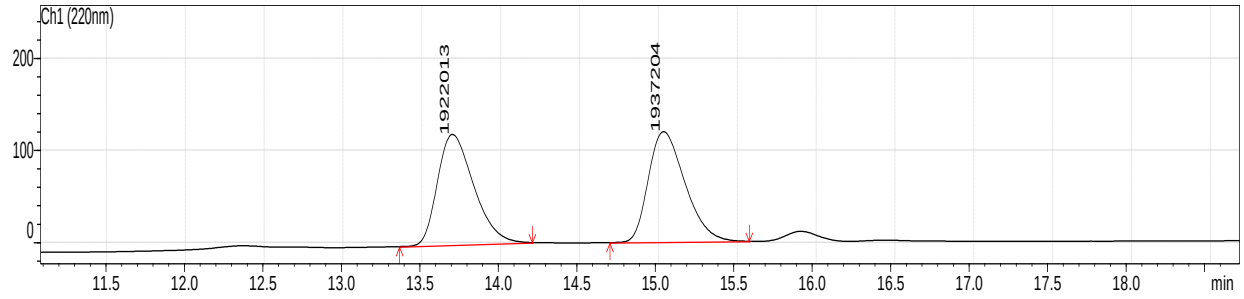

Peak #	Retention Time	Area	Area %
1	13.692	5016577	49.5
2	15.030	5122829	50.5

Enantioenriched **2.8a**:

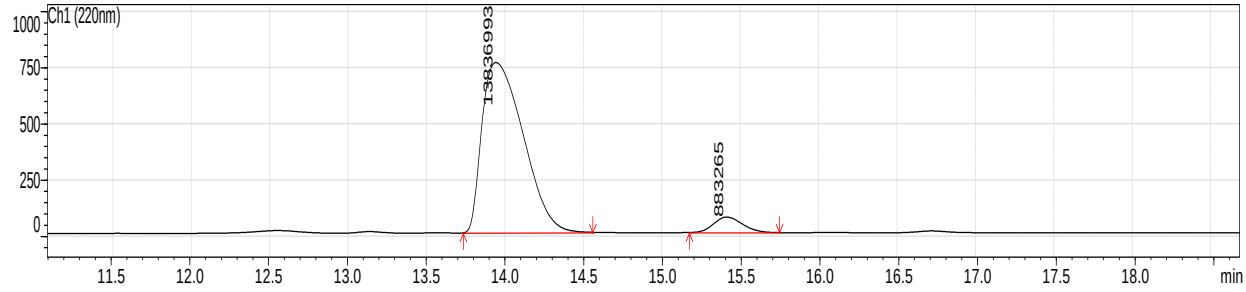

Peak #	Retention Time	Area	Area %
1	13.939	13836993	94.0
2	15.411	883265	6.0

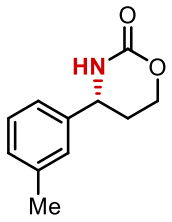

HPLC analysis for compound **2.9a** (CHIRALPAK® OJ-H, 5→35% iPrOH/hexane gradient over 22 min, 0.7 mL/min, 210 nm): t_R = 17.9 min (major), 18.6 min (minor); 90% ee

Racemic **2.9a**:

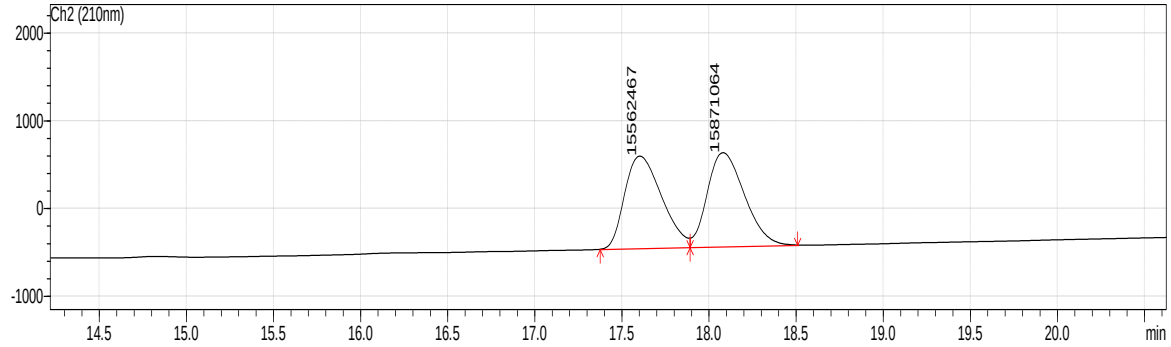

Peak #	Retention Time	Area	Area %
1	17.599	15562467	49.5
2	18.007	15871064	50.5

Enantioenriched **2.9a**:

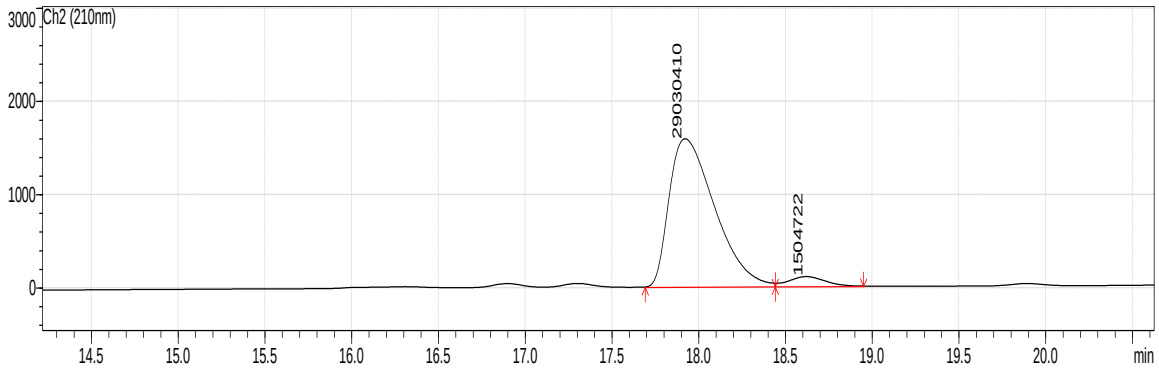

Peak #	Retention Time	Area	Area %
1	17.918	29030410	95.1
2	18.617	1504722	4.9

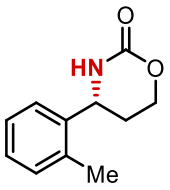

HPLC analysis for compound **2.10a** (CHIRALPAK® OJ-H, 5→35% iPrOH/hexane gradient over 22 min, 0.7 mL/min, 220 nm): t_R = 18.7 min (major), 20.2 min (minor); 80% ee

Racemic **2.10a**:

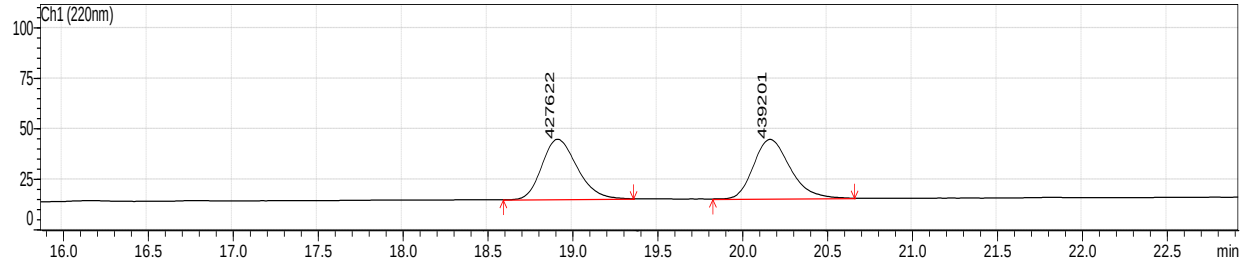

Peak #	Retention Time	Area	Area %
1	18.917	427622	49.3
2	20.167	439201	50.7

Enantioenriched **2.10a**:

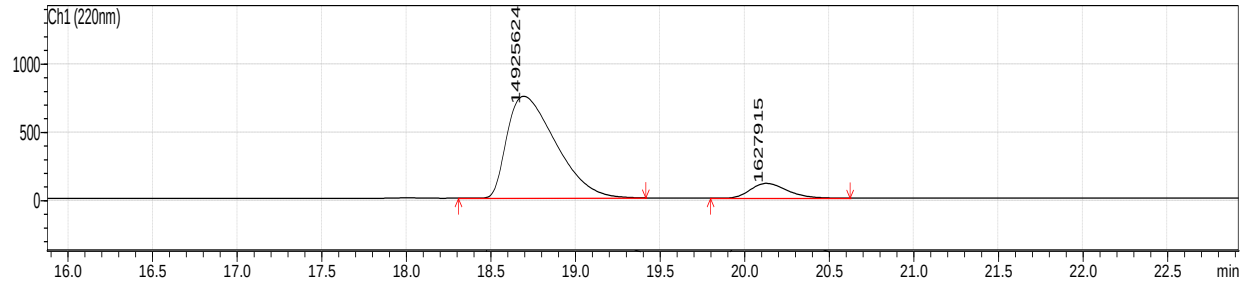

Peak #	Retention Time	Area	Area %
1	18.691	14925624	90.2
2	20.127	1627915	9.8

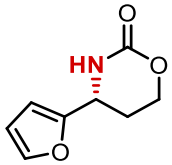

HPLC analysis for compound **2.11a** (CHIRALPAK® OJ-H, 5→35% iPrOH/hexane gradient over 22 min, 0.7 mL/min, 210 nm): t_R = 18.0 min (major), 19.1 min (minor); 84% ee

Racemic **2.11a**:

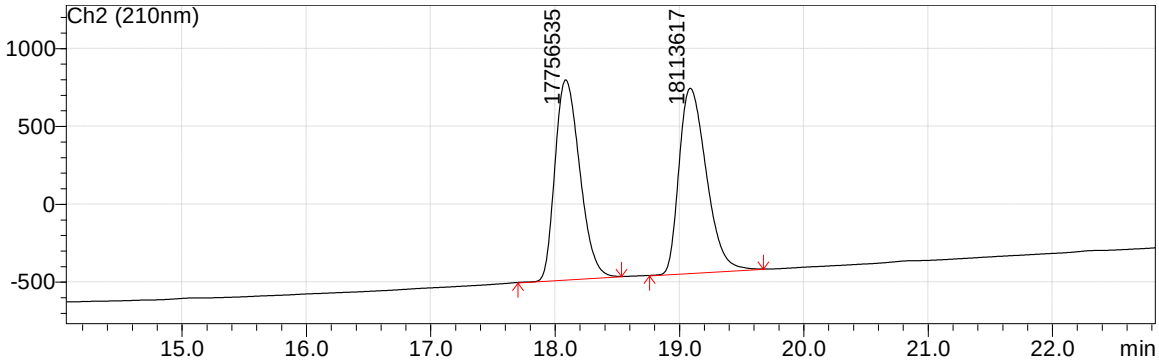

Peak #	Retention Time	Area	Area %
1	18.084	17756535	49.5
2	19.086	18113617	50.5

Enantioenriched **2.11a**:

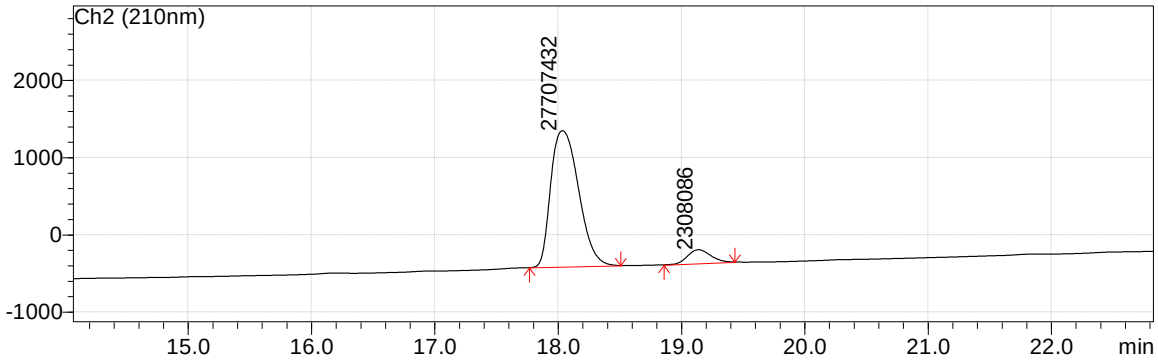

Peak #	Retention Time	Area	Area %
1	18.032	27707432	92.3
2	19.135	2308086	7.7

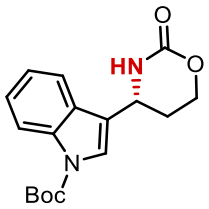

HPLC analysis for compound **2.12a** (CHIRALPAK® OJ-H, 5→35% iPrOH/hexane gradient over 22 min, 0.7 mL/min, 210 nm): t_R = 19.8 min (major), 21.0 min (minor); 72% ee

Racemic **2.12a**:

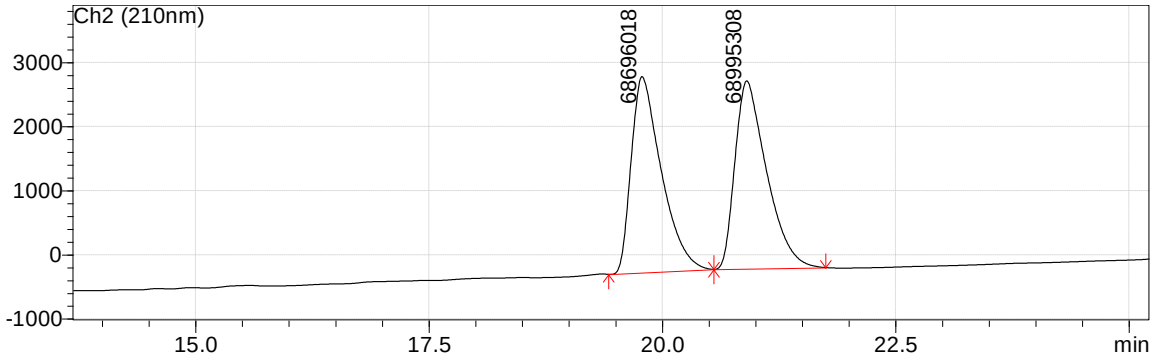

Peak #	Retention Time	Area	Area %
1	19.779	6869018	49.9
2	20.902	6899308	50.1

Enantioenriched **2.12a**:

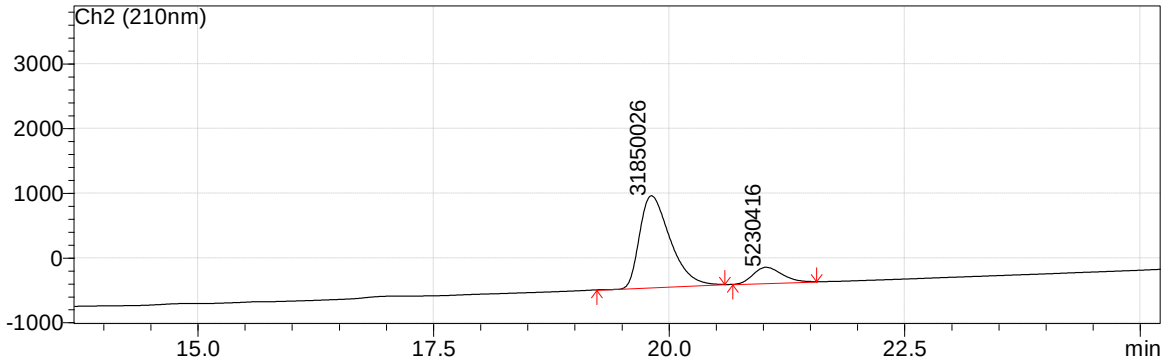

Peak #	Retention Time	Area	Area %
1	19.832	31850026	85.9
2	21.005	257561	14.1

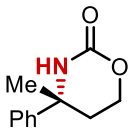

HPLC analysis for compound **2.15a** (CHIRALPAK® AD-H, 5→60% iPrOH/hexane gradient over 22 min, 0.7 mL/min, 210 nm): t_R = 12.9 min (major), 13.8 min (minor); 48% ee

Racemic **2.15a**:

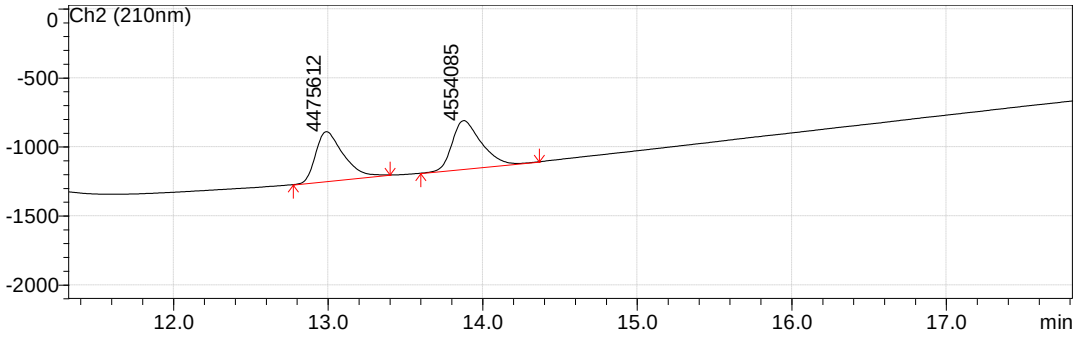

Peak #	Retention Time	Area	Area %
1	12.987	4475612	49.6
2	13.876	4554085	50.4

Enantioenriched **2.15a**:

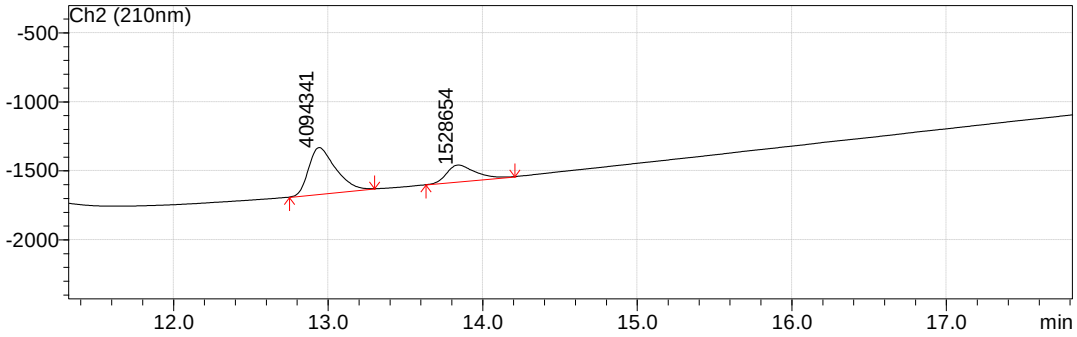

Peak #	Retention Time	Area	Area %
1	12.940	4094341	72.8
2	13.840	1528654	27.2

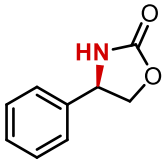

HPLC analysis for compound **2.16a** (CHIRALPAK® OJ-H, 5→35% iPrOH/hexane gradient over 22 min, 0.7 mL/min, 210 nm): t_R = 17.6 min (minor), 18.3 min (major); 34% ee

Racemic **2.16a**:

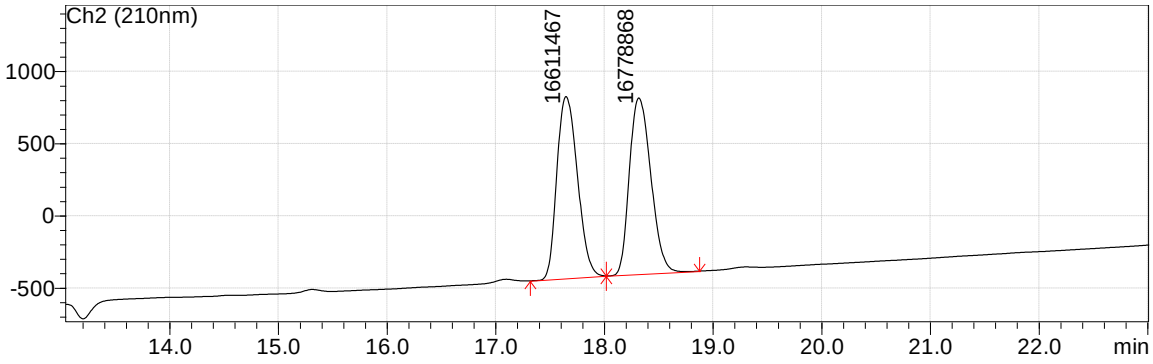

Peak #	Retention Time	Area	Area %
1	17.645	16611467	49.7
2	18.315	16778868	50.3

Enantioenriched **16a**:

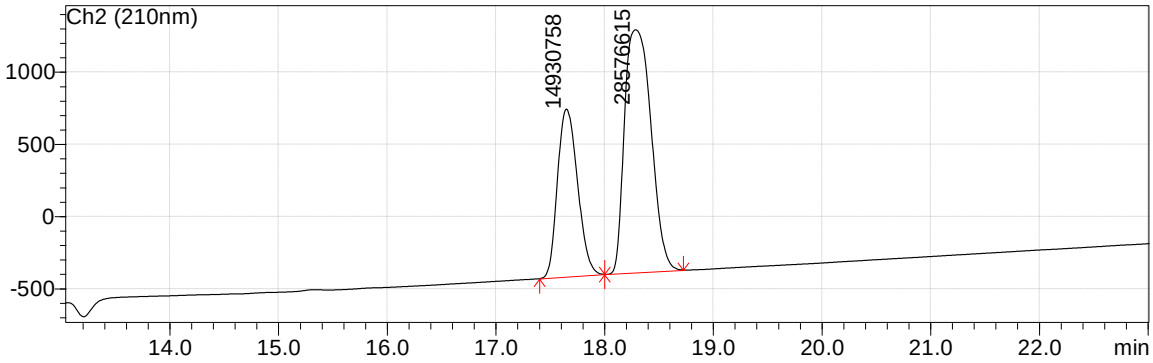

Peak #	Retention Time	Area	Area %
1	17.647	14930758	34.3
2	18.283	28576615	65.7

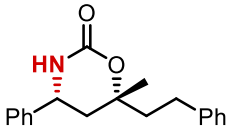

HPLC analysis for compound **2.17a** (CHIRALCEL® OJ-H, 5→35% iPrOH/hexane gradient over 22 min, 0.7 mL/min, 210 nm): t_R = 20.1 min (major), 28.1 min (minor); 91% ee

Racemic **2.17a**:

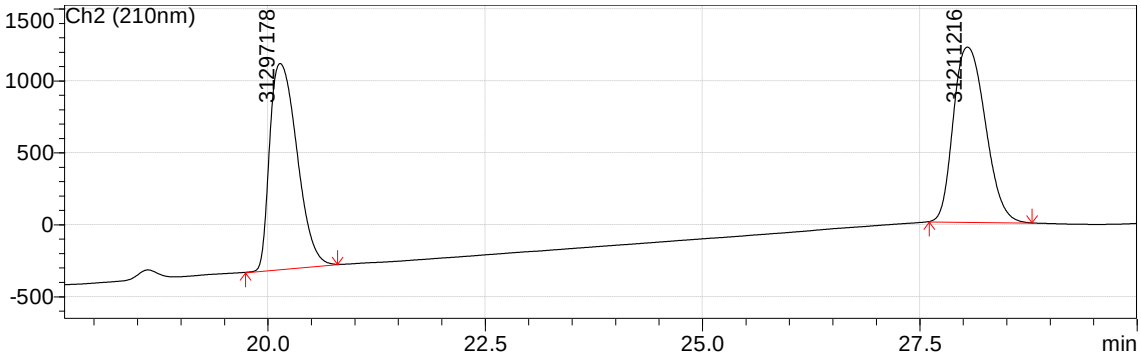

Peak #	Retention Time	Area	Area %
1	20.139	31297178	50.1
2	28.048	31211216	49.9

Enantioenriched **2.17a**:

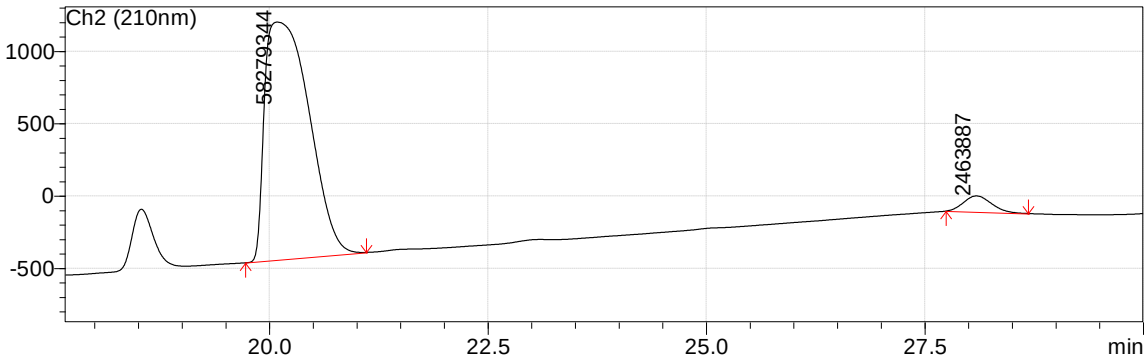

Peak #	Retention Time	Area	Area %
1	20.087	58279344	95.9
2	28.088	2463887	4.1

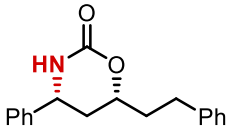

HPLC analysis for compound **2.18a** (CHIRALCEL® AD-H, 5→30% iPrOH/hexane gradient over 12 min, 0.7 mL/min, 220 nm): t_R = 15.9 min (major), 18.7 min (minor); 94% ee

Racemic **2.18a**:

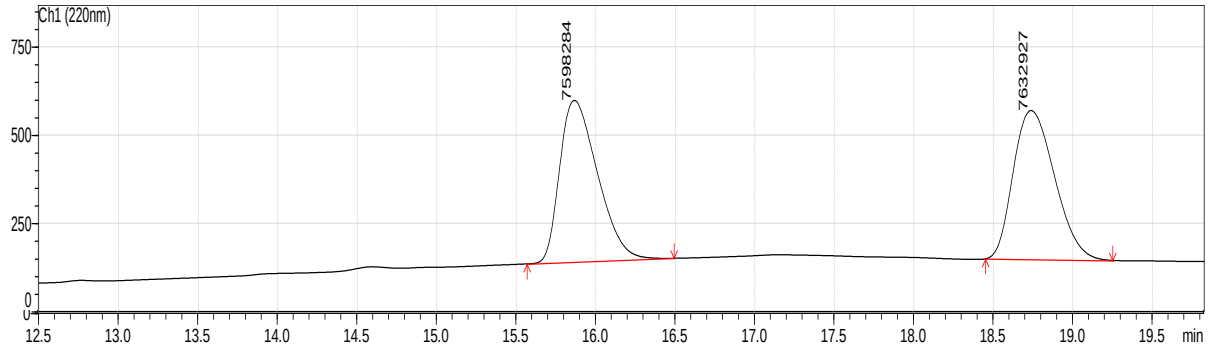

Peak #	Retention Time	Area	Area %
1	15.861	7598248	49.9
2	18.733	7632927	50.1

Enantioenriched **2.18a**:

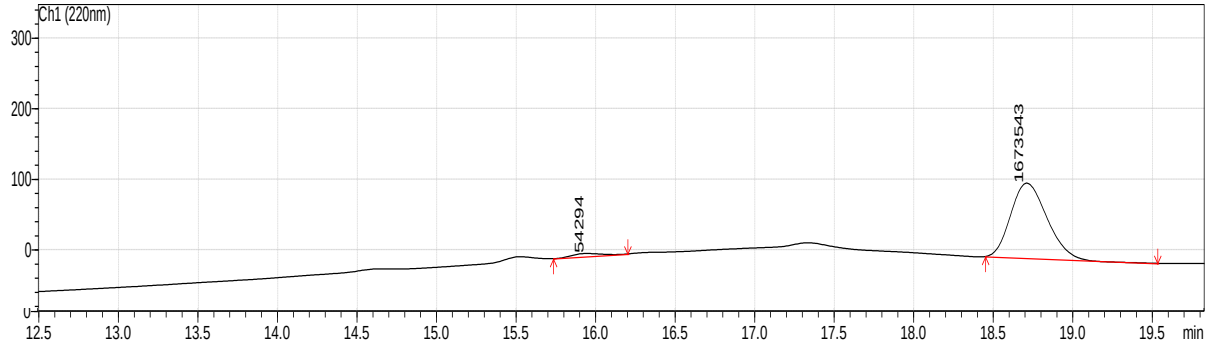

Peak #	Retention Time	Area	Area %
1	15.940	54294	3.1
2	18.706	1673543	96.9

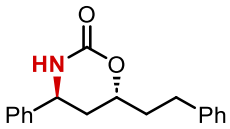

HPLC analysis for compound **2.18a-anti** (CHIRALCEL® OJH, 5→35% iPrOH/hexane gradient over 22 min, 0.7 mL/min, 210 nm): t_R = 24.7 min (major), 22.7 min (minor); 72% ee

Racemic **2.18a**:

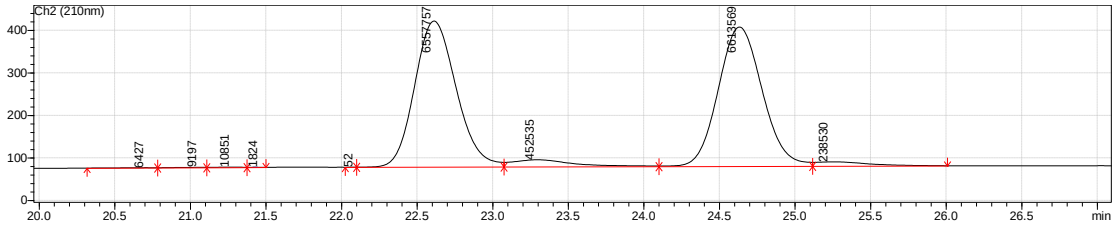

Peak #	Retention Time	Area	Area %
1	22.6	1859776	50.7
2	24.7	1806328	49.3

Enantioenriched **2.18a**:

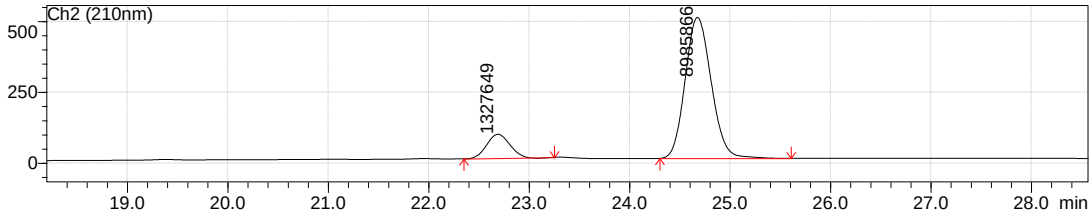

Peak #	Retention Time	Area	Area %
1	22.7	511646	13.9
2	24.7	3165079	86.1

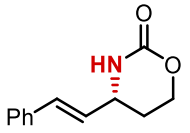

HPLC analysis for compound **2.19a** (CHIRALCEL® OJ-H, 5→35% iPrOH/hexane gradient over 27 min, 0.7 mL/min, 210 nm): t_R = 30.9 min (major), 33.8 min (minor); 83% ee

Racemic **2.19a**:

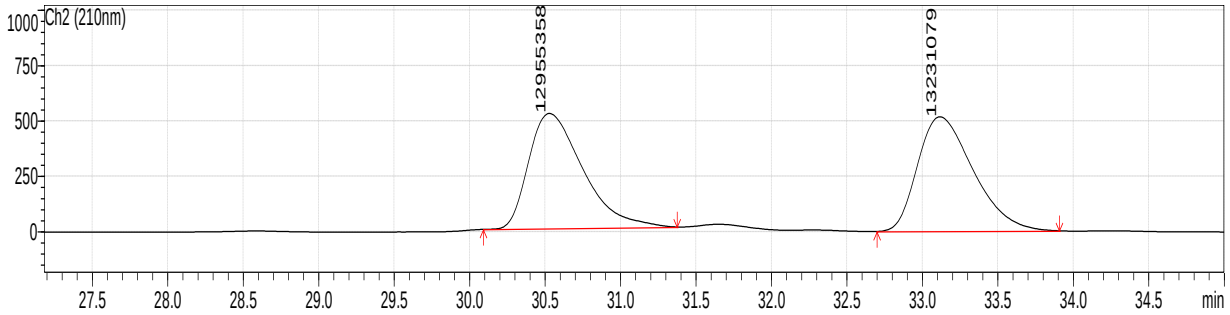

Peak #	Retention Time	Area	Area %
1	30.526	12955358	49.5
2	33.114	13231079	50.5

Enantioenriched **2.19a**:

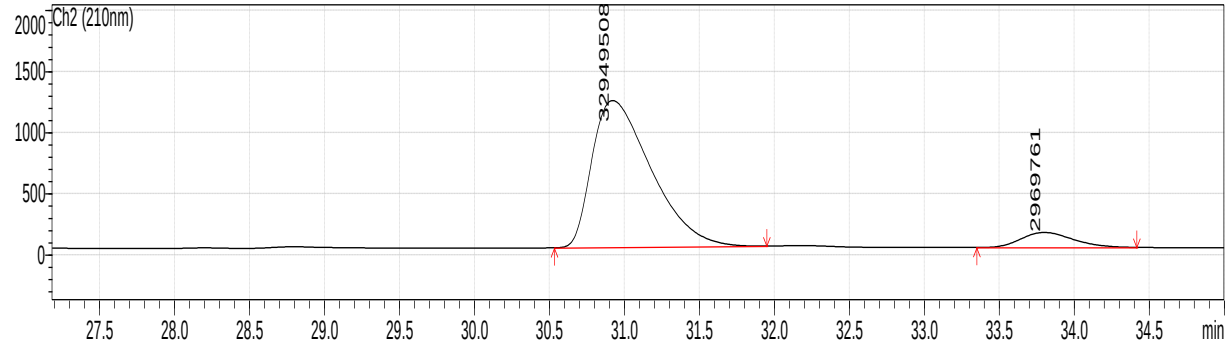

Peak #	Retention Time	Area	Area %
1	30.919	32949508	91.7
2	33.795	2969761	8.3

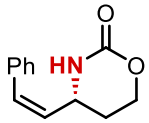

HPLC analysis for compound **2.20a** (CHIRALCEL® OJ-H, 5→35% iPrOH/hexane gradient over 27 min, 0.7 mL/min, 210 nm): t_R = 27.2 min (major), 29.3 min (minor); 31% ee

Racemic **2.20a**:

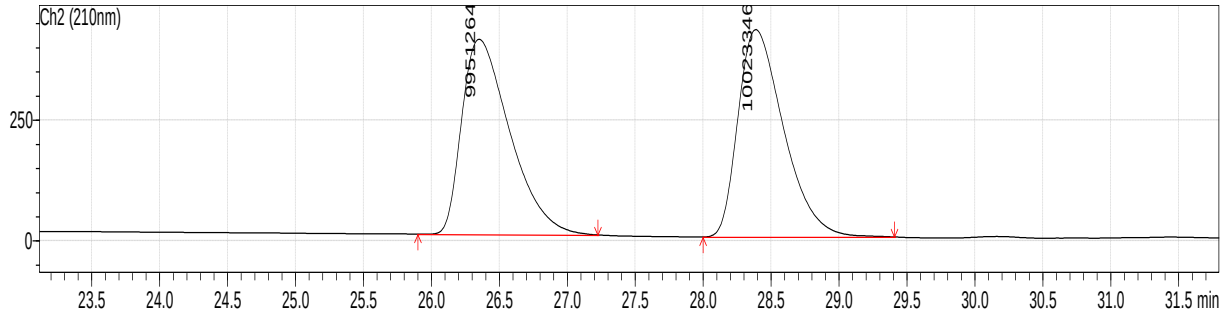

Peak #	Retention Time	Area	Area %
1	26.349	9951264	49.8
2	28.358	10023346	50.2

Enantioenriched **2.20a**:

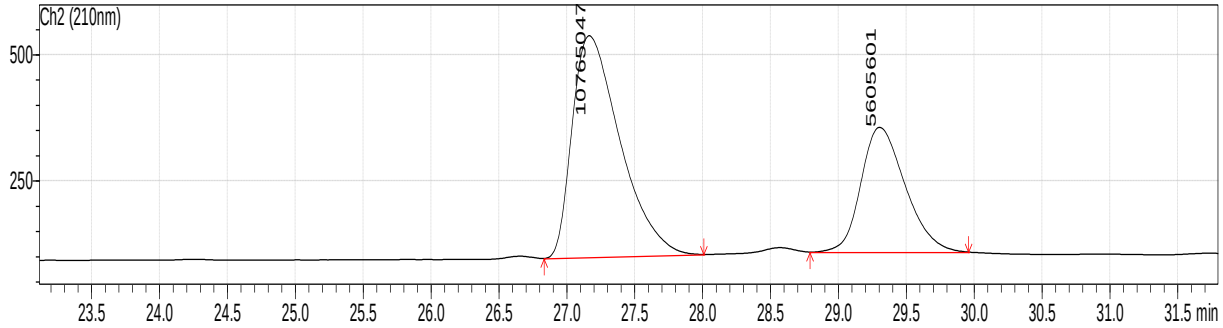

Peak #	Retention Time	Area	Area %
1	27.163	10765047	65.8
2	29.301	5305301	34.2

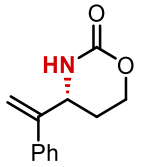

HPLC analysis for compound **2.21a** (CHIRALCEL® OJ-H, 5→35% iPrOH/hexane gradient over 22 min, 0.7 mL/min, 220 nm): t_R = 18.3 min (minor), 19.5 min (major); 80% ee

Racemic **2.21a**:

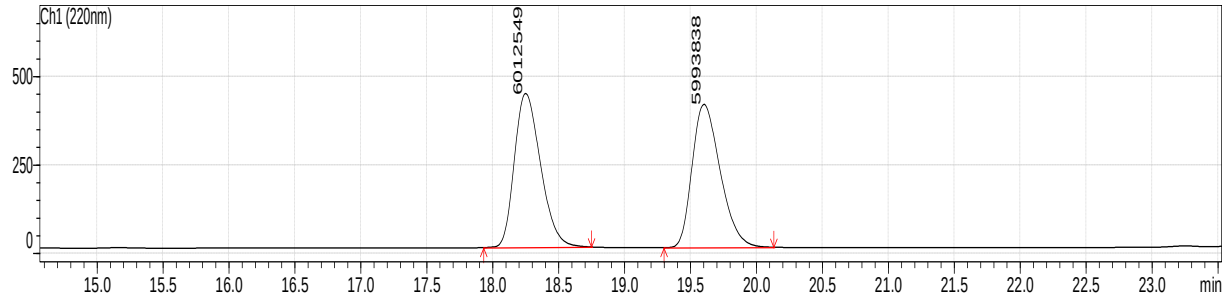

Peak #	Retention Time	Area	Area %
1	18.248	6012549	50.1
2	19.600	5993838	49.9

Enantioenriched **2.21a**:

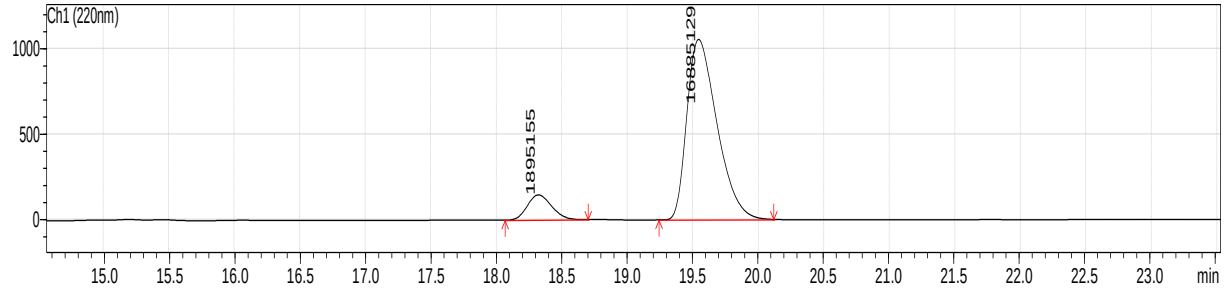

Peak #	Retention Time	Area	Area %
1	18.318	1895155	10.1
2	19.541	16885129	89.9

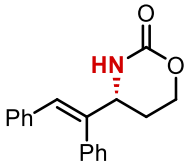

HPLC analysis for compound **2.22a** (CHIRALCEL® OJ-H, 5→35% iPrOH/hexane gradient over 22 min, 0.7 mL/min, 210 nm): t_R = 21.3 min (major), 33.7 min (minor); 76% ee

Racemic **2.22a**:

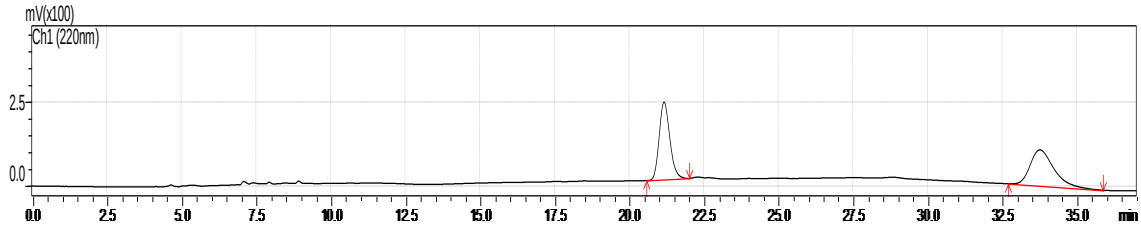

Peak #	Retention Time	Area	Area %
1	21.2	5745359	49.1
2	33.7	5958249	50.9

Enantioenriched **2.22a**:

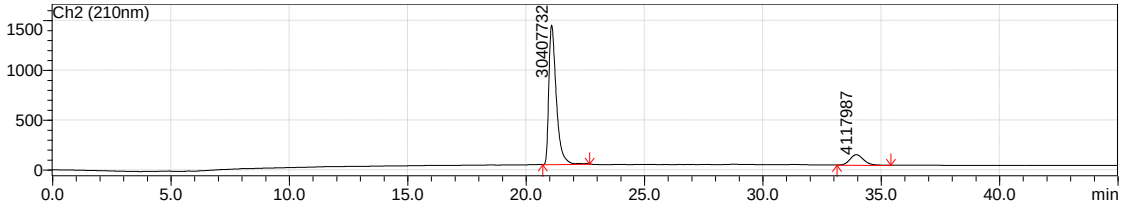

Peak #	Retention Time	Area	Area %
1	21.1	30074231	87.9
2	34.0	4139139	12.1

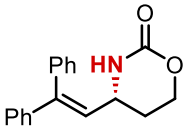

HPLC analysis for compound **2.23a** (CHIRALCEL® OJ-H, 5→35% iPrOH/hexane gradient over 22 min, 0.7 mL/min, 220 nm): t_R = 30.1 min (major), 36.4 min (minor); 99% ee

Racemic **2.23a**:

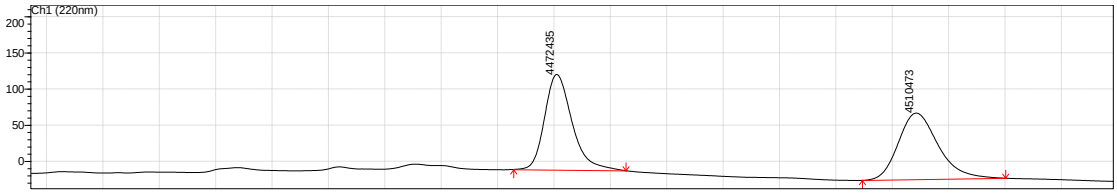

Peak #	Retention Time	Area	Area %
1	30.0	4472435	49.8
2	36.4	4510473	50.2

Enantioenriched **2.23a**:

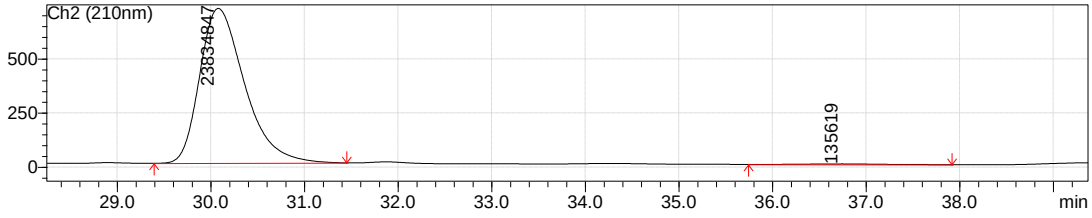

Peak #	Retention Time	Area	Area %
1	30.1	15784332	99.6
2	36.8	63877	0.4

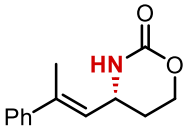

HPLC analysis for compound **2.24a** (CHIRALCEL® OJ-H, 5→35% iPrOH/hexane gradient over 27 min, 0.7 mL/min, 220 nm): t_R = 31.9 min (major), 34.0 min (minor); 77% ee

Racemic **2.24a**:

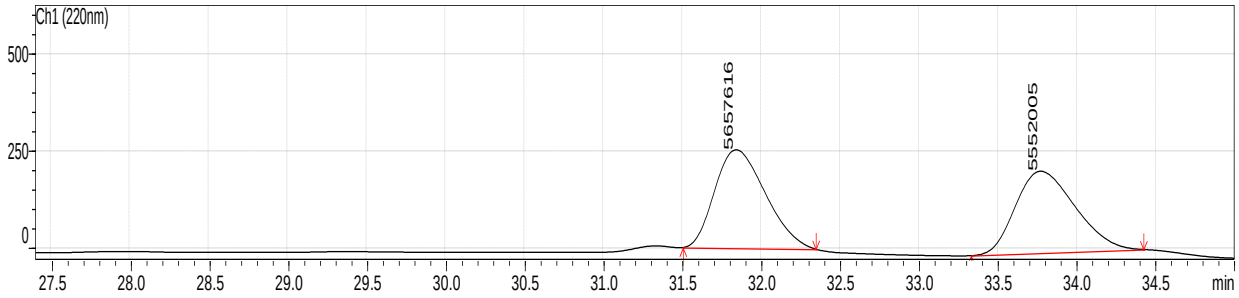

Peak #	Retention Time	Area	Area %
1	31.841	5657616	50.5
2	33.770	5552005	49.5

Enantioenriched **2.24a**:

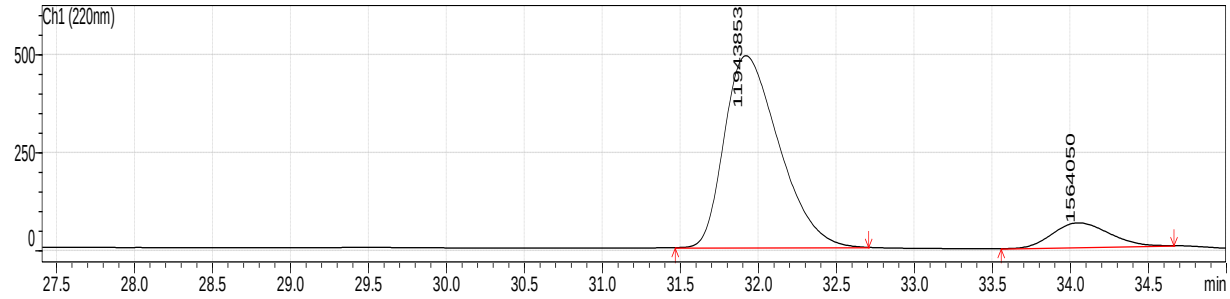

Peak #	Retention Time	Area	Area %
1	31.908	11943853	88.4
2	34.051	1564050	11.6

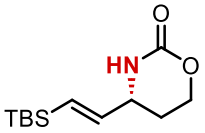

HPLC analysis for compound **2.25a** (CHIRALCEL® OJ-H, 5→20% iPrOH/hexane gradient over 12 min, 0.7 mL/min, 210 nm): t_R = 9.2 min (major), 10.4 min (minor); 94% ee

Racemic **2.25a**:

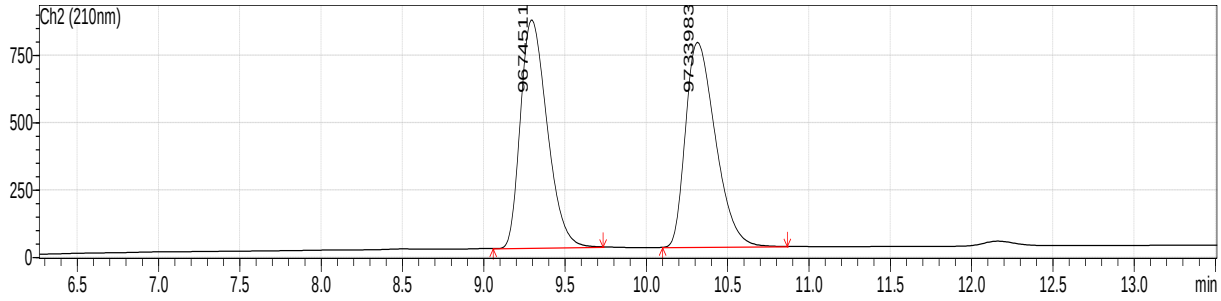

Peak #	Retention Time	Area	Area %
1	9.292	9674511	49.8
2	10.312	9733983	50.2

Enantioenriched **2.25a**:

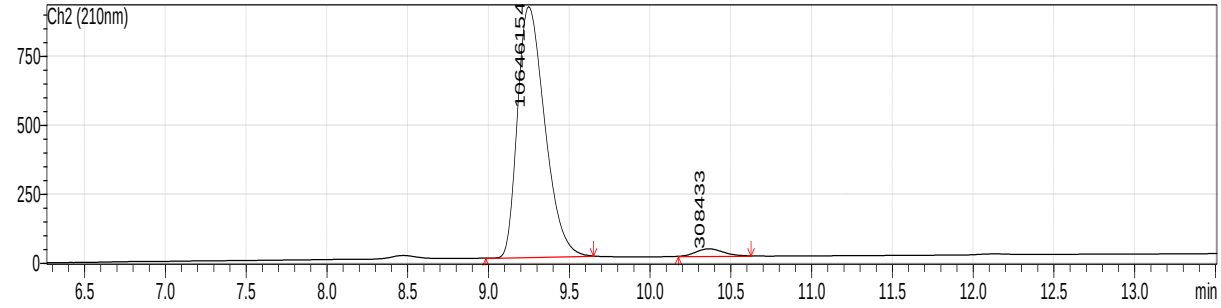

Peak #	Retention Time	Area	Area %
1	9.245	10646154	97.2
2	10.356	308433	2.8

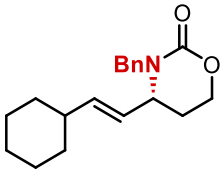

HPLC analysis for compound **2.26b** (CHIRALCEL® OJ-H, 5→20% iPrOH/hexane gradient over 22 min, 0.7 mL/min, 220 nm): t_R = 13.7 min (major), 14.3 min (minor); 85% ee

Racemic **2.26b**:

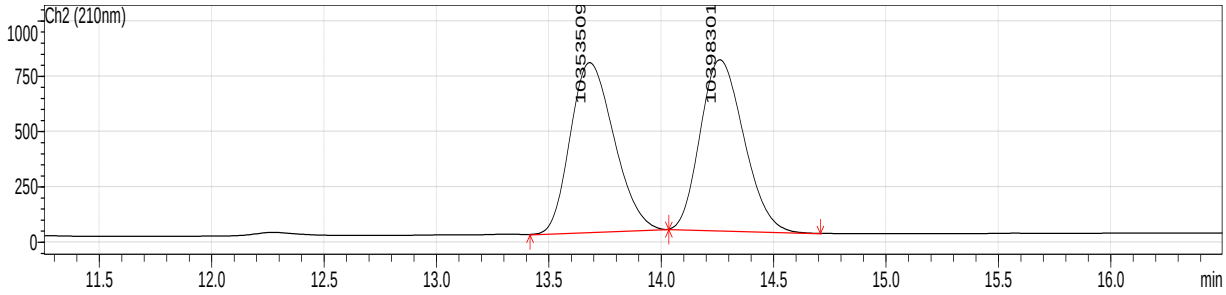

Peak #	Retention Time	Area	Area %
1	13.679	10353509	49.9
2	14.258	10398301	50.1

Enantioenriched **2.26b**:

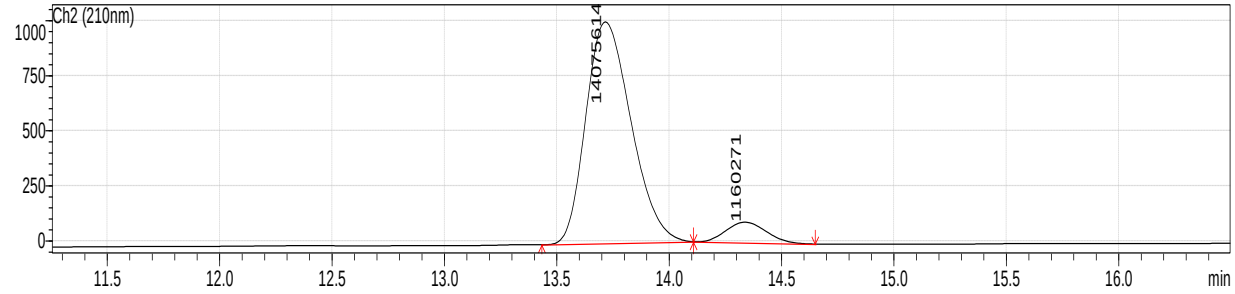

Peak #	Retention Time	Area	Area %
1	13.713	14075614	92.4
2	14.334	1160271	7.6

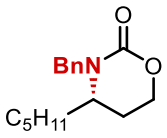

HPLC analysis for compound **2.27b** (CHIRALCEL® OD-H, 5→12% iPrOH/hexane gradient over 22 min, 0.7 mL/min, 210 nm): t_R = 19.6 min (major), 20.3 min (minor); 58% ee

Racemic **2.27b**:

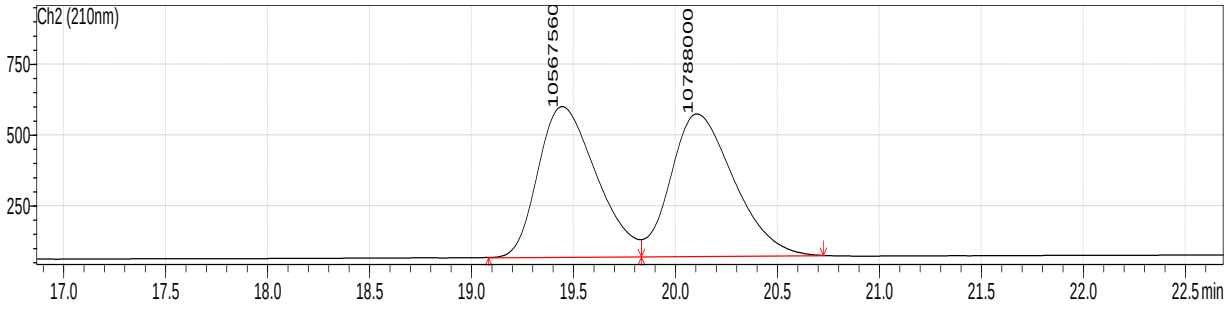

Peak #	Retention Time	Area	Area %
1	19.441	10567560	49.5
2	20.102	10788000	50.5

Enantioenriched **2.27b**:

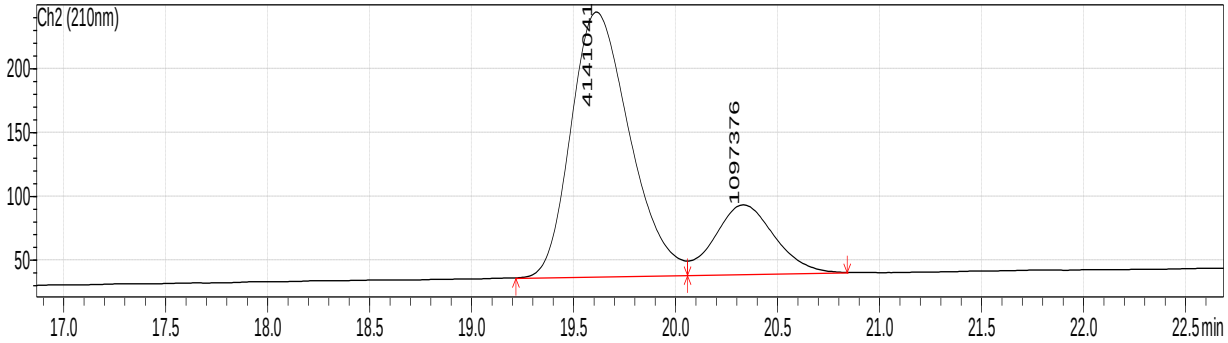

Peak #	Retention Time	Area	Area %
1	19.609	4141041	79.1
2	20.329	1097376	20.9

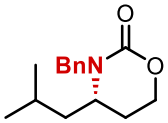

HPLC analysis for compound **2.28b** (CHIRALCEL® OJ-H, 5→20% iPrOH/hexane gradient over 22 min, 0.7 mL/min, 210 nm): t_R = 16.5 min (major), 17.7 min (minor); 54% ee

Racemic **2.28b**:

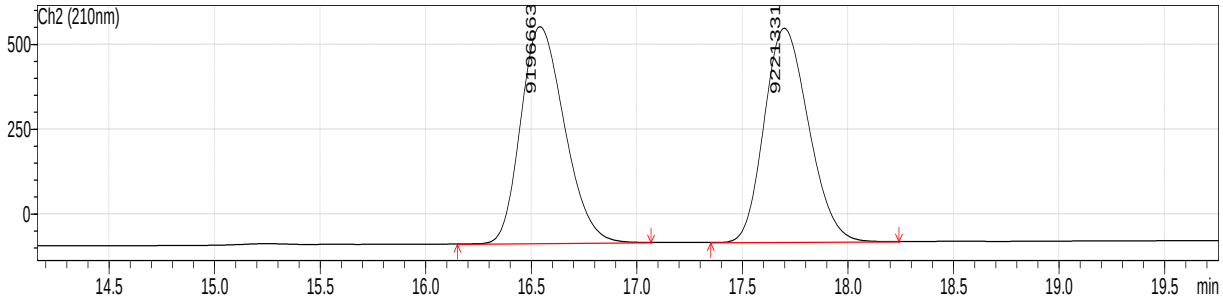

Peak #	Retention Time	Area	Area %
1	16.538	9196663	50.0
2	17.695	9221331	50.0

Enantioenriched **2.28b**:

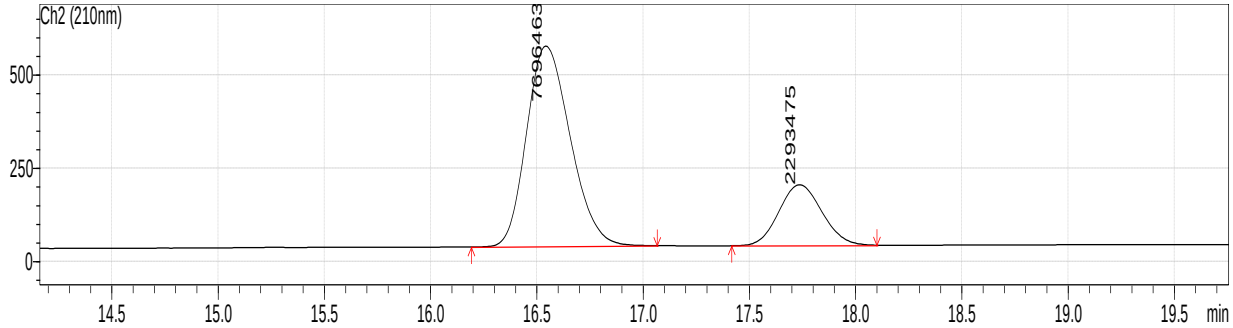

Peak #	Retention Time	Area	Area %
1	16.540	7696463	77.0
2	17.733	2293475	23.0

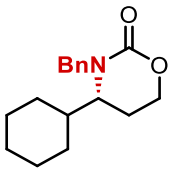

HPLC analysis for compound **2.29b** (CHIRALCEL® IC, 35→70% H_2O/acetonitrile (0.1% formic acid) gradient over 15 min, 0.7 mL/min, 210 nm): t_R = 10.4 min (major), 10.9 min (minor); 65% ee

Racemic **2.29a**:

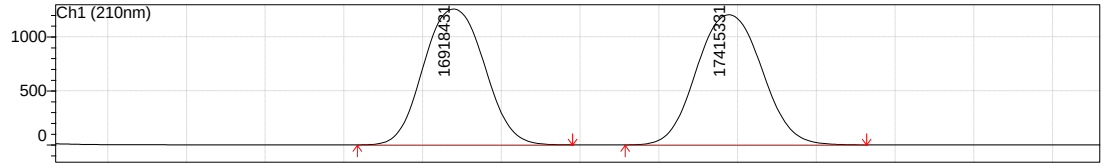

Peak #	Retention Time	Area	Area %
1	27.1	16934465	49.3
2	28.0	17436179	50.7

Enantioenriched **2.29a**:

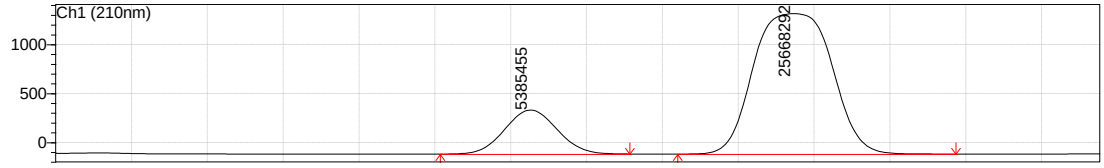

Peak #	Retention Time	Area	Area %
1	27.3	5385455	17.3
2	28.2	25668292	82.7

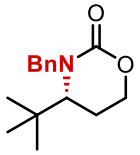

HPLC analysis for compound **2.30b** (CHIRALCEL® OJ-H, 5→20% iPrOH/hexane gradient over 22 min, 0.7 mL/min, 210 nm): t_R = 16.4 min (minor), 18.6 min (major); 52% ee

Racemic **2.30b**:

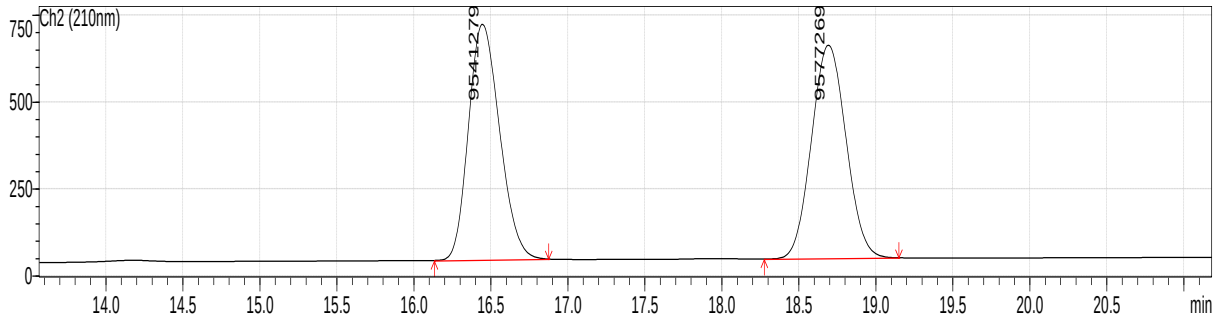

Peak #	Retention Time	Area	Area %
1	16.442	9541279	49.9
2	18.689	9577269	50.1

Enantioenriched **30b**:

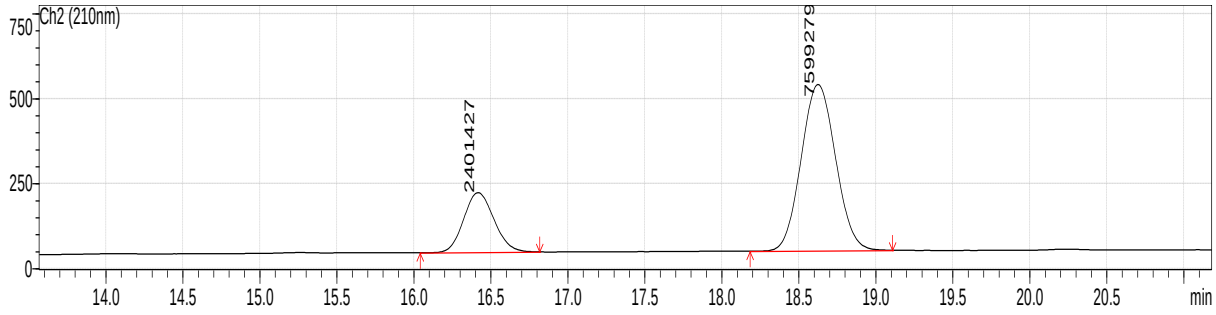

Peak #	Retention Time	Area	Area %
1	16.414	2401427	24.0
2	18.622	7599279	76.0

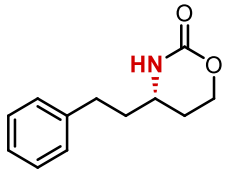

HPLC analysis for compound **2.31a** (CHIRALCEL® OD-H, 5→15% iPrOH/hexane gradient over 33 min, 0.7 mL/min, 220 nm): t_R = 28.4 min (major), 31.1 min (minor); 35% ee

Racemic **2.31a**:

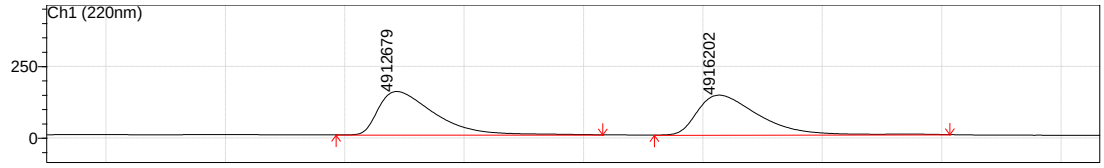

Peak #	Retention Time	Area	Area %
1	28.4	4912679	50.0
2	31.1	4916202	50.0

Enantioenriched **2.31a**:

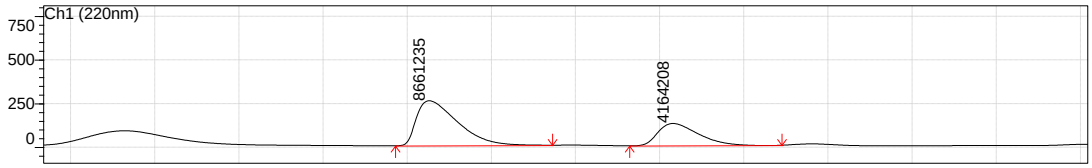

Peak #	Retention Time	Area	Area %
1	28.3	8661235	67.5
2	31.1	4164208	32.5

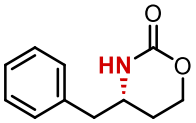

HPLC analysis for compound **2.32a** (CHIRALCEL® IC, 35→70% H_2O/acetonitrile (0.1% formic acid) gradient over 15 min, 0.7 mL/min, 210 nm): t_R = 10.4 min (major), 10.9 min (minor); 43% ee

Racemic **2.32a**:

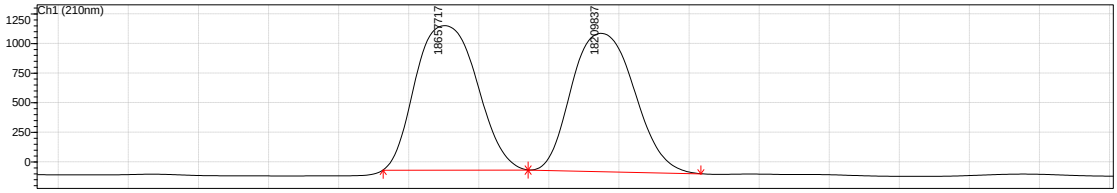

Peak #	Retention Time	Area	Area %
1	10.4	18657717	50.6
2	10.9	18209837	49.4

Enantioenriched **2.32a**:

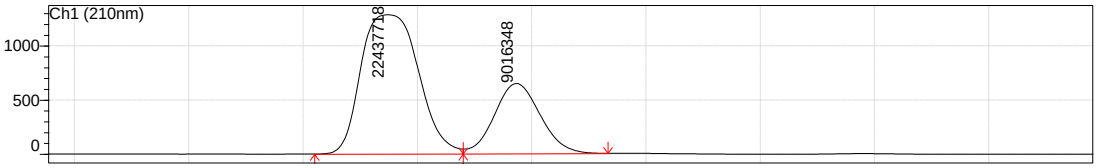

Peak #	Retention Time	Area	Area %
1	10.4	22437718	71.3
2	10.9	9016348	28.7

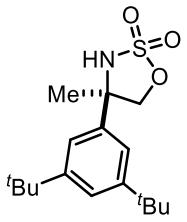

HPLC analysis for compound **2.34** (CHIRALCEL® AD-H, 5% iPrOH/hexane, 0.7 mL/min, 210 nm): t_R = 10.1 min (major), 11.4 min (minor); 99% *ee*

Racemic **2.34**:

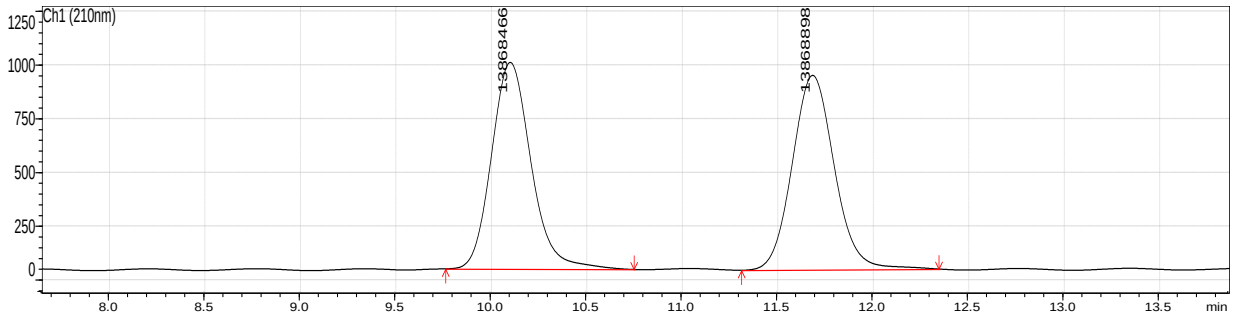

Peak #	Retention Time	Area	Area %
1	10.098	13868466	50.0
2	11.683	13868898	50.0

Enantioenriched **2.34**:

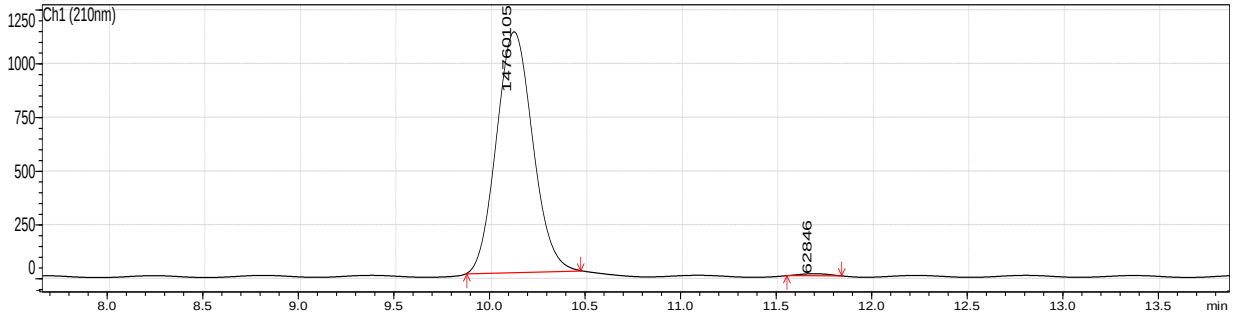

Peak #	Retention Time	Area	Area %
1	10.119	14760105	99.6
2	11.689	624846	0.4

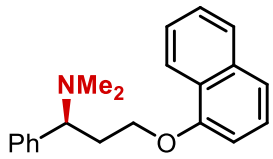

HPLC analysis for compound (*S*)-Dapoxetine (CHIRALCEL® OD-H, 0.2→1.6% iPrOH/hexane gradient over 12 min, 1.0 mL/min, 210 nm): t_R = t_R = 14.2 min (mino), 14.5 min (major); 90% *ee*

Racemic Dapoxetine:

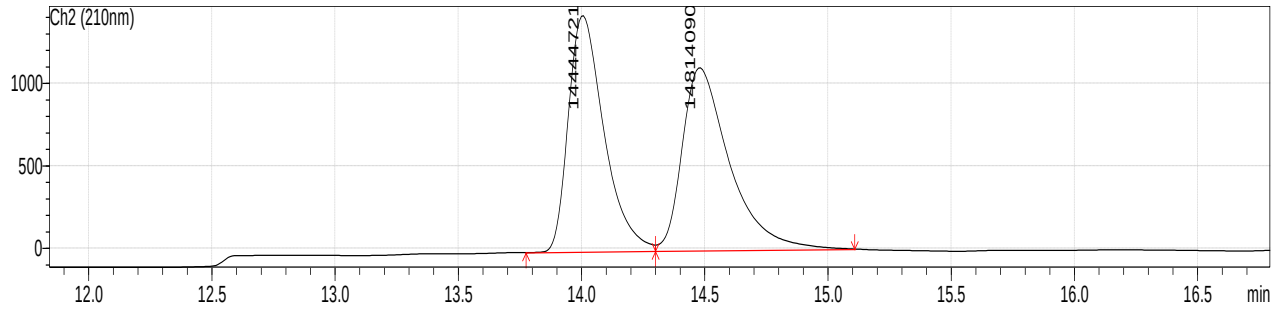

Peak #	Retention Time	Area	Area %
1	14.001	14444721	49.4
2	14.476	14814090	50.6

Enantioenriched (*S*)-Dapoxetine:

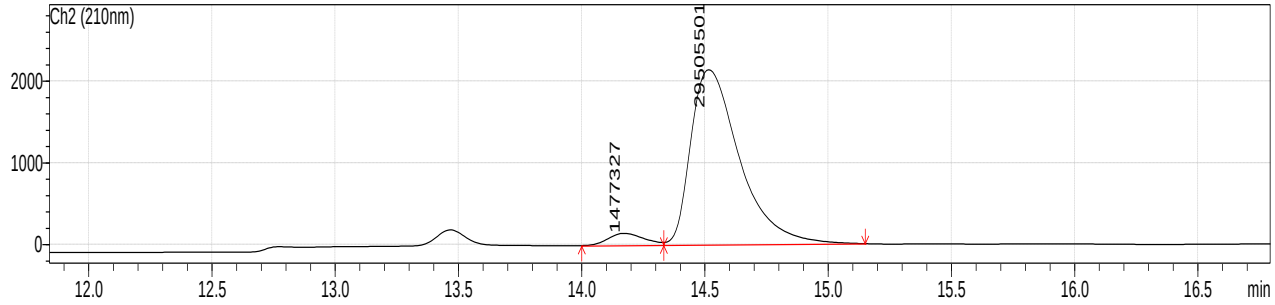

Peak #	Retention Time	Area	Area %
1	14.169	1477327	4.8
2	14.513	29505501	95.2

Chapter 3. *Chemoselective silver-catalyzed nitrene transfer for the synthesis of azepine and cyclic carbamimidate derivatives*

3.1. Introduction

N-heterocycles are common motifs in natural products and drugs; around 60% of FDA approved small-molecule drugs contain a of nitrogen-containing heterocycle.[1] Of this group of compounds, the majority is composed of a diverse set of five- and six-membered rings which are often much easier to synthesize than their four-, seven-, or eight-membered counterparts. Still, substituted seven-membered ring structures such as substituted azepanes and azepines are prevalent in natural products[2] and have shown potential as treatment for heart disease,[3] anti-diabetics,[4] anticancer agents,[5] anti-bacterials,[6] and anti-virals (Figure 3.1).[7] Thus, the development of divergent methodologies for the synthesis of these seven-membered heterocycles is highly desirable.

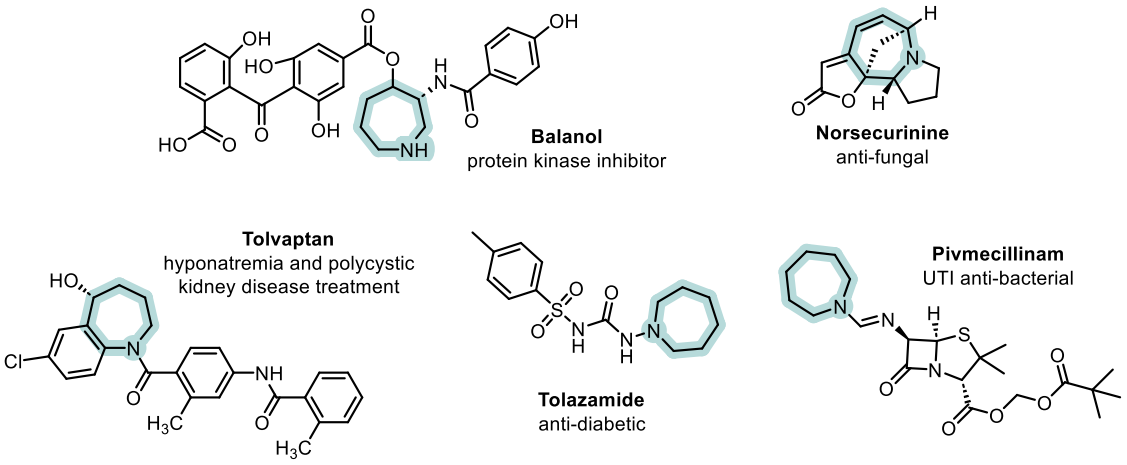

Figure 3.1 – Azepane and azepine derivitives in drugs and natural products.

Common methods for the synthesis of azepanes and related derivatives include [4+3] or [5+2] cycloadditions, ring expansion reactions, as well as various cyclization reactions such as *aza*-Prins cyclizations or ring closing metathesis reactions.[8] These *de novo* syntheses of the ring structure benefit from allowing functional groups to be intentionally installed in locations on the ring, however the synthesis of the necessary precursors can require multiple synthetic steps,

rendering the synthesis of compound libraries lengthy and challenging. An alternative and more modular synthetic approach would be to utilize prevalent aromatic rings as precursors and subsequently insert an atom into the ring to form the seven-membered heterocycle (Scheme 3.1). While many efforts have been expended towards utilizing skeletal editing to synthesize five- and six-membered rings,[9] the synthesis of medium-sized heterocycles is still limited. A common method of ring expansion is the Büchner reaction, which has often been utilized for the synthesis of medium-sized carbocycles.[10] More recently, the Büchner reaction has been used for the synthesis of azepines starting from pyridines and quinolines using carbene insertion strategies.[11]

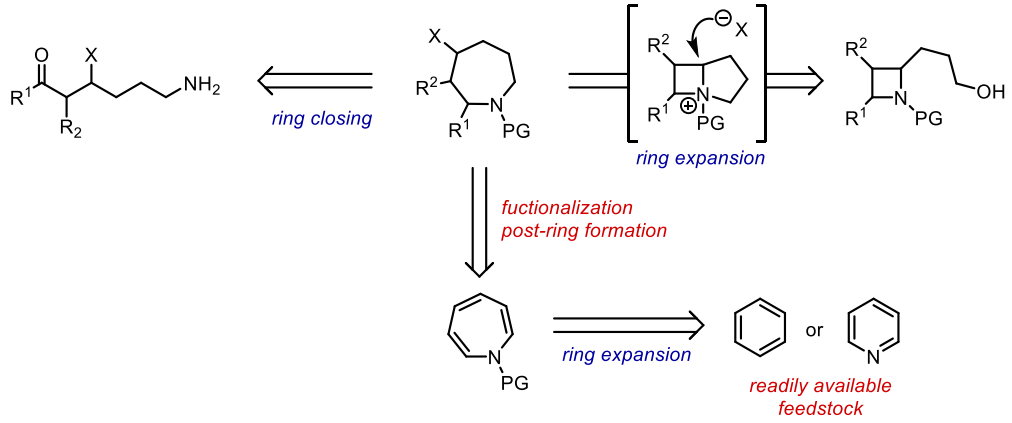

Scheme 3.1 – Potential synthetic approaches of substituted seven-membered heterocycles.

We envisioned an analogous approach, using nitrenes and phenyl rings together for an *aza*-Büchner-type ring expansion mechanism. This type of dearomatization reaction is precedented in the nitrene literature, however historical examples are limited by poor chemoselectivity and harsh, forcing conditions (Scheme 3.2a).[12] Transition metal catalysis allows for better control of highly reactive nitrene intermediates under much more mild conditions. However, a recent report using Rh_2esp_2 for this challenging dearomatization reaction still required high temperatures and catalyst loadings (Scheme 3.2b).[13] Additionally, though the

rhodium catalyst did impart selectivity for azepine formation over competing C(sp^2)–H insertion, selectivity of dearomatization versus C(sp^3)–H insertion was not shown.

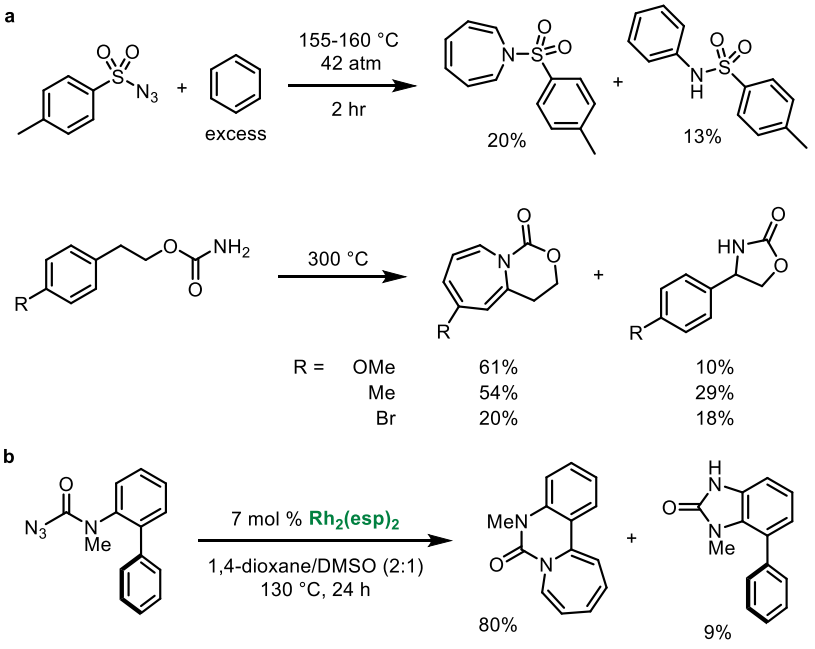

Scheme 3.2 – Precedent for chemodivergent reactivity. (a) Examples of uncontrolled selectivity from thermally generated nitrenes. (b) Example of transition metal catalyzed selectivity.

Our group has shown that silver can effectively control chemoselectivity, site-selectivity and enantioselectivity in nitrene transfer reactions by simply changing the ligand.[14] In particular, the group has shown that silver catalysts with a single bidentate ligand such as [Ag(dmbox)] are uniquely suited to controlling the site-selectivity of carbamates for the formation of six-membered rings.[14e] Additionally, we recently reported an asymmetric intramolecular aziridination using Tces-protected carbamimidates (Tces = trichloroethylsulfamate) as the nitrene precursor (Scheme 3.3a).[15] Carbamimidates were first reported as nitrene precursors by the Dauban group for use in C–H amination.[16] During the course of our investigations into intramolecular reactions with these precursors, we observed formation of a [3,7]-bicyclic aziridine which we had heretofore not observed with reactions of corresponding carbamates

(Scheme 3.3b). Therefore, we hypothesized that Tces-carbamimidates in combination with silver complexes may be able to access other previously unprecedented products of carbamates. Herein, we report a chemoselective method for synthesis of either azepines or cyclic carbamimidates using silver-catalyzed nitrene transfer (Scheme 3.3c).

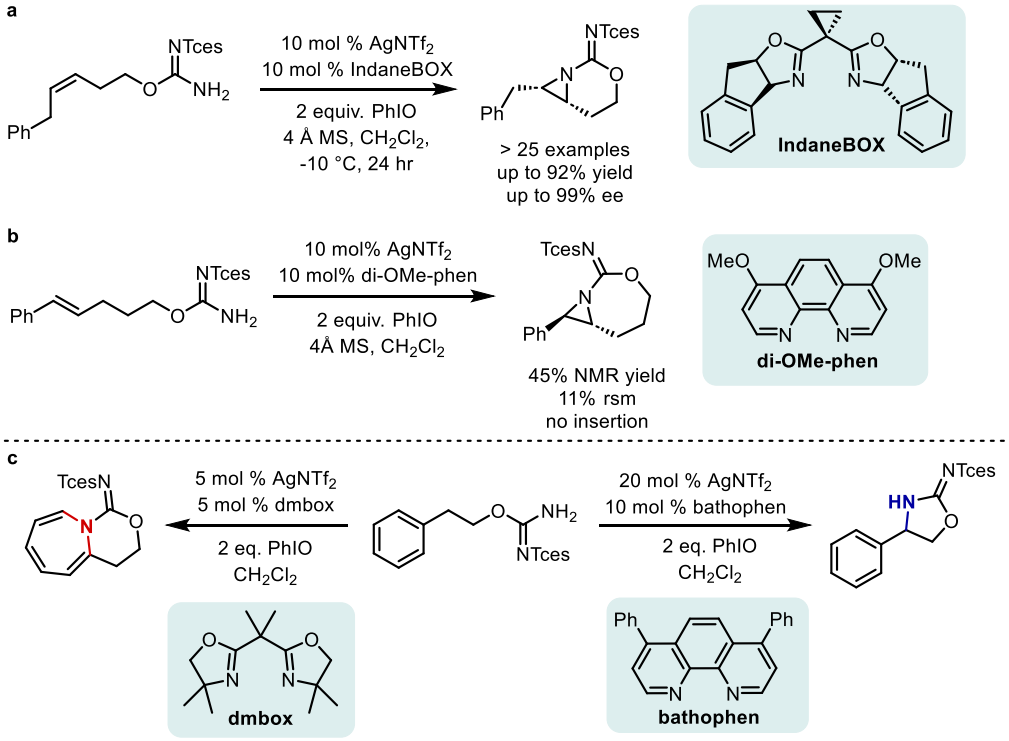

Scheme 3.3 – Reactivity of carbamimidates with silver complexes. (a) Asymmetric aziridination with IndaneBOX. (b) Unexpected reactivity of carbamimidate precursors with activated alkenes. (c) Chemodivergent nitrene reactivity controlled by ligand identity.

3.2. Results and discussion

3.2.1. Ligand effects on chemoselectivity

We began our investigation by subjecting carbamimidate **3.1** to nitrene transfer conditions with different types of bidentate silver complexes (Figure 3.2). Testing different ligand classes revealed interesting connections between the steric and electronic properties of the ligand and chemoselectivity. In general, ligands that enforce greater steric pressure on the

reaction site more strongly prefer formation of azepine **3.1b**, with all others preferring C–H insertion product **3.1a**. Neocuproine ligands (**L3.6**-**L3.8**) and dmbox ligand **L3.10** all favored formation of **3.1b** in moderate yields (60-65%). This strong steric influence does not apply to any of the previous chemoselective systems the group has developed, suggesting this effect is unique to the reaction with Tces-protected carbamimidates. However, computational insights from the group's previous work in asymmetric aziridination could explain this distinctive reactive and selectivity. In particular, computations indicate that the most stable transition state geometry at silver is a square-planar geometry, with the N of the imidate coordinating to silver.[15] This would put the sterically bulky Tces group in close proximity to any ligand substitution that is projecting in towards the silver center. We hypothesize that this negative steric interaction is key in disfavoring C–H insertion and instead allowing azepine formation to occur.

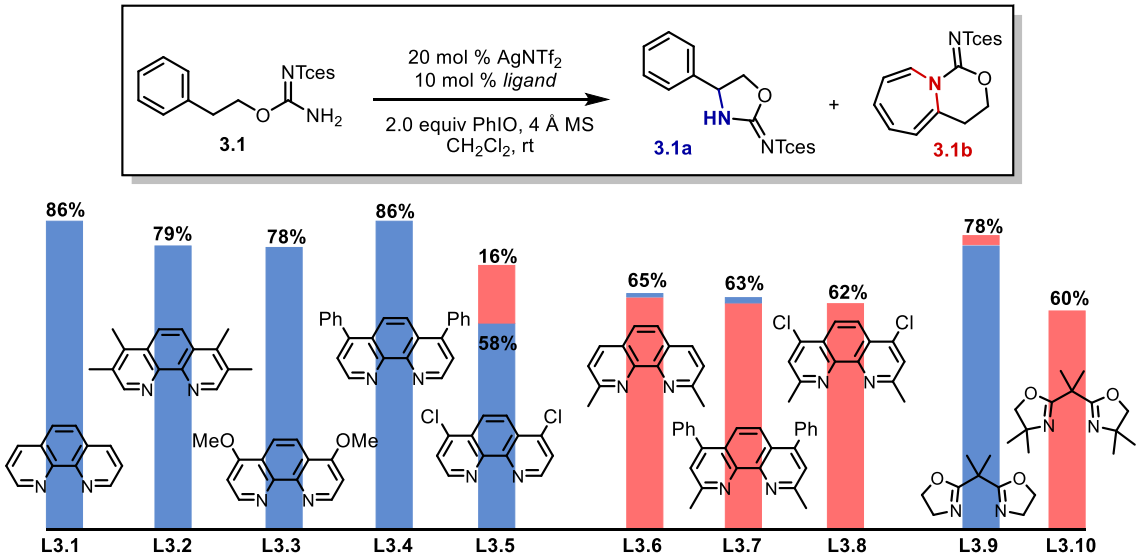

Figure 3.2 – Effect of bidentate ligand identity on chemoselectivity.

Nevertheless, sterics are not the only factor controlling selectivity in this reaction. For example, chemoselectivity for formation of **3.1b** was best when more electron-poor ligands **L3.8** and **L3.10** were used. Interestingly, this electronic effect extended to reactions that favored

formation of **3.1a** as well. In particular, ligands **L3.5** and **L3.9** both demonstrate that azepine formation can occur without steric influence provided that the accompanying ligand is electron-poor. More subtly, ligands that are more electron rich such as **L3.2** and **L3.3** generally perform slightly worse than their electron-neutral counterparts **L3.1** and **L3.4** (around 86% yield for the former pair and about 78% yield for the latter) which indicates that the nitrene formed from the carbamimidate is quite sensitive to small changes in the electronics of the ligand.

3.2.2. Scope of C–H insertion of carbamimidates

Efforts to improve the yields of the insertion reaction above 86% for carbamimidate **3.1** proved unfruitful so we proceeded with examining the scope (Table 3.1).

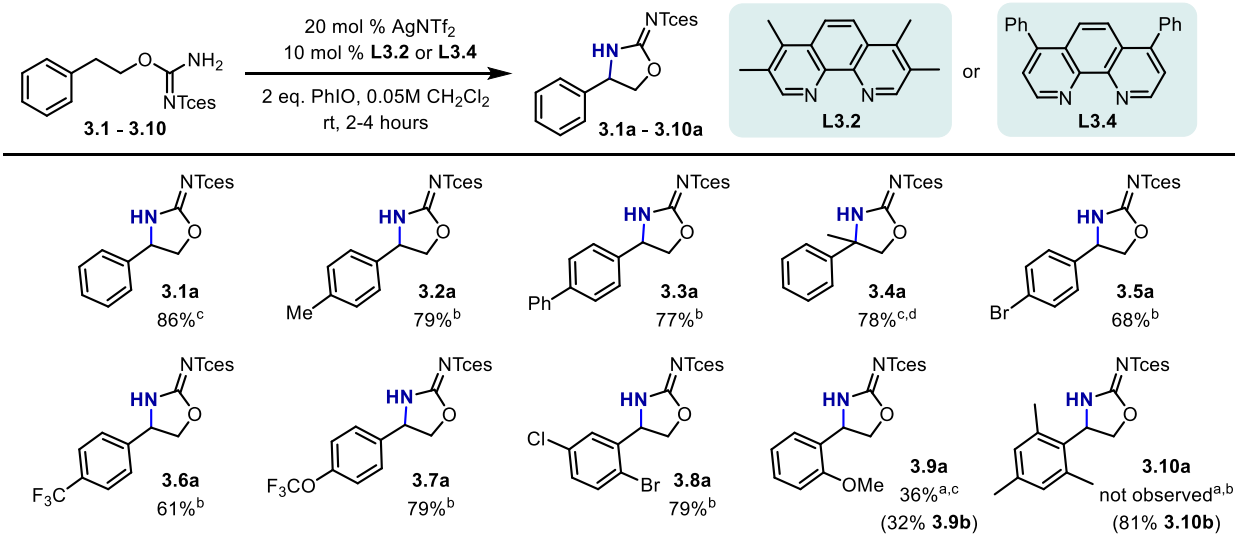

[a]Yields determined by ^{1}H NMR using trimethylphenyl silane as an internal standard. [b]Me_4phen was utilized. [c]bathophen was utilized. [d]3% of **3.4b** observed.

Table 3.1 – Scope of chemoselective silver-catalyzed amination of benzylic C(sp3)–H bonds.

In general, substrates with simple *para*-substitution on the arene (**3.2a**-**3.3a**, **3.5a**-**3.7a**) proceeded in good to excellent yields, with no azepine products observed. However, substrates that had an electron-donating group in the *para*-position underwent primarily degradation and

by-product formation, with small amounts of azepine formation. The problem of oxidative degradation is not present for reactions with carbamates, again highlighting the differences between that and the seemingly similar carbamimidate. Substrate **3.4** with an additional Me group in the benzylic position afforded **3.4a** in 78% yield with just a small reduction in chemoselectivity (3% of **3.4b** was observed). Disubstituted arene **3.8** yielded only 79% of C–H insertion product **3.8a**. Though electron-rich substitution was not tolerated at the *para*- and *meta*-positions, *ortho*-OMe substituted arene **3.9** afforded a mixture of about 1:1 **3.9a** to **3.9b**, with minimal degradation of the starting material. Interestingly, C–H insertion was never observed with carbamimidate **3.10**, and many different ligands were able to efficiently catalyze the formation of **3.10b** instead. It is likely that the combination of increased sterics near the benzylic position and increased electron-density of the arene ring hinder C–H insertion and favor dearomatization into the ring regardless of ligand identity.

3.3.3. Scope of dearomatization via NT

With the initial scope of the C–H insertion laid out, we set out to do the same with the azepine formation reaction. A brief optimization study revealed that yields could be improved from 60% up to 87% by reducing the concentration of the reaction from 0.05M to 0.025M and also lowering the catalyst loading from 20 mol % $AgNTf_2$ and 10 mol % **L3.10** down to 5 mol % for both. Presumably, this modification avoids over oxidation and degradation of the product while the reaction is running.

With the optimized conditions in hand, the reaction scope was explored (Table 3.2). In the majority of cases, the azepine product was formed exclusively. For electron-neutral substrates **3.2**-**3.4**, the reaction proceeded in excellent yields (>94%) to yield a stable, bright yellow solid.

Even though the slightly more electron-poor substrate **3.5** is slightly less efficient in terms of yield (69%), **3.5b** is the only product that is observed. Unfortunately, *para*-CF_3 substrate **3.6** is too electron-poor to undergo dearomatization under the reaction conditions. Instead, 25% of **3.6a** is recovered. On the other hand, substrate **3.7** provides azepine **3.7b** in 89% yield and excellent selectivity. Remarkably, carbamimidate **3.8** does not react when subjected to the reaction conditions. Presumably, the substrate itself is too electron-poor to allow for azepine formation, while the sterics of the substrate and the ligand inhibit C–H insertion.

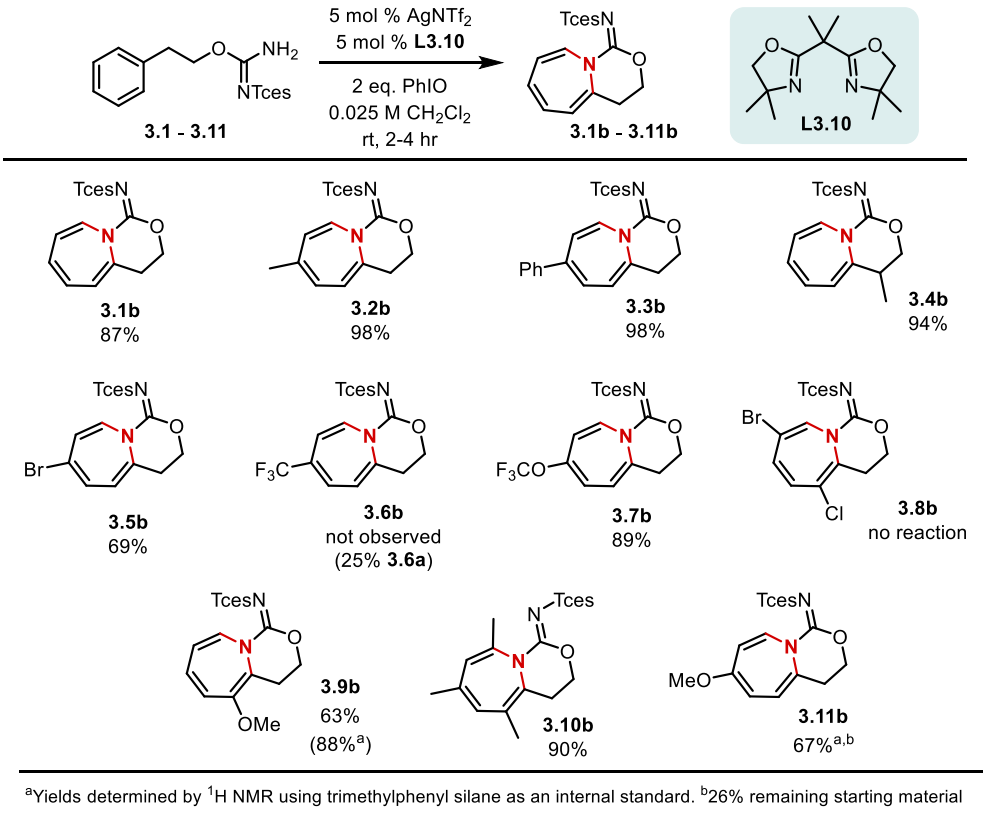

[a]Yields determined by ^{1}H NMR using trimethylphenyl silane as an internal standard. [b]26% remaining starting material

Table 3.2 – Scope of chemoselective silver-catalyzed dearomatization of arenes.

In contrast to the C–H insertion reaction, electron-rich arenes are well tolerated in the dearomatization reaction (**3.9b**-**3.11b**). As expected, carbamimidate **3.10** is easily converted to the corresponding azepine. Surprisingly, though most of the azepine products are very stable,

azepine **3.9b** showed signs of degradation and reduced yields between crude NMT analysis and isolation. Carbamimidate **3.11** can also be transformed into azepine **3.11b** in a 67% yield.

3.3.4. Diversification of bicyclic azepine products

After developing a mild and efficient method for the synthesis of these bicyclic azepine scaffolds, we were interested in seeing what types of further functionalized products could be made from these precursors. As expected, azepine 3.1b could be completely hydrogenated under standard conditions to form **3.12**, which could subsequently be hydrolyzed to form amino alcohol **3.13**. Other known chemistry such as the deprotection of the sulfamate protecting group also proceeded smoothly to form **3.14** in quantitative yield.[17]

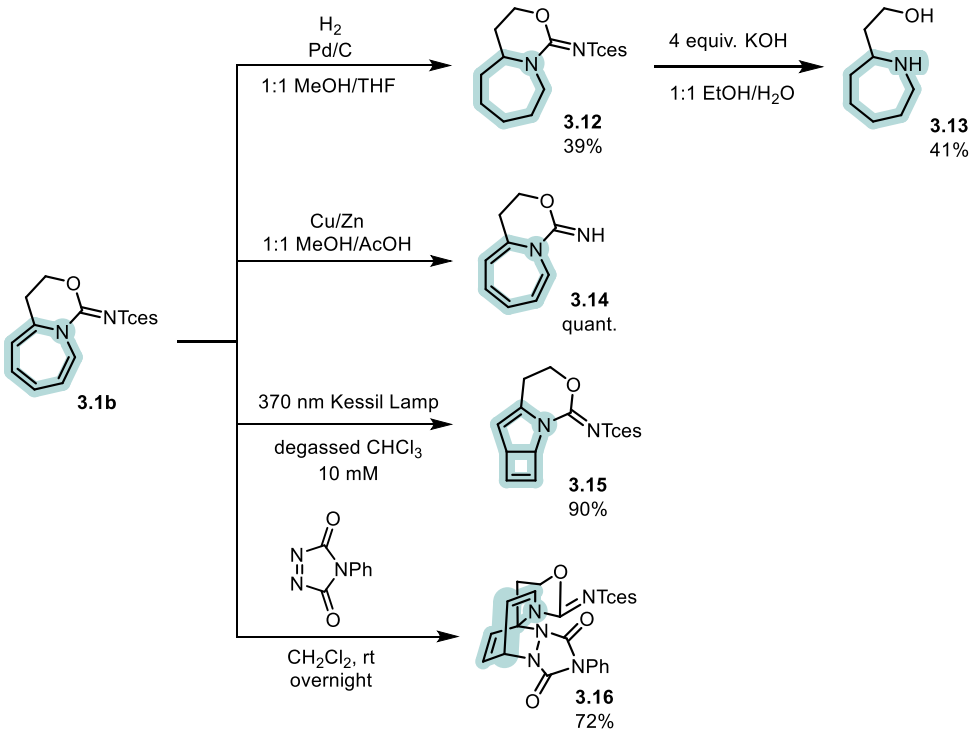

Scheme 3.4 – Successful diversification reactions of azepine **3.1b**.

Conjugated systems such as the one in azepine **3.1b** are also known for undergoing various cycloaddition reactions. In our case, a photoinduced [2+2] cyclization reaction resulted

in quick and clean formation of tricycle **3.15** in 90% yield.[18] Notably, similar bicyclic pyrrolidines have been proposed as potential bio isosteres for piperidines.[19] Finally, compound **3.1b** can also be converted into a complex bridging tricycle via a hetero-Diels-Alder [4+2] cycloaddition.[20]

3.3. Conclusions

In conclusion, we have developed a highly chemoselective reaction capable of selecting for either C–H insertion or for dearomatization by simply changing the ligand identity. We have demonstrated that bidentate ligands with steric bulking pointing into the reaction site prefer to undergo dearomatization, while unhindered ligands allow for facile C–H insertion. Electronic factors play a part in selectivity, but they are not the key to controlling it. The reaction is applicable to a wide range of substrates, however, substrates that are strongly electron-withdrawing or electron-donating are resistant to catalyst control and often undergo undesired reactivity. Still, interesting azepine products have been shown being brought forward to synthesize amino alcohol derivatives, along with bridging and fused tricycles.

Much work is left to be done on this project. From investigating bicyclic and heteroaromatic substrates, the true limits of this reaction have yet to be tested. Additionally, further work needs to be done to diversify these interesting products, including further investigations into manipulating individual alkenes in the unsaturated ring such as semi-reductions and alkene functionalizations. Ultimately, once we have completed these last experiments, we will have shown that *N*-dentate silver complexes are mild and highly selective catalyst for challenging selectivity problems such as dearomative aziridination versus C(sp3)–H insertion.

3.4. References

1. Vitaku, E.; Smith, D. T.; Njardarson, J. T. Analysis of the Structural Diversity, Substitution Patterns, and Frequency of Nitrogen Heterocycles among U.S. FDA Approved Pharmaceuticals. *J. Med. Chem.* **2014**, *57*, 10257–10274.
2. Reekie, T. A.; Kavanagh, M. E.; Longworth, M.; Kassiou, M. Synthesis of biologically active seven membered ring heterocycles. *Synthesis* **2013**, *45*, 3211–3227.
3. (a) Fukuda, H.; Ito, S.; Watari, K.; Mogi, C.; Arisawa, M.; Okajima, F.; Kurose, H.; Shuto, S. Identification of a potent and selective GPR4 antagonist as a drug lead for the treatment of myocardial infarction. *ACS Med. Chem. Lett.* **2016**, *7*, 493-497. (b) Nemerovski, C.; Hutchinson, D. J. Treatment of Hypervolemic or Euvolemic Hyponatremia Associated with Heart Failure, Cirrhosis, or the Syndrome of Inappropriate Antidiuretic Hormone with Tolvaptan: A Clinical Review. *Clin. Ther.* **2010**, *32*, 1015–1032. (c) Liu, X.; Wang, P.; Yu, S.; Wu, L. Eleclazine, a novel and selective late sodium current inhibitor, suppresses ventricular arrhythmias induced by acute global low-flow ischemia. *Circulation*. **2017**, *136*, A17138-A17138. (d) Messerli, F.H.; Oparil, S.; Feng, Z. Comparison of efficacy and side effects of combination therapy of angiotensin-converting enzyme inhibitor (benazepril) with calcium antagonist (either nifedipine or amlodipine) versus high-dose calcium antagonist monotherapy for systemic hypertension. *Am. J. Cardiol.* **2000**, *86*, 1182-1187.
4. (a) Haupt, E.; Köberich, W.; Beyer, J.; Schöffling, K. Pharmacodynamic aspects of tolbutamide, glibenclamide, glibornuride, and glisoxepide. II. Repeated administration in combination with glucose. *Diabetologia* **1971**, *7*, 455-460. (b) Firth, R.G.; Bell, P.M.; Rizza, R.A. Effects of tolazamide and exogenous insulin on insulin action in patients with non-insulin-dependent diabetes mellitus. *N. Engl. J. Med.* **1986**, *314*, 1280-1286.

5. (a) Kastrinsky, D.B.; Sangodkar, J.; Zaware, N.; Izadmehr, S.; Dhawan, N.S.; Narla, G.; Ohlmeyer, M. Reengineered tricyclic anti-cancer agents. *Bioorg. Med. Chem.* **2015**, *23*, 6528-6534. (b) Al-Qawasmeh, R.A.; Lee, Y.; Cao, M.Y.; Gu, X.; Viau, S.; Lightfoot, J.; Wright, J.A.; Young, A.H. 11-Phenyl-[b,e]-dibenzazepine compounds: novel antitumor agents. *Bioorg. Med. Chem. Lett.* **2009**, *19*, 104-107. (c) Kim, J.E.; Song, Y.J. Anti-varicella-zoster virus activity of cephalotaxine esters in vitro. *J. Microbiol.* **2019**, *57*, 74-79.
6. Graninger, W. Pivmecillinam - Therapy of Choice for Lower Urinary Tract Infection. *Int. J. Antimicrob. Agents* **2003**, *22*, 73–78.
7. (a) Zha, G. F.; Rakesh, K. P.; Manukumar, H. M.; Shantharam, C. S.; Long, S. Pharmaceutical Significance of Azepane Based Motifs for Drug Discovery: A Critical Review. *Eur. J. Med. Chem.* **2019**, *162*, 465–494. (b) Wu, S. F.; Lee, C. J.; Liao, C. L.; Dwek, R. A.; Zitzmann, N.; Lin, Y. L. Antiviral effects of an iminosugar derivative on flavivirus infections. *J. Virol.* **2002**, *76*, 3596–3604. (c) Block, T. M.; Jordan, R. Imino sugars as possible broad spectrum anti hepatitis virus agents: the alkovirs and glucovirs. *Antiviral Chem. Chemother.* **2002**, *12*, 317–326. (d) Greimel, P.; Spreitz, J.; Steutz, A. E. Iminosugars and relatives as antiviral and potential anti-infective agents. *Curr. Top. Med. Chem.* **2003**, *3*, 513–523.
8. For select reviews, see: (a) Kaur, M.; Garg, S.; Malhi, D. S.; Sohal, H. S. A Review on Synthesis, Reactions and Biological Properties of Seven Membered Heterocyclic Compounds: Azepine, Azepane, Azepinone. *Curr. Org. Chem.* **2021**, *25*, 449–506. (b) Chiacchio, M. A.; Legnani, L.; Chiacchio, U.; Lannazzo, D. Recent Advances on the Synthesis of Azepane-Based Compounds. *More Synth. Approaches to Nonaromatic Nitrogen Heterocycles, Vol. 2* **2022**, *2*, 529–558. (c) Ouyang, W.; Rao, J.; Li, Y.; Liu, X.; Huo, Y.; Chen, Q.; Li, X. Recent

Achievements in the Rhodium-Catalyzed Concise Construction of Medium N-Heterocycles, Azepines and Azocines. *Adv. Synth. Catal.* **2020**, *362*, 5576–5600.

9. (a) Dherange, B. D.; Kelly, P. Q.; Liles, J. P.; Sigman, M. S.; Levin, M. D. Carbon Atom Insertion into Pyrroles and Indoles Promoted by Chlorodiazirines. *J. Am. Chem. Soc.* **2021**, *143*, 11337–11344. (b) Patel, S. C.; Burns, N. Z. Conversion of Aryl Azides to Aminopyridines. *J. Am. Chem. Soc.* **2022**, *144*, 17797–17802. (c) Woo, J.; Christian, A. H.; Burgess, S. A.; Jiang, Y.; Mansoor, U. F.; Levin, M. D. Scaffold Hopping by Net Photochemical Carbon Deletion of Azaarenes. *Science* **2022**, *376*, 527–532. (d) Woo, J.; Stein, C.; Christian, A. H.; Levin, M. D. Carbon-to-Nitrogen Single-Atom Transmutation of Azaarenes. *Nature* **2023**, *623*, 77–82. (e) Li, G.; Lavagnino, M. N.; Ali, S. Z.; Hu, S.; Radosevich, A. T. Tandem C/N-Difunctionalization of Nitroarenes: Reductive Amination and Annulation by a Ring Expansion/Contraction Sequence. *J. Am. Chem. Soc.* **2023**, *145*, 41–46. (f) Pearson, T. J.; Shimazumi, R.; Driscoll, J. L.; Dherange, B. D.; Park, D. Il; Levin, M. D. Aromatic Nitrogen Scanning by Ipso-Selective Nitrene Internalization. *Science* **2023**, *381*, 1474–1479.
10. Reisman, S.; Nani, R.; Levin, S. Buchner and Beyond: Arene Cyclopropanation as Applied to Natural Product Total Synthesis. *Synlett* **2011**, *2011*, 2437–2442.
11. (a) Mailloux, M. J.; Fleming, G. S.; Kumta, S. S.; Beeler, A. B. Unified Synthesis of Azepines by Visible-Light-Mediated Dearomative Ring Expansion of Aromatic N-Ylides. *Org. Lett.* **2021**, *23*, 525–529. (b) Mamontov, A.; Chang, L.; Dossmann, H.; Bertrand, B.; Dechoux, L.; Thorimbert, S. Iron Catalyzed Dearomatization of Pyridines into Annelated Azepine Derivatives in a One-Step, Three-Component Reaction. *Org. Lett.* **2023**, *25*, 256–260. (c) Jiang, X. L.; Liu, Q.; Wei, K. F.; Zhang, T. T.; Ma, G.; Zhu, X. H.; Ru, G. X.; Liu, L.;

Hu, L. R.; Shen, W. B. Copper-Catalyzed Alkyne Oxidation/Büchner-Type Ring-Expansion to Access Benzo[6,7]Azepino[2,3-b]Quinolines and Pyridine-Based Diones. *Commun. Chem.* **2023**, *6*, 1–12.

12. (a) DeGraff, B. A.; Gillespie, D. W.; Sundberg, R. J. Phenyl Nitrene. A Flash Photolytic Investigation of the Reaction with Secondary Amines. *J. Am. Chem. Soc.* **1974**, *96*, 7491–7496. (b) Sundberg, R. J.; Heintzelman, R. W. Reactivity of Aryl Nitrenes. Competition between Carbazole Formation and Internal Bond Reorganization in Biphenylnitrenes. *J. Org. Chem.* **1974**, *39*, 2546–2552. (c) Ayyangar, N. R.; Bambal, R. B.; Lugade, A. G. Pressure-Induced Synthesis of an N-Sulphony1-1H-Azepine by Sulphonyl-Nitrene Insertion into Benzene. *J. Chem. Soc. Chem. Commun.* **1981**, 790–791. (d) Meth-Cohn, O.; Patel, D.; Rhouati, S. The Intramolecular Chemistry of Benzyl and Phenethyl Azidoformates. *Tetrahedron Lett.* **1982**, *23*, 5085–5088.
13. Li, H.; Li, N.; Wu, J.; Yu, T.; Zhang, R.; Xu, L. P.; Wei, H. Rhodium-Catalyzed Intramolecular Nitrogen Atom Insertion into Arene Rings. *J. Am. Chem. Soc.* **2023**, *145*, 17570–17576.
14. (a) Rigoli, J. W.; Weatherly, C. D.; Alderson, J. M.; Vo, B. T.; Schomaker, J. M. Tunable, Chemoselective Amination via Silver Catalysis. *J. Am. Chem. Soc.* **2013**, *135*, 17238–17241. (b) Weatherly, C.; Alderson, J. M.; Berry, J. F.; Hein, J. E.; Schomaker, J. M. Catalyst-Controlled Nitrene Transfer by Tuning Metal:Ligand Ratios: Insight into the Mechanisms of Chemoselectivity. *Organometallics* **2017**, *36*, 1649–1661. (c) Alderson, J. M.; Phelps, A. M.; Scamp, R. J.; Dolan, N. S.; Schomaker, J. M. Ligand-Controlled, Tunable Silver-Catalyzed C–H Amination. *J. Am. Chem. Soc.* **2014**, *136*, 16720–16723. (d) Huang, M.; Yang, T.; Paretsky, J. D.; Berry, J. F.; Schomaker, J. M. Inverting Steric Effects: Using “Attractive”

Noncovalent Interactions to Direct Silver-Catalyzed Nitrene Transfer. *J. Am. Chem. Soc.* **2017**, *139*, 17376–17386. (e) Ju, M.; Huang, M.; Vine, L. E.; Dehghany, M.; Roberts, J. M.; Schomaker, J. M. Tunable Catalyst-Controlled Syntheses of β- and γ-Amino Alcohols Enabled by Silver-Catalysed Nitrene Transfer. *Nat. Catal.* **2019**, *2*, 899–908.

15. Trinh, T. A.; Fu, Y.; Hu, D. B.; Zappia, S. A.; Guzei, I. A.; Liu, P.; Schomaker, J. M. Chemo- and Enantioselective Intramolecular Silver-Catalyzed Aziridinations of Carbamimidates. *Chem. Commun.* **2024**, *60*, 224–227.
16. Grelier, G.; Rey-Rodriguez, R.; Darses, B.; Retailleau, P.; Dauban, P. Catalytic Intramolecular C(sp^3)–H Amination of Carbamimidates. *European J. Org. Chem.* **2017**, *2017*, 1880–1883.
17. Clark, J. R.; Feng, K.; Sookezian, A.; White, M. C. Manganese-Catalysed Benzylic C(sp^3)–H Amination for Late-Stage Functionalization. *Nat. Chem.* **2018**, *10*, 583–591.
18. Fu, C.; Zhang, Y.; Xuan, J.; Zhu, C.; Wang, B.; Ding, H. Diastereoselective Total Synthesis of Salvileucalin C. *Org. Lett.* **2014**, *16*, 3376–3379.
19. Matador, E.; Tilby, M. J.; Saridakis, I.; Pedrón, M.; Tomczak, D.; Llaveria, J.; Atodiresei, I.; Merino, P.; Ruffoni, A.; Leonori, D. A Photochemical Strategy for the Conversion of Nitroarenes into Rigidified Pyrrolidine Analogues. *J. Am. Chem. Soc.* **2023**, *145*, 27810–27820.
20. Craig, D.; Spreadbury, S. R. J.; White, A. J. P. Synthesis and Hetero-Diels–Alder Reactions of Enantiomerically Pure Dihydro-1H-Azepines. *Chem. Commun.* **2020**, *56*, 9803–9806.

3.5. Experimental Details

3.5.1. General information

All glassware was either oven-dried overnight at 130 °C or flame-dried using a Bunsen burner. All glassware was then allowed to cool to room temperature in a desiccator filled with Drierite™ as a desiccant or under a stream of dry nitrogen prior to use. Unless otherwise specified, reagents were used as obtained from Sigma-Aldrich, Oakwood Products, Alfa Aesar, Tokyo Chemical Industry, Combi-Blocks, or Acros Organics and directly used without further purification. Tetrahydrofuran (THF) and dichloromethane (CH_2Cl_2)were passed through an alumina column before use. All other solvents were purified using accepted procedures from the sixth edition of "Purification of Laboratory Chemicals".[1] Air- and moisture-sensitive reactions were performed using standard Schlenk techniques under a nitrogen atmosphere. Analytical thin layer chromatography (TLC) was performed utilizing pre-coated silica gel 60 F_{24} plates containing a fluorescent indicator, while preparative chromatography was performed using SilicaFlash P60 silica gel (230-400 mesh) via Still's method.[2] Column chromatography was typically run using a gradient method employing mixtures of hexanes and ethyl acetate. Various stains were used to visualize reaction products, including *p*-anisaldehyde, $KMnO_4$, and ceric ammonium molybdate (CAM stain).. ^{1}H NMR and ^{13}C NMR spectra were obtained using Bruker Avance-400 (400 and 100 MHz) and Bruker Avance-500 (500 and 125 MHz) spectrometers. Chemical shifts were reported with reference to residual protiated solvent peaks (note: $CDCl_3$ referenced at δ 7.26 and 77.16 ppm, respectively). Accurate mass measurements were acquired at the University of Wisconsin-Madison using a Micromass LCT (electrospray ionization, time-of-flight analyzer or electron impact methods). The following instrumentation in the Paul Bender Chemistry Instrumentation Center was supported by: Thermo Q Exactive™ Plus by NIH 1S10 OD020022-1; Bruker Avance-500 by a generous gift from Paul J. and Margaret M. Bender; Bruker Avance-400 by NSF CHE-1048642 and the University of Wisconsin-Madison.

3.5.2. Synthesis and characterization of carbamimidate substrates

2,2,2-trichloroethyl carbamoylsulfamate was synthesized using known methods.[3]

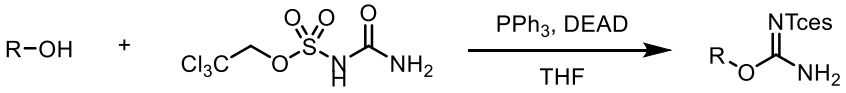

General procedure A. To a solution of alcohol (1.5 mmol, 1.0 equiv) in 8 mL dry THF was added triphenylphosphane (472.1 mg, 1.8 mmol, 1.2 equiv) and 2,2,2-trichloroethyl carbamoylsulfamate (488.7 mg, 1.8 mmol, 1.2 equiv). The mixture was cooled to 0 °C, and diethyl (E)-diazene-1,2-dicarboxylate (783.7 mg, 708.6 μL, 40 wt.%, 1.8 mmol, 1.2 equiv) was added. The reaction was warmed to room temp and stirred until complete by TLC (3-4 hours). Upon completion, the reaction was concentrated in vacuo. The combined organic layers were washed with brine, dried over $MgSO_4$, filtered, and concentrated under reduced pressure. The crude product was purified by silica gel column chromatography.

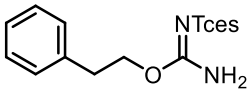

Compound 3.1. Carbamimidate **3.1** was prepared from 2-phenylethanol according to general procedure A on a 1.5 mmol scale. Purification was carried out by silica gel column chromatography (0→30% EtOAc/hexanes) to yield a white solid (393 mg, 70%); R_f = 0.45 (30% EtOAc/hexanes); ^{1}H NMR (500 MHz, $CDCl_3$) δ 7.35 – 7.29 (m, 2H), 7.28 – 7.24 (m, 1H), 7.23 – 7.18 (m, 2H), 7.02 (s, 1H), 5.47 (s, 1H), 4.64 (s, 2H), 4.48 (t, *J* = 6.9 Hz, 2H), 3.00 (t, *J* = 6.9 Hz, 2H); ^{13}C NMR (126 MHz, $CDCl_3$) δ 160.2, 136.7, 128.8, 128.7, 127.0, 93.7, 78.5, 69.4, 34.8; HRMS (ESI) m/z calcd. for $C_{11}H_{13}Cl_3N_2O_4S$ $[M+Na]^+$: 396.9554, found: 396.9546.

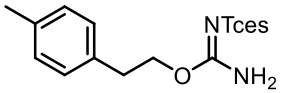

Compound 3.2. Carbamimidate **3.2** was prepared from 2-(4-methyl)ethanol according to general procedure A on a 4.0 mmol scale. Purification was carried out by silica gel column chromatography (0→30% EtOAc/hexanes) to yield a white solid (362 mg, 23%); R_f = 0.48 (30% EtOAc/hexanes); ^{1}H NMR (500 MHz, $CDCl_3$) δ 7.13 (d, *J* = 7.8 Hz, 2H), 7.09 (d, *J* = 8.2 Hz, 2H), 7.02 (s, 1H), 5.42 (s, 1H), 4.64 (s, 2H), 4.46 (t, *J* = 6.9 Hz, 2H), 2.96 (t, *J* = 6.9 Hz, 2H), 2.33 (s, 3H); ^{13}C NMR (126 MHz, $CDCl_3$) δ 160.2, 136.6, 133.6, 129.4, 128.7, 93.7, 78.5, 69.6, 34.4, 21.0; HRMS (ESI) m/z calcd. for $C_{12}H_{15}Cl_3N_2O_4S$ $[M+Na]^+$: 410.9710, found: 410.9701.

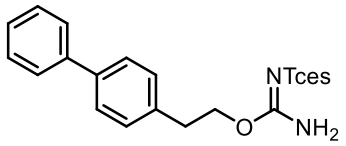

Compound 3.3. Carbamimidate **3.3** was prepared from 2-(biphenyl-4-yl)ethanol according to general procedure A on a 1.0 mmol scale. Purification was carried out by silica gel column chromatography (0→30% EtOAc/hexanes) to yield a white solid (183 mg, 40%); R_f = 0.42 (30% EtOAc/hexanes); ^{1}H NMR (500 MHz, $CDCl_3$) δ 7.64 – 7.50 (m, 4H), 7.44 (dd, *J* = 8.4, 6.9 Hz, 2H), 7.38 – 7.31 (m, 1H), 7.30 – 7.26 (m, 2H), 7.05 (s, 1H), 5.46 (s, 1H), 4.67 (s, 2H), 4.52 (t, *J* = 6.9 Hz, 2H), 3.05 (t, *J* = 6.9 Hz, 2H); ^{13}C NMR (126 MHz, $CDCl_3$) δ 160.2, 140.7, 140.0, 135.7, 129.2, 128.8, 127.4, 127.3, 127.0, 93.7, 78.5, 69.4, 34.4; HRMS (ESI) m/z calcd. for $C_{17}H_{17}Cl_3N_2O_4S$ $[M+Na]^+$: 472.9867, found: 472.9861.

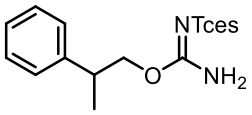

Compound 3.4. Carbamimidate **3.4** was prepared from 2-phenylpropa-1-nol according to general procedure A on a 2.0 mmol scale. Purification was carried out by silica gel column chromatography (0→30% EtOAc/hexanes) to yield a white solid (201 mg, 26%); R_f = 0.40 (30% EtOAc/hexanes); ^{1}H NMR (500 MHz, $CDCl_3$) δ 7.36 – 7.31 (m, 2H), 7.28 – 7.24 (m, 2H), 7.23 – 7.19 (m, 2H), 7.00 (s, 1H), 5.42 (s, 1H), 4.64 (s, 2H), 4.40 – 4.29 (m, 2H), 3.16 (h, *J* = 7.1 Hz, 1H), 1.32 (d, *J* = 7.0 Hz, 3H); ^{13}C NMR (126 MHz, $CDCl_3$) δ 160.3, 142.1, 128.7, 127.2, 127.1, 93.7, 78.5, 73.7, 38.8, 17.9; HRMS (ESI) m/z calcd. For $C_{12}H_{15}Cl_3N_2O_4S$ $[M+H]^+$: 388.9891, found: 388.9892.

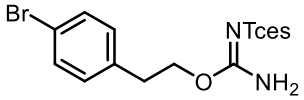

Compound 3.5. Carbamimidate **3.5** was prepared from 2-(4-bromophenyl)ethanol according to general procedure A on a 1.5 mmol scale. Purification was carried out by silica gel column chromatography (0→30% EtOAc/hexanes) to yield a white solid (192 mg, 28%); ^{1}H NMR (500 MHz, $CDCl_3$) δ 7.49 – 7.41 (m, 2H), 7.12 – 7.06 (m, 2H), 7.02 (s, 1H), 5.47 (s, 1H), 4.64 (s, 2H), 4.45 (t, *J* = 6.8 Hz, 2H), 2.96 (t, *J* = 6.8 Hz, 2H); ^{13}C NMR (126 MHz, $CDCl_3$) δ 160.1, 135.7, 131.8, 130.5, 120.9, 93.6, 78.5, 69.0, 34.2; HRMS (ESI) m/z calcd. For $C_{11}H_{12}BrCl_3N_2O_4S$ $[M+H]^+$: 452.8840, found: 452.8836.

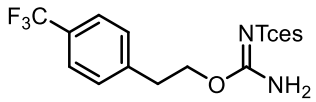

Compound 3.6. Carbamimidate **3.6** was prepared from 2-(4-(trifluoromethyl)phenyl)ethanol according to general procedure A on a 1.5 mmol scale. Purification was carried out by silica gel

column chromatography (0→30% EtOAc/hexanes) to yield a white solid (291 mg, 44%); R_f = 0.34 (30% EtOAc/hexanes); ^{1}H NMR (500 MHz, $CDCl_3$) δ 7.59 (d, *J* = 8.1 Hz, 2H), 7.33 (d, *J* = 8.0 Hz, 2H), 7.04 (s, 1H), 5.46 (s, 1H), 4.66 (s, 2H), 4.50 (t, *J* = 6.7 Hz, 2H), 3.07 (t, *J* = 6.7 Hz, 2H); ^{13}C NMR (126 MHz, $CDCl_3$) δ 160.1, 140.9, 129.41 (q, *J* = 32.6 Hz), 129.1, 125.65 (q, *J* = 3.8 Hz), 124.07 (q, *J* = 272.0 Hz), 93.6, 78.5, 68.8, 34.6; ^{19}F NMR (377 MHz, $CDCl_3$) δ -62.5; HRMS (ESI) m/z calcd. For $C_{12}H_{12}Cl_3F_3N_2O_4S$ $[M+Na]^+$: 464.9428, found: 464.9430.

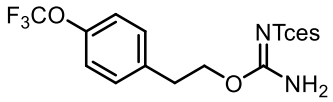

Compound 3.7. Carbamimidate **3.7** was prepared from 2-(4-(trifluoromethoxy)phenyl)ethanol according to general procedure A on a 2.0 mmol scale. Purification was carried out by silica gel column chromatography (0→30% EtOAc/hexanes) to yield a white solid (144 g, 16%); R_f = 0.39 (30% EtOAc/hexanes); ^{1}H NMR (500 MHz, $CDCl_3$) δ 7.25 – 7.20 (m, 2H), 7.20 – 7.14 (m, 2H), 7.05 (s, 1H), 5.44 (s, 1H), 4.66 (s, 2H), 4.47 (t, *J* = 6.8 Hz, 2H), 3.01 (t, *J* = 6.8 Hz, 2H); ^{13}C NMR (126 MHz, $CDCl_3$) δ 160.1, 148.22 (q, *J* = 2.0 Hz), 135.5, 130.1, 120.44 (q, *J* = 255.2 Hz), 121.3, 93.6, 78.5, 69.1, 34.1; ^{19}F NMR (377 MHz, $CDCl_3$) δ -57.9; HRMS (ESI) m/z calcd. For $C_{12}H_{12}Cl_3F_3N_2O_5S$ $[M+Na]^+$: 480.9377, found: 480.9368.

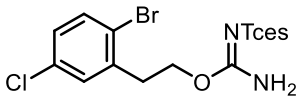

Compound 3.8. Carbamimidate **3.8** was prepared from 2-(2-bromo-5-chlorophenyl)ethanol according to general procedure A on a 1.2 mmol scale. Purification was carried out by silica gel column chromatography (0→30% EtOAc/hexanes) to yield a white solid. ^{1}H NMR (500 MHz, $CDCl_3$) δ 7.50 (d, *J* = 8.5 Hz, 1H), 7.22 (d, *J* = 2.5 Hz, 1H), 7.13 (dd, *J* = 8.5, 2.6 Hz, 1H), 7.09

(s, 1H), 5.50 (s, 1H), 4.67 (s, 2H), 4.49 (t, *J* = 6.7 Hz, 2H), 3.12 (t, *J* = 6.7 Hz, 2H); ^{13}C NMR (126 MHz, $CDCl_3$) δ 160.0, 138.0, 134.1, 133.6, 130.9, 128.9, 122.4, 93.6, 78.5, 67.4, 35.0; HRMS (ESI) m/z calcd. For $C_{11}H_{11}BrCl_4N_2O_4S$ $[M+H]^+$: 486.8450, found: 486.8447.

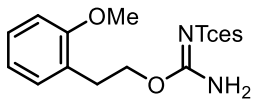

Compound 3.9. Carbamimidate **3.9** was prepared from 2-(2-methoxyphenyl)ethanol according to general procedure A on a 2.0 mmol scale. Purification was carried out by silica gel column chromatography (0→30% EtOAc/hexanes) to yield a white solid (288 mg, 36%); R_f = 0.42 (30% EtOAc/hexanes); ^{1}H NMR (500 MHz, $CDCl_3$) δ 7.27 – 7.22 (m, 1H), 7.13 (dd, *J* = 7.3, 1.7 Hz, 1H), 6.99 (s, 1H), 6.92 – 6.84 (m, 2H), 5.50 (s, 1H), 4.64 (s, 2H), 4.45 (t, *J* = 6.9 Hz, 2H), 3.84 (s, 3H), 3.01 (t, *J* = 6.9 Hz, 2H); ^{13}C NMR (126 MHz, $CDCl_3$) δ 160.4, 157.6, 130.7, 128.4, 124.9, 120.5, 110.4, 93.7, 78.5, 68.5, 55.3, 29.9; HRMS (ESI) m/z calcd. For $C_{12}H_{15}Cl_3N_2O_5S$ $[M+Na]^+$: 426.9659, found: 426.9651.

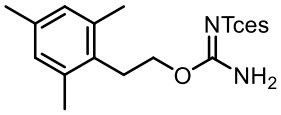

Compound 3.10. Carbamimidate **3.10** was prepared from 2-mesitylethanol according to general procedure A on a 1.5 mmol scale. Purification was carried out by silica gel column chromatography (0→30% EtOAc/hexanes) to yield a white solid (224 mg, 36%); R_f = 0.40 (30% EtOAc/hexanes); ^{1}H NMR (500 MHz, $CDCl_3$) δ 7.06 (s, 1H), 6.86 (s, 2H), 5.44 (s, 1H), 4.64 (s, 2H), 4.36 – 4.24 (m, 2H), 3.10 – 2.99 (m, 2H), 2.32 (s, 6H), 2.25 (s, 3H); ^{13}C NMR (126 MHz, $CDCl_3$) δ 160.2, 136.8, 136.4, 129.5, 129.2, 93.7, 78.4, 67.5, 28.4, 20.8, 19.9; HRMS (ESI) m/z calcd. For $C_{14}H_{19}Cl_3N_2O_4S$ $[M+Na]^+$: 439.0023, found: 439.0025.

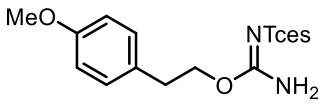

Compound 3.11. Carbamimidate **3.11** was prepared from 2-(4-methoxyphenyl)ethanol according to general procedure A on a 3.0 mmol scale. Purification was carried out by silica gel column chromatography (0→30% EtOAc/hexanes) to yield a white solid (544 mg, 45%); ^{1}H NMR (500 MHz, $CDCl_3$) δ 7.18 – 7.05 (m, 2H), 6.99 (s, 1H), 6.90 – 6.81 (m, 2H), 5.44 (s, 1H), 4.64 (s, 2H), 4.44 (t, *J* = 6.9 Hz, 2H), 3.80 (s, 3H), 2.94 (t, *J* = 6.9 Hz, 2H); ^{13}C NMR (126 MHz, $CDCl_3$) δ 160.2, 158.6, 129.8, 128.6, 114.1, 93.7, 78.5, 69.7, 55.3, 33.9; HRMS (ESI) m/z calcd. For $C_{12}H_{15}Cl_3N_2O_5S$ $[M+H]^+$: 404.9840, found: 404.9837.

3.5.3. Complete ligand screen

An example procedure for ligand optimization studies follows. An oven-dried vial equipped with a magnetic stir bar was charged with $AgNTf_2$ (7.8 mg, 20 μmol, 20 mol %), bathophen ligand (3.3 mg, 10 μmol, 10 mol %), and dry CH_2Cl_2 (2 mL). The reaction mixture was stirred vigorously for 15 min at room temperature. Powdered 4 Å molecular sieves (100 mg, 1 g of sieves/mmol of substrate) were added, followed by carbamimidate substrate (0.1 mmol, 1.0 equiv). Iodosobenzene (44 mg, 0.2 mmol, 2.0 equiv) was added in one portion and the reaction mixture was stirred at room temperature for 2 h. The mixture was filtered through a pad of silica rinsing with EtOAc, and the filtrate concentrated under reduced pressure. The yield of **3.1a** or **3.1b** was obtained by ^{1}H NMR spectroscopic analysis of the crude reaction mixture (relative to trimethylphenyl silane internal standard. For certain ligands, crude product was purified by silica gel column chromatography.

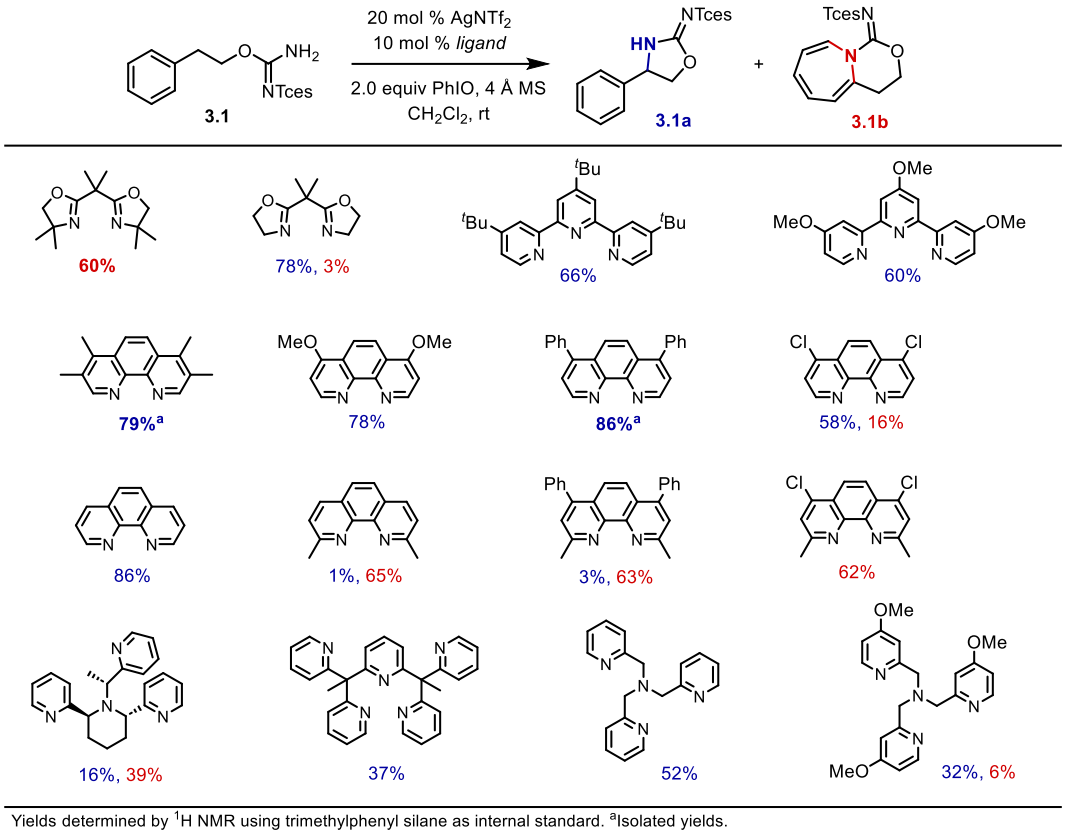

Yields determined by ^{1}H NMR using trimethylphenyl silane as internal standard. [a]Isolated yields.

Table S3.1 – *N*-dentate ligands screened for chemoselectivity with carbamimidates.

3.5.4. Selective C–H insertion of carbamimidates

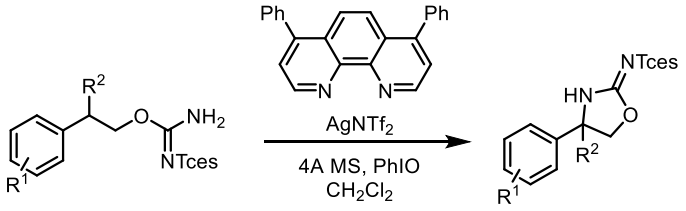

General procedure B for Ag-catalyzed C–H amination. An oven-dried vial equipped with a magnetic stir bar was charged with $AgNTf_2$ (7.8 mg, 20 μmol, 20 mol %), bathophen ligand (3.3 mg, 10 μmol, 10 mol %), and dry CH_2Cl_2 (2 mL). The reaction mixture was stirred vigorously for 15 min at room temperature. Powdered 4 Å molecular sieves (100 mg, 1 g of sieves/mmol of substrate) were added, followed by carbamimidate substrate (0.1 mmol, 1.0 equiv). Iodosobenzene (44 mg, 0.2 mmol, 2.0 equiv) was added in one portion and the reaction mixture

was stirred at room temperature for 2 h. The mixture was filtered through a pad of silica rinsing with EtOAc, and the filtrate concentrated under reduced pressure. The crude C–H amination product was purified by silica gel column chromatography.

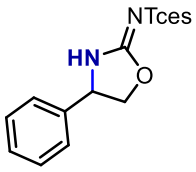

Compound 3.1a. The title compound was obtained from carbamimidate **3.1** following the general procedure B. Purification was carried out by silica gel column chromatography (0→50% EtOAc/hexanes) to yield a white solid (32.2 mg, 86%); ^{1}H NMR (500 MHz, $CDCl_3$) δ 7.63 (s, 1H), 7.50 – 7.39 (m, 3H), 7.35 – 7.29 (m, 2H), 5.20 (dd, *J* = 9.1, 7.1 Hz, 1H), 4.94 (t, *J* = 9.1 Hz, 1H), 4.76 – 4.67 (m, 2H), 4.43 (dd, *J* = 9.0, 7.1 Hz, 1H); ^{13}C NMR (126 MHz, $CDCl_3$) δ 162.9, 136.8, 129.7, 129.6, 126.2, 93.7, 78.7, 74.5, 58.8; HRMS (ESI) m/z calcd. for $C_{11}H_{11}Cl_3N_2O_4S$ $[M+H]^+$: 372.9578, found: 372.9575.

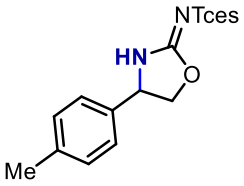

Compound 3.2a. The title compound was obtained from carbamimidate **3.2** following the general procedure B, except Me_4phen was used instead of bathophen. Purification was carried out by silica gel column chromatography (0→50% EtOAc/hexanes) to yield a white solid (30.6 mg, 79%); ^{1}H NMR (500 MHz, $CDCl_3$) δ 7.61 (s, 1H), 7.25 – 7.16 (m, 4H), 5.17 (dd, *J* = 9.1, 7.2 Hz, 1H), 4.91 (t, *J* = 9.1 Hz, 1H), 4.77 – 4.65 (m, 2H), 4.40 (dd, *J* = 9.0, 7.1 Hz, 1H), 2.37 (s, 3H); ^{13}C NMR (126 MHz, $CDCl_3$) δ 162.9, 139.8, 133.8, 130.2, 126.1, 93.7, 78.6, 74.6, 58.6, 21.2; HRMS (ESI) m/z calcd. for $C_{12}H_{13}Cl_3N_2O_4S$ $[M+H]^+$: 386.9734, found: 386.9730.

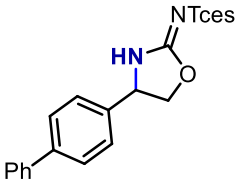

Compound 3.3a. The title compound was obtained from carbamimidate **3.3** following the general procedure B. Purification was carried out by silica gel column chromatography (0→50% EtOAc/hexanes) to yield a off-white solid (34.6 mg, 77%); ^{1}H NMR (500 MHz, $CDCl_3$) δ 7.70 – 7.63 (m, 3H), 7.60 – 7.56 (m, 2H), 7.49 – 7.44 (m, 2H), 7.42 – 7.36 (m, 3H), 5.25 (dd, *J* = 9.1, 7.1 Hz, 1H), 4.96 (t, *J* = 9.1 Hz, 1H), 4.78 – 4.66 (m, 2H), 4.47 (dd, *J* = 9.0, 7.1 Hz, 1H); ^{13}C NMR (126 MHz, $CDCl_3$) δ 162.9, 142.8, 139.8, 135.6, 129.0, 128.3, 127.9, 127.1, 126.7, 93.7, 78.7, 74.5, 58.6; HRMS (ESI) m/z calcd. for $C_{17}H_{15}Cl_3N_2O_4S$ $[M+H]^+$: 448.9891, found: 448.9889.

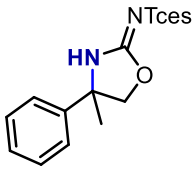

Compound 3.4a. The title compound was obtained from carbamimidate **3.4** following the general procedure B. Purification was carried out by silica gel column chromatography (0→50% EtOAc/hexanes) to yield a white solid (30.2 mg, 78%); ^{1}H NMR (500 MHz, $CDCl_3$) δ 7.79 (s, 1H), 7.47 – 7.40 (m, 2H), 7.40 – 7.31 (m, 3H), 4.75 – 4.67 (m, 2H), 4.55 (s, 2H), 1.86 (s, 3H); ^{13}C NMR (126 MHz, $CDCl_3$) δ 162.2, 141.2, 129.4, 128.8, 124.5, 93.7, 80.3, 78.6, 63.9, 26.9; HRMS (ESI) m/z calcd. for $C_{12}H_{13}Cl_3N_2O_4S$ $[M+H]^+$: 386.9734, found: 386.9731.

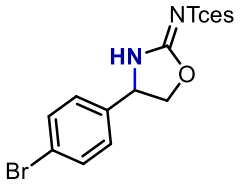

Compound 3.5a. The title compound was obtained from carbamimidate **3.5** following the general procedure B, except Me_4phen was used instead of bathophen. Purification was carried out by silica gel column chromatography (0→50% EtOAc/hexanes) to yield a white solid (31.2 mg, 69%); ^{1}H NMR (500 MHz, $CDCl_3$) δ 7.63 (s, 1H), 7.60 – 7.54 (m, 2H), 7.23 – 7.17 (m, 2H), 5.17 (dd, *J* = 9.1, 7.0 Hz, 1H), 4.93 (t, *J* = 9.1 Hz, 1H), 4.77 – 4.71 (m, 2H), 4.37 (dd, *J* = 9.1, 7.0 Hz, 1H); ^{13}C NMR (126 MHz, $CDCl_3$) δ 162.9, 135.8, 132.8, 127.8, 123.9, 99.3, 78.7, 74.2, 58.2; HRMS (ESI) m/z calcd. for $C_{11}H_{10}BrCl_3N_2O_4S$ $[M+H]^+$ 450.8683, found: 450.8682.

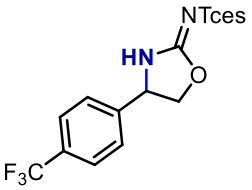

Compound 3.6a. The title compound was obtained from carbamimidate **3.6** following the general procedure B, except Me_4phen was used instead of bathophen. Purification was carried out by silica gel column chromatography (0→50% EtOAc/hexanes) to yield a white solid (27.0 mg, 61%); ^{1}H NMR (500 MHz, $CDCl_3$) δ 7.79 (s, 1H), 7.71 (d, *J* = 7.2 Hz, 2H), 7.47 (d, *J* = 8.1 Hz, 2H), 5.35 – 5.24 (m, 1H), 4.98 (t, *J* = 9.1 Hz, 1H), 4.76 – 4.60 (m, 2H), 4.40 (dd, *J* = 9.1, 6.8 Hz, 1H); ^{13}C NMR (126 MHz, $CDCl_3$) δ 162.9, 141.0, 131.95 (q, *J* = 33.2 Hz), 126.6, 123.55 (q, *J* = 272.5 Hz), 93.6, 78.7, 74.3, 58.2; ^{19}F NMR (377 MHz, $CDCl_3$) δ -62.9; HRMS (ESI) m/z calcd. for $C_{12}H_{10}Cl_3F_3N_2O_4S$ $[M+H]^+$: 440.9452, found: 440.9450.

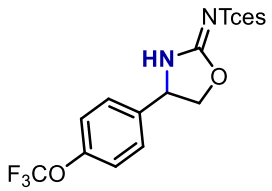

Compound 3.7a. The title compound was obtained from carbamimidate **3.7** following the general procedure B. Purification was carried out by silica gel column chromatography (0→50% EtOAc/hexanes) to yield a white solid (36.0 mg, 79%); ^{1}H NMR (500 MHz, $CDCl_3$) δ 7.73 (s, 1H), 7.41 – 7.35 (m, 2H), 7.33 – 7.27 (m, 2H), 5.32 – 5.18 (m, 1H), 4.95 (t, *J* = 9.1 Hz, 1H), 4.76 – 4.62 (m, 2H), 4.40 (dd, *J* = 9.1, 7.0 Hz, 1H); ^{13}C NMR (126 MHz, $CDCl_3$) δ 162.8, 150.0, 135.6, 127.9, 122.0, 120.3 (q, *J* = 258.2 Hz), 93.6, 78.7, 74.4, 58.1; ^{19}F NMR (377 MHz, $CDCl_3$) δ -57.9; HRMS (ESI) m/z calcd. for $C_{12}H_{10}Cl_3F_3N_2O_5S$ $[M+H]^+$: 456.9401, found: 456.9399.

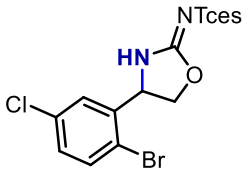

Compound 3.8a. The title compound was obtained from carbamimidate **3.8** following the general procedure B, except Me_4phen was used instead of bathophen. Purification was carried out by silica gel column chromatography (0→50% EtOAc/hexanes) to yield a white solid (38.5 mg, 79%); ^{1}H NMR (500 MHz, $CDCl_3$) δ 7.71 (s, 1H), 7.56 (d, *J* = 8.5 Hz, 1H), 7.38 (d, *J* = 2.4 Hz, 1H), 7.28 (dd, *J* = 8.5, 2.4 Hz, 1H), 5.55 (dd, *J* = 9.3, 6.2 Hz, 1H), 5.08 (t, *J* = 9.2 Hz, 1H), 4.81 – 4.68 (m, 2H), 4.36 (dd, *J* = 9.2, 6.2 Hz, 1H); ^{13}C NMR (126 MHz, $CDCl_3$) δ 163.3, 138.4, 135.1, 134.7, 131.0, 126.6, 119.5, 93.6, 78.8, 73.3, 57.5; HRMS (ESI) m/z calcd. for $C_{11}H_9BrCl_4N_2O_4S$ $[M+H]^+$: 484.8293, found: 484.8294.

3.5.5. Selective dearomative aziridination of carbamimidates

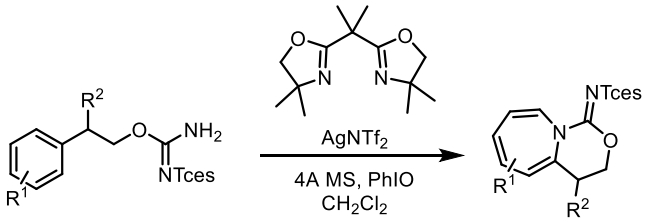

General procedure C for Ag-catalyzed dearomatization. An oven-dried vial equipped with a magnetic stir bar was charged with $AgNTf_2$ (1.9 mg, 5.0 μmol, 5 mol %), dmbox ligand (1.2 mg, 5.0 μmol, 5 mol %), and dry CH_2Cl_2 (4 mL). The reaction mixture was stirred vigorously for 15 min at room temperature. Powdered 4 Å molecular sieves (100 mg, 1 g of sieves/mmol of substrate) were added, followed by carbamimidate substrate (0.1 mmol, 1.0 equiv). Iodosobenzene (44 mg, 0.2 mmol, 2.0 equiv) was added in one portion and the reaction mixture was stirred at room temperature for 2 h. The mixture was filtered through a pad of silica rinsing with EtOAc, and the filtrate concentrated under reduced pressure. The crude azepine product was purified by silica gel column chromatography.

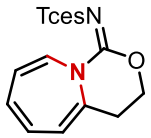

Compound 3.1b. The title compound was obtained from carbamimidate **3.1** following the general procedure C. Purification was carried out by silica gel column chromatography (0→50% EtOAc/hexanes) to yield a bright yellow solid (32.5 mg, 87%); ^{1}H NMR (500 MHz, $CDCl_3$) δ 6.07 (dd, *J* = 11.1, 5.7 Hz, 1H), 6.01 (dd, *J* = 11.3, 6.1 Hz, 1H), 5.84 (dd, *J* = 7.9, 1.0 Hz, 1H), 5.64 (dd, *J* = 8.1, 5.8 Hz, 1H), 5.52 (d, *J* = 6.1 Hz, 1H), 4.69 (s, 2H), 4.62 (t, *J* = 6.0 Hz, 2H), 2.59 (t, *J* = 5.9 Hz, 2H); ^{13}C NMR (126 MHz, $CDCl_3$) δ 151.7, 136.4, 130.2, 129.6, 127.8, 120.8, 117.2, 94.0, 78.7, 70.0, 28.6; HRMS (ESI) m/z calcd. for $C_{11}H_{13}Cl_3N_2O_4S$ $[M+H]^+$: 372.9578, found: 372.9574.

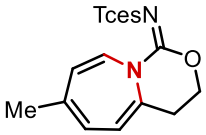

Compound 3.2b. The title compound was obtained from carbamimidate **3.2** following the general procedure C. Purification was carried out by silica gel column chromatography (0→50% EtOAc/hexanes) to yield a bright yellow solid (38.5 mg, 98%); ^{1}H NMR (500 MHz, $CDCl_3$) δ 5.86 (d, *J* = 8.1 Hz, 1H), 5.78 (dq, *J* = 6.6, 1.4 Hz, 1H), 5.50 (dd, *J* = 8.2, 1.2 Hz, 1H), 5.42 (d, *J* = 6.4 Hz, 1H), 4.70 – 4.68 (m, 2H), 4.61 (t, *J* = 5.9 Hz, 2H), 2.57 (t, *J* = 5.9 Hz, 2H), 1.86 (d, *J* = 1.5 Hz, 3H); ^{13}C NMR (126 MHz, $CDCl_3$) δ 151.7, 139.6, 133.8, 126.2, 125.4, 123.9, 117.0, 94.0, 78.7, 70.2, 28.3, 23.6; HRMS (ESI) m/z calcd. for $C_{12}H_{13}Cl_3N_2O_4S$ $[M+H]^+$: 386.9734, found: 386.9731.

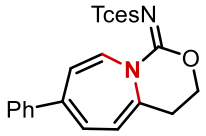

Compound 3.3b. The title compound was obtained from carbamimidate **3.3** following the general procedure C. Purification was carried out by silica gel column chromatography (0→50% EtOAc/hexanes) to yield a bright yellow solid (43.9 mg, 98%); ^{1}H NMR (500 MHz, $CDCl_3$) δ 7.42 – 7.30 (m, 5H), 6.30 (dt, *J* = 6.7, 1.1 Hz, 1H), 6.05 (dd, *J* = 8.3, 0.9 Hz, 1H), 5.92 (dd, *J* = 8.3, 1.2 Hz, 1H), 5.63 (d, *J* = 6.7 Hz, 1H), 4.72 (s, 2H), 4.65 (t, *J* = 5.9 Hz, 2H), 2.64 (t, *J* = 5.9 Hz, 2H); ^{13}C NMR (126 MHz, $CDCl_3$) δ 151.7, 141.9, 139.4, 135.7, 128.7, 128.5, 127.9, 125.8, 122.1, 116.9, 78.7, 69.9, 28.5; HRMS (ESI) m/z calcd. for $C_{17}H_{15}Cl_3N_2O_4S$ $[M+H]^+$: 448.9891, found: 448.9888.

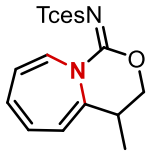

Compound 3.4b. The title compound was obtained from carbamimidate **3.4** following the general procedure C. Purification was carried out by silica gel column chromatography (0→50% EtOAc/hexanes) to yield a bright yellow solid (36.6 mg, 94%); ^{1}H NMR (500 MHz, $CDCl_3$) δ 6.09 (qd, *J* = 11.1, 5.7 Hz, 2H), 5.84 (dd, *J* = 7.9, 0.9 Hz, 1H), 5.68 (dd, *J* = 8.1, 5.7 Hz, 1H), 5.55 (d, *J* = 5.9 Hz, 1H), 4.74 – 4.64 (m, 2H), 4.60 (dd, *J* = 10.4, 4.9 Hz, 1H), 4.18 (dd, *J* = 10.5, 8.2 Hz, 1H), 2.68 (dddd, *J* = 8.3, 6.4, 5.1, 1.2 Hz, 1H), 1.22 (d, *J* = 6.7 Hz, 3H); ^{13}C NMR (126 MHz, $CDCl_3$) δ 151.9, 141.5, 130.2, 129.6, 127.8, 121.1, 114.7, 94.0, 78.7, 74.8, 32.1, 13.5; HRMS (ESI) m/z calcd. for $C_{12}H_{13}Cl_3N_2O_4S$ $[M+H]^+$: 386.9734, found: 386.9732.

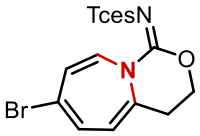

Compound 3.5b. The title compound was obtained from carbamimidate **3.5** following the general procedure C. Purification was carried out by silica gel column chromatography (0→50% EtOAc/hexanes) to yield a bright yellow solid (30.5 mg, 67%); ^{1}H NMR (500 MHz, $CDCl_3$) δ 6.40 (d, *J* = 6.7 Hz, 1H), 5.83 (d, *J* = 8.1 Hz, 1H), 5.74 (dd, *J* = 8.1, 1.1 Hz, 1H), 5.37 (d, *J* = 6.8 Hz, 1H), 4.69 (s, 2H), 4.62 (t, *J* = 5.9 Hz, 2H), 2.57 (t, *J* = 5.9 Hz, 2H); ^{13}C NMR (126 MHz, $CDCl_3$) δ 151.8, 136.6, 131.3, 128.5, 123.9, 123.5, 116.1, 93.9, 78.8, 69.9, 28.5; HRMS (ESI) m/z calcd. for $C_{11}H_{10}BrCl_3N_2O_4S$ $[M+H]^+$: 450.8683, found: 450.8682.

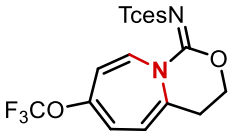

Compound 3.7b. The title compound was obtained from carbamimidate **3.7** following the general procedure C. Purification was carried out by silica gel column chromatography (0→50% EtOAc/hexanes) to yield a bright yellow solid (40.5 mg, 89%); ^{1}H NMR (500 MHz, $CDCl_3$) δ 6.01 (dd, *J* = 8.4, 3.2 Hz, 1H), 5.97 – 5.91 (m, 1H), 5.63 – 5.56 (m, 1H), 5.47 (dd, *J* = 7.3, 3.0 Hz, 1H), 4.71 – 4.66 (m, 2H), 4.64 (t, *J* = 5.9 Hz, 2H), 2.63 (t, *J* = 6.0 Hz, 2H); ^{13}C NMR (126 MHz, $CDCl_3$) δ 151.7, 148.0, 136.5, 129.8, 120.2 (q, *J* = 259.1 Hz), 118.4, 117.4, 113.5, 93.8, 78.8, 69.9, 28.5; ^{19}F NMR (377 MHz, $CDCl_3$) δ -57.6; HRMS (ESI) m/z calcd. for $C_{12}H_{10}Cl_3F_3N_2O_4S$ $[M+H]^+$: 456.9401, found: 956.9400.

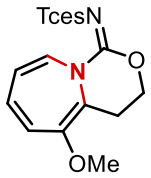

Compound 3.9b. The title compound was obtained from carbamimidate **3.9** following the general procedure C. Purification was carried out by silica gel column chromatography (0→50% EtOAc/hexanes) to yield a bright yellow solid (25.3 mg, 63%); ^{1}H NMR (500 MHz, $CDCl_3$) δ 6.19 (dd, *J* = 11.1, 6.1 Hz, 1H), 5.99 (dd, *J* = 11.1, 6.0 Hz, 1H), 5.78 (dd, *J* = 6.1, 1.3 Hz, 1H), 5.16 (d, *J* = 6.1 Hz, 1H), 4.84 (ddd, *J* = 10.6, 6.8, 1.5 Hz, 1H), 4.68 (d, *J* = 1.7 Hz, 2H), 4.52 (ddd, *J* = 12.2, 10.6, 5.4 Hz, 1H), 3.71 (s, 3H), 2.76 (ddd, *J* = 13.8, 5.4, 1.5 Hz, 1H), 2.68 (td, *J* = 13.0, 6.7 Hz, 1H); ^{13}C NMR (126 MHz, $CDCl_3$) δ 151.9, 142.6, 132.7, 128.4, 124.0, 118.6, 95.4, 94.0, 78.7, 71.0, 57.3, 28.9; HRMS (ESI) m/z calcd. for $C_{12}H_{13}Cl_3N_2O_5S$ $[M+H]^+$: 402.9684, found: 402.9680.

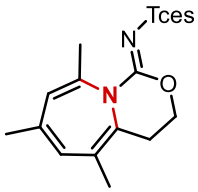

Compound 3.10b. The title compound was obtained from carbamimidate **3.10** following the general procedure C. Purification was carried out by silica gel column chromatography (0→50% EtOAc/hexanes) to yield a light yellow solid (37.5 mg, 90%); ^{1}H NMR (500 MHz, $CDCl_3$) δ 5.90 (s, 1H), 5.69 (s, 1H), 4.79 (ddd, *J* = 10.5, 6.7, 1.4 Hz, 1H), 4.71 – 4.61 (m, 2H), 4.42 (ddd, *J* = 12.5, 10.5, 5.2 Hz, 1H), 2.96 (ddd, *J* = 14.1, 5.2, 1.4 Hz, 1H), 2.40 (td, *J* = 13.3, 6.7 Hz, 1H), 2.12 (s, 3H), 1.90 (s, 3H), 1.81 (s, 3H); ^{13}C NMR (126 MHz, $CDCl_3$) δ 152.4, 137.9, 132.9, 129.9, 126.4, 126.3, 125.9, 94.2, 78.5, 70.7, 26.7, 23.6, 19.3, 17.7; HRMS (ESI) m/z calcd. for $C_{14}H_{17}Cl_3N_2O_4S$ $[M+H]^+$: 415.0047, found: 415.0048.

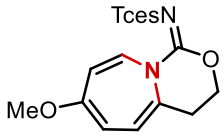

Compound 3.11b. The title compound was obtained from carbamimidate **3.11** following the general procedure C. The yield was determined by ^{1}H NMR using trimethylphenyl silane as the internal standard: (67%); ^{1}H NMR (500 MHz, $CDCl_3$) δ 6.06 (d, *J* = 8.5 Hz, 1H), 5.52 (dd, *J* = 8.5, 2.0 Hz, 1H), 5.44 (d, *J* = 7.2 Hz, 1H), 5.08 (dd, *J* = 7.3, 2.0 Hz, 1H), 4.69 (s, 2H), 4.61 (t, *J* = 5.9 Hz, 2H), 3.59 (s, 3H), 2.58 (t, *J* = 5.9 Hz, 2H); ^{13}C NMR (126 MHz, $CDCl_3$) δ 158.4, 151.7, 129.4, 128.4, 118.9, 115.6, 99.0, 94.0, 78.7, 70.5, 54.9, 28.3; HRMS (ESI) m/z calcd. for $C_{12}H_{13}Cl_3N_2O_5S$ $[M+H]^+$: 402.9684, found: 402.9682.

3.5.6. Other results from challenging substrates

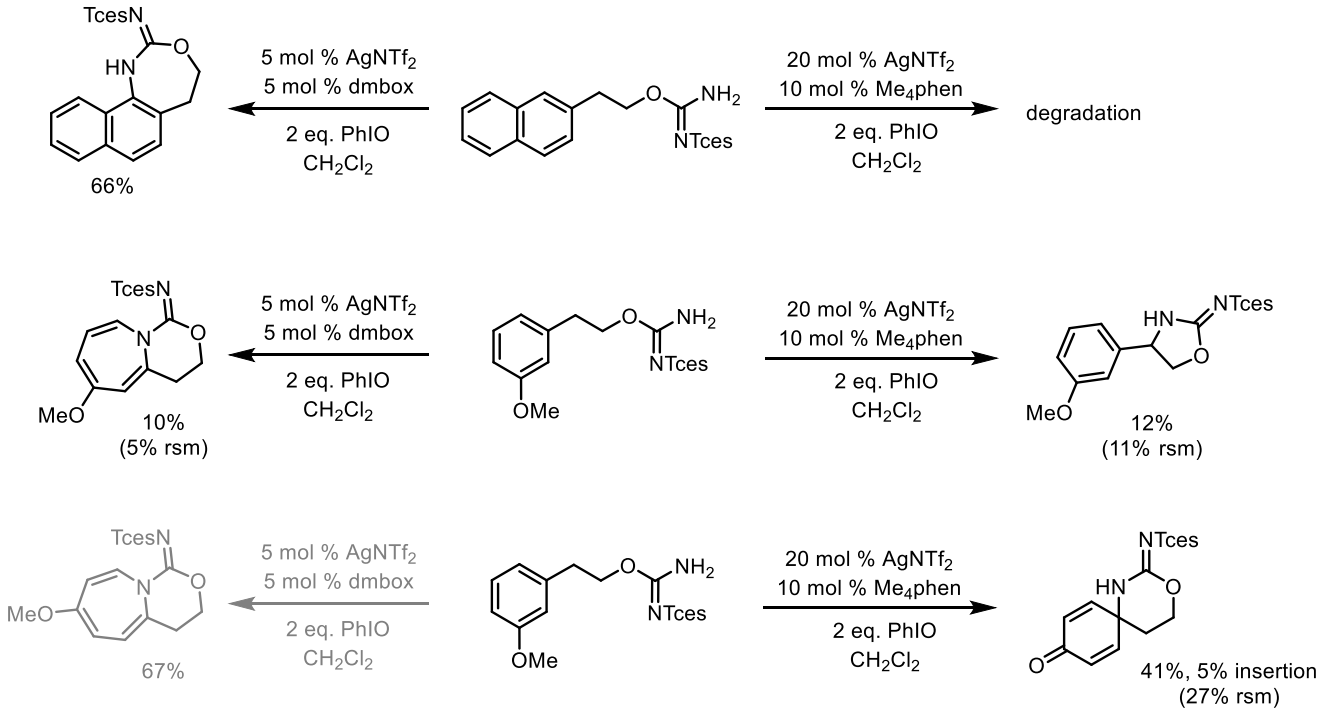

Scheme S3.1 – Example substrates that were not amenable to optimization.

Various substrates that were tested under the optimized reaction conditions did not produce the desired products (Scheme S3.1). Significant efforts were made to achieve desired reactivity, including changing the ligand identity, temperature, reaction time, amount of oxidant, and oxidant identity. None of the attempted optimizations were successful in manipulating the reaction to produce the desired product. The majority of substrates that were unsuccessful in achieving C–H insertion suffered from oxidative degradation. In many cases, this was exemplified by poor mass balance and a messy crude NMR. Sometimes other oxidative by-products could be observed in appreciable amounts, though these were often unstable under the reaction conditions. Another interesting result was detected while attempting to form the azepine product using 2-naphthylethanol-derived carbamimidate. With this substrate, all reactions with ligands that would typically produce azepine instead led to the C(sp^2)–H insertion product. Other

problematic substrates can be found in Figure S3.1. These substrates either failed at the starting material synthesis step or the nitrene transfer step. The explanations for each substrate can be seen below.

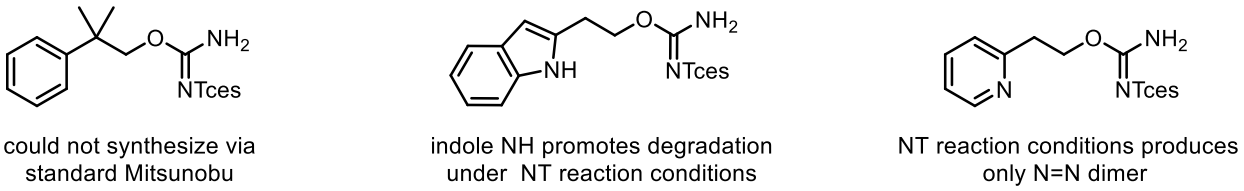

Figure S3.1 – Other substrates which produced undesired results.

3.5.7. Procedures for diversification of compound **3.1b**

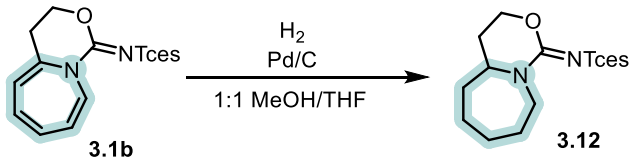

Compound 3.12. To a flame-dried round-bottom flask equipped with a magnetic stir bar was charged with **3.1b** (56.0 mg, 0.15 mmol, 1 equiv.), palladium on carbon (10 wt %, 16 mg, 0.15 mmol, 1 equiv) and 1:1 mixture of methanol/THF (1 mL). The reaction mixture was stirred at room temperature under balloon pressure of hydrogen for 2 hours. The catalyst was removed by filtration over celite, and the filter bed was washed with ethyl acetate. Purification was carried out by silica gel column chromatography (0→50% EtOAc/hexanes) to yield a white solid (22.4 mg, 39%); ^{1}H NMR (500 MHz, $CDCl_3$) δ 4.72 – 4.57 (m, 2H), 4.45 (dddd, *J* = 40.2, 11.3, 7.4, 3.8 Hz, 2H), 4.16 (ddd, *J* = 14.0, 5.0, 3.8 Hz, 1H), 3.69 (dq, *J* = 7.4, 5.4 Hz, 1H), 3.05 (ddd, *J* = 13.8, 10.8, 2.8 Hz, 1H), 2.21 – 1.49 (m, 10H); ^{13}C NMR (126 MHz, $CDCl_3$) δ 156.2, 94.4, 78.5, 65.7, 55.0, 49.6, 34.9, 27.6, 27.5, 26.2, 23.6; HRMS (ESI) m/z calcd. for $C_{11}H_{17}Cl_3N_2O_4S$ $[M+H]^+$: 379.0047, found: 379.0044.

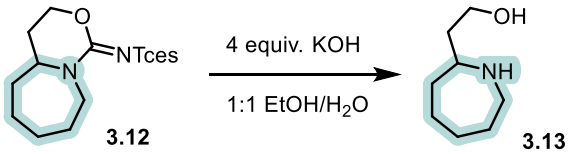

Compound 3.13. To a flame-dried round-bottom flask equipped with a magnetic stir bar was charged with **3.1b** (37.4 mg, 0.1 mmol, 1 equiv.), potassium hydroxide (22.4 mg, 0.4 mmol, 4 equiv.) in 1:1 mixture of ethanol/water (2 mL). The reaction mixture was refluxed overnight. After cooling to room temperature, the reaction mixture was extracted three times with dichloromethane, and the combined organic layer was washed with brine, dried over magnesium sulfate, filtered, and concentrated under reduced pressure. Purification was carried out by silica gel column chromatography (0→50% EtOAc/hexanes) to yield white solid (8.6 mg, 41%); ^{1}H NMR (500 MHz, $CDCl_3$) δ 4.28 (ddd, *J* = 10.5, 6.4, 3.8 Hz, 1H), 4.20 (ddd, *J* = 11.2, 8.3, 3.4 Hz, 1H), 4.06 (dt, *J* = 14.1, 4.4 Hz, 1H), 3.63 (dq, *J* = 7.8, 5.4 Hz, 1H), 2.90 (ddd, *J* = 13.9, 10.9, 2.7 Hz, 1H), 1.99 – 1.47 (m, 12H); ^{13}C NMR (126 MHz, $CDCl_3$) δ 64.2, 55.2, 47.6, 35.4, 28.8, 28.1, 27.4, 23.7.

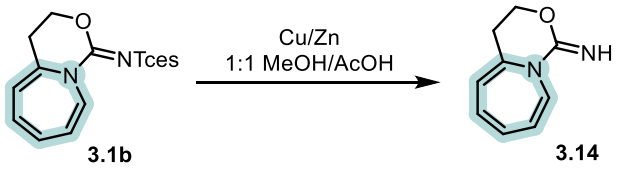

Compound 3.14. To a flame-dried round-bottom flask equipped with a magnetic stir bar was charged with **3.1b** (37.4 mg, 0.1 mmol, 1 equiv.) and zinc-copper couple (80.5 mg, 0.5 mmol, 5 equiv.) in 1:1 mixture of methanol/acetic acid (4 mL). The reaction mixture was stirred at room temperature overnight, filtered over celite, and washed thoroughly with methanol. The acetic acid was removed by azeotrope with toluene, and the crude product was purified by silica gel column chromatography (0→10% methanol/dichloromethane) to yield white solid (16.2 mg,

99.9%); ^{1}H NMR (500 MHz, Methanol-d_4) δ 5.95 (dd, J = 3.8, 2.6 Hz, 2H), 5.78 (d, J = 7.9 Hz, 1H), 5.51 – 5.39 (m, 2H), 4.43 (t, J = 6.0 Hz, 2H), 2.53 (t, J = 6.0 Hz, 2H); ^{13}C NMR (126 MHz, MeOD) δ 151.6, 140.8, 131.3, 130.6, 130.4, 120.3, 116.4, 70.3, 49.8, 29.7; HRMS (ESI) m/z calcd. for $C_9H_{10}N_2O$ $[M+H]^+$: 163.0866, found: 163.0865.

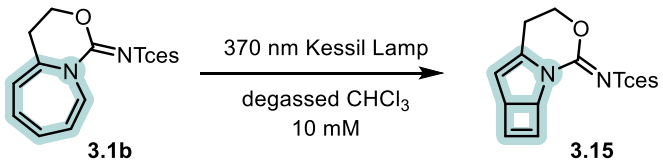

Compound 3.15. To an oven-dried Schlenk tube equipped with a magnetic stir bar was charged with **3.1b** (14.9 mg, 0.04 mmol, 1 equiv.) and degassed chloroform (10 mM, 4 mL). The reaction mixture was irradiated with 370 nm Kessel lamp at room temperature for 15 minutes. The crude product was concentrated under reduced pressure and purified by silica gel column chromatography (0→50% EtOAc/hexanes) to yield white solid (13.5 mg, 90%); ^{1}H NMR (500 MHz, $CDCl_3$) δ 6.43 (t, J = 2.2 Hz, 1H), 6.16 (d, J = 1.7 Hz, 1H), 5.30 (dt, J = 3.0, 1.6 Hz, 1H), 5.08 (dd, J = 3.8, 1.8 Hz, 1H), 4.73 – 4.64 (m, 2H), 4.54 (dt, J = 10.9, 4.8 Hz, 1H), 4.37 (ddd, J = 10.9, 8.9, 4.8 Hz, 1H), 3.90 (ddd, J = 4.0, 2.8, 1.4 Hz, 1H), 2.84 – 2.67 (m, 2H); ^{13}C NMR (126 MHz, $CDCl_3$) δ 153.1, 145.8, 135.2, 134.3, 110.8, 94.1, 78.7, 66.8, 62.3, 50.1, 23.3; HRMS (ESI) m/z calcd. for $C_{11}H_{11}Cl_3N_2O_4S$ $[M+H]^+$: 372.9578, found: 372.9574.

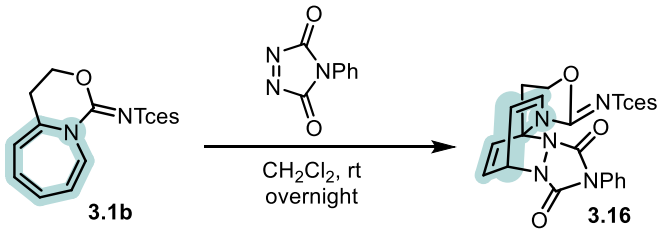

Compound 3.16. To an oven-dried vial equipped with a magnetic stir bar was charged with **3.1b** (24.0 mg, 0.064 mmol, 1 equiv.), 4-phenyl-1,2,4-triazole-3,5-dione (12.0 mg, 0.71 mmol, 1.1

equiv.) and anhydrous dichloromethane (0.17 mM, 0.38 mL). The reaction mixture was stirred at room temperature overnight. The crude product was concentrated under reduced pressure and purified by silica gel column chromatography (0→50% EtOAc/hexanes) to yield white solid (25.5 mg, 72%); ^{1}H NMR (500 MHz, $CDCl_3$) δ 7.54 – 7.35 (m, 5H), 7.12 (d, *J* = 9.6 Hz, 1H), 6.81 (dd, *J* = 8.9, 7.1 Hz, 1H), 6.01 (dd, *J* = 8.9, 1.1 Hz, 1H), 5.50 (dd, *J* = 9.7, 7.4 Hz, 1H), 5.04 – 4.97 (m, 1H), 4.95 (ddd, *J* = 11.7, 5.8, 3.8 Hz, 1H), 4.68 (s, 2H), 4.62 (ddd, *J* = 12.0, 9.5, 2.8 Hz, 1H), 3.93 (ddd, *J* = 15.0, 9.5, 3.8 Hz, 1H), 2.52 (ddd, *J* = 15.0, 5.7, 2.9 Hz, 1H); ^{13}C NMR (126 MHz, $CDCl_3$) δ 154.9, 152.2, 150.4, 131.7, 130.5, 129.3, 128.9, 128.7, 125.6, 123.9, 106.9, 93.7, 78.9, 71.8, 64.9, 48.6, 31.6; HRMS (ESI) m/z calcd. for $C_{19}H_{16}Cl_3N_5O_6S$ $[M+Na]^+$: 569.9779, found: 569.9773.

3.5.8. References

1. Armarego, W. L. F.; Chai, C. L. L. *Purification of Laboratory Chemicals*; 2013.
2. Still, W. C., Kahn, M., Mitra, A. J. Rapid chromatographic technique for preparative separations with moderate resolution. *J. Org. Chem.* **1978**, *43*, 2923–2925.
3. Kim, M.; Mulcahy, J. V.; Espino, C. G.; Du Bois, J. Expanding the Substrate Scope for C-H Amination Reactions: Oxidative Cyclization of Urea and Guanidine Derivatives. *Org. Lett.* **2006**, *8*, 1073–1076.

Appendix 1. NMR Spectra.

^{1}H NMR (500 MHz, Chloroform-*d*) and ^{13}C NMR (126 MHz, $CDCl_3$) for compound **2.5.**

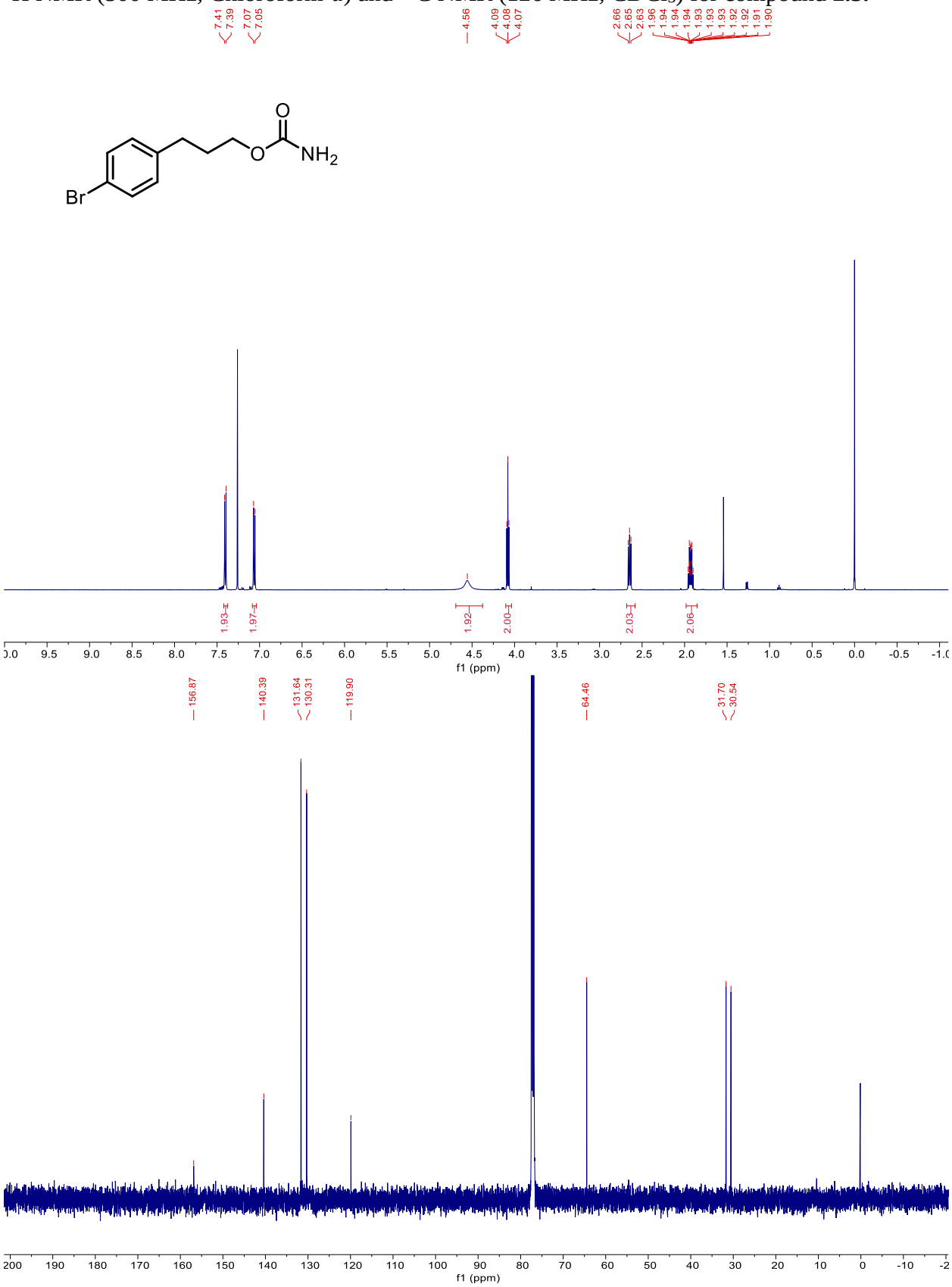

^{1}H NMR (500 MHz, Chloroform-*d*) and ^{13}C NMR (126 MHz, $CDCl_3$) for compound **2.6.**

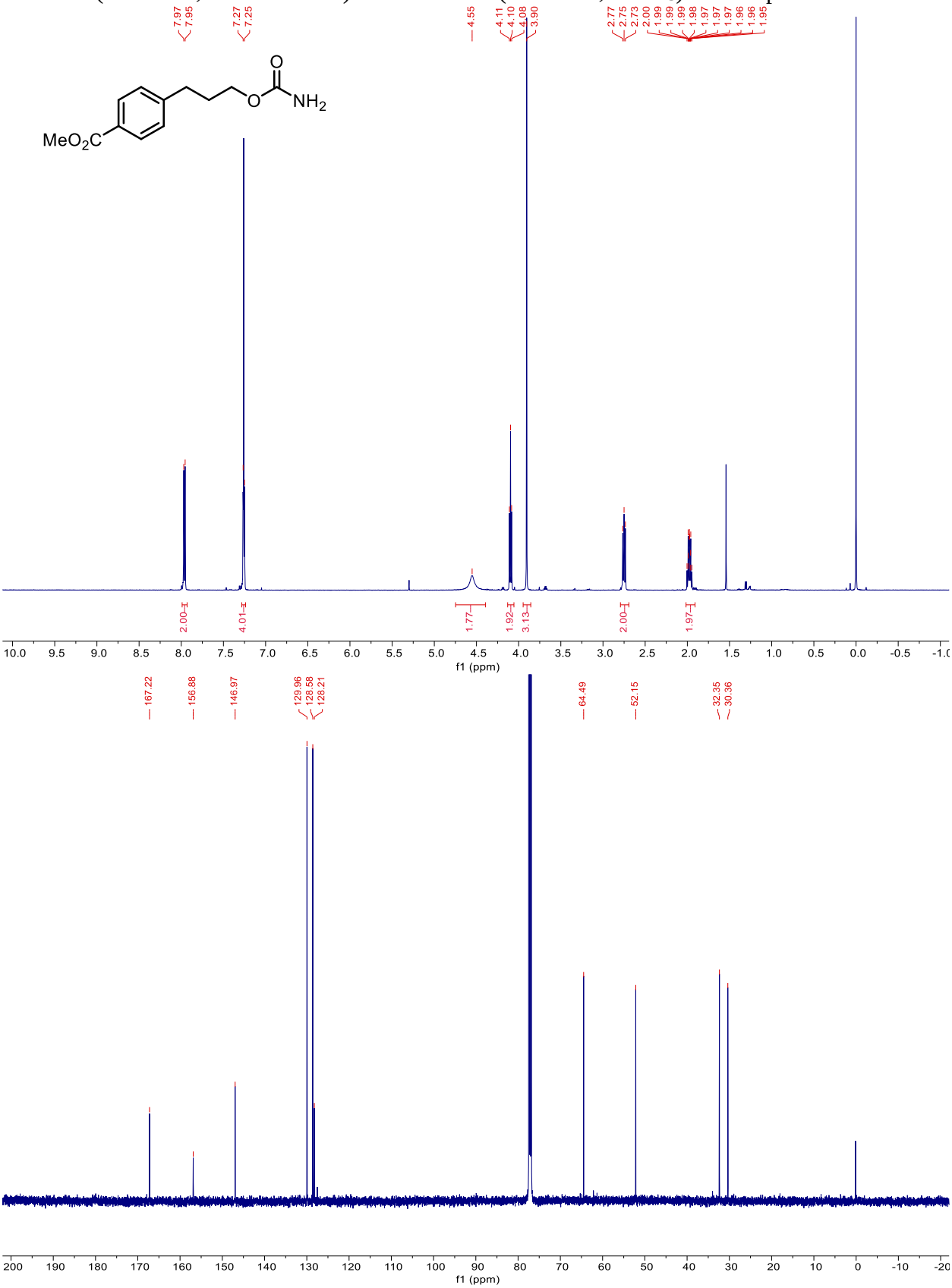

^{1}H NMR (500 MHz, Chloroform-*d*) and ^{13}C NMR (126 MHz, $CDCl_3$) for compound **2.10.**

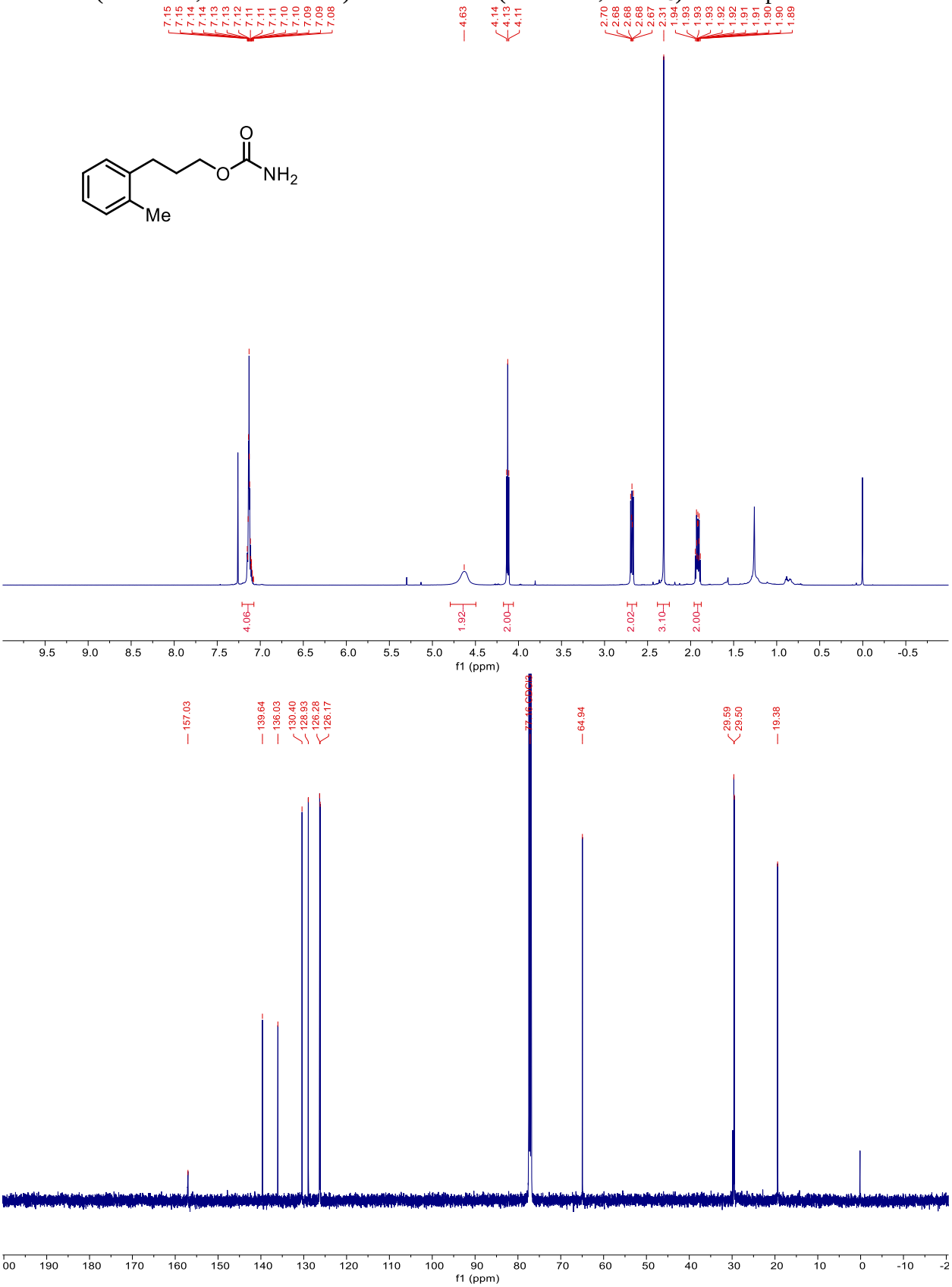

^{1}H NMR (500 MHz, Chloroform-*d*) and ^{13}C NMR (126 MHz, $CDCl_3$) for compound **2.11.**

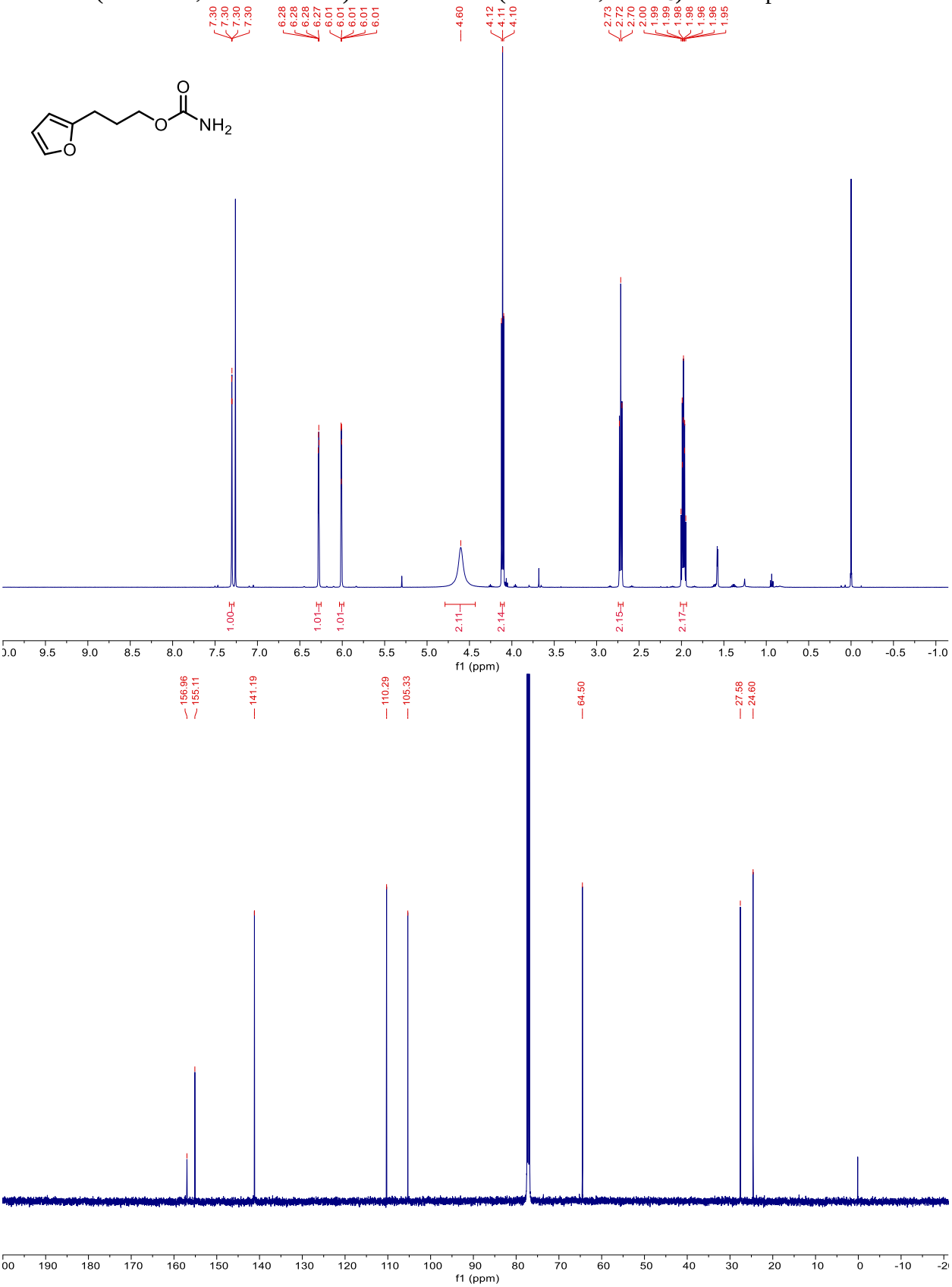

^{1}H NMR (500 MHz, Chloroform-*d*) and ^{13}C NMR (126 MHz, $CDCl_3$) for compound **2.12.**

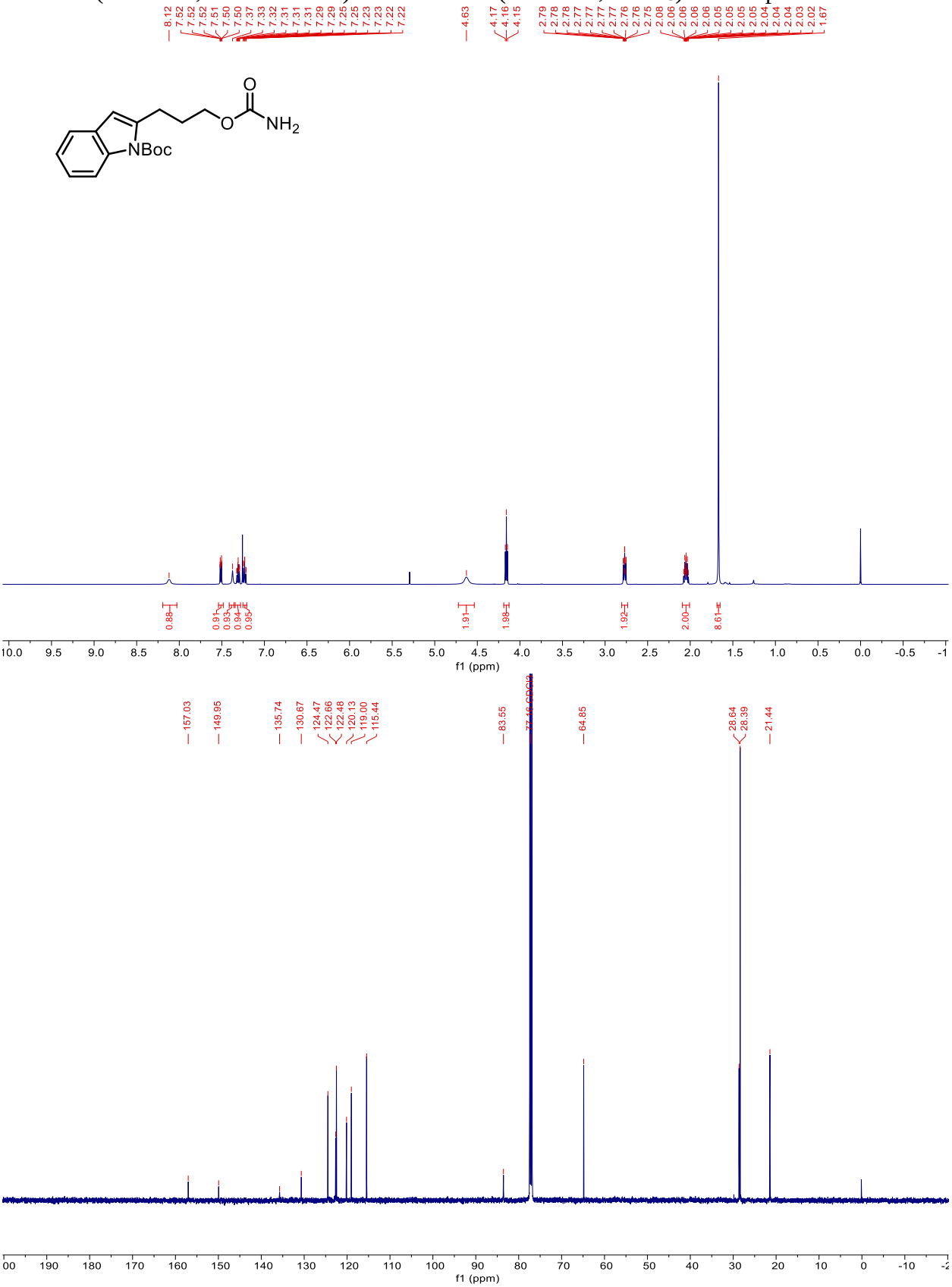

^{1}H NMR (500 MHz, Chloroform-*d*) and ^{13}C NMR (126 MHz, $CDCl_3$) for compound **2.13.**

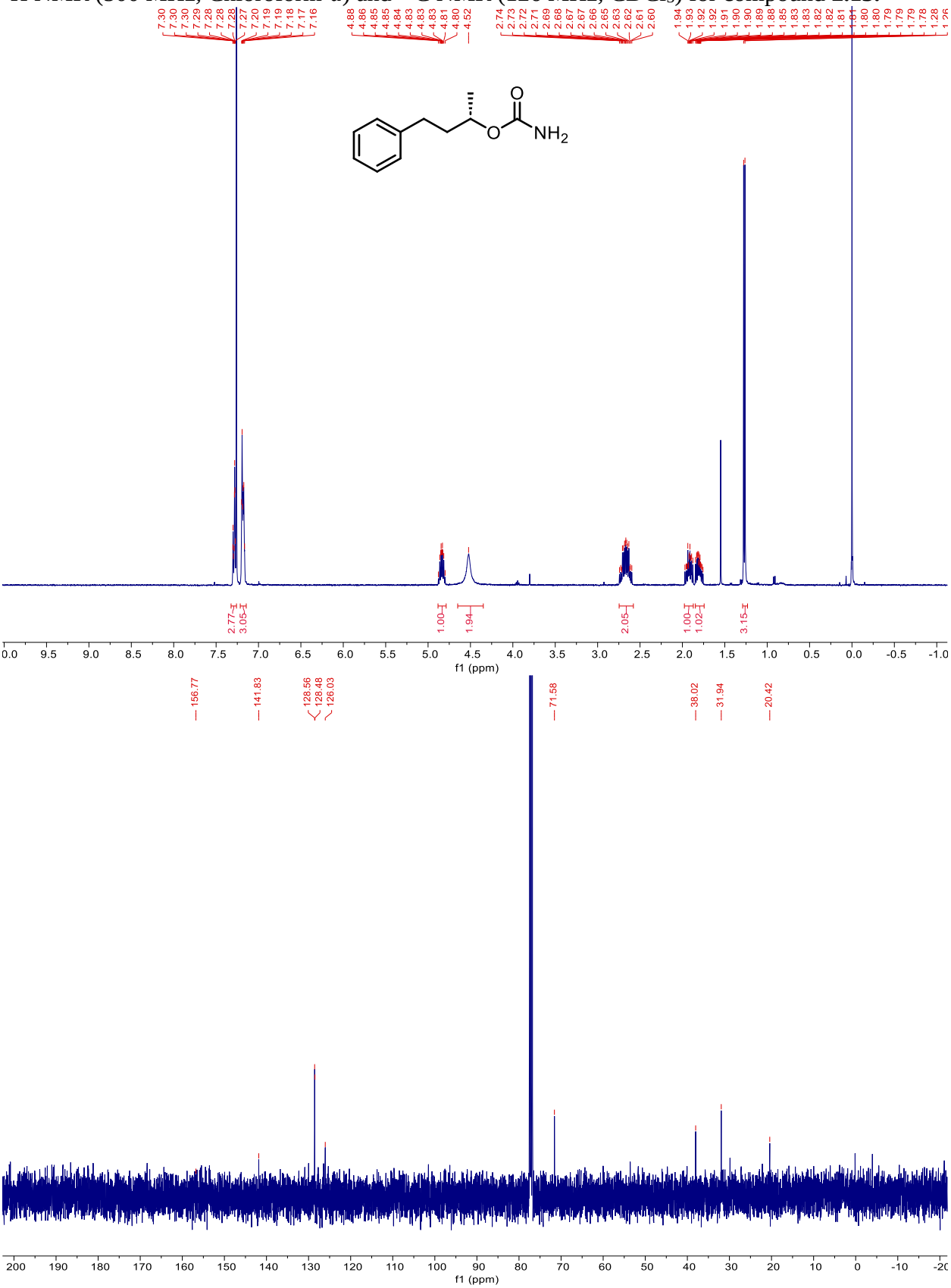

^{1}H NMR (500 MHz, Chloroform-*d*) and ^{13}C NMR (126 MHz, $CDCl_3$) for compound **2.14.**

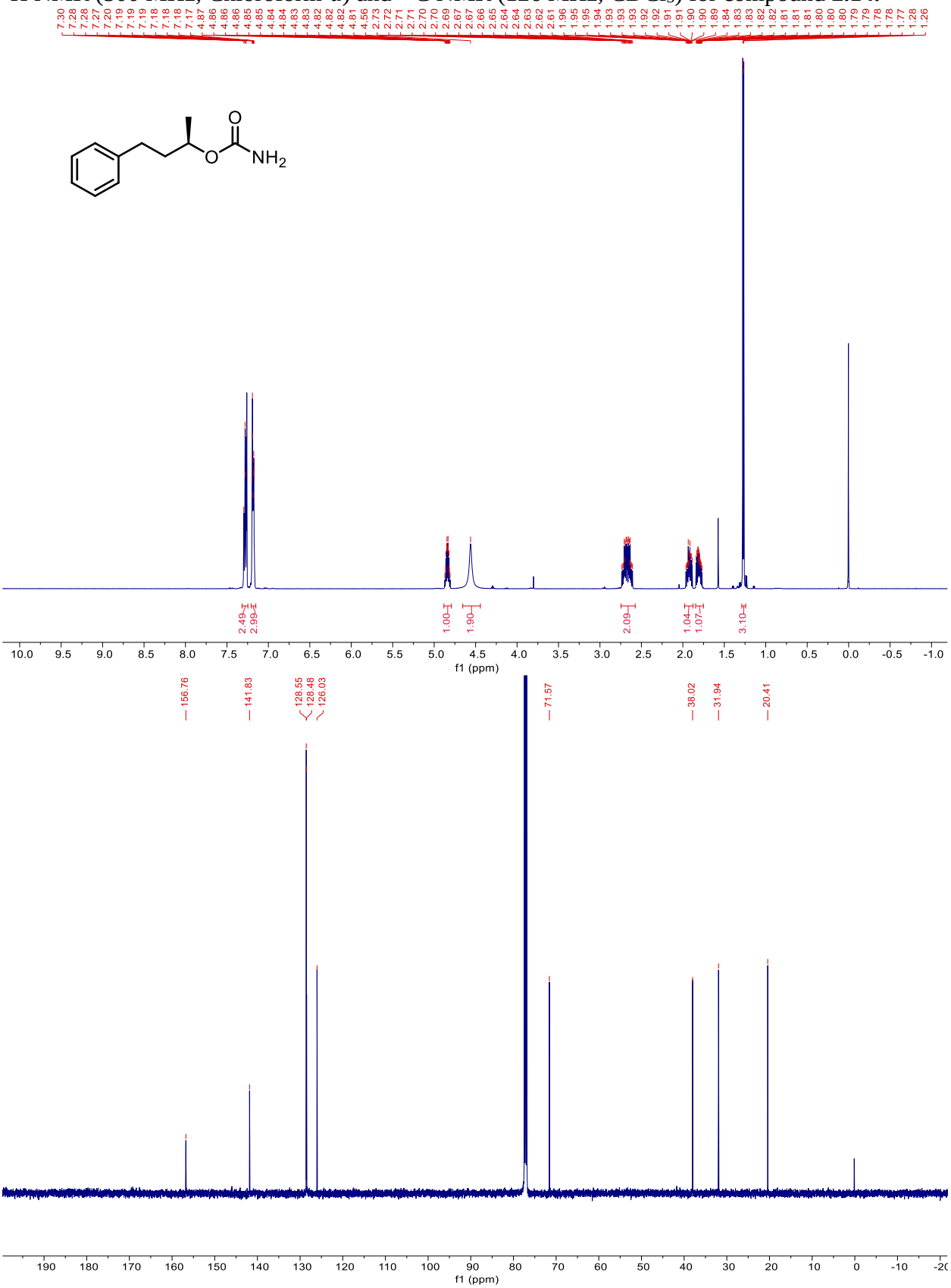

^{1}H NMR (500 MHz, Chloroform-*d*) and ^{13}C NMR (126 MHz, $CDCl_3$) for compound **2.15.**

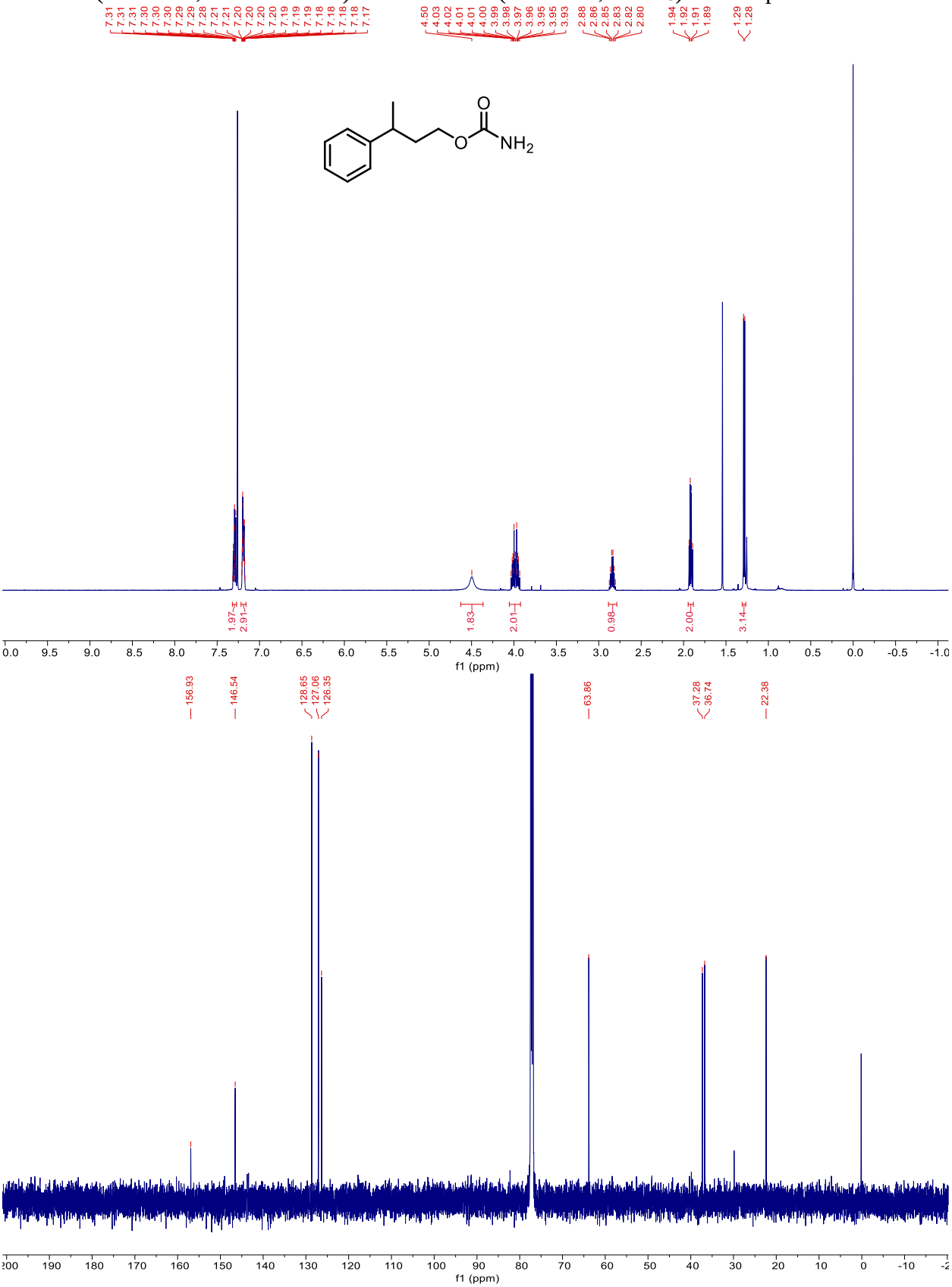

^{1}H NMR (500 MHz, Chloroform-*d*) and ^{13}C NMR (126 MHz, $CDCl_3$) for compound **2.16.**

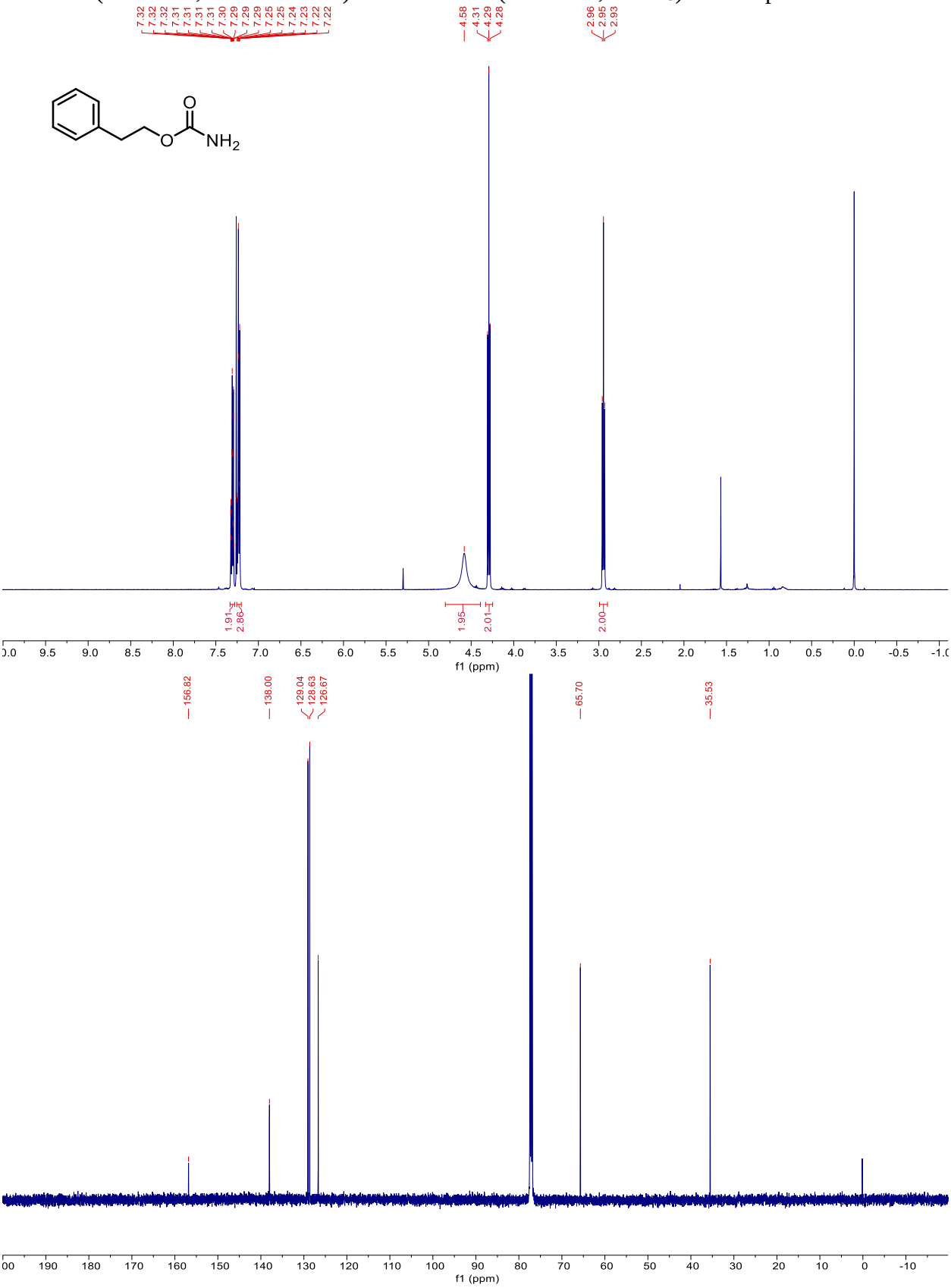

^{1}H NMR (500 MHz, Chloroform-*d*) and ^{13}C NMR (126 MHz, $CDCl_3$) for compound **2.17.**

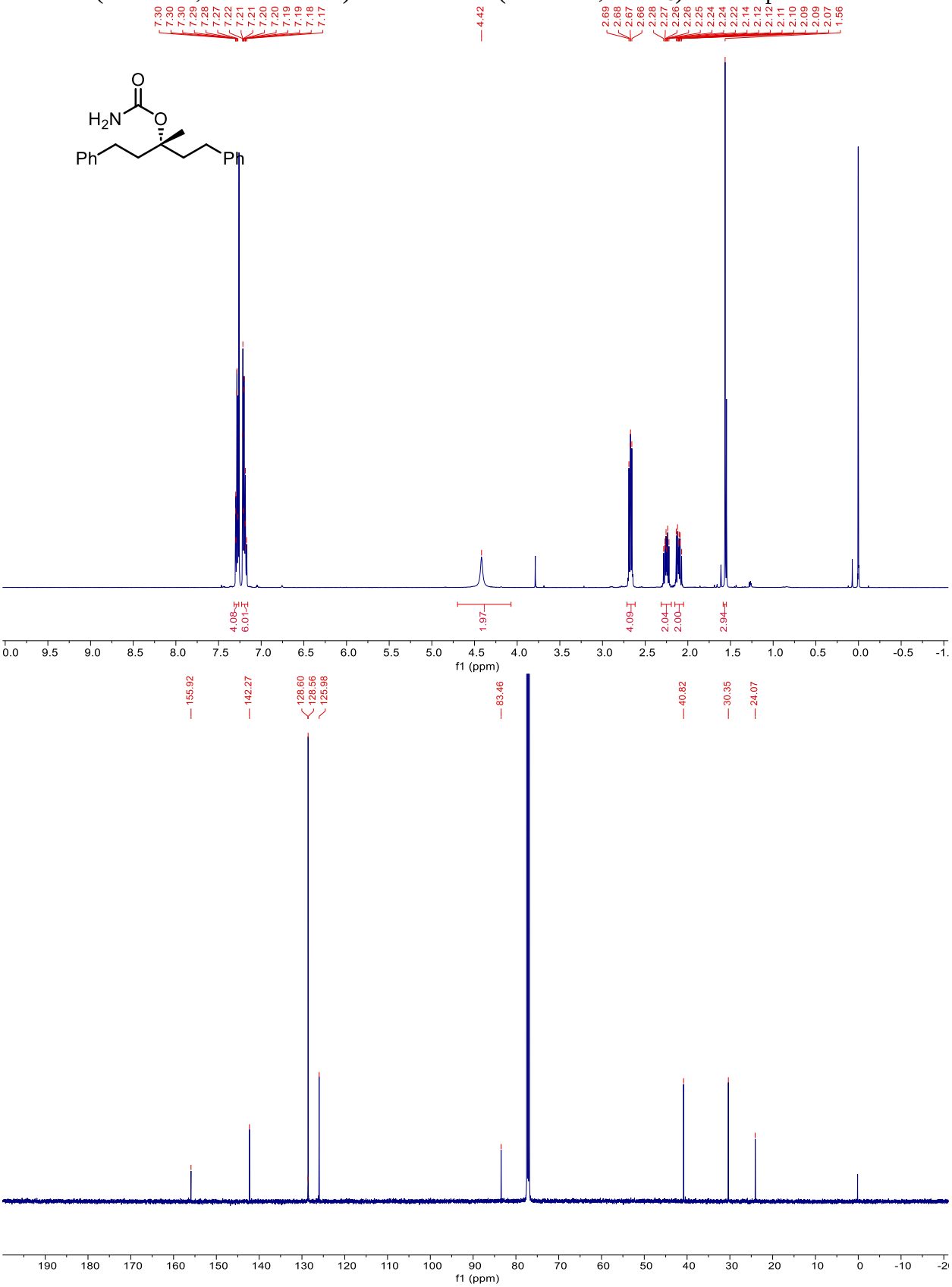

^{1}H NMR (500 MHz, Chloroform-*d*) and ^{13}C NMR (126 MHz, $CDCl_3$) for compound **2.18.**

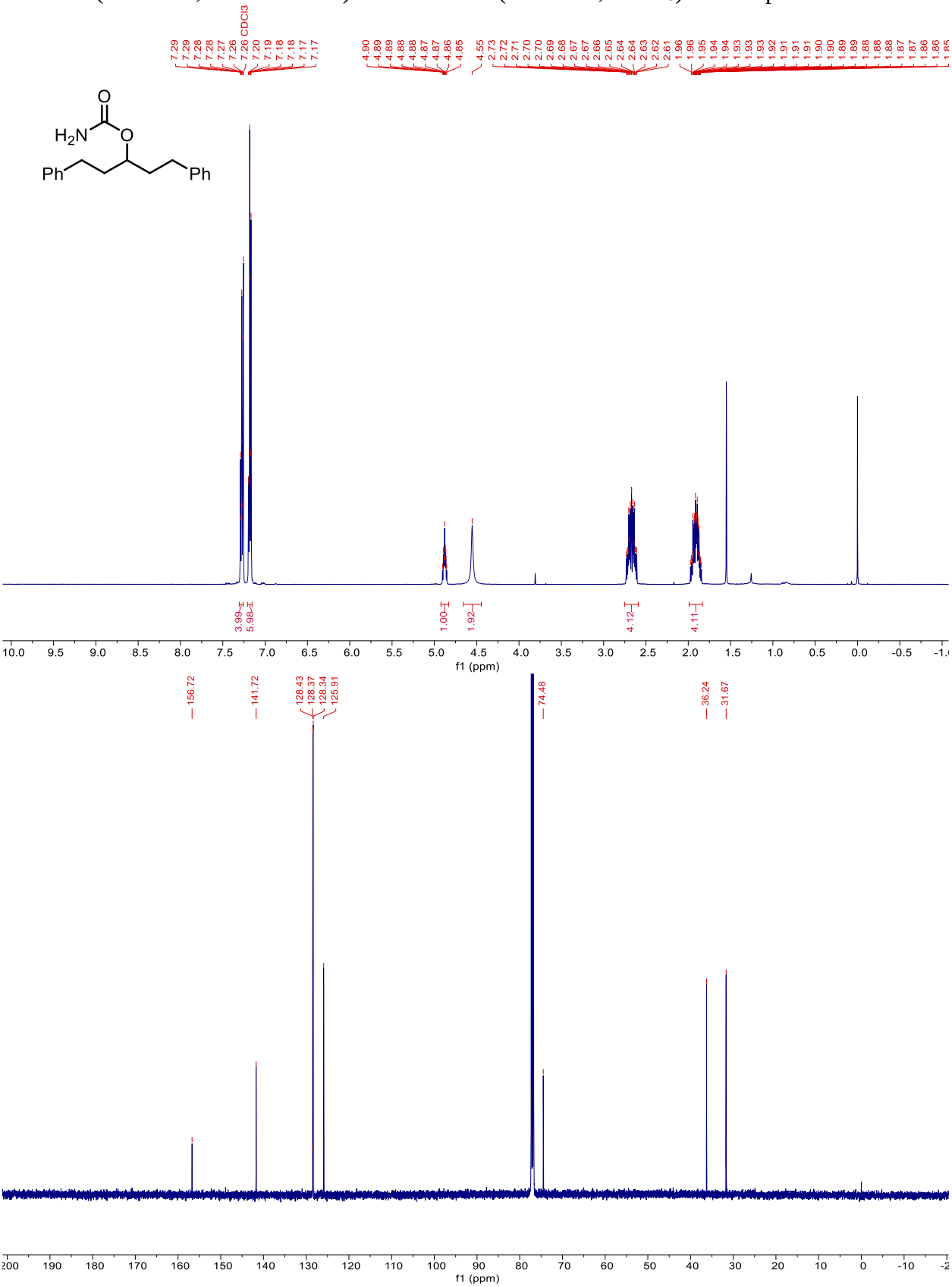

^{1}H NMR (500 MHz, Chloroform-*d*) and ^{13}C NMR (126 MHz, $CDCl_3$) for compound **2.19.**

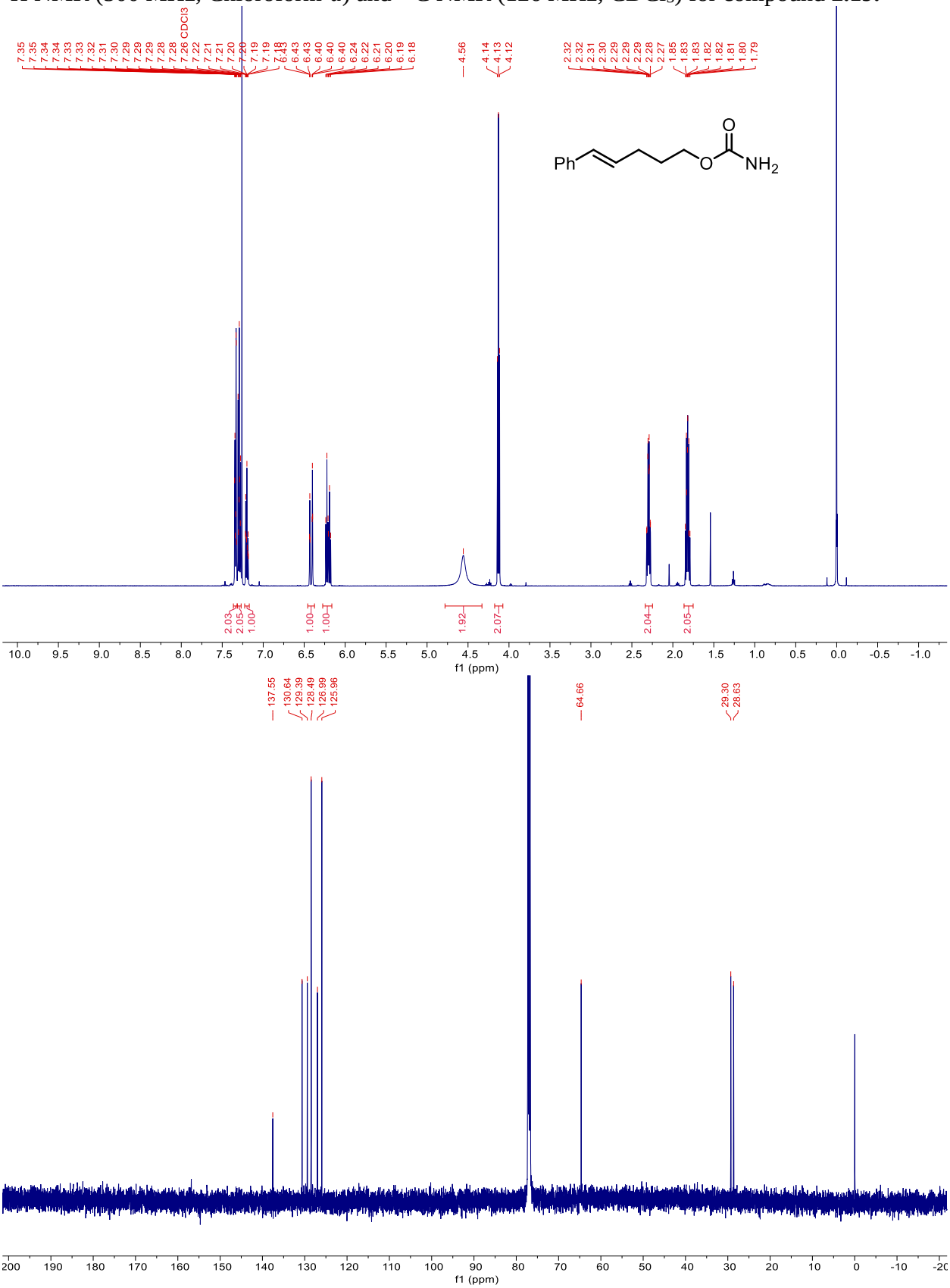

^{1}H NMR (500 MHz, Chloroform-*d*) and ^{13}C NMR (126 MHz, $CDCl_3$) for compound **2.20.**

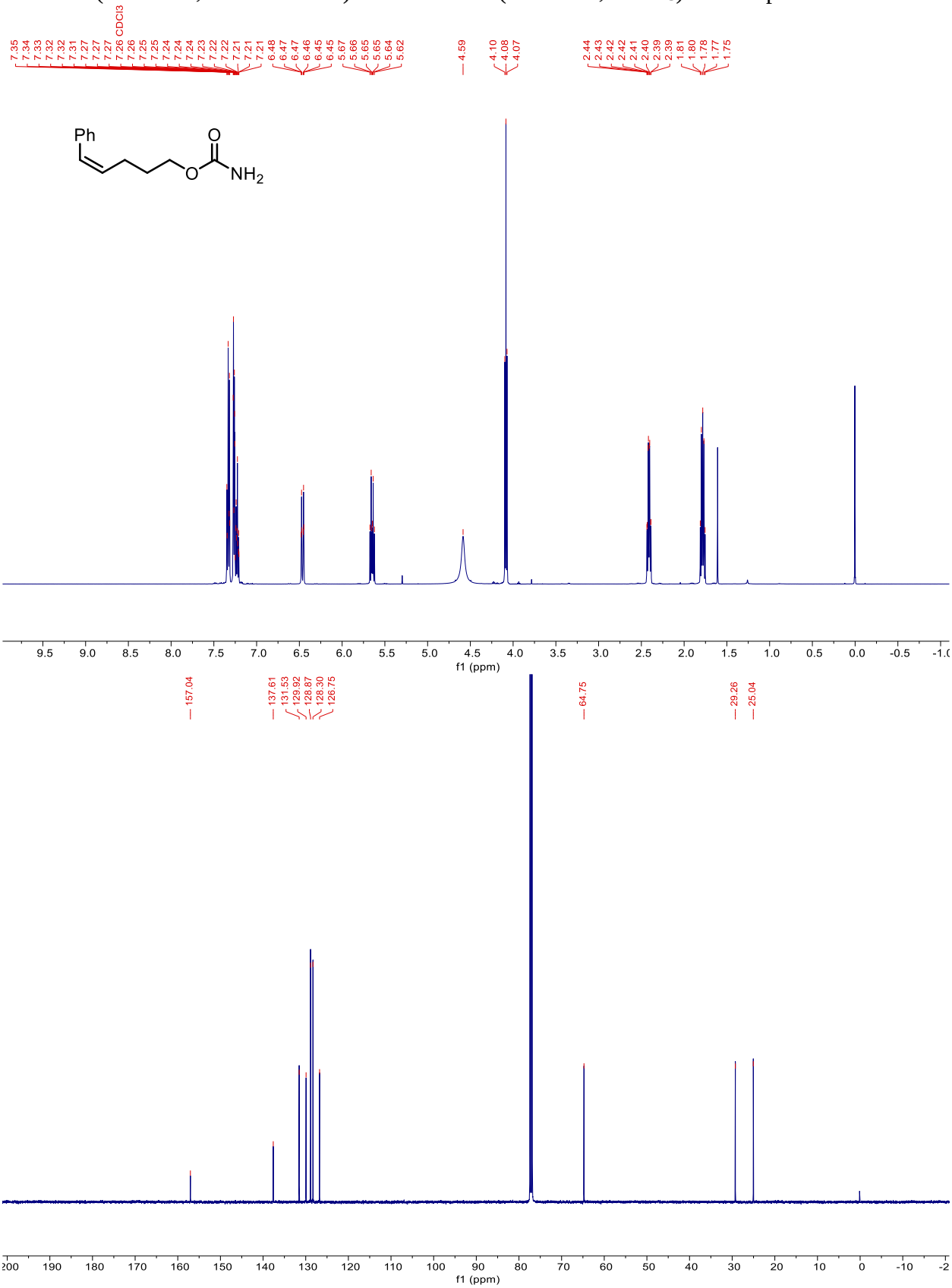

^{1}H NMR (500 MHz, Chloroform-*d*) and ^{13}C NMR (126 MHz, $CDCl_3$) for compound **2.21.**

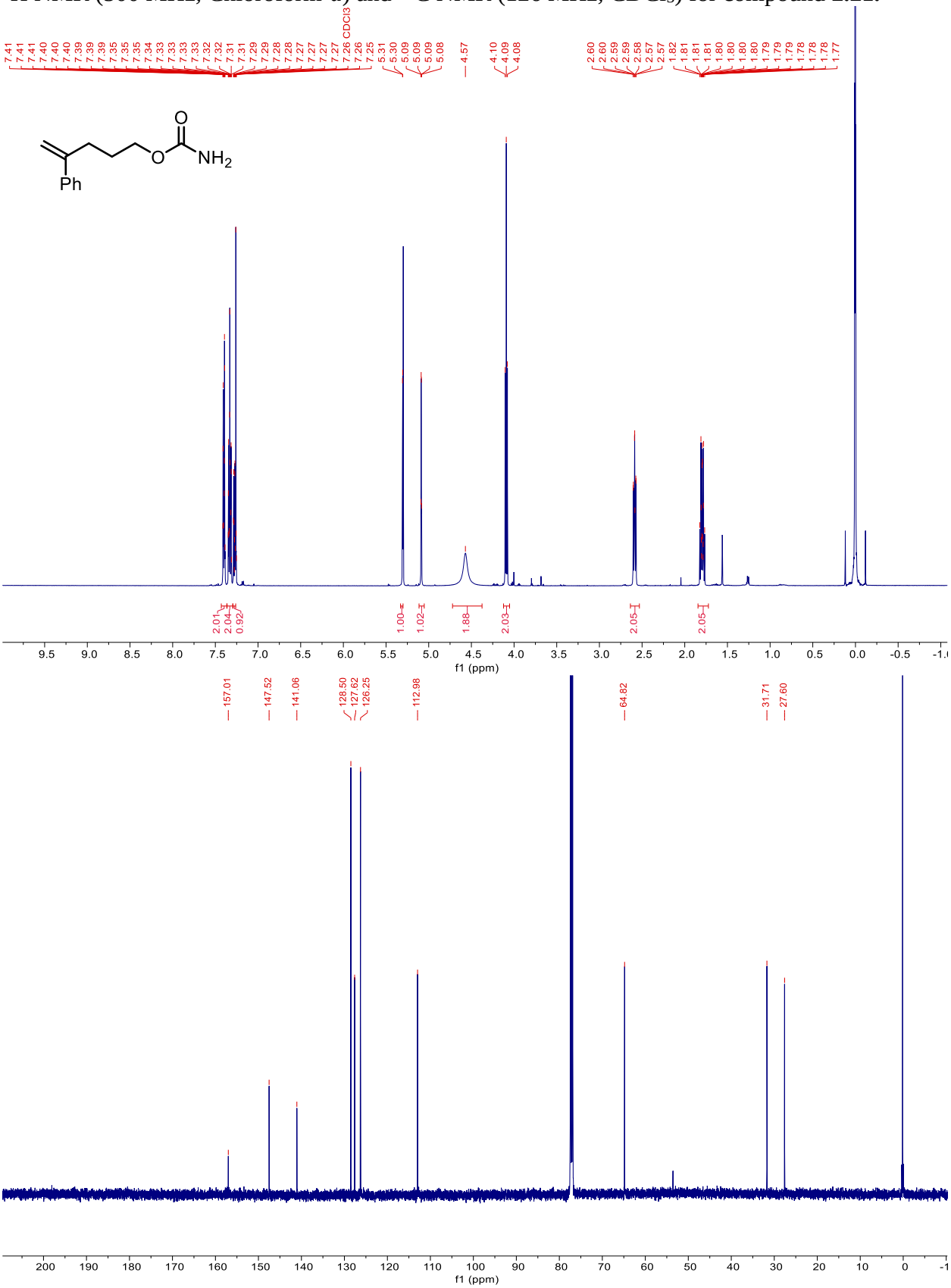

^{1}H NMR (500 MHz, Chloroform-*d*) and ^{13}C NMR (126 MHz, $CDCl_3$) for compound **2.22.**

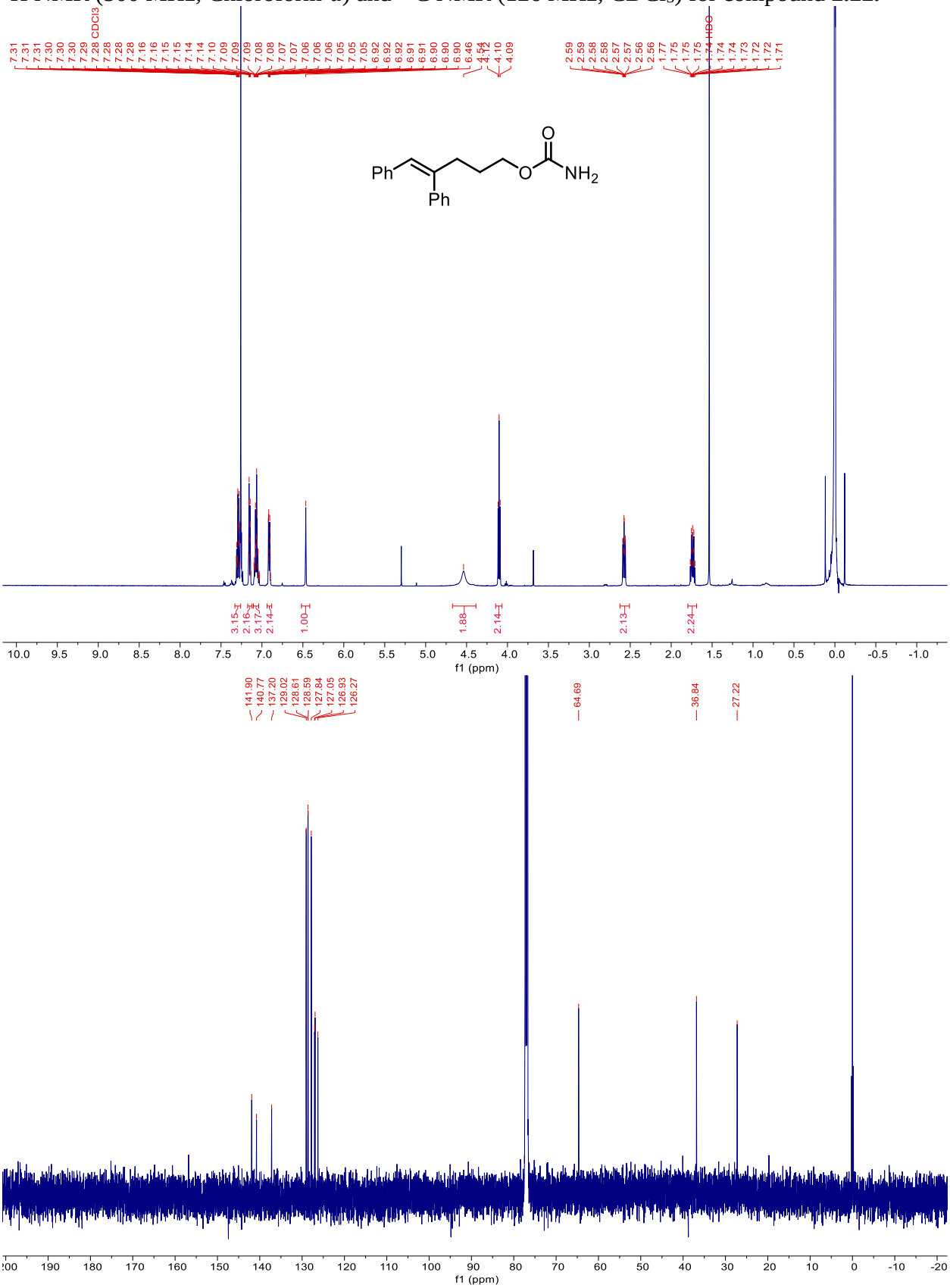

^{1}H NMR (500 MHz, Chloroform-*d*) and ^{13}C NMR (126 MHz, $CDCl_3$) for compound **2.23.**

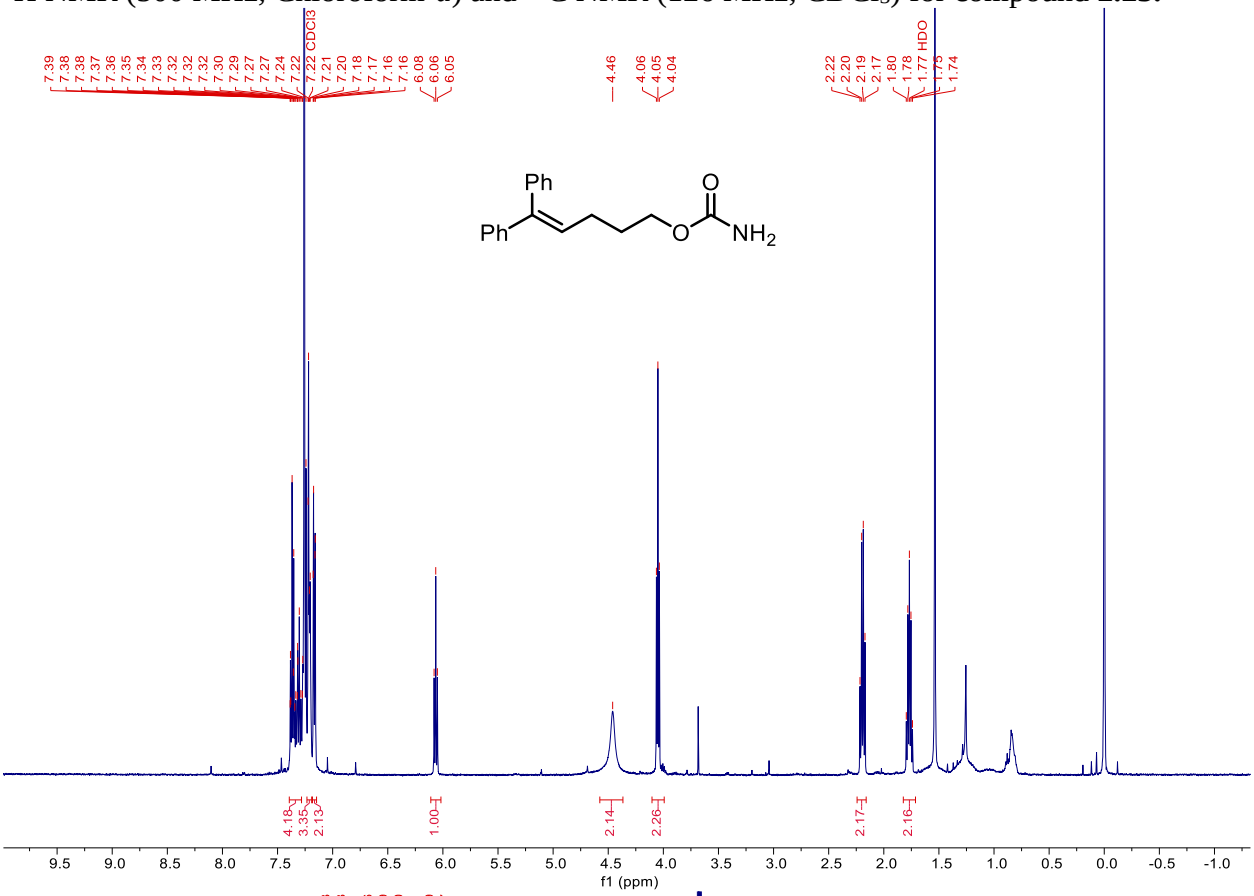

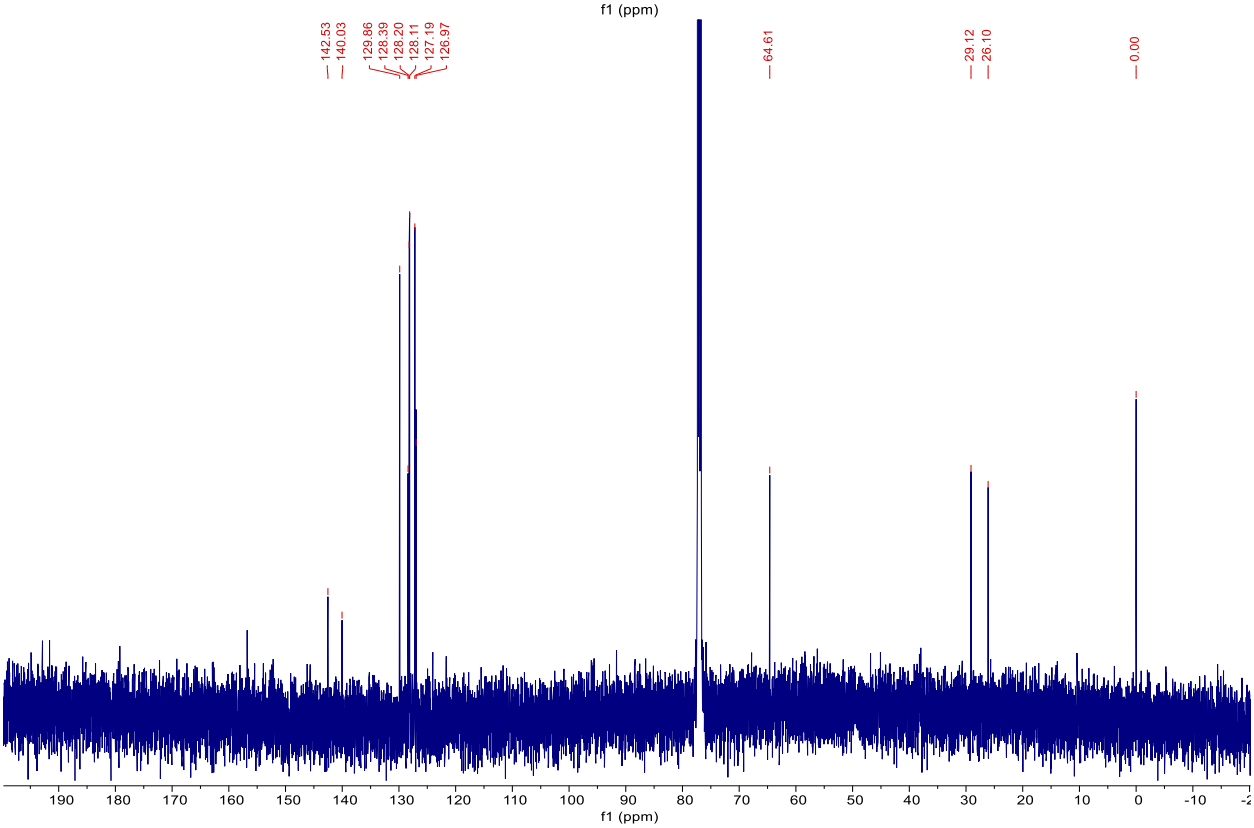

^{1}H NMR (500 MHz, Chloroform-*d*) and ^{13}C NMR (126 MHz, $CDCl_3$) for compound **2.24.**

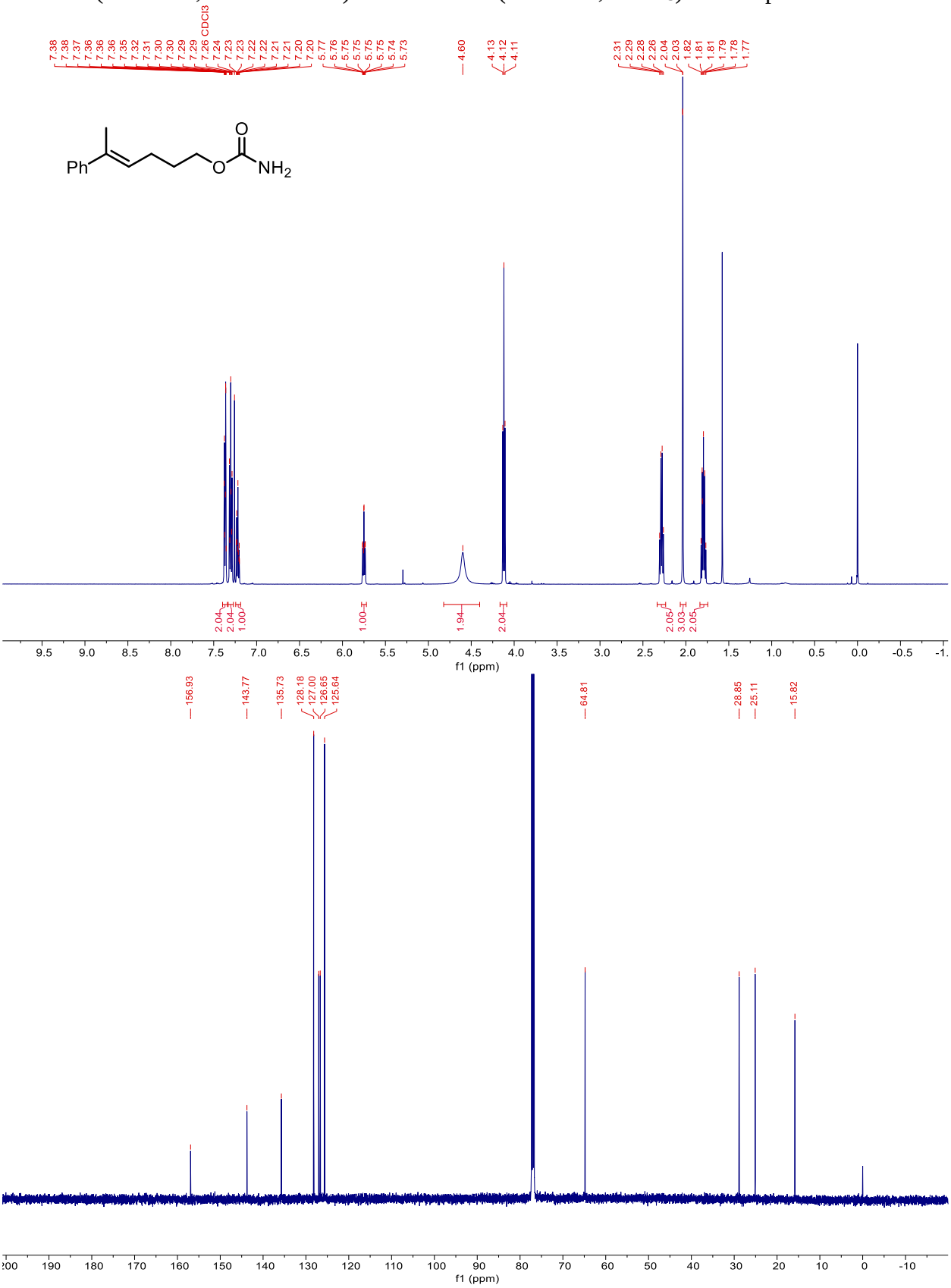

^{1}H NMR (500 MHz, Chloroform-*d*) and ^{13}C NMR (126 MHz, $CDCl_3$) for compound **2.25.**

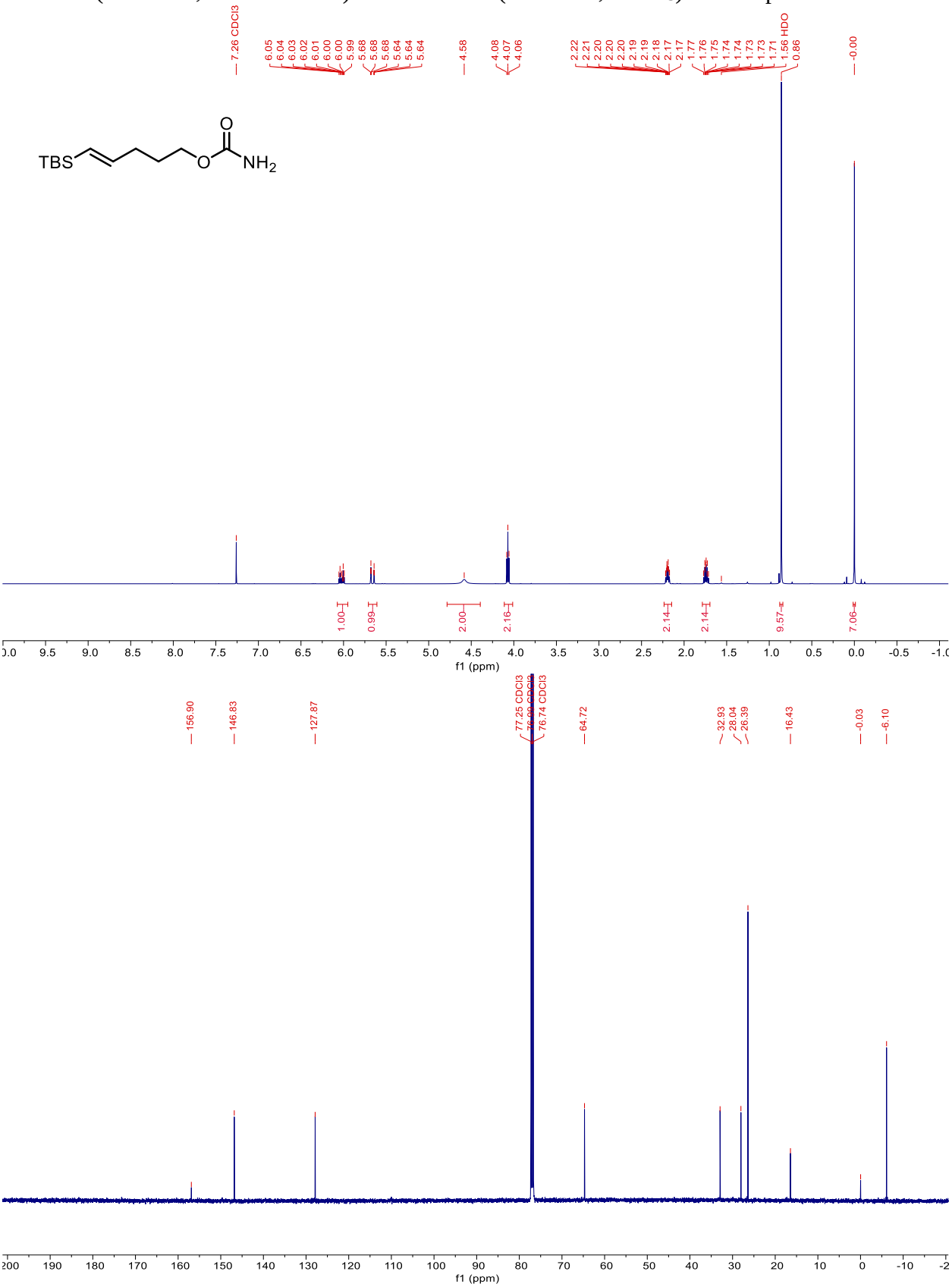

^{1}H NMR (500 MHz, Chloroform-*d*) and ^{13}C NMR (126 MHz, $CDCl_3$) for compound **2.26.**

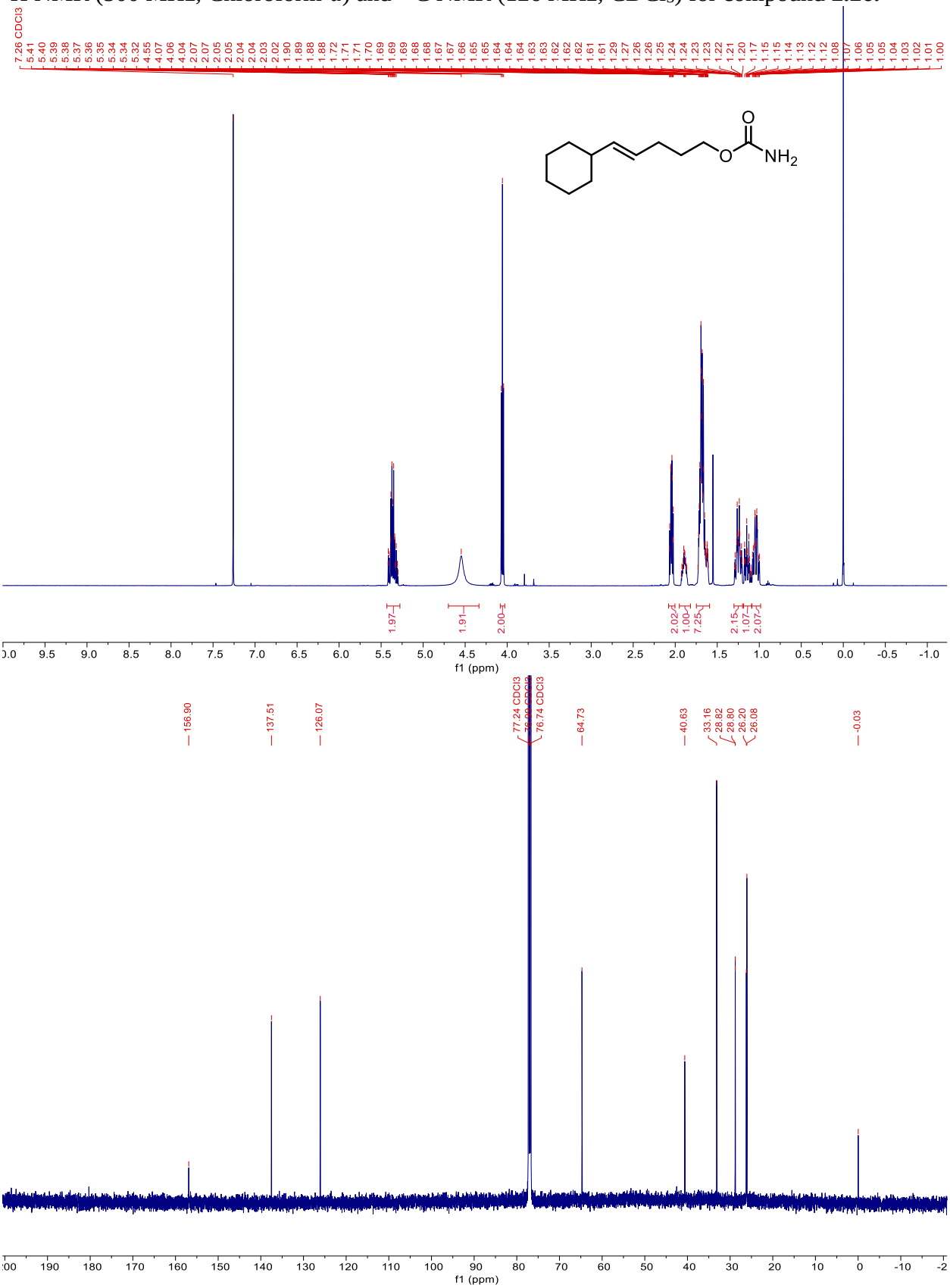

^{1}H NMR (500 MHz, Chloroform-*d*) and ^{13}C NMR (126 MHz, $CDCl_3$) for compound **2.27.**

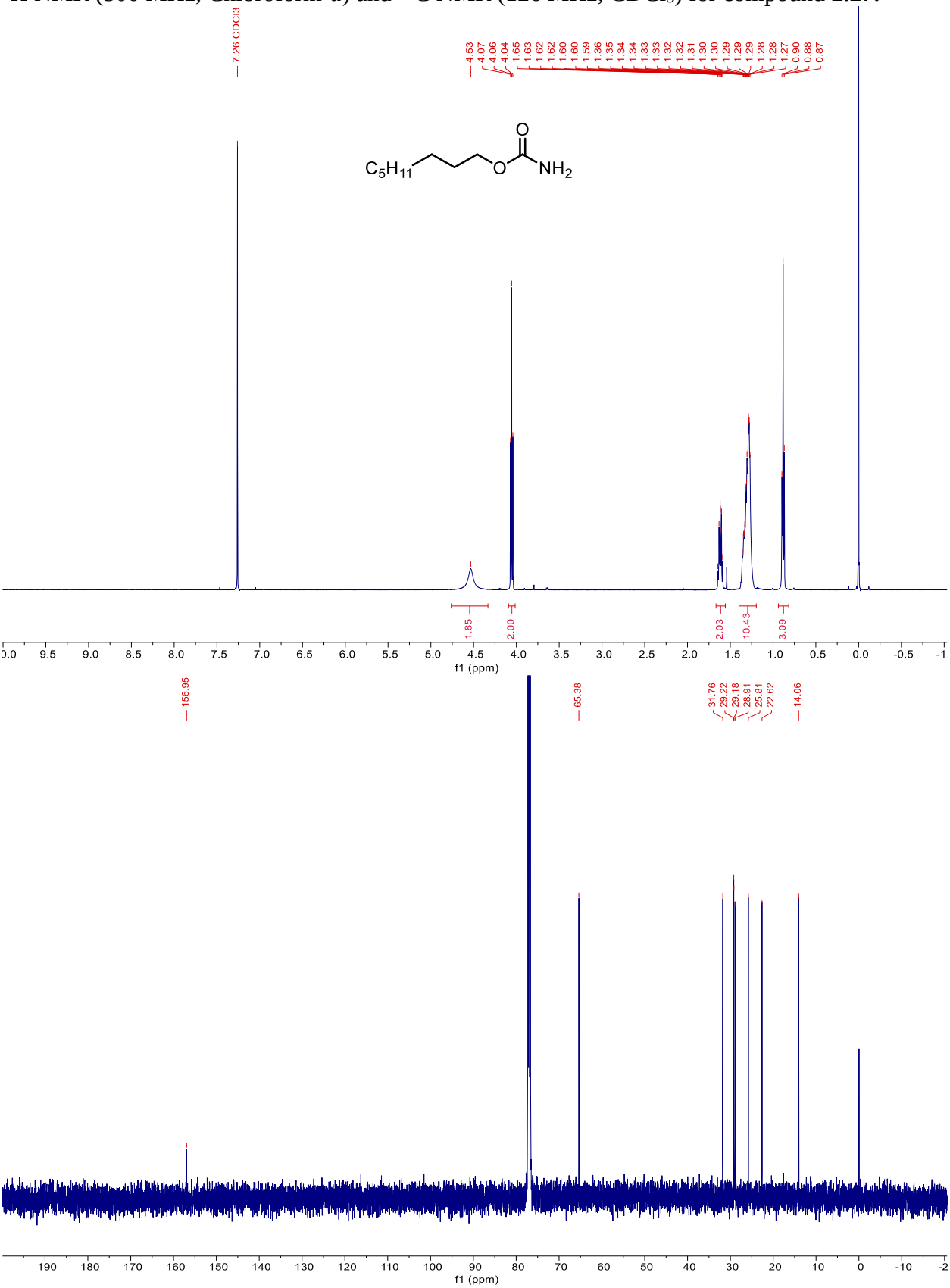

^{1}H NMR (500 MHz, Chloroform-*d*) and ^{13}C NMR (126 MHz, $CDCl_3$) for compound **2.28.**

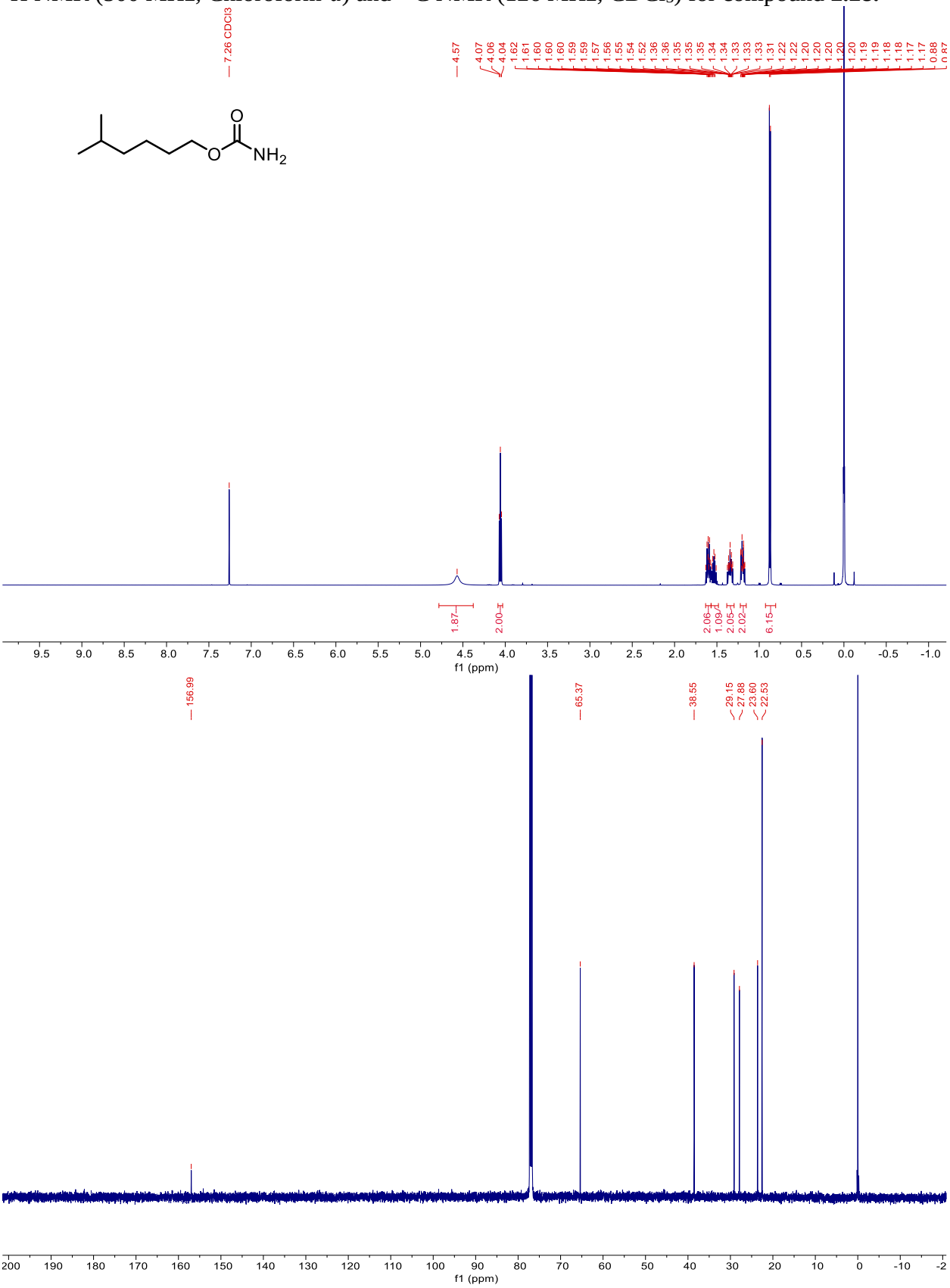

^{1}H NMR (500 MHz, Chloroform-*d*) and ^{13}C NMR (126 MHz, $CDCl_3$) for compound **2.29.**

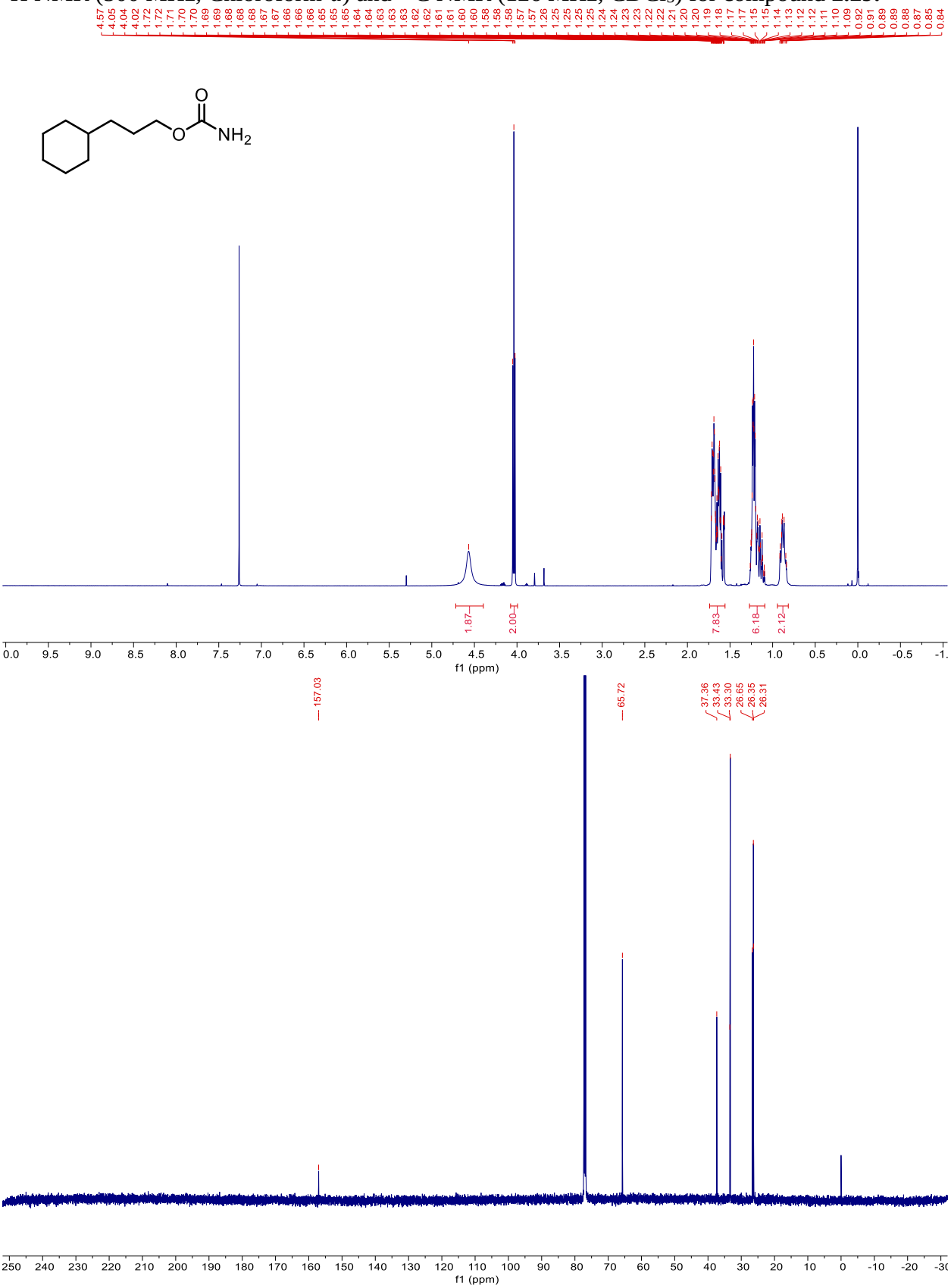

^{1}H NMR (500 MHz, Chloroform-*d*) and ^{13}C NMR (126 MHz, $CDCl_3$) for compound **2.30.**

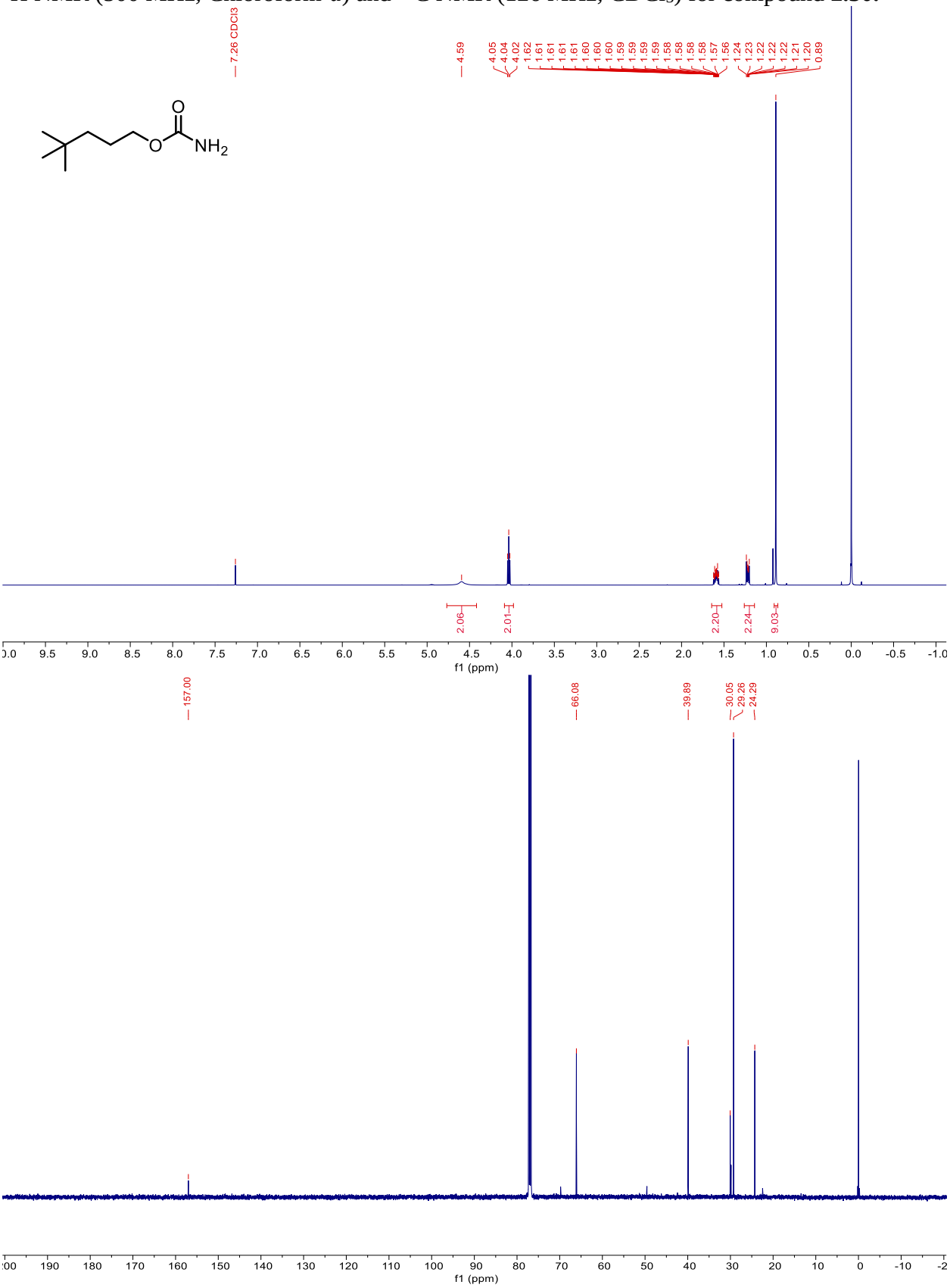

^{1}H NMR (500 MHz, Chloroform-*d*) and ^{13}C NMR (126 MHz, $CDCl_3$) for compound **2.31.**

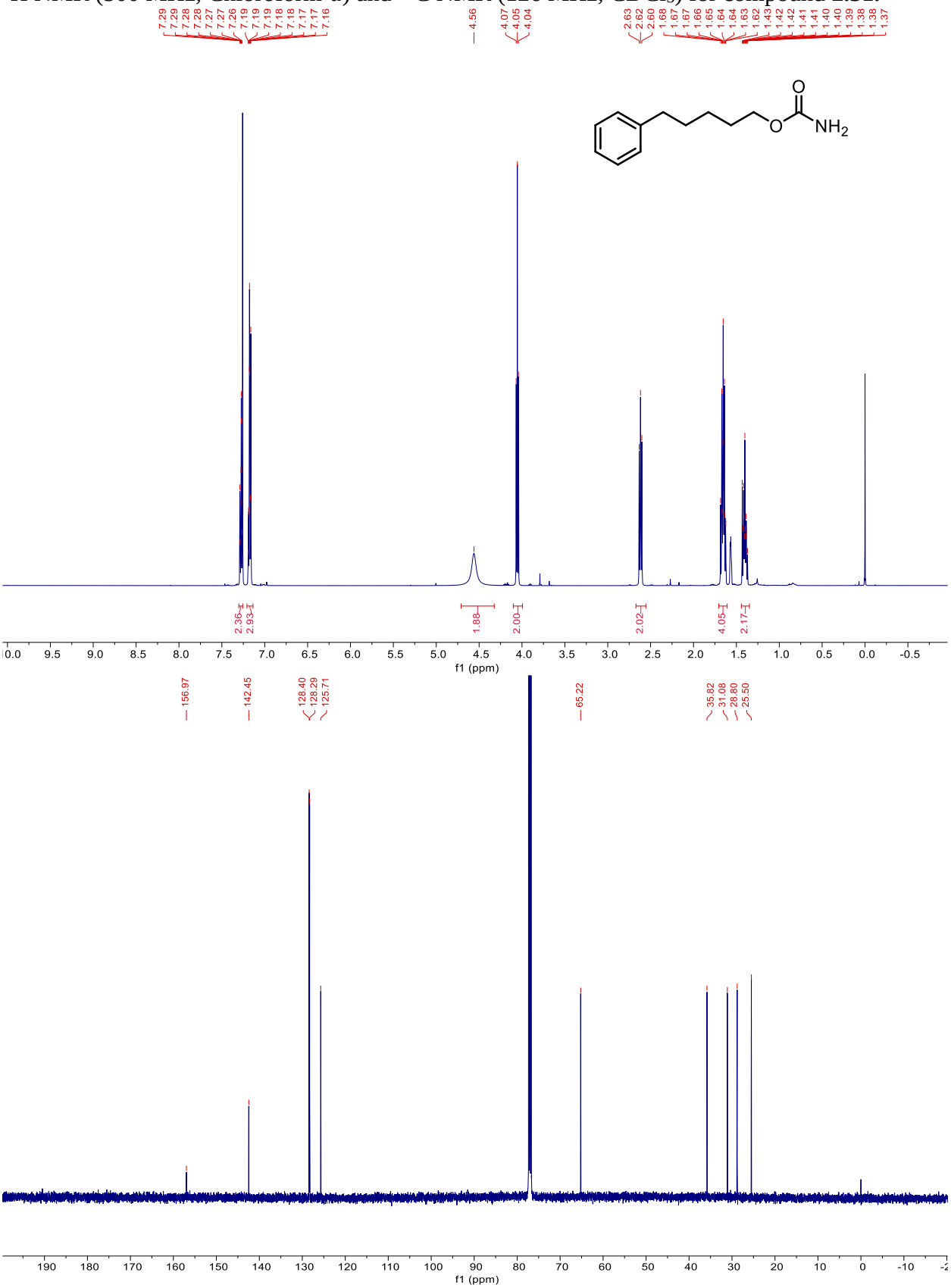

^{1}H NMR (500 MHz, Chloroform-*d*) and ^{13}C NMR (126 MHz, $CDCl_3$) for compound **2.32.**

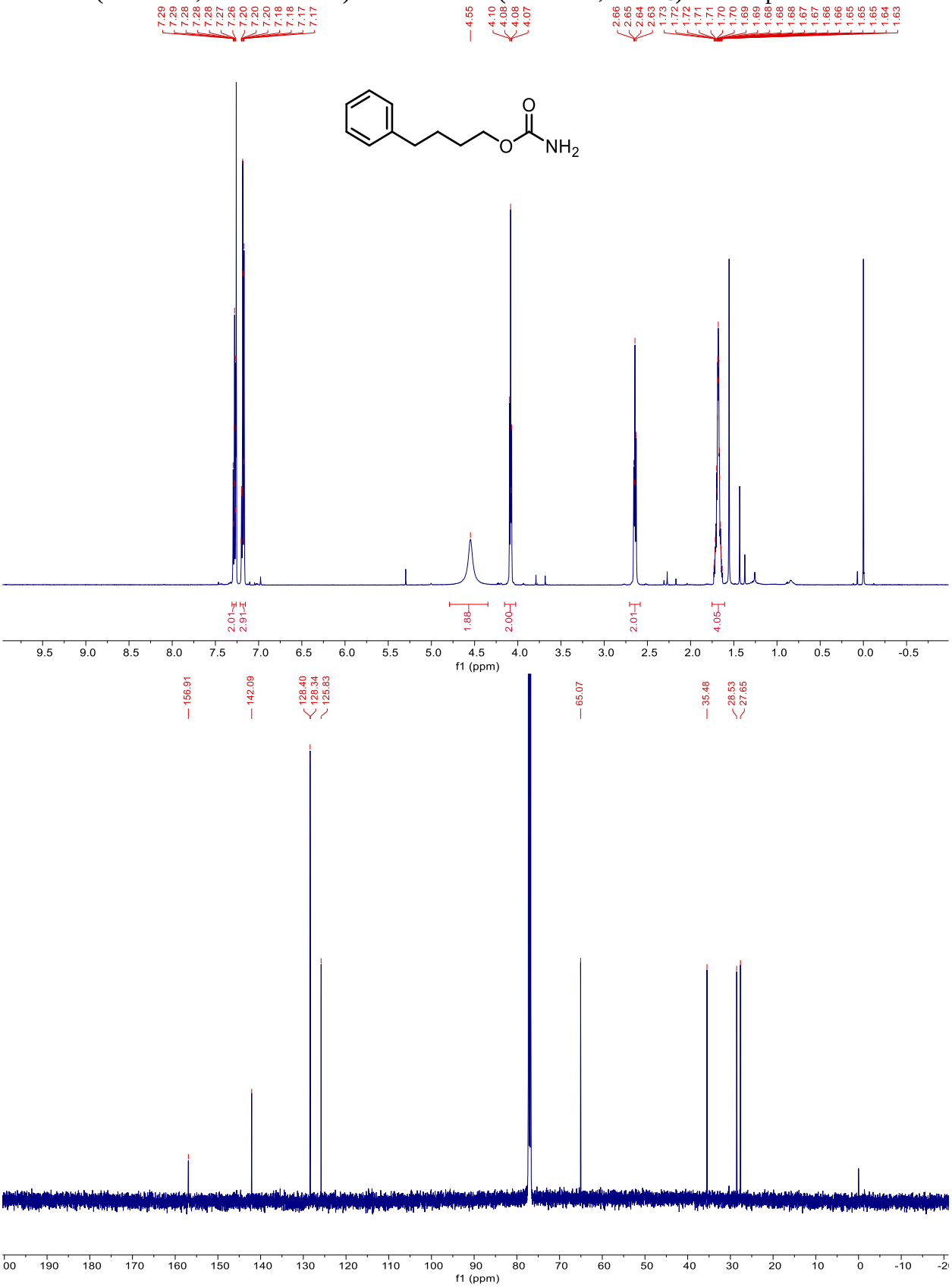

^{1}H NMR (500 MHz, Chloroform-*d*) and ^{13}C NMR (126 MHz, $CDCl_3$) for compound **2.2a.**

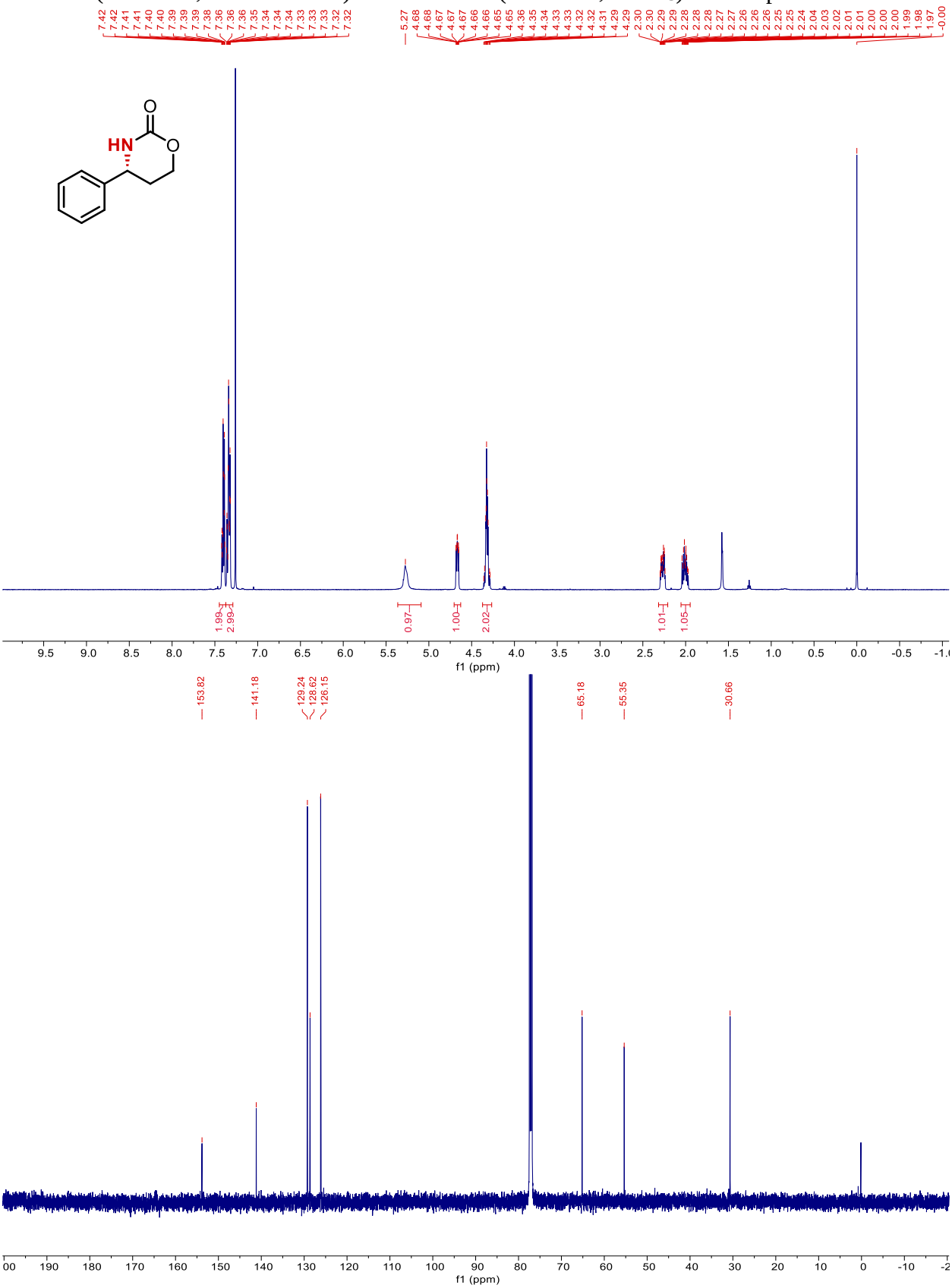

^{1}H NMR (500 MHz, Chloroform-*d*) and ^{13}C NMR (126 MHz, $CDCl_3$) for compound **2.2b.**

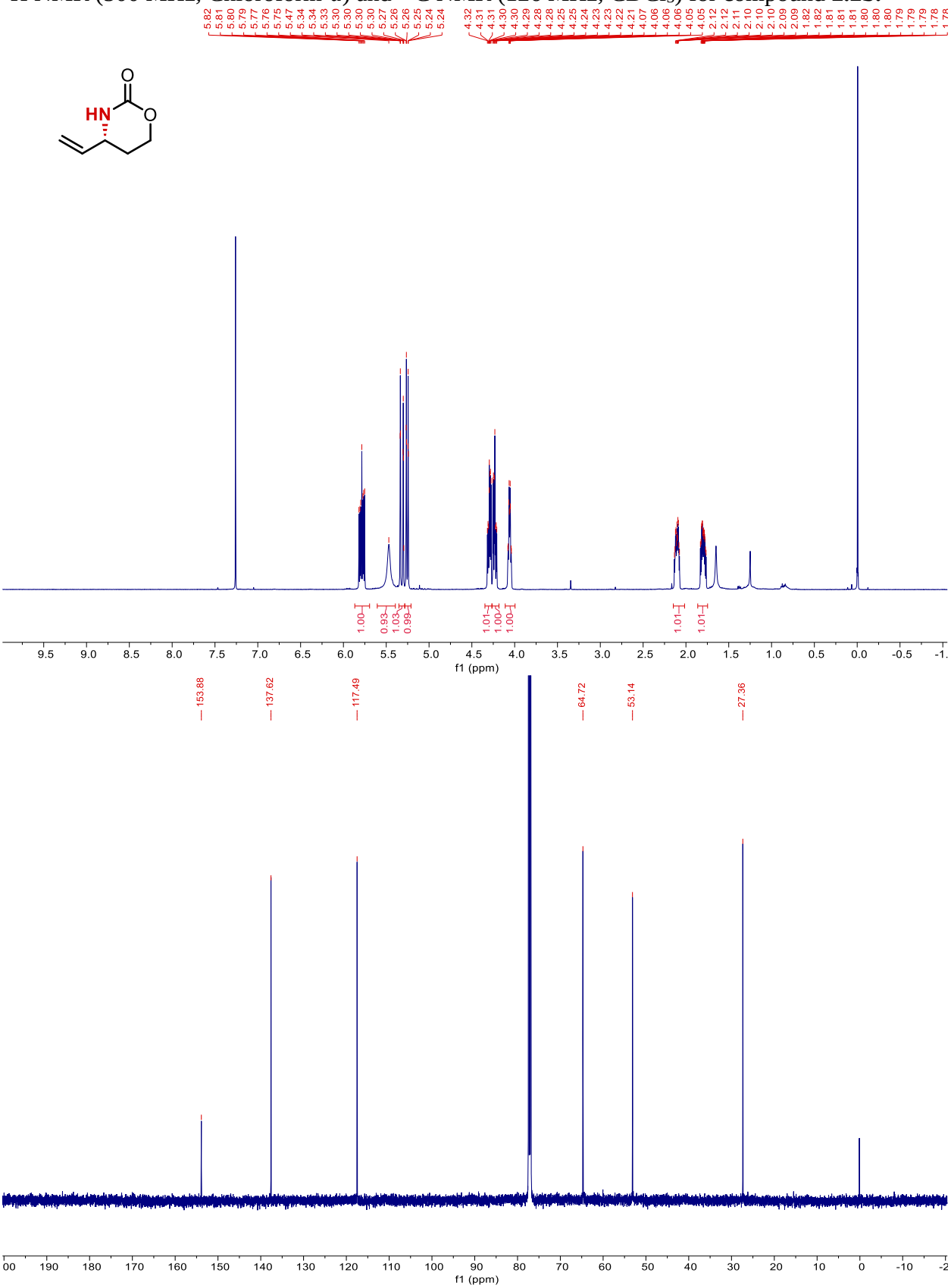

^{1}H NMR (500 MHz, Chloroform-*d*) and ^{13}C NMR (126 MHz, $CDCl_3$) for compound **2.2c.**

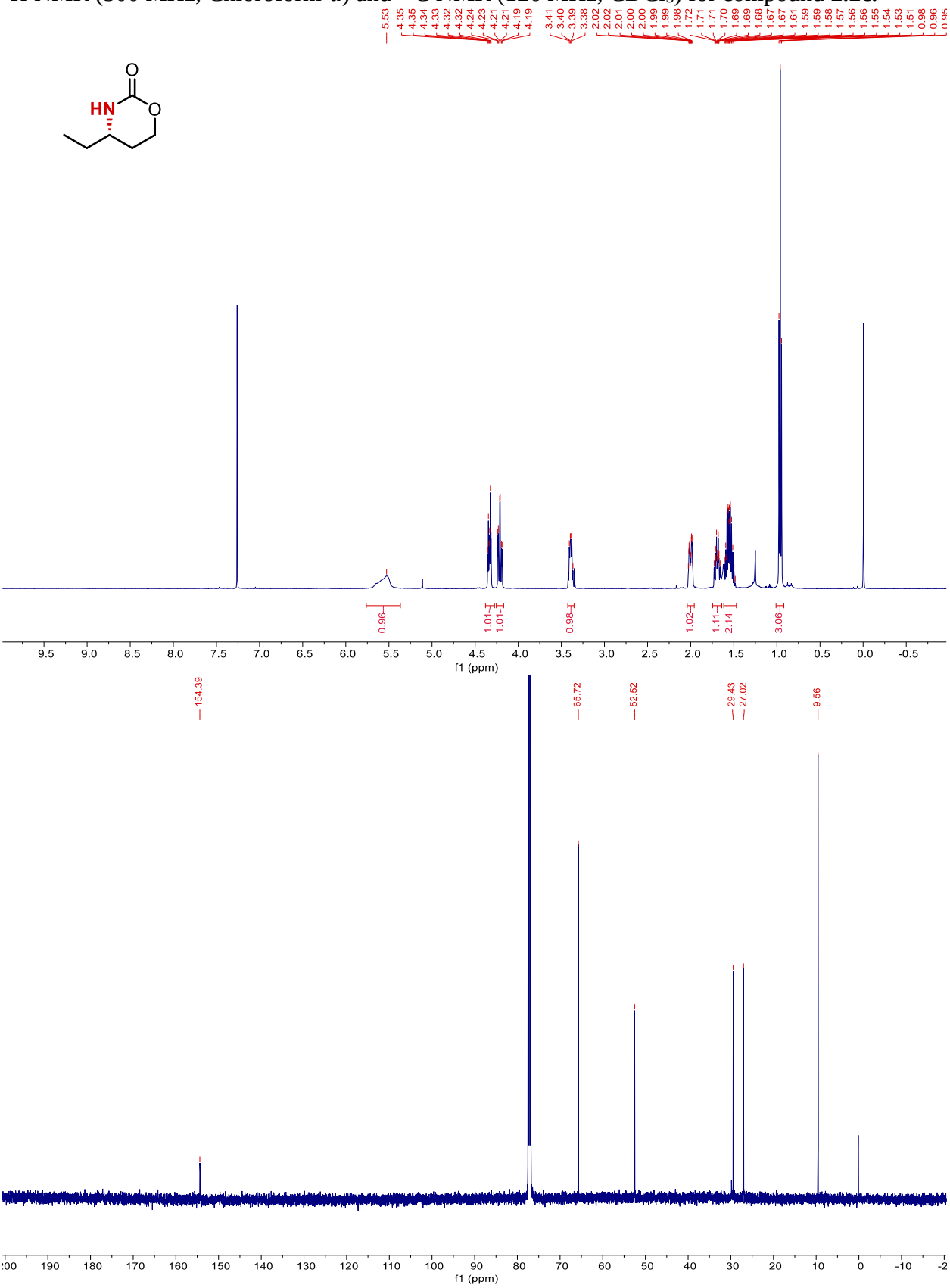

^{1}H NMR (500 MHz, Chloroform-*d*) and ^{13}C NMR (126 MHz, $CDCl_3$) for compound **2.3a.**

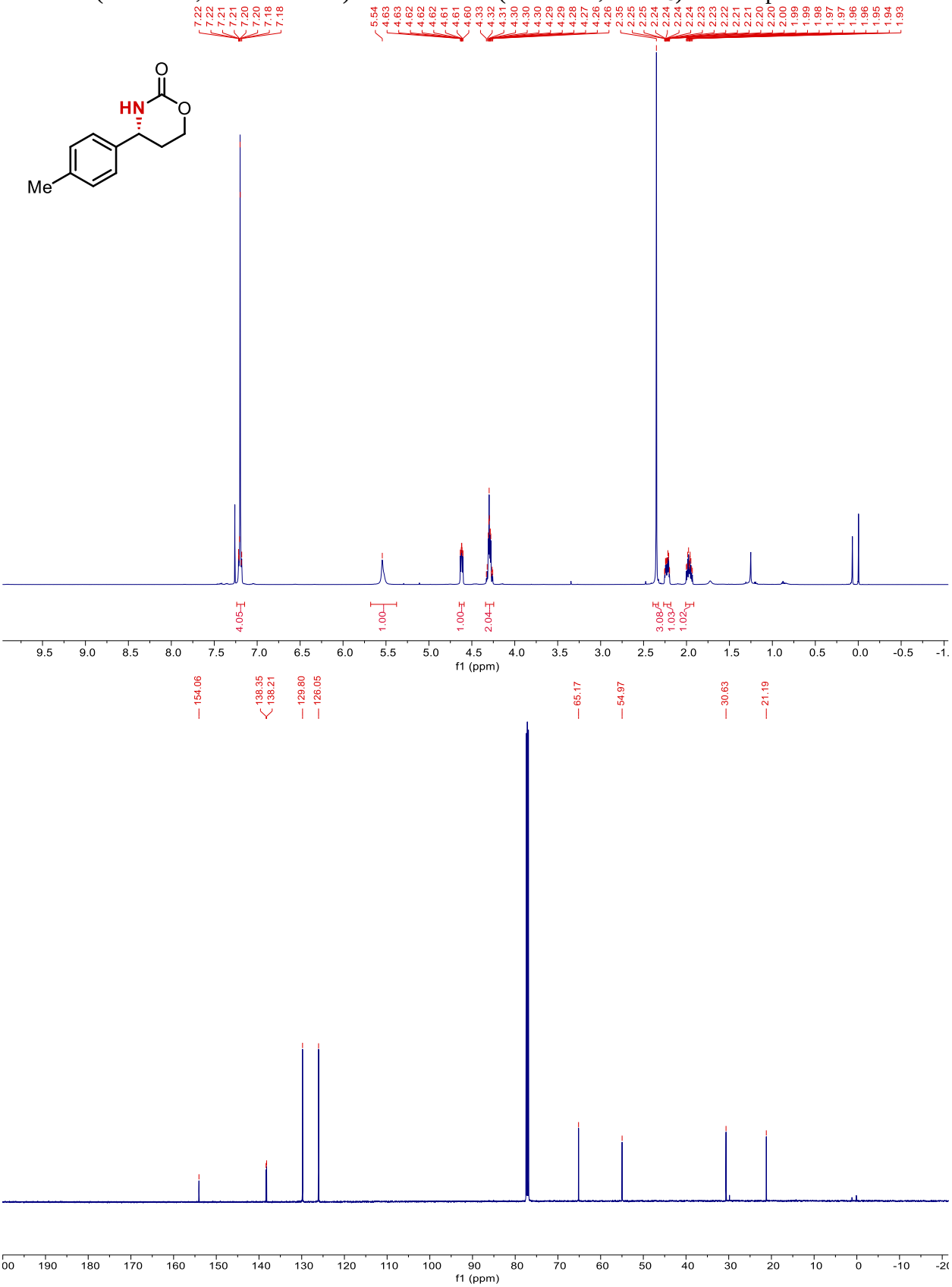

^{1}H NMR (500 MHz, Chloroform-*d*) and ^{13}C NMR (126 MHz, $CDCl_3$) for compound **2.4a.**

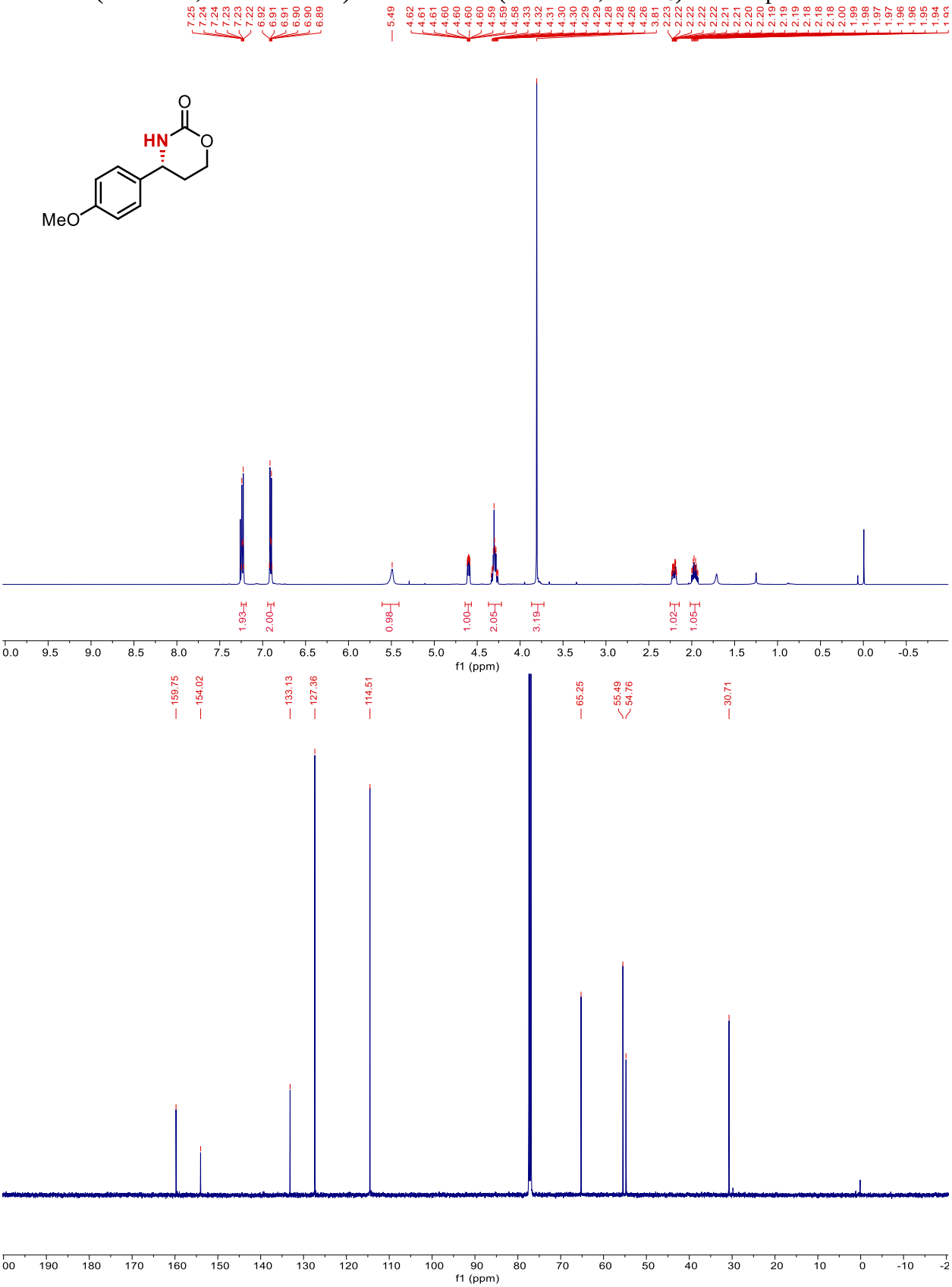

^{1}H NMR (500 MHz, Chloroform-*d*) and ^{13}C NMR (126 MHz, $CDCl_3$) for compound **2.5a.**

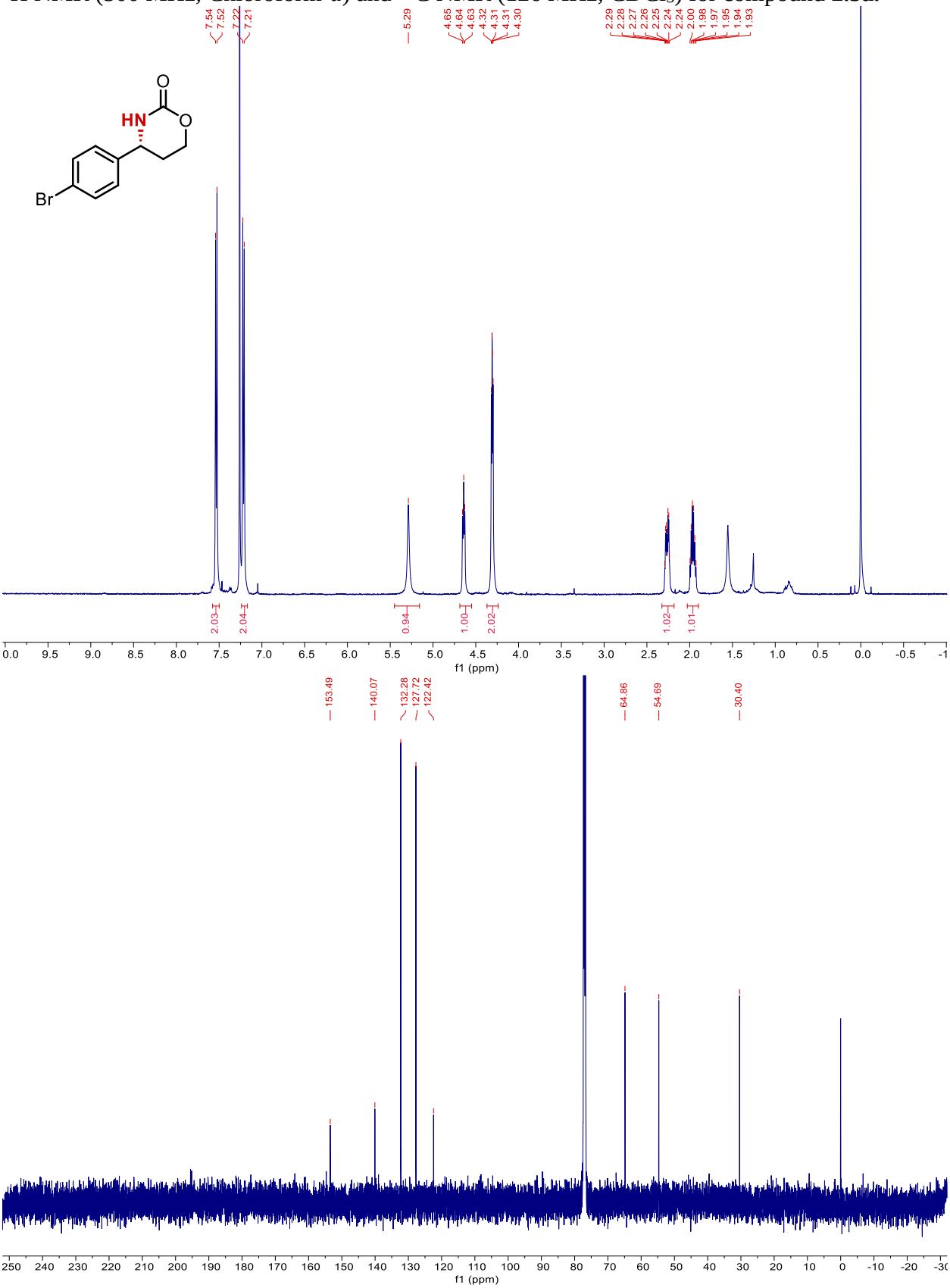

^{1}H NMR (400 MHz, Chloroform-*d*) and ^{13}C NMR (101 MHz, $CDCl_3$) for compound **2.6a.**

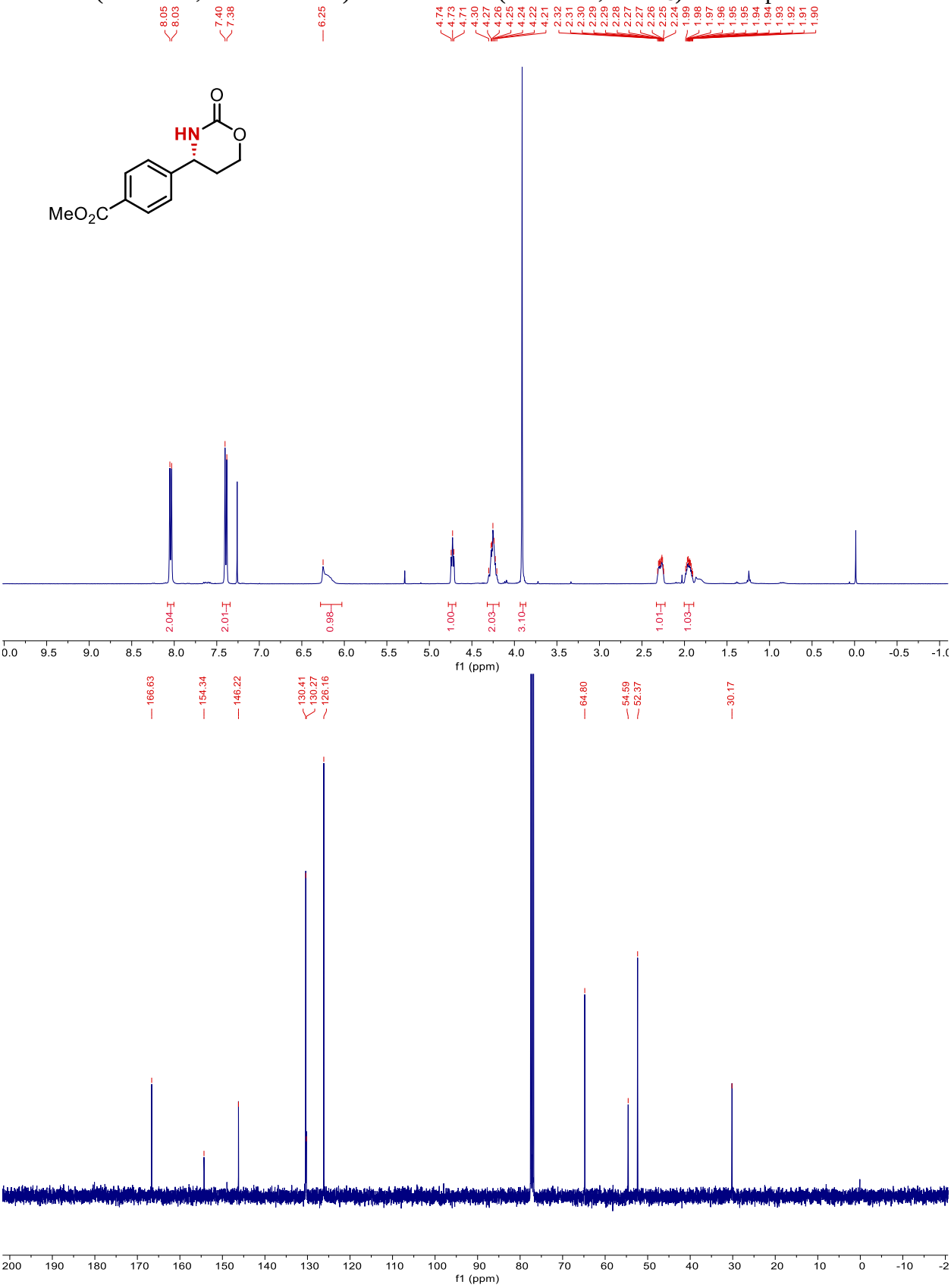

^{1}H NMR (500 MHz, Chloroform-*d*), ^{13}C NMR (126 MHz, $CDCl_3$), and ^{19}F NMR (377 MHz, $CDCl_3$) for compound **2.7a.**

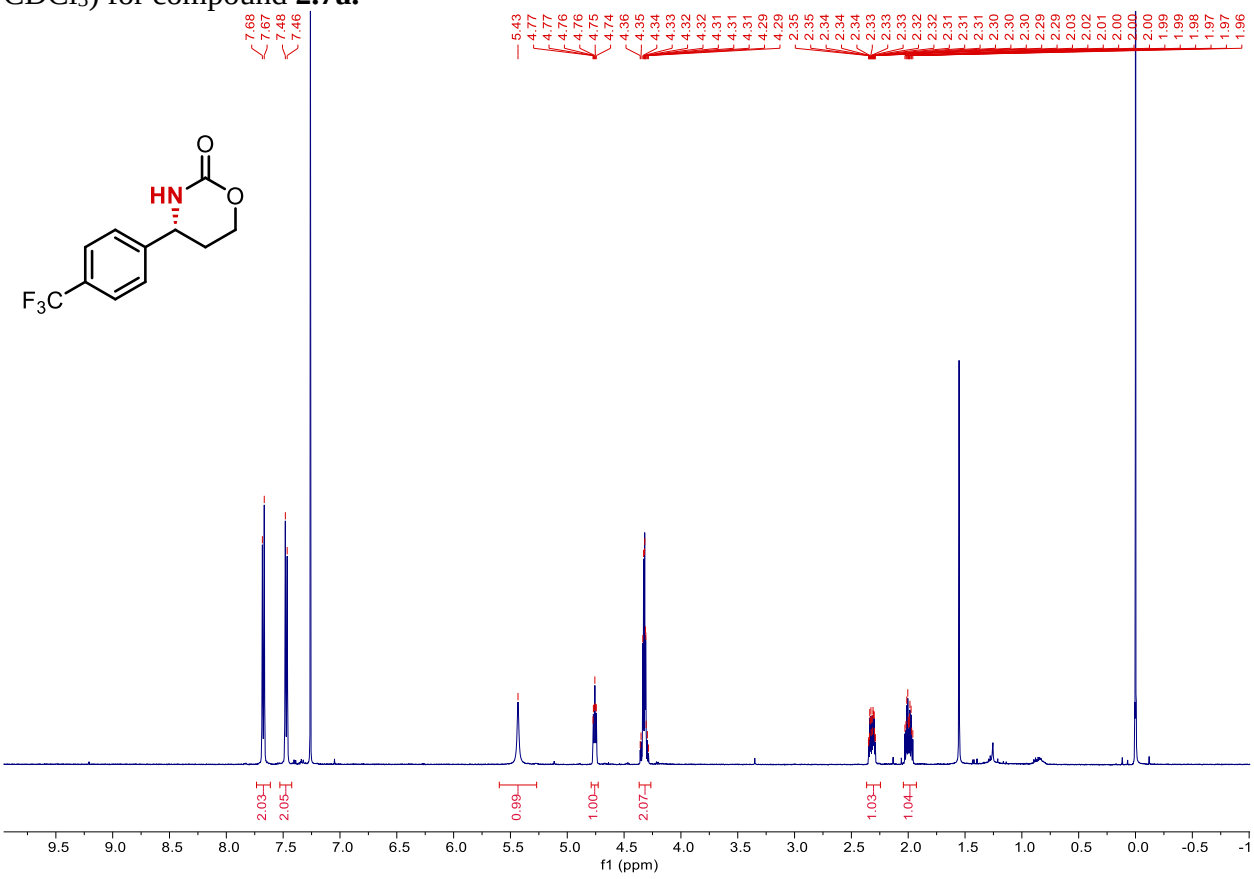

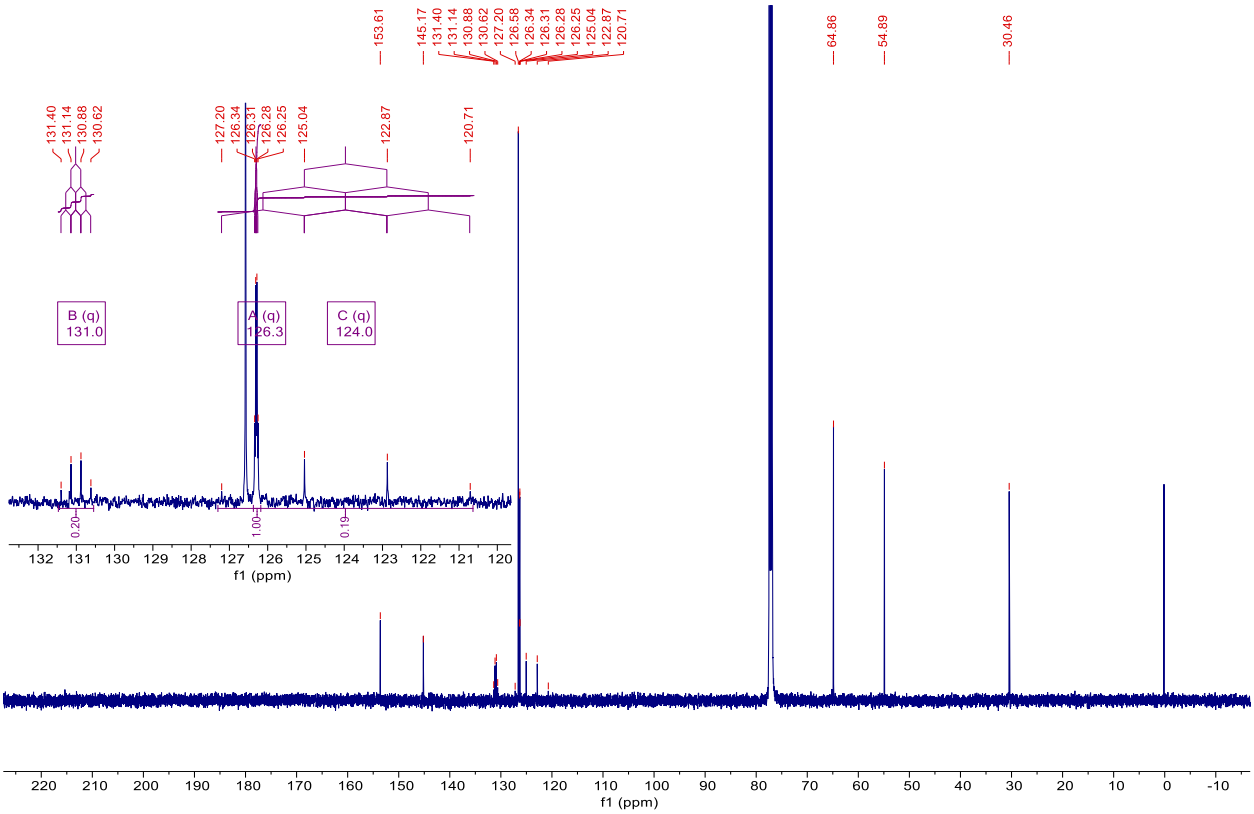
153.61
145.17
131.40
131.14
130.88
130.62
127.20
126.58
126.34
126.31
126.28
126.25
125.04
122.87
120.71
64.86
54.89
30.46
B (q)
131.0
A (q)
126.3
C (q)
124.0
0.20
1.00
0.19
f1 (ppm)

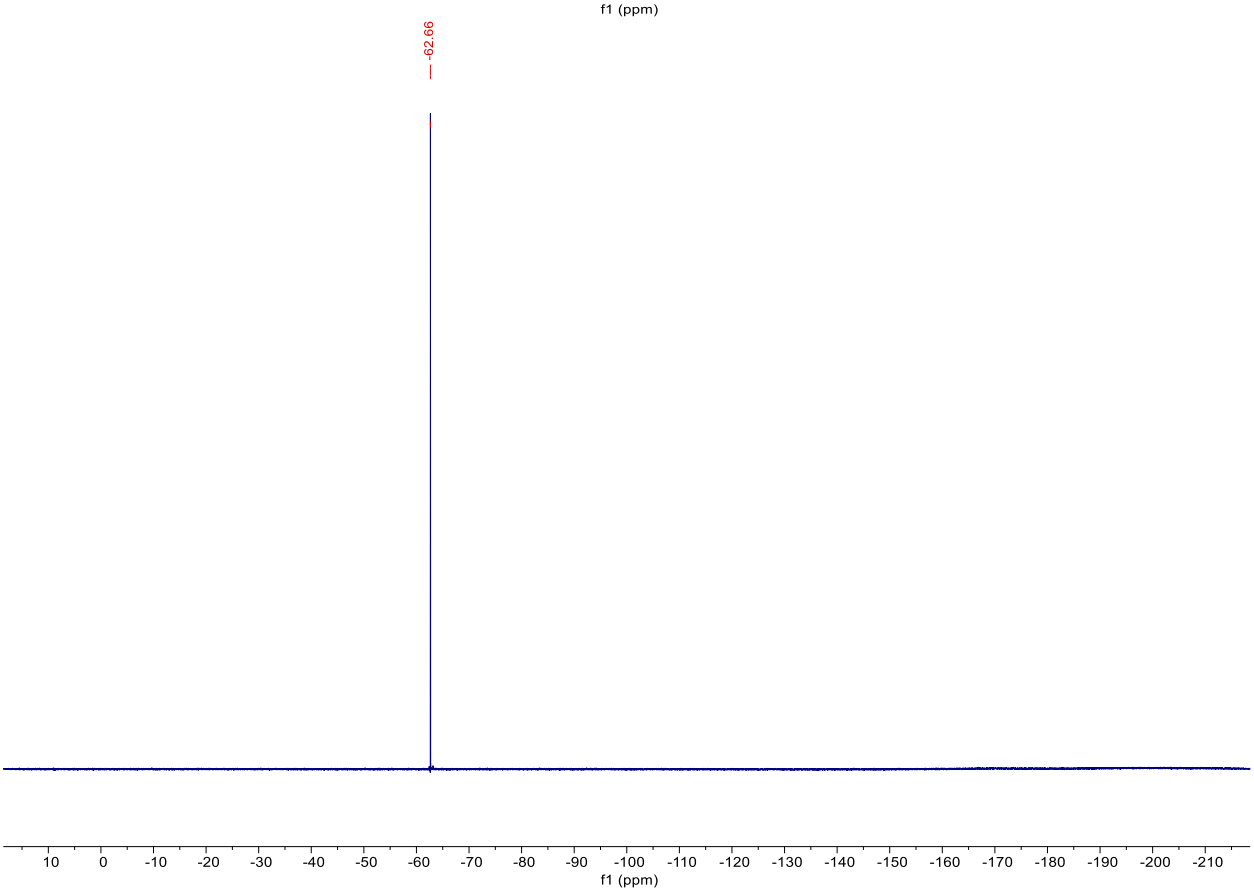
-62.66
f1 (ppm)

^{1}H NMR (500 MHz, Chloroform-*d*) and ^{13}C NMR (126 MHz, $CDCl_3$) for compound **2.8a.**

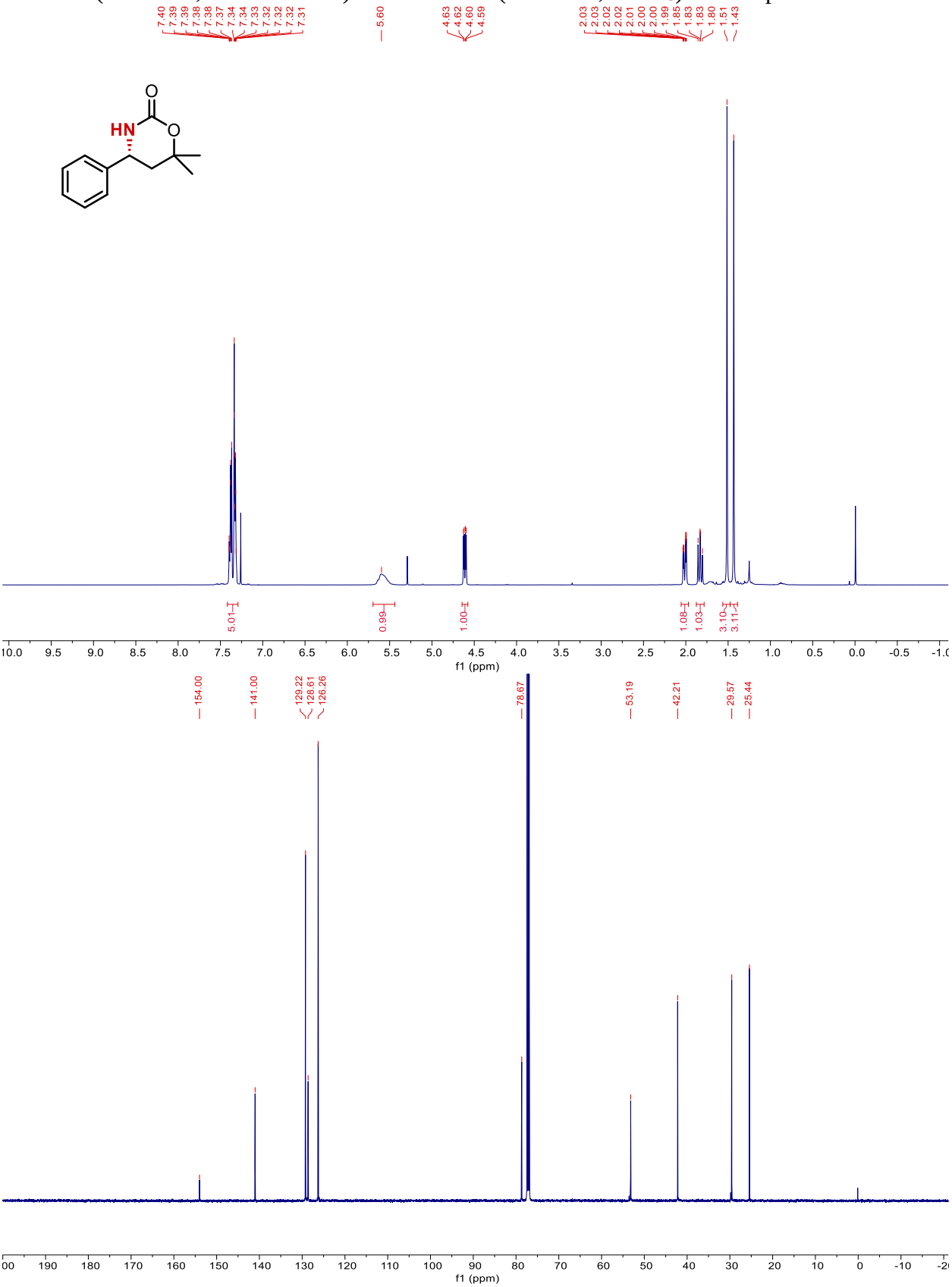

^{1}H NMR (500 MHz, Chloroform-*d*) and ^{13}C NMR (126 MHz, $CDCl_3$) for compound **2.9a.**

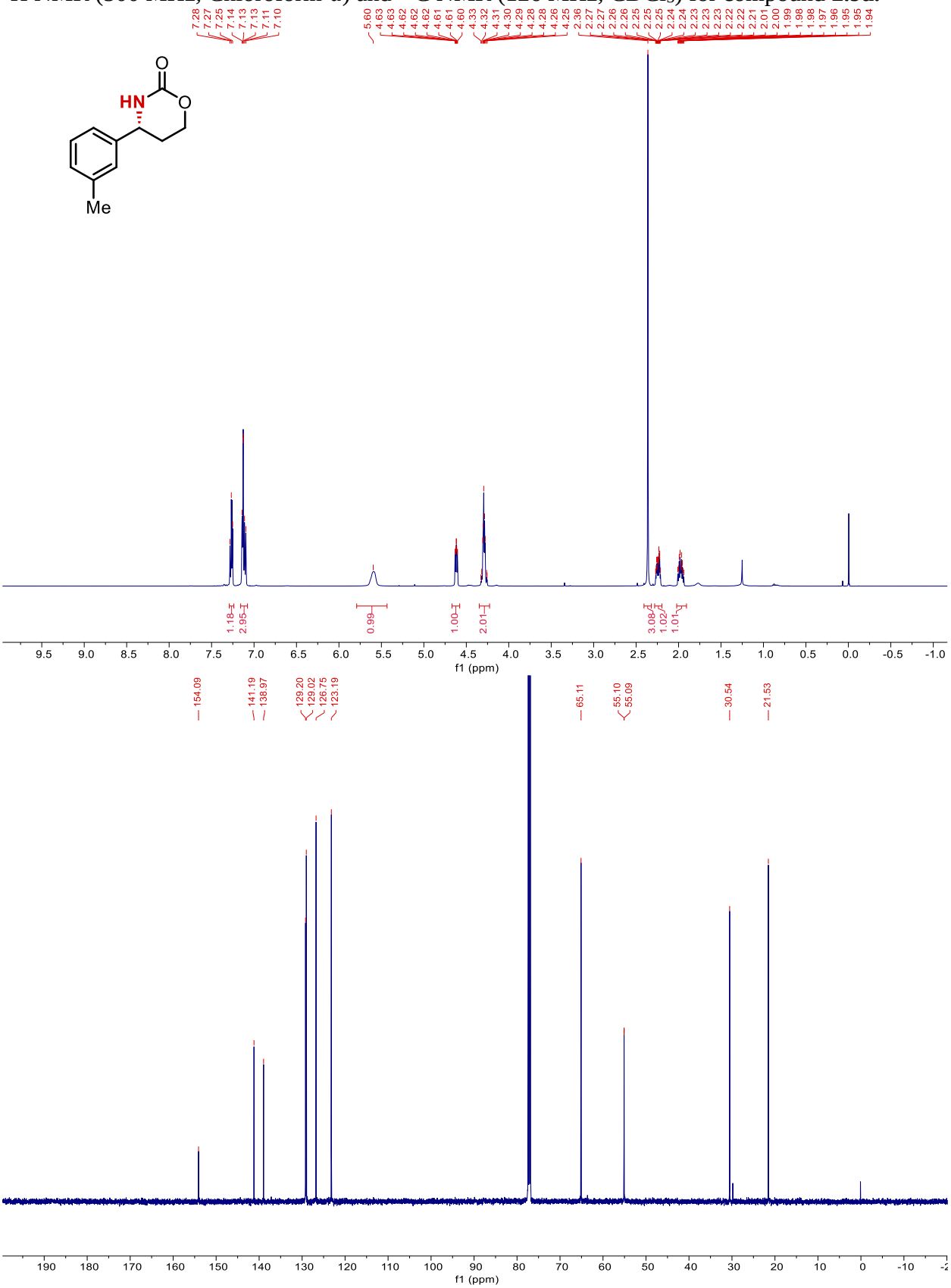

^{1}H NMR (500 MHz, Chloroform-*d*) and ^{13}C NMR (126 MHz, $CDCl_3$) for compound **2.10a.**

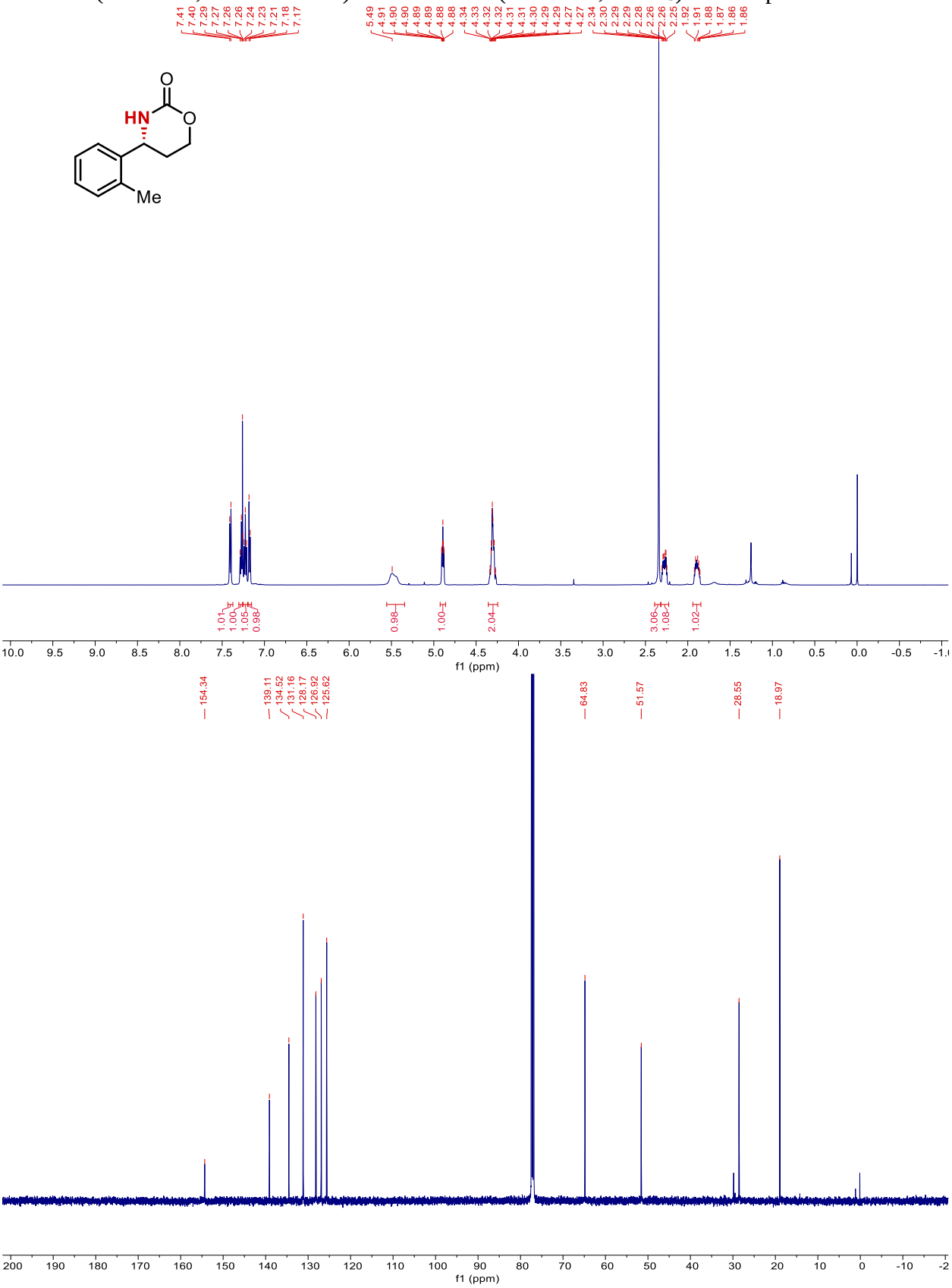

^{1}H NMR (500 MHz, Chloroform-*d*) and ^{13}C NMR (126 MHz, $CDCl_3$) for compound **2.11a.**

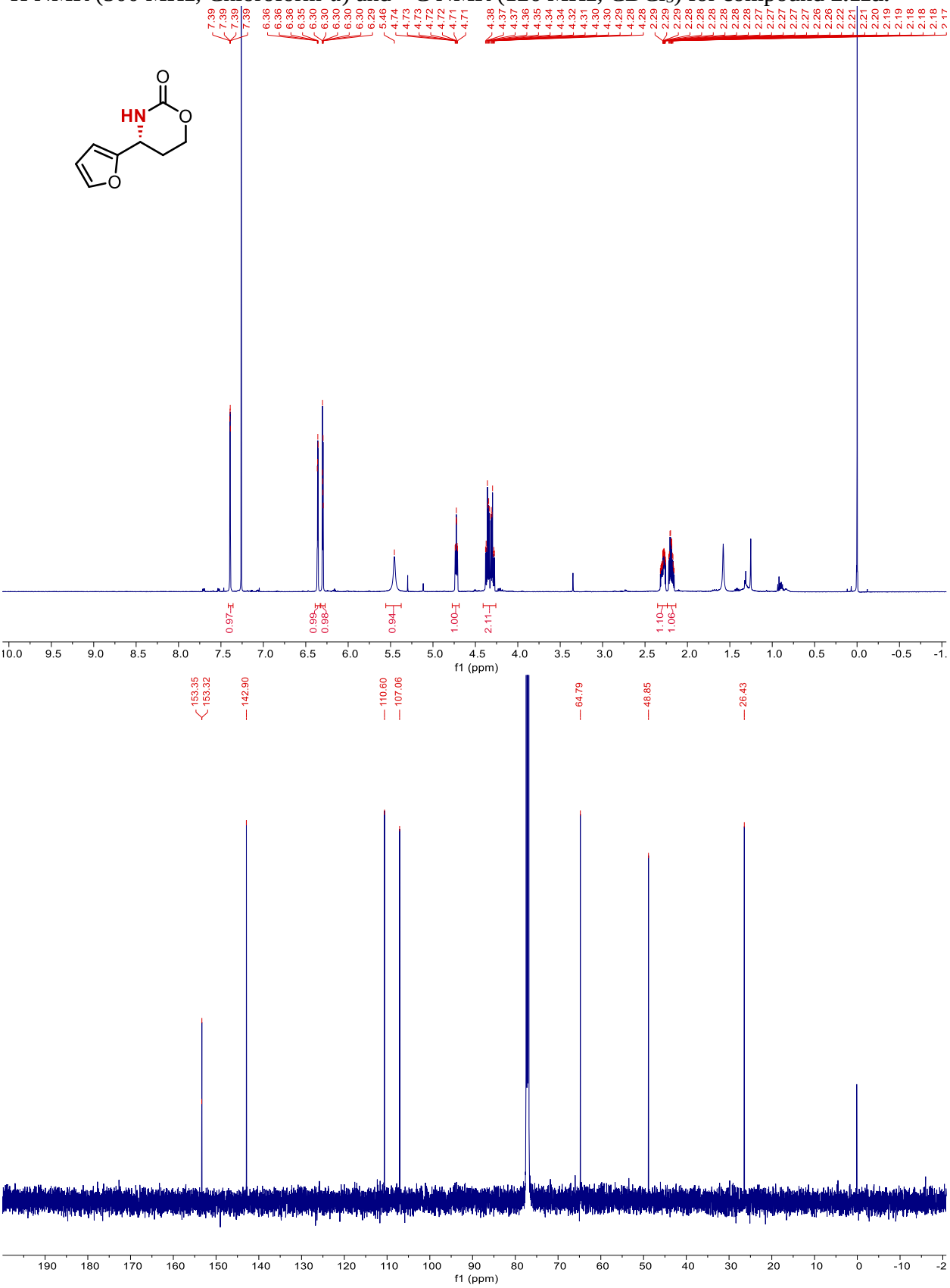

^{1}H NMR (500 MHz, Chloroform-*d*) and ^{13}C NMR (126 MHz, $CDCl_3$) for compound **2.12a.**

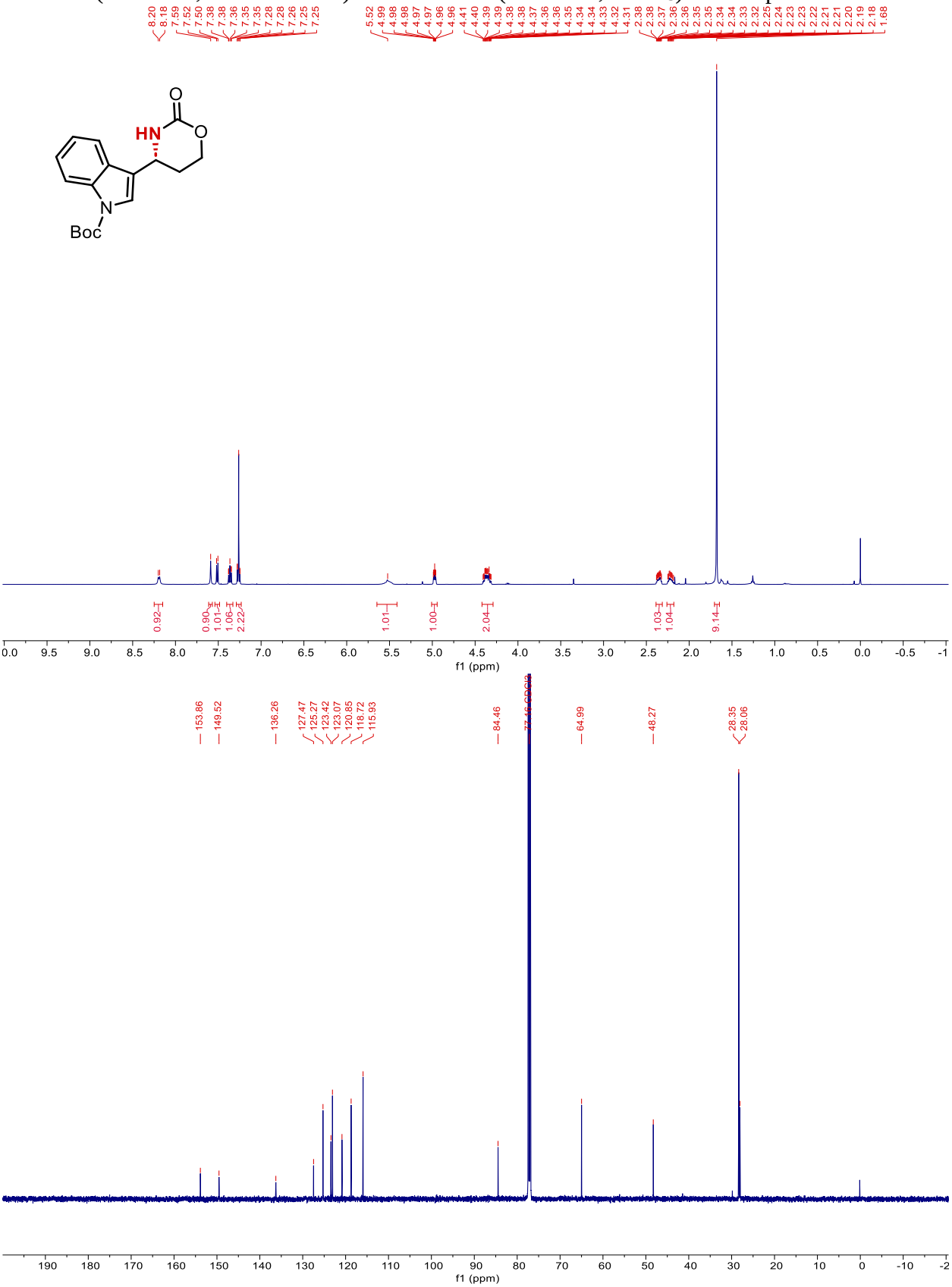

^{1}H NMR (500 MHz, Chloroform-*d*) and ^{13}C NMR (126 MHz, $CDCl_3$) for compound **2.13a.**

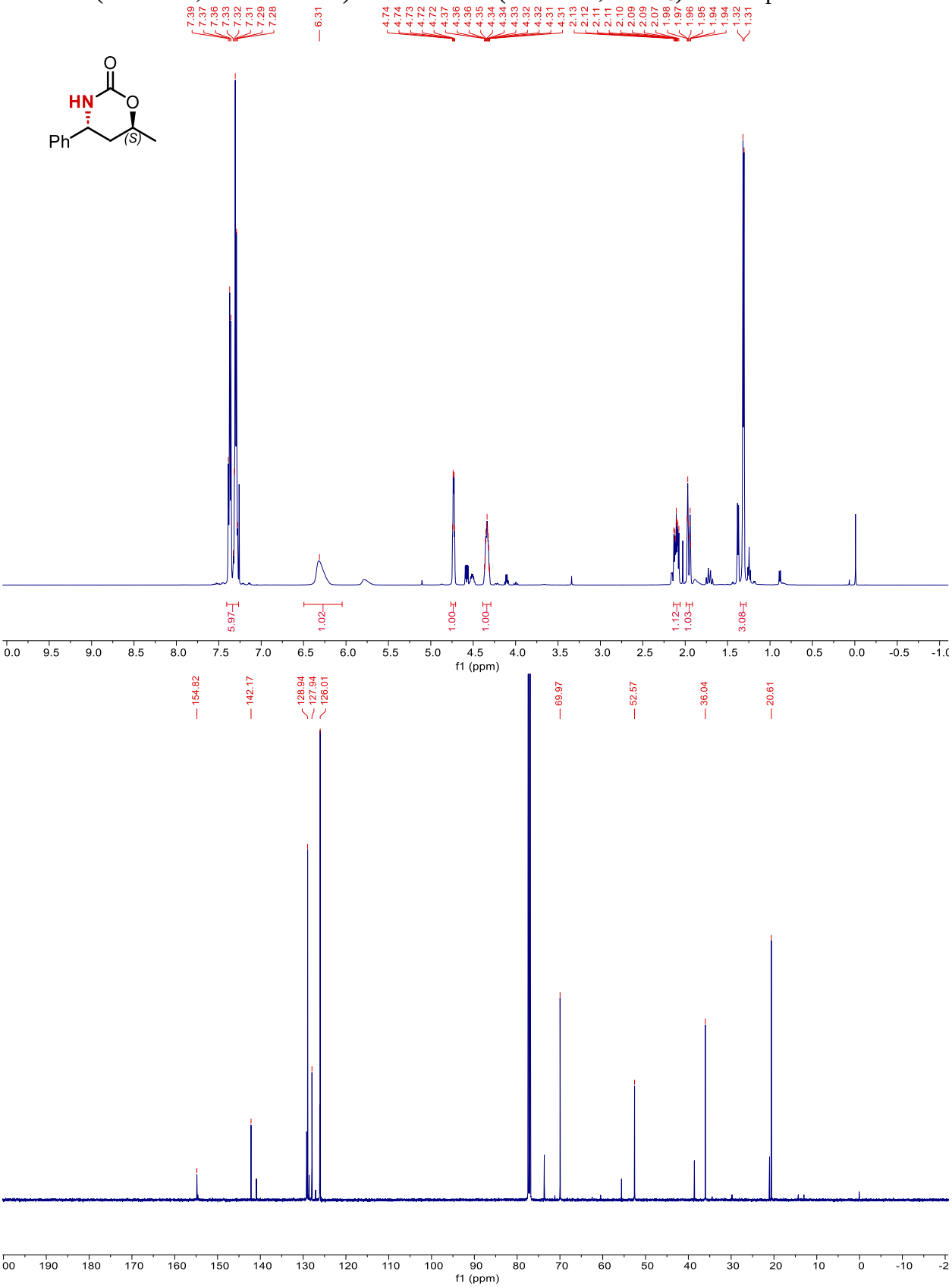

^{1}H NMR (500 MHz, Chloroform-*d*) and ^{13}C NMR (126 MHz, $CDCl_3$) for compound **2.14a.**

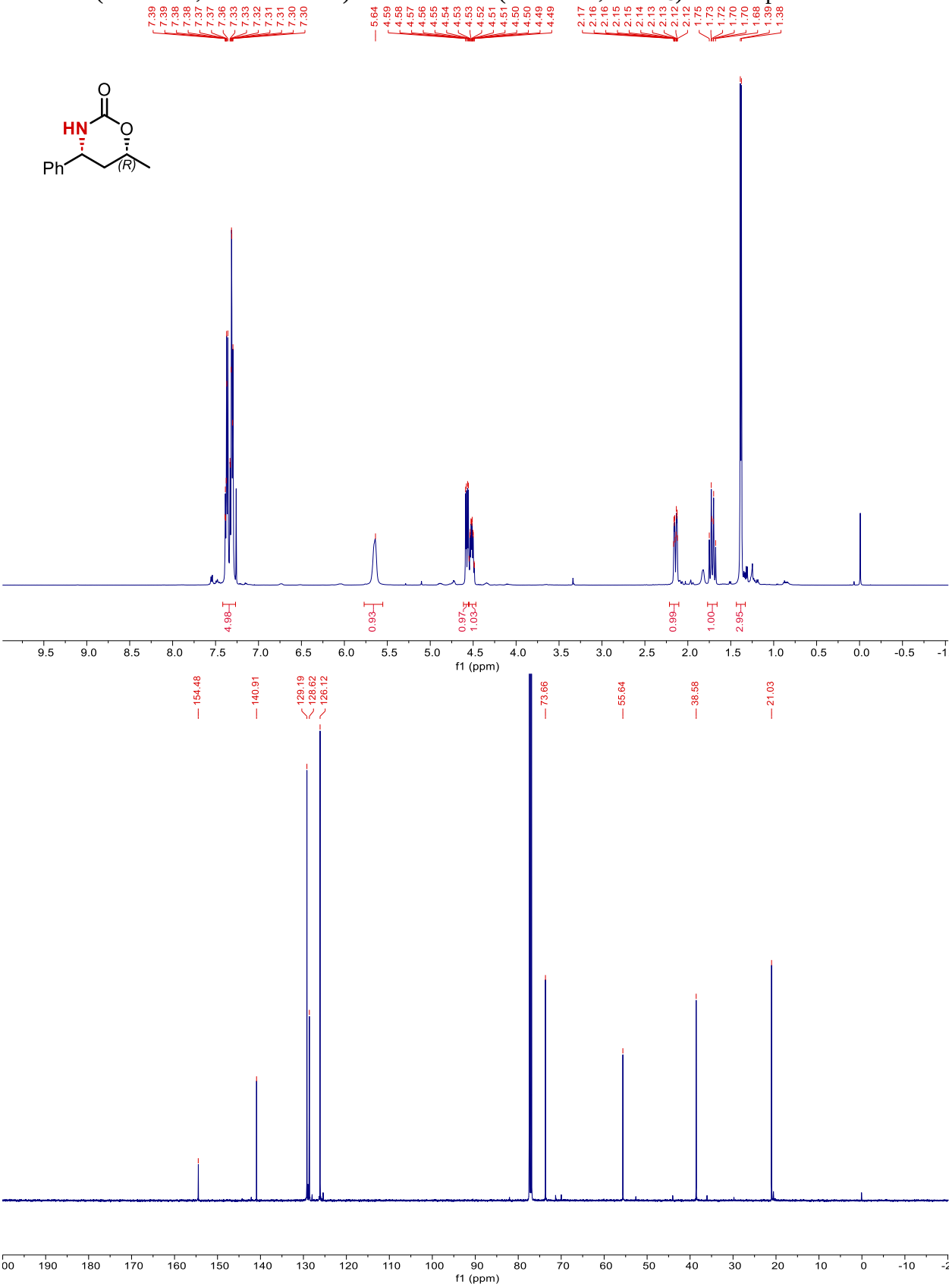

^{1}H NMR (500 MHz, Chloroform-*d*) and ^{13}C NMR (126 MHz, $CDCl_3$) for compound **2.15a.**

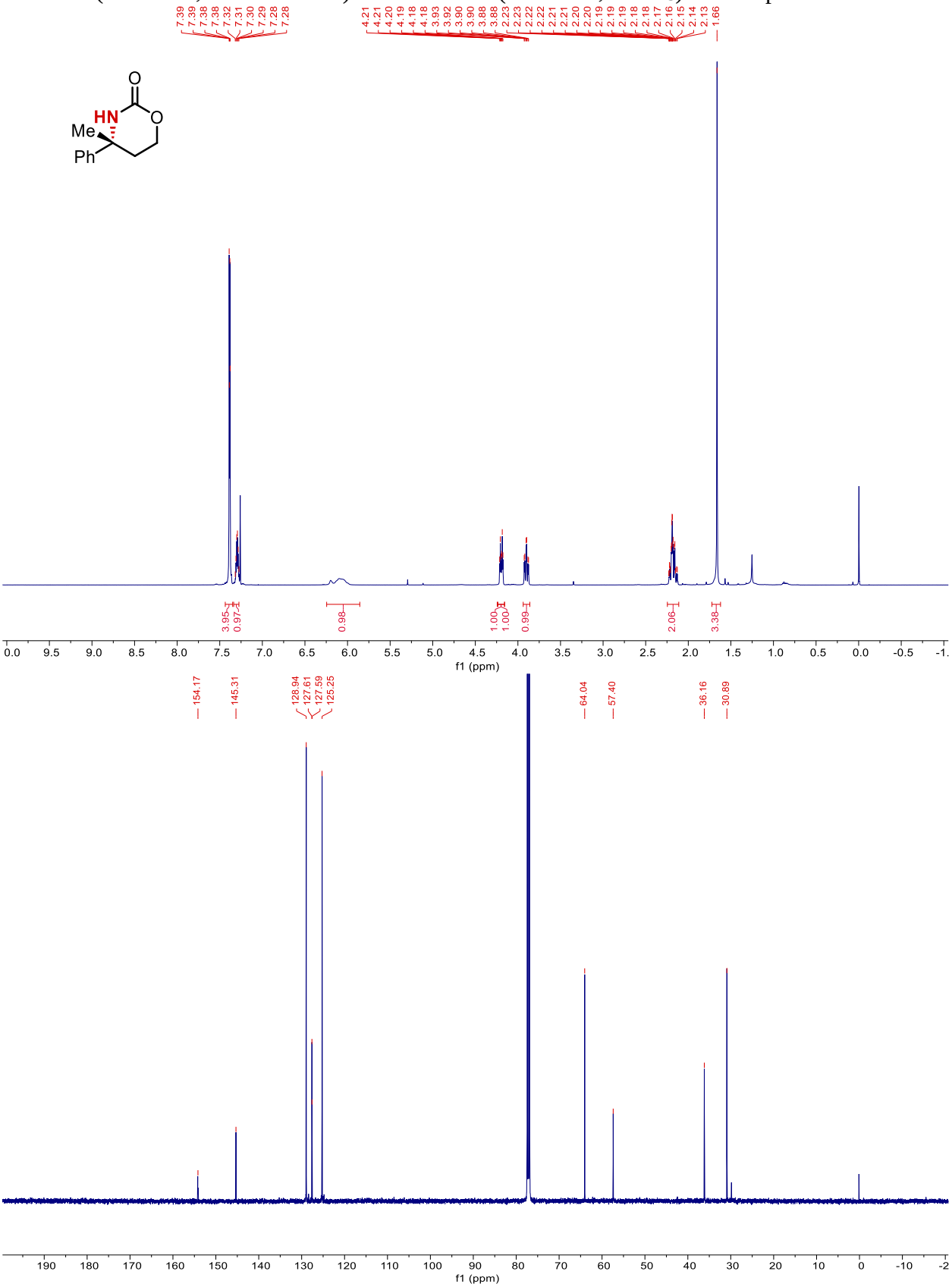

^{1}H NMR (500 MHz, Chloroform-*d*) and ^{13}C NMR (126 MHz, $CDCl_3$) for compound **2.16a.**

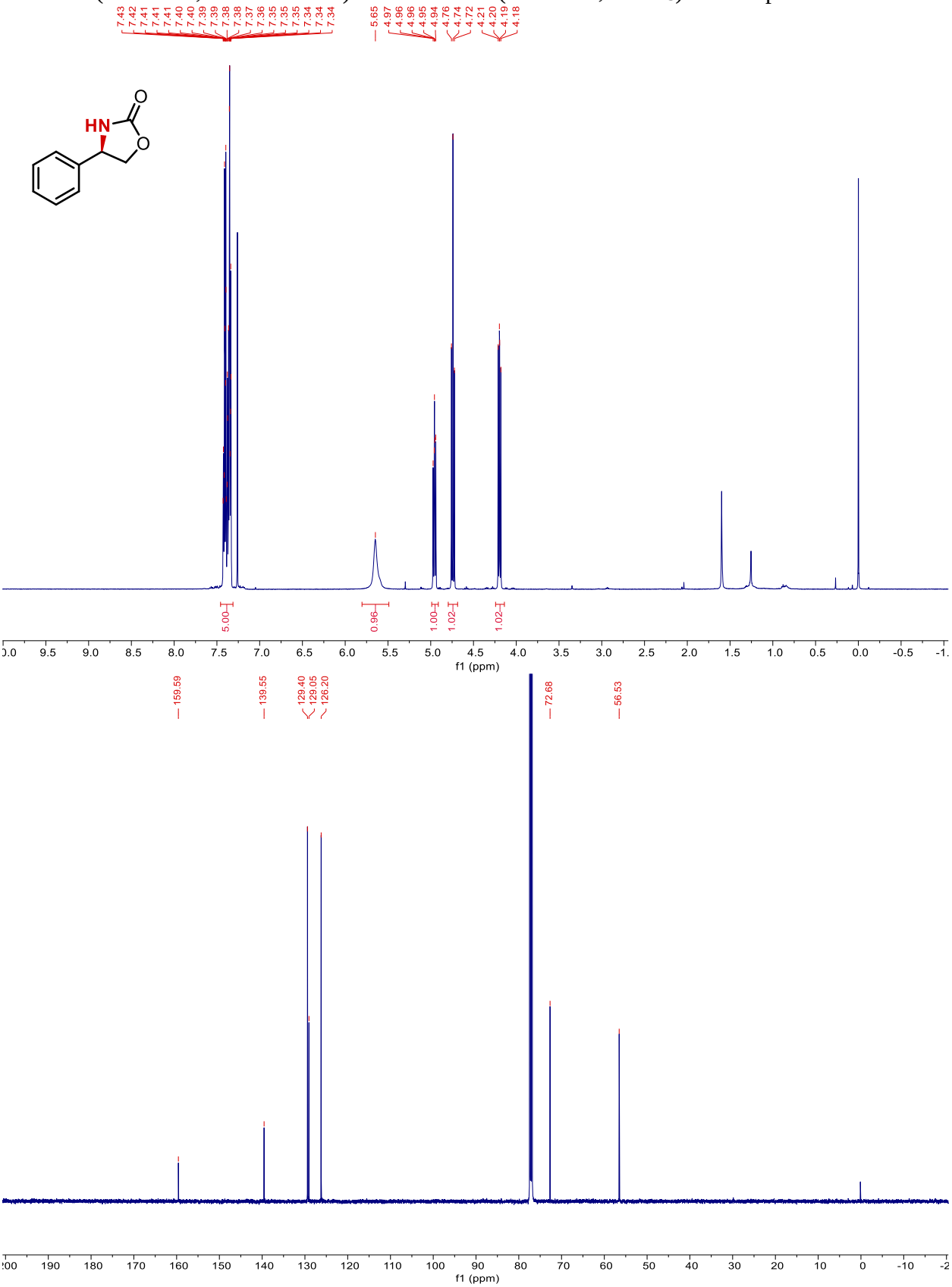

^{1}H NMR (500 MHz, Chloroform-*d*) and ^{13}C NMR (126 MHz, $CDCl_3$) for compound **2.17a.**

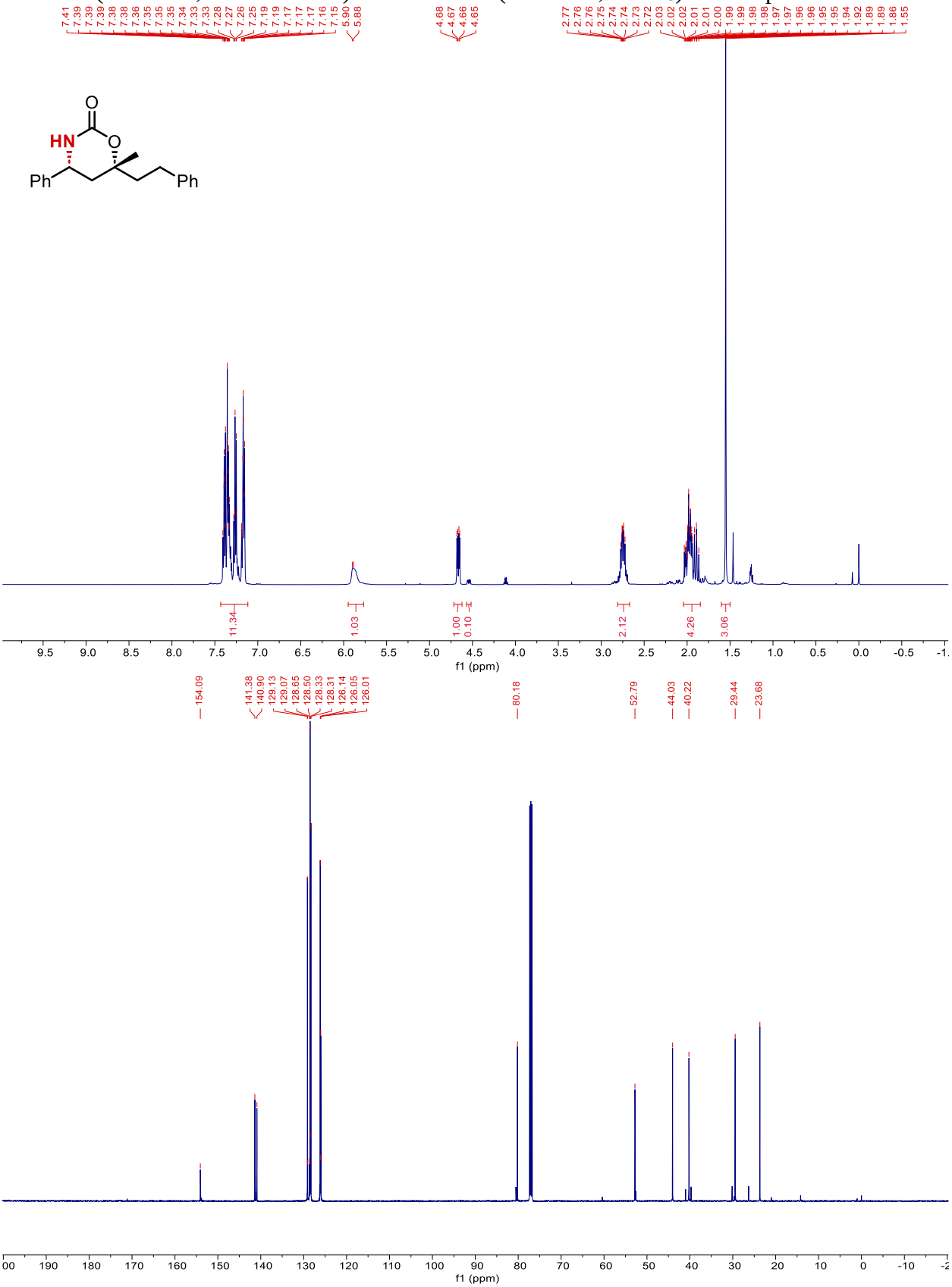

^{1}H NMR (500 MHz, Chloroform-*d*) and ^{13}C NMR (126 MHz, $CDCl_3$) for compound **2.18a-*syn*.**

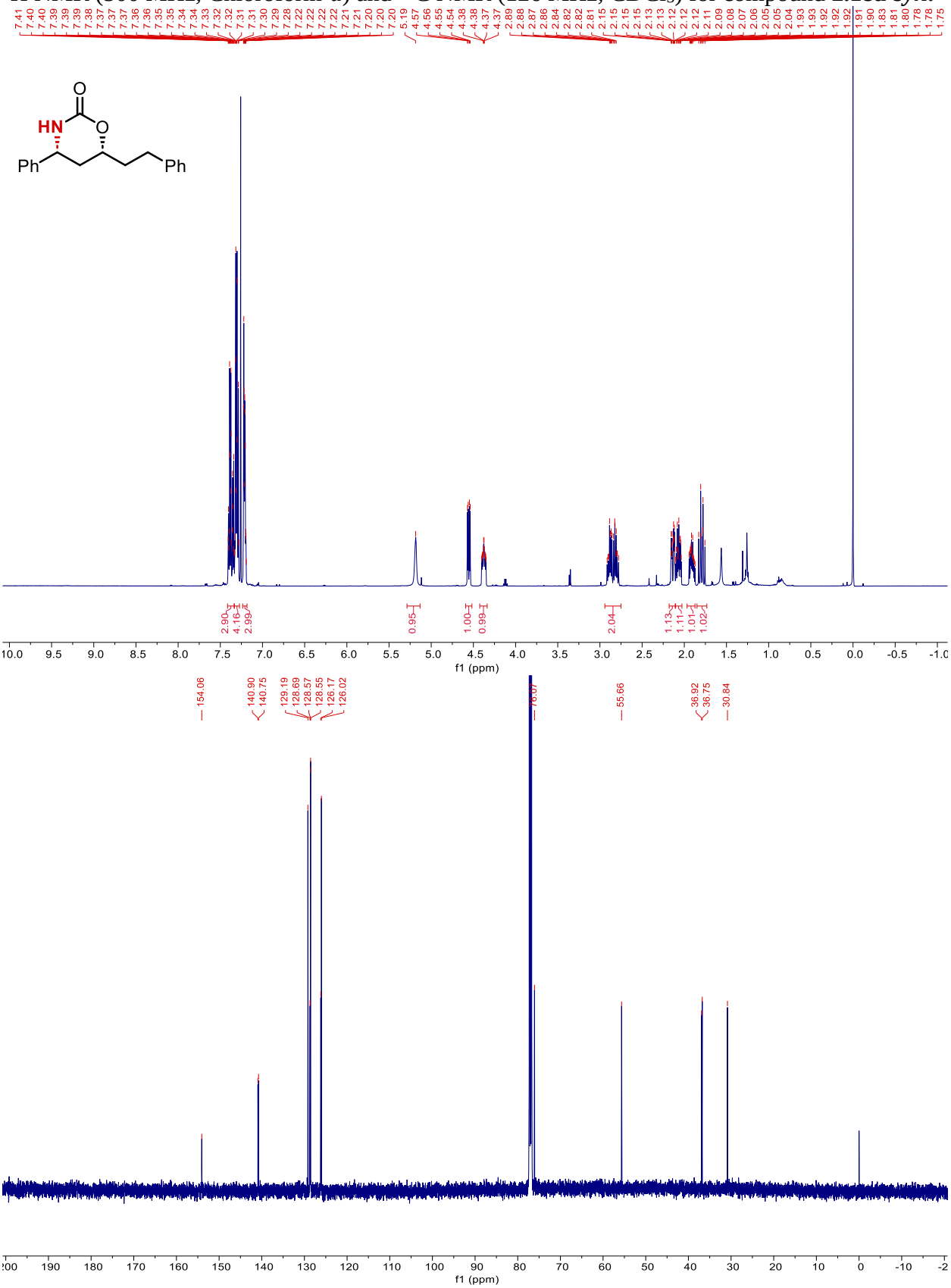

^{1}H NMR (500 MHz, Chloroform-*d*) and ^{13}C NMR (126 MHz, $CDCl_3$) for compound **2.18a-*anti*.**

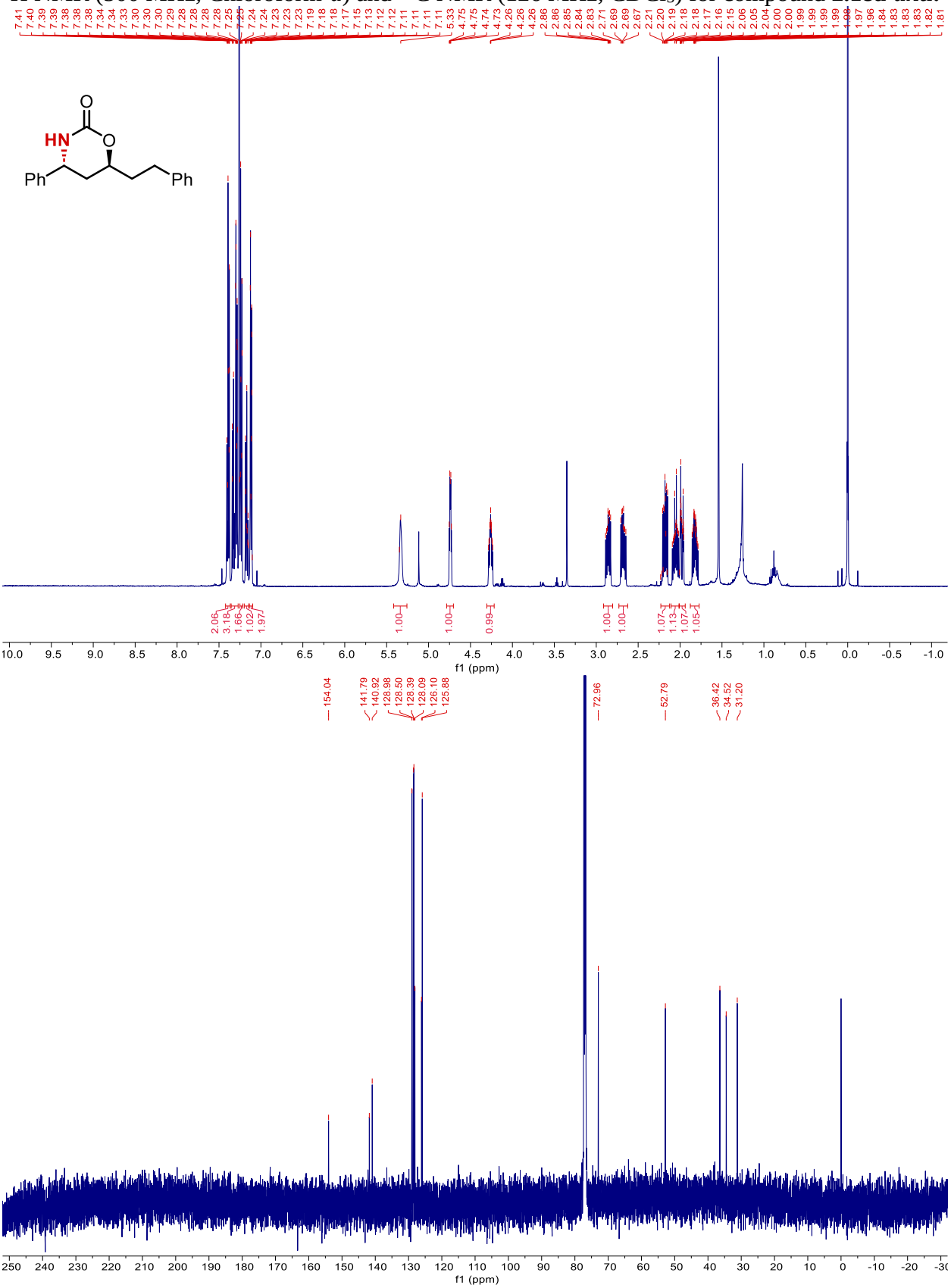

^{1}H NMR (500 MHz, Chloroform-*d*) and ^{13}C NMR (126 MHz, $CDCl_3$) for compound **2.19a.**

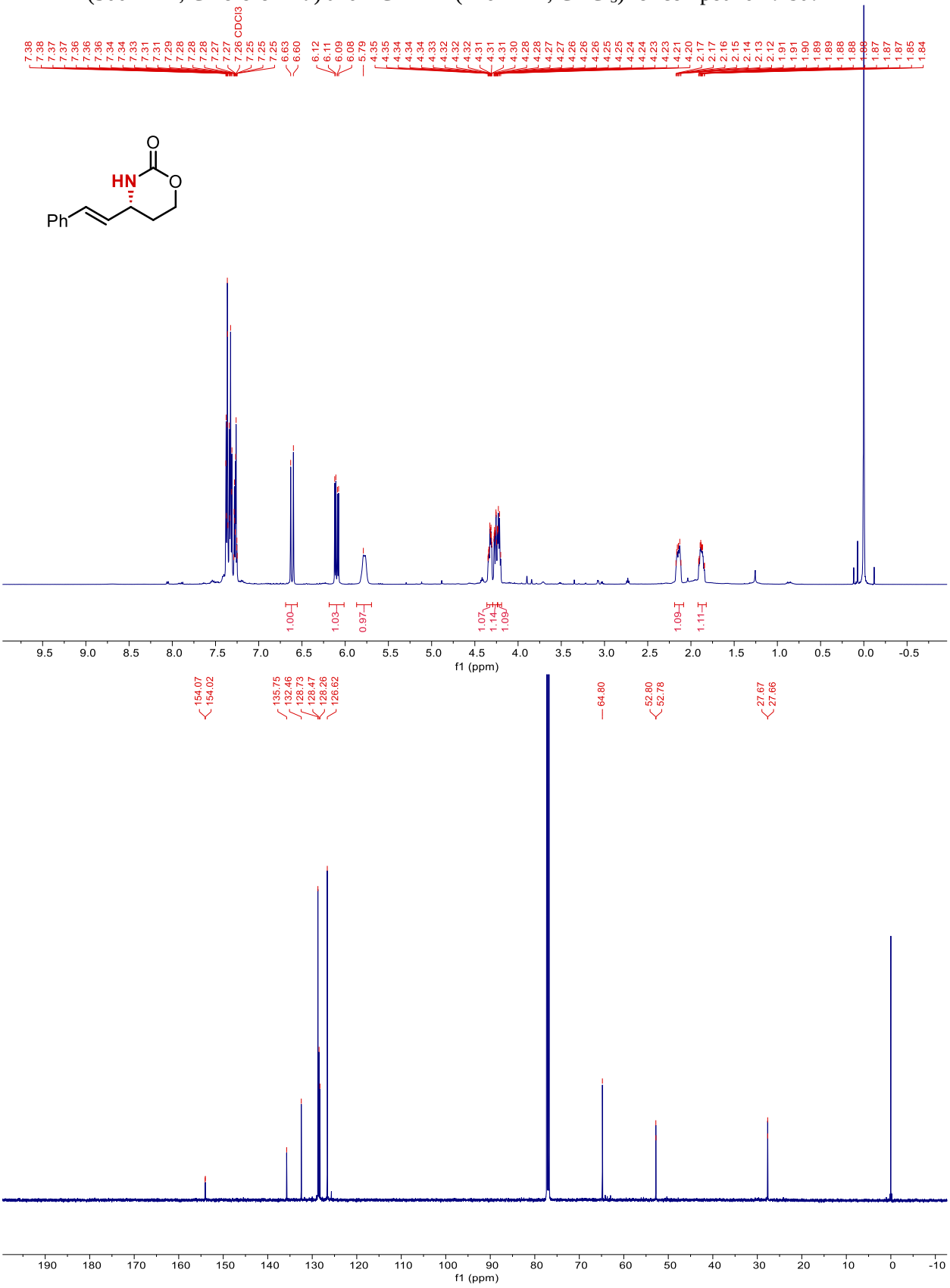

^{1}H NMR (500 MHz, Chloroform-*d*) and ^{13}C NMR (126 MHz, $CDCl_3$) for compound **2.20a.**

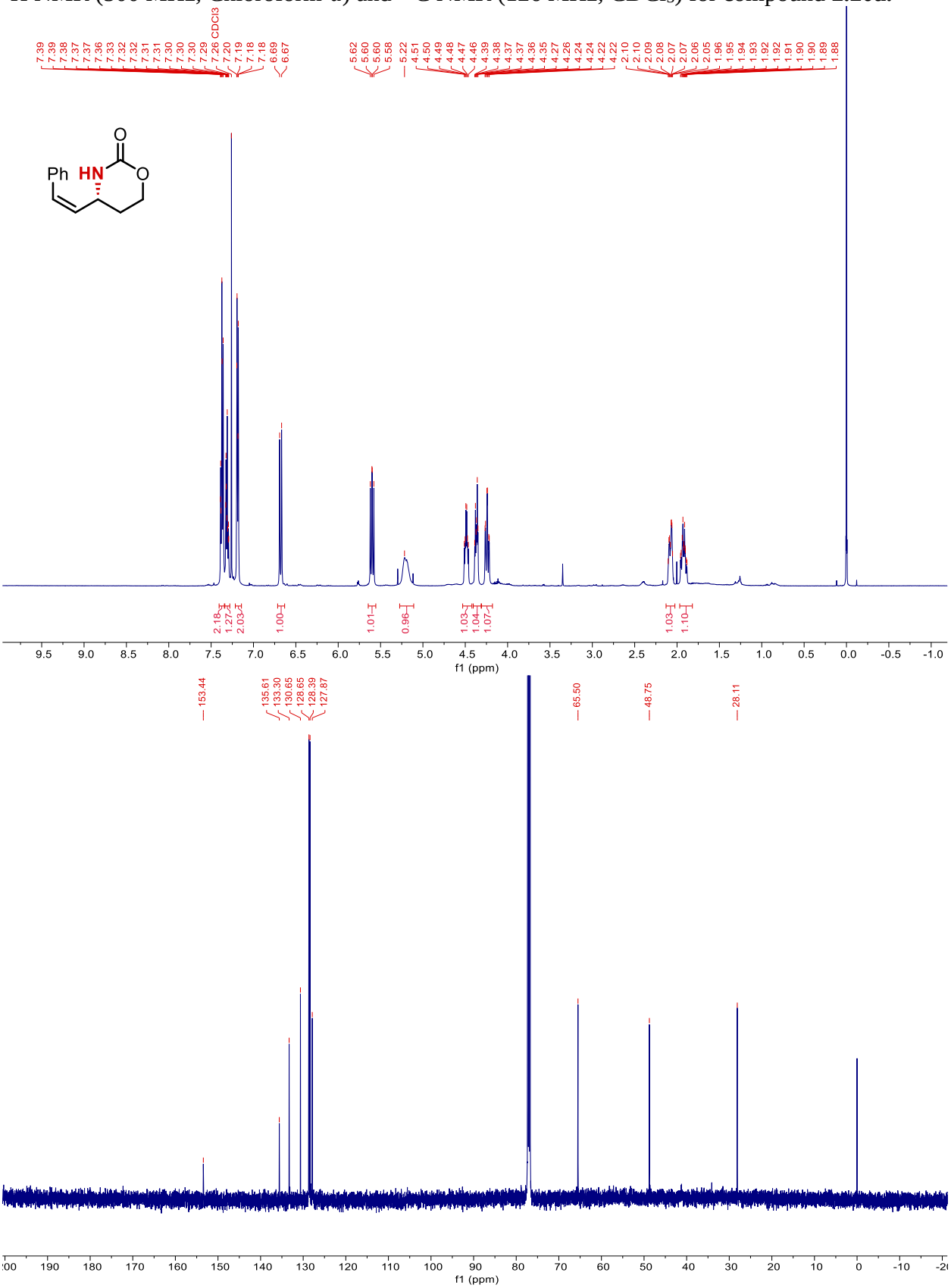

^{1}H NMR (500 MHz, Chloroform-*d*) and ^{13}C NMR (126 MHz, $CDCl_3$) for compound **2.21a.**

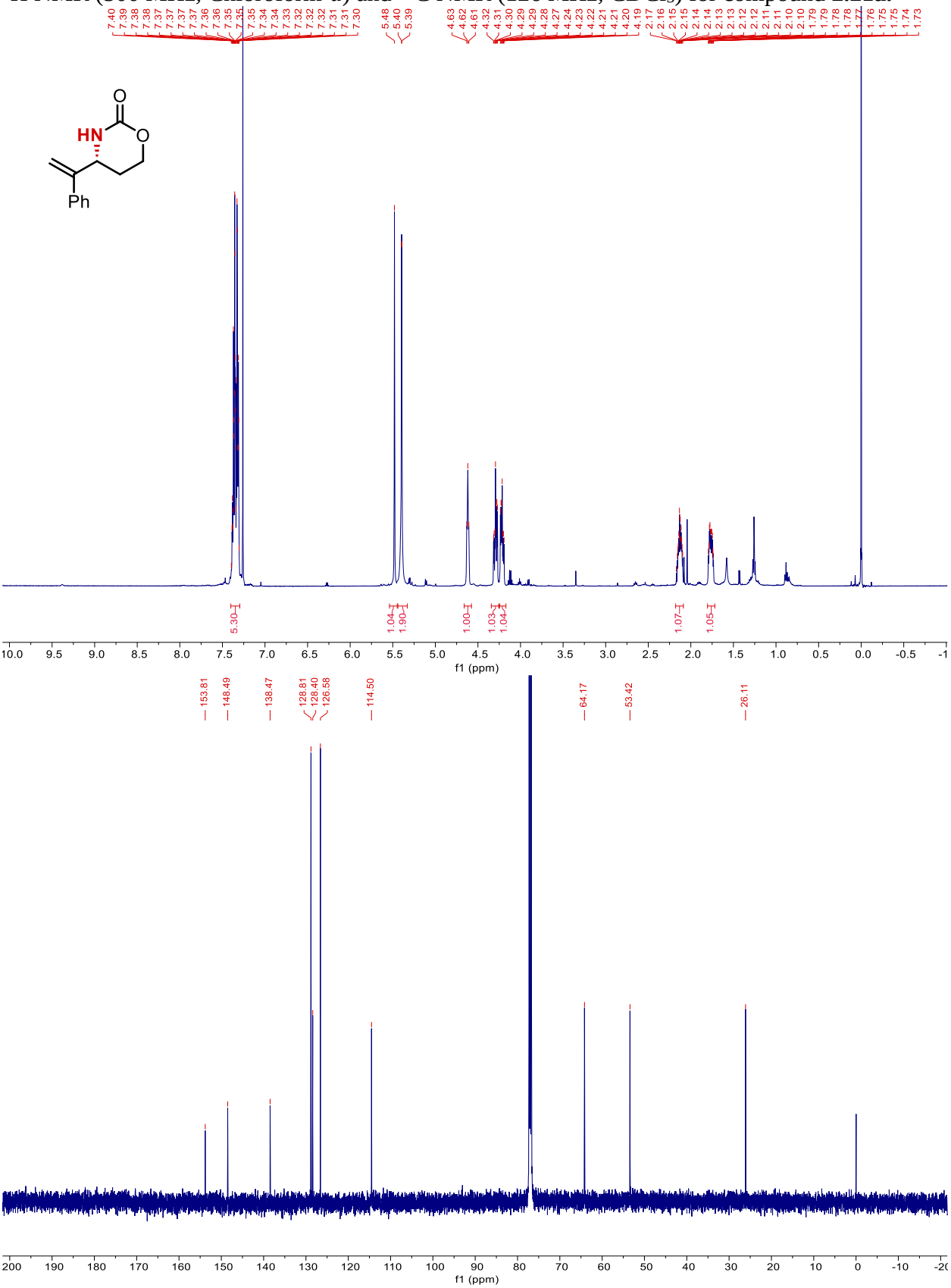

^{1}H NMR (500 MHz, Chloroform-*d*) and ^{13}C NMR (126 MHz, $CDCl_3$) for compound **2.22a.**

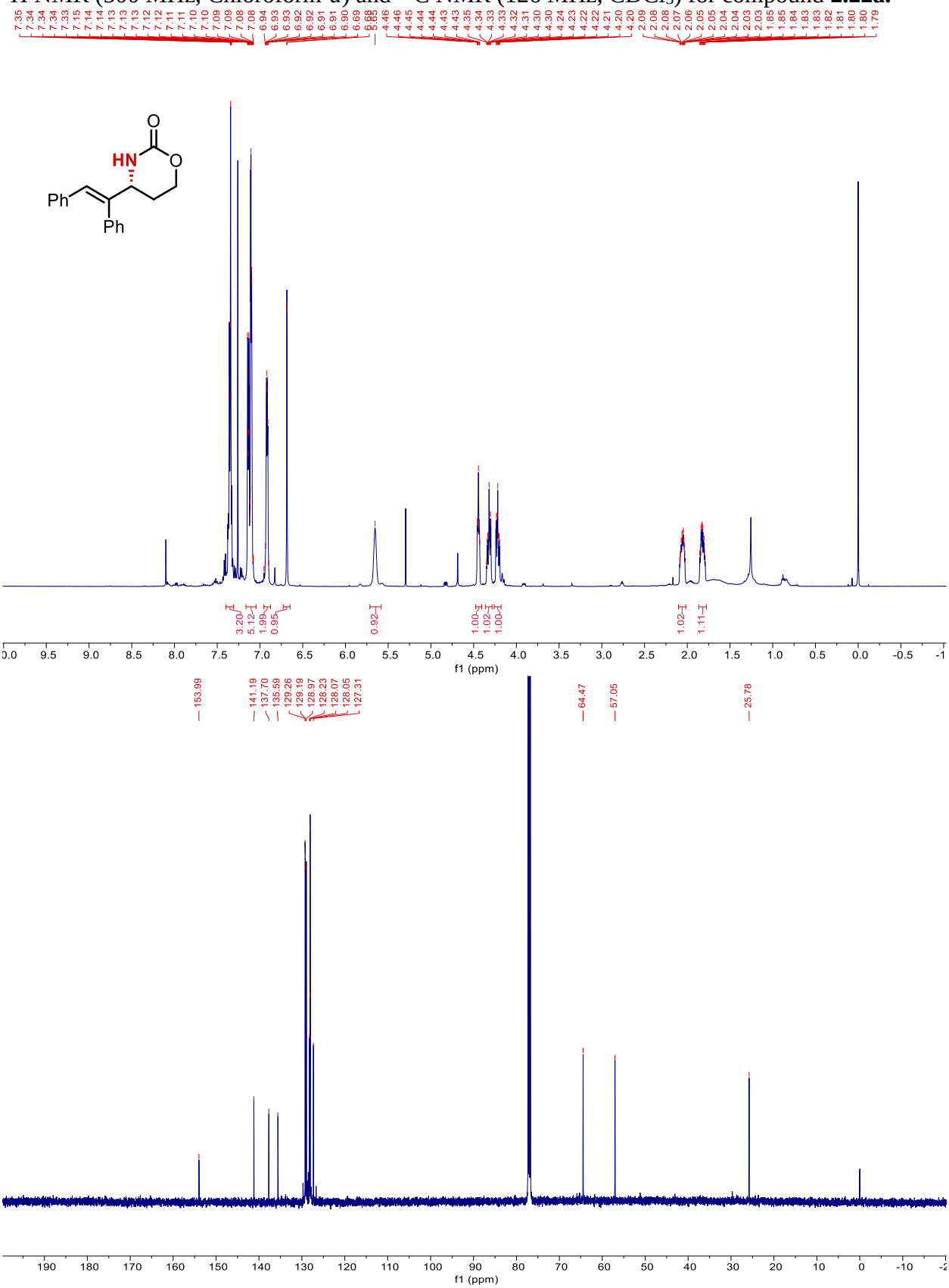

^{1}H NMR (500 MHz, Chloroform-*d*) and ^{13}C NMR (126 MHz, $CDCl_3$) for compound **2.23a.**

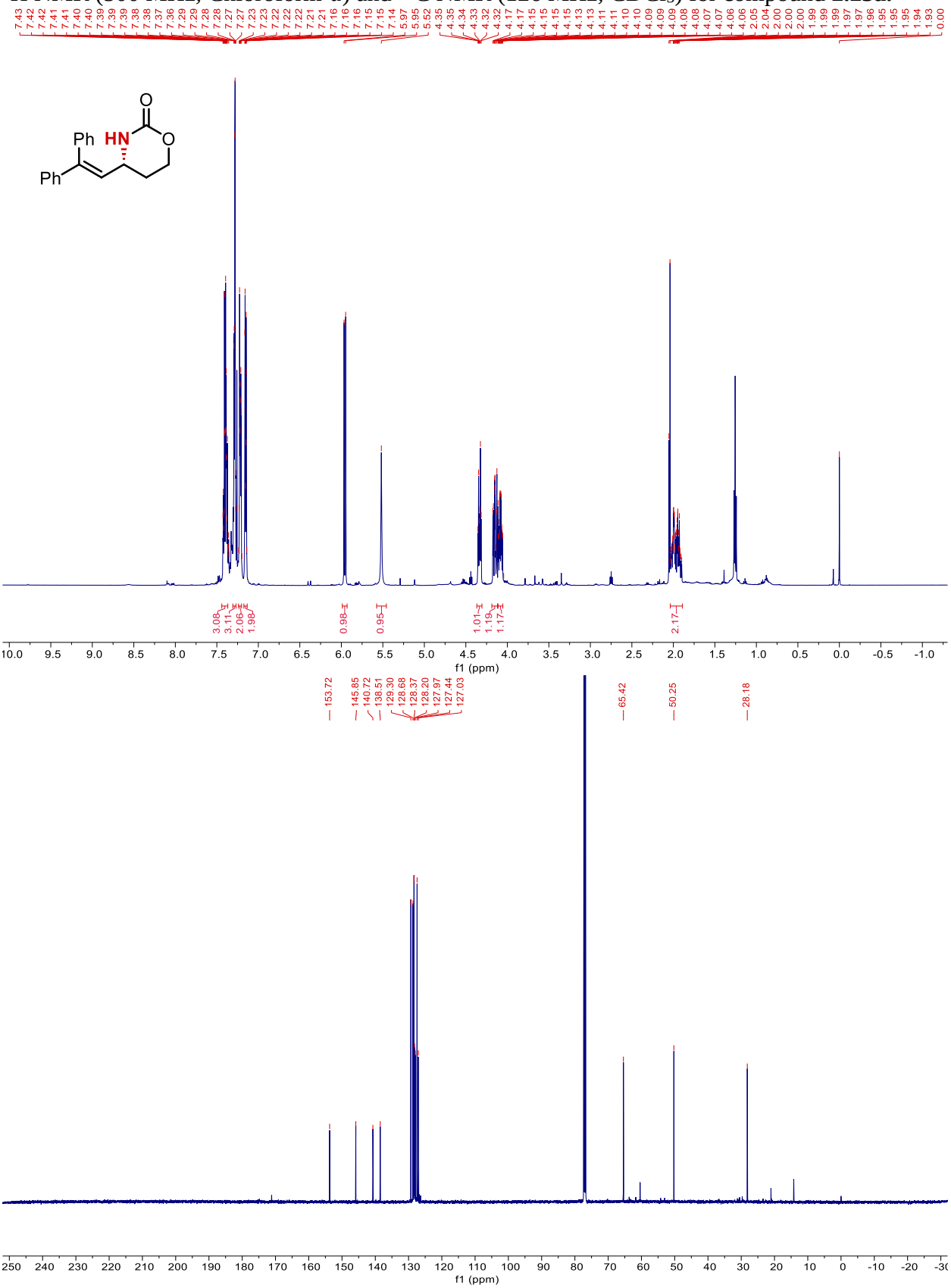

^{1}H NMR (500 MHz, Chloroform-*d*) and ^{13}C NMR (126 MHz, $CDCl_3$) for compound **2.24a.**

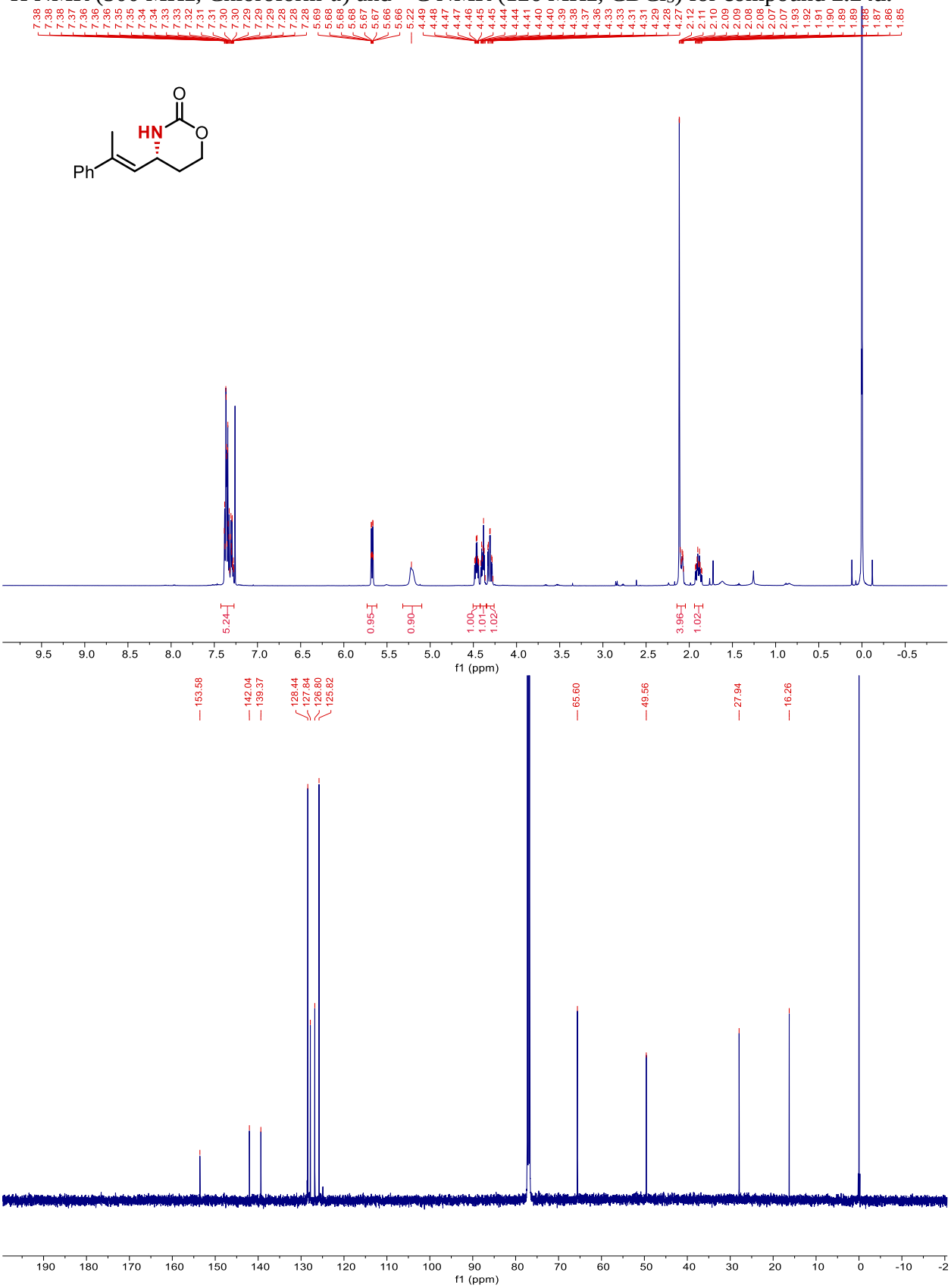

^{1}H NMR (500 MHz, Chloroform-*d*) and ^{13}C NMR (126 MHz, $CDCl_3$) for compound **2.25a.**

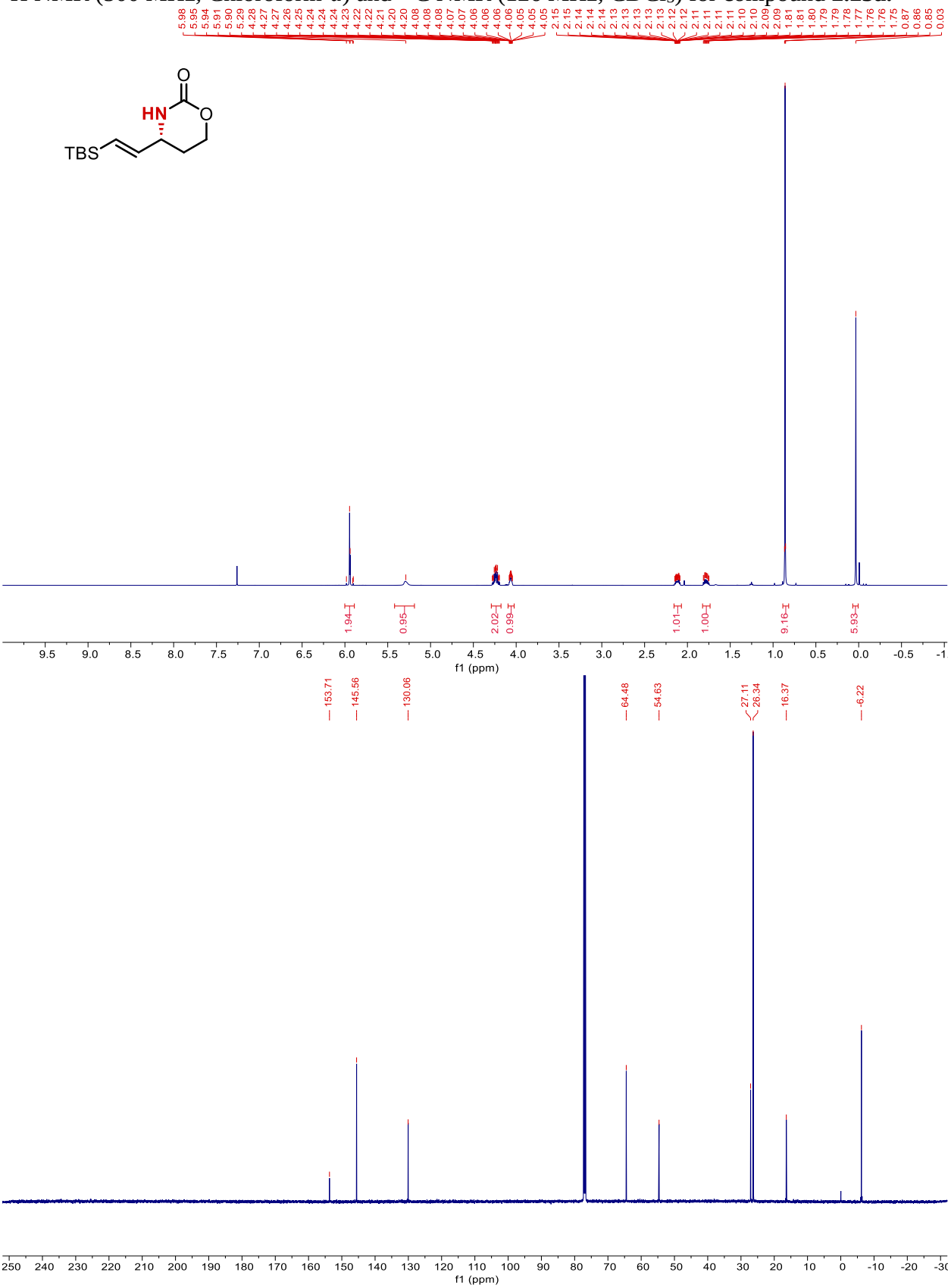

^{1}H NMR (500 MHz, Chloroform-*d*) and ^{13}C NMR (126 MHz, $CDCl_3$) for compound **2.26a.**

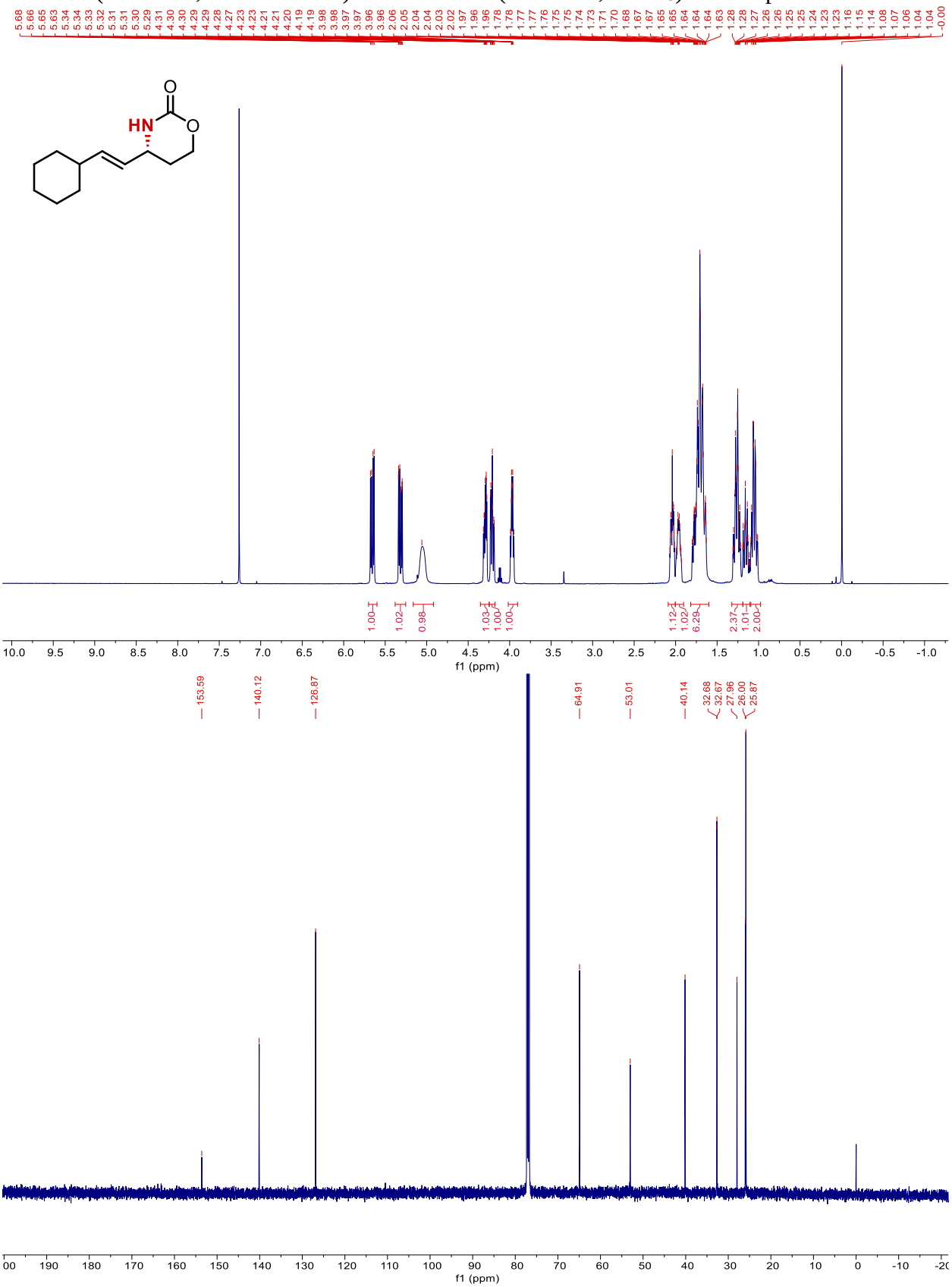

^{1}H NMR (500 MHz, Chloroform-*d*) and ^{13}C NMR (126 MHz, $CDCl_3$) for compound **2.27a.**

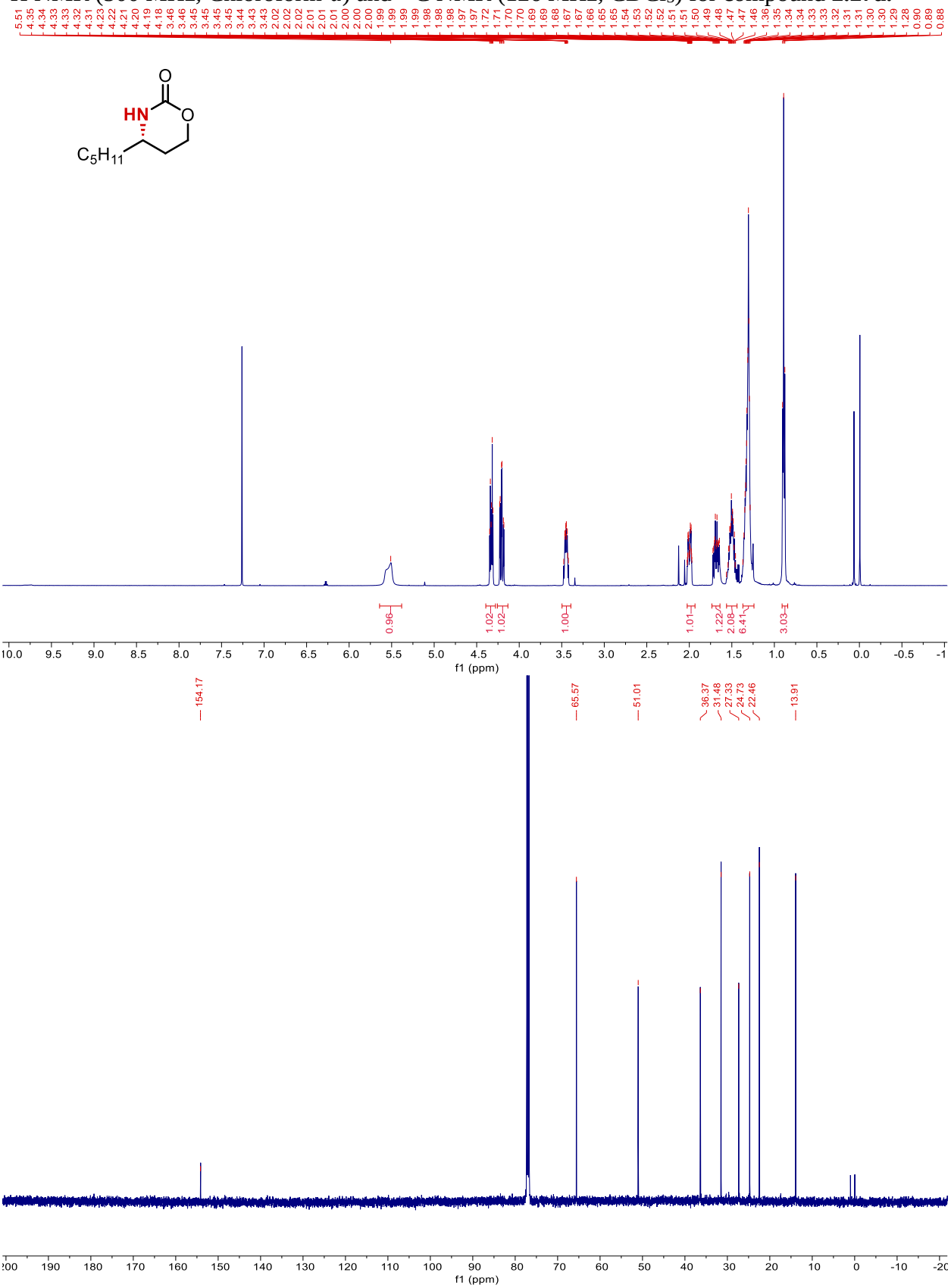

^{1}H NMR (500 MHz, Chloroform-*d*) and ^{13}C NMR (126 MHz, $CDCl_3$) for compound **2.28a.**

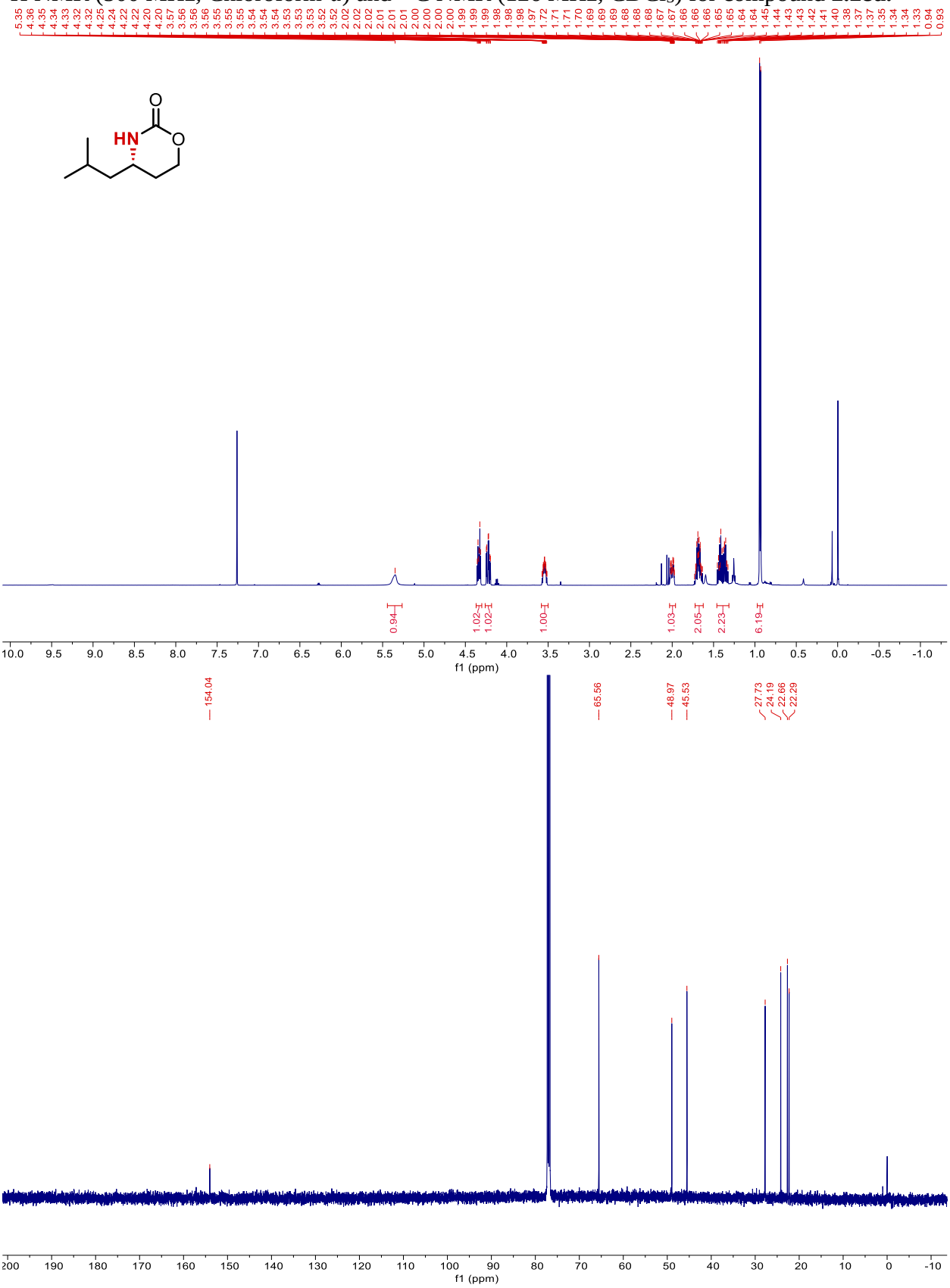

^{1}H NMR (500 MHz, Chloroform-*d*) and ^{13}C NMR (126 MHz, $CDCl_3$) for compound **2.29a.**

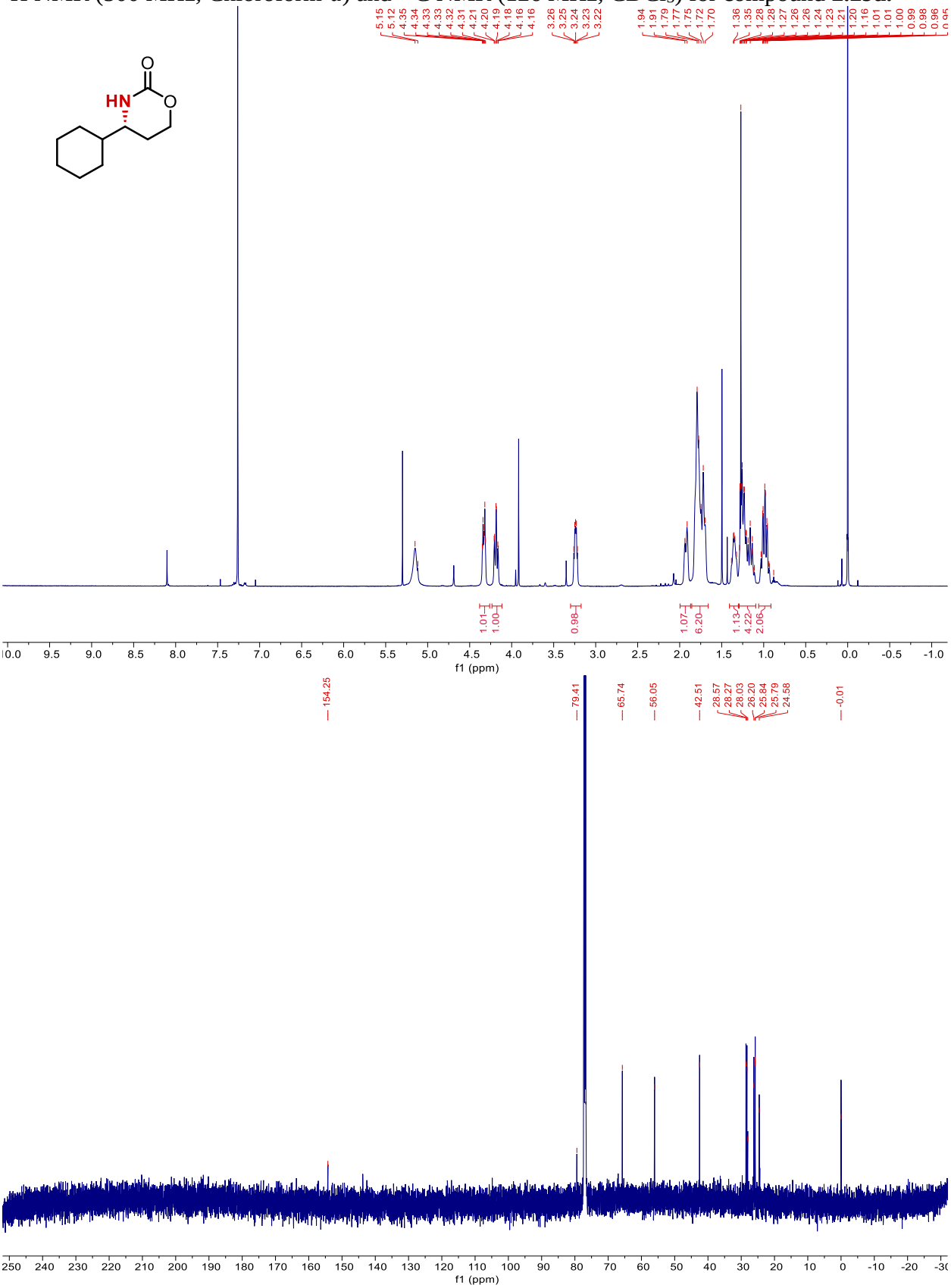

^{1}H NMR (500 MHz, Chloroform-*d*) and ^{13}C NMR (126 MHz, $CDCl_3$) for compound **2.30a.**

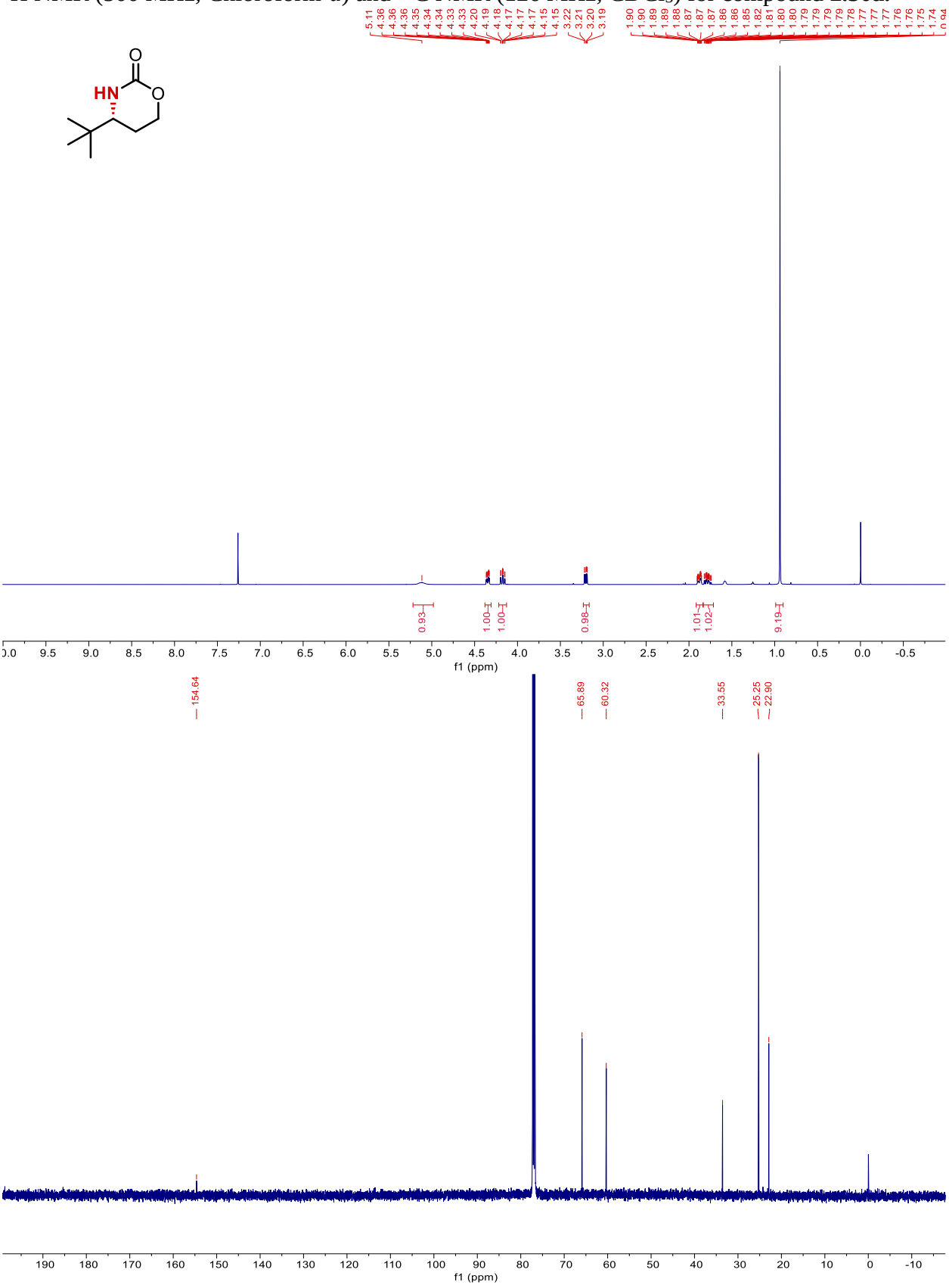

^{1}H NMR (500 MHz, Chloroform-*d*) and ^{13}C NMR (126 MHz, $CDCl_3$) for compound **2.31a.**

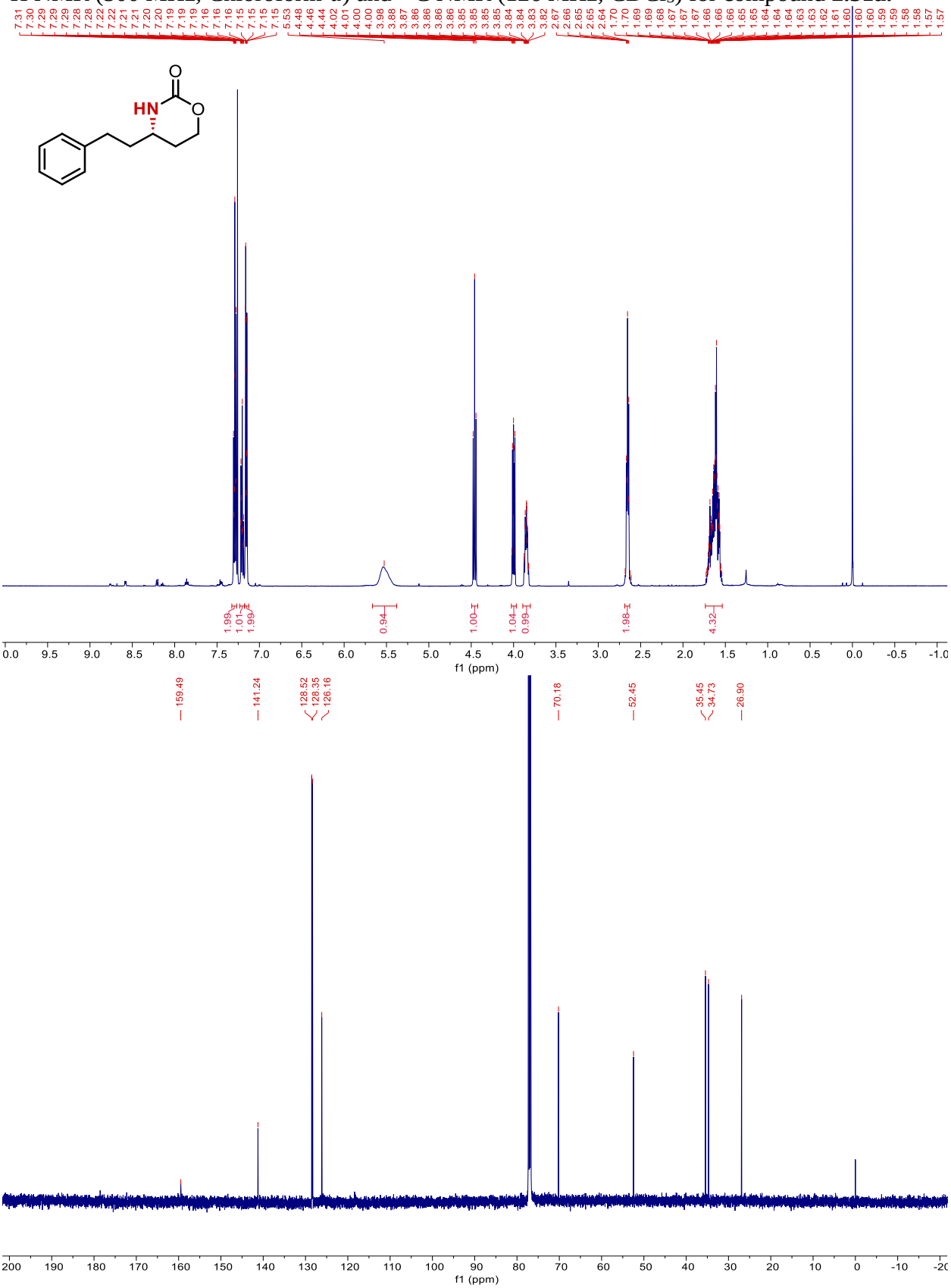

^{1}H NMR (500 MHz, Chloroform-*d*) and ^{13}C NMR (126 MHz, $CDCl_3$) for compound **2.32a.**

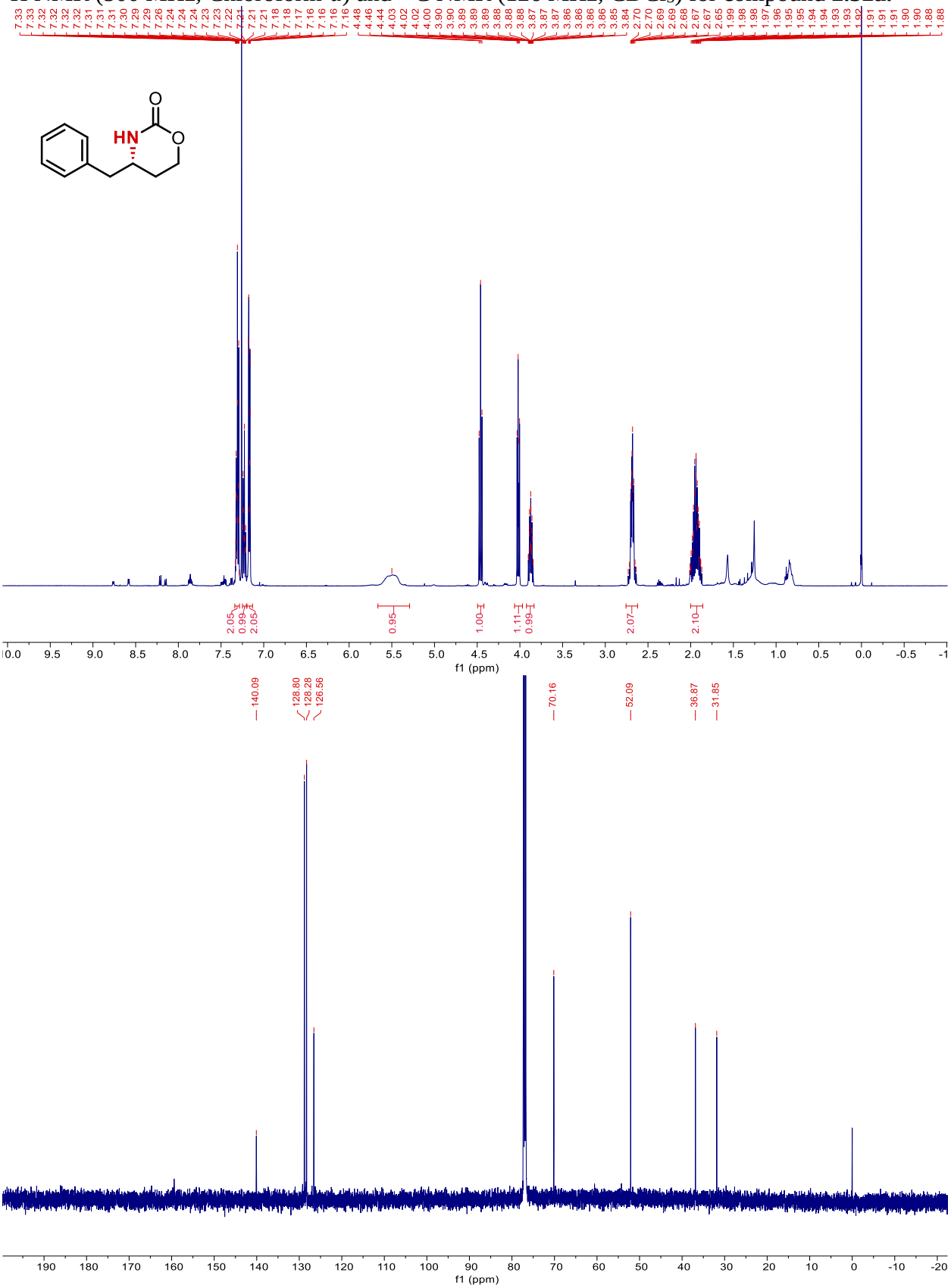

^{1}H NMR (500 MHz, $CDCl_3$) and ^{13}C NMR (126 MHz, $CDCl_3$) for compound **(*S*)-Dapoxetine.**

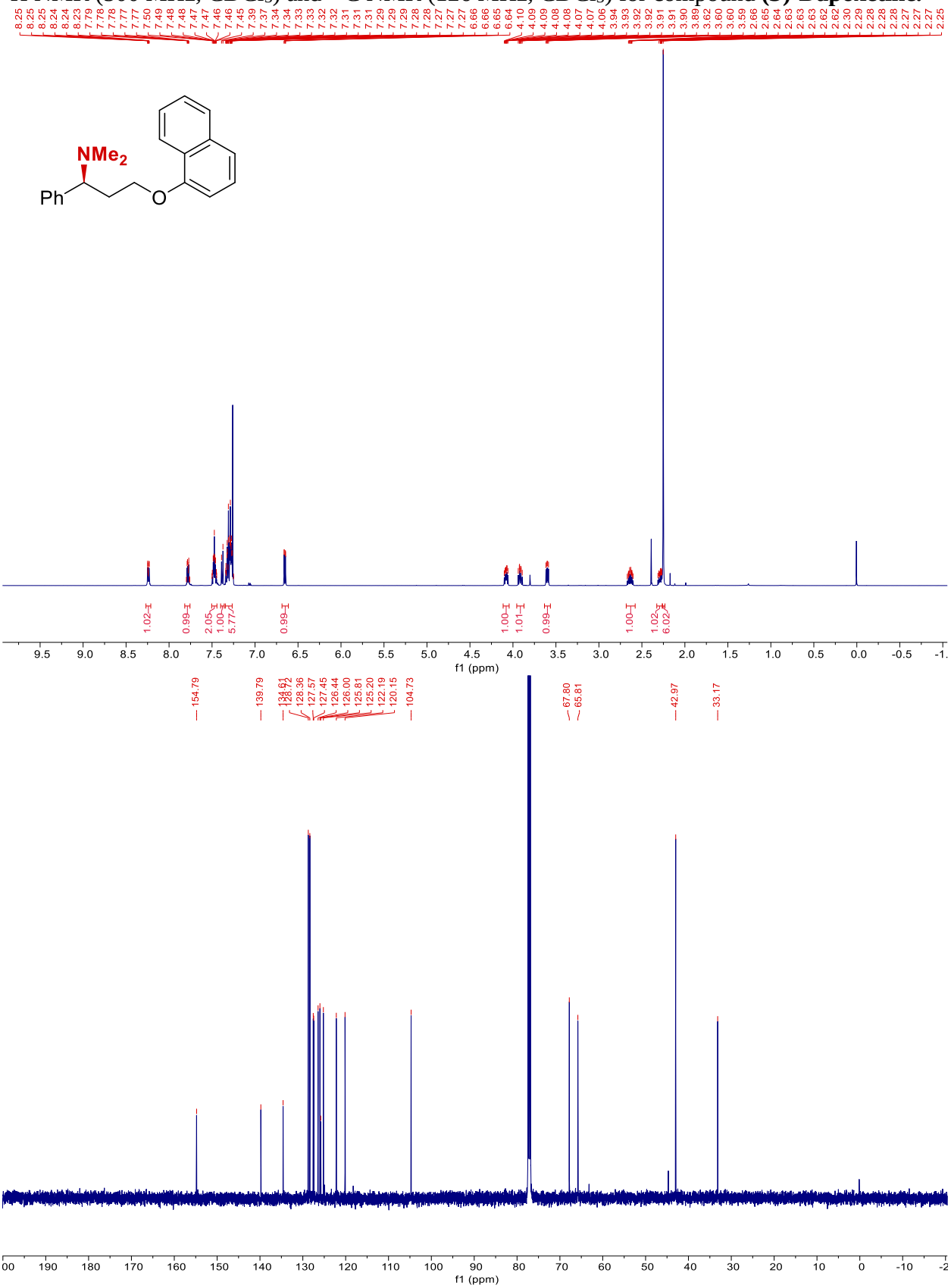

^{1}H NMR (500 MHz, Chloroform-*d*) and ^{13}C NMR (126 MHz, $CDCl_3$) for compound **2.33.**

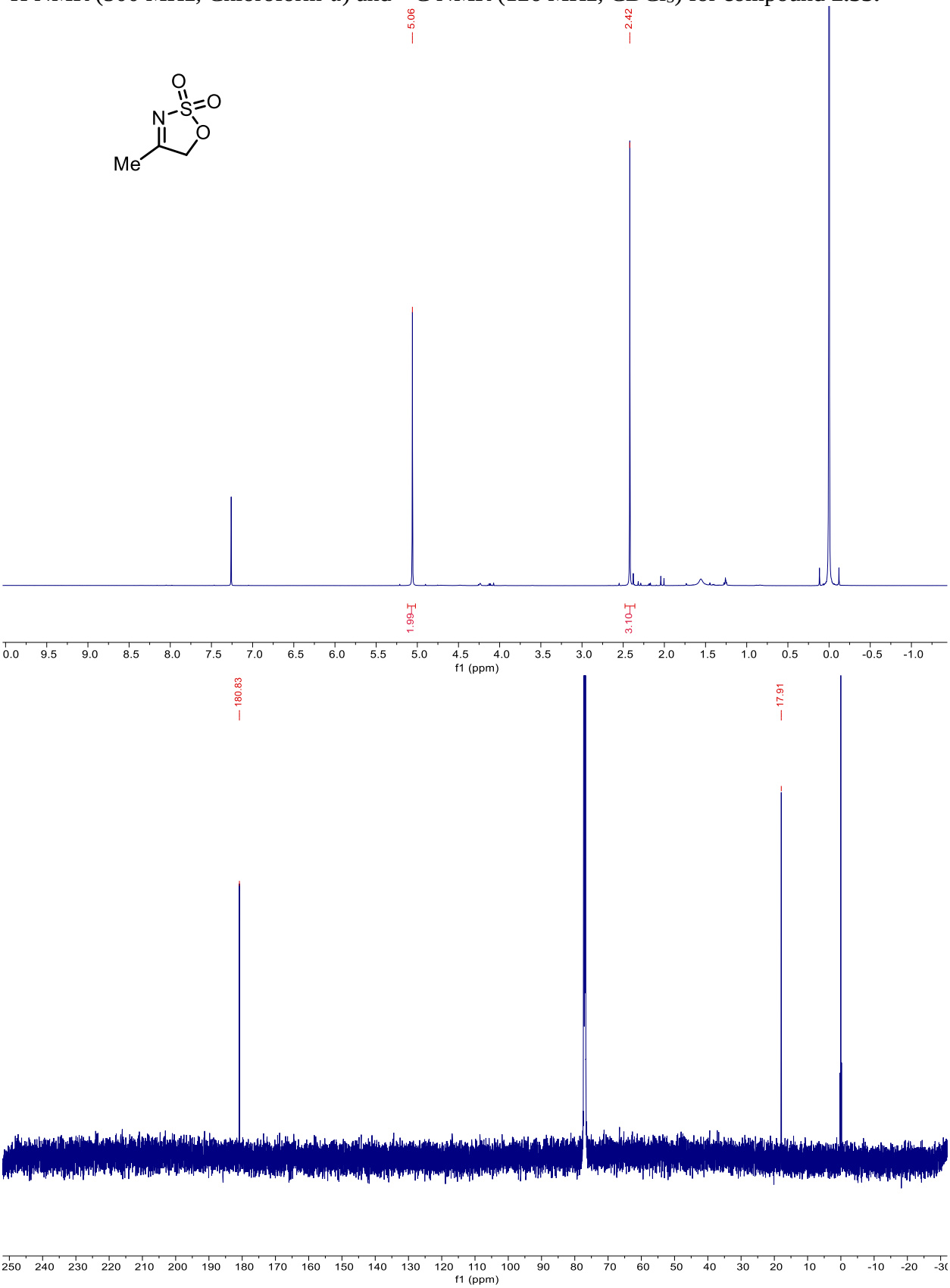

^{1}H NMR (500 MHz, Chloroform-*d*) and ^{13}C NMR (126 MHz, $CDCl_3$) for compound **2.34.**

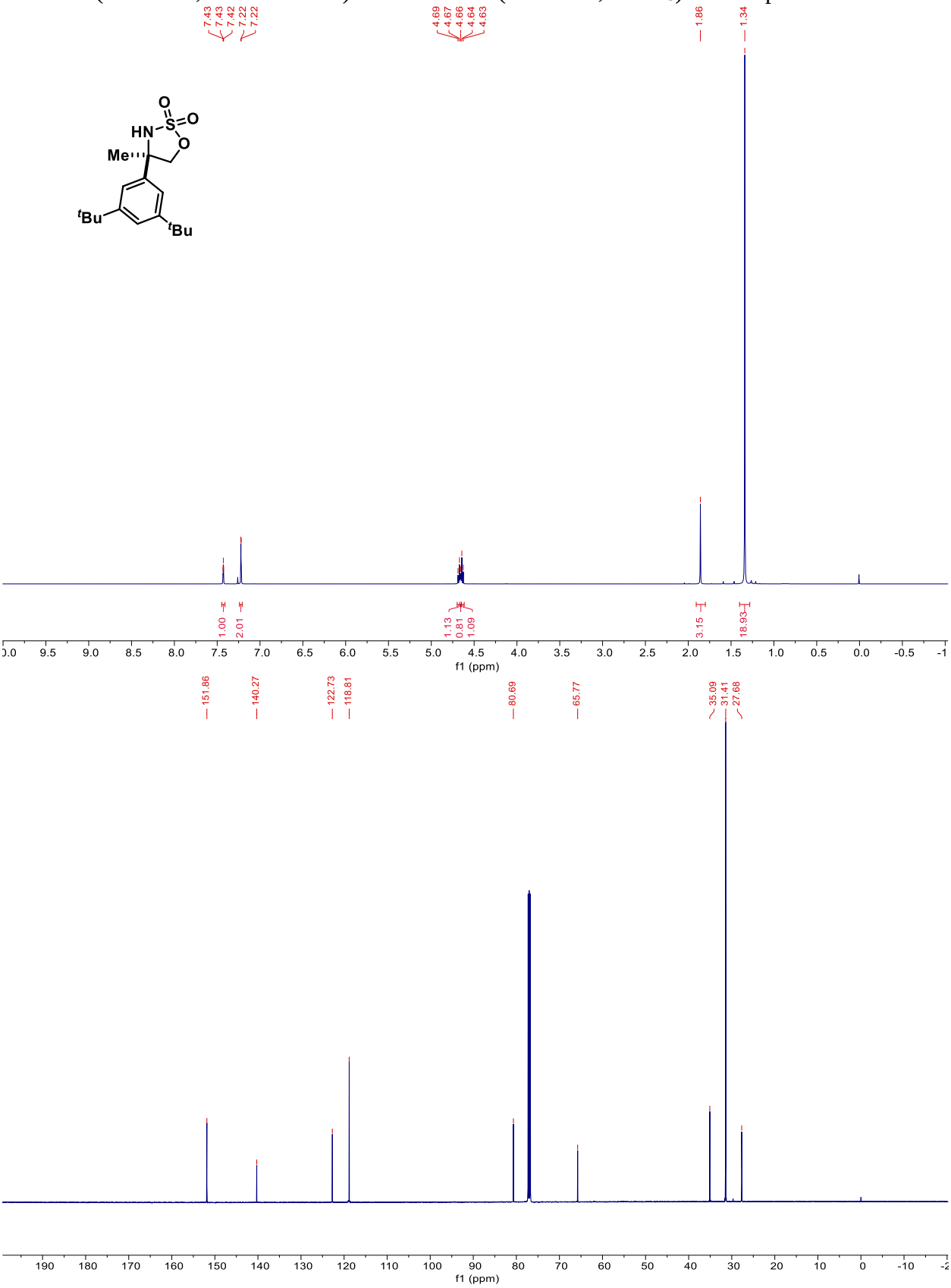

^{1}H NMR (500 MHz, Chloroform-*d*) and ^{13}C NMR (126 MHz, $CDCl_3$) for compound **2.35.**

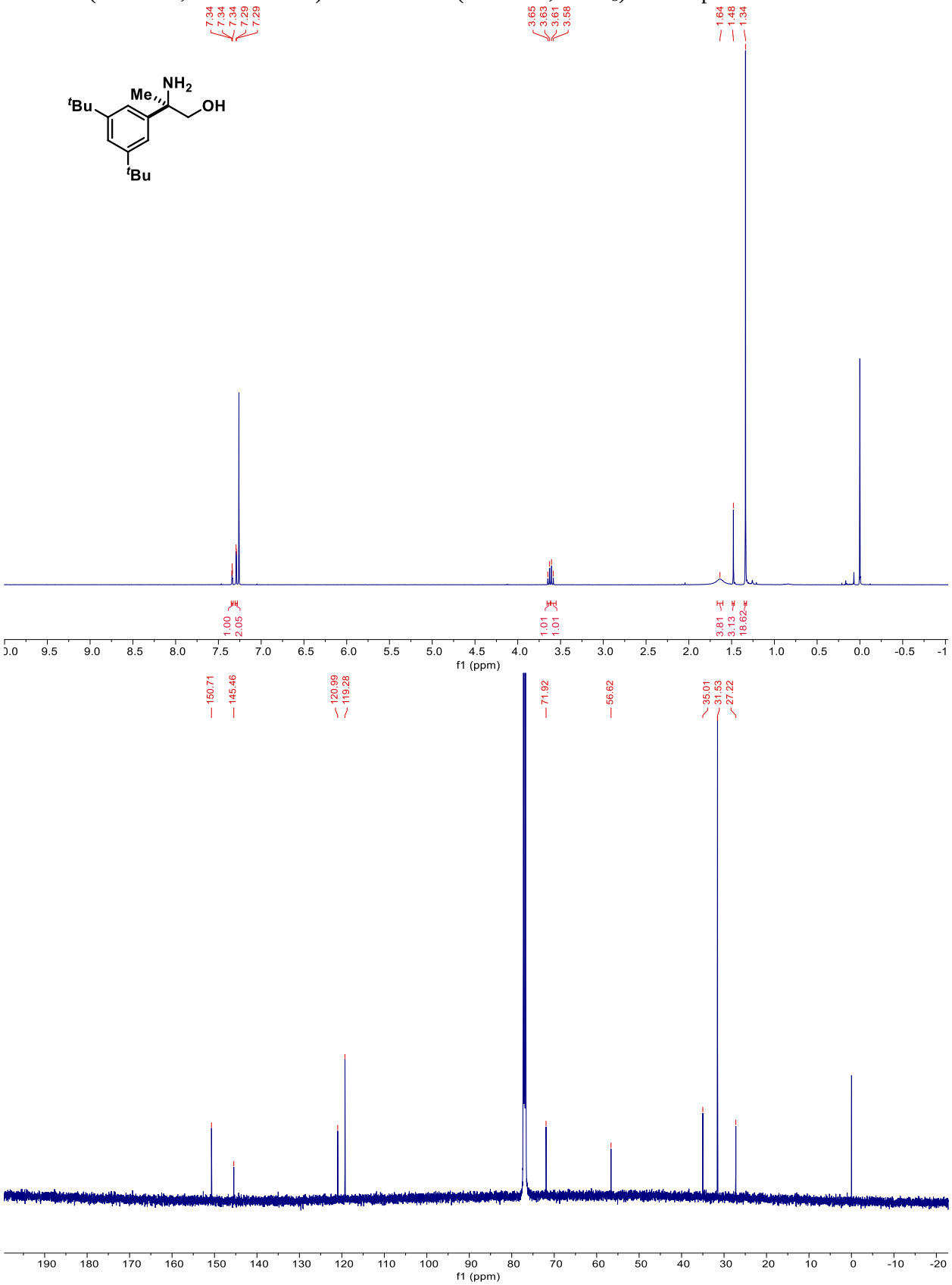

^{1}H NMR (500 MHz, Chloroform-*d*) and ^{13}C NMR (126 MHz, $CDCl_3$) for **(*R*,*R*)-MinBOX.**

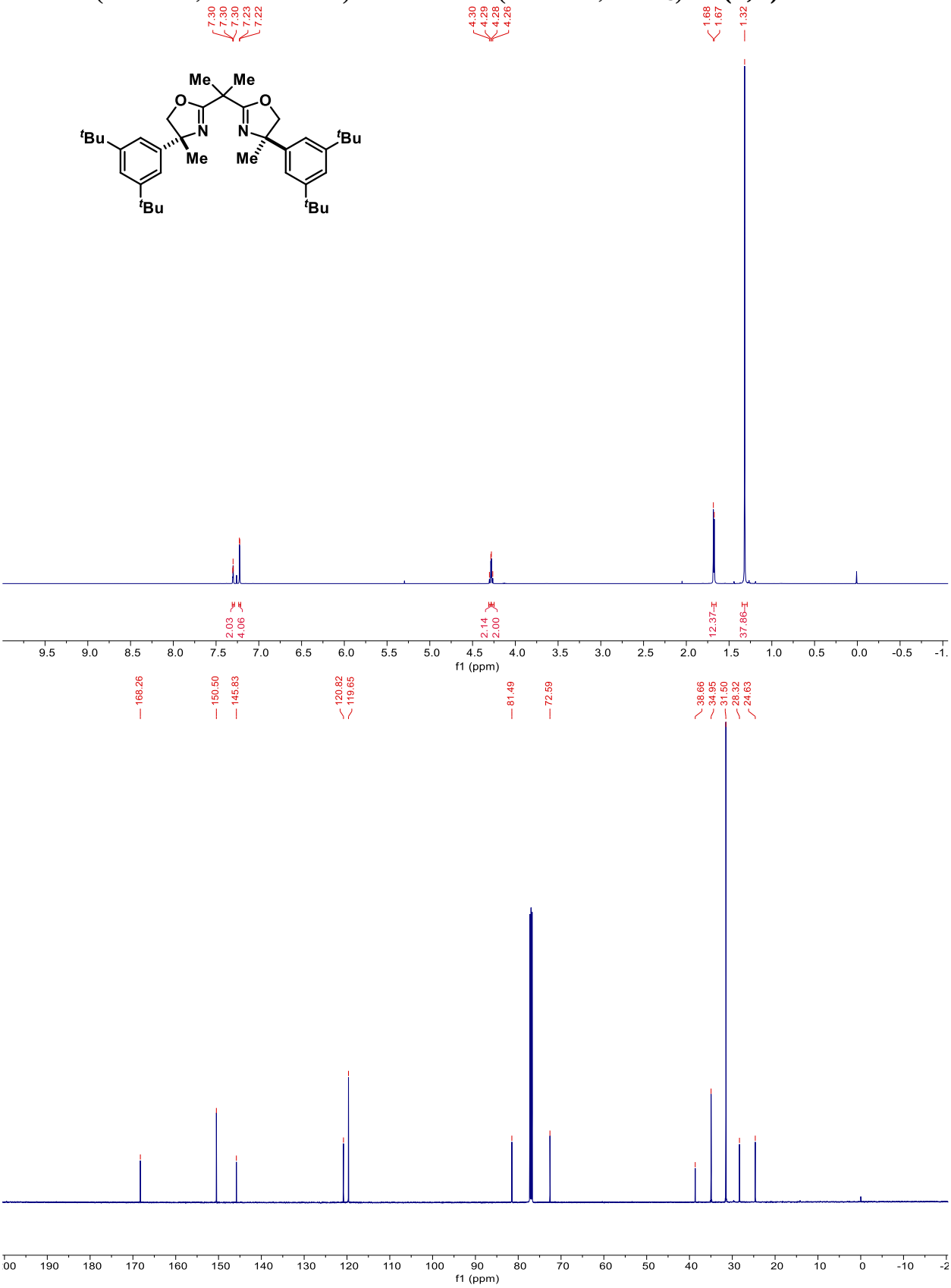

^{1}H NMR (500 MHz, Chloroform-*d*) and ^{13}C NMR (126 MHz, $CDCl_3$) for compound **S2.1.**

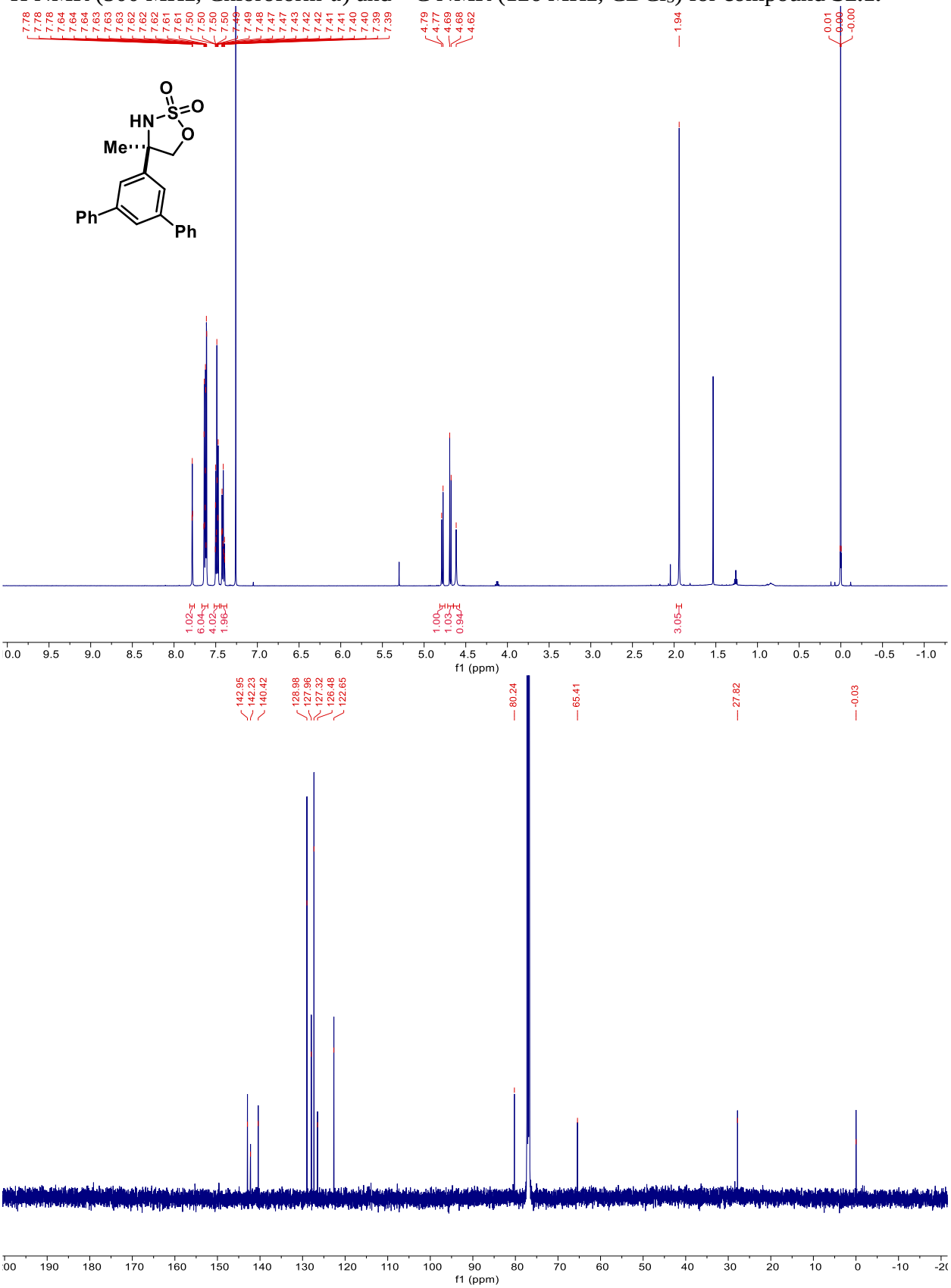

^{1}H NMR (500 MHz, Chloroform-*d*) and ^{13}C NMR (126 MHz, $CDCl_3$) for compound **S2.2.**

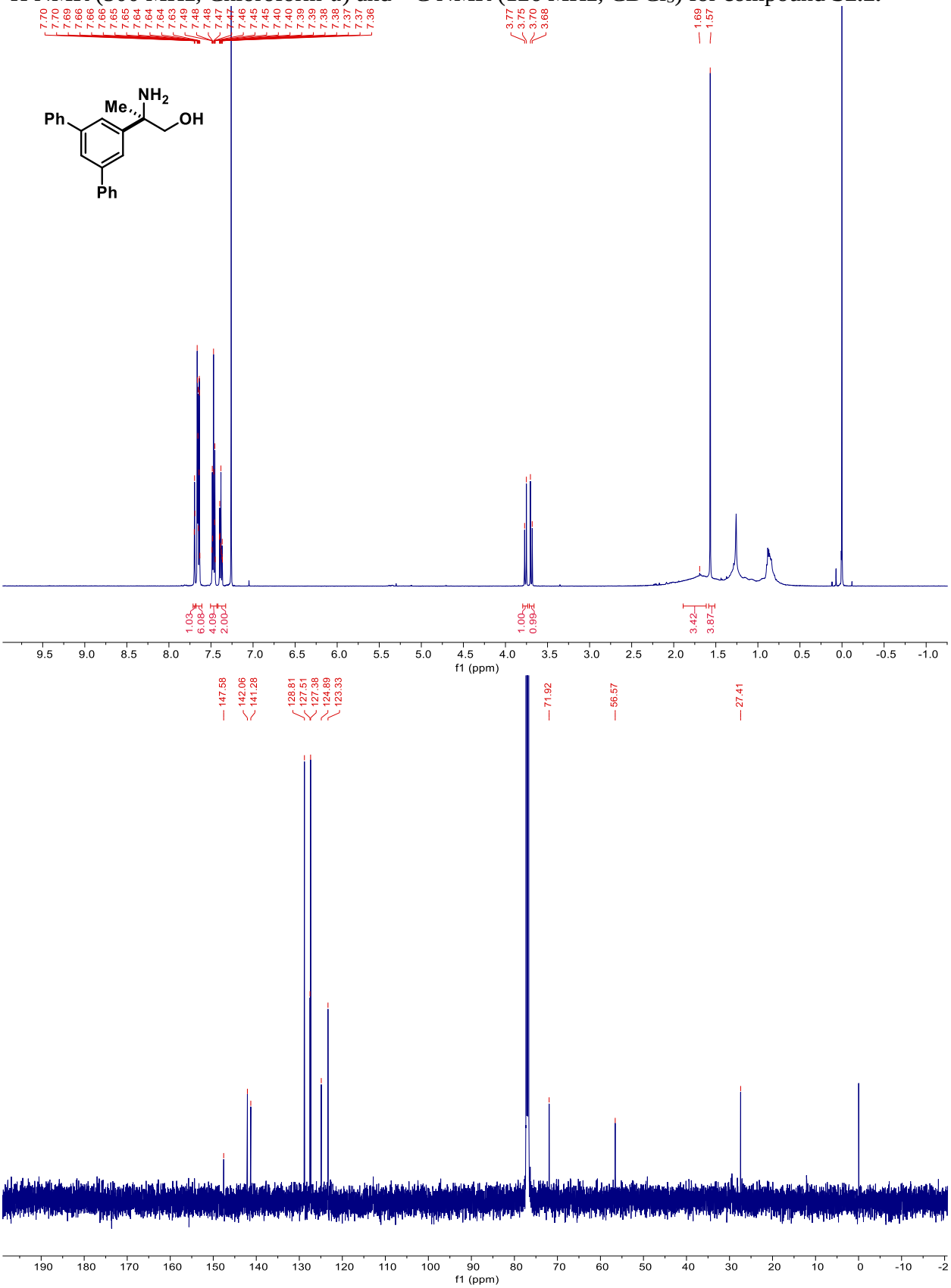

^{1}H NMR (500 MHz, Chloroform-*d*) and ^{13}C NMR (126 MHz, $CDCl_3$) for **(*R*,*R*)-WenBOX.**

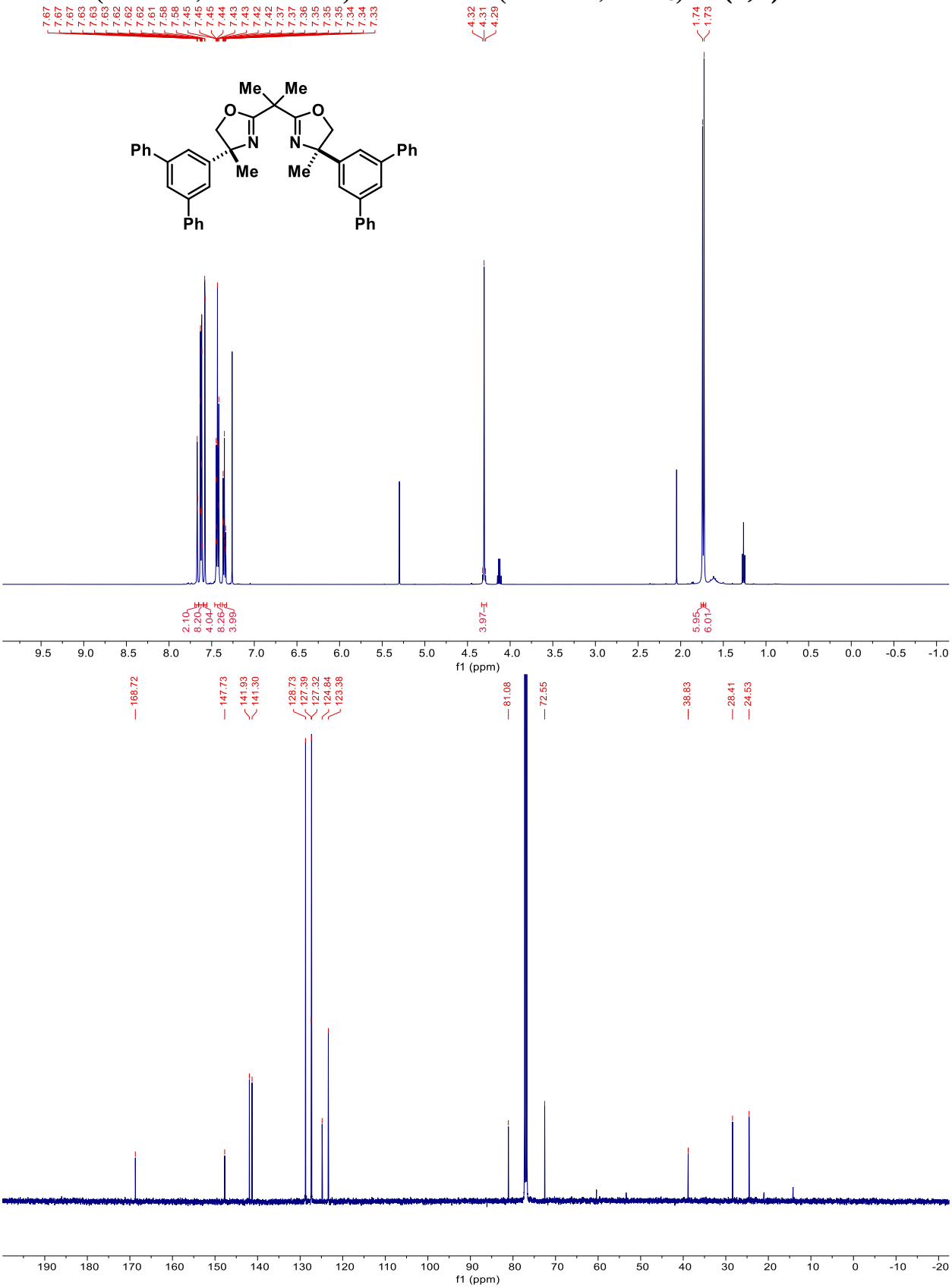

^{1}H NMR (500 MHz, Chloroform-*d*) and ^{13}C NMR (126 MHz, $CDCl_3$) for compound **S2.3.**

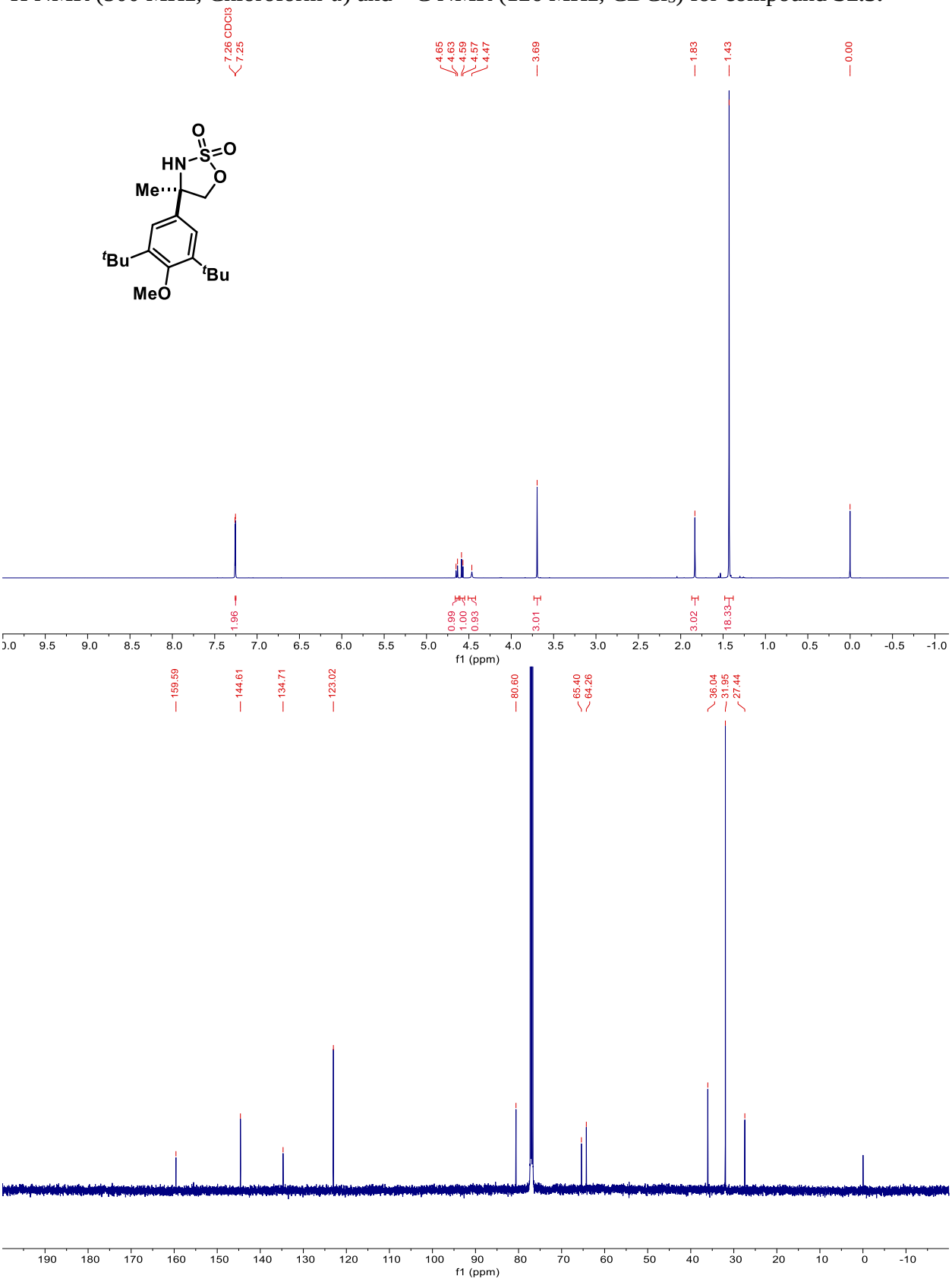

^{1}H NMR (500 MHz, Chloroform-*d*) and ^{13}C NMR (126 MHz, $CDCl_3$) for compound **S2.4.**

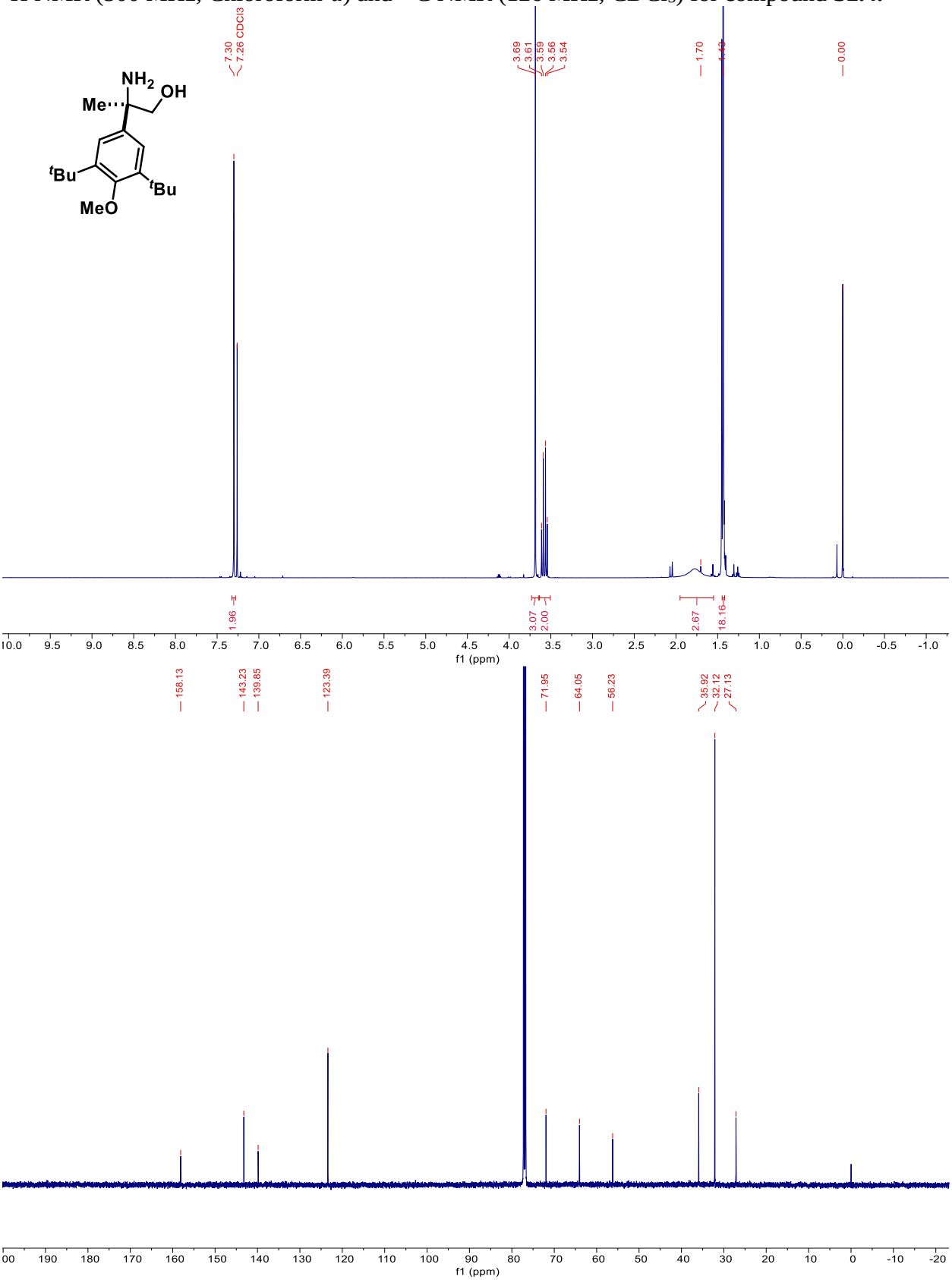

^{1}H NMR (500 MHz, $CDCl_3$) and ^{13}C NMR (126 MHz, $CDCl_3$) for **(*R*,*R*)-*p*-OMe-MinBOX.**

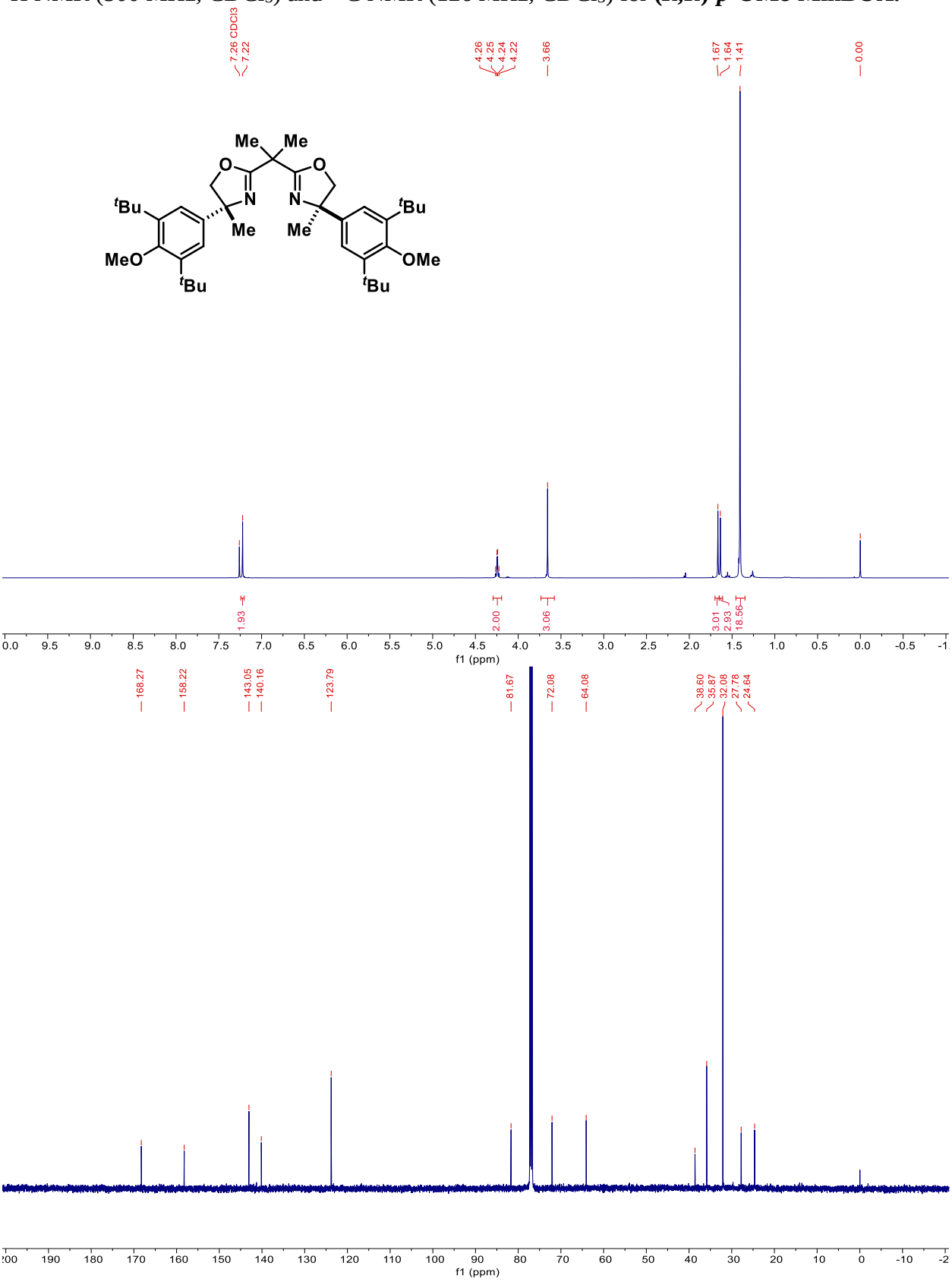

^{1}H NMR (500 MHz, $CDCl_3$) and ^{13}C NMR (126 MHz, $CDCl_3$) for compound **3.1.**

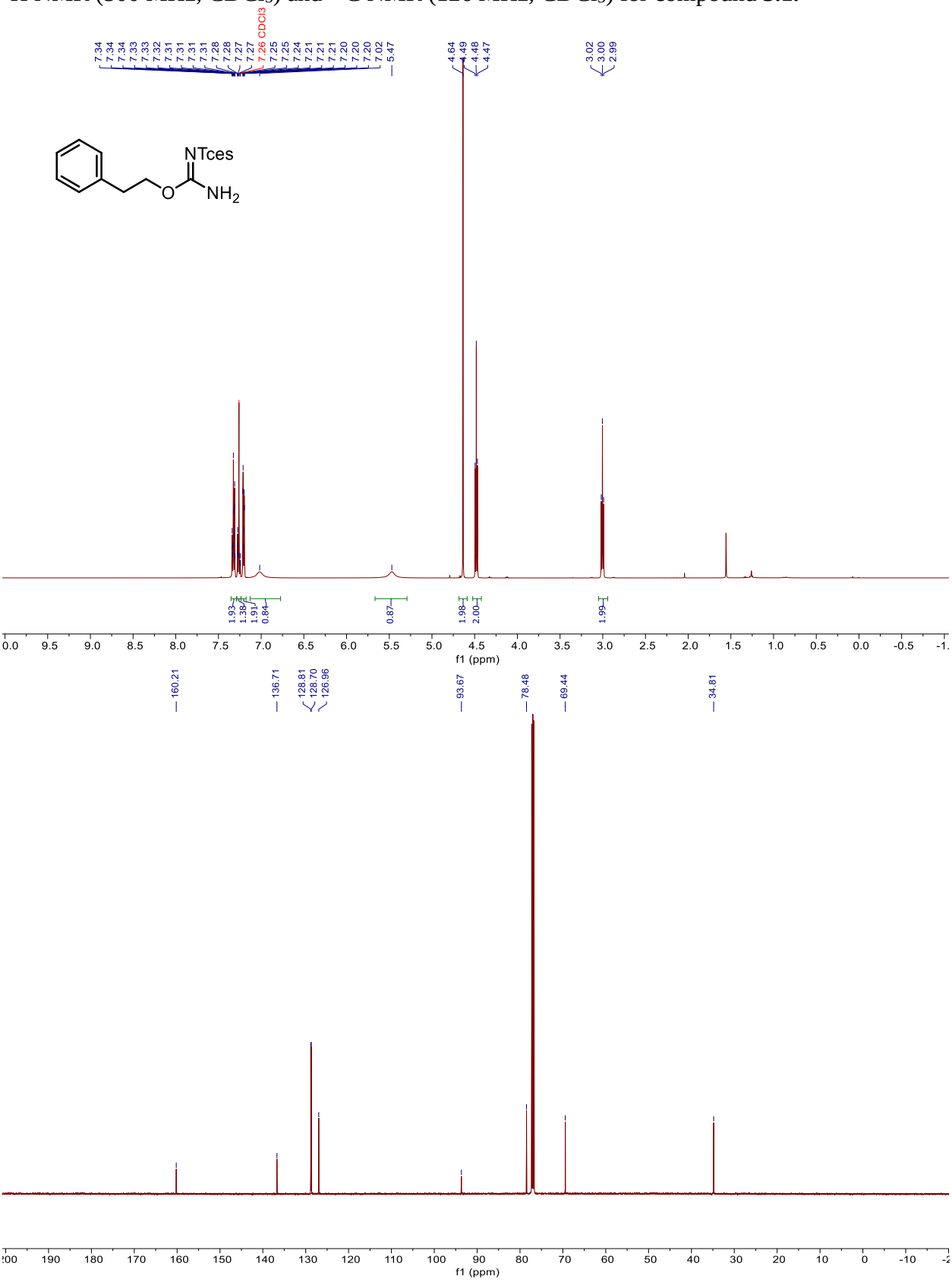

^{1}H NMR (500 MHz, $CDCl_3$) and ^{13}C NMR (126 MHz, $CDCl_3$) for compound **3.2.**

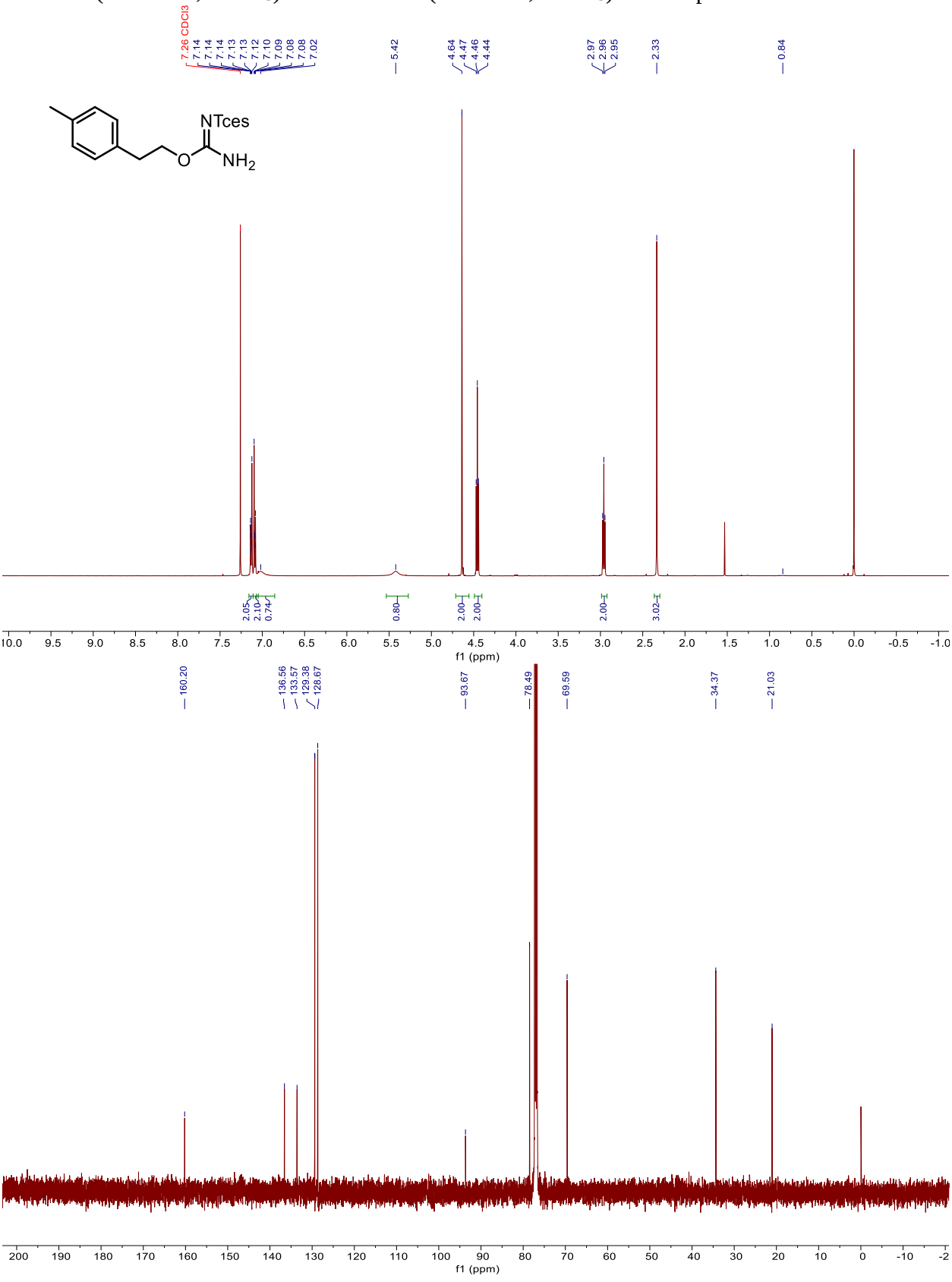

^{1}H NMR (500 MHz, $CDCl_3$) and ^{13}C NMR (126 MHz, $CDCl_3$) for compound **3.3.**

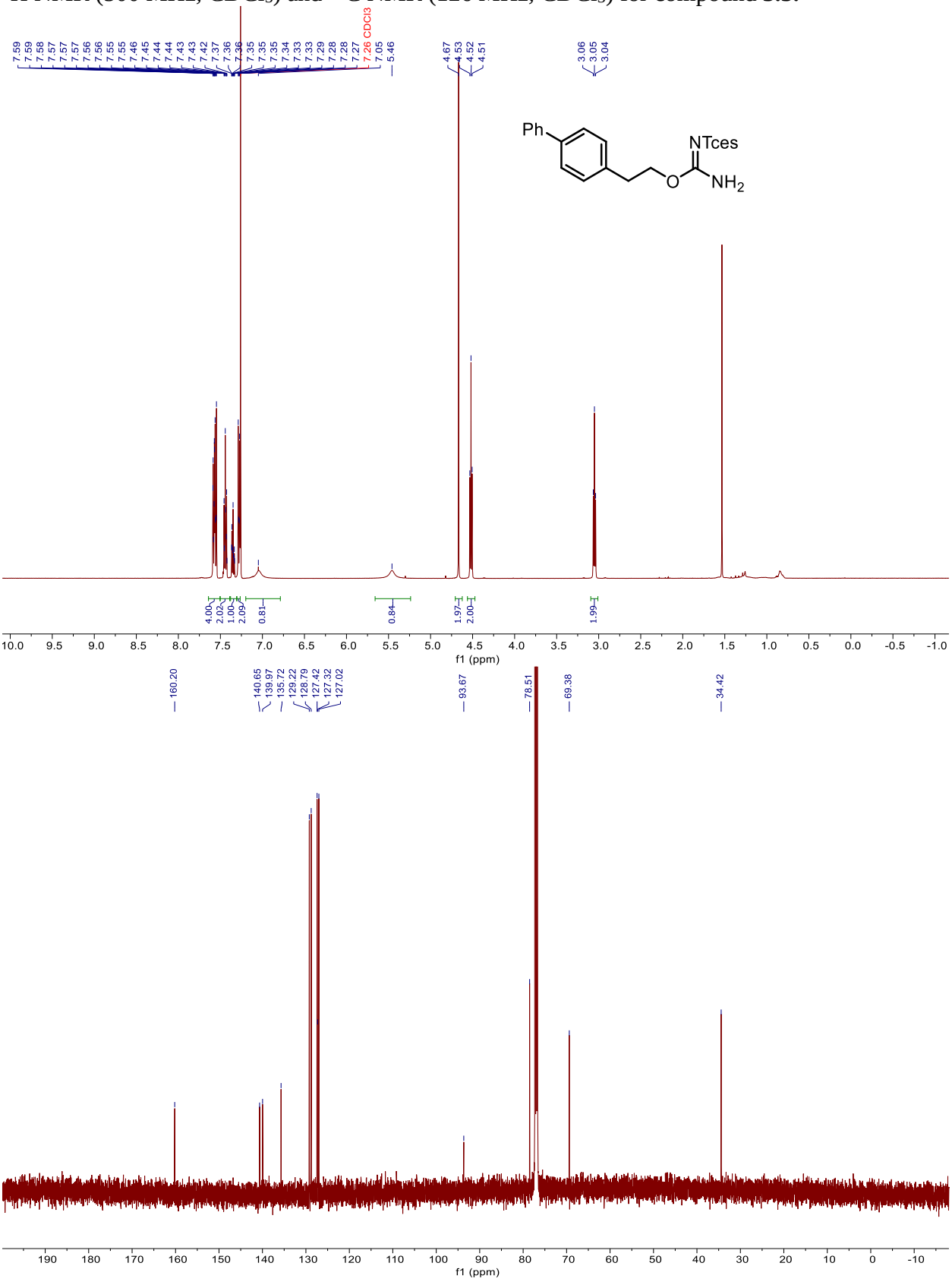

^{1}H NMR (500 MHz, $CDCl_3$) and ^{13}C NMR (126 MHz, $CDCl_3$) for compound **3.4.**

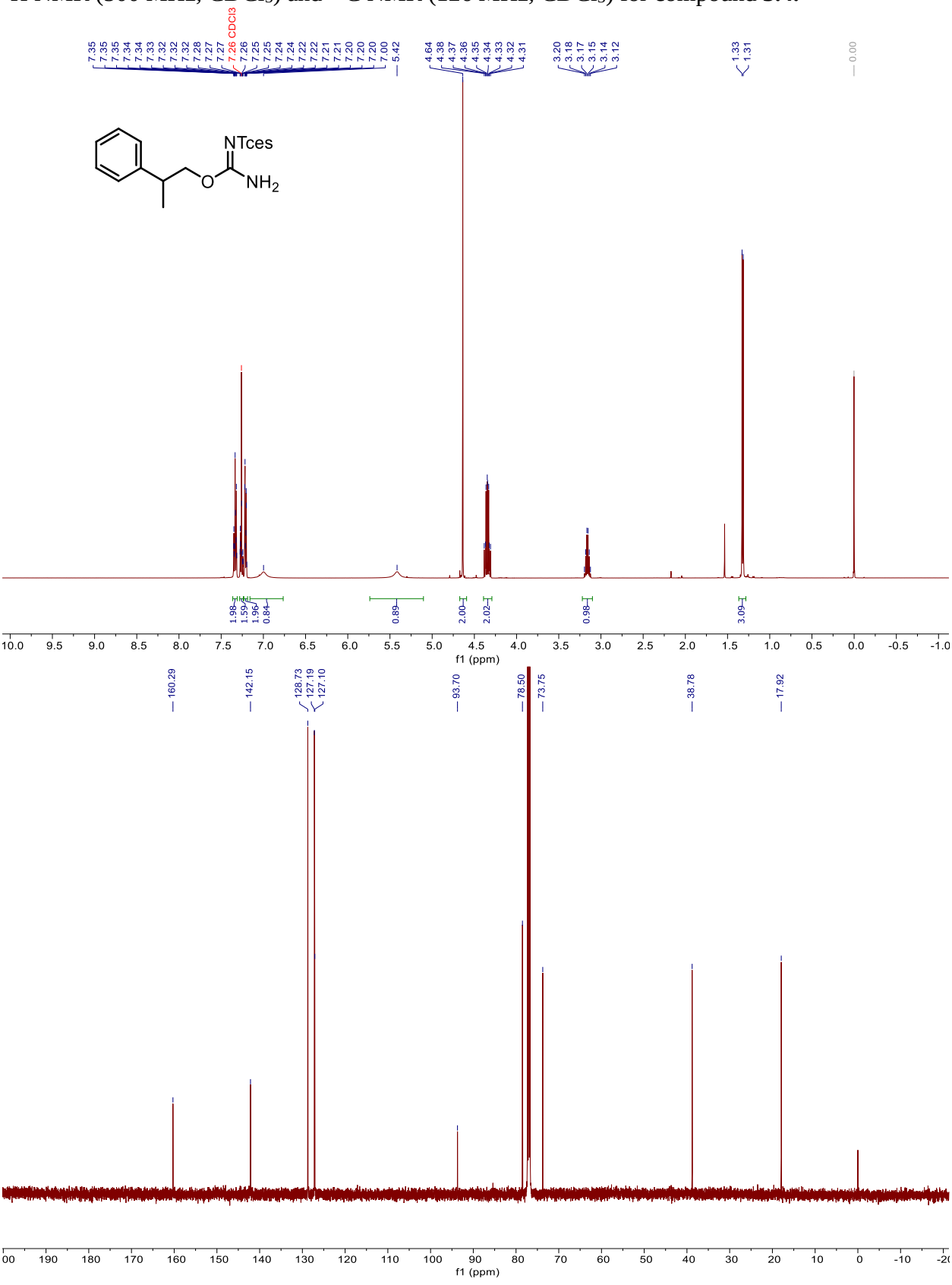

^{1}H NMR (500 MHz, $CDCl_3$) and ^{13}C NMR (126 MHz, $CDCl_3$) for compound **3.5.**

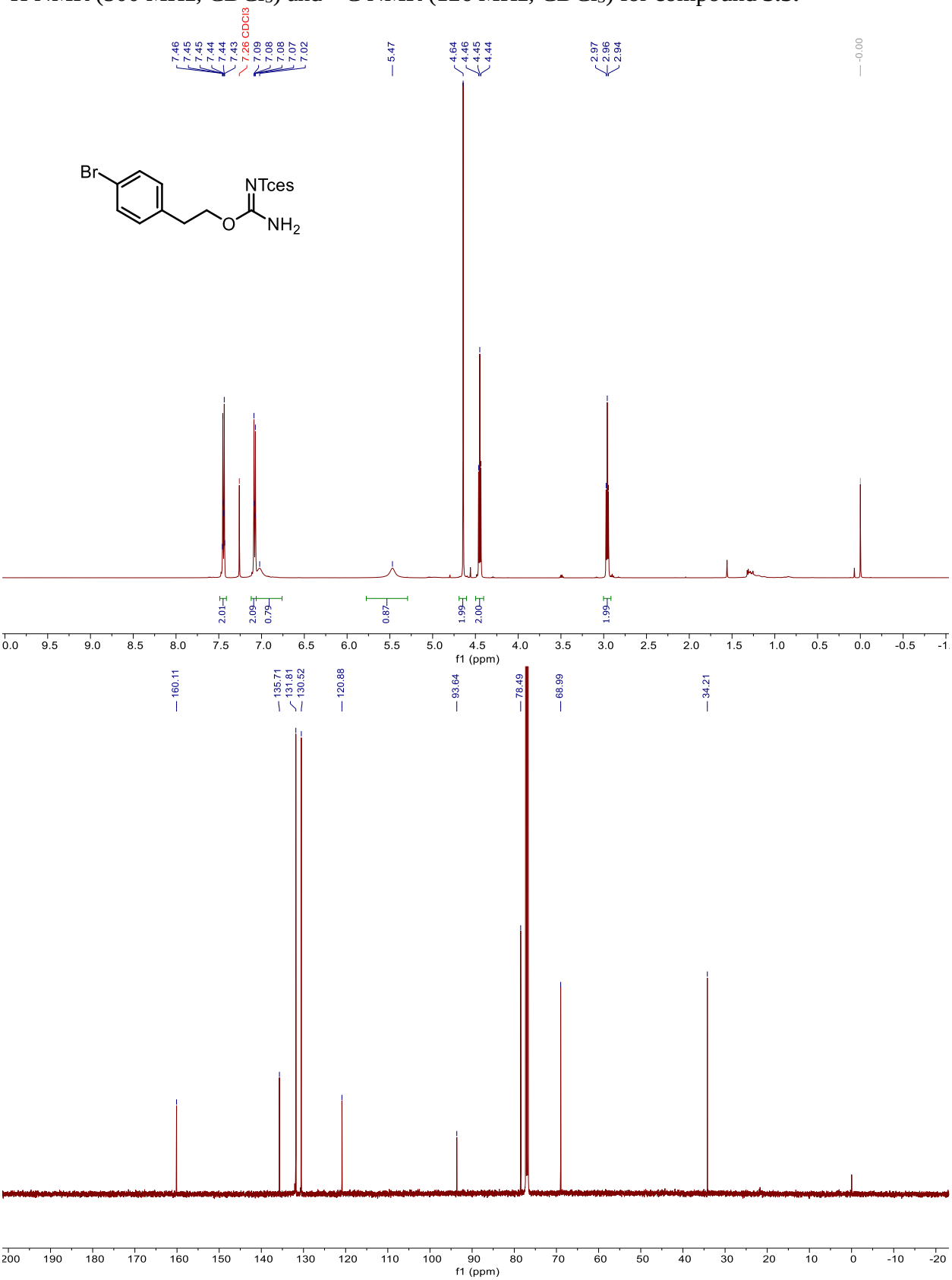

^{1}H NMR (500 MHz, $CDCl_3$), ^{13}C NMR (126 MHz, $CDCl_3$), and ^{19}F NMR (377 MHz, $CDCl_3$) for compound **3.6.**

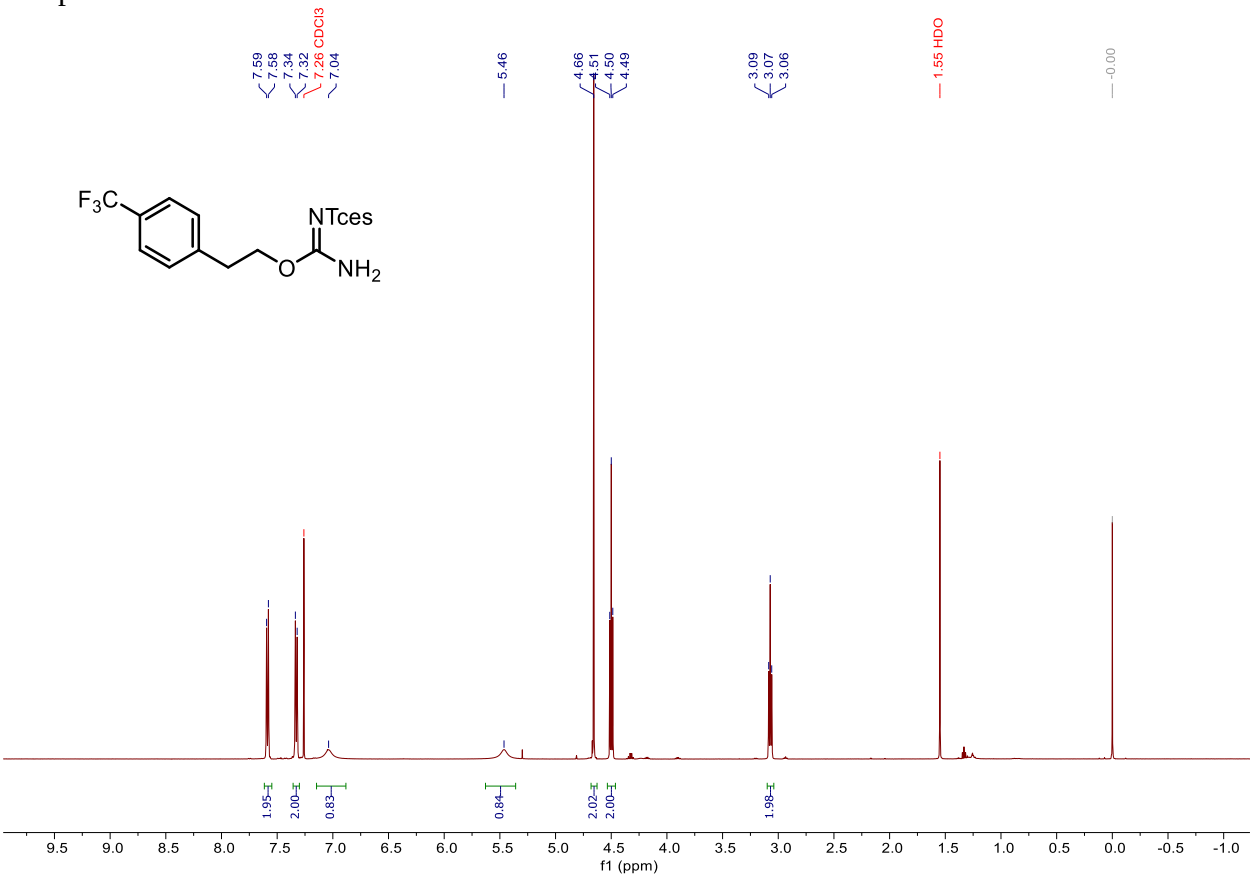

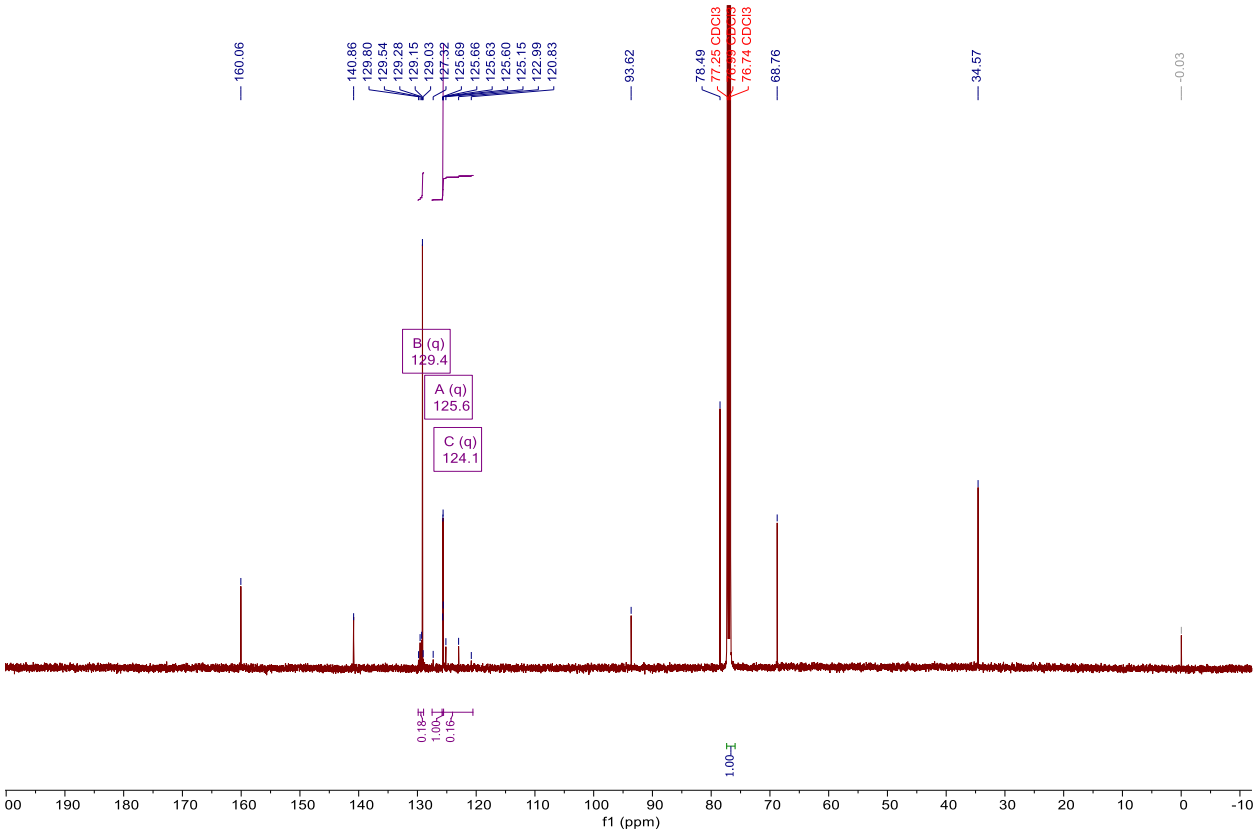
160.06
140.86
129.80
129.54
129.28
129.15
129.03
127.32
125.69
125.66
125.63
125.60
125.15
122.99
120.83
93.62
78.49
77.25 CDCl3
76.74 CDCl3
68.76
34.57
-0.03
B (q)
129.4
A (q)
125.6
C (q)
124.1
0.18
1.00
0.16
1.00
f1 (ppm)

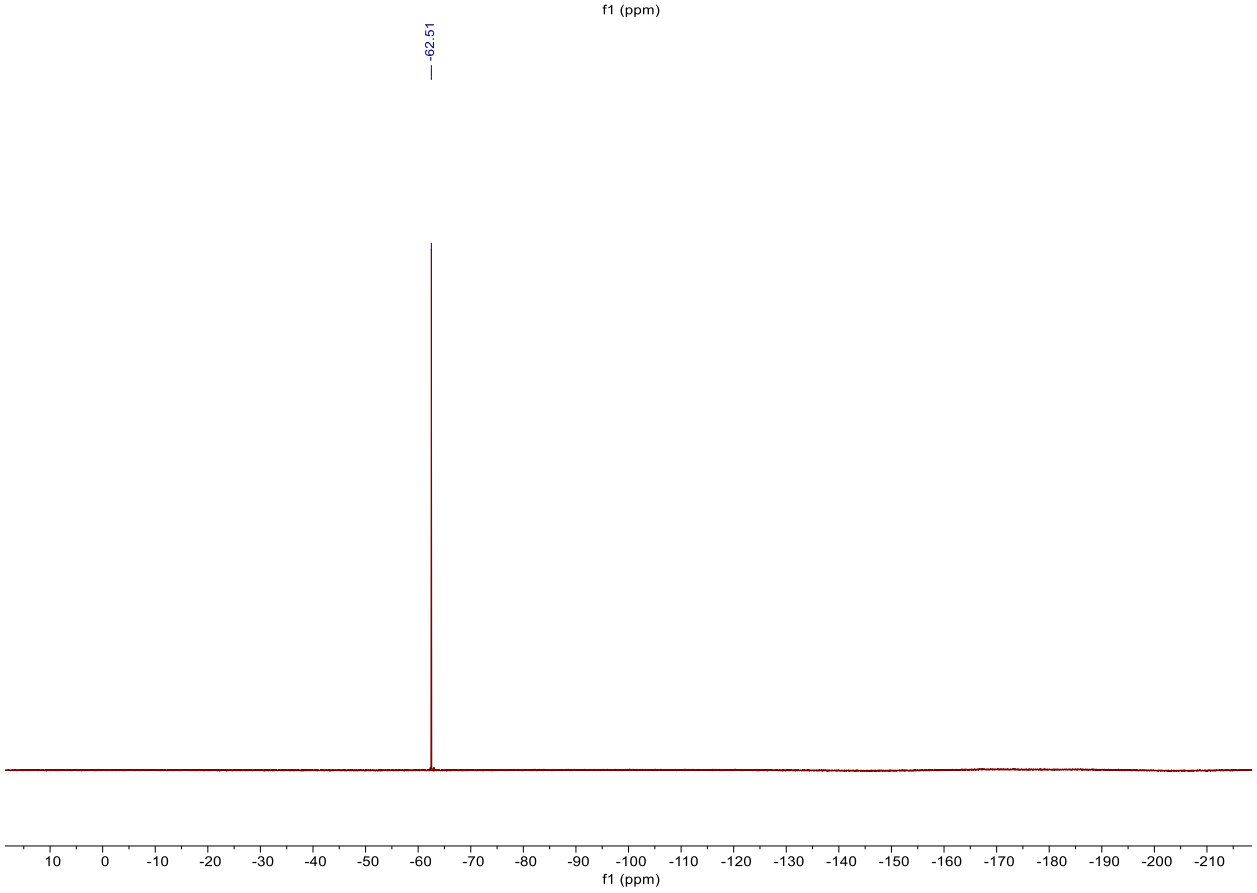
-62.51
f1 (ppm)

^{1}H NMR (500 MHz, $CDCl_3$), ^{13}C NMR (126 MHz, $CDCl_3$), and ^{19}F NMR (377 MHz, $CDCl_3$) for compound **3.7.**

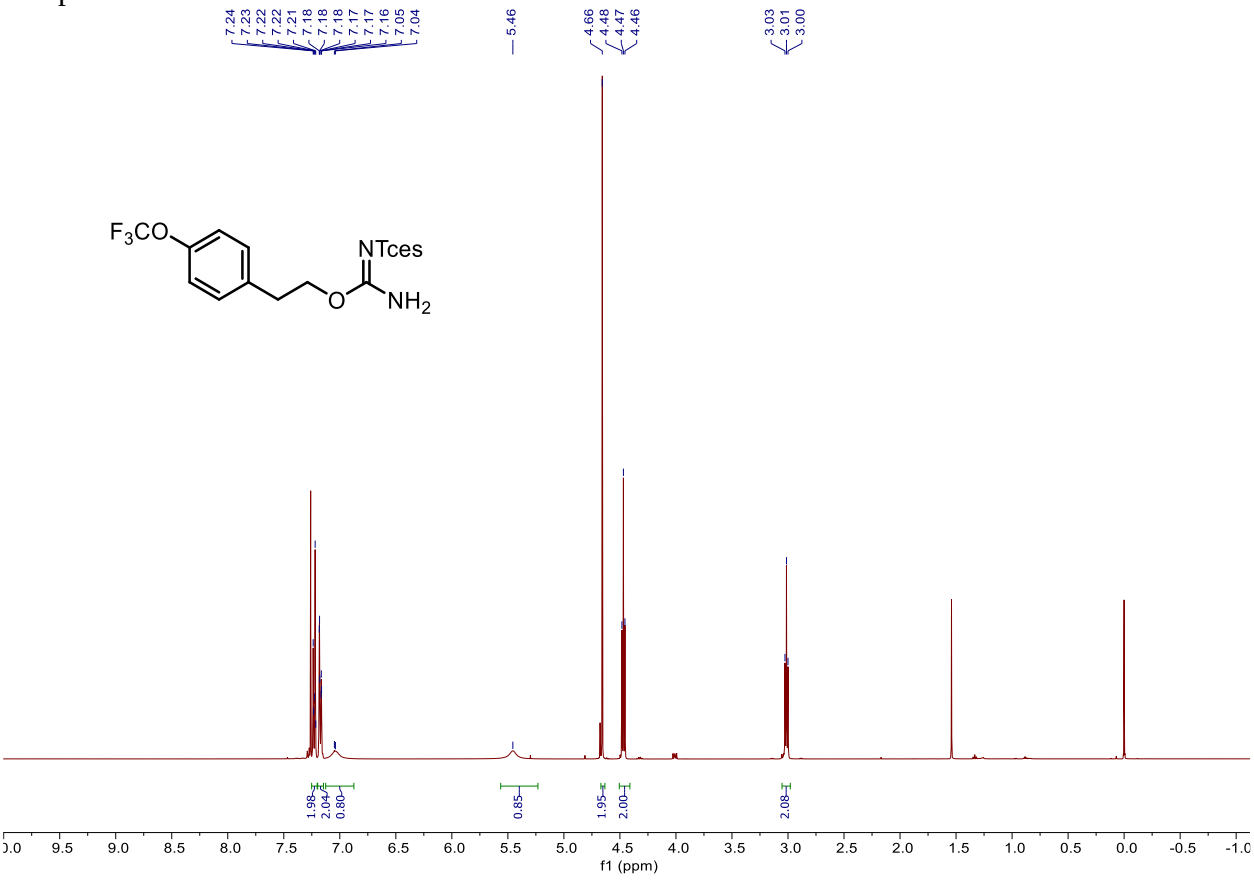

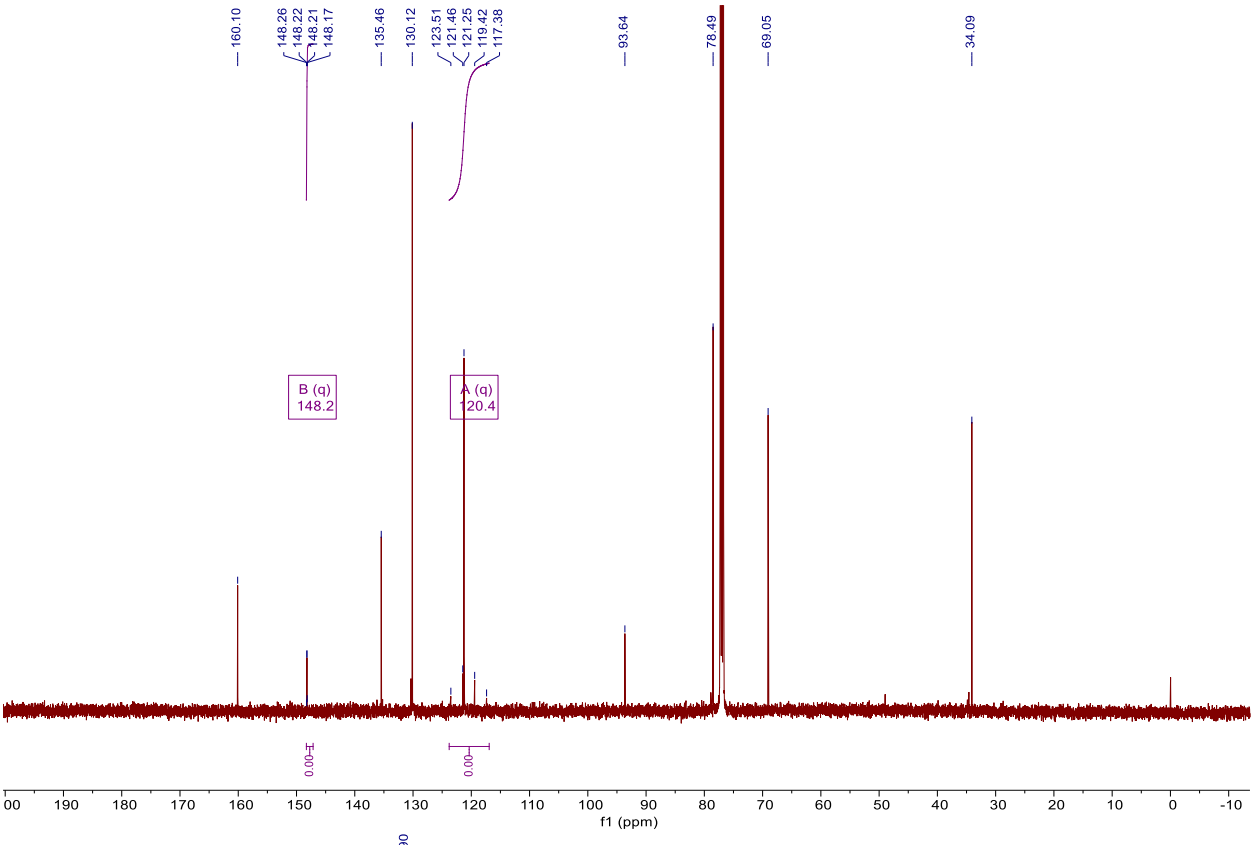
160.10
148.26
148.22
148.21
148.17
135.46
130.12
123.51
121.46
121.25
119.42
117.38
93.64
78.49
69.05
34.09
B (q)
148.2
A (q)
120.4
0.00
0.00
f1 (ppm)

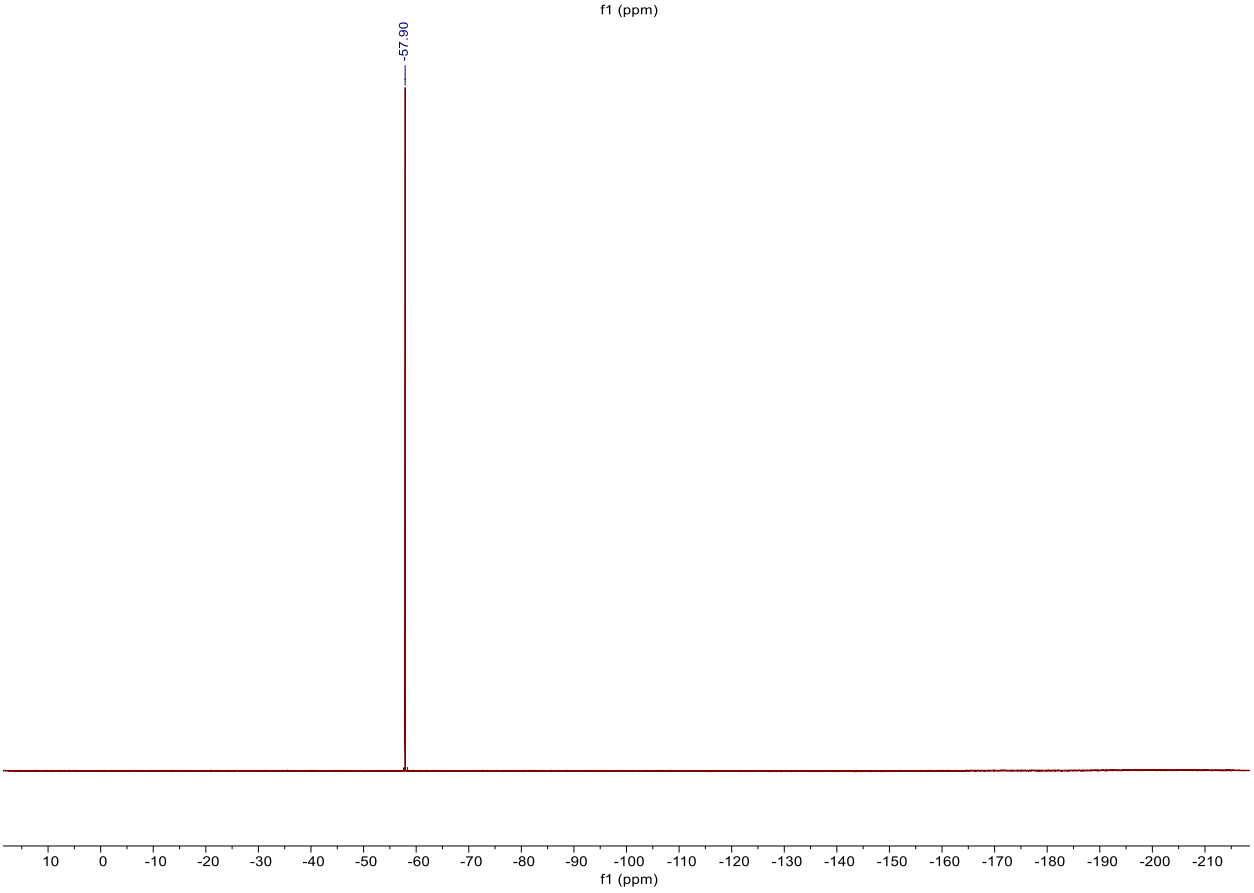
-57.90
f1 (ppm)

^{1}H NMR (500 MHz, $CDCl_3$) and ^{13}C NMR (126 MHz, $CDCl_3$) for compound **3.8.**

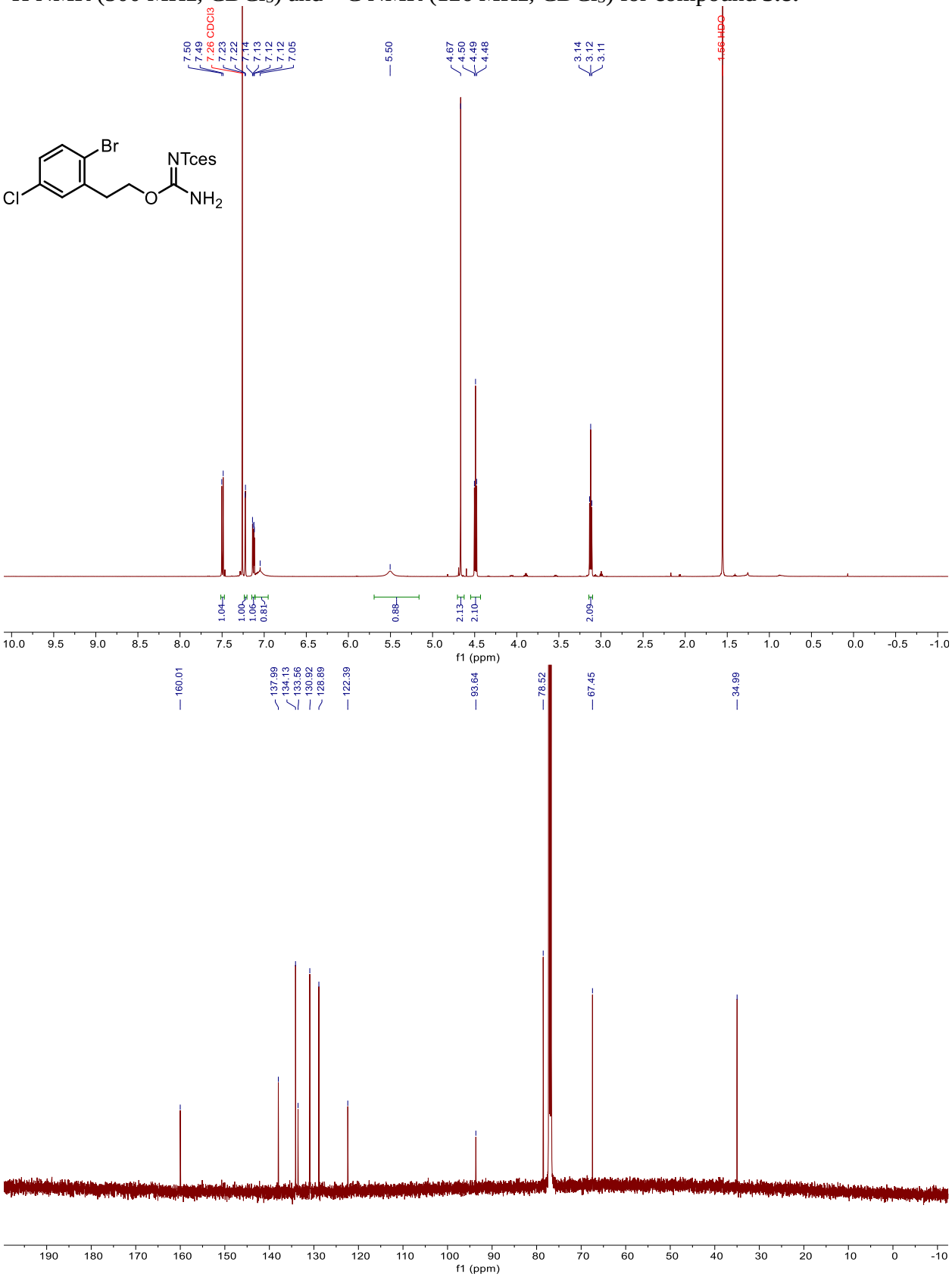

^{1}H NMR (500 MHz, $CDCl_3$) and ^{13}C NMR (126 MHz, $CDCl_3$) for compound **3.9.**

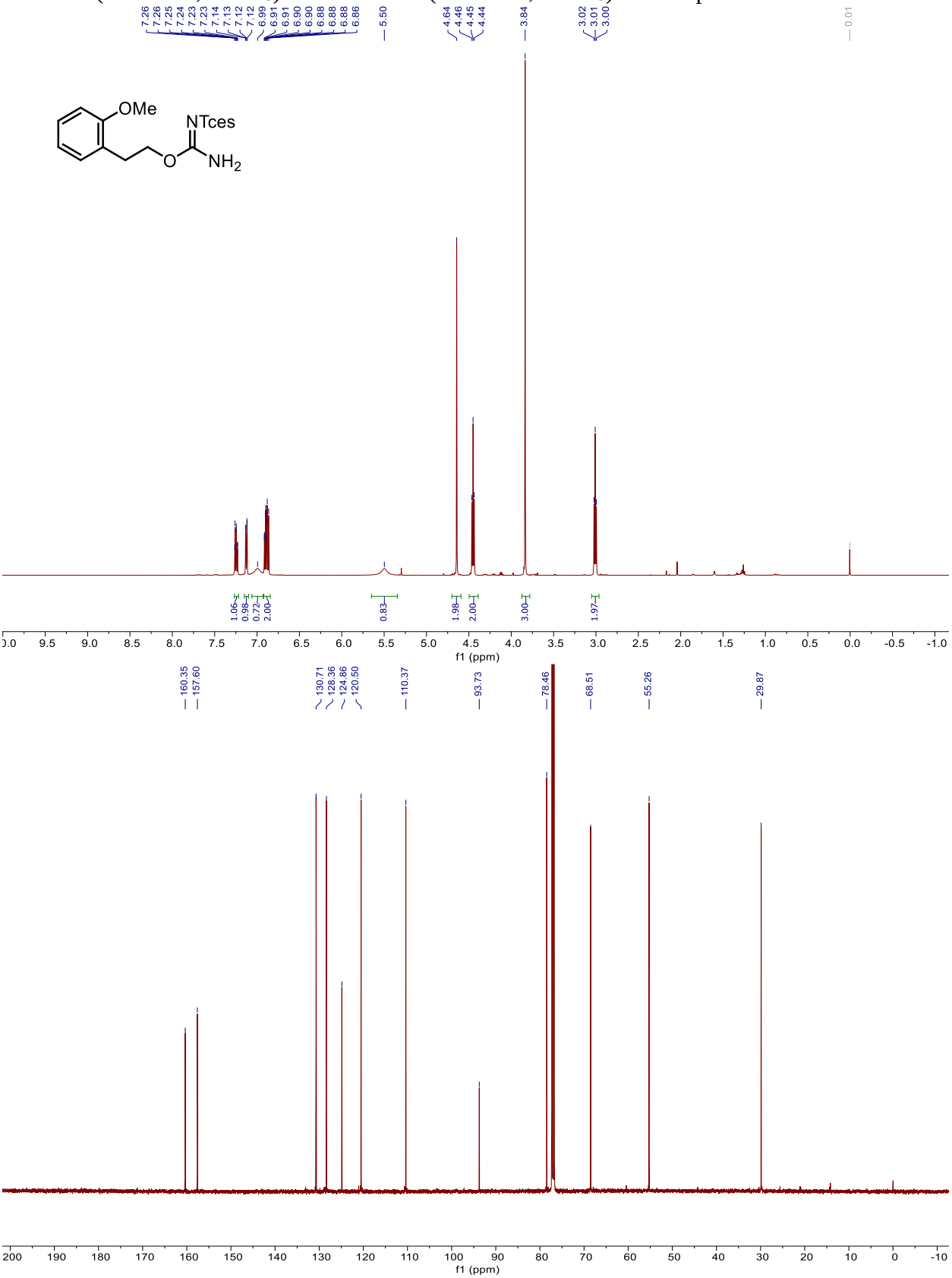

^{1}H NMR (500 MHz, $CDCl_3$) and ^{13}C NMR (126 MHz, $CDCl_3$) for compound **3.10.**

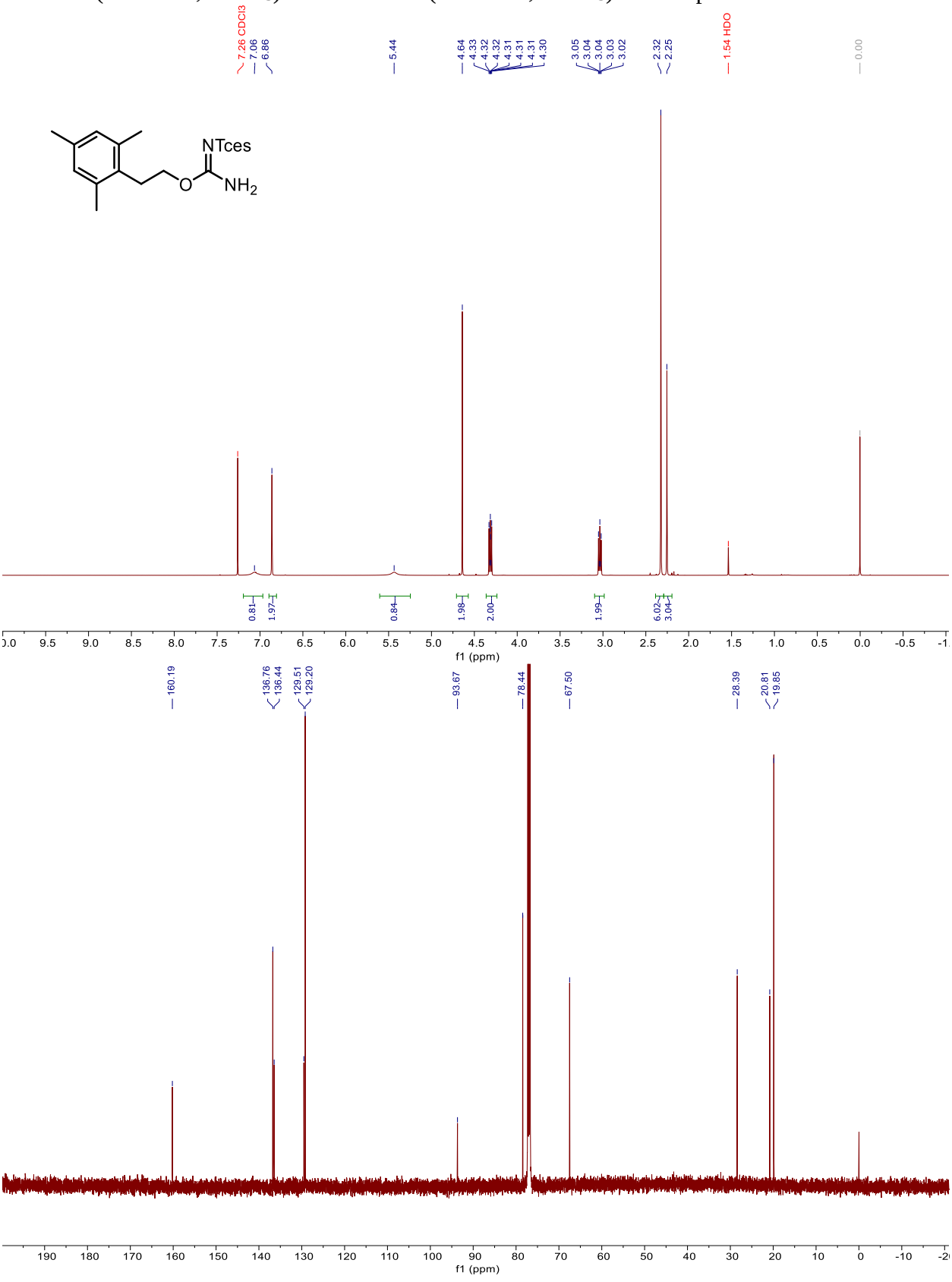

^{1}H NMR (500 MHz, $CDCl_3$) and ^{13}C NMR (126 MHz, $CDCl_3$) for compound **3.11.**

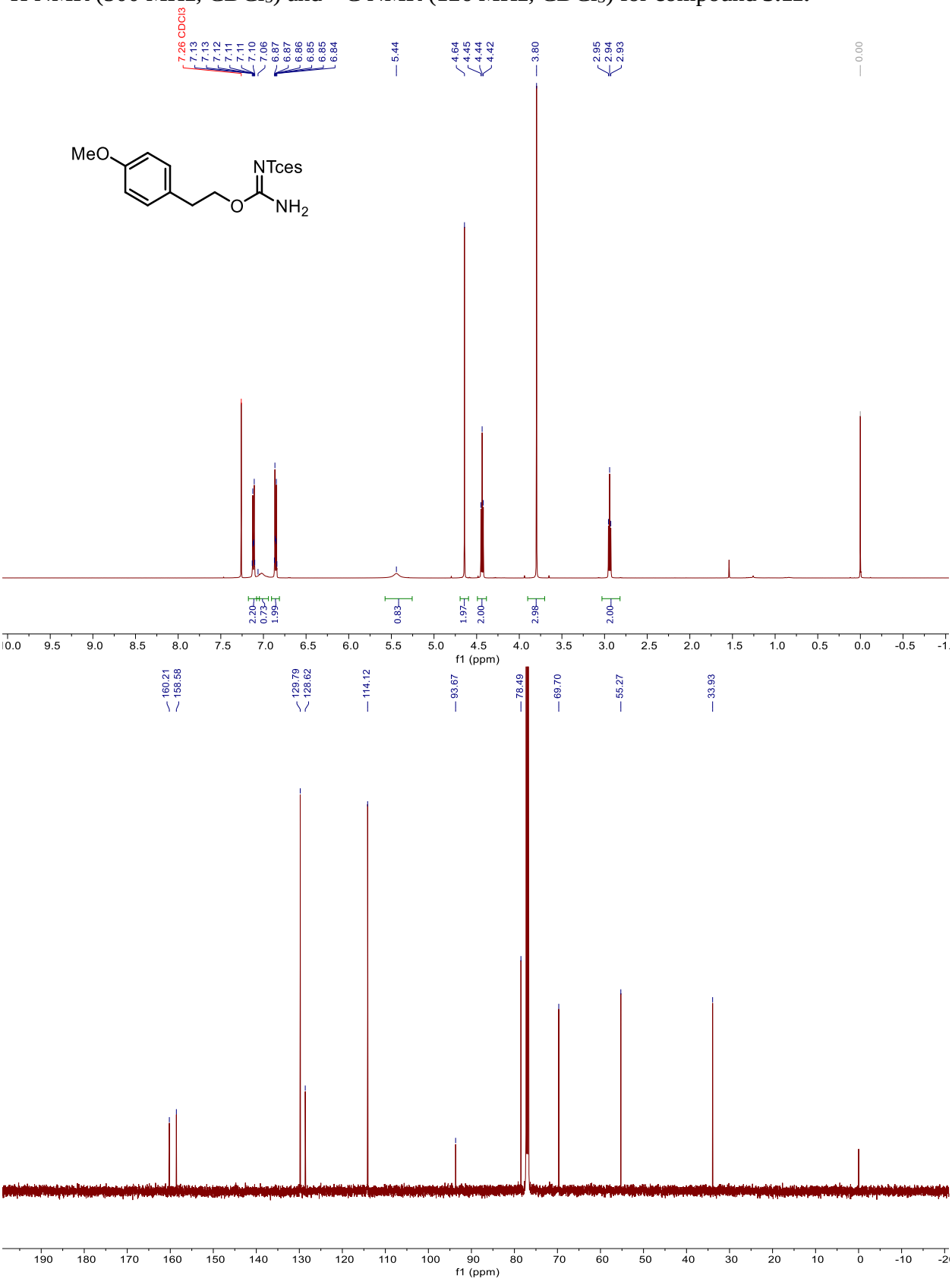

^{1}H NMR (500 MHz, $CDCl_3$) and ^{13}C NMR (126 MHz, $CDCl_3$) for compound **3.1a.**

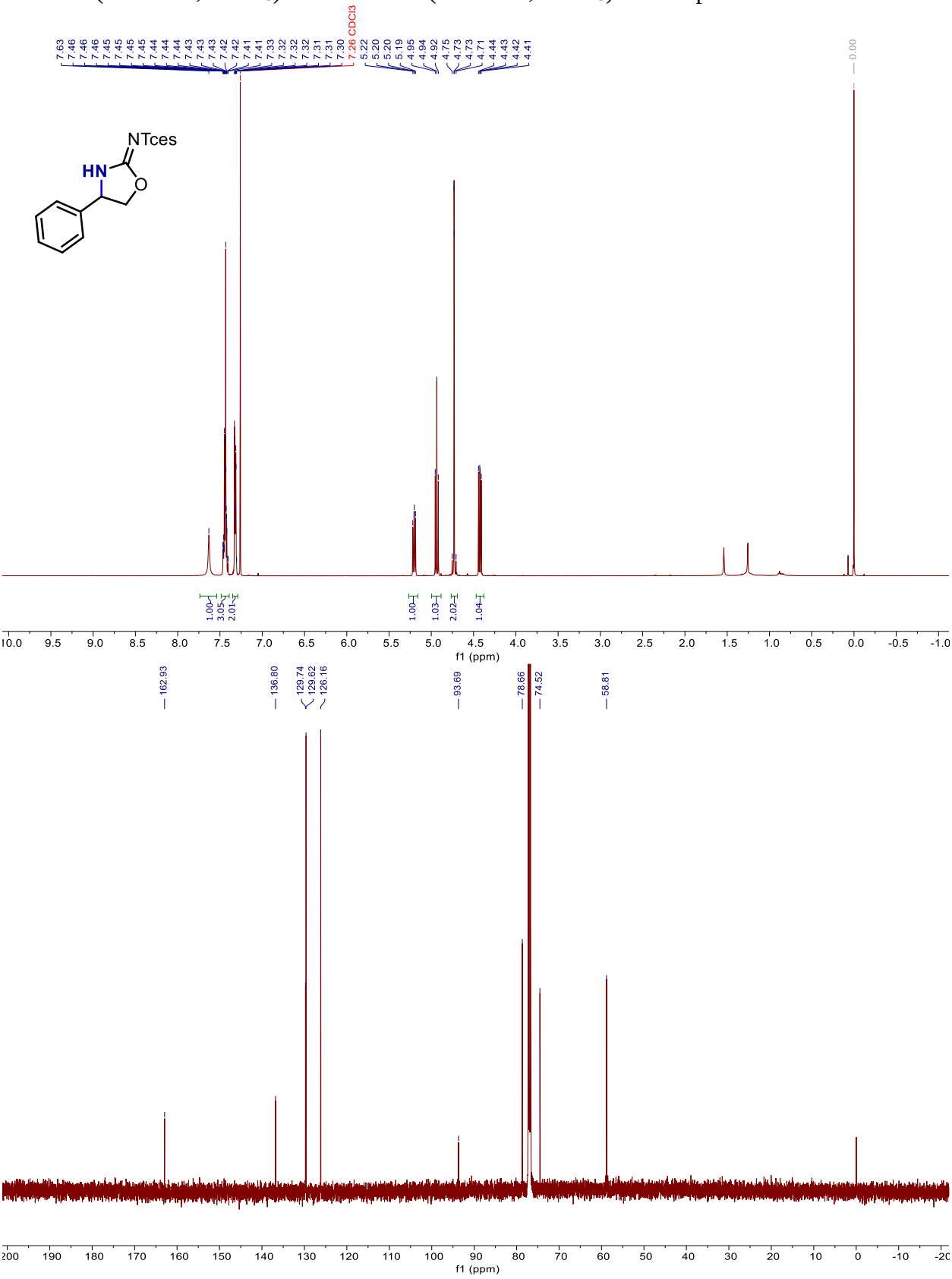

^{1}H NMR (500 MHz, $CDCl_3$) and ^{13}C NMR (126 MHz, $CDCl_3$) for compound **3.2a.**

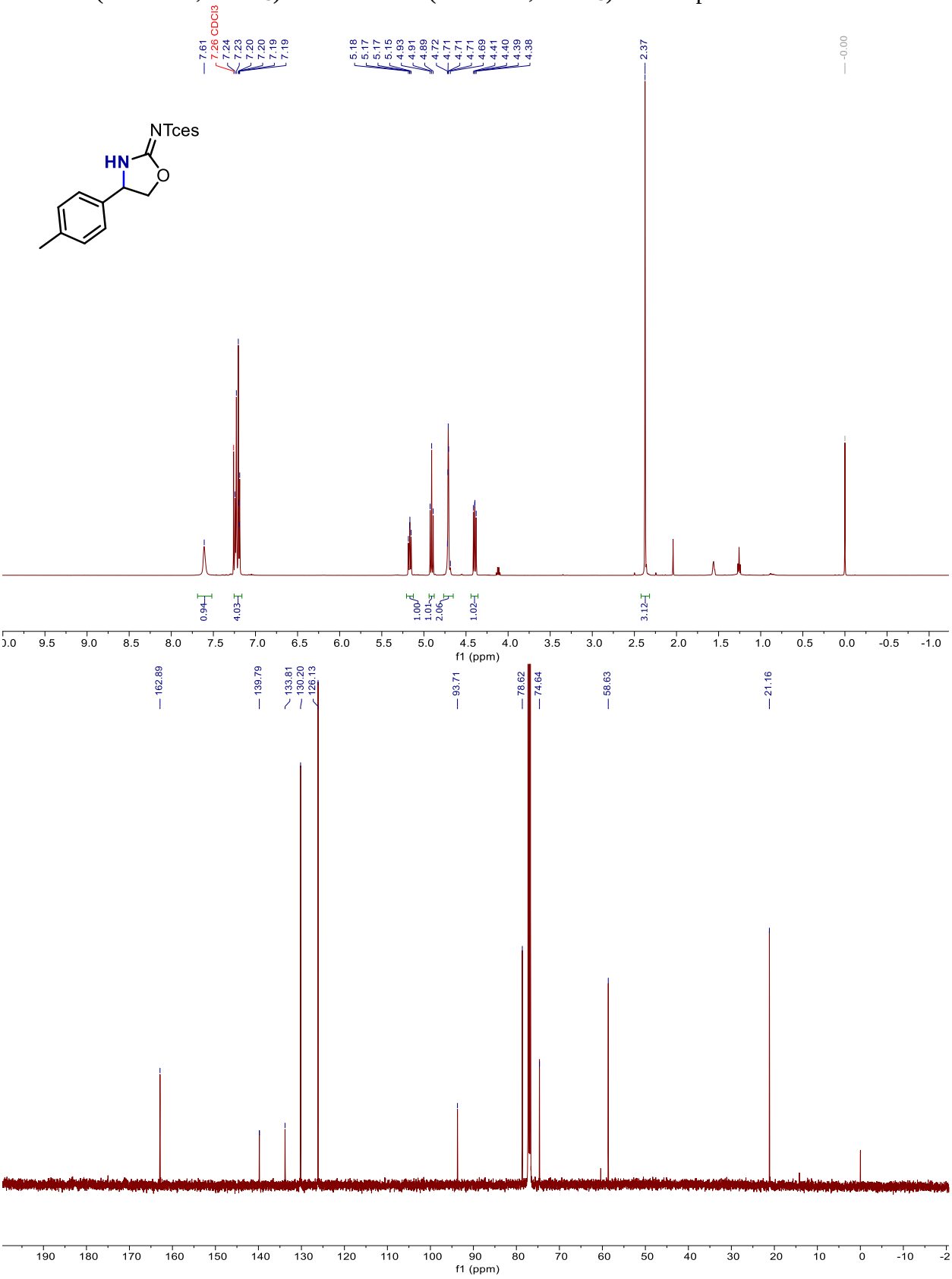

^{1}H NMR (500 MHz, $CDCl_3$) and ^{13}C NMR (126 MHz, $CDCl_3$) for compound **3.3a.**

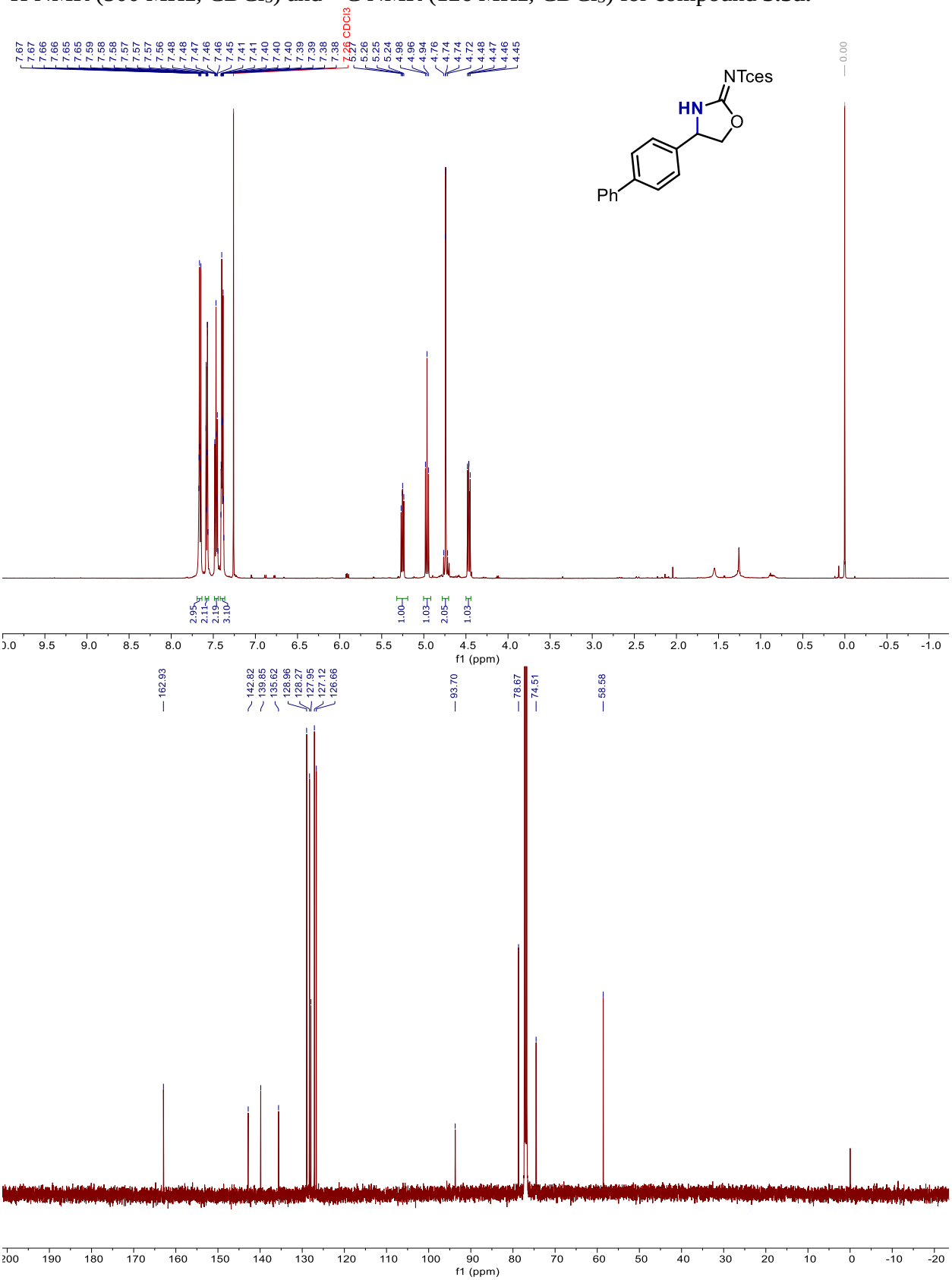

^{1}H NMR (500 MHz, $CDCl_3$) and ^{13}C NMR (126 MHz, $CDCl_3$) for compound **3.4a.**

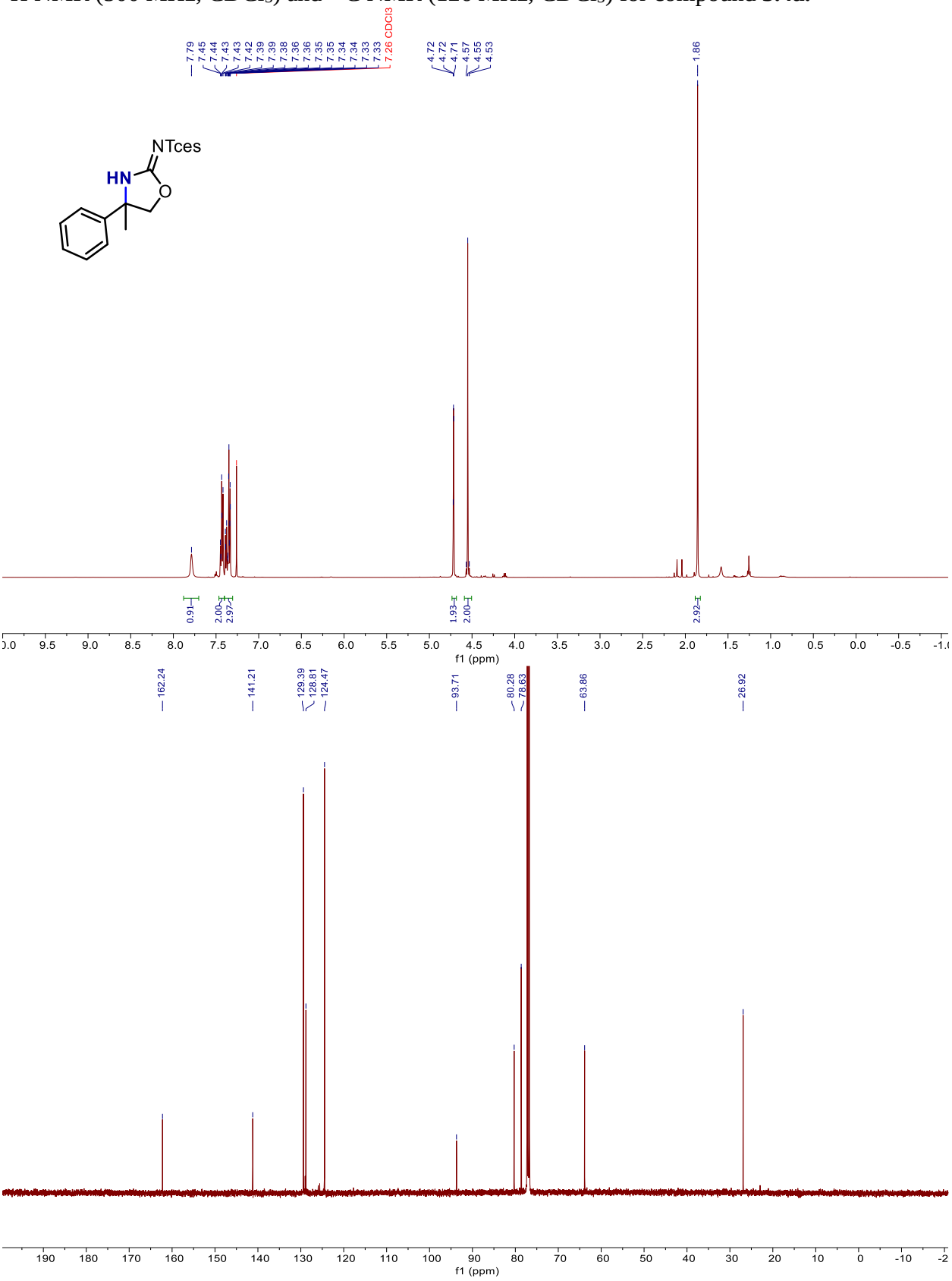

^{1}H NMR (500 MHz, $CDCl_3$), ^{13}C NMR (126 MHz, $CDCl_3$), and ^{19}F NMR (377 MHz, $CDCl_3$)for compound **3.6a.**

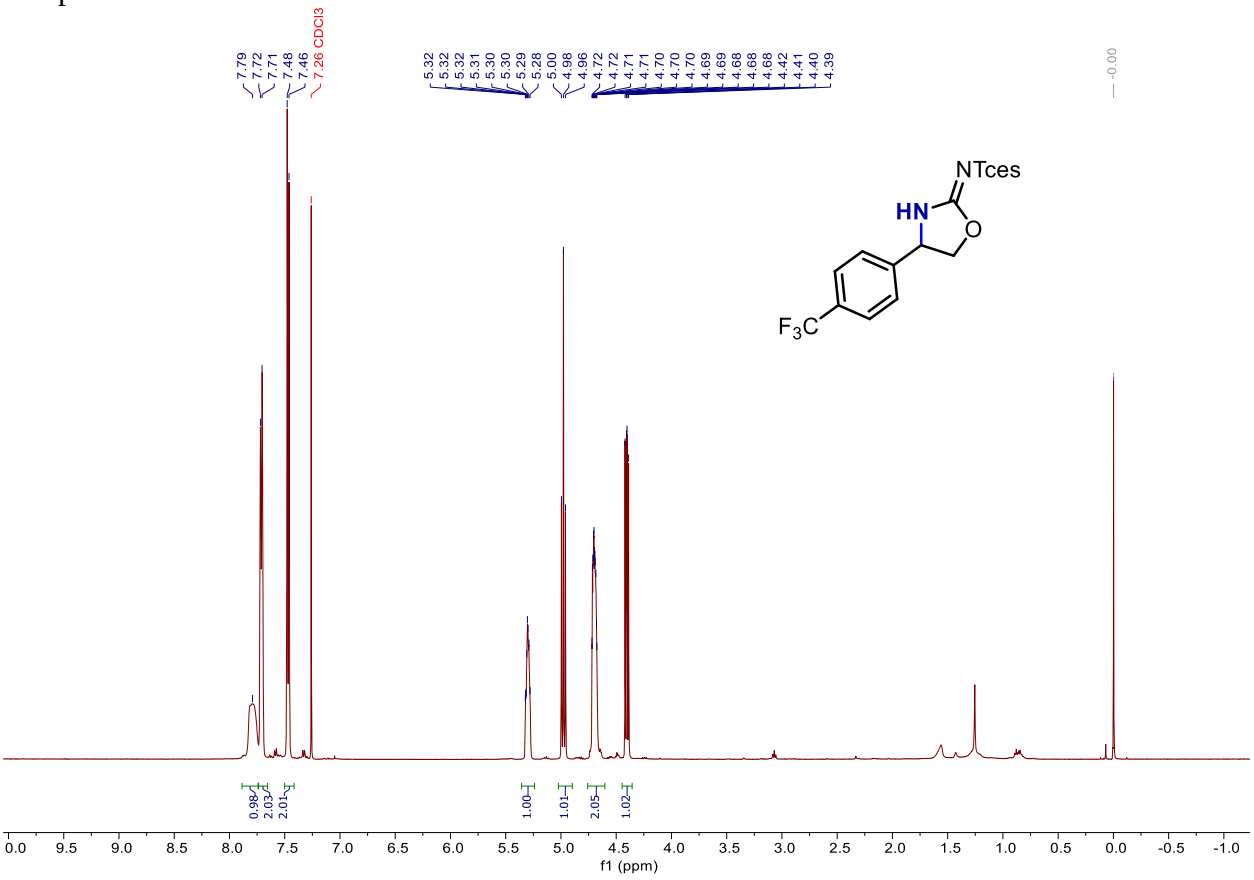

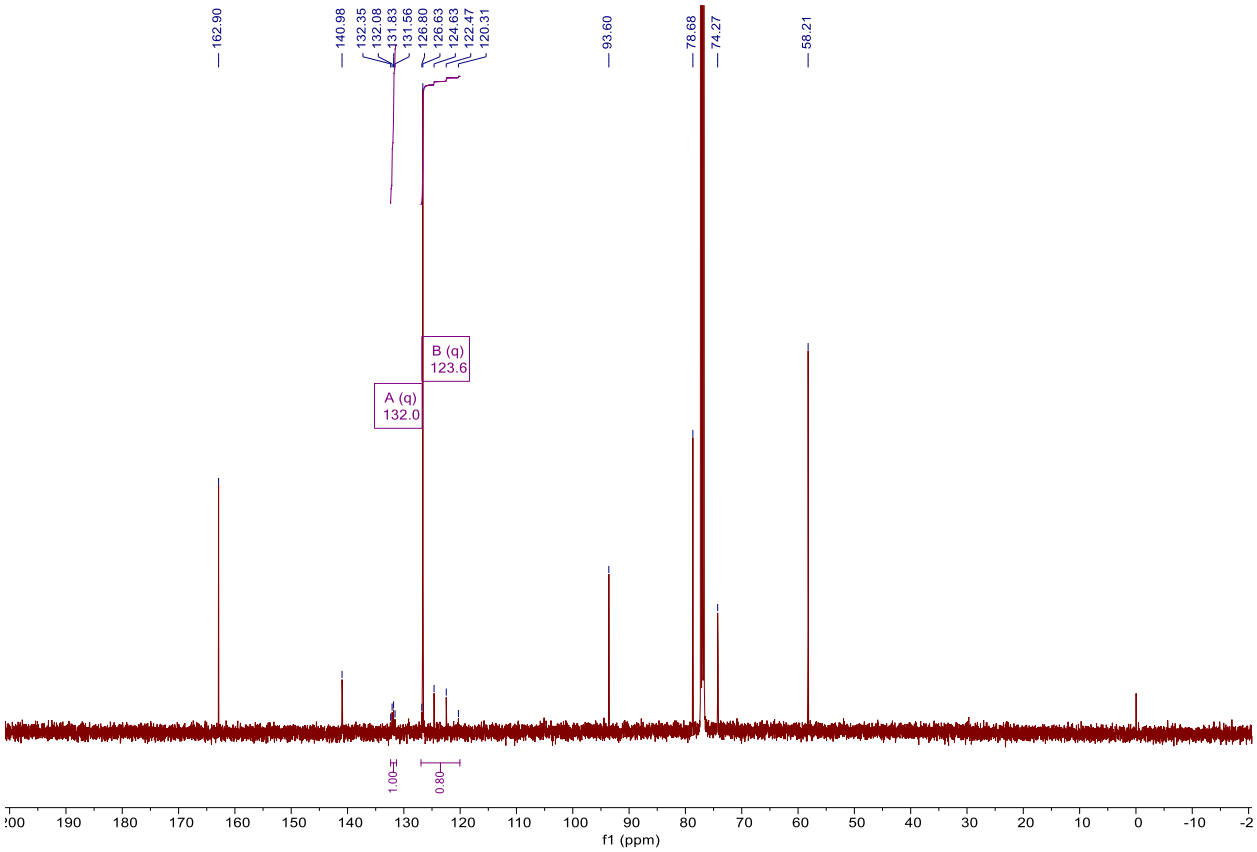
162.90
140.98
132.35
132.08
131.83
131.56
126.80
126.63
124.63
122.47
120.31
93.60
78.68
74.27
58.21
B (q)
123.6
A (q)
132.0
1.00
0.80
f1 (ppm)

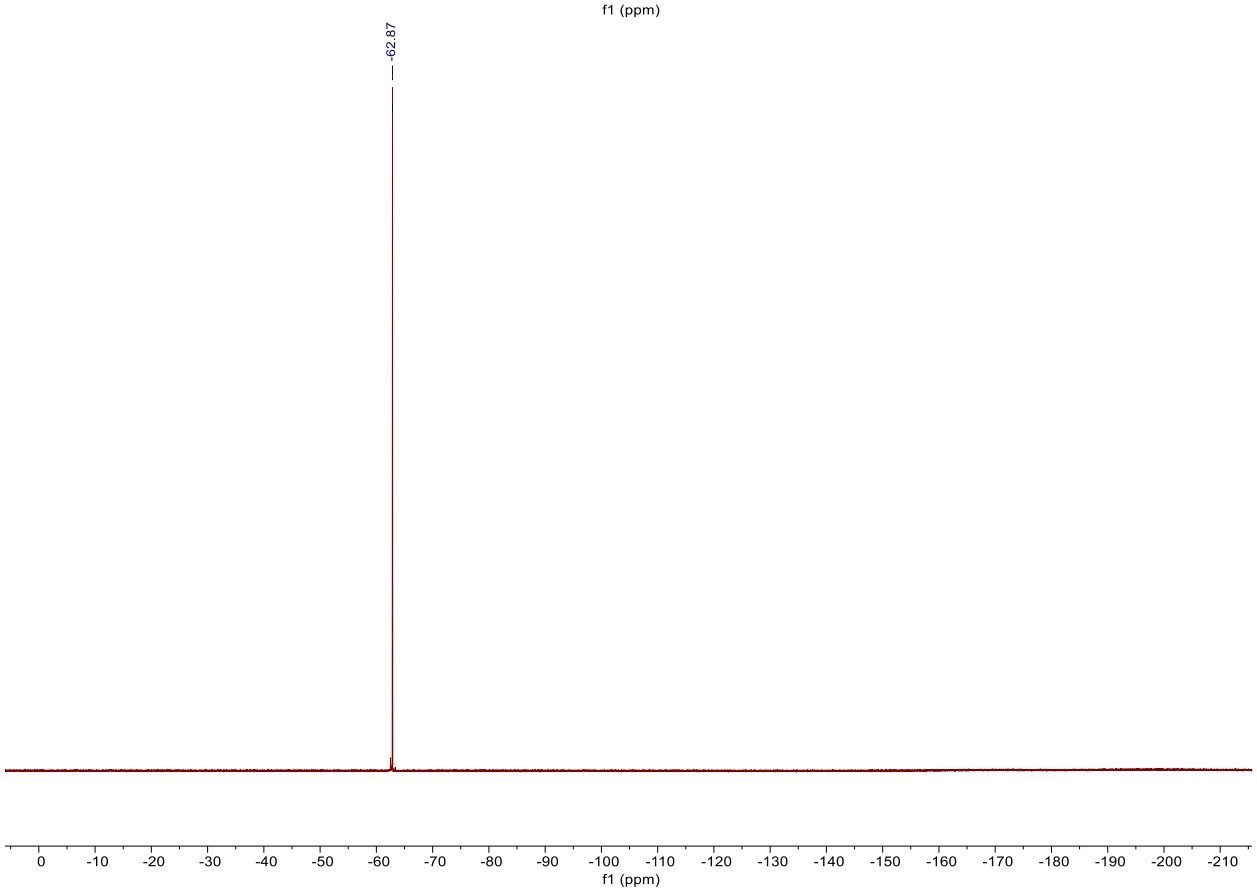
-62.87
f1 (ppm)

^{1}H NMR (500 MHz, $CDCl_3$), ^{13}C NMR (126 MHz, $CDCl_3$), and ^{19}F NMR (377 MHz, $CDCl_3$)for compound **3.7a.**

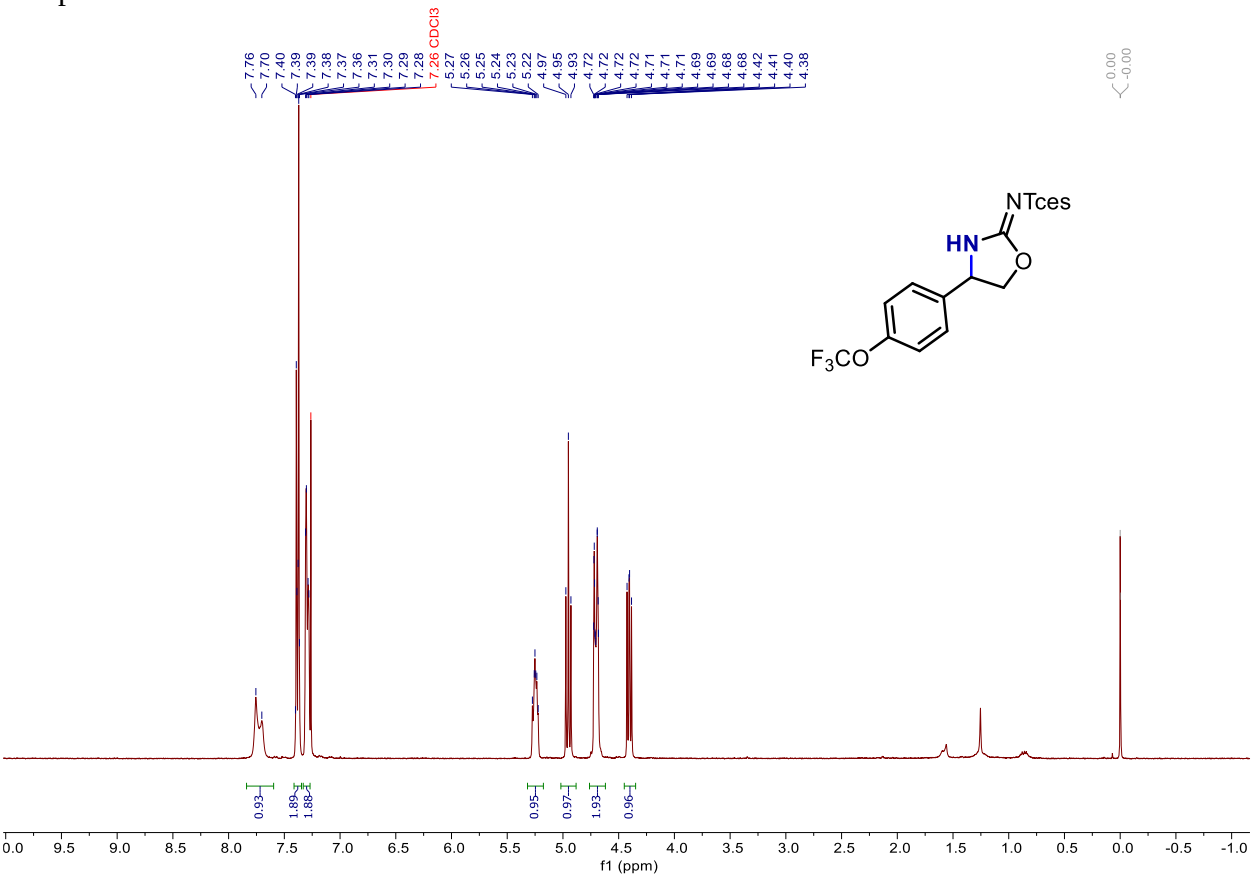

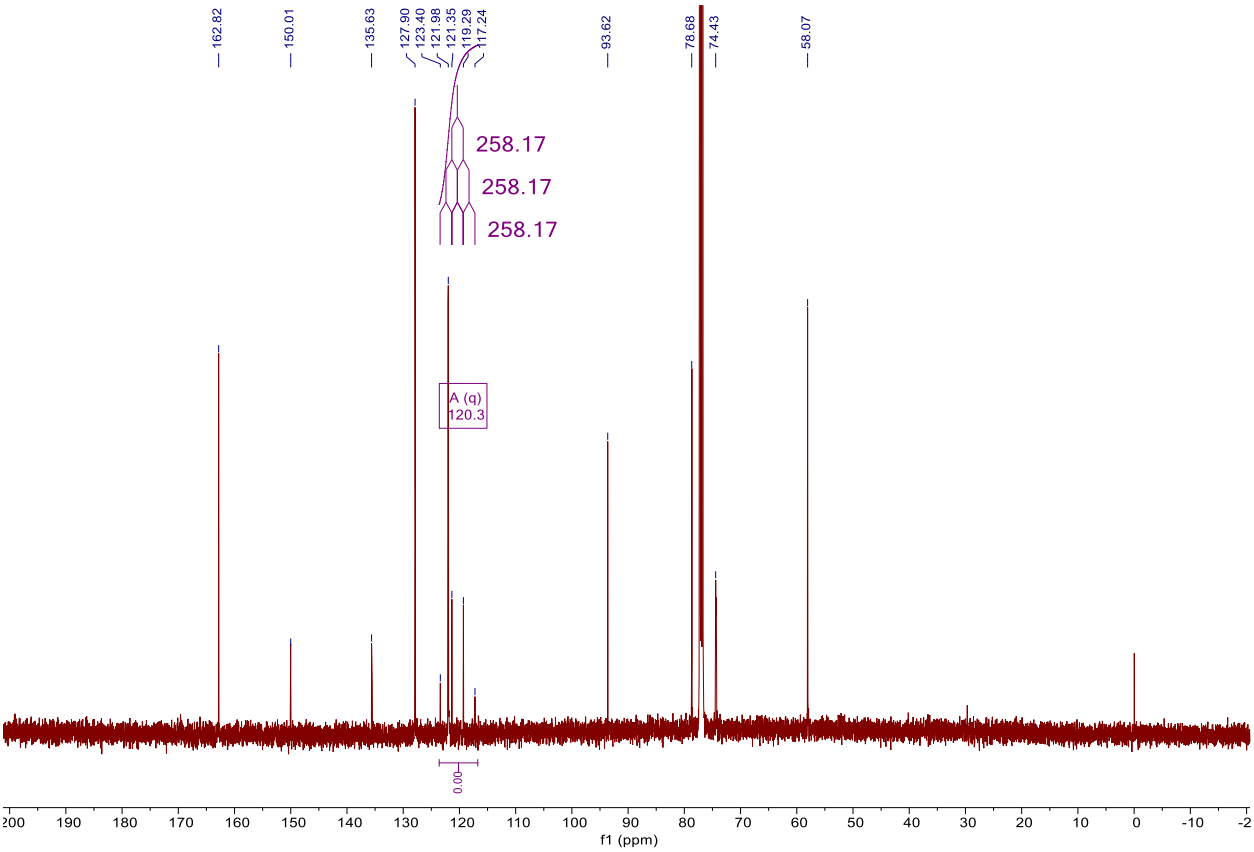
162.82
150.01
135.63
127.90
123.40
121.98
121.35
119.29
117.24
93.62
78.68
74.43
58.07
258.17
258.17
258.17
A (q)
120.3
0.00
f1 (ppm)

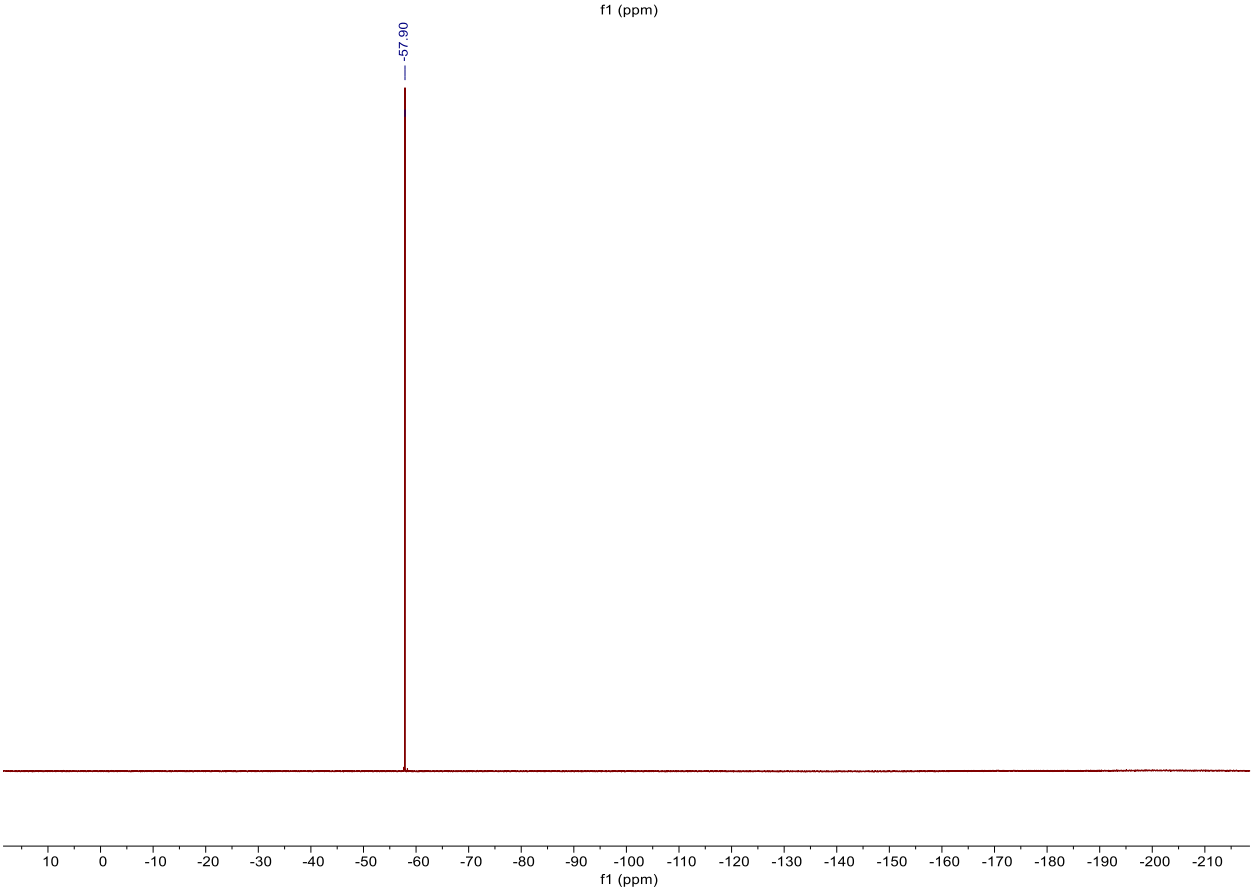
-57.90
f1 (ppm)

^{1}H NMR (500 MHz, $CDCl_3$) and ^{13}C NMR (126 MHz, $CDCl_3$) for compound **3.8a.**

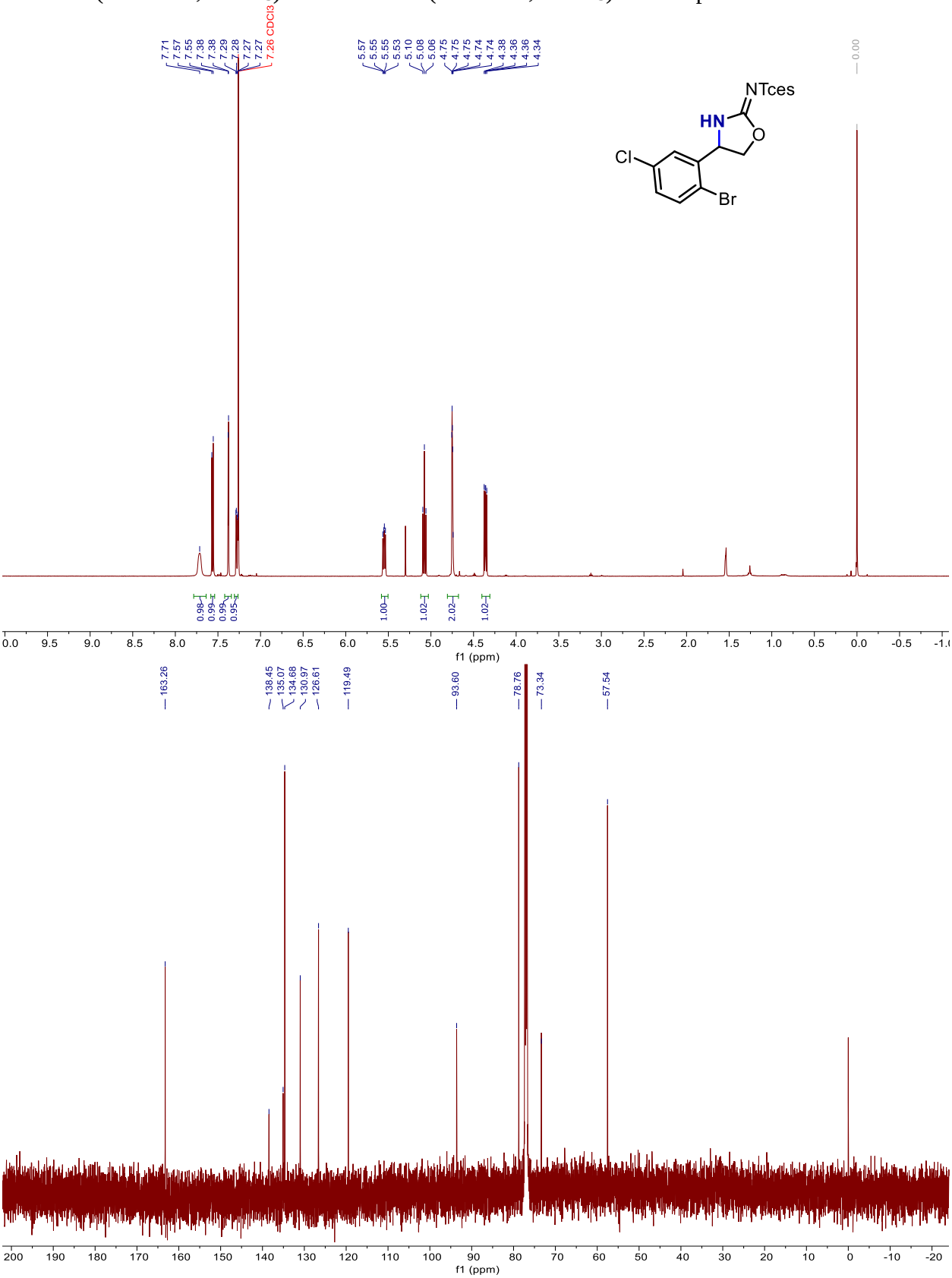

^{1}H NMR (500 MHz, $CDCl_3$) and ^{13}C NMR (126 MHz, $CDCl_3$) for compound **3.1b.**

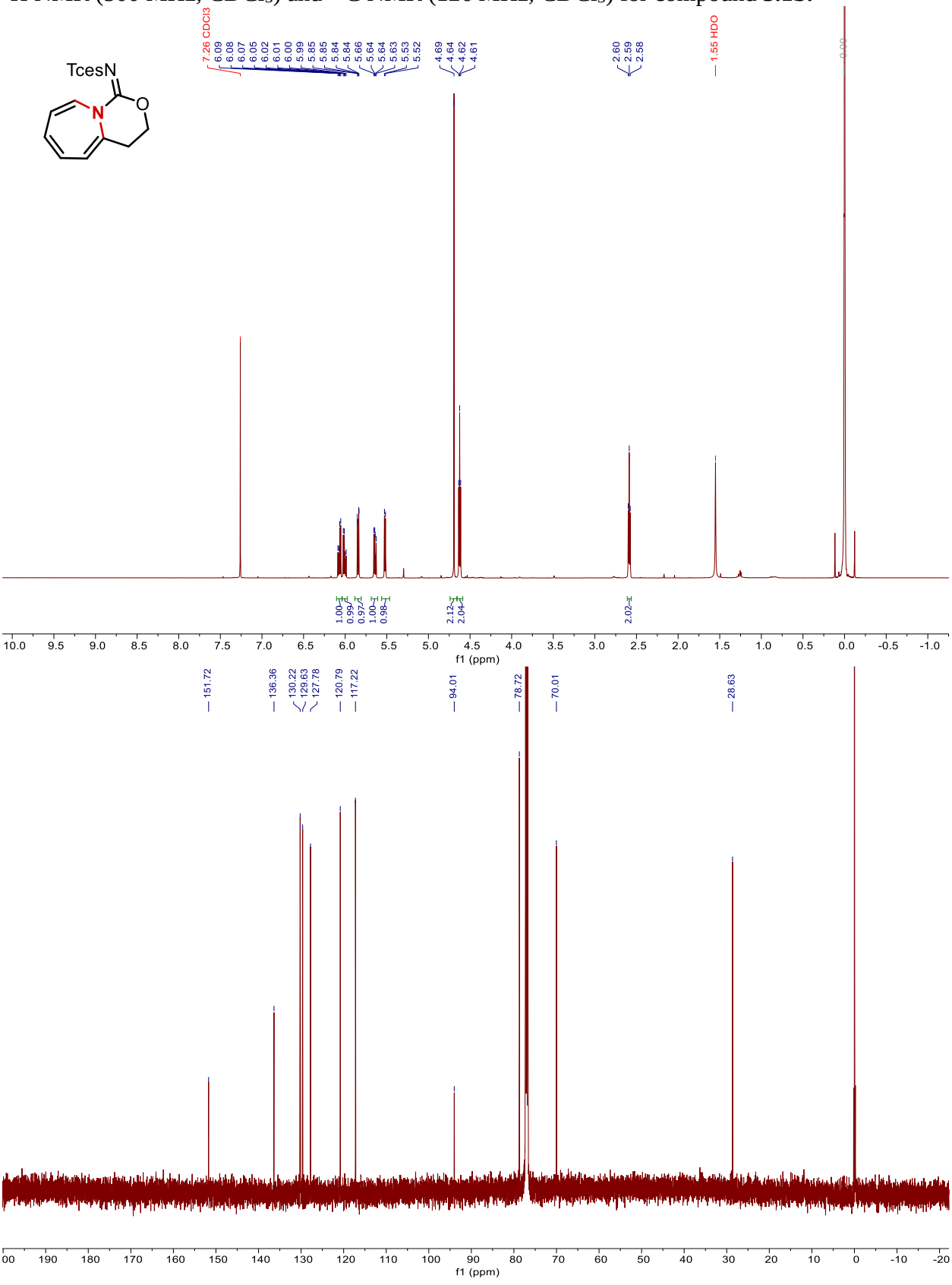

^{1}H NMR (500 MHz, $CDCl_3$) and ^{13}C NMR (126 MHz, $CDCl_3$) for compound **3.2b.**

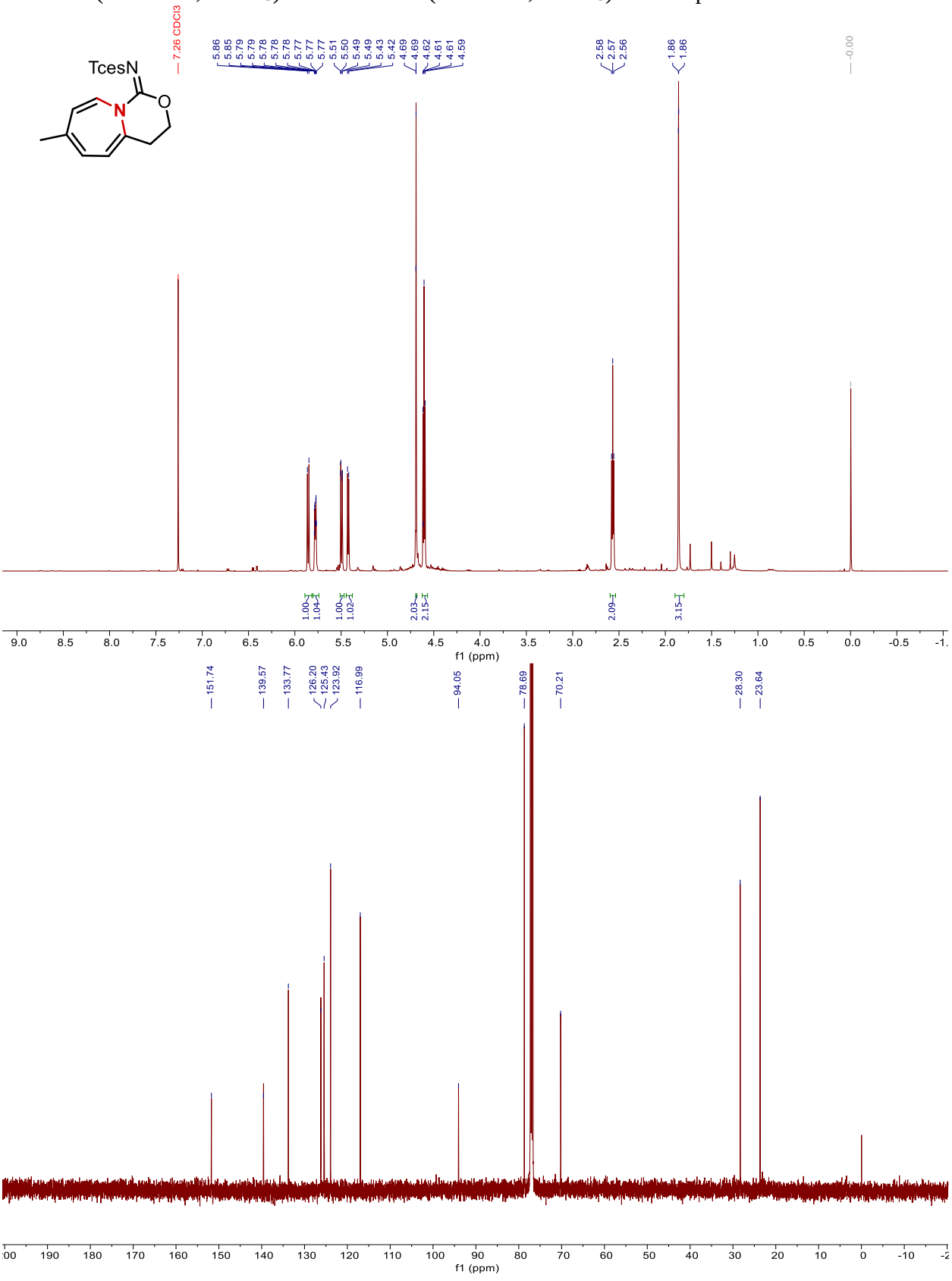

^{1}H NMR (500 MHz, $CDCl_3$) and ^{13}C NMR (126 MHz, $CDCl_3$) for compound **3.3b.**

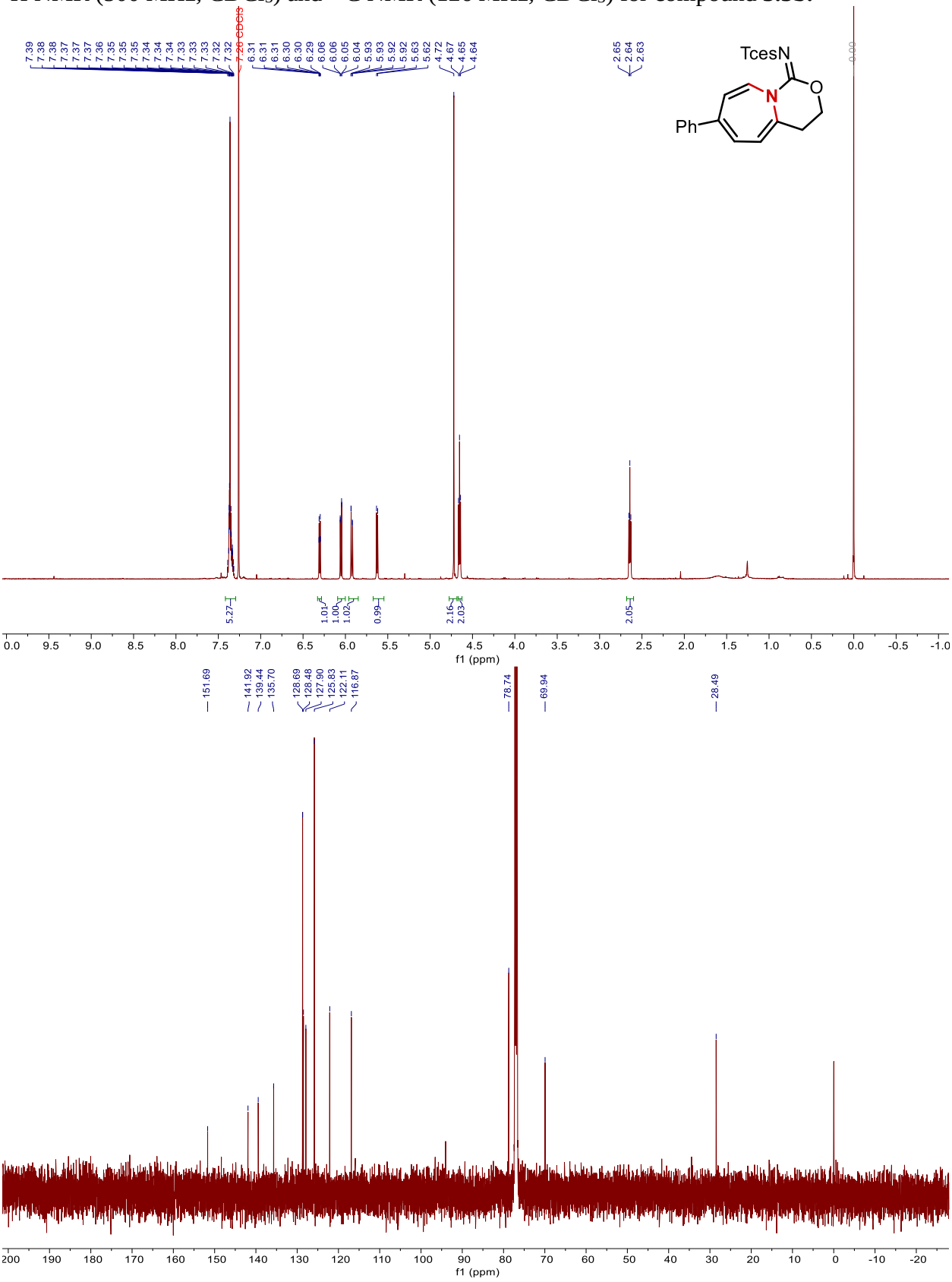

^{1}H NMR (500 MHz, $CDCl_3$) and ^{13}C NMR (126 MHz, $CDCl_3$) for compound **3.4b.**

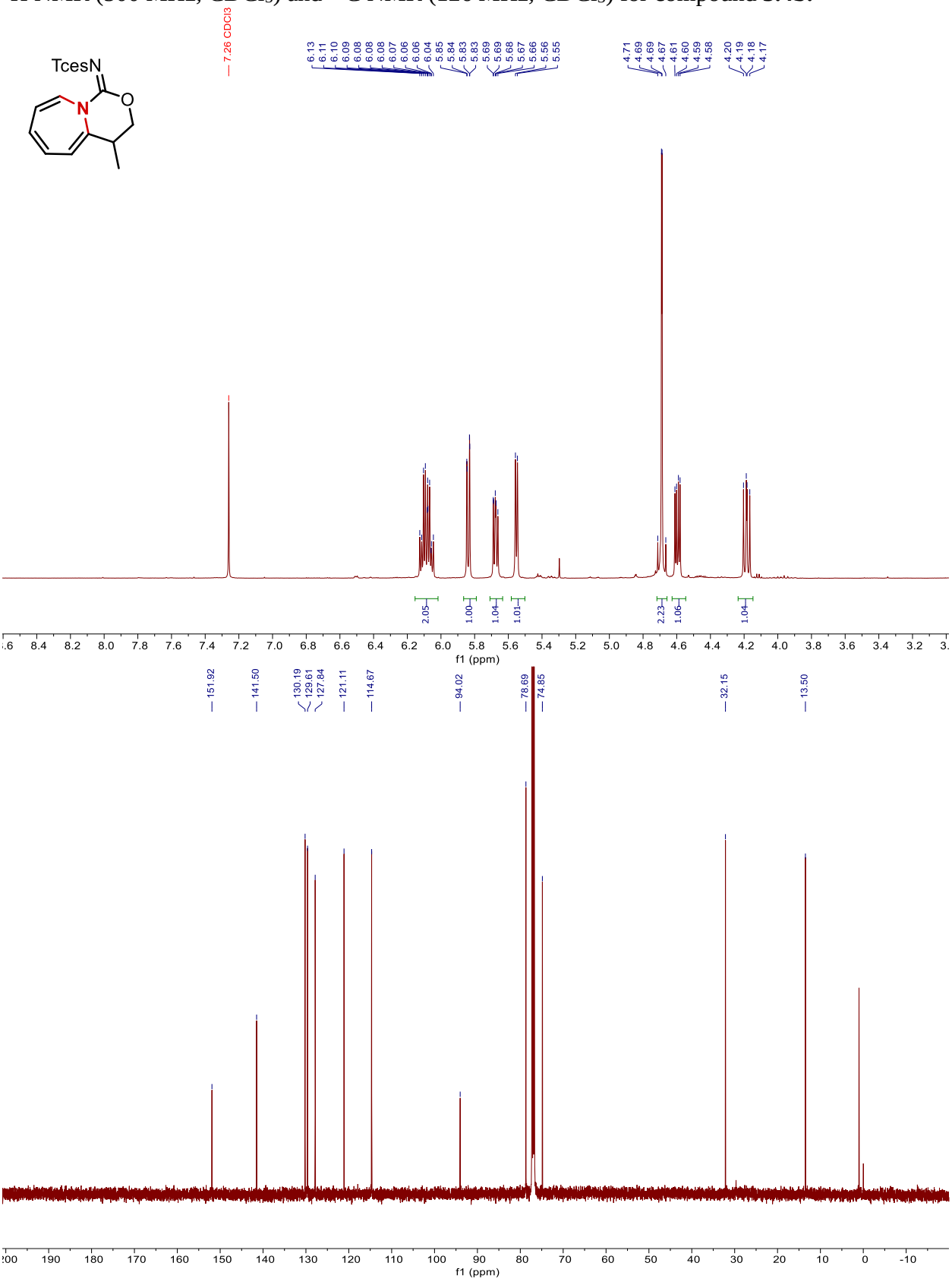

^{1}H NMR (500 MHz, $CDCl_3$) and ^{13}C NMR (126 MHz, $CDCl_3$) for compound **3.5b.**

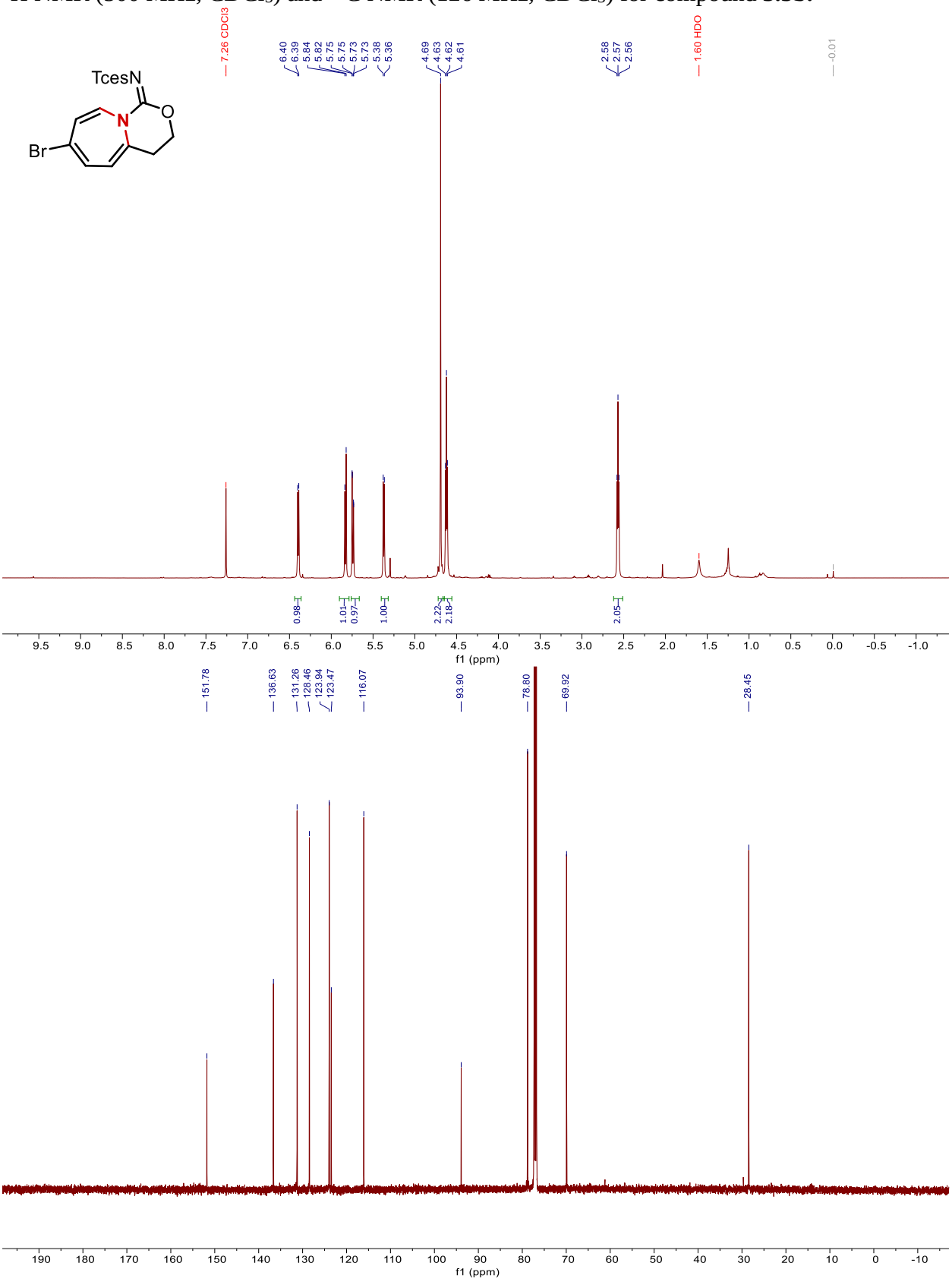

^{1}H NMR (500 MHz, $CDCl_3$), ^{13}C NMR (126 MHz, $CDCl_3$), and ^{19}F NMR (377 MHz, $CDCl_3$)for compound **3.7b.**

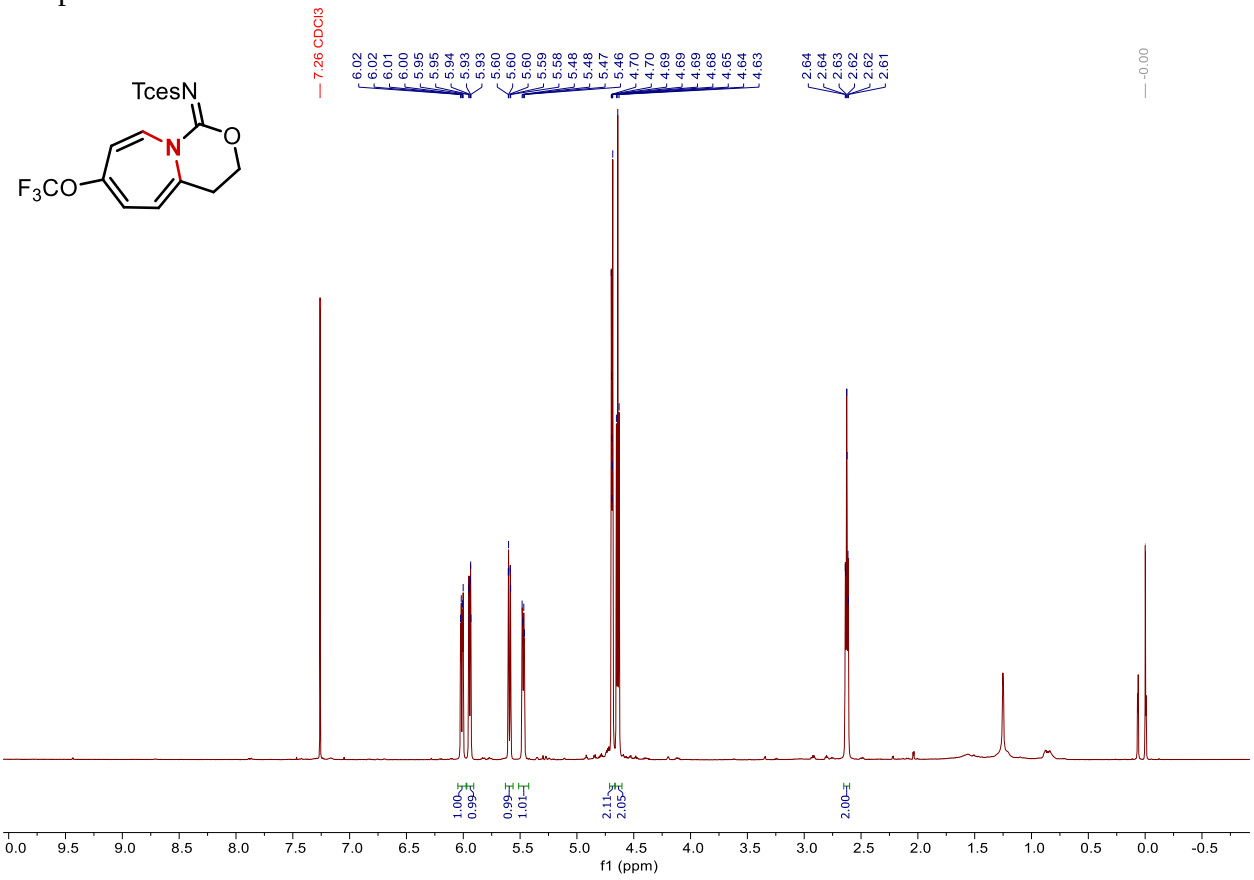

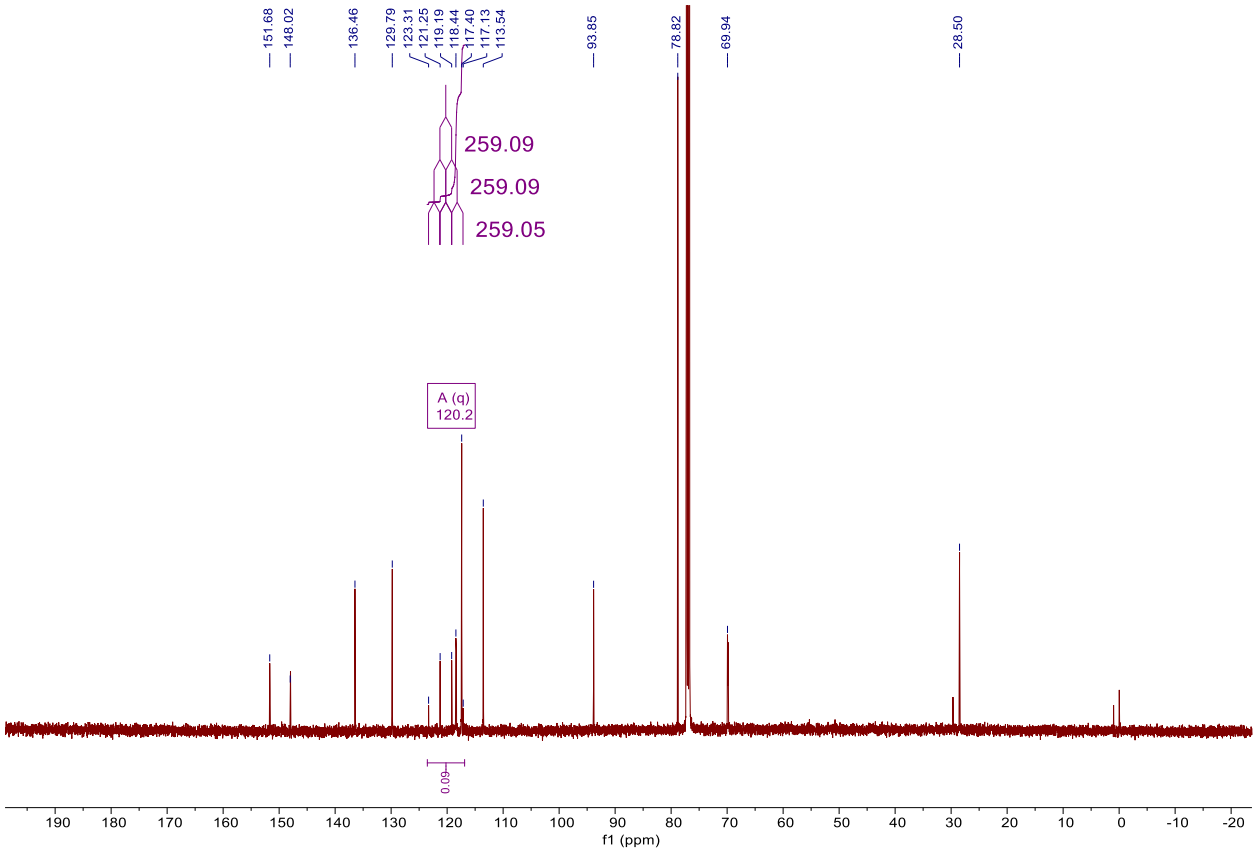
151.68
148.02
136.46
129.79
123.31
121.25
119.19
118.44
117.40
117.13
113.54
93.85
78.82
69.94
28.50
259.09
259.09
259.05
A (q)
120.2
0.09
190 180 170 160 150 140 130 120 110 100 90 80 70 60 50 40 30 20 10 0 -10 -20
f1 (ppm)

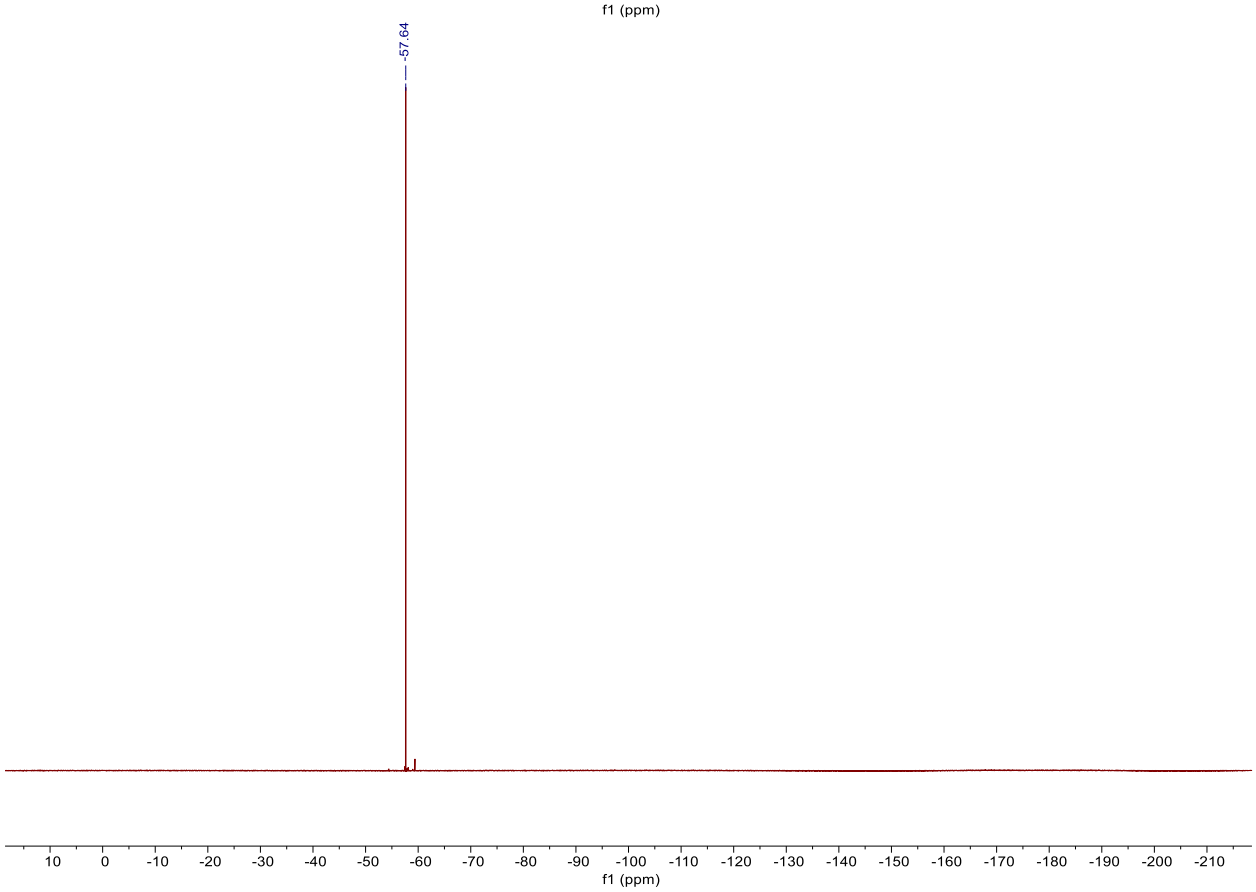
-57.64
10 0 -10 -20 -30 -40 -50 -60 -70 -80 -90 -100 -110 -120 -130 -140 -150 -160 -170 -180 -190 -200 -210
f1 (ppm)

^{1}H NMR (500 MHz, $CDCl_3$) and ^{13}C NMR (126 MHz, $CDCl_3$) for compound **3.9b.**

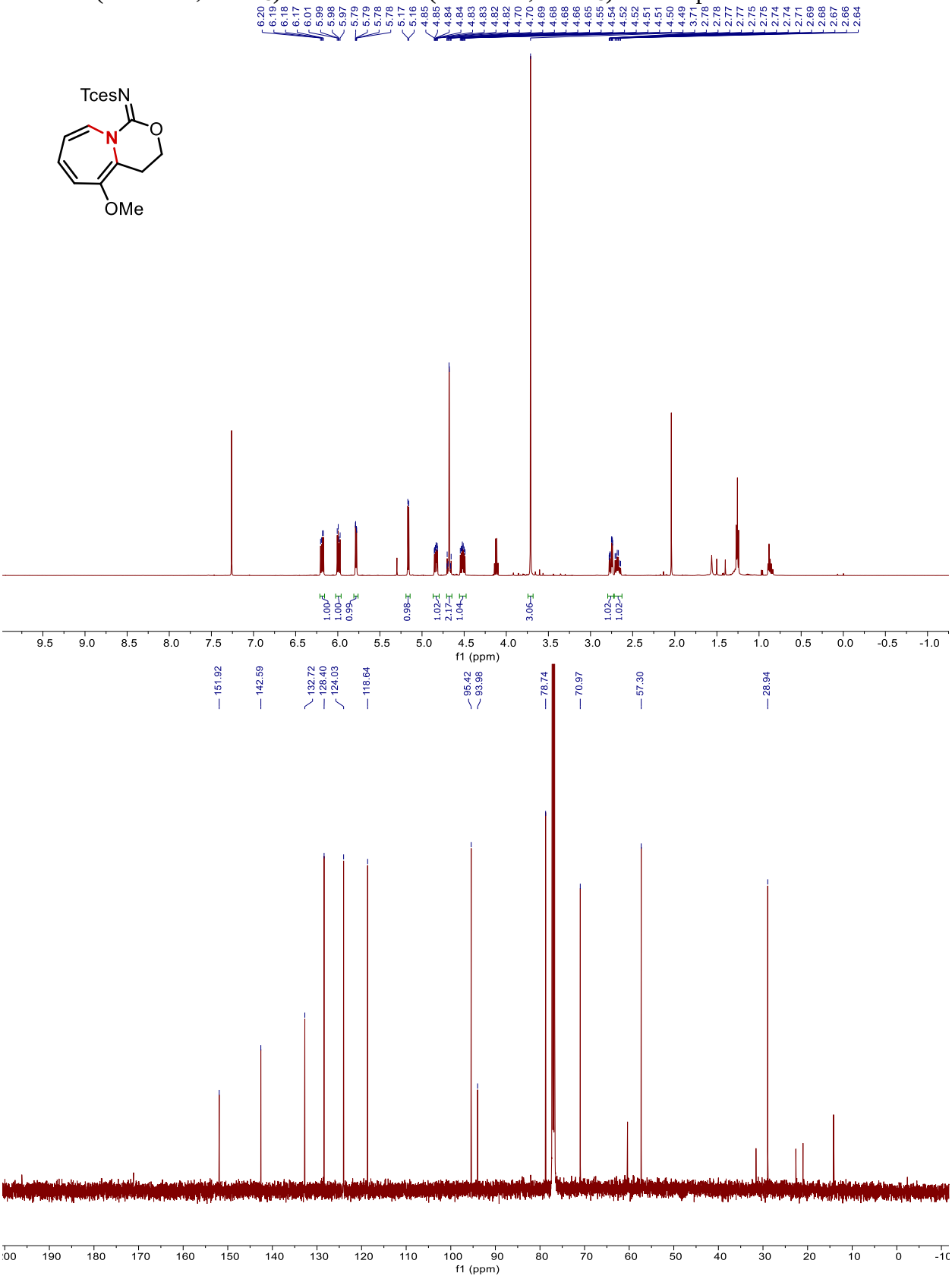

^{1}H NMR (500 MHz, $CDCl_3$) and ^{13}C NMR (126 MHz, $CDCl_3$) for compound **3.10b.**

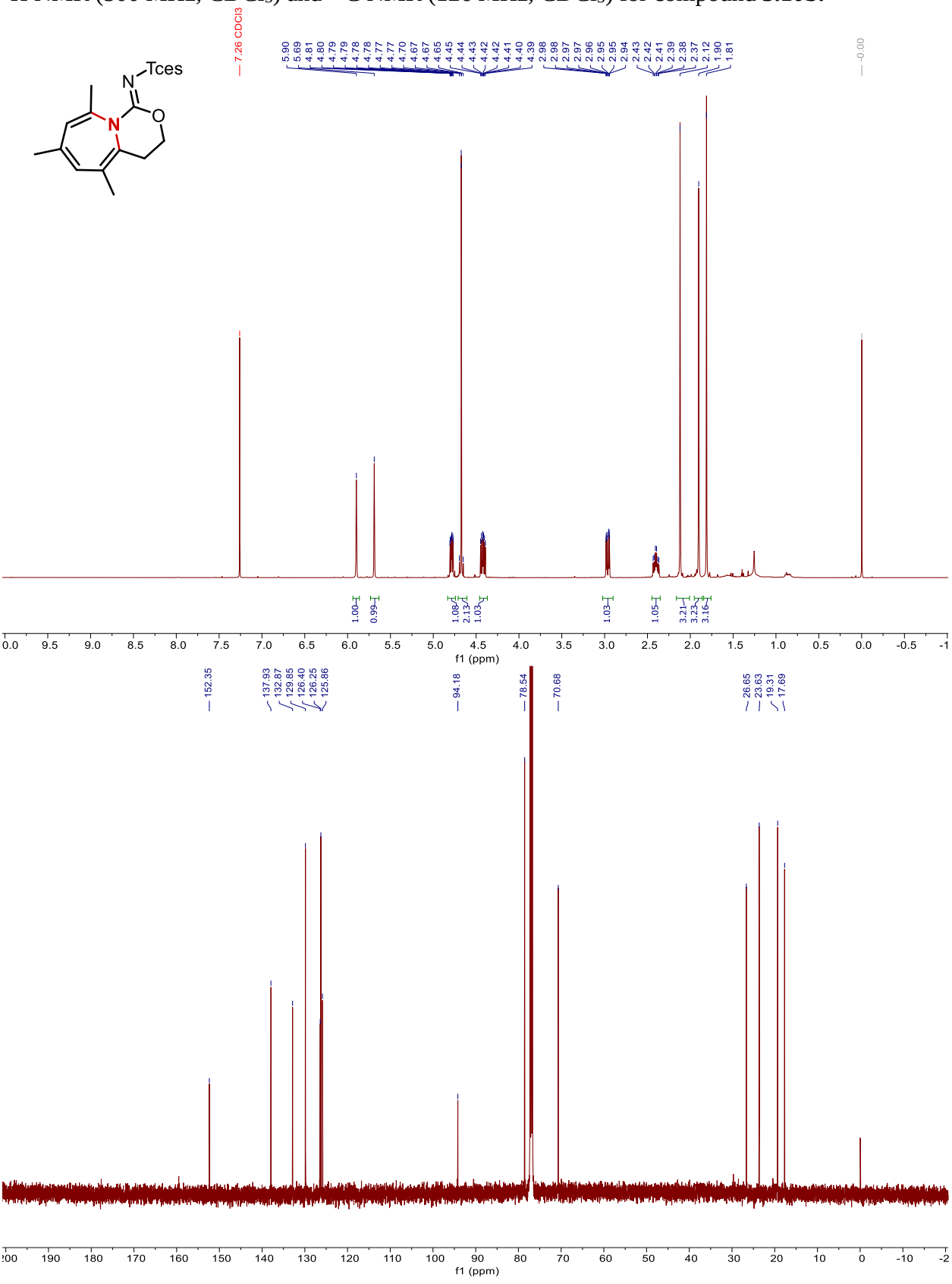

^{1}H NMR (500 MHz, $CDCl_3$) and ^{13}C NMR (126 MHz, $CDCl_3$) for compound **3.11b.**

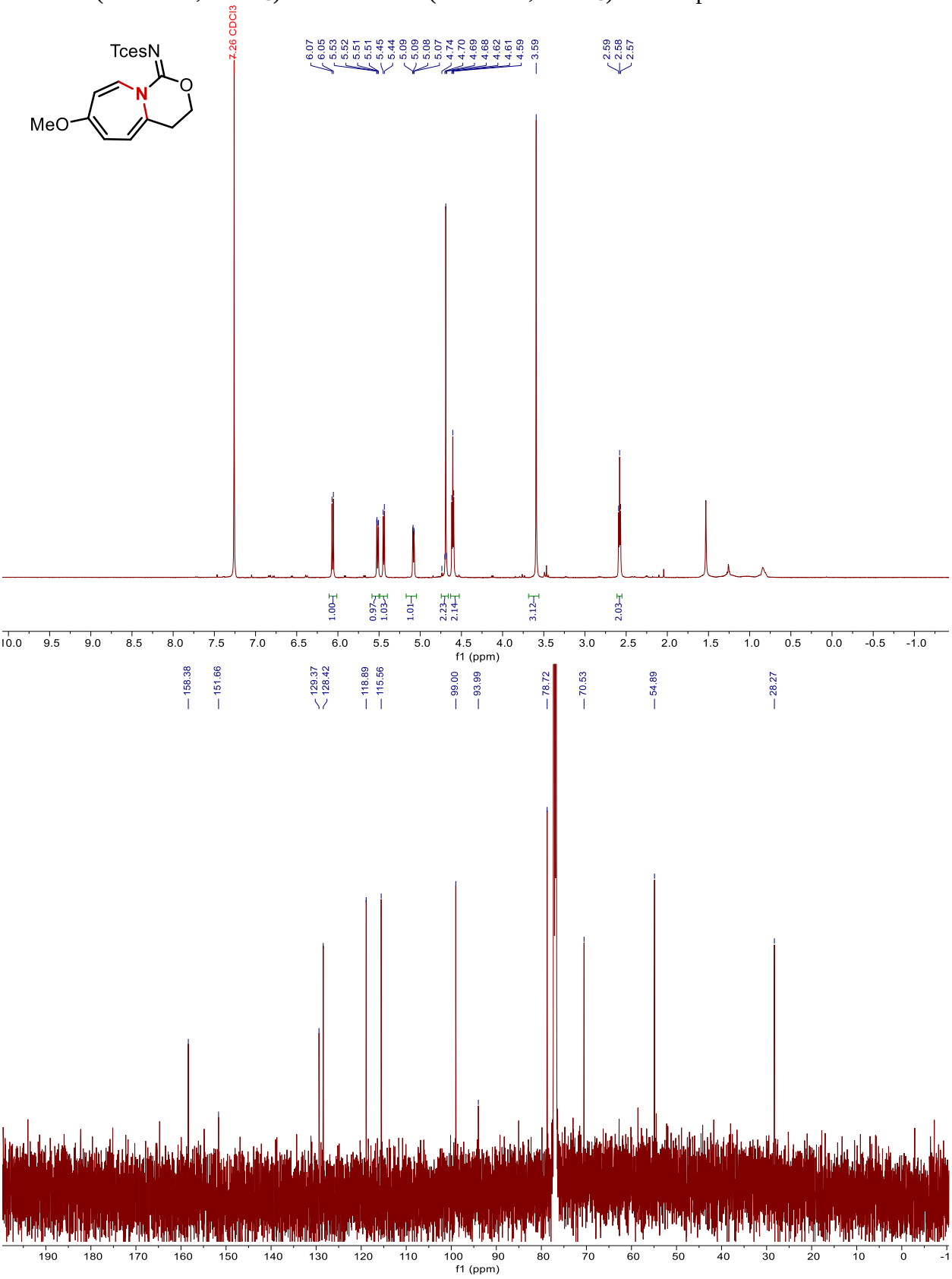

^{1}H NMR (500 MHz, $CDCl_3$) and ^{13}C NMR (126 MHz, $CDCl_3$) for compound **3.12.**

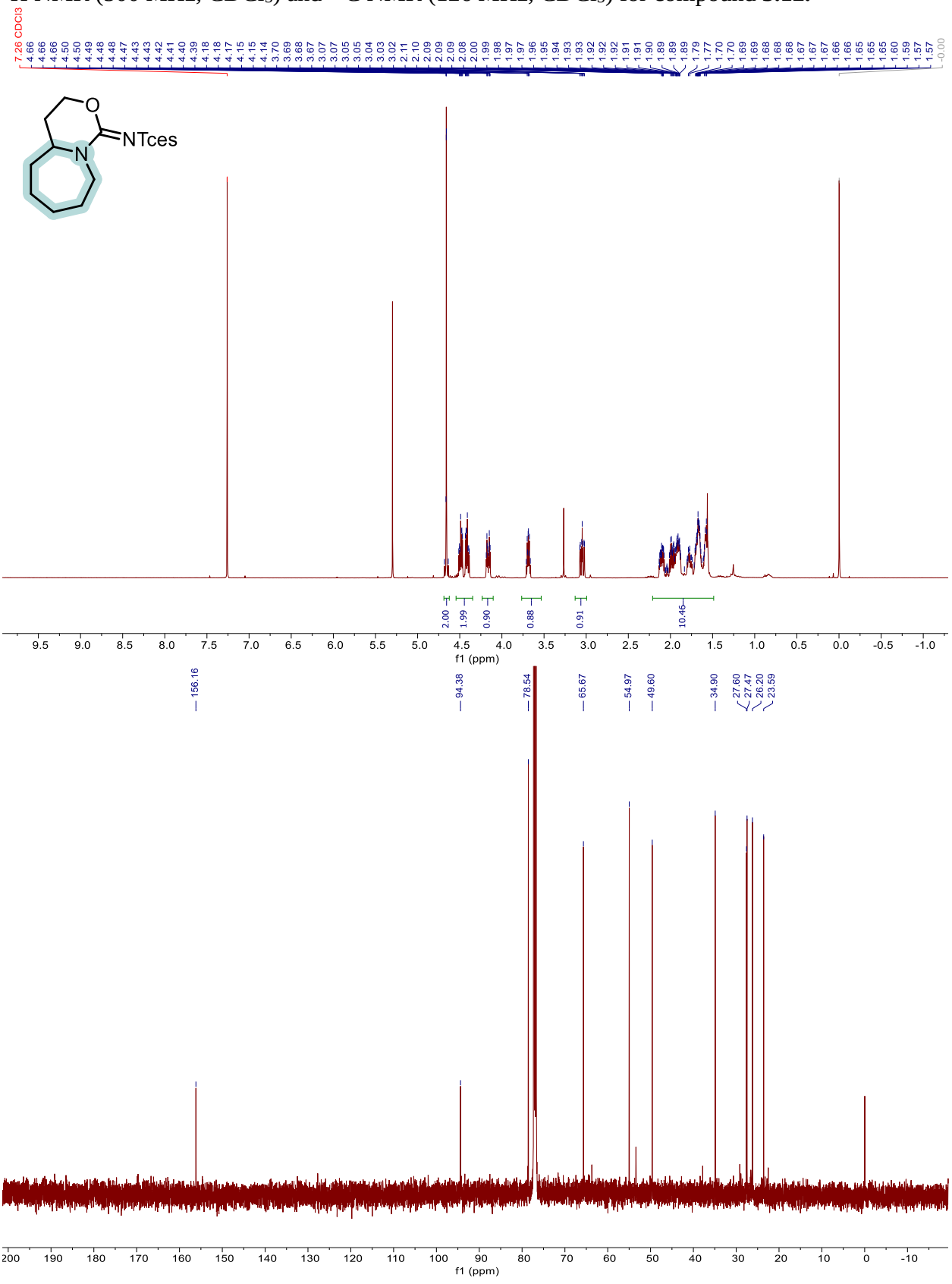

^{1}H NMR (500 MHz, $CDCl_3$) and ^{13}C NMR (126 MHz, $CDCl_3$) for compound **3.13.**

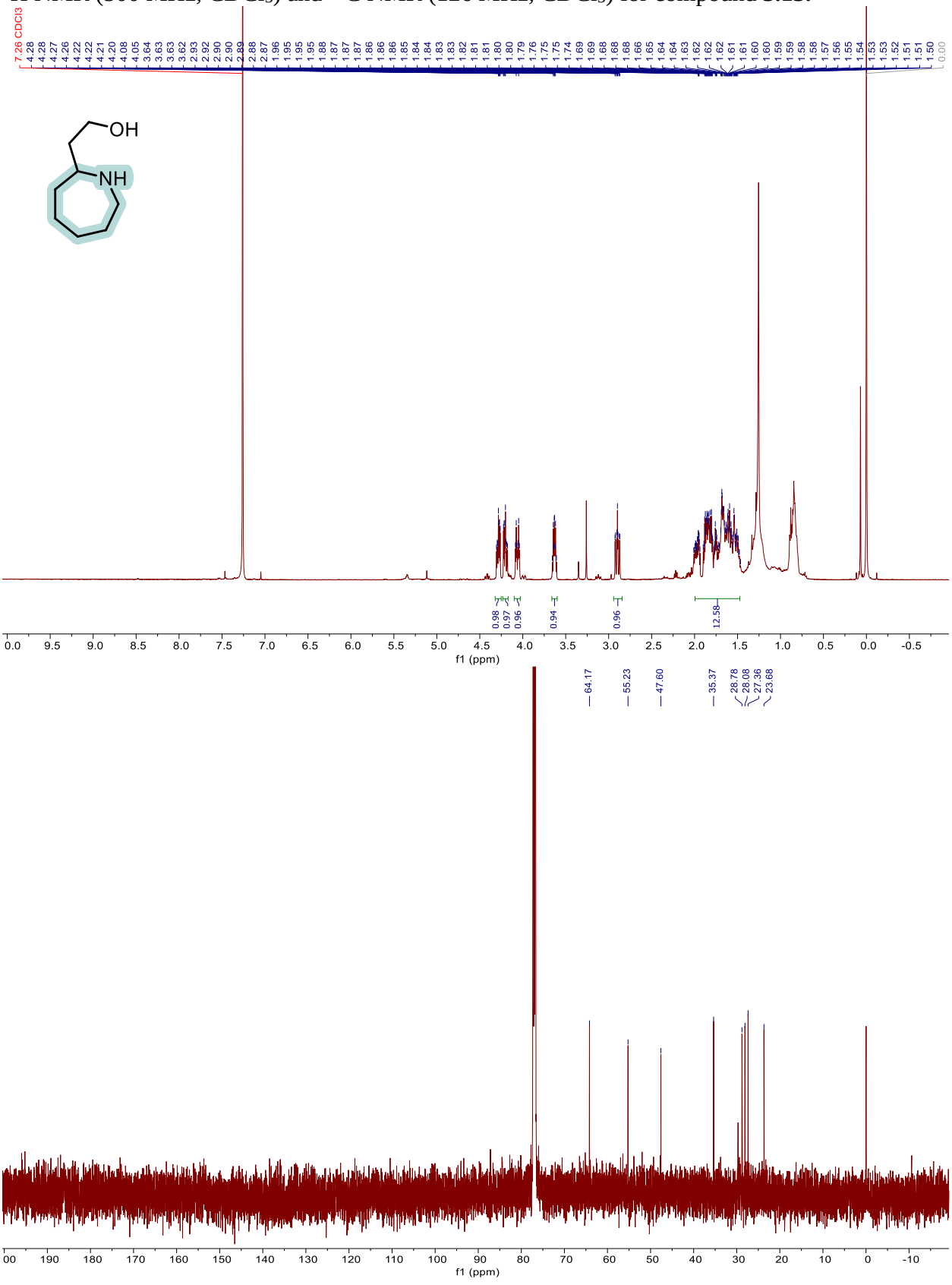

^{1}H NMR (500 MHz, MeOD) and ^{13}C NMR (126 MHz, MeOD) for compound **3.14.**

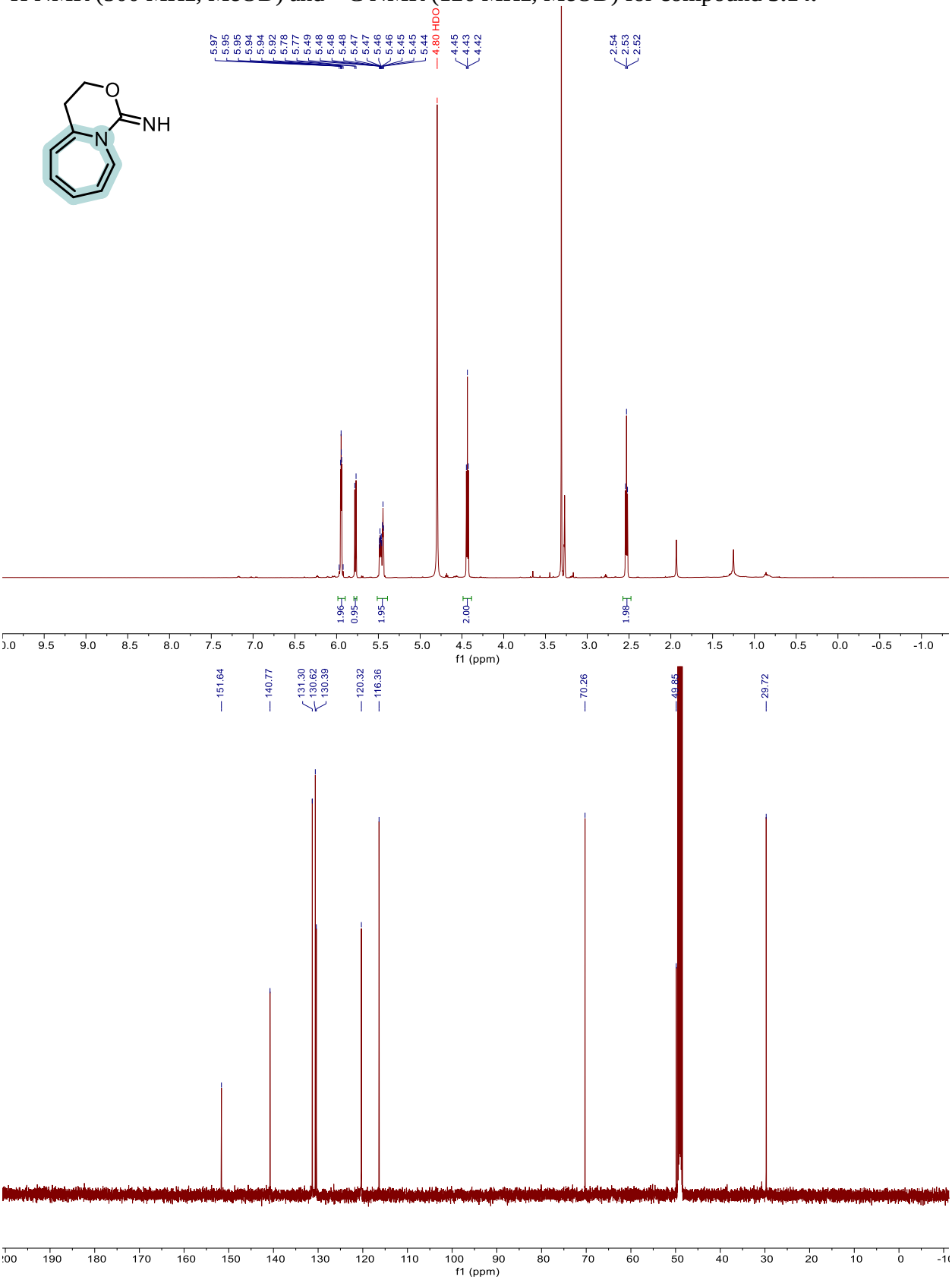

^{1}H NMR (500 MHz, $CDCl_3$) and ^{13}C NMR (126 MHz, $CDCl_3$) for compound **3.15.**

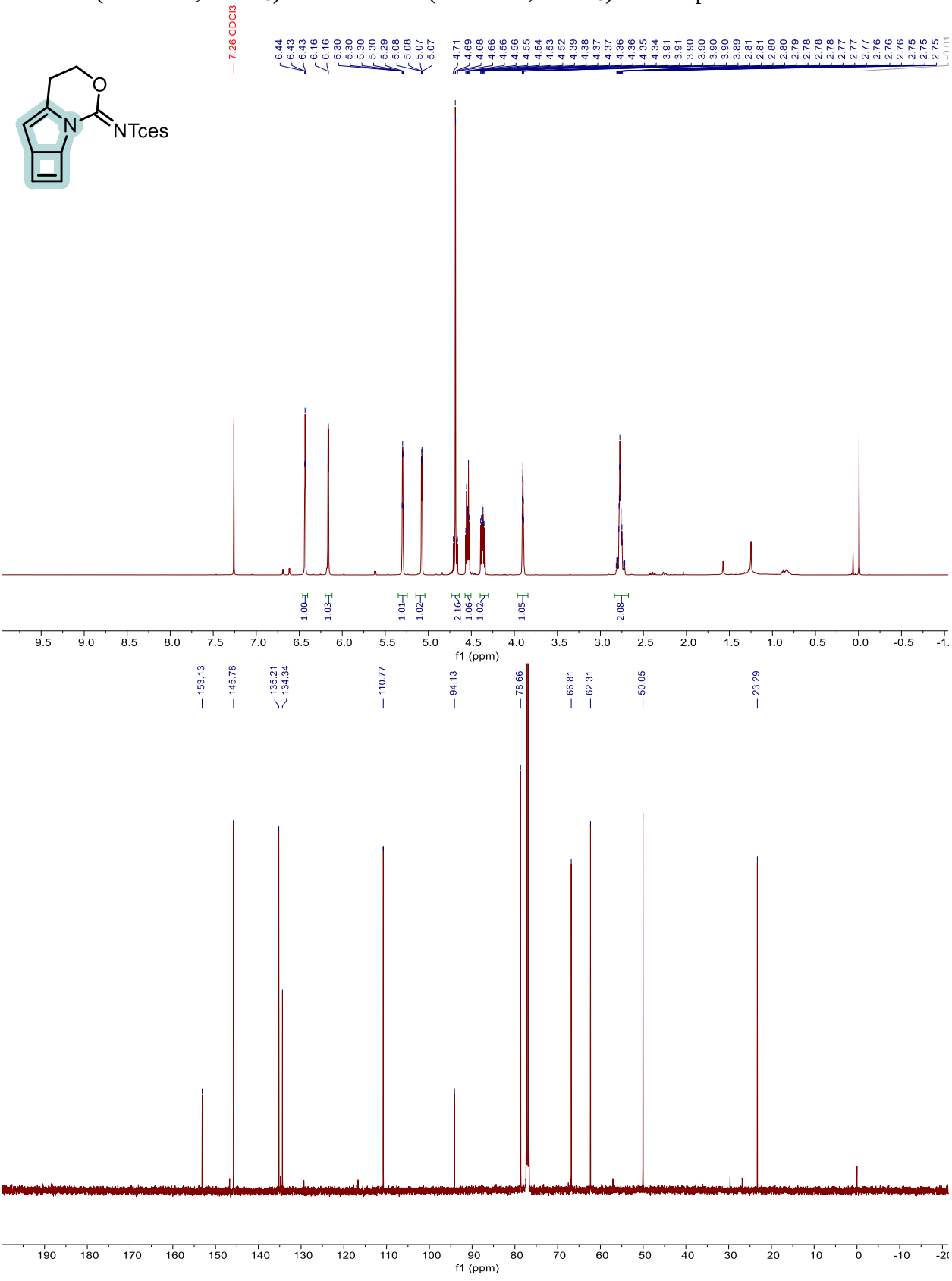

^{1}H NMR (500 MHz, $CDCl_3$) and ^{13}C NMR (126 MHz, $CDCl_3$) for compound **3.16.**